frontiers | Research Topics

The immune response to therapeutic antibodies

Edited by
Daniel T. Mytych, Michael Tovey and
Arno J. Kromminga

Published in
Frontiers in Immunology

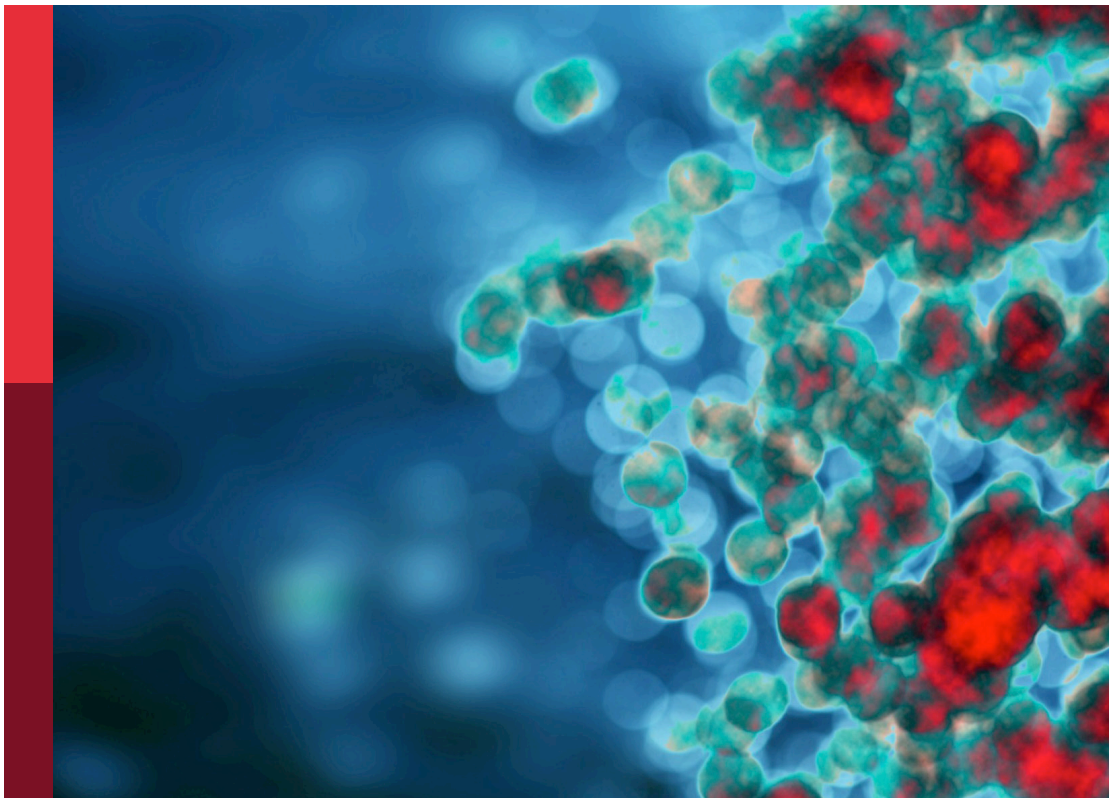

ISSN 1664-8714
ISBN 978-2-8325-6035-8
DOI 10.3389/978-2-8325-6035-8

About Frontiers

Frontiers is more than just an open access publisher of scholarly articles: it is a pioneering approach to the world of academia, radically improving the way scholarly research is managed. The grand vision of Frontiers is a world where all people have an equal opportunity to seek, share and generate knowledge. Frontiers provides immediate and permanent online open access to all its publications, but this alone is not enough to realize our grand goals.

Frontiers journal series

The Frontiers journal series is a multi-tier and interdisciplinary set of open-access, online journals, promising a paradigm shift from the current review, selection and dissemination processes in academic publishing. All Frontiers journals are driven by researchers for researchers; therefore, they constitute a service to the scholarly community. At the same time, the *Frontiers journal series* operates on a revolutionary invention, the tiered publishing system, initially addressing specific communities of scholars, and gradually climbing up to broader public understanding, thus serving the interests of the lay society, too.

Dedication to quality

Each Frontiers article is a landmark of the highest quality, thanks to genuinely collaborative interactions between authors and review editors, who include some of the world's best academicians. Research must be certified by peers before entering a stream of knowledge that may eventually reach the public - and shape society; therefore, Frontiers only applies the most rigorous and unbiased reviews. Frontiers revolutionizes research publishing by freely delivering the most outstanding research, evaluated with no bias from both the academic and social point of view. By applying the most advanced information technologies, Frontiers is catapulting scholarly publishing into a new generation.

What are Frontiers Research Topics?

Frontiers Research Topics are very popular trademarks of the *Frontiers journals series*: they are collections of at least ten articles, all centered on a particular subject. With their unique mix of varied contributions from Original Research to Review Articles, Frontiers Research Topics unify the most influential researchers, the latest key findings and historical advances in a hot research area.

Find out more on how to host your own Frontiers Research Topic or contribute to one as an author by contacting the Frontiers editorial office: frontiersin.org/about/contact

The immune response to therapeutic antibodies

Topic editors
Daniel T. Mytych — Amgen, United States
Michael Tovey — Svar Life Science, France
Arno J. Kromminga — BioNTech, Germany

Citation
Mytych, D. T., Tovey, M., Kromminga, A. J., eds. (2025). *The immune response to therapeutic antibodies*. Lausanne: Frontiers Media SA.
doi: 10.3389/978-2-8325-6035-8

Topic Editor Dr. Michael Tovey is MD of Svar France which develops reporter-gene cell lines that could be used to detect neutralizing antibodies against therapeutic agents. Dr. Arno Kromminga is also affiliated with BioNTech which works in the field of therapeutic antibodies; The other Topic Editors declare no competing interests with regard to the Research Topic subject.

Table of contents

frontiers | Frontiers in Immunology

TYPE Editorial
PUBLISHED 10 February 2025
DOI 10.3389/fimmu.2025.1554297

OPEN ACCESS

EDITED AND REVIEWED BY
Harry W. Schroeder,
University of Alabama at Birmingham,
United States

*CORRESPONDENCE
Michael G. Tovey
michael.tovey@svarlifescience.com

RECEIVED 01 January 2025
ACCEPTED 27 January 2025
PUBLISHED 10 February 2025

CITATION
Tovey MG, Kromminga AJ and Mytych DT (2025) Editorial: The immune response to therapeutic antibodies.
Front. Immunol. 16:1554297.
doi: 10.3389/fimmu.2025.1554297

Editorial: The immune response to therapeutic antibodies

Michael G. Tovey[1]*, Arno J. Kromminga[2] and Daniel T. Mytych[3]

[1]Department of Research & Development Svar Lifescience AB, Villejuif, France, [2]Department of Biolytics BioNtech, Mainz, Germany, [3]Department of Clinical Immunology Amgen, Thousand Oaks, CA, United States

KEYWORDS

therapeutic antibodies, MAPPS, monoclonal antibodies, anti-drug antibodies, neutralizing antibodies

Editorial on the Research Topic
The immune response to therapeutic antibodies

The objective of the Research Topic of Frontiers in Immunology on the "*Immune Response to Therapeutic Antibodies*" was to provide a forum for articles that contribute to our understanding of the advances that have helped make therapeutic antibodies one of the most successful classes of therapeutic proteins, and how the field continues to develop and what are the principal challenges that limit this development. The development of an unwanted immune response including the formation of anti-drug antibodies (ADAs) remains one of the principal concerns limiting the use of therapeutic antibodies as illustrated by the recent draft guidance from the Food and Drug Administration (FDA) on how the incidence and clinical significance of ADAs should be reported on product labels. An analysis of this guidance is outlined in detail in one of the articles in the Research Topic (Swanson). The effect of ADAs can range from mere detection to a substantial effect on efficacy and safety most severe in the rare cases when the ADAs cross-react with an endogenous non-redundant counterpart. The diversity of the manuscripts received reflects the vitality of the field some 26 years after the approval of Remicade (infliximab) initially for the treatment of Crohn's disease. These include a better understanding of the factors that predict immunogenicity risk and the outcome in patients treated with anti-tumor necrosis factor alpha antibodies (Spencer et al.; Spencer et al.). The articles published in the Research Topic demonstrate that the field continues to be innovative in terms of the techniques used to render therapeutic antibodies less immunogenic, including computational humanization of antibodies and nanobodies (Gordon et al.), and sufficiently mature to be able to compare framework shuffling and complementarity determining region (CDR) grafting for the humanization of a murine antibody (Wang et al.). Although the reduction in the immunogenicity of therapeutic antibodies has been attained primarily through sequence optimization, the introduction of chemical modifications such as PEGylation to improve serum half-life and glycosylation of the Fc domain to improve effector function can create potentially immunogenic neoepitopes that require the development of additional assays (Hagman et al.). ADAs directed against therapeutic antibodies can reduce bioavailability and alter pharmacokinetics, necessitating comprehensive immunogenicity risk assessments starting at an early stage of drug development. Given the complexity of immunogenicity, no single assay can universally predict the immune response leading to the formation of anti-drug antibodies, requiring an integrated analytical platform to comprehensively evaluate ADA against a therapeutic

antibody (Ding et al.). A trend appears to be the use of a risk-centered approach involving extensive characterization and multiple assays to assess both binding and neutralizing antibodies to support the clinical development of complex multiple-domain protein therapeutics (Hagman et al.). This is illustrated by articles describing the use of a pharmacokinetic (PK) assay as the basis for the characterization of the ADA response to a T-cell engager bispecific antibody (Lotz et al.) and immunogenicity data in a non-human primate (NHP) study that informed on non-sequence, mechanism-based immunogenicity risk of a bi-functional fusion protein combining an anti-PD-1 antibody domain and a single IL-21 mutein domain on the C-terminus that translated to clinical immunogenicity risk (Kroenke et al.). The latter study showed that the cytokine domain can enhance the antibody response directed against the antibody domain, again increasing the complexity of what drives an ADA response. The importance of preclinical immunogenicity risk evaluation was illustrated by a report that showed that the ADA response to a T-cell engager administered by the subcutaneous route in patients with metastatic castration-resistant prostate cancer was markedly reduced when administered by intravenous infusion due most probably to the presence of non-tolerant T-cell epitopes within the amino acid sequence of the T-cell engager that was exposed upon subcutaneous administration (Penny et al.).

ADA production is triggered by a cascade of events initiated by antigen uptake by professional antigen-presenting cells (APCs), particularly dendritic cells (DCs). These cells process the internalized antigen and display peptide fragments as peptide–MHC-II complexes on their surface. T cells that recognize these complexes, along with receiving additional co-stimulatory signals, can trigger B-cell activation, leading to the production of ADAs (Siegel et al.). Given the pivotal role of DCs in this process, assays such as MHC-II-associated peptide proteomics (MAPPs) are frequently employed in drug development to evaluate their capacity to present drug-derived peptides (Jankowski et al.). Several articles describe *in vitro* methods to assess the immunogenicity of therapeutic antibodies based on their ability to be presented by HLA alleles to T cells (Walsh et al.) and how this can differ between geographically diverse populations and how it is crucial to predict potential adverse events and design safer biologics (Siegel et al.). The MAPPs assay has emerged as the predominant method to evaluate the immunogenic potential of engineered variants of immunogenic proteins including therapeutic antibodies (Jankowski et al.). The numerous manuscripts of high quality submitted for publication in the Research Topic of Frontiers in Immunology on the "*Immune Response to Therapeutic Antibodies*" attest to the vitality of the field and will lead to the preparation of a subsequent volume.

Author contributions

MT: Writing – original draft. AK: Writing – review & editing. DM: Writing – review & editing.

Conflict of interest

Author MT was employed by company Svar Lifescience AB. Author AK was employed by company BioNtech. Author DM was employed by company Amgen.

Publisher's note

frontiers | Frontiers in Immunology

TYPE Original Research
PUBLISHED 16 October 2023
DOI 10.3389/fimmu.2023.1271120

OPEN ACCESS

EDITED BY
Michael Tovey,
Svar Life Science, France

REVIEWED BY
Hao Li,
Beth Israel Deaconess Medical Center and Harvard Medical School, United States
Meenu Wadhwa,
National Institute for Biological Standards and Control (NIBSC), United Kingdom

*CORRESPONDENCE
Zuben E. Sauna
Zuben.Sauna@fda.hhs.gov

†These authors have contributed equally to this work

RECEIVED 01 August 2023
ACCEPTED 13 September 2023
PUBLISHED 16 October 2023

CITATION
Jankowski W, Kidchob C, Bunce C, Cloake E, Resende R and Sauna ZE (2023) The MHC Associated Peptide Proteomics assay is a useful tool for the non-clinical assessment of immunogenicity. *Front. Immunol.* 14:1271120. doi: 10.3389/fimmu.2023.1271120

The MHC Associated Peptide Proteomics assay is a useful tool for the non-clinical assessment of immunogenicity

Wojciech Jankowski[1†], Christopher Kidchob[1†], Campbell Bunce[2], Edward Cloake[2], Ricardo Resende[2] and Zuben E. Sauna[1*]

[1]Hemostasis Branch 1, Division of Hemostasis, Office of Plasma Protein Therapeutics, Center for Biologics Evaluation and Research, Food and Drug Administration, Silver Spring, MD, United States, [2]Abzena, Cambridge, United Kingdom

The propensity of therapeutic proteins to elicit an immune response, poses a significant challenge in clinical development and safety of the patients. Assessment of immunogenicity is crucial to predict potential adverse events and design safer biologics. In this study, we employed MHC Associated Peptide Proteomics (MAPPS) to comprehensively evaluate the immunogenic potential of re-engineered variants of immunogenic FVIIa analog (Vatreptacog Alfa). Our finding revealed the correlation between the protein sequence affinity for MHCII and the number of peptides identified in a MAPPS assay and this further correlates with the reduced T-cell responses. Moreover, MAPPS enable the identification of "relevant" T cell epitopes and may contribute to the development of biologics with lower immunogenic potential.

KEYWORDS

therapeutic protein, immunogenicity, MAPPS, HLA, protein engineering, anti-drug antibodies

Introduction

Therapeutic proteins are used to address serious clinical conditions and have emerged as an important class of therapeutics. Despite their many advantages over small molecule drugs, therapeutic proteins have one important drawback; protein-drugs can elicit immune responses in the patient. Anti-drug antibodies (ADAs) that do not directly affect the therapeutic protein are referred to as binding antibodies and immunogenicity risks are limited. On the other hand, neutralizing antibodies (NABs) can affect the efficacy of the medication, alter the PK/PD profile of the drug, or interact with, and neutralize endogenous proteins (1, 2). ADAs can also elicit hypersensitivity responses in the patient and be life threatening. Consequently, immunogenicity is a serious concern

during the development of any therapeutic proteins and has been the subject of many white papers and guidance documents (3–7).

The development of some drugs has been discontinued due to immunogenicity issues (8–11). However, even protein drugs that are licensed and marketed continue to be sub-optimal due to immune responses in some patients (12). The evaluation of the immunogenicity risk of putative protein drugs early in drug development is thus increasingly carried out. To estimate the immunogenicity of candidate drugs several computational tools, *in vitro* and *in vivo* assays have been developed in the last two decades [for an overview see (13)].

The early (and necessary) steps in such an immune response to therapeutic proteins involve: (i) Internalization of the therapeutic protein into antigen presenting cells (APCs). (ii) Degradation of the therapeutic protein into peptide fragments. (iii) Presentation of the therapeutic peptide-derived fragments on Major Histocompatibility Complex Class II (MHCII) molecules on APCs. (iv) Recognition of the peptide-MHC-II complex by T cell receptors (TCRs) on $CD4^+$ T cells. (v) Proliferation of the $CD4^+$ T cells.

Most tools and assays used to assess immunogenicity risk of therapeutic proteins prior to the initiation of clinical trials interrogate one or more of the early steps in the immune response described above. For instance, computational assessments can predict with considerable accuracy the binding affinity of the therapeutic protein derived peptides to MHCII molecules which is an indicator of whether a specific peptide will be presented by the MHCII repertoire of an individual (14). Similarly, *in vitro* methods can be used to experimentally measure the peptide-MHCII affinities (15). These assessments however assume that all potential peptides can be generated from a therapeutic protein, which is not the case. Consequently, there is the possibility of overestimating immunogenicity because some peptides from the therapeutic protein are found to bind strongly to MHCII molecules, however these may never be generated by APCs (16, 17). Other methods, that determine T cell proliferation following incubation with the therapeutic protein (1, 15) involve protein internalization, peptide processing, MHCII presentation, recognition by TCRs and T cell proliferation. The drawback of these methods is that they provide information about the overall immunogenicity of the protein, however, do not allow identification of specific T cell epitopes.

Here we discuss a method that has been gaining momentum in assessing the immunogenicity of therapeutic proteins, namely, the MHC associated peptide proteomics (MAPPs) assay (18). This method is more expensive, complex and resource intense compared to other methods and it is important to demonstrate its value.

The MAPPs assay allows identification of naturally presented, therapeutic protein-derived peptides on MHC proteins. The workflow involves exposure of the full-length therapeutic protein to APCs, and the identification of peptides bound to the MHC complexes. Consequently, this is the only assay that provides information about both processing of the protein to generate peptides and the presentation of these peptides on the MHC. Nonetheless, the considerable resources demanded by a MAPPs assay necessitate that the utility of the assay is demonstrated. In this study we use well characterized variants of recombinant Factor VIIa (FVIIa) to evaluate the MAPPs assay.

Recombinant FVIIa is licensed as bypass therapy for hemophilia A patients who develop neutralizing anti-drug antibodies to Factor VIII (FVIII) (19). From an immunological perspective, patients treated with recombinant FVIIa are not deficient in FVII, they are consequently tolerized to FVII and no anti-FVIIa antidrug antibodies have been reported. However, an analog of FVIIa with 3 amino acid substitutions elicited anti-drug antibodies in 11% of the patient population during a phase 3 clinical trial (8). The clinically relevant neo-epitopes were used, *post-hoc*, to evaluate concordance between *in silico*, *in vitro* and *ex vivo* assessments and clinical immunogenicity (20). Subsequently, the immunogenic variant of FVIIa was re-engineered to be less immunogenic (21). This set of molecules; wild type FVIIa, immunogenic variant and de-immunized analogs were used to evaluate the utility of the MAPPs assay for obtaining clinically relevant information.

Materials and methods

Isolation of PBMCs

Peripheral blood mononuclear cells (PBMCs) were obtained from healthy community subject buffy coats (from blood drawn within 24 hours), under consent, from commercial vendors. PBMC were isolated from buffy coats using Lymphocyte separation medium (Corning, Amsterdam, The Netherlands) density centrifugation and $CD8^+$ T-cell depleted using $CD8^+$ RosetteSep (StemCell Technologies Inc., London, United Kingdom).

T-cell proliferation assay

A cohort of 50 subjects was selected to best represent the number and frequency of HLA-DR and HLA-DQ allotypes expressed in the world population. PBMC were counted, viability assessed by acridine orange and propidium iodide using a Luna-FL Automated Cell Counter (Logos Biosystems, Annandale, VA), and suspended in AIM-V culture medium (Invitrogen, Paisley, United Kingdom) at 4 to 6×10^6 PBMC/mL. Bulk cultures were established for each subject where cells were added to a 24-well plate (Corning Life Science) along with peptide to give a final concentration of 5 μM. For each subject a clinically relevant positive control (cells incubated with exenatide [Bydureon, AstraZeneca, United Kingdom]) and a negative control (cells incubated with culture medium alone) were also included. An additional positive control used in the assay was Keyhole limpet hemocyanin. Proliferation of $CD4^+$ T cells within the culture was measured on days 5, 6, 7, and 8 poststimulation by gently resuspending the cells and removal of 3 × 100 μL samples, which were transferred to a round bottomed 96-well plate and pulsed with 0.75 μCi/well tritiated thymidine (Perkin Elmer, Buckingham, United Kingdom). After 18 hours, the cultures were harvested onto filter mats (Perkin Elmer) using a TomTec Mach III cell harvester and counts per minute (cpm) for each well determined by Meltilex (Perkin Elmer) scintillation counting on a

1450 Microbeta Wallac Trilux Liquid Scintillation Counter (Perkin Elmer) in parallax, low background counting mode. All assays were performed in triplicate. Stimulation index (SI) was calculated by dividing the average counts per minute from peptide cultures by the average counts per minute in medium control cultures.

MAPPs assay

Monocyte derived Dendritic cells (MoDC) were prepared using PBMC from 11 donors using RoboSep™ negative human monocyte isolation kits and RoboSep™ cell isolation instrument (StemCell Technologies, Cambridge, UK) according to the manufacturer's instructions. Monocytes were re-suspended in MoDC differentiation medium and incubated at 37°C, 5% CO2. On day 7, the test samples were added to the cells in MoDC culture medium, and incubated at 37°C, 5% CO2. Following incubation, cells were matured by the addition of LPS (Sigma Aldrich, Poole, UK) and incubated at 37°C, 5% CO2 for 18 hours. On day 8, MoDC were harvested, washed and pelleted prior to flash-freezing at -80°C and cell lysis.

Following cell lysis, the HLA-DR / peptide complexes were purified from the cell lysate by immunoprecipitation and peptides bound to HLA-DR were eluted under acidic conditions. Peptides were analysed using nano liquid chromatography coupled to an Orbitrap mass spectrometer and were identified using the Sequest algorithm, built in the Proteome Discoverer software v2.1 (ThermoFisher Scientific) against a proprietary database and the sequences of the test samples.

Once the final list of identified peptides was completed, the sequence heatmaps were generated using MATLAB (MathWorks®, Cambridge, UK) to allow visualization of the sequence location and frequency of the identified peptides.

In silico peptide-MHC-II binding affinity computations

The set of 4 molecules; wild type FVIIa, the immunogenic variant, Vatreptacog alfa (VA), and two de-immunized analogs of VA, DI-1 and DI-2 were evaluated with their respect to common MHC-II variants. The computation involved generating overlapping 15 mer ammino acid sequences from the primary sequence of each of the 4 molecules. Using the algorithm, NetMHCIIpan 3.2, a machine learning algorithm we predicted the binding of each of the peptides generated to a set of 38 MHC-II molecules. NETMHCIIpan 3.2 utilizes training with randomly generated sets of peptides to generate binding distribution curves for each MHC-II allele (14) which permits binding affinity to be expressed as a percentile rank. Our analyses used a set of 38 DRB1 alleles which represent 99.12% of the allele coverage for the North American population. The peptide-MHC-II binding affinity data set was presented as a promiscuity score [] as a surrogate measure of immunogenicity in the population. The promiscuity score is the sum of the allele frequencies of the MHC-II alleles that binding with high affinity (percentile rank<10%).

Density plots of peptides identified in the MAPPs assay

The probability density plot was generated individually from MAPPs data obtained for each donor. For the set of FVIIa-derived peptides identified in the MAPPs assay, the minimum percent-rank score of each peptide for that subject's HLA alleles was estimated using netMHCIIpan version 3.2.40. The scores were plotted as histograms.

Calculation of cluster frequencies

The frequency of each cluster in the cohort was calculated according to the equation below:

$$\begin{aligned} &Cluster\ \ frequency \\ &= (number\ \ of\ \ donors\ \ common\ \ to\ \ a\ \ cluster \\ &\div total\ \ number\ \ of\ \ donors) \times 100 \end{aligned}$$

Results

Immunogenicity of proteins used in this study

The FVIIa analog, Vatreptacog alfa (VA) elicited anti-drug antibodies in 11% of the population in a clinical trial (8). Two deimmunized variants (DI-1 and DI-2) of VA were designed for reduced immunogenicity (21). We determined the reduction in binding affinities of DI-1 (Figure 1A) and DI-2 (Figure 1B) peptides compared to the equivalent VA peptides for common MHCII variants. Together the MHCII variants depicted in Figures 1A, B, occur in >90% of the North American (NA) population. Similarly, the deimmunized variants show a significant ($p = 0.0113$ for DI-1 and $p = 0.0299$ for DI-2) decrease in the promiscuity score compared to VA (Figure 1C). The promiscuity score describes the fraction of MHC-II variants a peptide binds to with high affinity (percentile score<10) weighted for the frequency with which each MHC-II variant occurs in the NA population (22).

We also evaluated the wild type FVIIa, the engineered analog VA and the two de-immunized variants DI-1 and DI-2 in an *in vitro* T cell proliferation assay. For the T cell proliferation assay (see Methods) we used PBMCs obtained from 50 donors. The relative frequencies of MHC-II variants in our cohort were comparable to those found in the NA population (Figure 1D). Cells from a donor were considered responsive in the assay if the stimulation index (SI) was >2 (see Methods for definition of SI). Consistent with clinical experience, no donors responded to the wild type FVIIa while almost all donors responded to VA. 2 and 0% of donors responded

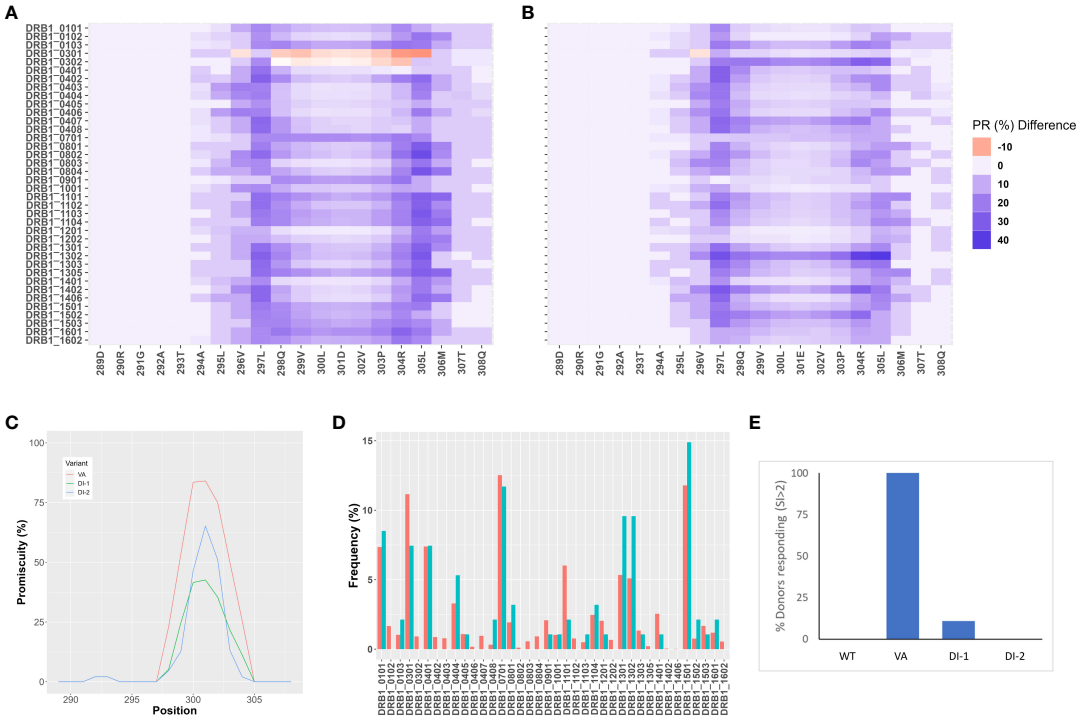

FIGURE 1
In-silico and *in vitro* immunogenicity assessments of deimmunized variants DI-1 and DI-2. **(A,B)** Peptide-MHC-II affinity for 15 mer overlapping peptides in the region of the VA mutations, E296V, and M298Q were determined as percentile ranks. The Y-axis shows the individual MHC-II DRB1 variants, and the X-axis shows the amino acid position. Each position depicts a 15 mer peptide and the amino acid depicted on the figure represents the central peptide in that peptide (i.e., position 9). The percentile rank change between VA and the two variants, DI-1 **(A)** and DI-2 **(B)** are shown. The darker blue color represents an increase in percentile rank (i.e., decrease in affinity) for the de-immunized variant as compared to VA. **(C)** Promiscuity scores (22) for VA, DI-1, and DI-2 derived 15 mer peptides in the region of the mutations introduced in VA. The promiscuity score describes the fraction of MHC-II variants a peptide binds to with high affinity (percentile score<10) weighted for the frequency with which each MHC-II variant occurs in the North American population. **(D)** Distribution of MHC-II variants in the donor cohort used for a T cell proliferation assay (results depicted in (E). The frequencies at which each MHC-II DRB1 variant occurs in the donor cohort (blue bars) and in the North American population (red bars) are shown. **(E)** Cells from the same donor cohort depicted in **(D)** were subjected to a 3H-incorporation T-cell proliferation assay. The per-cent of donors responding to each of the 4 proteins (WT, VA, DI-1, and DI-2) are depicted. Cells from a donor were considered 'responders' if the day 8 stimulation index (SI) value was >2 (see Methods for definition of SI).

to the deimmunized variants DI-1 and DI-2, respectively (Figure 1E). Thus, the potential immunogenicity (based on this assay) of the deimmunized variants was comparable to that of the wild-type protein which has not been associated with immunogenicity in the clinic (23).

The four variants of FVIIa (wild type, VA, DI-1, and DI-2) have distinctive T cell mediated immune responses. The immune responses are likely based on differences in the presentation of peptides by MHC-II proteins on APCs (24). Consequently, these variants were used to assess the utility of the MAPPs assay in immunogenicity assessments.

Mutant FVIIa peptides identified in a MAPPs assay

We carried out the MAPPs assay using PBMCs from 11 donors (see Methods for details). All donors were HLA typed and the MHC-II DRB1 alleles identified in the cohort represent >75% of higher frequency alleles identified in the NA population. Moreover, the relative frequency of each MHC-II DRB1 allele in the cohort is comparable to the frequency of that allele in the NA population (Figure 2A). MoDC from the same cohort of donors were incubated with each of the four variants of FVIIa (wild type, VA, DI-1, and DI-2) to identify peptides presented on the MHC-II DRB1 proteins. The workflow in this study involved affinity capture of MHC-II DRB1 alleles. Thus, while the HLA typing shows the DR, DP and DQ variants for each donor, the peptides identified in the assay are only those associated with the DR alleles. We have included this limitation in the results section. Previously, we identified peptides that were presented by the DR, DP and DQ alleles separately (25). We determined that most of the peptides (~80 %) were presented by the DRB1 alleles.

The total number of sample-specific peptides identified on MHC-II proteins isolated from each donor when incubated with the four FVIIa variants are shown in Figure 2B. In addition to the total number of peptides, we also tabulated the number of peptides that included the E296V and M298Q mutations introduced into VA (Figure 2C).

We have previously demonstrated that peptides identified in a MAPPs assay have a higher affinity to the MHC-II proteins of the donor/patient (25). We estimated the peptide-MHC-II affinities for

10.3389/fimmu.2023.1271120

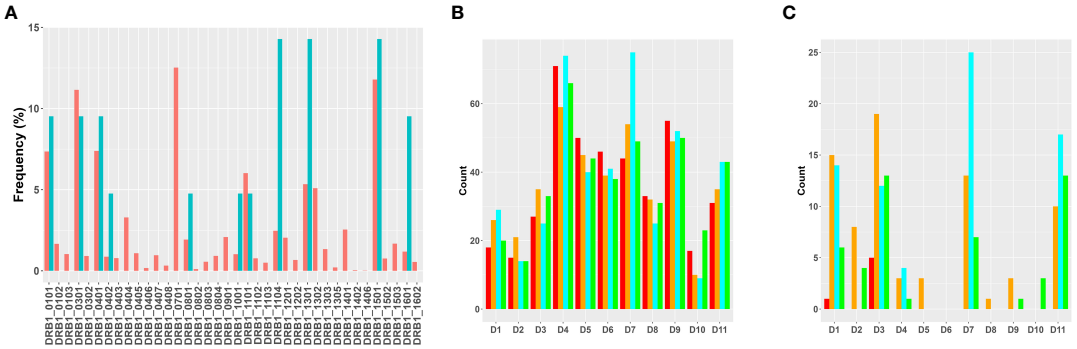

FIGURE 2
Overview of results of the MAPPs assay. **(A)** Distribution of MHC-II variants in the donor cohort used for MAPPs assays. The frequencies at which each MHC-II DRB1 variant occurs in the donor cohort (blue bars) and in the North American population (red bars) are shown. **(B)** The total number of FVIIa-derived peptides recovered from dendritic cells from each of the donors when matured in the presence of WT (red bars), VA (orange bars), DI-1 (blue bars) or DI-2 (green bars) are shown. **(C)** The total number of FVIIa-derived peptides in the region of the VA mutations (E296, and M298) recovered from dendritic cells from each of the donors when matured in the presence of WT (red bars), VA (orange bars), DI-1 (blue bars) or DI-2 (green bars) are shown.

each of the peptides identified in the MAPPs assay using the MHC-II allotype of the donor. The peptide-MHC-II binding affinities were converted to a percentile rank. We demonstrate that the peptides identified in the MAPPs assay are skewed to the left of the plot (Figure 3), i.e., there is a greater probability of finding peptides with lower percentile rank scores (higher affinity). An overview of the characteristic of FVIIa-derived peptides identified in the MAPPs assay is provided in Tables 1A, B.

FVIIa peptides identified in the MAPPs assay locate to 10 clusters

The heat maps depicted in Figure 4 show all the FVIIa-derived peptides identified in the MAPPs assay following incubation of APCs with the FVIIa variants. All peptides were incubated with cells from the same cohort of donors, i.e., an identical distribution of HLA alleles. Although the relative number of peptides varies, all FVIIa variants result in the identification of peptides from the same 10 clusters. This suggests similar processing of the FVIIa variants by the proteolytic machinery of the APCs. This cohort of donors all have a functional FVIIa. Thus, the peptides are mostly self, i.e., they have the same sequence as the endogenous FVIIa expressed by the donor. The peptides found in cluster 8, include mutations in the wild-type sequence to generate the VA and DI-1 and DI-2 variants. These foreign/non-self-peptides are the ones that are relevant vis-à-vis immunogenicity as these are most likely to initiate an immune response to the FVIIa variants. The peptides identified in cluster 8 are listed in Tables 2A–D. It is important to note that, compared to VA, far fewer wild-type peptides are presented by the APCs. This finding demonstrates that the mutations introduced in the VA variant enhance the processing and/or presentation of FVIIa-peptides by the APCs. That the VA peptides are also foreign peptides further increases the probability

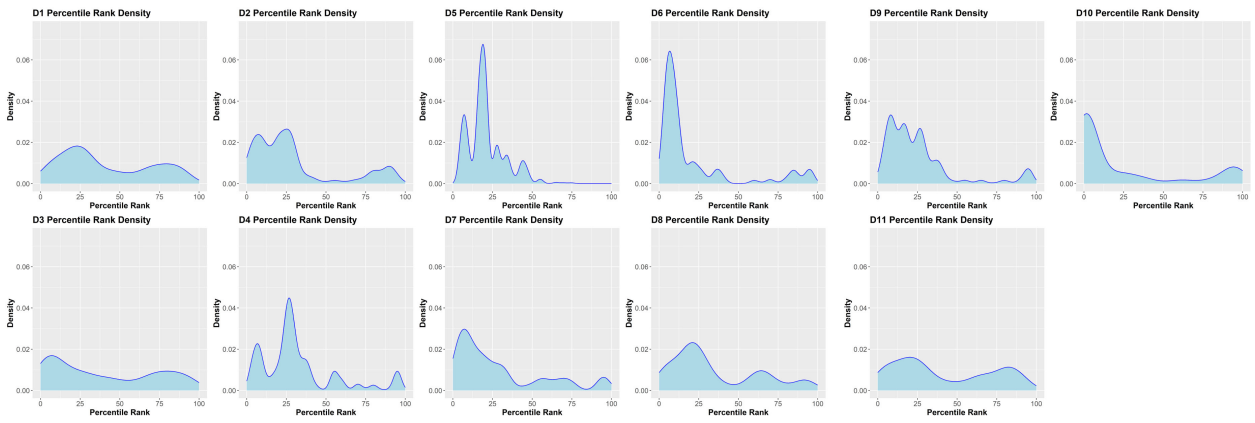

FIGURE 3
Density plots of FVIII peptides identified on donor MHC-II variants in the MAPPs assay. The distributions of percentile rank scores predicted by netMHCIIpan3.2 for all peptides found in the MAPPs assay for all 11 donors used in the study are depicted. Peptides found in the MAPPs assay were more likely to have high binding affinity to the patients' alleles as shown by the greater probability of finding lower percentile rank scores for these peptide/MHC-II binding pairs.

10.3389/fimmu.2023.1271120

TABLE 1A Overview of peptides found for each donor in the MAPPS assay.

Donor	Total Number of Peptides[1]	Number of Unique Peptides[2]	Average Peptide Length[3]	Minimum Peptide Length[4]	Maximum Peptide Length[5]
D1	93	55	17	13	26
D2	64	31	17	13	24
D3	120	74	17	13	25
D4	270	80	18	12	25
D5	179	55	17	12	24
D6	164	43	16	12	21
D7	222	96	17	10	25
D8	121	37	17	13	25
D9	206	60	18	11	25
D10	59	24	17	13	20
D11	152	72	16	11	26

1. Total number of peptides found for each donor across all four variants of FVIIa.
2. Number of unique peptides found after removing duplicate sequences.
3. Average peptide length for peptides found in each donor.
4. For each donor, the peptide with the shortest length was recorded.
5. For each donor, the peptide with the longest length was recorded.

TABLE 1B Overview of peptides found for each donor-construct pair in the MAPPS assay.

Donor Construct	Total Number of Peptides	Number of Unique Peptides	Average Peptide Length	Minimum Peptide Length	Maximum Peptide Length
D1-DI-1	29	29	16	13	19
D1_DI-2	20	20	17	14	24
D1_VA	26	25	17	13	26
D1_WT	18	18	17	14	19
D2_DI-1	14	12	16	13	22
D2_DI-2	14	11	16	13	18
D2_VA	21	17	17	14	24
D2_WT	15	14	17	14	23
D3_DI-1	25	24	16	13	19
D3_DI-2	33	30	17	13	24
D3_VA	35	31	17	13	24
D3_WT	27	25	18	14	25
D4_DI-1	74	69	18	12	25
D4_DI-2	66	64	18	13	25
D4_VA	59	58	18	13	25
D4_WT	71	69	18	12	25
D5_DI-1	40	38	17	13	22
D5_DI-2	44	42	17	12	22
D5_VA	45	43	17	12	24
D5_WT	50	47	17	12	22

(Continued)

10.3389/fimmu.2023.1271120

TABLE 1B Continued

Donor Construct	Total Number of Peptides	Number of Unique Peptides	Average Peptide Length	Minimum Peptide Length	Maximum Peptide Length
D6_DI-1	41	37	16	13	21
D6_DI-2	38	33	16	13	21
D6_VA	39	34	16	12	21
D6_WT	46	39	16	12	21
D7_DI-1	75	68	17	10	25
D7_DI-2	49	48	16	10	25
D7_VA	54	52	17	10	25
D7_WT	44	43	17	10	25
D8_DI-1	25	23	17	13	23
D8_DI-2	31	29	17	13	25
D8_VA	32	29	18	13	25
D8_WT	33	29	17	13	23
D9_DI-1	52	50	17	13	25
D9_DI-2	50	48	18	13	25
D9_VA	49	47	17	13	25
D9_WT	55	52	18	11	25
D10_DI-1	9	6	18	16	20
D10_DI-2	23	21	17	13	20
D10_VA	10	7	18	14	20
D10_WT	17	16	16	14	20
D11_DI-1	43	40	16	11	20
D11_DI-2	43	40	16	13	26
D11_VA	35	33	17	13	26
D11_WT	31	29	17	13	25

1. Total number of peptides found for each donor and FVIIa protein combination.
2. Number of unique peptides found after removing duplicate sequences.
3. Average peptide length for peptides found in each donor and FVIII protein.
4. For each donor and FVIII protein, the peptide with the shortest length was recorded.
5. For each donor and FVIII protein, the peptide with the longest length was recorded.

of these peptides being identified by T cell receptors (TCRs) resulting in a potential initiation of the immune response.

Mutant FVIIa peptides identified on APCs from each donor when incubated with the different FVIIa variants

Monocyte-derived Dendritic cells isolated from the same cohort of donors were incubated with the wild-type FVIIa, VA and the two de-immunized variants, DI-1 and DI-2 and subjected to a MAPPs assay (see methods). The FVIIa-derived peptides in the region of the VA mutations (E296V, and M298Q) identified in the MAPPs assay for each of the FVIIa variants are shown in Tables 2A–D. For each donor we compared the number of peptides identified when the dendritic cells were incubated with VA and each of the two de-immunized variants DI-1 and DI-2. The de-immunized variants were designed to bind with lower affinity to diverse MHC-II variants. For each of the donors in the cohort used we determined: (i) If the mutations introduced in the de-immunized variant resulted in a decrease in binding affinity for the MHC-DRB1 alleles of the donor. (ii) If incubation of the de-immunized variant with the APCs resulted in fewer FVIIa peptides as compared to incubation of VA. The results (Figure 5A) show that when incubated with the variants DI-1 and DI-2, 66.7% and 88.9% of donors respectively exhibited fewer FVIIa peptides on the MHC-II proteins. The percent decrease in the number of peptides (compared to VA) for DI-1 and DI-2 are depicted in Figures 5B, C, respectively. For the deimmunized variant, D1-1: No peptides were detected when the deimmunized variant was incubated with

10.3389/fimmu.2023.1271120

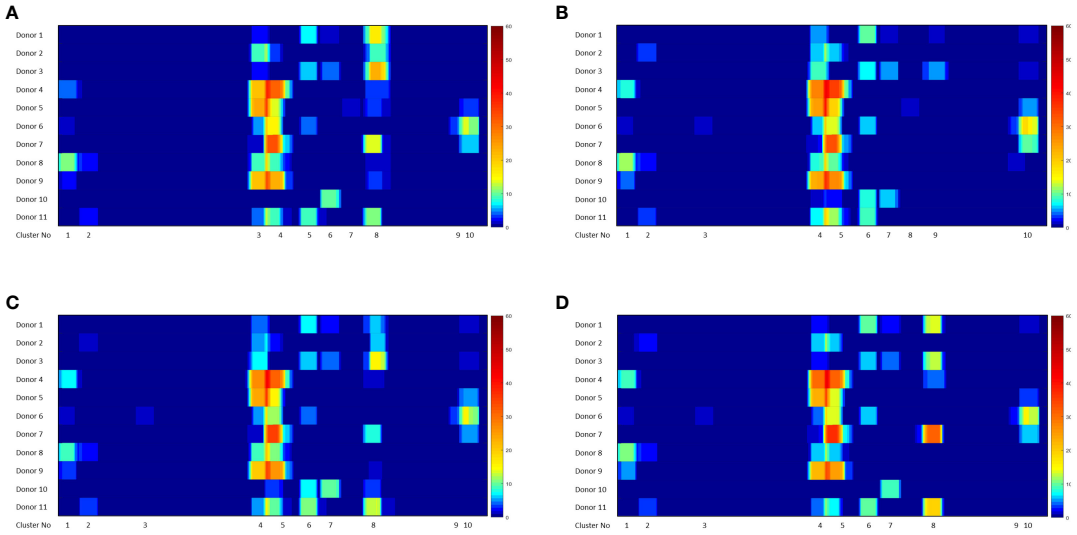

FIGURE 4
Heatmaps showing FVIIa-derived peptides identified in the MAPPs assay. The position of the FVIIa amino acid sequence and all identified clusters are shown on the X-axis. The heatmaps depicts the number of peptides identified in the MAPPs assay at each position following incubation with VA **(A)**, WT **(B)**, DI-1 **(C)** and DI-2 **(D)** proteins. Note that 8 clusters of peptides (shown on the figure) were identified for all treatments.

TABLE 2A Peptides from the Wild Type FVII found in the MAPPS assay and associated HLA alleles.

WT	Halotypes						
Sequences	DRB1	DRB1	DRB3	DRB3	DRB4	DQB1	DQB1
DRGATALELMVLNVPRLMTQD	**03:01:01:01**	**11:04:01**	**01:01:02:01**	**02:02:01:01**	**N/A**	**2:01:01**	**06:02:01:01**
DRGATALELMVLNVPRLMTQDCLQ	**03:01:01:01**	**11:04:01**	**01:01:02:01**	**02:02:01:01**	**N/A**	**2:01:01**	**06:02:01:01**
DRGATALELMVLNVPRLMTQDCLQQ	**03:01:01:01**	**11:04:01**	**01:01:02:01**	**02:02:01:01**	**N/A**	**2:01:01**	**06:02:01:01**
LELMVLNVPRLMTQD	**04:01:01:01** **03:01:01:01**	**11:04:01** **N/A**	**02:02:01:01** **01:01:02:01**	**N/A** **N/A**	**01:03:01:01** **N/A**	**03:01:01:01** **02:01:01**	**N/A** **06:02:01:01**
LELMVLNVPRLMTQDC	**03:01:01:01**	**11:04:01**	**01:01:02:01**	**02:02:01:01**	**N/A**	**2:01:01**	**06:02:01:01**

N/A, Not Available.

TABLE 2B Peptides from VA construct found in the MAPPS assay and associated HLA alleles.

VA	Halotypes							
Sequence	DRB1	DRB1	DRB3	DRB3	DRB4	DRB5	DQB1	DQB1
LLDRGATALVLQVLNVPRL	**4:02:01**	**13:01:01:01**	**01:01:02:01**	**N/A**	**01:03:01:01**	**N/A**	**03:02:01:01**	**06:03:01:01**
LDRGATALVLQVLNVPR	**04:01:01:01**	**15:01:01:01**	**N/A**	**N/A**	**01:03:01:01**	**1:01:01**	**03:02:01:01**	**06:02:01:01**
LDRGATALVLQVLNVPRL	**04:01:01:01**	**15:01:01:01**	**N/A**	**N/A**	**01:03:01:01**	**1:01:01**	**03:02:01:01**	**06:02:01:01**
LDRGATALVLQVLNVPRLM	**4:02:01**	**13:01:01:01**	**01:01:02:01**	**N/A**	**01:03:01:01**	**N/A**	**03:02:01:01**	**06:03:01:01**
DRGATALVLQVLNVPR	**04:01:01:01** **03:01:01:01** **04:02:01**	**11:04:01** **N/A** **13:01:01:01**	**02:02:01:01** **01:01:02:01**	**N/A** **N/A** **N/A**	**01:03:01:01** **N/A** **N/A**	**N/A** **N/A** **N/A**	**03:01:01:01** **02:01:01** **03:02:01:01**	**N/A** **06:02:01:01** **06:03:01:01**
DRGATALVLQVLNVPRL	**04:01:01:01** **03:01:01:01** **04:02:01** **15:01:01:01**	**11:04:01** **N/A** **13:01:01:01** **N/A**	**02:02:01:01** **01:01:02:01** **N/A** **N/A**	**N/A** **N/A** **N/A** **N/A**	**01:03:01:01** **N/A** **N/A** **N/A**	**N/A** **N/A** **N/A** **01:01:01**	**03:01:01:01** **02:01:01** **03:02:01:01** **N/A**	**N/A** **06:02:01:01** **06:03:01:01** **N/A**

(Continued)

10.3389/fimmu.2023.1271120

TABLE 2B Continued

VA	Halotypes							
Sequence	DRB1	DRB1	DRB3	DRB3	DRB4	DRB5	DQB1	DQB1
DRGATALVLQVLNVPRLM	04:01:01:01 03:01:01:01 01:01:01 04:02:01 15:01:01:01	11:04:01 N/A 10:01:01:01 13:01:01:01 N/A	02:02:01:01 01:01:02:01 N/A N/A N/A	N/A N/A N/A N/A N/A	01:03:01:01 N/A N/A N/A N/A	N/A N/A N/A N/A 01:01:01	03:01:01:01 02:01:01 05:01:01:01 03:02:01:01 N/A	N/A 06:02:01:01 N/A 06:03:01:01 N/A
DRGATALVLQVLNVPRLMT	4:02:01	13:01:01:01	01:01:02:01	N/A	01:03:01:01	N/A	03:02:01:01	06:03:01:01
DRGATALVLQVLNVPRLMTQDCLQ	11:04:01 03:01:01:01	15:01:01:01 N/A	02:02:01:01 01:01:02:01	N/A N/A	N/A N/A	01:01:01 N/A	03:01:01:01 02:01:01	06:02:01:01 N/A
DRGATALVLQVLNVPRLMTQDCLQQ	04:01:01:01	11:04:01	02:02:01:01	N/A	01:03:01:01	N/A	03:01:01:01	N/A
DRGATALVLQVLNVPRLMTQDCLQQS	04:01:01:01	11:04:01	02:02:01:01	N/A	01:03:01:01	N/A	03:01:01:01	N/A
RGATALVLQVLNVPRL	04:02:01 04:01:01:01	13:01:01:01 15:01:01:01	01:01:02:01 N/A	N/A N/A	01:03:01:01 N/A	N/A 01:01:01	03:02:01:01 06:02:01:01	06:03:01:01 N/A
RGATALVLQVLNVPRLM	4:02:01	13:01:01:01	01:01:02:01	N/A	01:03:01:01	N/A	03:02:01:01	06:03:01:01
GATALVLQVLNVPR	04:01:01:01 03:01:01:01 04:02:01 15:01:01:01	11:04:01 N/A 13:01:01:01 N/A	02:02:01:01 01:01:02:01 N/A N/A	N/A N/A N/A N/A	01:03:01:01 N/A N/A N/A	N/A N/A N/A 01:01:01	03:01:01:01 02:01:01 03:02:01:01 N/A	N/A 06:02:01:01 06:03:01:01 N/A
GATALVLQVLNVPRL	04:01:01:01 03:01:01:01 04:02:01 15:01:01:01	11:04:01 N/A 13:01:01:01 N/A	02:02:01:01 01:01:02:01 N/A N/A	N/A N/A N/A N/A	01:03:01:01 N/A N/A N/A	N/A N/A N/A 01:01:01	03:01:01:01 02:01:01 03:02:01:01 N/A	N/A 06:02:01:01 06:03:01:01 N/A
GATALVLQVLNVPRLM	04:01:01:01	15:01:01:01	N/A	N/A	01:03:01:01	1:01:01	03:02:01:01	06:02:01:01
GATALVLQVLNVPRLMTQDCLQ	04:01:01:01 15:01:01:01 03:01:01:01 13:01:01:01	11:04:01 N/A N/A 16:01:01	02:02:01:01 N/A 01:01:02:01 N/A	N/A N/A N/A N/A	01:03:01:01 N/A N/A 02:02:01	N/A 01:01:01 N/A N/A	03:01:01:01 06:02:01:01 02:01:01 05:02:01:01	N/A N/A N/A 06:03:01:01
GATALVLQVLNVPRLMTQDCLQQ	13:01:01:01	16:01:01	01:01:02:01	N/A	N/A	2:02:01	05:02:01:01	06:03:01:01
GATALVLQVLNVPRLMTQDCLQQS	04:01:01:01 15:01:01:01 03:01:01:01 13:01:01:01 01:01:01 04:02:01 11:01:01:01	11:04:01 N/A N/A 16:01:01 10:01:01:01 N/A N/A	02:02:01:01 N/A 01:01:02:01 N/A N/A N/A N/A	N/A N/A N/A N/A N/A N/A N/A	01:03:01:01 N/A N/A N/A N/A N/A N/A	N/A 01:01:01 N/A 02:02:01 N/A N/A N/A	03:01:01:01 06:02:01:01 02:01:01 05:02:01:01 05:01:01:01 03:02:01:01 06:01:01:01	N/A N/A N/A 06:03:01:01 N/A N/A
ATALVLQVLNVPR	04:02:01 04:01:01:01	13:01:01:01 15:01:01:01	01:01:02:01 N/A	N/A N/A	01:03:01:01 N/A	N/A N/A	03:02:01:01 01:01:01	06:03:01:01 06:02:01:01
ATALVLQVLNVPRL	04:02:01 04:01:01:01	13:01:01:01 15:01:01:01	01:01:02:01 N/A	N/A N/A	01:03:01:01 N/A	N/A 01:01:01	03:02:01:01 06:02:01:01	06:03:01:01 N/A
ATALVLQVLNVPRLMTQDCLQQS	11:04:01	15:01:01:01	02:02:01:01	N/A	N/A	1:01:01	03:01:01:01	06:02:01:01
TALVLQVLNVPRL	1:01:01	10:01:01:01	N/A	N/A	N/A	N/A	05:01:01:01	N/A
TALVLQVLNVPRLM	1:01:01	16:01:01	N/A	N/A	N/A	2:02:01	05:01:01:01	05:02:01:01
ALVLQVLNVPRLM	1:01:01	16:01:01	N/A	N/A	N/A	2:02:01	05:01:01:01	05:02:01:01
ALVLQVLNVPRLMTQD	03:01:01:01	11:04:01	01:01:02:01	02:02:01:01	N/A	N/A	2:01:01	06:02:01:01
ALVLQVLNVPRLMTQDCL	04:01:01:01	11:04:01	02:02:01:01	N/A	01:03:01:01	N/A	03:01:01:01	N/A
ALVLQVLNVPRLMTQDCLQ	04:01:01:01 03:01:01:01	11:04:01 N/A	02:02:01:01 01:01:02:01	N/A N/A	01:03:01:01 N/A	N/A N/A	03:01:01:01 02:01:01	N/A 06:02:01:01
ALVLQVLNVPRLMTQDCLQQS	03:01:01:01	11:04:01	01:01:02:01	02:02:01:01	N/A	N/A	2:01:01	06:02:01:01
LVLQVLNVPRLMTQ	03:01:01:01	11:04:01	01:01:02:01	02:02:01:01	N/A	N/A	2:01:01	06:02:01:01

(Continued)

10.3389/fimmu.2023.1271120

TABLE 2B Continued

VA	Halotypes							
Sequence	DRB1	DRB1	DRB3	DRB3	DRB4	DRB5	DQB1	DQB1
LVLQVLNVPRLMTQD	04:01:01:01 15:01:01:01 03:01:01:01	11:04:01 N/A N/A	02:02:01:01 N/A 01:01:02:01	N/A N/A N/A	01:03:01:01 N/A N/A	N/A 01:01:01 N/A	03:01:01:01 06:02:01:01 02:01:01	N/A N/A N/A
LVLQVLNVPRLMTQDC	11:04:01	15:01:01:01	02:02:01:01	N/A	N/A	1:01:01	03:01:01:01	06:02:01:01
LVLQVLNVPRLMTQDCL	04:01:01:01 03:01:01:01	11:04:01 N/A	02:02:01:01 01:01:02:01	N/A N/A	01:03:01:01 N/A	N/A N/A	03:01:01:01 02:01:01	N/A 06:02:01:01
LVLQVLNVPRLMTQDCLQ	11:04:01 03:01:01:01	15:01:01:01 N/A	02:02:01:01 01:01:02:01	N/A N/A	N/A N/A	01:01:01 N/A	03:01:01:01 02:01:01	06:02:01:01 N/A
VLQVLNVPRLMTQ	04:01:01:01 03:01:01:01	11:04:01 N/A	02:02:01:01 01:01:02:01	N/A N/A	01:03:01:01 N/A	N/A N/A	03:01:01:01 02:01:01	N/A 06:02:01:01
VLQVLNVPRLMTQD	04:01:01:01 15:01:01:01 03:01:01:01	11:04:01 N/A N/A	02:02:01:01 N/A 01:01:02:01	N/A N/A N/A	01:03:01:01 N/A N/A	N/A 01:01:01 N/A	03:01:01:01 06:02:01:01 02:01:01	N/A N/A N/A
VLQVLNVPRLMTQDC	03:01:01:01	11:04:01	01:01:02:01	02:02:01:01	N/A	N/A	2:01:01	06:02:01:01
VLQVLNVPRLMTQDCL	03:01:01:01	11:04:01	01:01:02:01	02:02:01:01	N/A	N/A	2:01:01	06:02:01:01

N/A, Not Available.

cells from 4 donors, i.e., a 100% decrease in the number of peptides. There was a 30% decrease in number of peptides following incubation with DI-1 compared to VA for 1 donor. When the experiment was carried out in the remaining 4 donors there was no or minimal (0-10%) decrease in the number of peptides. The deimmunized variant DI-2 too showed a decrease in the number of peptides identified: Only one donor showed no decrease in the number of peptides while the other donors showed a 30-100% decrease in the number of peptides. The mean decrease in the number of peptides presented by DI-1 and DI-2 was 49.3% and 59.3%. The deimmunizing strategy selected mutants that resulted in the largest decrease in the promiscuity scores, i.e., the largest decrease in affinity for the maximum fraction of the population. As illustrated in Figures 5B, C, the effect with respect to individual donors can be variable.

Cluster peptide frequency within donor

Determining the frequency with which peptides of interest occur in a donor offers a biologically relevant parameter. The greater the frequency at which a specific foreign peptide of interest (cluster peptide) is identified the higher the theoretical probability of eliciting an immune response. The cluster-peptide frequencies for each of the FVIIa molecules (wild-type, VA, DI-1, and DI-2) are depicted in Table 3. We calculated the percent inhibition in the cluster frequency compared to VA for the wild-type, DI-1, and DI-2 FVIIa proteins (see methods for details). We have shown above, that the wild-type, DI-1, and DI-2 FVIIa proteins exhibit a decrease in T cell proliferation compared to VA (Figure 1B). Consistent with this finding, we demonstrate a significant increase in the percent inhibition in the cluster frequency for the wild-type, DI-1, and DI-2 FVIIa molecules compared to VA (Figures 6A, B). The percent of donors who showed a decrease in the cluster peptide frequency following deimmunization is depicted in Figure 6C.

Discussion

Both antigen processing and presentation are necessary for eliciting T cell responses. To evaluate these steps of the immune response to therapeutic proteins, conventional methods incubate APCs with the therapeutic protein and/or overlapping peptides derived from the therapeutic protein and then measure T cell responses. The primary drawback of these approaches is that: (i) If over-lapping peptides are used in the assay, many peptides that are found to elicit a T-cell response may not be generated by the proteolytic machinery of the cell (i.e., identification of false positives). (ii) If a protein is used in the assay, it is impossible to determine which of the peptides in the protein elicit the response. A mass spectrometry-based strategy, the so-called MHC-associated peptide proteomics (MAPPs) assay, identifies therapeutic protein derived peptides presented and eluted from the MHC proteins. The assay is finding increasing use in the early non-clinical assessment of therapeutic proteins as it is the only experimental strategy that permits identification of therapeutic-protein derived peptides which are both processed and presented by the immune system. However, the MAPPs assay is both technically demanding and expensive and its value and utility need to be assessed.

To assess the value of any *in vitro* assay to provide results that are predictive of clinical outcomes is difficult. This is because the immunogenicity risk of candidate therapeutic entities using *in vitro* assays are carried out early in drug development. Drug candidates determined to be high-risk are generally not moved forward to

TABLE 2C Peptides from the DI-1 construct found in the MAPPS assay and associated HLA alleles.

DI-1	Halotypes								
Sequence	DRB1	DRB1	DRB3	DRB3	DRB4	DRB5	DRB5	DQB1	DQB1
VSGWGQLLDRGATALVLQVLDVPR	4:02:01	13:01:01:01	01:01:02:01	N/A	01:03:01:01	N/A	N/A	03:02:01:01	06:03:01:01
GWGQLLDRGATALVLQVLDVPR	4:02:01	13:01:01:01	01:01:02:01	N/A	01:03:01:01	N/A	N/A	03:02:01:01	06:03:01:01
LLDRGATALVLQVLDVPR	04:01:01:01	15:01:01:01	N/A	N/A	01:03:01:01	N/A	1:01:01	03:02:01:01	06:02:01:01
LLDRGATALVLQVLDVPRL	4:02:01	13:01:01:01	01:01:02:01	N/A	01:03:01:01	N/A	N/A	03:02:01:01	06:03:01:01
LLDRGATALVLQVLDVPRLM	4:02:01	13:01:01:01	01:01:02:01	N/A	01:03:01:01	N/A	N/A	03:02:01:01	06:03:01:01
LDRGATALVLQVLDVPR	04:01:01:01 04:02:01 15:01:01:01	11:04:01 N/A N/A	02:02:01:01 13:01:01:01 N/A	N/A 01:01:02:01 N/A	01:03:01:01 N/A N/A	N/A N/A 01:01:01	N/A N/A N/A	03:01:01:01 03:01:01:01 06:02:01:01	N/A 06:03:01:01 N/A
LDRGATALVLQVLDVPRL	04:01:01:01 03:01:01:01 04:02:01 15:01:01:01	11:04:01 N/A 13:01:01:01 N/A	02:02:01:01 01:01:02:01 N/A N/A	N/A N/A N/A N/A	01:03:01:01 N/A N/A N/A	N/A N/A N/A 01:01:01	N/A N/A N/A N/A	03:01:01:01 02:01:01 03:02:01:01 N/A	N/A 06:02:01:01 06:03:01:01 N/A
LDRGATALVLQVLDVPRLM	03:01:01:01 04:02:01 04:01:01:01	11:04:01 13:01:01:01 15:01:01:01	01:01:02:01 N/A N/A	02:02:01:01 N/A N/A	N/A 01:03:01:01 N/A	N/A N/A 01:01:01	N/A N/A N/A	02:01:01 03:02:01:01 N/A	06:02:01:01 06:03:01:01 N/A
DRGATALVLQVLDVPR	04:01:01:01 03:01:01:01 04:02:01 15:01:01:01	11:04:01 N/A 13:01:01:01 N/A	02:02:01:01 01:01:02:01 N/A N/A	N/A N/A N/A N/A	01:03:01:01 N/A N/A N/A	N/A N/A N/A 01:01:01	N/A N/A N/A N/A	03:01:01:01 02:01:01 03:02:01:01 N/A	N/A 06:02:01:01 06:03:01:01 N/A
DRGATALVLQVLDVPRL	04:01:01:01 03:01:01:01 04:02:01	11:04:01 N/A 13:01:01:01	02:02:01:01 01:01:02:01 N/A	N/A N/A N/A	01:03:01:01 N/A N/A	N/A N/A N/A	N/A N/A N/A	03:01:01:01 02:01:01 03:02:01:01	N/A 06:02:01:01 06:03:01:01
DRGATALVLQVLDVPRLM	04:01:01:01 03:01:01:01 04:02:01 15:01:01:01	11:04:01 N/A 13:01:01:01 N/A	02:02:01:01 01:01:02:01 N/A N/A	N/A N/A N/A N/A	01:03:01:01 N/A N/A N/A	N/A N/A N/A 01:01:01	N/A N/A N/A N/A	03:01:01:01 02:01:01 03:02:01:01 N/A	N/A 06:02:01:01 06:03:01:01 N/A
DRGATALVLQVLDVPRLMT	04:01:01:01 03:01:01:01 04:02:01 15:01:01:01	11:04:01 N/A 13:01:01:01 N/A	02:02:01:01 01:01:02:01 N/A N/A	N/A N/A N/A N/A	01:03:01:01 N/A N/A N/A	N/A N/A N/A 01:01:01	N/A N/A N/A N/A	03:01:01:01 02:01:01 03:02:01:01 N/A	N/A 06:02:01:01 06:03:01:01 N/A
DRGATALVLQVLDVPRLMTQ	13:01:01:01 04:02:01 04:01:01:01	16:01:01 N/A 15:01:01:01	01:01:02:01 N/A N/A	N/A N/A N/A	N/A 01:03:01:01 N/A	02:02:01 N/A 01:01:01	N/A N/A N/A	05:02:01:01 03:02:01:01 06:02:01:01	06:03:01:01 N/A N/A
DRGATALVLQVLDVPRLMTQD	13:01:01:01	16:01:01	01:01:02:01	N/A	N/A	2:02:01	N/A	05:02:01:01	06:03:01:01

(Continued)

10.3389/fimmu.2023.1271120

TABLE 2C Continued

DI-1	Halotypes								
Sequence	DRB1	DRB1	DRB3	DRB3	DRB4	DRB5	DRB5	DQB1	DQB1
DRGATALVLQVLDVPRLMTQDC	13:01:01:01	16:01:01	01:01:02:01	N/A	N/A	2:02:01	N/A	05:02:01:01	06:03:01:01
RGATALVLQVLDVPR	04:01:01:01 04:02:01 15:01:01:01	11:04:01 13:01:01:01 N/A	02:02:01:01 01:01:02:01 N/A	N/A N/A N/A	01:03:01:01 N/A N/A	N/A N/A 01:01:01	N/A N/A N/A	03:01:01:01 03:02:01:0106:02:01:01	N/A 06:03:01:01 N/A
RGATALVLQVLDVPRL	4:02:01	13:01:01:01	01:01:02:01	N/A	01:03:01:01	N/A	N/A	03:02:01:01	06:03:01:01
RGATALVLQVLDVPRLM	04:01:01:01 04:02:01 15:01:01:01	11:04:01 13:01:01:01 N/A	02:02:01:01 01:01:02:01 N/A	N/A N/A N/A	01:03:01:01 N/A N/A	N/A N/A 01:01:01	N/A N/A N/A	03:01:01:01 03:02:01:01 06:02:01:01	N/A 06:03:01:01 N/A
GATALVLQVLDVP	4:02:01	13:01:01:01	01:01:02:01	N/A	01:03:01:01	N/A	N/A	03:02:01:01	06:03:01:01
GATALVLQVLDVPR	04:01:01:01 03:01:01:01 04:02:01 15:01:01:01	11:04:01 N/A 13:01:01:01 N/A	02:02:01:01 01:01:02:01 N/A N/A	N/A N/A N/A N/A	01:03:01:01 N/A N/A N/A	N/A N/A N/A 01:01:01	N/A N/A N/A N/A	03:01:01:01 02:01:01 03:02:01:01 N/A	N/A 06:02:01:01 06:03:01:01 N/A
GATALVLQVLDVPRL	04:01:01:01 03:01:01:01 04:02:01 15:01:01:01	11:04:01 N/A 13:01:01:01 N/A	02:02:01:01 01:01:02:01 N/A N/A	N/A N/A N/A N/A	01:03:01:01 N/A N/A N/A	N/A N/A N/A 01:01:01	N/A N/A N/A N/A	03:01:01:01 02:01:01 03:02:01:01 N/A	N/A 06:02:01:01 06:03:01:01 N/A
GATALVLQVLDVPRLM	04:01:01:01 04:02:01 15:01:01:01 N/A	11:04:01 13:01:01:01 N/A N/A	02:02:01:01 01:01:02:01 N/A N/A	N/A N/A N/A N/A	01:03:01:01 N/A N/A N/A	N/A N/A 01:01:01 N/A	N/A N/A N/A N/A	03:01:01:01 03:02:01:01 06:02:01:01 N/A	N/A 06:03:01:01 N/A N/A
ATALVLQVLDVPR	04:01:01:01 03:01:01:01 04:02:01 15:01:01:01	11:04:01 N/A 13:01:01:01 N/A	02:02:01:01 01:01:02:01 N/A N/A	N/A N/A N/A N/A	01:03:01:01 N/A N/A N/A	N/A N/A N/A 01:01:01	N/A N/A N/A N/A	03:01:01:01 02:01:01 03:02:01:01 N/A	N/A 06:02:01:01 06:03:01:01 N/A
ATALVLQVLDVPRL	04:01:01:01 03:01:01:0104:02:01 15:01:01:01	11:04:01 N/A 13:01:01:01 N/A	02:02:01:01 01:01:02:01 N/A N/A	N/A N/A N/A N/A	01:03:01:01 N/A N/A N/A	N/A N/A N/A 01:01:01	N/A N/A N/A N/A	03:01:01:01 02:01:01 03:02:01:01 N/A	N/A 06:02:01:0106:03:01:01 N/A
ATALVLQVLDVPRLM	04:02:01 N/A N/A N/A	13:01:01:01 N/A N/A N/A	01:01:02:01 N/A N/A N/A	N/A N/A N/A N/A	01:03:01:01 N/A N/A N/A	N/A N/A N/A N/A	N/A N/A N/A N/A	03:02:01:01 N/A N/A N/A	06:03:01:01 N/A N/A N/A
TALVLQVLDVPR	04:02:01 N/A	13:01:01:01 N/A	01:01:02:01 N/A	N/A N/A	01:03:01:01 N/A	N/A N/A	N/A N/A	03:02:01:01 N/A	06:03:01:01 N/A

(Continued)

10.3389/fimmu.2023.1271120

TABLE 2C Continued

DI-1	Halotypes								
Sequence	DRB1	DRB1	DRB3	DRB3	DRB4	DRB5	DRB5	DQB1	DQB1
	N/A N/A	N/A N/A	N/A N/A	N/A N/A	N/A N/A	N/A N/A	N/A N/A	N/A N/A	N/A N/A
TALVLQVLDVPRL	04:02:01 04:01:01:01 N/A N/A	13:01:01:01 15:01:01:01 N/A N/A	01:01:02:01 N/A N/A N/A	N/A N/A N/A N/A	01:03:01:01 N/A N/A N/A	N/A 01:01:01 N/A N/A	N/A N/A N/A N/A	03:02:01:01 06:02:01:01 N/A N/A	06:03:01:01 N/A N/A N/A
TALVLQVLDVPRLMTQ	13:01:01:01 N/A N/A N/A	16:01:01 N/A N/A N/A	01:01:02:01 N/A N/A N/A	N/A N/A N/A N/A	N/A N/A N/A N/A	02:02:01 N/A N/A N/A	N/A N/A N/A N/A	05:02:01:01 N/A N/A N/A	06:03:01:01 N/A N/A N/A
ALVLQVLDVPR	04:02:01 04:01:01:01 N/A N/A	13:01:01:01 15:01:01:01 N/A N/A	01:01:02:01 N/A N/A N/A	N/A N/A N/A N/A	01:03:01:01 N/A N/A N/A	N/A 01:01:01 N/A	N/A N/A N/A N/A	03:02:01:01 06:02:01:01 N/A N/A	06:03:01:01 N/A N/A N/A
LVLQVLDVPRLMTQD	03:01:01:01 N/A N/A N/A	11:04:01 N/A N/A N/A	01:01:02:01 N/A N/A N/A	02:02:01:01 N/A N/A	N/A N/A N/A N/A	N/A N/A N/A N/A	N/A N/A N/A N/A	02:01:01 N/A N/A N/A	06:02:01:01 N/A N/A N/A
VLQVLDVPRLMTQD	04:01:01:01 03:01:01:01 N/A N/A	11:04:01 N/A N/A N/A	02:02:01:01 01:01:02:01 N/A N/A	N/A N/A N/A N/A	01:03:01:01 N/A N/A N/A	N/A N/A N/A N/A	N/A N/A N/A N/A	03:01:01:01 02:01:01 N/A N/A	N/A 06:02:01:01 N/A N/A

N/A, Not Available.

10.3389/fimmu.2023.1271120

10.3389/fimmu.2023.1271120

TABLE 2D Peptides from the DI-2 construct found in the MAPPS assay and associated HLA alleles.

DI-2	Halotypes							
Sequence	DRB1	DRB1	DRB3	DRB3	DRB4	DRB5	DQB1	DQB1
LDRGATALVLQVLEVPR	04:01:01:01 N/A N/A N/A	15:01:01:01 N/A N/A N/A	N/A N/A N/A N/A	N/A N/A N/A N/A	01:03:01:01 N/A N/A N/A	01:01:01 N/A N/A N/A	03:02:01:01 N/A N/A N/A	06:02:01:01 N/A N/A N/A
LDRGATALVLQVLEVPRL	04:02:01 04:01:01:01 N/A N/A	13:01:01:01 15:01:01:01 N/A N/A	01:01:02:01 N/A N/A N/A	N/A N/A N/A N/A	01:03:01:01 N/A N/A N/A	N/A 01:01:01 N/A N/A	03:02:01:01 06:02:01:01 N/A N/A	06:03:01:01 N/A N/A N/A
DRGATALVLQVLE	04:01:01:01 N/A N/A N/A	15:01:01:01 N/A N/A N/A	N/A N/A N/A N/A	N/A N/A N/A N/A	01:03:01:01 N/A N/A N/A	01:01:01 N/A N/A N/A	03:02:01:01 N/A N/A N/A	06:02:01:01 N/A N/A N/A
DRGATALVLQVLEVPR	04:01:01:01 03:01:01:01 04:02:01 15:01:01:01	11:04:01 N/A 13:01:01:01 N/A	02:02:01:01 01:01:02:01 N/A N/A	N/A N/A N/A N/A	01:03:01:01 N/A N/A N/A	N/A N/A N/A 01:01:01	03:01:01:01 02:01:01 03:02:01:01 N/A	N/A 06:02:01:01 06:03:01:01 N/A
DRGATALVLQVLEVPRL	04:01:01:01 N/A 04:02:01 15:01:01:01	11:04:01 N/A 13:01:01:01 N/A	02:02:01:01 01:01:02:01 N/A N/A	N/A N/A N/A N/A	01:03:01:01 N/A N/A N/A	N/A N/A N/A 01:01:01	03:01:01:01 02:01:01 03:02:01:01 N/A	03:01:01:01 06:02:01:01 06:03:01:01 N/A
DRGATALVLQVLEVPRLM	04:02:01 04:01:01:01 N/A N/A	13:01:01:01 15:01:01:01 N/A N/A	01:01:02:01 N/A N/A N/A	N/A N/A N/A N/A	01:03:01:01 N/A N/A N/A	N/A 01:01:01 N/A N/A	03:02:01:01 06:02:01:01 N/A N/A	06:03:01:01 N/A N/A N/A
DRGATALVLQVLEVPRLMTQ	13:01:01:01 N/A N/A N/A	16:01:01 N/A N/A N/A	01:01:02:01 N/A N/A N/A	N/A N/A N/A N/A	N/A N/A N/A N/A	02:02:01 N/A N/A N/A	05:02:01:01 N/A N/A N/A	06:03:01:01 N/A N/A N/A
DRGATALVLQVLEVPRLMTQDCLQ	04:01:01:01 03:01:01:01 N/A N/A	11:04:01 N/A N/A N/A	02:02:01:01 01:01:02:01 N/A N/A	N/A N/A N/A N/A	01:03:01:01 N/A N/A N/A	N/A N/A N/A N/A	03:01:01:01 02:01:01 N/A N/A	N/A 06:02:01:01 N/A N/A
RGATALVLQVLEVPR	04:01:01:01 N/A N/A N/A	15:01:01:01 N/A N/A N/A	N/A N/A N/A N/A	N/A N/A N/A N/A	01:03:01:01 N/A N/A N/A	01:01:01 N/A N/A N/A	03:02:01:01 N/A N/A N/A	06:02:01:01 N/A N/A N/A
RGATALVLQVLEVPRL	04:01:01:01 N/A N/A N/A	15:01:01:01 N/A N/A N/A	N/A N/A N/A N/A	N/A N/A N/A N/A	01:03:01:01 N/A N/A N/A	01:01:01 N/A N/A N/A	03:02:01:01 N/A N/A N/A	06:02:01:01 N/A N/A N/A
GATALVLQVLEVPR	04:02:01 04:01:01:01 N/A N/A	13:01:01:01 15:01:01:01 N/A N/A	01:01:02:01 N/A N/A N/A	N/A N/A N/A N/A	01:03:01:01 N/A N/A N/A	N/A 01:01:01 N/A N/A	03:02:01:01 06:02:01:01 N/A N/A	06:03:01:01 N/A N/A N/A
GATALVLQVLEVPRL	04:02:01 03:01:01:01 04:01:01:01 N/A	13:01:01:01 N/A 15:01:01:01 N/A	01:01:02:01 02:02:01:01 N/A N/A	N/A N/A N/A N/A	01:03:01:01 N/A N/A N/A	N/A N/A 01:01:01 N/A	03:01:01:01 02:01:01 06:02:01:01 N/A	06:03:01:01 N/A N/A N/A
ATALVLQVLEVPR	04:02:01 04:01:01:01 N/A N/A	13:01:01:01 15:01:01:01 N/A N/A	01:01:02:01 N/A N/A N/A	N/A N/A N/A N/A	01:03:01:01 N/A N/A N/A	N/A 01:01:01 N/A N/A	03:02:01:01 06:02:01:01 N/A N/A	06:03:01:01 N/A N/A N/A
ATALVLQVLEVPRL	04:01:01:01 N/A N/A N/A	15:01:01:01 N/A N/A N/A	N/A N/A N/A N/A	N/A N/A N/A N/A	01:03:01:01 N/A N/A N/A	01:01:01 N/A N/A N/A	03:02:01:01 N/A N/A N/A	06:02:01:01 N/A N/A N/A

(Continued)

10.3389/fimmu.2023.1271120

TABLE 2D Continued

DI-2	Halotypes							
Sequence	DRB1	DRB1	DRB3	DRB3	DRB4	DRB5	DQB1	DQB1
ALVLQVLEVPRLM	01:01:01 N/A N/A N/A	16:01:01 N/A N/A N/A	N/A N/A N/A N/A	N/A N/A N/A N/A	N/A N/A N/A N/A	02:02:01 N/A N/A N/A	05:01:01:01 N/A N/A N/A	05:02:01:01 N/A N/A N/A
ALVLQVLEVPRLMTQD	03:01:01:01 N/A N/A N/A	11:04:01 N/A N/A N/A	01:01:02:01 N/A N/A N/A	02:02:01:01 N/A N/A N/A	N/A N/A N/A N/A	N/A N/A N/A N/A	02:01:01 N/A N/A N/A	06:02:01:01 N/A N/A N/A
ALVLQVLEVPRLMTQDCLQ	03:01:01:01 N/A N/A N/A	11:04:01 N/A N/A N/A	01:01:02:01 N/A N/A N/A	02:02:01:01 N/A N/A N/A	N/A N/A N/A N/A	N/A N/A N/A N/A	02:01:01 N/A N/A N/A	06:02:01:01 N/A N/A N/A
LVLQVLEVPRLMTQ	04:01:01:01 03:01:01:01 N/A N/A	11:04:01 N/A N/A N/A	02:02:01:01 01:01:02:01 N/A N/A	N/A N/A N/A N/A	01:03:01:01 N/A N/A N/A	N/A N/A N/A N/A	03:01:01:01 02:01:01 N/A N/A	N/A 06:02:01:01 N/A N/A
LVLQVLEVPRLMTQD	04:01:01:01 15:01:01:01 03:01:01:01 N/A	11:04:01 N/A N/A N/A	02:02:01:01 N/A 01:01:02:01 N/A	N/A N/A N/A N/A	01:03:01:01 N/A N/A N/A	N/A 01:01:01 N/A N/A	03:01:01:01 06:02:01:01 02:01:01 N/A	N/A N/A N/A N/A
LVLQVLEVPRLMTQDC	03:01:01:01 N/A N/A N/A	11:04:01 N/A N/A N/A	01:01:02:01 N/A N/A N/A	02:02:01:01 N/A N/A N/A	N/A N/A N/A N/A	N/A N/A N/A N/A	02:01:01 N/A N/A N/A	06:02:01:01 N/A N/A N/A
LVLQVLEVPRLMTQDCL	03:01:01:01 N/A N/A N/A	11:04:01 N/A N/A N/A	01:01:02:01 N/A N/A N/A	02:02:01:01 N/A N/A N/A	N/A N/A N/A N/A	N/A N/A N/A N/A	02:01:01 N/A N/A N/A	06:02:01:01 N/A N/A N/A
LVLQVLEVPRLMTQDCLQ	11:04:01 N/A N/A N/A	15:01:01:01 N/A N/A N/A	02:02:01:01 N/A N/A N/A	N/A N/A N/A N/A	N/A N/A N/A N/A	01:01:01 N/A N/A N/A	03:01:01:01 N/A N/A N/A	06:02:01:01 N/A N/A N/A
VLQVLEVPRLMTQ	11:04:01 03:01:01:01 N/A N/A	15:01:01:01 N/A N/A N/A	02:02:01:01 01:01:02:01 N/A N/A	N/A N/A N/A N/A	N/A N/A N/A N/A	01:01:01 N/A N/A N/A	03:01:01:01 02:01:01 N/A N/A	06:02:01:01 N/A N/A N/A
VLQVLEVPRLMTQD	04:01:01:01 15:01:01:01 03:01:01:01 N/A	11:04:01 N/A N/A N/A	02:02:01:01 N/A 01:01:02:01 N/A	N/A N/A N/A N/A	01:03:01:01 N/A N/A N/A	N/A 01:01:01 N/A N/A	03:01:01:01 06:02:01:01 02:01:01 N/A	N/A N/A N/A N/A
VLQVLEVPRLMTQDC	03:01:01:01 N/A N/A N/A	11:04:01 N/A N/A N/A	01:01:02:01 N/A N/A N/A	02:02:01:01 N/A N/A N/A	N/A N/A N/A N/A	N/A N/A N/A N/A	02:01:01 N/A N/A N/A	06:02:01:01 N/A N/A N/A
VLQVLEVPRLMTQDCL	03:01:01:01 N/A N/A N/A	11:04:01 N/A N/A N/A	01:01:02:01 N/A N/A N/A	02:02:01:01 N/A N/A N/A	N/A N/A N/A N/A	N/A N/A N/A N/A	02:01:01 N/A N/A N/A	06:02:01:01 N/A N/A N/A
EVPRLMTQDCLQQSRKVG	04:01:01:01 N/A N/A N/A	15:01:01:01 N/A N/A N/A	N/A N/A N/A N/A	N/A N/A N/A N/A	01:03:01:01 N/A N/A N/A	01:01:01 N/A N/A N/A	03:02:01:01 N/A N/A N/A	06:02:01:01 N/A N/A N/A

N/A, Not Available.

10.3389/fimmu.2023.1271120

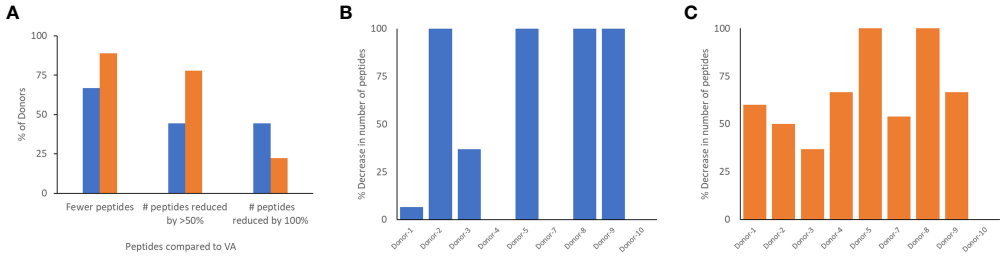

FIGURE 5
Comparison of peptides identified in the MAPPs assay following incubation of dendritic cells with VA and de-immunized FVIIa proteins. **(A)** The number of peptides from the region of the FVIIa mutation were computed when donor cells were treated with VA, DI-1 (blue), or DI-2 (orange). The graph shows the percent of donors that showed a reduction in the number of peptides when cells were treated with DI-1 or DI-2 compared to VA. We also show the fraction of donors with a 50% and 100% decrease in the number of peptides following treatment with DI-1 or DI-2. In addition, for each of the 11 donors, we depict the per-cent decrease in the number of peptides when treated with DI-1 **(B)** or DI-2 **(C)** compared to VA. Note that VA derived peptides were not identified on some donors thus it is not possible to calculate a decrease in the number of peptides for those donors.

clinical studies. Once a candidate drug enters clinical trials it is challenging to obtain samples from patients for the purpose of replicating assays carried out in the non-clinical phase(s). In this study we leveraged an analog of recombinant FVIIa, VA to assess the results from the MAPPs assay. The wild type recombinant FVIIa has been used as a drug for almost 3 decades and there are no reports of immunogenicity for the approved indication. A variant of FVIIa (VA), with an improved safety profile was designed (26) however drug development was discontinued during phase 3 clinical trials because 11% of patients developed anti-drug antibodies (8). In a *post-hoc* study we previously demonstrated that the results of *in vitro* and *ex vivo* assays comparing wild-type FVIIa and VA showed concordance with the clinical outcome (20). We found that 100% of patients with anti-drug antibodies exhibited at least one MHC-II allele that bound with high affinity to VA peptides (compared to 44% of patients with no anti-drug antibodies). T cell–mediated immune responses can be driven by the peptides that bind MHC-II proteins with high affinity. The VA peptide-MHC-II affinity was significantly higher for antidrug antibody positive patients compared to patients which were antidrug antibody negative (no patient with low VA peptide-MHC-II affinity for both HLA-DRB1 alleles developed antidrug antibodies. Taken together, our results indicated T cell mediated development of antidrug antibodies in patients treated with VA. Subsequently, using this information we designed and characterized two de-immunized variants of VA (21) (designated DI-1 and DI-2 in this study).

Compared to the wild-type FVIIa, VA elicited stronger T cell responses (Figure 1D) which is consistent with the results of clinical studies (8) and previous *in vitro* findings (20). The DI-1 and DI-2 variants were designed to bind MHCII variants with lower affinity (21) and show T cell responses in a significantly lower number of donors (Figure 1D). In these experiments we ensured, (a) that the donor cohort represented 75% of higher frequency DRB1 MHCII variants found in the NA population and (b) that the relative frequencies of the MHCII variants in the donor cohort were comparable to that found in the NA population (Figure 1C). Thus, based on the results of clinical studies (8) and *in vitro* assays (Figure 1) VA was determined to be a more immunogenic molecule than wild-type FVIIa, DI-1 or DI-2. With this background, wild-type FVIIa, VA, DI-1 and DI-2, which are variants of the same protein but have distinct and well characterized immune responses, were used to evaluate the utility of the MAPPs approach in determining immunogenicity risk for therapeutic proteins.

The donor cohort for the MAPPs assay included MHCII-DRB1 variants found in 75% of the NA population and the more common MHCII-DRB1 variants occur at comparable frequencies in the NA population and in the donor cohort. In general, most peptides identified in the MAPPs assay exhibit high affinity for the MHCII variants identified on the individual donors (Figure 1D). We (25) and others (27–29) have shown that peptides identified in MAPPs assays consistently show high affinity for the MHCII variants of the donor and the density plot provides a quality control measure for the MAPPs assay. Similarly, other characteristics of the peptides (e.g., the average, maximum and minimum lengths of the peptides) are also consistent with the biology of MHCII-mediated presentation of exogenous protein-derived peptides.

Numerous peptides, most of which are derived from endogenous proteins expressed and subsequently catabolized by the donor, are identified in a MAPPs assay. From this large dataset we identified the peptides derived from the different FVIIa molecules. We found that for all 4 FVIIa molecules (wild-type, VA, DE-1, and DE-2) 10 clusters of peptides were identified (Figure 4). While the relative numbers of peptides differ, all FVIIa molecules present peptides from the same regions of the FVIIa protein. By incubating the different FVIIa molecules with dendritic cells from the same donor cohort, our results suggest comparable protein proteolysis across donors.

From the perspective of immunogenicity risk of therapeutic proteins, foreign peptides that are presented by the MHCII are the ones most likely to drive an immune response (15). As FVIIa is approved for use in hemophilia A patients with inhibitors (23), the patients are not deficient in FVIIa. Consequently, patients who are treated with FVIIa, as well as the donor cohort used in this study, are tolerized to wild-type FVIIa. This postulate is reinforced by the clinical experience (spanning several decades) using recombinant FVIIa wherein there are no reports of immunogenicity for this

10.3389/fimmu.2023.1271120

TABLE 3 Cluster peptide frequency for each variant*.

Variant	Cluster location	Cluster sequence	Frequency within Cohort (%)	% within Donor	Donor 1	Donor 2	Donor 3	Donor 4	Donor 5	Donor 6	Donor 7	Donor 8	Donor 9	Donor 10	Donor 11
WT	291 - 315	DRGATALELMVLNVPRLMTQDCLQQ	18		6	0	19	0	0	0	0	0	0	0	0
VA	289 - 316	LLDRGATALVLQVLNVPRLMTQDCLQQS	82		58	38	54	5	7		24	3	6		29
DI-1	283 - 312	VSGWGQLLDRGATALVLQVLDVPRLMTQDC	45		48	0	48	5	0	0	33	0	0	0	40
DI-2	290 - 320	LDRGATALVLQVLEVPRLMTQDCLQQSRKVG	73		30	29	73	2	0	0	14	0	2	13	30

*See text and methods for the definition of cluster peptide frequency.

biologic. However, the introduction of mutations E296V and M298Q into the FVIIa variant (VA) render these peptides foreign. Thus, identification of peptides that include these mutations would be biologically and clinically important. Peptides that include the mutations introduced into VA were detected in Cluster 8 in the heat maps shown in Figure 4. The peptides with E296V and M298Q mutations identified in each donor are listed in Tables 2A–D. This finding provides an important measure of the utility of the MAPPs assay as it provides a mechanistic explanation for the higher incidence of immunogenicity associated with VA (8).

The DI-1 and DI-2 variants of VA offer an alternate approach to evaluating the MAPPs assay. Both variants were specifically designed to decrease the peptide-MHCII binding affinity of the peptides with the E296V and M298Q mutations to diverse MHCII variants. We show that, compared to VA, DI-1 and DI-2 show lower affinity for MHCII DRB1 alleles expressed by the donors in our cohort. Thus, we hypothesize that incubation of DI-1 or DI-2 would result in fewer peptides from Cluster 8 (i.e., those that include the E296V and M298Q mutations introduced into VA). Our results (Figure 5A) show that when incubated with the variants DI-1 or DI-2, 66.7% and 88.8% of donors respectively exhibited fewer peptides on the MHC-II proteins (when compared to VA). For DI-1, 45% of donors showed a 100% decrease in the number of peptides identified. For DI-2, 75% showed a 50% reduction in the number of peptides while 25% of donors showed a 100% decrease in the number of peptides (Figure 5A). Taken together our data shows that de-immunization of proteins by decreasing the affinity for MHCII alleles results in fewer peptides identified in a MAPPs assay (Figure 5) and reduced T-cell proliferation (Figure 1).

The cluster frequency is another useful measure that can be obtained from MAPPs data. The frequency that each cluster is presented in the donor cohort is a representation The cluster frequency indicates the percentage of donors that present a specific peptide cluster therefore a high frequency peptide cluster indicates a more promiscuous binding peptide that may indicate a greater risk of immunogenicity. Here, we show that the wild-type FVIIa as well as DI-1 and DI-2 show a significant increase in the per-cent inhibition in cluster frequency compared to VA (Figure 6). We determined that 67% and 78% of donors were deemed to respond as expected to DI-1 and DI-2 respectively (i.e., a reduction in the cluster frequency as compared to VA).

The limitations of this study include a relatively small donor cohort of 11 because the MAPPs method is resource intensive and expensive. However, we have endeavored to include a broad and representative set of MHC-II variants (at least with respect to the North American population). Another drawback is that due to the numbers of cells needed and other logistical issues we were unable to carry out the MAPPs assay and T cell proliferation assays on the same donor cohort. As MAPPs assays become more routine, efficient (with respect to the number of cells required) and less expensive more extensive studies to benchmark the results of the MAPPs assay to other *in vitro/ex vivo* methods and clinical outcomes will be possible. We would also like to emphasize that the current study addresses the intrinsic immunogenicity of a therapeutic protein. Many other important variables that are

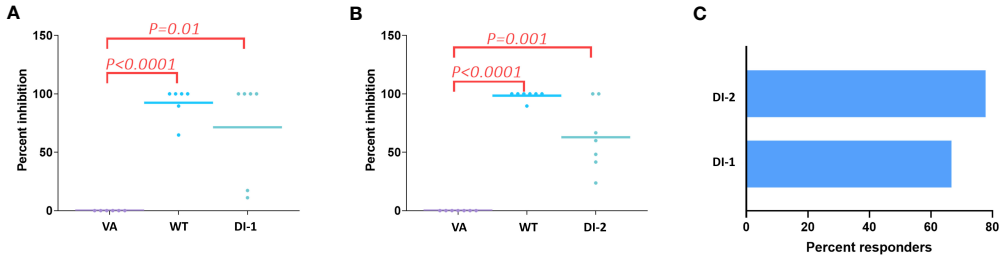

FIGURE 6
Decrease in cluster peptide frequency for deimmunized FVIIa proteins. Using VA as the positive control we computed the percent inhibition in the cluster frequency (see text) when cells from all 11 donors were treated with the WT FVIIa or DI-1 **(A)** or DI-2 **(B)**. Significant (p-values are depicted on the figure) increases in the percent inhibition of cluster frequencies were observed when cells were treated with WT, DI-1, and DI-2 FVIIa proteins. **(C)** Using cluster frequency as the measure the percent of donors who responded to DI-1 or DI-2 are show. A responder shows a decrease in cluster frequency compared to VA.

associated with immunogenicity (1) such as impurities, aggregates and leachables from the container and/closure are not studied here.

Here we show that the MAPPs assay used in conjunction with *in-silico* assessments and T cell proliferation assays could provide a useful immunogenicity risk assessment of a candidate protein therapeutic prior to initiation of clinical studies. Additionally, the MAPPs assay allows direct identification of therapeutic protein-derived peptides on HLA variants. These peptides thus represent T cell epitopes which could be relevant for de-immunization programs. We also show that while several scores/parameters can be derived from the MAPPs data, some (e.g., the cluster frequency) show better associations with clinical outcomes.

Data availability statement

The data presented in the study are deposited in the Harvard Dataverse repository, accession number https://doi.org/10.7910/DVN/7WIZCP.

Ethics statement

Ethical approval was not required for the studies on humans in accordance with the local legislation and institutional requirements because only commercially available established cell lines were used.

Author contributions

ZS: Conceptualization, Data curation, Formal Analysis, Funding acquisition, Investigation, Supervision, Writing – original draft, Writing – review & editing. WJ: Conceptualization, Data curation, Formal Analysis, Investigation, Visualization, Writing – original draft, Writing – review & editing. CK: Data curation, Formal Analysis, Visualization, Writing – review & editing. CB: Data curation, Formal Analysis, Investigation, Methodology, Writing – review & editing. EC: Data curation, Formal Analysis, Investigation, Methodology, Writing – review & editing. RR: Data curation, Formal Analysis, Investigation, Methodology, Writing – review & editing.

Funding

The authors declare financial support was received for the research, authorship, and/or publication of this article. Research conducted in the laboratory of ZS is funded by US Food and Drug Administration (FDA) intramural grants from the Chief Scientist's Challenge Grant and the Critical Path Initiative. This project was supported in part by an appointment of CK to the Research Participation Program at the Office of Therapeutics, Center for Biologics Evaluation and Research, US Food and Drug Administration, administered by the Oak Ridge Institute for Science and Education through an interagency agreement between the US Department of Energy and the FDA.

Conflict of interest

CB and EC are employed by Abzena. RR was employed by Abzena when this study was carried out and is currently employed by Lonza.

The remaining authors declare that the research was conducted in the absence of any commercial or financial relationships that could be construed as a potential conflict of interest.

Publisher's note

References

1. Sauna ZE, Lagasse D, Pedras-Vasconcelos J, Golding B, Rosenberg AS. Evaluating and mitigating the immunogenicity of therapeutic proteins. *Trends Biotechnol* (2018) 36(10):1068–84. doi: 10.1016/j.tibtech.2018.05.008

2. Rosenberg AS, Sauna ZE. Immunogenicity assessment during the development of protein therapeutics. *J Pharm Pharmacol* (2018) 70(5):584–94. doi: 10.1111/jphp.12810

3. Shankar G, Shores E, Wagner C, Mire-Sluis A. Scientific and regulatory considerations on the immunogenicity of biologics. *Trends Biotechnol* (2006) 24 (6):274–80. doi: 10.1016/j.tibtech.2006.04.001

4. Shankar G, Pendley C, Stein KE. A risk-based bioanalytical strategy for the assessment of antibody immune responses against biological drugs. *Nat Biotechnol* (2007) 25(5):555–61. doi: 10.1038/nbt1303

5. Gorovits B, Wakshull E, Pillutla R, Xu Y, Manning MS, Goyal J. Recommendations for the characterization of immunogenicity response to multiple domain biotherapeutics. *J Immunol Methods* (2014) 408:1–12. doi: 10.1016/j.jim.2014.05.010

6. FDA. *Guidance for industry: immunogenicity testing of therapeutic protein products - developing and validating assays for anti-drug antibody detection*. Silver Spring MD, USA: U.S. Department of Health and Human Services, Food and Drug Administration (2019).

7. FDA. *Guidance for industry: immunogenicity assessment for therapeutic protein products*. Silver Spring MD, USA: U.S. Department of Health and Human Services, Food and Drug Administration (2014).

8. Mahlangu JN, Weldingh KN, Lentz SR, Kaicker S, Karim FA, Matsushita T, et al. Changes in the amino acid sequence of the recombinant human factor VIIa analog, vatreptacog alfa, are associated with clinical immunogenicity. *J Thromb Haemost.* (2015) 13(11):1989–98. doi: 10.1111/jth.13141

9. Casadevall N, Nataf J, Viron B, Kolta A, Kiladjian JJ, Martin-Dupont P, et al. Pure red-cell aplasia and antierythropoietin antibodies in patients treated with recombinant erythropoietin. *N Engl J Med* (2002) 346(7):469–75. doi: 10.1056/NEJMoa011931

10. Li J, Yang C, Xia Y, Bertino A, Glaspy J, Roberts M, et al. Thrombocytopenia caused by the development of antibodies to thrombopoietin. *Blood.* (2001) 98 (12):3241–8. doi: 10.1182/blood.V98.12.3241

11. Ridker PM, Tardif JC, Amarenco P, Duggan W, Glynn RJ, Jukema JW, et al. Lipid-reduction variability and antidrug-antibody formation with bococizumab. *N Engl J Med* (2017) 376(16):1517–26. doi: 10.1056/NEJMoa1614062

12. Lagasse HAD, McCormick Q, Sauna ZE. Secondary failure: immune responses to approved protein therapeutics. *Trends Mol Med* (2021) 27(11):1074–83. doi: 10.1016/j.molmed.2021.08.003

13. Sauna ZE, Richards SM, Maillere B, Jury EC, Rosenberg AS. Editorial: immunogenicity of proteins used as therapeutics. *Front Immunol* (2020) 11:614856. doi: 10.3389/fimmu.2020.614856

14. Jensen KK, Andreatta M, Marcatili P, Buus S, Greenbaum JA, Yan Z, et al. Improved methods for predicting peptide binding affinity to MHC class II molecules. *Immunology.* (2018) 154(3):394–406. doi: 10.1111/imm.12889

15. Jawa V, Cousens LP, Awwad M, Wakshull E, Kropshofer H, De Groot AS. T-cell dependent immunogenicity of protein therapeutics: Preclinical assessment and mitigation. *Clin Immunol* (2013) 149(3):534–55. doi: 10.1016/j.clim.2013.09.006

16. Roche PA, Furuta K. The ins and outs of MHC class II-mediated antigen processing and presentation. *Nat Rev Immunol* (2015) 15(4):203–16. doi: 10.1038/nri3818

17. Vyas JM, van der Veen AG, Ploegh HL. The known unknowns of antigen processing and presentation. *Nat Rev Immunol* (2008) 8(8):607–18. doi: 10.1038/nri2368

18. Karle AC. Applying MAPPs assays to assess drug immunogenicity. *Front Immunol* (2020) 11:698. doi: 10.3389/fimmu.2020.00698

19. Scharrer I. Recombinant factor VIIa for patients with inhibitors to factor VIII or IX or factor VII deficiency. *Haemophilia.* (1999) 5(4):253–9. doi: 10.1046/j.1365-2516.1999.00319.x

20. Lamberth K, Reedtz-Runge SL, Simon J, Klementyeva K, Pandey GS, Padkjaer SB, et al. *Post hoc* assessment of the immunogenicity of bioengineered factor VIIa demonstrates the use of preclinical tools. *Sci Transl Med* (2017) 9(372):eaag1286. doi: 10.1126/scitranslmed.aag1286

21. Jankowski W, McGill J, Lagasse HAD, Surov S, Bembridge G, Bunce C, et al. Mitigation of T-cell dependent immunogenicity by reengineering factor VIIa analogue. *Blood Adv* (2019) 3(17):2668–78. doi: 10.1182/bloodadvances.2019000338

22. Pandey GS, Yanover C, Howard TE, Sauna ZE. Polymorphisms in the F8 gene and MHC-II variants as risk factors for the development of inhibitory anti-factor VIII antibodies during the treatment of hemophilia a: a computational assessment. *PloS Comput Biol* (2013) 9(5):e1003066. doi: 10.1371/journal.pcbi.1003066

23. Abshire T, Kenet G. Recombinant factor VIIa: review of efficacy, dosing regimens and safety in patients with congenital and acquired factor VIII or IX inhibitors. *J Thromb Haemost.* (2004) 2(6):899–909. doi: 10.1111/j.1538-7836.2004.00759.x

24. McGill JR, Yogurtcu ON, Verthelyi D, Yang H, Sauna ZE. SampPick: selection of a cohort of subjects matching a population HLA distribution. *Front Immunol* (2019) 10:2894. doi: 10.3389/fimmu.2019.02894

25. Jankowski W, Park Y, McGill J, Maraskovsky E, Hofmann M, Diego VP, et al. Peptides identified on monocyte-derived dendritic cells: a marker for clinical immunogenicity to FVIII products. *Blood Adv* (2019) 3(9):1429–40. doi: 10.1182/bloodadvances.2018030452

26. Persson E, Kjalke M, Olsen OH. Rational design of coagulation factor VIIa variants with substantially increased intrinsic activity. *Proc Natl Acad Sci U S A.* (2001) 98(24):13583–8. doi: 10.1073/pnas.241339498

27. Meunier S, Hamze M, Karle A, de Bourayne M, Gdoura A, Spindeldreher S, et al. Impact of human sequences in variable domains of therapeutic antibodies on the location of CD4 T-cell epitopes. *Cell Mol Immunol* (2020) 17(6):656–8. doi: 10.1038/s41423-019-0304-3

28. Sekiguchi N, Kubo C, Takahashi A, Muraoka K, Takeiri A, Ito S, et al. MHC-associated peptide proteomics enabling highly sensitive detection of immunogenic sequences for the development of therapeutic antibodies with low immunogenicity. *MAbs.* (2018) 10(8):1168–81. doi: 10.1080/19420862.2018.1518888

29. Cassotta A, Mikol V, Bertrand T, Pouzieux S, Le Parc J, Ferrari P, et al. A single T cell epitope drives the neutralizing anti-drug antibody response to natalizumab in multiple sclerosis patients. *Nat Med* (2019) 25(9):1402–7. doi: 10.1038/s41591-019-0568-2

frontiers | Frontiers in Immunology

TYPE Original Research
PUBLISHED 23 October 2023
DOI 10.3389/fimmu.2023.1261070

OPEN ACCESS

EDITED BY
Sudhir Paul,
University of Texas Health Science Center at Houston, United States

REVIEWED BY
Sebastian Spindeldreher,
Integrated Biologix GmbH, Switzerland
Stephanie Planque,
University of Texas Health Science Center at Houston, United States

*CORRESPONDENCE
Daniel T. Mytych
dmytych@amgen.com

RECEIVED 18 July 2023
ACCEPTED 02 October 2023
PUBLISHED 23 October 2023

CITATION
Penny HL, Hainline K, Theoharis N, Wu B, Brandl C, Webhofer C, McComb M, Wittemer-Rump S, Koca G, Stienen S, Bargou RC, Hummel H-D, Loidl W, Grüllich C, Eggert T, Tran B and Mytych DT (2023) Characterization and root cause analysis of immunogenicity to pasotuxizumab (AMG 212), a prostate-specific membrane antigen-targeting bispecific T-cell engager therapy. *Front. Immunol.* 14:1261070. doi: 10.3389/fimmu.2023.1261070

Characterization and root cause analysis of immunogenicity to pasotuxizumab (AMG 212), a prostate-specific membrane antigen-targeting bispecific T-cell engager therapy

Hweixian Leong Penny[1], Kelly Hainline[1], Nathaniel Theoharis[2], Bin Wu[3], Christian Brandl[4], Christian Webhofer[5], Mason McComb[6], Sabine Wittemer-Rump[7], Gökben Koca[7], Sabine Stienen[8], Ralf C. Bargou[9], Horst-Dieter Hummel[9], Wolfgang Loidl[10], Carsten Grüllich[11], Tobias Eggert[12], Ben Tran[13] and Daniel T. Mytych[1]*

[1]Department of Clinical Immunology, Amgen, Thousand Oaks, CA, United States, [2]Labcorp, Translational Biomarker Solutions, Greenfield, IN, United States, [3]Department of Biologics, Amgen, Thousand Oaks, CA, United States, [4]Department of Translational Safety & Bioanalytical Sciences, Amgen Research (Munich) GmbH, Munich, Germany, [5]Department of Process Development, Amgen Research (Munich) GmbH, Munich, Germany, [6]Department of Clinical Pharmacology, Modeling & Simulation, Amgen, Thousand Oaks, CA, United States, [7]Bayer AG, Research and Development Oncology (RED Onc), Pharmaceuticals, Berlin, Germany, [8]Department of Early Development (Oncology), Amgen Research (Munich) GmbH, Munich, Germany, [9]Translational Oncology/Early Clinical Trial Unit (ECTU), Comprehensive Cancer Center Mainfranken, University Hospital Wurzburg, Wurzburg, Germany, [10]Department of Urology, Ordensklinikum Linz GmbH, Linz, Austria, [11]Department of Medical Oncology, National Center for Tumor Diseases, Heidelberg University Medical Center, Heidelberg, Germany, [12]Department of Early Development (Oncology), Amgen, Thousand Oaks, CA, United States, [13]Department of Medical Oncology, Peter MacCallum Cancer Centre, Melbourne, VIC, Australia

Introduction: In oncology, anti-drug antibody (ADA) development that significantly curtails response durability has not historically risen to a level of concern. The relevance and attention ascribed to ADAs in oncology clinical studies have therefore been limited, and the extant literature on this subject scarce. In recent years, T cell engagers have gained preeminence within the prolific field of cancer immunotherapy. These drugs whose mode of action is expected to potently stimulate anti-tumor immunity, may potentially induce ADAs as an unintended corollary due to an overall augmentation of the immune response. ADA formation is therefore emerging as an important determinant in the successful clinical development of such biologics.

Methods: Here we describe the immunogenicity and its impact observed to pasotuxizumab (AMG 212), a prostate-specific membrane antigen (PSMA)-targeting bispecific T cell engager (BiTE®) molecule in NCT01723475, a first-in-human (FIH), multicenter, dose-escalation study in patients with metastatic castration-resistant prostate cancer (mCRPC). To explain the disparity in ADA incidence observed between the SC and CIV arms of the study, we interrogated other patient and product-specific factors that may have explained the difference beyond the route of administration.

10.3389/fimmu.2023.1261070

Results: Treatment-emergent ADAs (TE-ADA) developed in all subjects treated with at least 1 cycle of AMG 212 in the subcutaneous (SC) arm. These ADAs were neutralizing and resulted in profound exposure loss that was associated with contemporaneous reversal of initial Prostate Surface Antigen (PSA) responses, curtailing durability of PSA response in patients. Pivoting from SC to a continuous intravenous (CIV) administration route remarkably yielded no subjects developing ADA to AMG 212. Through a series of stepwise functional assays, our investigation revealed that alongside a more historically immunogenic route of administration, non-tolerant T cell epitopes within the AMG 212 amino acid sequence were likely driving the high-titer, sustained ADA response observed in the SC arm.

Discussion: These mechanistic insights into the AMG 212 ADA response underscore the importance of performing preclinical immunogenicity risk evaluation as well as advocate for continuous iteration to better our biologics.

KEYWORDS

immunogenicity, BiTE®, T cell engager, ADA, prostate cancer

Introduction

Biologics such as monoclonal antibodies and their associated bispecific antibody constructs consist of large and complex structures. Some of these amino acid sequences and structural motifs, may induce humoral immune responses due to non-self recognition by the patient's immune repertoire, resulting in the formation of specific anti-drug antibodies (ADAs).

The ADA response is initiated by antigen-presenting cells (APCs) that phagocytose, internalize, and process the drug into smaller peptides. These peptides are loaded onto major histocompatibility complex (MHC) class II at the APC cell surface for presentation to CD4+ T cell clones that recognize the specific peptide-MHCII complex (pMHC) (1–3). At the same time, B cells recognizing structural motifs in the tertiary structure of the protein therapeutic are stimulated to produce IgM. However, IgM responses are often transient. For a sustained humoral response, B cells must be further activated to differentiate into plasma cells, which subsequently affinity mature and isotype class-switch to become potent IgG producers. This additional "help" is accomplished mainly by CD4+ T cells which have been activated by pMHC recognized on the APC (1–3). Therefore, sustained ADA formation is a coordinated response engaging several immune cell types: APC capture, processing and presentation; B cell recognition of conformational epitopes and T cell recognition of sequence-based epitopes from the same antigen.

ADAs can cause unintended clinical consequences affecting exposure and safety, with effects ranging from none to life-threatening. ADAs may impact the pharmacokinetics (PK) of a drug (4–6), maintaining or more often, decreasing, exposure depending on whether the ADAs are sustaining or clearing antibodies respectively (7). Even though ADAs can affect PK, this does not necessarily translate to impaired efficacy of the drug. Patients risk experiencing reduced efficacy particularly in cases where early-onset, high magnitude, high-affinity neutralizing ADAs (NAb) are induced (4–6). NAbs bind to the variable regions of the antibody to prevent engagement of the target antigen, effectively stymying therapeutic activity. In contrast, binding ADAs that bind to other parts of the antibody, such as the Fc region, may not directly result in loss of therapeutic activity. However, both binding and neutralizing ADAs may lead to formation of large drug-antibody immune complexes that can be rapidly cleared by phagocytes in the spleen and liver, resulting in suboptimal exposure and eventual loss of efficacy (4–7). In oncology, ADAs may rise to the level of concern when there is potential for clear differences in key Response Evaluation Criteria in Solid Tumors (RECIST) response parameters such as progression-free survival (PFS) and overall survival (OS) between ADA-positive and ADA-negative subgroups. Patients in whom ADAs develop are also at increased risk for certain adverse events such as complement-mediated reactions, infusion-related reactions, or other Type III hypersensitivity events due to the deposition of these immune complexes in microvessels (8).

In addition to treatment-induced ADAs, pre-existing reactivity has been detected in drug-naïve individuals (9). While the origin of pre-existing reactivity is not well-understood, and the clinical impact of which can be highly variable, pre-existing reactivity represents an additional layer of immunogenicity monitoring when evaluating novel protein therapeutics. However, clinically significant pre-existing reactivity against biologics is rare and is not often boosted upon dosing with investigational drug.

In oncology, the risk of ADA development may be lower in patients due to their disease state itself, or in patients who have recently completed chemotherapy and whose immune systems may still be recovering from these myeloablative regimens. The suppressed ability to mount a robust antibody response may have

accounted for the historically low rates of ADAs observed to tumor-associated antigen targeted, monoclonal antibody-based investigational drugs.

Clinical immunogenicity has gained renewed interest of late, as immunotherapies exhibiting ability to potently trigger an immune response have brought the topic of drug-induced immunogenicity into active discourse. In a focused review consolidating immunogenicity data from 81 clinical trials with anti-cancer biologics, Van Brummelen and colleagues observed that 63% of these studies report ADA formation (10), suggesting that many compounds currently being investigated in oncology are potentially immunogenic. However, the clinical relevance of some of these ADAs remain unclear.

In a similar assessment, Davda and colleagues reviewed the incidence of ADA and NAb across multiple, approved, anti-cancer antibody-based immunomodulatory agents and found that the data is suggestive of a higher likelihood of immunogenicity to antibodies with T cell or APC targets compared to B cell targets (11). Not surprisingly, in a more recent review focused on bispecific antibody constructs in the immuno-oncology (IO) space, Zhou and colleagues reappraise the need for immunogenicity risk assessment throughout development for this class of biologics and have provided specific recommendations (12). Taken together, this underscores the need for close monitoring of potential immunogenicity to drugs being advanced in IO studies, particularly drugs which target T cell priming and activation.

Pasotuxizumab (henceforth referred to as AMG 212) is a 55 kD protein with an anti-PSMA target binding domain linked to an anti-CD3 binding domain. It is a Bispecific T cell engager (BiTE®) molecule, a class of biologics whose mode of action is such that when the BiTE® molecule is bound on one end to target protein on the surface of a target cell and bound to CD3 on a T cell at the other end, proximity-induced, redirected T cell lysis of target cells can occur. In NCT01723475, a FIH study, AMG 212 was tested in mCRPC patients, who were refractory to novel anti-androgen therapy (abiraterone and/or enzalutamide) and had failed at least one (but not more than two) taxane regimen.

It has been previously reported that anti-androgen therapy can modulate the immune milieu in the tumor microenvironment, promoting an immunosuppressed state in mCRPC patients. However, Gardner and colleagues showed that a vaccine based on a novel recombinant soluble PSMA protein was able to elicit anti-PSMA antibodies in patients with progressive prostate cancer (13). These antibodies reacted strongly with prostate cancer cells and increased with multiple dosing. Taken together, the data show that despite immunomodulation by prior therapy, along with tumor escape and immune resistance mechanisms in this patient population, mCRPC patients are still capable of mounting an antigen-specific humoral response to a biologic.

Here we report the clinical immunogenicity to AMG 212 and its impact as observed in NCT01723475. We characterize how ADA onset, magnitude and kinetics impacted the PK, pharmacodynamic (PD) response and adverse events observed on study. We also describe a measure implemented mid-study to mitigate the ADAs detected in the SC arm. Further, we performed a root cause analysis to explain the immunogenicity observed, by assessing potential contributing factors such as the baseline immune status of subjects and product quality attributes of the drug lots administered to subjects. Finally, through a series of *in vitro* assays, we identified non-tolerant sequence-based epitopes contributing to the robust and clinically impactful ADA response to AMG 212 delivered subcutaneously.

Materials and methods

AMG 212 study design

This was an open-label, multicenter, Phase I, dose-escalation study (ClinicalTrials.gov, NCT01723475) conducted at five clinical study centers in Germany and Austria and sponsored by Bayer AG, Leverkusen, Germany. It was designed to determine the safety and maximum tolerated dose (MTD) of AMG 212 (primary objectives) and to assess pharmacokinetics, PSA and tumor response (secondary objectives) and biomarkers (exploratory objective) of AMG 212 administered either by daily SC injection or CIV infusion. An independent data monitoring committee was established to regularly review safety data. The starting doses for the SC and CIV arms were 0.5 and 5 µg daily, respectively. A cycle for this study, in both the SC and CIV arms, was defined as 21 days (or 3 weeks).

In the SC arm, AMG 212 was administered daily by SC injection, with no breaks between cycles. The SC dosing schema is shown in Supplementary Figure S1A. SC injection sites included four abdominal regions around the navel, upper arm and thighs. The 2 ml syringes for SC administration were prepared by the local pharmacy and administered either in the clinic by a healthcare professional or at home by the patient.

In the CIV arm, AMG 212 was administered as a continuous IV infusion, using an on-body portable infusion pump and central venous port system. In the first 4 cycles (first 12 weeks on study), patients received treatment on a "5 week on-1 week off" schedule, whereby AMG 212 was administered over 5 weeks, followed by a treatment-free interval of 1 week. From cycle 5 onwards, patients could continue treatment on the "5 week on-1 week off" schedule or switch to a "4 week on-2 week off" schedule, at the discretion of the investigator and the subject. The CIV dosing schema is shown in Supplementary Figure S1B.

In both the CIV arm and the higher dose-level SC cohorts, prophylactic oral or IV dexamethasone was administered before the administration of AMG 212 to mitigate cytokine release syndrome (CRS) risk. At the discretion of the investigators, concomitant therapy was allowed. For each patient, treatment continued until tumor progression, unacceptable toxicity, consent withdrawal, or withdrawal from the study. Further details on study design can be found in Hummel et al., 2021 (14).

AMG 212 patients

Men aged ≥ 18 years old with histologically or cytologically confirmed advanced CRPC with treatment failure after ≥ 1 taxane regimen and who were refractory to abiraterone and/or

enzalutamide or refused any other standard therapy were eligible for inclusion in the study. Eligible patients had undergone bilateral orchiectomy or received continuous androgen deprivation therapy and had evidence of progressive disease after discontinuation of anti-androgen therapy (i.e., flutamide, bicalutamide or nilutamide) before study drug treatment. Additional inclusion and exclusion criteria have been described in Hummel et al., 2021 (14).

AMG 160 study design

This was an open-label, multi-center, phase 1, dose-exploration/dose-expansion study in patients with mCRPC from North America, Europe, Asia, and Australia (NCT03792841) and sponsored by Amgen. The primary objectives of the study were to evaluate the safety and tolerability of AMG 160, to determine the MTD and/or recommended phase 2 dose (RP2D). The secondary objectives were to evaluate the preliminary antitumor activity and characterize the PK and pharmacodynamics of AMG 160.

AMG 160 was administered intravenously in 28-day cycles. Once the target dose was reached, AMG 160 was administered by short-term IV infusion over 1 hr, every 2 weeks. In the dose exploration phase, to mitigate against CRS, step-dosing was implemented. Similar to the premedications used in the AMG 212 study, prophylactic oral and/or IV dexamethasone was administered before the administration of AMG 160 to mitigate CRS risk.

Following the dose exploration phase, a dose expansion study was conducted to confirm the safety, PK, and pharmacodynamics of AMG 160 at the RP2D, and to obtain further safety and efficacy data and carry out correlative biomarker analysis.

AMG 160 patients

The AMG 160 patient population enrolled in NCT03792841 was comparable to that enrolled for AMG 212 in NCT01723475. In brief, men aged ≥18 years of age were included if they had histologically or cytologically confirmed mCRPC that was refractory to novel hormonal therapy, had failed 1–2 taxane regimens (or were unsuitable for or had refused treatment with taxanes), and had evidence of progressive disease as defined by the Prostate Cancer Working Group 3 (PCWG3) guidelines. Patients were excluded if they had active autoimmune disease or required immunosuppressive therapy, had received prior PSMA–targeted therapy (patients treated with PSMA radionuclide therapy were considered eligible), or had evidence of central nervous system metastases, leptomeningeal disease, or spinal cord compression.

AMG 212 and AMG 160 patients

Both the AMG 212 and AMG 160 clinical studies were conducted in accordance with the ethical principles derived from international guidelines, including the Declaration of Helsinki, Council for International Organizations of Medical Sciences International Ethical Guidelines, and applicable International Conference on Harmonisation guidelines, laws, and regulations. The study protocols were approved by the Institutional Review Board/Independent Ethics Committee at each study site. All patients provided written informed consent.

Anti-AMG 212 antibody assessments (binding and neutralizing antibody assays)

ADA sampling timepoints

In the SC arm, blood samples for immunogenicity evaluation were collected predose on Cycle 1 Day 1, 8 and 15, on Day 1 of each cycle from Cycle 2 to 8, on Day 1 of every second cycle thereafter and at least 36 hr after the last dose of AMG 212. In the CIV arm, blood samples were collected predose on Cycle 1 Day 1, 8 and 15, on Day 1 of each subsequent cycle and at least 36 hr after the last dose of AMG 212. The ADA collection schedule for the SC and CIV arms is shown in Supplementary Figures S1A, B.

Binding ADA assay

Anti-AMG 212 antibodies were measured using a validated electrochemiluminescence-based bridging assay. This immunoassay method followed a two-tiered assay approach consisting of a screening assay and confirmatory assay. Samples were diluted 1:10 in D-PBS (Gibco Cat# 14190-094) or D-PBS and soluble drug (confirmatory assay only) prior to analysis. The samples were then incubated with conjugate mixture consisting of biotinylated-AMG 212 and ruthenylated-AMG 212. During this incubation, the two antigen binding sites of anti-AMG 212 antibodies were able to form a bridge between the labeled AMG 212 molecules. The sample mixture was then added to a blocked streptavidin microtiter plate, washed, and analyzed on a plate reader. The result was a series of electrically induced oxidation-reduction reactions involving ruthenium (from the captured complex) and tripropylamine. In this immunogenicity screening assay, a subject-specific floating cut point was calculated by adding a specific normalization factor to the pre-dose subject sample. Samples with results equal to or greater than the assay cut point were then tested to confirm specificity of the response. Samples classified as positive in the confirmatory assay were further titrated in 10% human serum pool and reported at the highest dilution titer at which a positive response was determined. The normalization factor and the confirmatory assay cut point were calculated from 40 prostate cancer donor serum samples. The assay sensitivity was 8.6 ng/mL based on a goat polyclonal positive control antibody. At 12, 120 and 1,200 ng/mL of anti-AMG 212 antibody, the assay tolerated at least 10,000 pg/mL of excess AMG 212.

Neutralizing ADA assay

The resulting immunoassay-positive samples were analyzed using a cell-based bioassay to determine whether the detected binding antibodies have neutralizing properties. This AMG 212 neutralizing assay was based on an *in-vitro* cell-based competitive ligand binding assay. Effector cells (CD3-positive MC15 cells) were incubated with target cells (human PSMA-positive C4-2 cells),

serum samples and AMG 212. After overnight incubation, the cytotoxic activity was measured with the luminescent CytoTox-Glo™ Cytotoxicity Assay kit (Promega). The CytoTox-Glo™ Cytotoxicity Assay uses a luminogenic peptide substrate, the AAF-Glo™ Substrate, to measure dead-cell protease activity released from cells that have lost membrane integrity. When the serum sample contained AMG 212 neutralizing antibodies, cytotoxicity was reduced. A sample was considered positive for neutralizing antibodies if the decrease of the cytotoxicity was greater than the cut point compared to the maximal toxicity sample. The cut point was calculated from 45 healthy donor serum samples. The assay sensitivity was 780 ng/mL based on a goat polyclonal positive control antibody. At 13,500 ng/mL of anti-AMG 212 antibody, the assay tolerated at least 3,000 pg/mL of excess AMG 212.

AMG 212 pharmacokinetics assessment

PK sampling timepoints

In the SC arm, blood samples for PK assessment were collected predose at Cycle 1 Day 1 and 15, and at 1, 2, 4, 6, 8, 12 and 24 hr post-infusion at these two timepoints. Samples were also collected predose on Cycle 1 Day 3, 4 and 8. From Cycle 2 to 8, and every second cycle thereafter, a blood sample was collected on Day 1 within 2 to 6 hr post-dose. In the CIV arm, blood samples were collected on Cycle 1 Day 1 predose, at the 2-3 hr and 4-6 hr post-start of infusion timepoints, and on Day 2, 8 and 15. From Cycle 2 onwards, a blood sample was collected on Day 1 and 15 with every subsequent even cycle, and collected on Day 1, 2 and 15 with every subsequent odd cycle.

PK assay

The assay to quantify AMG 212 was based on a sandwich immunoassay format in which capture antibodies (goat polyclonal anti-AMG 212 antibodies) were coated on a plate. After sample incubation, a mouse anti-idiotype monoclonal antibody against the CD3 binding domain of AMG 212 was bound to the captured AMG 212 and detected with ruthenylated anti-mouse antibody. The assay range was 0.150 to 111 ng/mL.

AMG 212 pharmacodynamic assessments (PSA and peripheral blood immune cell biomarkers)

Efficacy was assessed according to the Prostate Cancer Clinical Trials Working Group 2 recommendations (15). RECIST responses are not described in this manuscript but were reported in Hummel et al., 2021 (14). Changes in serum PSA levels were assessed predose on days 1, 8 and 15 of cycle 1, at the beginning of each subsequent cycle and at the end of treatment visit. A PSA response was defined as a 50% reduction in the PSA level from baseline that was confirmed by a second test value at least 3 weeks later. Other pharmacodynamic markers, including peripheral blood biomarkers of T-cell activation (including CD69) and monocyte activation (including HLA-DR) were assessed by flow cytometry and were conducted before and during treatment.

Epibase® MHC class II-associated peptide proteomics assay

The Epibase® MAPPS assay was performed at Lonza. Monocytes were isolated from frozen PBMC samples by positive magnetic bead selection (Miltenyi Biotec). Monocytes were seeded into T12.5 flasks with 5 X 10^6 monocytes per flask in differentiation medium (Dendritic Cell (DC) medium containing 100 ng/mL IL-4, 50ng/mL GM-CSF) and incubated for 5 days at 37°C, 5% CO2 to differentiate into DC. The DC were then loaded with AMG 212 (or medium alone for the Blank) and matured with Lipoprotein polysaccharide (LPS) for 24 hr. After maturation, the DC were lysed and the membrane fraction containing the HLA:peptide complexes was solubilized and incubated with Protein A mag sepharose beads (GE Healthcare) coated with anti-HLA-DR antibody (Lonza) at 4°C overnight. The following morning the beads were washed in Tris Buffer Solution (TBS) and the peptides eluted from the HLA-DR complex with 0.1% Trifluoroacetic acid (TFA). Finally, the peptides were purified by passing through a 10kDa Molecular Weight Cut-Off (MWCO) spin column and stored at -80°C for mass spectrometry (MS) analysis. MS data analysis was carried out using the PEAKS® Studio Software package. The identified peptides are then mapped back to the full-length AMG 212 protein sequence and compared to an Epibase® in silico analysis to identify which HLA-DR alleles are responsible for the peptide binding. Albumin was also included as an internal control in the samples to verify assay performance. Comparable numbers of total (173 vs 171) and distinct (85 vs 77) albumin peptides were detected in the AMG 212 sample in the first and second round of MAPPS respectively, indicating that the assay was consistent and sensitive across repeats.

Test and control peptides

Along with the MAPPS-identified sequences (#1-5, #8, #8.5, 11), peptides spanning the rest of the Complementarity Determining Regions (CDR) regions of AMG 212 were proactively synthesized. These additional sequences were labeled Peptide #6, 7, 9, 10 and 12. A separate peptide, Peptide #13, was synthesized as a known self-tolerant peptide and acted as a negative control peptide that demonstrated MHC class II-binding but was not expected to confer T cell reactivity. A total of 14 peptides were synthesized.

Pool 1 consisted of 5 peptides (Peptide #1, 2, 3, 4 and 5) and Pool 2 consisted of 8 peptides (#6, 7, 8, 9, 10, 11, 12 and 13). Peptide #8.5 was inadvertently missed in Pool 2. CEFTA, a peptide pool consisting of 35 MHC class II-restricted peptides from human CMV, EBV, influenza virus, tetanus toxin, and adenovirus 5, and PADRE (Pan DR-binding epitope), were used as positive controls as these peptides are designed to stimulate T cells with a broad array of HLA types.

Restimulated T cell line assay

Isolated CD4+ T cells were stimulated with multiple rounds of autologous monocyte-derived DCs (moDCs) pulsed with our test peptides in a 4-week co-culture. For the first 3 weeks, the T cells were stimulated weekly with freshly-derived moDCs pulsed with peptide pools in the first 3 stimulations, and then with individual peptides from a pool, for a fourth and final stimulation.

On Day 1, CD14+ cells were isolated from PBMC using positive selection magnetic microbeads (Miltenyi Biotech). The CD14+ cells were differentiated into immature DCs by seeding at 1 X 10^6/mL into a 96 well plate (200 µL/well) in Cellgenix DC GMP Medium (Sartorius) supplemented with 100 ng/mL IL-4 (Peprotech) and 50 ng/mL GM-CSF (Peprotech). After 5 days, the immature DCs were separately loaded with 5 µg/mL CEFTA peptide (Mabtech) pool, 5 µM PADRE peptide (Mayflower Biosciences), or 5 µM test peptide pool and matured with 10 ng/mL TNF-α (R&D Systems) and 5 ng/mL IL-1β (Peprotech) for 48 hours. The quality of the matured DCs was assessed by labeling of markers HLA-DR, CD14, CD80, CD83, CD86, CD209, and CD11b. CD4+ T cells were isolated from PBMC using negative selection magnetic microbeads (Miltenyi Biotech). CD4+ T cells (2 X 10^5/well) were stimulated by peptide-loaded DC and cultured initially in AIM-V supplemented with 2% Human AB Serum (Sigma-Aldrich) for 21 days. Freshly loaded and matured DCs were added to the T cell culture every 7 days, and the culture medium was refreshed every 7 days with AIM-V supplemented with 2% Human AB Serum (Sigma-Aldrich), 10 U/mL IL-2 (Peprotech), and 5 ng/mL IL-7 (Peprotech).

On Day 21, a fraction (4-5 X 10^4) of CD4+ T cells were taken from each well and stimulated with peptide pool-loaded DCs in pre-coated Human Interferon-γ PVDF Plates (ImmunoSpot®). After 48 h incubation, the manufacturer's plate development instructions were followed to detect secreted IFN-γ. Spots were counted using a CTL ImmunoSpo® S6 Ultra M2 Analyzer. Wells with unloaded DCs (absence of peptide, but with T cells) and wells with T cells only (no DCs, no peptide), served as negative controls. T cell lines reactive to individual peptides were determined as wells that had spot counts at least two-fold higher in the presence of peptide compared to the unloaded DC negative control, with a minimal difference of 30 spots, as described previously (16, 17). The identified antigen-specific T cell lines were then divided and stimulated with individual peptide-loaded DCs in the fourth week of co-culture. The same ELISpot protocol was applied, and the same parameters were used to determine if a T cell line was specific to an individual peptide (2-fold higher than negative controls, with a minimal difference of 30 spots).

Clinical memory recall assay

Ten ml of whole blood at the end-of-treatment (EOT) timepoint was collected per subject, according to the Schedule of Assessments in the AMG 160 FIH Study 20180101 (NCT03792841). The blood was sent ambient on the same day of collection to the central lab for PBMC processing using the CTL protocol (18) within a 48 hr window from time of collection. The PBMCs were enumerated and stored in liquid nitrogen at a cell concentration of 10 X 10^6/ml before onward batch shipment to Labcorp Translational Biomarker Solutions. Upon thawing of the patient PBMCs, we noted poor viability and functionality in the majority of samples. Thus, we performed a pilot experiment to bulk stimulate a known reactive donor's PBMCs using a test peptide pool of our suspect sequences to clonally expand peptide-specific T cell memory clones over 10 days. This was a strategy undertaken previously by other groups in non-oncology disease indications (19). However, our efforts were unsuccessful in sustaining viability of these mCRPC patient PBMCs despite providing multiple cytokines to stimulate growth and proliferation such as IL-2, IL-4, and an anti-CD28 antibody.

Ultimately, to perform the clinical memory recall assay, freshly-thawed patient PBMCs were seeded at 2 X 10^5/well into pre-coated Human Interferon-γ PVDF Plates (ImmunoSpot®) and incubated with individual test peptides at 5 µM each, in CTL-Test Medium supplemented with 2mM GlutaMAX and 10 ng/mL of GM-CSF (Peprotech). The peptides tested were #1, 2, 8, 8.5, 11, along with peptides #13 and #4 which we had established previously from the restimulated T cell line assays to be negative controls (did not demonstrate T cell reactivity). Phytohemagglutinin (PHA) at 2 µg/mL was used as a strong, non-specific stimulator for a technical positive control. PBMCs from an AMG 160-naive healthy donor, acted as an additional negative control for the assay. After 72 hr of incubation (37°C, 5% CO2, humidified chamber), manufacturer's plate development instructions were followed to detect secreted IFN-γ. Spots were counted using a CTL Immunospot® Series 5 Macro Analyzer.

Statistical analysis

Analyses of AMG 212 immunogenicity, PK and signs of activity were descriptive in nature and presented using summary statistics and individual subject profiles. ADA status, exposure impact and PSA response correlation analyses were performed using a logistic regression model with SAS (version 9.4) software. Further details on sample sizes, dose-limiting toxicities (DLTs) and safety summary statistics to fulfill the study objectives can be found in a prior clinical report summarizing the overall results of the AMG 212 FIH study (14). Patients who completed the study without any major protocol violations were included in the PK, ADA, PD and where applicable, PSA response evaluation sets. In figures where specific parameters are being compared between the SC and CIV subjects, statistical significance was determined by the Student's t-test (two-tailed), whereby p values of < 0.05 were considered significant and denoted by a single asterisk*, and n.s. refers to "not significant".

Results

Incidence, magnitude, and kinetics of TE-ADA to AMG 212 in the SC arm

NCT01723475 was first initiated in a cohort of 31 subjects who were subcutaneously administered AMG 212 into four regions

around the navel (other injection sites were permitted) (14). Doses were given daily for 21 days per cycle, at dose levels ranging from 0.5 µg to 172 µg per day until confirmed disease progression if there were no other reasons to discontinue AMG 212 treatment. At appropriate timepoints, patient serum samples were collected and screened for binding and neutralizing antibodies to AMG 212.

Pre-existing reactivity was not observed to AMG 212. However, as an aggregate across all doses in the SC dose escalation study, treatment-emergent ADA (TE-ADA) developed in 30/31 subjects (96.7%) who had a post-baseline result (Table 1.1). None of the ADAs developed on-study were transient (Table 1.1). Except for one subject who did not receive AMG 212 past Cycle 1 Day 8, all 30 subjects who completed at least one treatment cycle of AMG 212 developed TE binding ADAs (30/30, 100% incidence). Of these 30 binding ADA-positive subjects, all except two with very low titer ADA (1:30 and 1:90), had binding ADA that was also neutralizing (28/30, 93.3% incidence). Therefore, the validated neutralizing antibody assay used to test AMG 212 clinical study samples had sufficient drug tolerance and was sensitive enough to capture almost all subjects positive for binding ADA.

The majority of ADAs had an onset spanning Cycle 1 Day 15 to Cycle 4 Day 1, with median onset at Cycle 2 Day 1, or Day 22 (Figure 1A) (14). Ten subjects had ADAs whose maximum titers were achieved at follow-up (FU) (data not shown). Since patients in the SC arm were treated for an overall median time of 91 days, this indicated that peak ADA titers were not yet reached even at the final scheduled antibody collection timepoint tested, about 3 months from the initiation of AMG 212 dosing. The median ADA titer across the 30 binding ADA+ subjects was 218, 700 (Figure 1B). Nineteen of the 31 subjects had approximated ADA concentrations above 1 µg/ml (Signal-to-Noise, S/N extrapolated using goat anti-AMG 212 antibody positive control). Both measures of ADA magnitude (titer and S/N) indicate that the ADA responses in these patients were significant. The ADA response was not dose-dependent i.ea higher ADA incidence, an earlier onset of ADA development, or a greater magnitude of ADA, was not observed at higher dose levels compared to lower dose levels (Figures 1A, B).

Taken together, TE-ADA observed in the subcutaneous cohort (i) developed early, within the first 2 cycles of AMG 212 treatment, (ii) often progressed to high titers that neutralized AMG 212 activity and (iii) was sustained till end of study as none of the ADAs were transient.

TE-ADA in the SC arm: clinical impact to exposure, PSA response and safety

Exposure-ADA correlation analyses were performed to determine the impact of the TE-ADA on exposure and efficacy. Following subcutaneous administration, PK was not consistently detectable at lower dose levels. Therefore, it was not reasonable to make any PK-ADA associations at these lower dose levels.

From the 72 µg to 172 µg dose level, PK was detectable in all subjects at first. However, of the 17 TE-ADA+ subjects, 14 subjects had PK samples measuring below the lower limit of quantitation (LLOQ) and 3 subjects had PK samples measuring close to LLOQ, either at the same timepoint as the first positive ADA sample, or at timepoints thereafter (Supplementary Figures S2A, B). This profound loss of exposure, which coincided with ADA onset, was most likely due to the development of TE-ADA that cleared AMG 212 to undetectable levels in these subjects.

A key pharmacodynamic (PD) marker in prostate cancer is Prostate Surface Antigen (PSA), which acts as a clinically validated marker of disease progression and therefore a surrogate marker for drug activity. From the 36 to 172 µg dose level, reductions in PSA > 50% relative to baseline were observed in nine patients (14). In these initial PSA responders, ADA-mediated loss of exposure likely resulted in an elimination of initial PSA decline, with subsequent progressing PSA. Four examples of such subjects are shown in Figures 2A–D. These examples show contemporaneous association of ADA onset with drug clearance, an ensuing rise of PSA and loss of drug activity gains made in the first cycle. In addition, 3 subjects who had stable PSA initially, also recorded rising PSA levels upon developing ADA. Two such examples are shown in Figures 2E, F. In total, of the 14 ADA+ subjects who had an exposure impact (PK<LLOQ at or after ADA onset), 13 had a PSA rebound from an initial PSA decline or PSA stable status (Supplementary Figure S2C).

Given the high titers of ADAs observed in the SC arm, the ADAs were assessed for any association with immune-complex related safety events known to be associated with ADAs, such as infusion reactions or other hypersensitivity events (8). While infusion reactions and hypersensitivity events were not reported, out of 30 ADA-positive subjects, 24 were observed to develop injection site reactions (14). These were localized injection site erythemas indicating cutaneous inflammation. However, there were 6 ADA-positive subjects that did not develop injection site reactions. Therefore, based on the analysis of this small sample size, an association of these ADAs with injection site reactions could not be identified.

Taken together, TE-ADA observed in the SC cohort was not clearly associated with adverse events but did result in uniform exposure loss. This most likely accounted for the curtailment of the PSA response observed initially.

Topical glucocorticoid co-treatment at SC injection sites to mitigate ADAs

In the SC cohort, due to the consistent formation of ADAs and the observation of localized injection site reactions in many ADA-positive subjects, it was hypothesized that ADA development was induced by the skin-resident DCs, which are well-established to be excellent APCs (20, 21). To prevent, reduce and/or delay ADA development, topical glucocorticoid (GC) treatment including clobetasol propionate and methylprednisolone was introduced mid-study in a protocol amendment, due to their known ability to reduce DC numbers and inhibit their function (22–24). Parallel cohorts of subjects dosed at the 144 µg (Cohort 11) and 172 µg (Cohort 10) dose levels received an aggressive regimen of topical GC (Figure 3). Designated injection sites at the abdomen were pre-treated with clobetasol propionate 0.05% cream for 7 days before

TABLE 1.1 Anti-AMG 212 Antibody Incidence in Subcutaneous (SC) Arm.

	Cohort 1 0.5 µg/d (N = 1)	Cohort 2 1.5 µg/d (N = 1)	Cohort 3 4.5 µg/d (N = 1)	Cohort 4 9.0 µg/d (N = 3)	Cohort 5 18 µg/d (N = 3)	Cohort 6 36 µg/d (N = 4)	Cohort 7 72 µg/d (N = 3)	Cohort 8 144 µg/d (N = 3)	Cohort 9 172 µg/d (N = 3)	Cohort 10 172 µg/d + GC (N = 6)	Cohort 11 144 µg/d + GC (N = 3)	Total (All cohorts) (N = 31)
Subjects with a result at baseline	1	1	1	3	3	4	3	3	3	6	3	31
Pre-existing Ab incidence - n (%)												
Binding antibody positive at baseline	0/1 (0.0)	0/1 (0.0)	0/1 (0.0)	0/3 (0.0)	0/3 (0.0)	0/4 (0.0)	0/3 (0.0)	0/3 (0.0)	0/3 (0.0)	0/6 (0.0)	0/3 (0.0)	0/31 (0.0)
Subjects with a postbaseline result	1	1	1	3	3	4	3	3	3	6	3	31
Treatment-emergent Ab incidence - n (%)												
Binding antibody positive postbaseline with a negative result at baseline	1/1 (100.0)	1/1 (100.0)	1/1 (100.0)	3/3 (100.0)	3/3 (100.0)	4/4 (100.0)	3/3 (100.0)	2/3 (66.7)	3/3 (100.0)	6/6 (100.0)	3/3 (100.0)	30/31 (96.7)
Neutralizing antibody positive postbaseline with a negative result at baseline	1/1 (100.0)	1/1 (100.0)	1/1 (100.0)	3/3 (100.0)	3/3 (100.0)	4/4 (100.0)	2/3 (66.7)	2/2 (100.0)	2/3 (66.7)	6/6 (100.0)	3/3 (100.0)	28/30 (93.3)
Transient [a]	0/1 (0.0)	0/1 (0.0)	0/1 (0.0)	0/3 (0.0)	0/3 (0.0)	0/4 (0.0)	0/3 (0.0)	0/2 (0.0)	0/3 (0.0)	0/6 (0.0)	0/3 (0.0)	0/30 (0.0)

N = Number of subjects who received ≥ 1 dose of investigational productAb = Antibody.
n = number of subjects with a result.
[a] Negative result at the subject's last timepoint tested within the study period.
GC = topical glucocorticoid treatment at SC injection sites.
Tables 1.1 and 1.2 has been previously reported as Supplementary Tables S5 and S6 respectively in Hummel et al., 2021 (14).

10.3389/fimmu.2023.1261070

10.3389/fimmu.2023.1261070

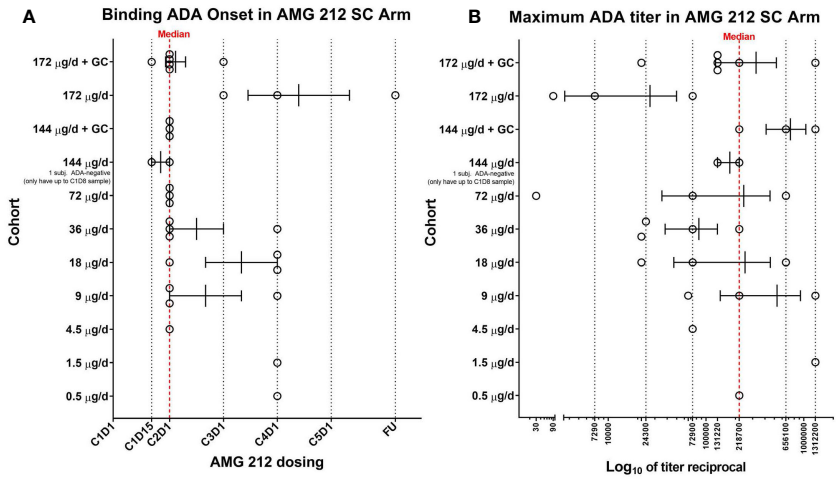

FIGURE 1
Binding ADA onset and maximum ADA titer in the SC arm of the AMG 212 first-in-human study. At appropriate timepoints, patient serum samples were collected and screened for binding antibodies to AMG 212 using a fully validated, electrochemiluminescence-based antibody assay. 30 of the 31 subjects enrolled in the SC arm completed at least 1 cycle of AMG 212 SC dosing. All 30 subjects developed binding ADA and are shown in the scatter plots **(A, B)**. Each circle represents a single subject. Each row represents individual cohorts, starting from Cohort 1 (bottom, 0.5 μg/d) to Cohort 10 (top, 172 μg/d + topical glucocorticoid (GC) treatment at the SC injection sites). Subjects were enrolled in single-subject cohorts for the first 3 cohorts and in multiple-subject cohorts thereafter. The scatter plot in **(A)** shows the range of binding ADA onset in each cohort, plotted as cycle number, day number (CXDX) upon initiation of AMG 212 dosing. FU refers to the 30-day follow-up period after the end of treatment. Error bars depict the mean and standard error of mean (SEM) of the binding ADA onset within each cohort. The red dotted line at Cycle 2 Day 1 (or Day 22) represents the median binding ADA onset across the dose escalation phase in the AMG 212 SC arm. The scatter plot in **(B)** shows the range of maximum ADA titer in each cohort, plotted as the reciprocal of the maximum ADA titer registered by each subject at any time on study. Error bars depict the mean and SEM of the maximum ADA titer reciprocal within each cohort. The red dotted line at titer reciprocal 218700 represents the median maximum ADA titer across the dose escalation phase in the AMG 212 SC arm.

the Cycle 1 Day 1 AMG 212 SC dose to induce apoptosis of skin APCs. The same injection sites were then further treated with methylprednisolone aceponate 0.1% cream during the 21-day cycle to suppress APC function. This was repeated through the third cycle (Figure 3).

The ability of the topical GC to eliminate or suppress skin APCs was not confirmed, as skin biopsies were not retrieved from GC-treated subjects. As a surrogate marker of whether the topical GC eliminated or suppressed skin APCs, peripheral blood monocyte counts were analyzed. There were no significant differences in this parameter, at the 144 and 172 μg/d dose levels, between the paired cohorts comparing subjects treated with or without GC (Supplementary Figures 3A, B).

Despite utilizing topical GC to forestall APC engagement, this strategy was not successful in preventing, delaying or suppressing the magnitude of ADA development (Table 1.1, comparing Cohort 10 to Cohort 9, and Cohort 11 to Cohort 8; Figures 1A, B: top 4 rows).

TE-ADA in the CIV arm

As the ADAs observed in the SC cohort could not be mitigated, it was not feasible to continue dose escalation in the SC setting as exposure could not be reasonably sustained past the second cycle. A new arm of the study testing AMG 212 via continuous intravenous (CIV) administration was initiated. In stark contrast to the SC cohort, 0/16 subjects (0% incidence) developed ADAs in the CIV cohort when administered AMG 212 at dose levels ranging from 5 μg/d to 80 μg/d (Table 1.2). This result was not due to false negatives, as the drug tolerance for the ADA assay was satisfactory and drug interference could be ruled out. As expected, in these ADA-negative subjects, clinically-observed exposure was sustained, dose-proportional, and fell within the normal range of variability (Supplementary Figure S1 of Hummel et al., 2021 (14)).

From the 5 to 80 μg/d dose levels, confirmed PSA responses (PSA 30 or PSA 50) were recorded in 5/16 subjects (14). Out of these 5 PSA responders, 3 subjects had an initial PSA decline that was reversed, despite sustained exposure in the absence of TE-ADA. These 3 subjects were dosed at lower dose levels at which a sustained pharmacodynamic response from AMG 212 may not be expected, and for which other resistance mechanisms may have played a role in the observed loss of response as well. Remarkably, 1 subject each at the two highest dose levels tested, 40 μg/d and 80 μg/d, had sustained PSA 50 responses for 12 cycles and 25 cycles respectively (Figures 2G, H).

Taken together, in contrast to the SC route, AMG 212 did not induce any TE-ADAs when administered by CIV infusion. This enabled maintenance of exposure, yielding an exceptional durability of response in two subjects at the higher dose levels.

10.3389/fimmu.2023.1261070

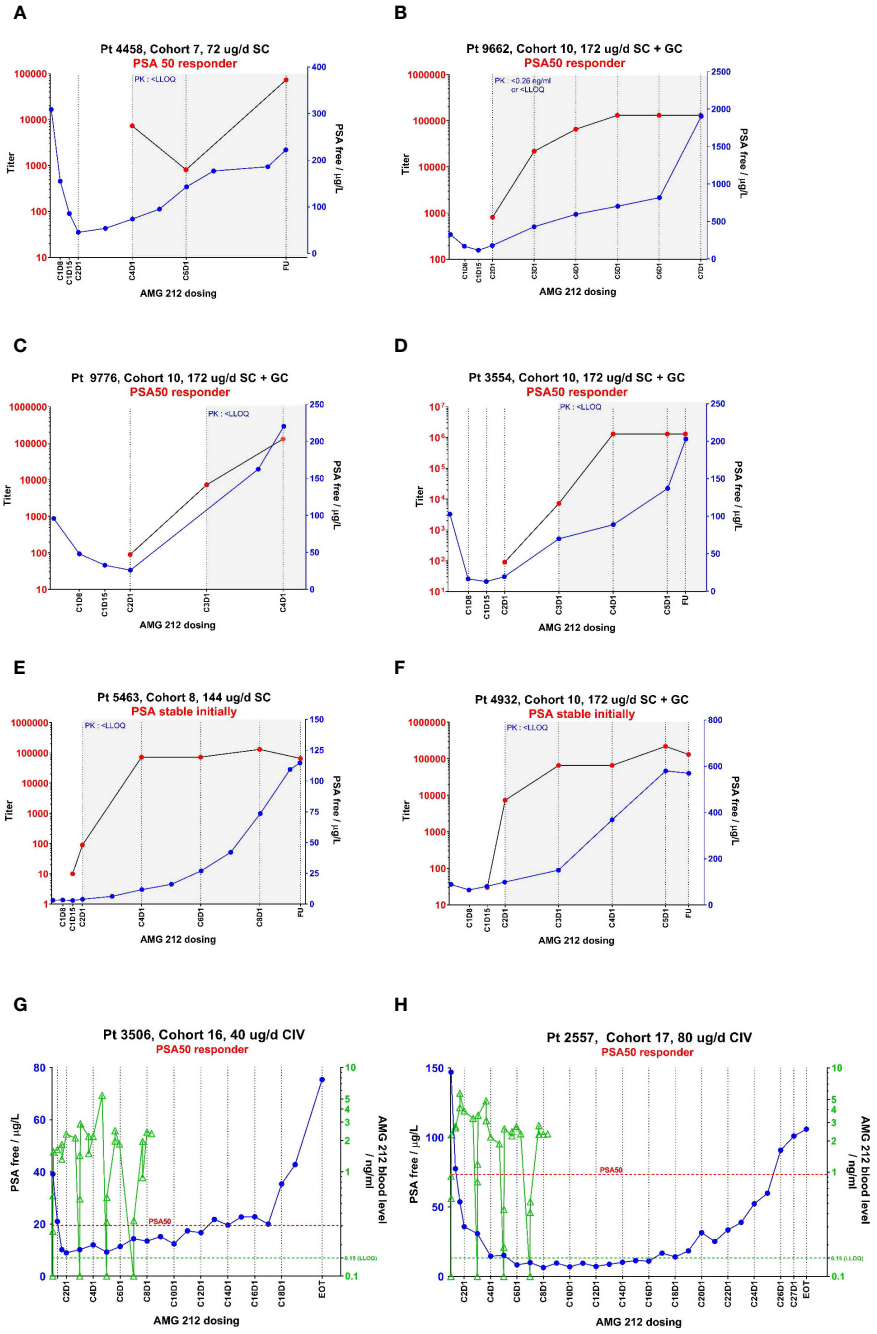

FIGURE 2
PK, ADA and PSA profiles from select individual subjects in the AMG 212 SC and CIV arm showing temporal correlation between these 3 parameters. The temporal relationship between pharmacokinetics (PK, as represented by drug concentration), ADA magnitude (as represented by titer) and a pharmacodynamic marker of biochemical disease progression (as represented by Prostate Surface Antigen (PSA)), are plotted in line graphs **(A–H)**. CXDX refers to the cycle number and day number upon initiation of AMG 212 dosing. "EOT" refers to End-of-Treatment. FU refers to the 30-day follow-up period after the end of treatment. **(A–F)** show the profiles of six subjects from the SC arm, which include four PSA 50 responders **(A–D)** and two PSA stable subjects **(E, F)**. **(G, H)** show the profiles of two subjects from the CIV arm who were both PSA 50 responders. In the SC arm, AMG 212 PK was not consistently detectable among subjects in the same cohort until Cohort 7, the 72 µg/d dose level. At Cohort 7 and onwards, while PK was detectable initially, the onset of ADAs correlated with an impact to PK, whereby PK fell to below the lower limit of quantitation (LLOQ). The time period at which PK measured <LLOQ is depicted by a gray shaded area on the graphs **(A–F)**. In the CIV arm, ADAs did not develop in all treated subjects, and PK was detectable in all cohorts (no gray shaded areas in **(G, H)**). In **(A–F)**, ADA titer is shown on the left y-axis, and PSA on the right y-axis. In G-H, PSA is shown on the left y-axis and PK on the right y-axis. In **(G, H)** the PK trace stops at Cycle 8 Day 8 for both Subject 3506 and Subject 2557, as that was the last PK timepoint collected for these patients on study. The legend for the line graphs is as follows - PK: green triangles, ADA-positive status: red circles, PSA: blue circles, green dotted line at 0.15 ng/ml is the LLOQ of the PK assay; red dotted line represents the PSA value at which 50% reduction from baseline was observed.

10.3389/fimmu.2023.1261070

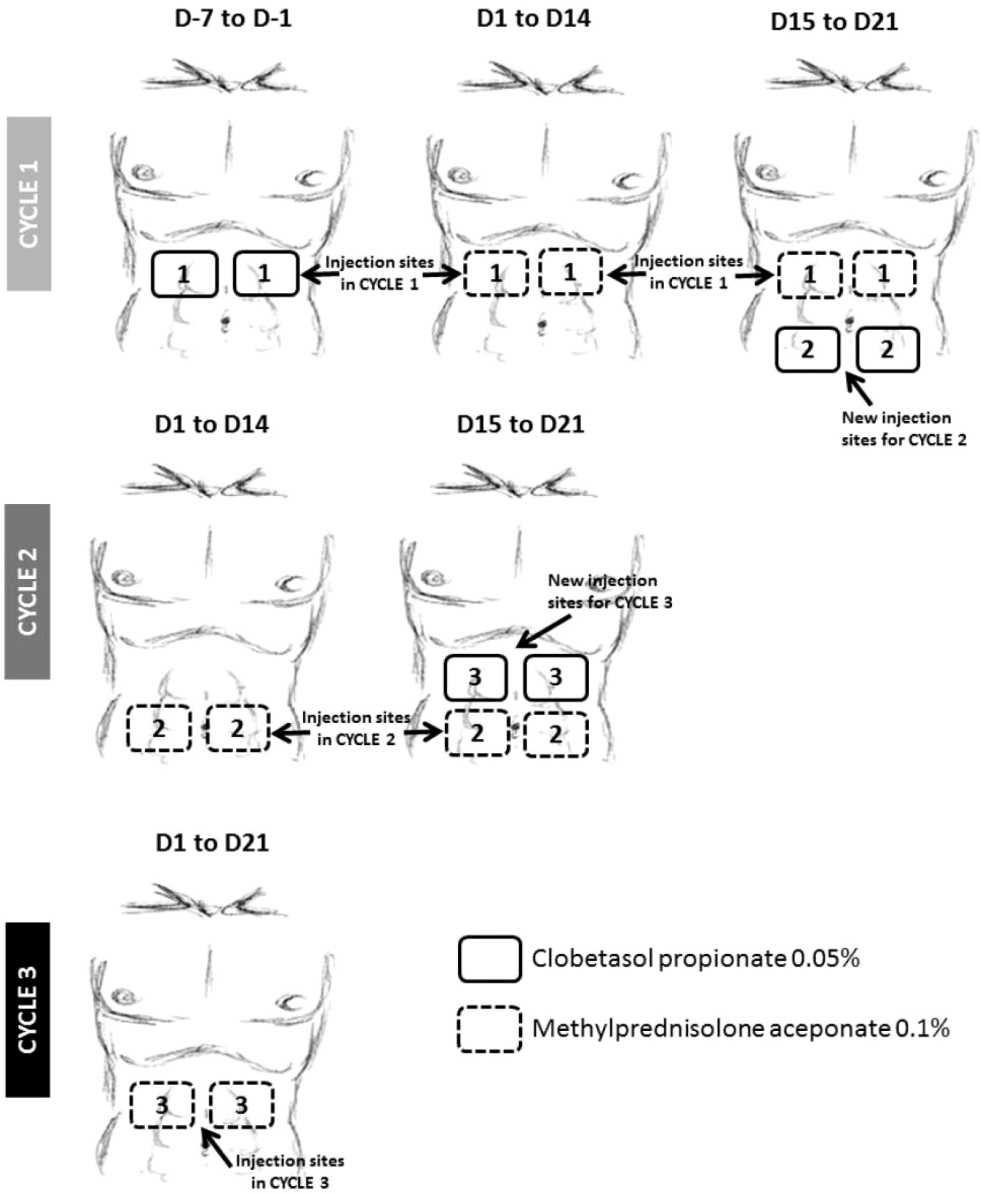

FIGURE 3
Topical glucocorticoid (GC) treatment at AMG 212 SC injection sites implemented at the 144 and 172 µg/d dose levels. To mitigate the ADA observed during dose escalation, a daily topical GC treatment of SC injection sites for the first 3 cycles was introduced mid-study, with the goal of suppressing skin antigen presenting cell (APC) function. The above schema provided instructions on administering the topical GC in patients who injected AMG 212 at 4 regions around the navel. On Cycle 1, Day minus 7 to Cycle 1 Day minus 1, i.e. 1 week to 1 day prior to start of AMG 212, subjects applied a hazelnut-sized amount of clobetasol propionate 0.05% cream in a uniform layer on each of 2 abdominal skin areas for a 7-day daily topical administration. Upon initiation of the AMG 212 SC daily dosing cycle, from Cycle 1 Day 1 to Cycle 1 Day 21, subjects continued applying daily topical GC on the same 2 marked skin areas where SC injections were performed, with methylprednisolone aceponate 0.1% cream. The AMG 212 SC injection was always performed before the administration of the topical GC on the same day. This "7-day clobetasol premedication, 21-day methylprednisolone concomitant medication" topical GC regimen was repeated for Cycle 2 and Cycle 3, on 2 other abdominal skin areas distinct from the injection sites of the previous cycle. A subject stopped administration of topical GC if a local reaction related to the AMG 212 SC injections or a Grade ≥2 local or systemic reaction related to GC treatment occurred. Further daily injections were then performed outside the marked skin areas selected for the ongoing cycle.

10.3389/fimmu.2023.1261070

TABLE 1.2 Anti-AMG 212 Antibody Incidence in Continuous Intravenous Infusion (CIV) Arm.

	Cohort 13 5 µg/d (N = 3)	Cohort 14 10 µg/d (N = 4)	Cohort 15 20 µg/d (N = 3)	Cohort 16 40 µg/d (N = 4)	Cohort 17 80 µg/d (N = 2)	Total (All cohorts) (N = 16)
Subjects with a result at baseline	3	4	3	4	2	16
Pre-existing Ab incidence - n (%)						
Binding antibody positive at baseline	0/3 (0.0)	0/4 (0.0)	0/3 (0.0)	0/4 (0.0)	0/2 (0.0)	0/16 (0.0)
Subjects with a postbaseline result						
Treatment-emergent Ab incidence –n (%)						
Binding antibody positive postbaseline with a negative or no result at baseline	0/3 (0.0)	0/4 (0.0)	0/3 (0.0)	0/4 (0.0)	0/2 (0.0)	0/16 (0.0)
Transient [a]	0/0 (–)	0/0 (-)	0/0 (-)	0/0 (-)	0/0 (-)	**0/16** (0.0)

N = Number of subjects who received ≥ 1 dose of investigational product.
Ab = Antibody.
n = number of subjects with a result.
[a]Negative result at the subject's last timepoint tested within the study period.
GC = topical glucocorticoid treatment at SC injection sites.
Tables 1.1 and 1.2 has been previously reported as Supplementary Tables S5 and S6 respectively in Hummel et al., 2021 (14).

Root cause analysis of the difference in clinical immunogenicity observed between the SC and CIV cohorts

Several factors contribute to a therapeutic's immunogenic risk and observed immunogenicity in the clinic. We sought to explain the polar difference in TE-ADA incidence observed between the SC (near 100%) and CIV (0%) cohorts by systematically interrogating both product-related and patient-specific factors, beyond the route of administration.

Immune status of SC and CIV subjects

To determine if an elevated baseline immune status in the SC subjects played a role in predisposing them to developing ADA, activation status (CD69+) on CD4+ T cells and MHC class II upregulation (HLA-DR^{hi}) on monocytes were assessed by flow cytometry in peripheral blood at the time of screening (7 days before Cycle 1 day 1). At the screening timepoint, no significant differences in CD14+ HLA-DR+ counts (Figure 4A), HLA-DR^{hi} median fluorescence intensity (MFI) (Figure 4B), CD4+ CD69+ counts (Figure 4C) and percentages (Figure 4D), were observed between SC and CIV subjects. TE-ADA+ subjects in the SC cohort were further spliced into those who had a maximum ADA titer corresponding to more than (high titer) or less than (low titer) of 1: 10, 000, at any time on study. Subjects with high titer TE-ADA did not exhibit significantly greater monocyte MHC class II upregulation (Figure 4E) or T cell activation (Figure 4F) compared to those with low titer TE-ADA at screening. Taken together, the data suggest that SC subjects were not inadvertently biased to developing TE-ADA from higher predose immune parameters relevant to generating an ADA response that may have occurred by chance.

In addition, as most of the TE-ADA developed by the end of cycle 1, we assessed peripheral CD4+ T cell activation at all timepoints in the first cycle for which flow cytometry data was available. Although CIV subjects had lower CD4+CD69+ counts at baseline compared to SC subjects, the CD4+ T cell activation status did not appear to be increased in SC subjects compared to CIV subjects over the period of Cycle 1 Day 8 to Cycle 2 Day 1, when the majority of TE-ADA developed (Figure 4G). Flow cytometry assessing B cell markers of activation was not performed in this study. Thus, CD4+ T cell activation documented over time in the peripheral blood, was unable to capture the ongoing ADA response generated in the secondary lymphoid tissue.

Product quality attributes of Good Manufacturing Practice lots used in the SC and CIV arms

Of a drug product's various attributes, high molecular weight species (HMWS) (larger than dimer) is an attribute widely acknowledged as a primary risk to immunogenicity (25–27). The AMG 212 SC and CIV Good Manufacturing Practice (GMP) lots were formulated the same as a lyophilisate, for reconstitution with sterile water for injection (WFI). Upon review of the drug product quality profile of AMG 212 GMP lots, drug product monomer purity was comparable at 97-98% in each of the SC and CIV GMP lots, indicating that HMWS levels were low and comparable between the lots used in the SC and CIV arms of the study (Table 2). Other product quality attributes with immunogenicity risk potential, such as visible particles, and particulate matter, including the pH of the formulations, were comparable between the SC and CIV GMP lots as well (Table 2). Taken together, the drug product quality attribute data suggest that SC subjects were not inadvertently biased to developing TE-ADA due to higher

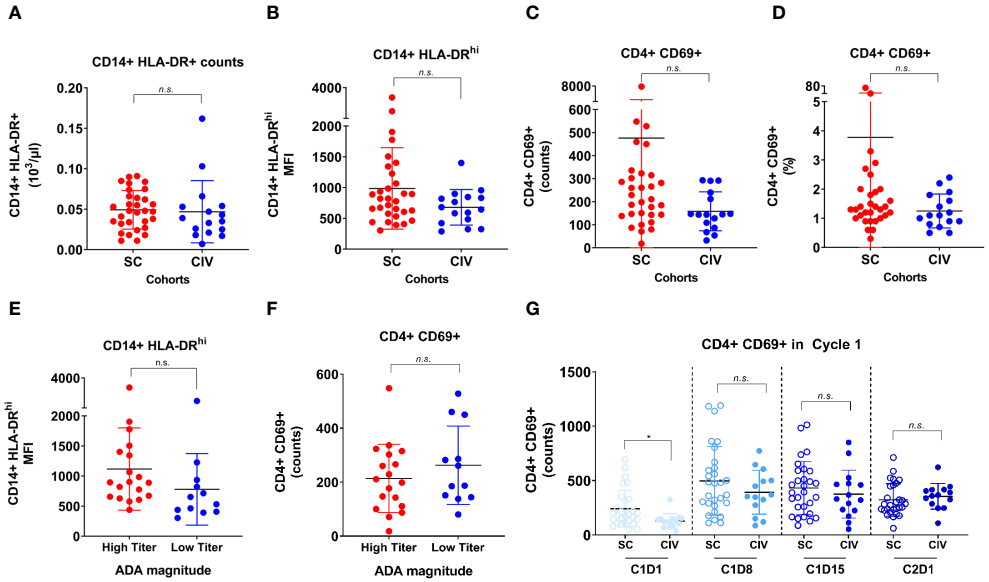

FIGURE 4
Flow cytometric analysis of CD14+ monocyte and CD4+ T cell activation between SC and CIV arms of AMG 212. MHC class II upregulation on CD14+ monocytes, as evaluated by HLA-DR+ counts and HLA-DR^{hi} median fluorescence intensity (MFI) **(A, B)**, and the activation status of CD4+ T cells, as evaluated by CD69+ counts and CD69+ cells as a percentage of CD4+ T cells **(C, D)**, were assessed by flow cytometry in peripheral blood at the time of screening (7 days before cycle 1 day 1). ADA+ subjects in the SC arm were further sub-grouped into those who had a maximum ADA titer corresponding to more than (high titer) or less than (low titer) of 1: 10, 000 at any time on study **(E, F)**. Peripheral CD4+ T cell activation status between the SC and CIV arms was analyzed at predose timepoints through the first cycle (on day 1, 8, 15) and on cycle 2 day 1 **(G)**. Each circle represents an individual subject. Unpaired t tests were used to compare between the SC and CIV subjects. n.s. is not significant. *p-value < 0.05.

amounts of immunogenicity-risk related attributes in the SC GMP lots that may have occurred by chance.

In addition, we examined stability assays that tested whether AMG 212 was stable over time after reconstitution. AMG 212 consisted of over 97% monomer species as measured by size-exclusion chromatography, after 7 days at 5 ± 3°C, and an additional 4 days at 37 ± 2°C with agitation (data not shown). This data suggests that it was unlikely that AMG 212 drug product could have developed HMWS in concerning amounts over time at human body temperature for at least 4 days. Taken together, an assessment of HMWS in AMG 212 drug substance and drug product ruled out this attribute as a potential cause for the immunogenicity observed in the SC arm.

Given the above, patient baseline immune status (peripheral blood), and drug product quality attributes related to immunogenicity risk, did not appear to contribute to ADA formation in SC-administered subjects.

The immunogenicity observed to SC-dosed AMG 212 may be most evidently explained by the route of administration. However, relying on this factor alone would be an oversimplification, as not all SC-injected protein therapeutics above 20kD in size, which are known to first encounter the lymphatic system before entering the peripheral circulation (28, 29), elicit ADA responses. Table 1.1 shows that TE-ADAs developed in every dose level of the SC cohort, from the lowest to the highest dose level tested. This indicates a lack of dose-dependency in the induction of the ADA response. It also suggests that a characteristic inherent in the drug may be driving immunogenicity.

To determine where the AMG 212 SC ADAs were binding to on AMG 212, we performed exploratory work evaluating the domain specificity of these ADAs. Using 8 ADA-positive and 14 ADA-negative samples from 4 subjects (1 subject each from the 0.5, 1.5, 4.5 and 9.0 µg/d cohorts) in an exploratory assay and with appropriate reagents, these results demonstrated that AMG 212 ADAs bound predominantly to the PSMA binder, and not to the CD3 binder or the linker (data not shown).

However, sustained, clinically impactful ADA responses such as those observed in the AMG 212 SC arm are often driven not by structural epitopes recognized by B cells alone, but by CD4+ T cells recognizing sequence-based epitopes located within the drug's amino acid sequence. We therefore focused our efforts on seeking out potential T cell epitope(s) in AMG 212. Here we hypothesized that the combination of the SC drug delivery regimen and the existence of potentially immunogenic sequences in AMG 212 were responsible for driving the robust clinical ADA response.

To address the latter part of this hypothesis, we performed a series of *in vitro* experiments to determine whether AMG 212 contained potentially non-tolerant, sequence-based, T cell epitopes.

Identification of potential sequence-based epitopes in AMG 212

MAPPS, restimulated T cell line assay and clinical memory recall assay

We applied a tiered approach in seeking out potential T cell epitopes in AMG 212. Starting at the level of APC recognition and presentation, we narrowed down suspect sequences through their reactivity in healthy donor T cells, and eventually tested the peptides in clinical memory recall assays using patient samples.

First, we sought to determine whether there were specific sequences in AMG 212 that were being presented on the APC surface to T cells by employing MHC class II-associated peptide proteomics (MAPPS) (30, 31). While MAPPS does not assess the ability of peptide-MHC complexes to elicit a T cell response directly, it seeks to identify MHC class II-binding peptide sequences that are naturally processed and presented by MHC class II on the surface of APCs. These sequences can then be identified by mass spectrometry, allowing for precise location mapping onto the full-length sequence.

MAPPS was performed on AMG 212 twice, evaluating a total of 20 donors that included a variety of HLA-DRB alleles representing the major subtypes in the human population (Supplementary Table 1). MAPPS identified 8 distinct sequence regions across the full-length amino acid sequence of AMG 212 that was being presented on HLA-DRB alleles. These were labeled as Sequence Region #1, 2, 3, 4, 5, 8, 8.5 and 11 (Figure 5A). Sequence region #1-5 were located in the CD3 binder, while sequence region #8, 8.5 and 11 were located in the PSMA binder of AMG 212 (Figure 5A). The overall number of donors that presented each sequence region are shown in Figure 5B. Although there were a few sequence regions that appeared to be presented by multiple donors, MAPPS did not reveal any one sequence region as a potentially immunodominant epitope over the rest of the regions based on incidence (Figure 5B).

While MAPPS helps to vastly narrow down possibilities of culprit epitopes, this assay does not verify that these putative sequences are immunogenic (32). Therefore, each putative sequence region identified by MAPPS needed to be confirmed for their ability to stimulate a specific T cell response. To further filter which of these 8 sequence regions presented on the APC surface could be conferring specific T cell reactivity, peptides spanning these 8 sequence regions were synthesized. In addition, peptides spanning the rest of the CDR regions of AMG 212 were proactively synthesized alongside the MAPPS-identified sequence regions to completely account for AMG 212's most novel sequence regions with the highest potential for immunogenicity.

To determine which of these suspect epitopes could confer T cell reactivity, a restimulated T cell line assay using healthy donor PBMCs was developed in-house, with modifications to what has been described previously (16, 17, 33). The restimulated T cell line assay is in essence, an extension of the traditional DC:T assay that evaluates sequence-based immunogenicity risk (32). A key differentiating factor is that the restimulated T cell line assay utilizes multiple rounds of stimulation instead of one. This serves two purposes. First, this approach recapitulates the chronic dosing regimen that AMG 212 patients experienced and therefore simulates an antigen-experienced memory response. Second, because naïve healthy donors were being used in this assay, multiple stimulations aid in increasing the rare antigen-specific precursor T cell clonal frequencies found in naive individuals ($1:10^7$) to those found in memory responses ($\sim 1:10^{3\text{-}5}$) (34). The assay schema for the restimulated T cell line assay is shown in Figure 6A. The restimulated T cell line assay was performed 3 times, with a total of 10 donors. The HLA allele subtypes of these donors are shown in Supplementary Table 2.

The accrued assay results showed that of the 13 suspect peptides tested, 4 peptides showed T cell reactivity in more than 1 donor (Figure 6B). These 4 peptides were Peptide #1, 2, 8 and 11. Of the 10 donors, 3 donors were reactive to Peptide #1, 5 donors to Peptide #2, 4 donors to Peptide #8 and 2 donors to Peptide #11 (Figure 6B). In assays where the same donor was repeated, specific peptide reactivity could be reproduced. Representative ELISPOT images along with corresponding spot counts showing the individual peptide reactivity profile of 2 donors are shown in Figure 6C. In these examples, Donor 8945 was observed to react to Peptides #1 and 2 from Pool 1, while Donor 6445 was observed to react to Peptides #8 and 11 from Pool 2 (Figure 6C). Notably, peptides such as peptide #4-7, 9-10, 12 and our self-tolerant peptide #13 negative control, did not show T cell reactivity consistently across assays. Peptide #4 and #5, despite being presented by 7 and 8 out of 20 donors respectively in the MAPPS assay (Figure 5B), failed to confer T cell reactivity in the restimulated T cell line assay. MAPPS can be under-predictive if the appropriate sensitivity is not applied (12, 32). However, this was not the case in our MAPPS assays, as we had sufficient consistency and sensitivity across both rounds of MAPPS assays (see Methods).The results from the restimulated T cell line assay align with our expectations that only a subset of sequences identified from the MAPPS assay, translate into T cell reactivity.

With our top suspect sequence regions in hand, we sought to ascertain which of these sequences could be driving AMG 212 immunogenicity in a clinical memory recall assay (19) using patient PBMCs. The recall assay capitalizes on an antigen-experienced memory response from ADA+ subjects, in which the patient's peptide-specific T cell clonal frequency has been expanded. In this assay, upon *ex vivo* stimulation from the immunogenic peptide(s), this pool of peptide-specific memory T cell clones within ADA+ patient PBMCs can be recalled upon to secrete Interferon-γ, detectable by ELISPOT.

Ideally, we would have performed this recall assay using PBMCs from AMG 212 ADA+ patients. However, at this point in our investigation, the AMG 212 FIH clinical trial had already concluded, and we were unable to obtain PBMCs from AMG 212 ADA+ subjects retrospectively. However, a follow-on molecule to AMG 212, AMG 160 (half-life extended BiTE® molecule), was being investigated in a FIH trial at that time (ClinicalTrials.gov, NCT03792841).

AMG 212 and AMG 160 were observed to have 98.4% sequence identity. Importantly, comparing our top peptide sequence suspects #1, 2, 8, 8.5 and 11 in AMG 212 to analogous regions in AMG 160, we found Peptide #1, 2, 8 and 8.5 to be identical. Peptide #11 was 2 amino acids different compared to the analogous sequence in AMG 160. To determine if this difference could affect HLA class II

A

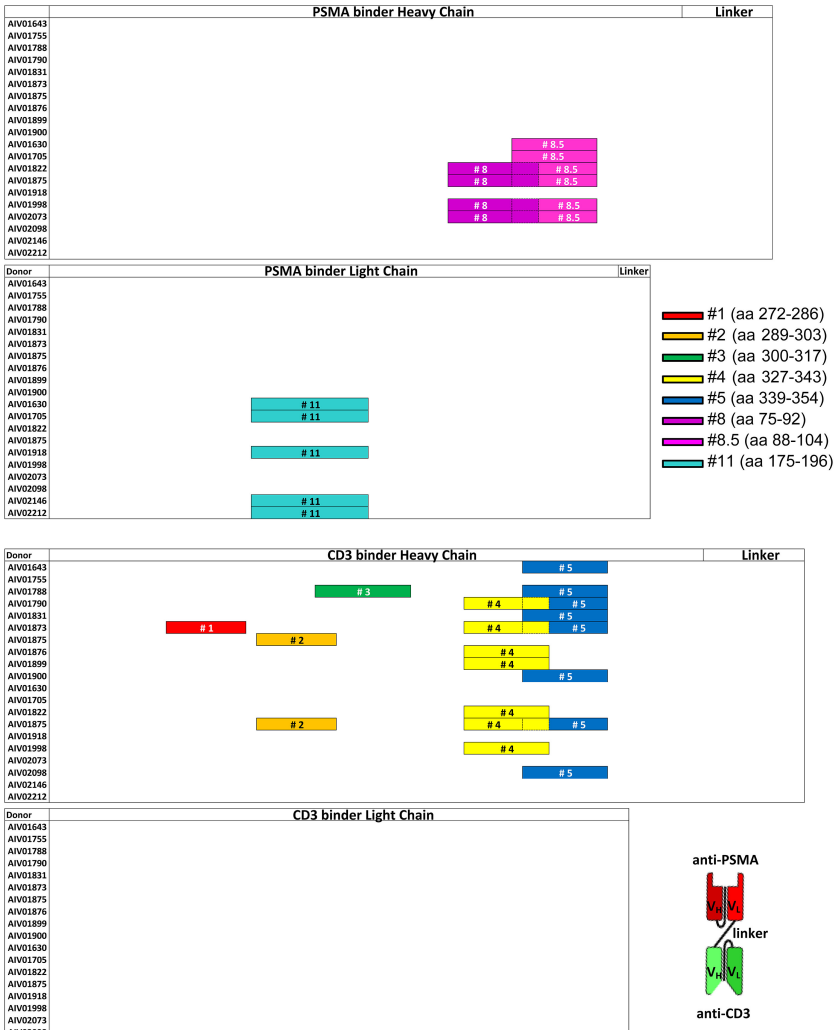

B

Binder	Sequence Region #	MAPPS-identified (n=20 donors)
CD3	1	1/20
	2	2/20
	3	1/20
	4	7/20
	5	8/20
PSMA	8	4/20
	8.5	6/20
	11	5/20

FIGURE 5
MHC class II-associated peptide proteomics (MAPPS) assay identified sequences within full-length AMG 212 that were naturally processed and presented on the APC surface for presentation to T cells. Immature DCs were loaded with AMG 212 to allow for capture, processing and formation of peptide major histocompatibility complex (pMHC) complexes. Cells were harvested and lysed to immunoprecipitate the pMHC complexes from the DC surface. Peptides were eluted off the presenting MHC class II molecules, and their sequences identified by mass spectrometry, allowing for precise location mapping onto the full-length sequence. **(A)** This sequence map depicts the full-length AMG 212 sequence, divided into four sub-sections: the PSMA binder, heavy and light chains (top half; top two sub-sections) and the CD3 binder, heavy and light chains (bottom half; bottom two sub-sections). Each row within each sub-section represents a single donor. The different color bars mapped onto each of the rows denote the location and length of the distinct sequence regions #1-5, #8, 8.5 and 11. These sequences ranged from 14 – 20 amino acids long and their amino acid (aa) residue numbers (start and end) are shown alongside their respective bars in the legend. The overlap between sequence region #8 and #8.5, #4 and 5, are depicted by a dotted border. Several donors presented multiple peptides within the same sequence region, but a single color bar is shown to account for all sequences within that region that were detected from that donor. A schematic of the overall structure of AMG 212 is shown next to the sequence maps for reference. V_H and V_L refer to the single chain variable heavy and single chain variable light regions of the antibody construct respectively. MAPPS was performed on AMG 212 twice, evaluating a total of 20 donors that included a variety of HLA-DRB alleles representing the major subtypes in the human population. The table in **(B)** shows the aggregate number of donors that presented each sequence region as an incidence of the 20 donors utilized in the MAPPS assays. The HLA allele subtypes of these 20 donors are found in Supplementary Table 1.

10.3389/fimmu.2023.1261070

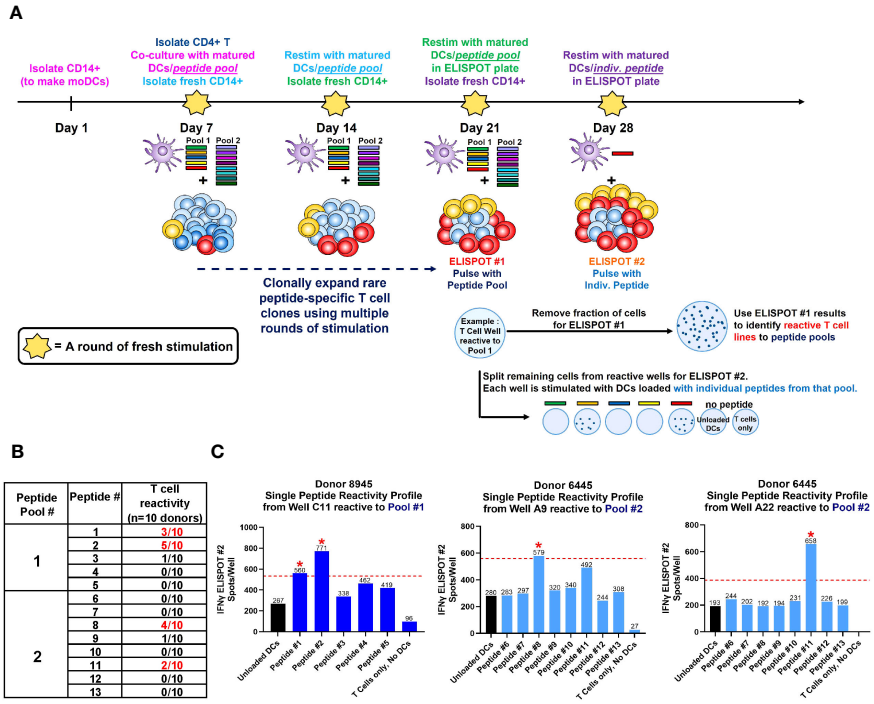

Peptide Pool #	Peptide #	T cell reactivity (n=10 donors)
1	1	3/10
	2	5/10
	3	1/10
	4	0/10
	5	0/10
2	6	0/10
	7	0/10
	8	4/10
	9	1/10
	10	0/10
	11	2/10
	12	0/10
	13	0/10

FIGURE 6
Restimulated T cell line assay on healthy donor PBMCs. A schema of the restimulated T cell assay is shown in **(A)**. To simulate an antigen-experienced memory response, isolated CD4+ T cells were stimulated with multiple rounds of autologous monocyte-derived DCs (moDCs) pulsed with our suspect peptides in a 4-week co-culture. In the week prior to each stimulation, CD14+ cells were isolated from healthy donor PBMC, differentiated into immature DCs with IL-4 and GM-CSF, then separately loaded with 5 μg/mL CEFTA peptide pool or 5 μM PADRE peptide (positive controls), or 5 μM of Peptide Pool #1 or #2 (test peptides) and matured with TNF-α and IL-1β for 48 hours. On Day 7, autologous CD4+ T cells were isolated and seeded at 2 X 10^5/well and stimulated with peptide-loaded DC weekly for the next 21 days. Freshly-loaded and matured DCs were added to the T cell culture every 7 days, and the culture medium was refreshed every 7 days with IL-2 and IL-7. On Day 21, a fraction (4-5 X 10^4) of CD4+ T cells were removed from each well and stimulated with peptide pool-loaded DCs in pre-coated Human Interferon-γ ELISPOT plates, visualized and counted for spots after a 48 hr incubation. On Day 28, peptide pool-specific T cell lines identified from ELISPOT #1 were then fractionated and stimulated with individual peptide-loaded DCs in pre-coated Human Interferon-γ ELISPOT plates, visualized and counted for spots 48 hr later as before. The table in **(B)** shows the aggregate incidence of individual peptide reactivity among the 10 donors tested, after performing this assay 3 times. The bar graphs in **(C)** show the individual peptide reactivity profile (as determined by ELISPOT #2) of Donor 8945 and Donor 6445. A T cell line was deemed reactive to an individual peptide if the spot counts were 2-fold higher than unloaded DC controls, with a minimal difference of 30 spots (above the cut-off value). The red dotted line represents the cut-off value in each plot for that T cell line, which may be different between wells based on the unloaded DC control. Reactive peptides are denoted with a red asterix *. The HLA allele subtypes of the 10 donors used in this assay are found in Supplementary Table 2.

binding, we utilized structural modeling to determine where the critical nonamer binding core could exist within that sequence. The results of these modeling efforts predicted that those 2 amino acid positions were not anchor residues for HLA class II binding. Therefore, Peptide #11 would likely be bound to HLA class II similarly to the analogous AMG 160 peptide sequence, and hence recognized similarly by AMG 160 patients' T cell clones.

Unlike AMG 212, which was administered by continuous IV infusion, AMG 160 was administered by short-term IV infusion over 1 hour, every 2 weeks, after the target dose was reached. Yet, despite being administered intravenously, AMG 160 engendered clinically significant immunogenicity. As of Sep 19th 2020 (an earlier data-cut), as disclosed in the virtual ESMO 2020 presentation describing interim results of the AMG 160 FIH study, 6 of 30 (20.0%) patients evaluated developed ADAs which affected drug exposure between cycles 1 and 10 (35). The full AMG 160 ADA dataset, which evaluated a greater number of subjects, will be disclosed in an upcoming publication (in preparation). By comparison, the clinically meaningful AMG 160 ADA incidence was not as high as that of AMG 212, to which TE-ADA developed in 30/31 subjects (96.7%) within the first 6 cycles upon SC administration of AMG 212 (Table 1.1; Figure 1A).

Due to the high sequence identity, we postulated that the sequences driving immunogenicity to AMG 212 and AMG 160 were most likely the same. In addition, the disease population treated was comparable in the AMG 212 and AMG 160 FIH trials, further supporting the rationale to test our suspect AMG 212 peptide sequences using AMG 160 patient samples. We obtained End of Treatment (EOT) PBMC samples from patients in the AMG 160 FIH trial, to evaluate Peptide #1, 2, 8, 8.5 and 11 in the clinical memory recall assay. In total, PBMC samples from 9 ADA-positive and 8 ADA-negative patients from the AMG 160 FIH trial were assessed in this assay.

Of the suspect sequences tested, Peptide #1, 8 and 11, but not #2 or 8.5, exhibited a recall response in a single AMG 160 ADA+ subject (Figures 7A, B). This was not observed in AMG 160 ADA-negative subjects or in AMG 160-naive healthy donor controls (Figures 7A, B). Notably, this subject with detectable peptide

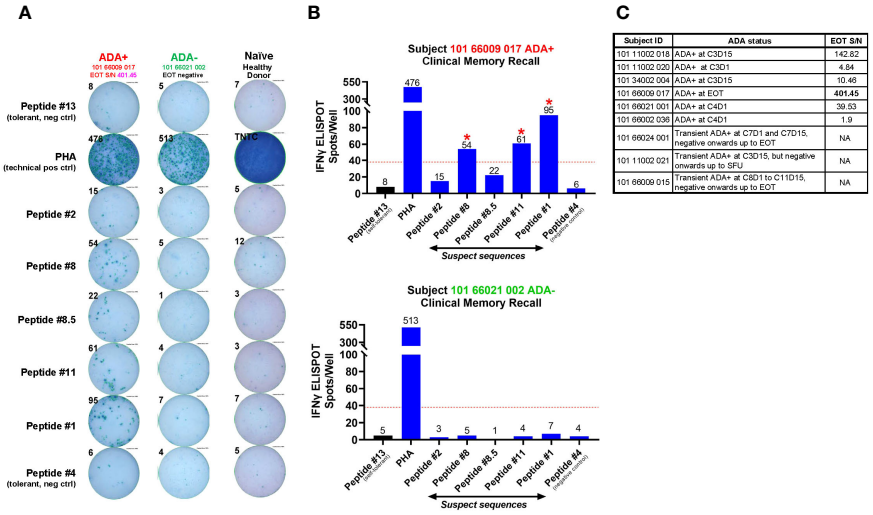

FIGURE 7
Clinical memory recall assay on patient PBMCs obtained at EOT from the AMG 160 FIH trial. Regardless of ADA status, 10 ml of whole blood was collected at the end of treatment (EOT) timepoint from patients enrolled in the AMG 160 First-in-Human (FIH) trial, Study 20180101. Whole blood was sent ambient to the central lab for same-day processing into PBMCs and stored frozen. Freshly thawed patient PBMCs were plated at 2 X 10^5 cells per well, pulsed with individual peptides at 5 μM for 72 hr, and evaluated for a recall response via IFNγ ELISPOT. 10 ng/ml of GM-CSF was provided in the culture. Peptides # 1, 2, 8, 8.5 and 11 were experimental "suspect" sequences. Peptides #13 and #4 were negative control sequences that did not confer T cell reactivity, which we established previously from the restimulated T cell line assays. PBMC from an AMG 160-naive healthy donor was used as an additional negative control. Phytohemagglutinin (PHA) was used as a non-specific T cell activator and acted as a technical positive control for the ELISPOT assay. TNTC refers to "Too-numerous-to-count". The ELISPOT image enumerating the IFNγ spot counts in response to *ex vivo* stimulation from these individual peptides is shown for ADA-positive subject 101 66009 017 and ADA-negative subject 101 66021 002 **(A)**, and depicted as bar plots in **(B)**. The red dotted line in the bar graphs represents the cut-off value calculated as a number with two-fold more spots in the presence of that individual peptide compared to self-tolerant Peptide #13 within the same subject, with a minimal difference of 30 spots. Peptides producing spot counts above the cut-off value were considered able to promote a recall response in these patient PBMCs (denoted by red asterix *). In total, PBMC samples from 9 ADA-positive and 8 ADA-negative patients from the AMG 160 FIH trial were assessed in this assay. The 9 ADA-positive subjects, their binding ADA onset and the magnitude (Signal-to-Noise, S/N) of ADA response at EOT (if found positive at EOT), are shown in the table in **(C)**.

reactivity, had the highest magnitude of ADA at the EOT timepoint among our 9 ADA-positive subjects (Figure 7C). Five other ADA-positive subjects had comparatively lower magnitude (1-2 logs lower) of ADA response at the EOT timepoint, while the remaining 3 ADA-positive subjects had a transient ADA response and was found ADA-negative at the EOT timepoint (Figure 7C). Subsequent discontinuation of the AMG 160 FIH study precluded our ability to obtain more ADA+ patient PBMCs and perform additional recall assays.

Taken together, our multi-assay approach sequentially filtering potential epitopes starting from the level of MHC class II binding to recalling a clinical memory ADA response *ex vivo*, yielded at least 3 possible non-tolerant sequence-based epitopes in AMG 212.

In conclusion, the totality of data from our root cause investigation supports our hypothesis explaining the disparate TE-ADA incidence between the AMG 212 SC and CIV cohorts. The unfavorable combination of a subcutaneous drug delivery, in which a >20 kD protein such as AMG 212 would have had to traffic through secondary lymphoid tissue first, together with at least three non-tolerant T cell epitopes present within the AMG 212 sequence, most likely contributed to the sustained, high-titer ADA response to AMG 212.

Discussion

The emergence of clinically impactful immunogenicity during development is potentially detrimental to patients from two standpoints. First, if the ADAs are associated with certain adverse events. Second, if the ADAs are neutralizing and/or significantly reduce exposure, this may prevent any efficacy response or curtail durability of response. The AMG 212 FIH study's SC arm was an unfortunate case-in-point illustrating the latter in an oncology indication. The decision to switch route of administration from SC to CIV mid-study enabled signs of drug activity to be observed, likely in part because ADAs did not develop in the CIV arm and exposure was sustained. Remarkably, in two CIV subjects, durable PSA responses lasting more than one year were achieved.

The root cause of the immunogenicity observed in the SC arm was initially attributed to the route of administration and treatment regimen. Preclinical and clinical data, including internal Amgen clinical data, support our current understanding that IV administration, in general, has a lower immunogenicity risk than SC administration (36–39). However, there are several instances where there are no differences in immunogenicity rates to the same biologic administered SC and IV, such as in the case of ACTEMRA® (tocilizumab) and ORENCIA® (abatacept) (40, 41).

In certain cases, a lower dose administered intermittently may be more immunogenic than a larger dose administered without interruption (42). Due to the very short half-life (2-3 hr) and fast clearance of AMG 212, a more frequent dosing (once daily dosing) was necessitated to preserve exposure in subjects receiving AMG 212 by the SC route. In contrast, for the CIV dose administrations, subjects received AMG 212 as a continuous IV infusion at a constant flow rate given over 5 consecutive weeks followed by a treatment-free interval of 1 week.

When a foreign protein such as AMG 212 was injected subcutaneously at microgram levels, the frequent daily administration in this setting may have elicited ADA formation due to repeated boosting. Thus, the combination of low-dose, high-frequency and historically more immunogenic route of administration may have elicited the ADA response in the SC arm. As the SC portion of the study was terminated early, strategies such as optimizing dosing frequency to mitigate ADA development was not attempted.

Apart from the dose and dosing frequency, we considered aspects of SC drug delivery that could influence the induction of an ADA response. Drug delivery via the SC route relies on uptake from the interstitial domain of the subcutis. It is well-established that the molecular size of proteins injected SC determines their fate and path to the systemic circulation (28, 29). They have two potential routes for uptake and biodistribution. Lower molecular weight drugs (<20 kD), including small molecules such as insulin, can enter the general circulation directly through blood capillaries. However, higher molecular weight (>20kD) drugs, which include BiTE® molecules such as AMG 212, must traffic through the interstitial matrix of the subcutis to the peripheral lymphatic system first, before entering the systemic circulation (28, 29).

Thus, SC-delivered AMG 212 would have encountered APCs and other immune cells through a series of lymph nodes enroute to the thoracic duct, before reaching the peripheral circulation. This likely provided more opportunity and time for APCs to phagocytose the drug and engender an immune response to AMG 212. CIV-delivered AMG 212 however, directly entered the bloodstream from inception, bypassing the peripheral lymphatic system on the first pass through the body. However, relying on this explanation alone would be an oversimplification, as not all SC-injected protein therapeutics above 20kD in size elicit ADA responses. Conversely, IV-injected protein therapeutics still run the risk of engendering clinically meaningful immunogenicity, as we observed in the case of AMG 160.

Other factors associated with the anatomy of the skin were considered as well. The rapid egress of the drug product into the skin, an organ containing a high frequency of APCs (43), together with a possible depot effect where the drug product forms or stays in aggregates in the interstitial SC space (44, 45) compared to dispersal in high-flow, fluid-rich IV environment, were all plausible reasons why the immunogenic response was triggered in SC-administered patients. However, despite intense topical GC treatment at the injection site to suppress local APC response, this mitigation strategy proved unsuccessful. This suggested that the induction of immunogenicity to SC-delivered AMG 212, was not skin-deep and belied a different and/or further root cause.

Apart from the route of administration, the causes of an immunogenic response to therapeutic proteins include patient-related factors, such as genetic background, baseline immunologic status from either disease state or concomitant medications, and product-related factors, such as attributes incurred during manufacture of the drug and the amino acid sequence of the drug itself. In this report, we investigated as many of these potentially contributing factors as we were able.

As the patients' prior lines of therapies and disease indication were comparable between the patients enrolled into the SC and CIV arms, such patient-specific factors were first ruled out. Baseline immune status (Figure 4) and product quality attributes such as HMWS in the GMP lots (Table 2) were comparable between the SC and CIV arms, thus ruling these factors out as well. We therefore focused our efforts on intrinsic factors of the drug, such as structure-based B cell epitopes and more importantly, sequence-based, T cell epitope(s) that may explain the immunogenicity to AMG 212.

Identification of immunogenic epitopes in biologics is not without precedent, and several groups have recently successfully done so for T cell epitopes (17, 19) and even B cell epitopes (46). Through a series of *in vitro* assays including MAPPS, restimulated T cell line and clinical memory recall assays, we identified at least 3 possible sequence drivers of AMG 212 immunogenicity (Figures 5–7).

While considered the gold standard, obtaining patient PBMC samples for the clinical memory recall assay proved a unique challenge because the AMG 160 FIH study was nearing conclusion by the time we introduced this novel PBMC sample collection for the purposes of performing the recall assay. A limited number of AMG 160 patient PBMC samples were ultimately collected to evaluate the suspect sequence regions. Low cell viability in the patient PBMCs precluded our ability to perform high throughput analyses evaluating more sequences.

Furthermore, we observed that the recall assay was successful in detecting a memory response only in an ADA+ subject with a robust magnitude of ADA at the time of PBMC collection. This is presumably due to an ongoing high-affinity antibody response, in which expanding CD4+ T cell clones continue to provide classical help via the CD40-CD40L axis to perpetuate the antibody response. The ability to detect recall responses may therefore be largely dependent on the strength of the ADA response at the point of PBMC sample collection, which is variable and unpredictable in the clinic. These factors should be carefully deliberated upon when seeking out culprit T cell epitopes responsible for clinical immunogenicity using recall assays.

Both the MAPPS and restimulated T cell assays utilized healthy donor cells. This may not recapitulate the diseased condition where differential proteasomal processing of antigens and post-translational modifications of the epitopes may be taking place. Therefore, sequences showing T cell reactivity in assays using cells derived from healthy donor PBMC, may not fully replicate the epitopes driving a clinical ADA response to the same biologic in a disease setting. Even in a clinical memory recall assay that utilizes patient PBMCs, the number of possible suspect sequences that can be tested is ultimately limited by the PBMC viability and numbers

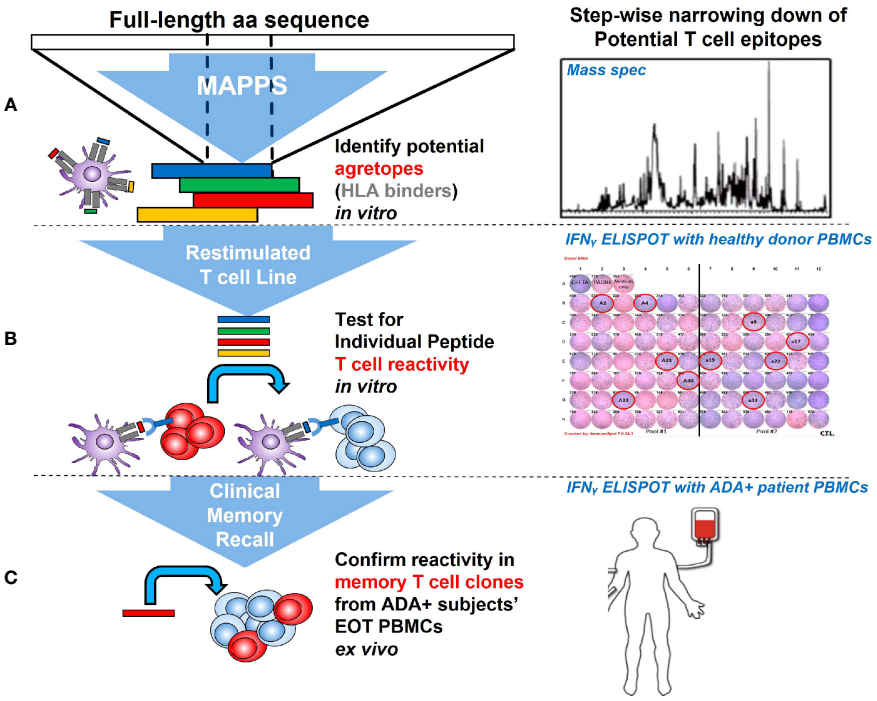

FIGURE 8
Stepwise approach used to identify sequence-based T cell epitopes driving AMG 212 immunogenicity. Starting at the level of APC recognition and presentation, MHC class II-associated peptide proteomics (MAPPS) was used to parse out sequence regions that were naturally processed and presented by HLA class II on the APC surface **(A)**. To further narrow down suspect sequences, peptides representing the MAPPS-identified sequence regions and all other CDR regions were synthesized and tested for individual peptide reactivity in a restimulated T cell line assay, which recapitulates an antigen-specific memory response in healthy donors **(B)**. Peptides that conferred T cell reactivity through this assay were then tested in a clinical memory recall assay, to confirm the peptide's ability to produce a recall response in patients who have developed a robust anti-drug antibody response in the clinic **(C)**.

collected in the patient sample. In addition, although this report focused largely on finding epitopes driving a T-dependent ADA response, a potential role of T-independent B cell responses driving AMG 212 immunogenicity cannot be excluded.

In this manuscript, we disclosed the amino acid residue numbering of the suspect sequence regions but not the amino acid sequences as the latter represent proprietary information. However, not disclosing the actual sequences themselves does not compromise the interpretations and conclusions of this report. In general, ADAs have the greatest potential to develop in response to antigen-specific sequences in the CDRs of even fully-human antibodies as they are deemed the most foreign part of the biologic (6). Indeed, 2 of the 3 identified non-tolerant epitopes spanned the CDR regions of AMG 212. This result was not unexpected. However, some outstanding questions remain.

Of the 3 non-tolerant epitopes identified, was one more immunodominant than the other two? Were there more epitopes we would have identified had we been able to perform more recall assays? AMG 160 differs structurally from AMG 212 as it has an additional "add-on" of a single chain Fc on the C-terminus end of

TABLE 2 Comparison of selected drug product quality attributes related to immunogenicity risk between SC and CIV lots used in the AMG 212 study.

Attribute	SC GMP Lot #1	SC GMP Lot #2	CIV GMP Lot #1	CIV GMP Lot #2
Appearance, visible particles	Free from particles	Free from particles	Free from particles	Free from particles
Subvisible particles (per container)				
≥ 25 μm	0	1	1	0
≥ 10 μm	3	4	9	15
Purity, % monomer by SE-HPLC	98	97	98	97
pH-value	6.0	5.9	6.0	6.2

Attributes known to potentially contribute to immunogenicity risk were evaluated to rule out differences between the SC and CIV GMP lots that could have accounted for the disparity in ADA incidence between the two arms. The attributes of (1) visible particles, (2) subvisible particles, (3) AMG 212 drug product purity (% monomer by size exclusion-high performance liquid chromatography (SE-HPLC) and (4) pH-value are shown in Table 2. A near 100% drug product purity (% monomer by SE-HPLC) indicate low levels of other size variants including high molecular weight species (HMWS). Both the SC and CIV GMP lots passed acceptance criteria for these attributes and are considered comparable to each other.

the CD3 binder, for the purposes of half-life extension. With the additional Fc portion on AMG 160, could this key structural difference, which would inherently generate different overall B cell epitopes, result in different ADA responses to AMG 212 and AMG 160? The additional Fc portion could also result in differential antigen uptake and proteasomal processing of AMG 160 in APCs. Could epitopes have been missed in using AMG 160 subject PBMCs, instead of AMG 212 subject PBMCs? If there were intrinsic immunogenic regions within the AMG 212 amino acid sequence itself that was likely driving the ADA responses, why were ADAs not observed in the CIV arm as well? Could the continuous IV administration have induced immune tolerance over time to AMG 212, permitting AMG 212 to go "unseen" by the immune system?

Another potential explanation for the lack of ADAs in the CIV arm pertains to the dose levels administered. The maximum tolerated dose was not reached before the study was discontinued (not due to lack of efficacy or safety reasons). Anecdotally, across several T cell engager trials, we have observed that intra-subject dose-escalation can sometimes result in *de novo* development of ADAs. This has been observed even in situations where a patient had been ADA-negative for a significant amount of time prior to the intra-subject dose-escalation. In the AMG 212 FIH study, it is possible that had dose escalation in the CIV arm been pursued, clinically meaningful ADAs may have been detected at higher dose levels. However, as we did not continue further dose escalation past 80 µg/d, we acknowledge that this remains mere speculation.

This body of work, built upon many others, establishes a thought process and a systematic approach in addressing how a sponsor may identify culprit T cell epitopes driving clinical immunogenicity (Figure 8). Upon their identification, culprit T cell epitopes can be removed or de-immunized in the next iteration of the biologic. However, such re-engineering efforts face an arguably uphill task. Although it has been done previously (47–50), de-immunizing key amino acid residues requires extensive modeling to determine the nonamer cores (51) within the identified suspect sequences. Unlike the closed binding pocket of MHC class I, the MHC class II binding pocket is open and more flexible (52). Within the nonamer cores, determining anchor residues in the binding pocket or those protruding into the TCR for possible replacement, would be key to de-immunization. Importantly, while disruption of HLA class II binding would be the goal of these modeling efforts, these point mutational analyses must fulfill other pertinent, non-trivial criteria. These include ensuring that upon modifying the CDRs, the binding affinity and potency of the target binders are not affected, and that the overall antibody construct remains stable and intact, such that the drug retains its intended functionality.

When a biologic exhibits high sequence-based risk based on available prediction tools, downstream assays to confirm possible epitopes should be initiated. One can envision that the tiered approach we utilized to identify culprit epitopes retrospectively, can also be implemented prospectively, to de-risk molecules before they enter the clinic. Indeed, others have built mechanistic models that additionally account for the drug's mode of action when attempting to predict a molecule's clinical immunogenic risk (53). Clearly, there exists a concerted effort from industry and regulators alike to shift from viewing ADA development as an aleatory risk to an informed one.

Clinical immunogenicity may still accompany development of immunomodulatory drugs despite best efforts in predicting immunogenic risk and de-immunizing as much as possible upfront. Biologics whose mode of action potently ablates B cells or inhibits their maturation and differentiation, discernibly run a much lower risk of developing clinically meaningful ADAs, even when administered in the SC setting. Notably, the first approved T cell engager worldwide, BLINCYTO® (blinatumomab) (CD19-targeting), although approved as a CIV formulation, has since been tested as a SC formulation in both Relapsed/Refractory indolent Non-Hodgkin's Lymphoma (NHL) and Acute Lymphoblastic Leukemia (ALL). In both of these trials, anti-blinatumomab antibodies were not detected (54, 55).

In the absence of early-onset, clinically impactful, "showstopping" ADAs, sponsors and regulatory agencies alike may consider raising their tolerance threshold to ADAs for biologics exhibiting a favorable risk: benefit ratio, and in which the ADA impact to clinical response is none, unclear or unknown.

The recent approval of KIMMTRAK® (tebentafusp-tebn), a first-in-class T cell engager for HLA-A 02:01-positive metastatic uveal melanoma patients may be a case-in-point. A 29-33% binding ADA incidence graces the label of KIMMTRAK®. High-titer ADA was shown to decrease exposure by 97% (56). However, the ADAs did not appear to impact overall survival. Such approvals suggest that an increased tolerance of biologics with significant ADA in light of a favorable risk: benefit ratio may already be underway.

Mitigation of ADAs with a variety of strategies during early clinical development have been considered over the years for different disease indications (57). This may be feasible in a disease population where the mitigation strategy is part of standard of care. However, such added interventions are generally not feasible in an already heavily pre-treated oncology population, and where other weakly or non-immunogenic therapies may be available as alternatives. In an age where immunomodulatory drugs dominate oncology pipelines across industry, we propose that clinical monitoring of immunogenicity for this class of drugs in early phase trials is no longer obligatory, but an imperative for onward progress to pivotal stage development.

Data availability statement

The original contributions presented in the study are included in the article/Supplementary Material. Further inquiries can be directed to the corresponding author.

Ethics statement

The studies involving humans were approved by (1) Krankenhaus der Barmherzigen Schwestern Linz,

Ethikkommission der Barmherzigen Schwestern Linz, Seilerstätte 4, 4010 Linz, Austria (2); Ethikkommission des Landes Oberösterreich, Kepler Universitätsklinikum Neuromed Campus, Wagner-Jauregg Weg 15, 4020 Linz, Austria (3); Universitätsklinikum Heidelberg, Ethikkommission der Med. Fakultät Heidelberg, Alte Glockengießerei 11/1, 69115 Heidelberg, Germany (4); Klinikum der Universität Würzburg, Ethik-Kommission bei der Medizinischen Fakultät, Institut für Pharmakologie und Toxikologie, Versbach Str. 9, 97078 Würzburg, Germany (5); Landesamt für Gesundheit und Soziales, Geschäftsstelle der Ethik-Kommission des Landes Berlin, Fehrbelliner Platz 1 (Dienstgebäude), 10707 Berlin, Germany. The studies were conducted in accordance with the local legislation and institutional requirements. The participants provided their written informed consent to participate in this study. Written informed consent was obtained from the individual (s) for the publication of any potentially identifiable images or data included in this article.

Author contributions

HP: Conceptualization, Data curation, Formal Analysis, Investigation, Methodology, Writing – original draft, Writing – review & editing. KH: Formal Analysis, Methodology, Writing – review & editing. NT: Formal Analysis, Methodology, Writing – review & editing. BW: Writing – review & editing, Methodology. CB: Formal Analysis, Methodology, Writing – review & editing. CW: Formal Analysis, Methodology, Writing – review & editing. MM: Formal Analysis, Methodology, Writing – review & editing. SW-R: Conceptualization, Formal Analysis, Funding acquisition, Writing – review & editing. GK: Conceptualization, Formal Analysis, Funding acquisition, Writing – review & editing. SS: Conceptualization, Data curation, Formal Analysis, Investigation, Methodology, Project administration, Supervision, Writing – review & editing. RB: Conceptualization, Investigation, Writing – review & editing. H-DH: Conceptualization, Investigation, Writing – review & editing. WL: Conceptualization, Investigation, Writing – review & editing. CG: Conceptualization, Investigation, Writing – review & editing. TE: Data curation, Formal Analysis, Investigation, Methodology, Project administration, Supervision, Writing – review & editing. BT: Investigation, Writing – review & editing. DM: Formal Analysis, Funding acquisition, Methodology, Project administration, Supervision, Writing – original draft, Writing – review & editing, Conceptualization, Data curation.

Funding

The author(s) declare financial support was received for the research, authorship, and/or publication of this article. The AMG 212 clinical study was funded by Bayer. The root cause analysis behind AMG 212 immunogenicity was performed and funded by Amgen.

Acknowledgments

The authors would like to thank M Salvati, H Kouros-Mehr and M Janat-Amsbury for their leadership, medical and scientific oversight of the AMG 160 clinical trial; C Pompe for his work assessing drug product stability of AMG 212; G Juan for reviewing the AMG 212 peripheral blood immune cell biomarker data; J Volkland for Bayer-Amgen data transfers and program administration; N Smith from Lonza Biologics for assistance with performing the MAPPS assay; G Keller and C Tinberg for the modeling efforts de-immunizing our suspect sequences; J Chung and J Huh for perspective on SC drug delivery; S Treichel, P Gokani, Z Yang for statistical evaluation; L Chea and S Mudalagiriyappa for the editing and review of updated figures. Current affiliations for M Salvati is Regeneron Pharmaceuticals, for H Kouros-Mehr is Sana Biotechnology, for M Janat-Amsbury is Halia Therapeutics, and for C Pompe is Leukocare AG.

Conflict of interest

All authors, except for NT, SW-R, GK, RB, H-DH, WL, CG, and BT, were/are employees of Amgen during the time this study and associated analyses were being conducted. SW-R and GK are employees of Bayer AG. Author WL was employed by Ordensklinikum Linz GmbH. RB is a patent holder for blinatumomab, from which he receives royalty payments, and has consulted for and received honoraria from Amgen, Cellex and Gemoab. H-DH has received travel, accommodations or other expenses from Johnson & Johnson, Boehringer Ingelheim, Amgen Inc. and Bristol Myers Squibb. WL has received honoraria from Accord and Novartis. BT has received a grant, consulting fees, and honoraria from Amgen Inc. NT was an employee of Labcorp Translational Biomarker Solutions at the time of this study and has no conflicts to disclose.

The remaining authors declare that the research was conducted in the absence of any commercial or financial relationships that could be construed as a potential conflict of interest.

The authors declare that this study received funding from Bayer and Amgen. The funders were involved in the study design, collection, analysis, interpretation of results, the writing of this article and the decision to submit it for publication.

Publisher's note

Supplementary material

The Supplementary Material for this article can be found online at: https://www.frontiersin.org/articles/10.3389/fimmu.2023.1261070/full#supplementary-material

SUPPLEMENTARY FIGURE 1
Dosing schema and ADA sampling timepoints of the subcutaneous (SC) **(A)** and continuous IV (CIV) infusion **(B)** arms of the AMG 212 First-in-Human clinical study. Cycles are depicted by green arrows; dosing schedules depicted by blue font and ADA sampling timepoints depicted by red arrows. The terms "C" refers to cycle, "D" refers to day and "EOIP" refers to End-of-Investigational Product. In the SC arm, AMG 212 was administered daily by SC injection, with no breaks between cycles **(A)**. In the SC arm, ADA samples were collected predose on Cycle 1 Day 1, 8 and 15, on Day 1 of each cycle from Cycle 2 to 8, on Day 1 of every second cycle thereafter and at least 36 hr after the last dose of AMG 212 **(A)**. In the CIV arm, AMG 212 was administered as a continuous IV infusion, using an on-body portable infusion pump and central venous port system. In the first 4 cycles (first 12 weeks on study), patients received treatment on a "5 week on-1 week off" schedule, whereby AMG 212 was administered over 5 weeks, followed by a treatment-free interval of 1 week. From cycle 5 onwards, patients could continue treatment on the "5 week on-1 week off" schedule or switch to a "4 week on-2 week off" schedule, at the discretion of the investigator and the subject **(B)**. In the CIV arm, ADA samples were collected predose on Cycle 1 Day 1, 8 and 15, on Day 1 of each subsequent cycle and at least 36 hr after the last dose of AMG 212 **(B)**.

SUPPLEMENTARY FIGURE 2
Comparison of AMG 212 concentration (ng/mL, y-axis, log-10 scale) from SC-dosed subjects receiving 72 µg/day (top), 144 µg/day (middle) and 172 µg/day (bottom) by ADA positivity status per subject with available PK data **(A)**; ADA status, exposure impact and PSA response correlation analyses using 2X2 tables **(B, C)**. The 1-hour post-dose concentration (x-axis) for cycle 1 day 1 (C1D1HR1), day 15 (C1D15HR1), cycle 2 day 1 (C2D1HR1), cycle 3 day 1 (C3D1HR1) and cycle 4 day 1 (C4D1HR1) are shown for comparison. Negative ADA status is shown in gray and positive ADA status is shown in dark red. All subjects with available data from the subcutaneous cohort including subjects with co-administration of glucocorticoid treatment are included. Samples below the lower limit of quantitation (LLOQ) were assigned 0.15 ng/mL **(A)**. To determine the correlation between ADA status and exposure impact (PK < LLOQ at or after ADA onset), the 2X2 table shown in **(B)** was utilized and a logistic regression model applied. The results show that the odds ratio is 0.080 (95% CI: <0.001, 8.698), *p-value=0.2915*. While the numbers in the table show a trend of exposure impact in ADA-positive subjects, due to the small sample size, this trend is not statistically significant. To determine the correlation of Exposure Impact with PSA rebound, the 2X2 table shown in **(C)** was utilized and a logistic regression model applied. The results show that the odds ratio is 25.998 (95% CI: 1.118, 604.431), *p-value=0.0424*. The numbers in the table show a clear trend of PSA rebound in exposure-impacted subjects, with a p-value reaching significance (<0.05). Due to the limited sample size of these correlation analyses, these analyses are presented herein in a descriptive manner.

SUPPLEMENTARY FIGURE 3
Peripheral blood CD14+ monocyte counts over time between patients who did or did not receive topical glucorticosteroids (GC) at the 144 µg/d **(A)** and 172 µg/d **(B)** dose levels in the SC arm of the AMG 212 clinical study. Monocyte counts were tabulated over time, before and during AMG 212 SC dosing. "C" refers to cycle and "D" refers to day. "PRE" refers to predose. Each symbol/connecting line represents individual subjects who did apply topical GC (+GC) or did not (-GC) on their injection sites. The apparent decrease in monocyte count from Day -7 to Cycle 1 Day 1, during which clobetasol propionate is administered, may be confounded by the prophylactic Dexamethasone to mitigate against Cytokine Release Syndrome (CRS) before the start of dosing in these subjects. To determine whether GC impacted peripheral blood monocyte counts over time, an unpaired t test was applied to the data comparing both groups at each time point. At the 144 ug/d cohort, monocyte counts of +GC (n=3) compared to -GC (n=3) subjects showed a *p-value* of 0.28, 0.15 and 0.44 at the screening, Cycle 1 Day 1 (C1D1) predose and Cycle 1 Day 15 (C1D15) predose timepoints respectively. At the 172 ug/d cohort, monocyte counts of +GC (n=6) compared to -GC (n=3) subjects showed a *p-value* of 0.43, 0.15 and 0.99 at the screening, C1D1 predose and C1D15 predose timepoints respectively. Collectively, the data show that the use of topical GC did not significantly change peripheral blood monocyte counts.

SUPPLEMENTARY TABLE 1
HLA subtypes.

SUPPLEMENTARY TABLE 2
HLA subtypes.

References

1. Baker M, Reynolds HM, Lumicisi B, Bryson CJ. Immunogenicity of protein therapeutics: The key causes, consequences and challenges. *Self/Nonself* (2010) 1 (4):314–22. doi: 10.4161/self.1.4.13904

2. Harding FA, Stickler MM, Razo J, DuBridge R. The immunogenicity of humanized and fully human antibodies. *mAbs* (2010) 2(3):256–65. doi: 10.4161/mabs.2.3.11641

3. Jawa V, Terry F, Gokemeijer J, Mitra-Kaushik S, Roberts BJ, Tourdot S, et al. T-cell dependent immunogenicity of protein therapeutics pre-clinical assessment and mitigation–updated consensus and review. *Front Immunol* (2020) 2020:11. doi: 10.3389/fimmu.2020.01301

4. Boehncke W-H, Brembilla NC. Immunogenicity of biologic therapies: causes and consequences. *Expert Rev Clin Immunol* (2018) 14(6):513–23. doi: 10.1080/1744666X.2018.1468753

5. Bray-French K, Hartman K, Steiner G, Marban-Doran C, Bessa J, Campbell N, et al. Managing the impact of immunogenicity in an era of immunotherapy: from bench to bedside. *J Pharm Sci* (2021) 110(7):2575–84. doi: 10.1016/j.xphs.2021.03.027

6. Sauna ZE, Lagassé D, Pedras-Vasconcelos J, Golding B, Rosenberg AS. Evaluating and mitigating the immunogenicity of therapeutic proteins. *Trends Biotechnol* (2018) 36(10):1068–84. doi: 10.1016/j.tibtech.2018.05.008

7. Chirmule N, Jawa V, Meibohm B. Immunogenicity to therapeutic proteins: impact on PK/PD and efficacy. *AAPS J* (2012) 14(2):296–302. doi: 10.1208/s12248-012-9340-y

8. Krishna M, Nadler SG. Immunogenicity to biotherapeutics – the role of anti-drug immune complexes. *Front Immunol* (2016) 7(21):1–13. doi: 10.3389/fimmu.2016.00021

9. Xue L, Rup B. Evaluation of pre-existing antibody presence as a risk factor for posttreatment anti-drug antibody induction: analysis of human clinical study data for multiple biotherapeutics. *AAPS J* (2013) 15(3):893–6. doi: 10.1208/s12248-013-9497-z

10. van Brummelen EM, Ros W, Wolbink G, Beijnen JH, Schellens JH. Antidrug antibody formation in oncology: clinical relevance and challenges. *Oncologist* (2016) 21 (10):1260–8. doi: 10.1634/theoncologist.2016-0061

11. Davda J, Declerck P, Hu-Lieskovan S, Hickling TP, Jacobs IA, Chou J, et al. Immunogenicity of immunomodulatory, antibody-based, oncology therapeutics. *J ImmunoTher Cancer* (2019) 7(1):105. doi: 10.1186/s40425-019-0586-0

12. Zhou Y, Penny HL, Kroenke MA, Bautista B, Hainline K, Chea LS, et al. Immunogenicity assessment of bispecific antibody-based immunotherapy in oncology. *J Immunother Cancer* (2022) 10(4):1–11. doi: 10.1136/jitc-2021-004225

13. Gardner JP, Durso RJ, Jacques S, Arrigale R, Maughan M, Donovan GP, et al. Novel prime-boost combinations of PSMA-based vaccines for prostate cancer. *J Clin Oncol* (2005) 23(16_suppl):2572–. doi: 10.1200/jco.2005.23.16_suppl.2572

14. Hummel HD, Kufer P, Grullich C, Seggewiss-Bernhardt R, Deschler-Baier B, Chatterjee M, et al. Pasotuxizumab, a BiTE((R)) immune therapy for castration-resistant prostate cancer: Phase I, dose-escalation study findings. *Immunotherapy* (2021) 13(2):125–41. doi: 10.2217/imt-2020-0256

15. Scher HI, Halabi S, Tannock I, Morris M, Sternberg CN, Carducci MA, et al. Design and end points of clinical trials for patients with progressive prostate cancer and castrate levels of testosterone: recommendations of the prostate cancer clinical trials working group. *J Clin Oncol* (2008) 26(7):1148–59. doi: 10.1200/JCO.2007.12.4487

16. Delluc S, Ravot G, Maillere B. Quantitative analysis of the CD4 T-cell repertoire specific to therapeutic antibodies in healthy donors. *FASEB J Off Publ Fed Am Societies Exp Biol* (2011) 25(6):2040–8. doi: 10.1096/fj.10-173872

17. Spindeldreher S, Karle A, Correia E, Tenon M, Gottlieb S, Huber T, et al. T cell epitope mapping of secukinumab and ixekizumab in healthy donors. *MAbs* (2020) 12 (1):1707418. doi: 10.1080/19420862.2019.1707418

18. (CTL) CTL. *Protocols and guidelines for working with human PBMC in ELISPOT assays* . Available at: www.immunospot.com.

19. Hamze M, Meunier S, Karle A, Gdoura A, Goudet A, Szely N, et al. Characterization of CD4 T cell epitopes of infliximab and rituximab identified from healthy donors. *Front Immunol* (2017) 8:500. doi: 10.3389/fimmu.2017.00500

20. Itano AA, McSorley SJ, Reinhardt RL, Ehst BD, Ingulli E, Rudensky AY, et al. Distinct dendritic cell populations sequentially present antigen to CD4 T cells and stimulate different aspects of cell-mediated immunity. *Immunity* (2003) 19(1):47–57. doi: 10.1016/S1074-7613(03)00175-4

21. Ruedl C, Koebel P, Bachmann M, Hess M, Karjalainen K. Anatomical origin of dendritic cells determines their life span in peripheral lymph nodes. *J Immunol* (2000) 165(9):4910–6. doi: 10.4049/jimmunol.165.9.4910

22. Gruver-Yates AL, Quinn MA, Cidlowski JA. Analysis of glucocorticoid receptors and their apoptotic response to dexamethasone in male murine B cells during development. *Endocrinology* (2014) 155(2):463–74. doi: 10.1210/en.2013-1473

23. Hoetzenecker W, Meingassner JG, Ecker R, Stingl G, Stuetz A, Elbe-Bürger A. Corticosteroids but not pimecrolimus affect viability, maturation and immune function of murine epidermal langerhans cells. *J Invest Dermatol* (2004) 122(3):673–84. doi: 10.1111/j.0022-202X.2004.22324.x

24. Vanderheyde N, Verhasselt V, Goldman M, Willems F. Inhibition of human dendritic cell functions by methylprednisolone. *Transplantation* (1999) 67(10):1342–7. doi: 10.1097/00007890-199905270-00009

25. Joubert MK, Hokom M, Eakin C, Zhou L, Deshpande M, Baker MP, et al. Highly aggregated antibody therapeutics can enhance the in *vitro* innate and late-stage T-cell immune responses. *J Biol Chem* (2012) 287(30):25266–79. doi: 10.1074/jbc.M111.330902

26. Lundahl MLE, Fogli S, Colavita PE, Scanlan EM. Aggregation of protein therapeutics enhances their immunogenicity: causes and mitigation strategies. *RSC Chem Biol* (2021) 2(4):1004–20. doi: 10.1039/D1CB00067E

27. Moussa EM, Panchal JP, Moorthy BS, Blum JS, Joubert MK, Narhi LO, et al. Immunogenicity of therapeutic protein aggregates. *J Pharm Sci* (2016) 105(2):417–30. doi: 10.1016/j.xphs.2015.11.002

28. Jones GB, Collins DS, Harrison MW, Thyagarajapuram NR, Wright JM. Subcutaneous drug delivery: An evolving enterprise. *Sci Transl Med* (2017) 9(405):. doi: 10.1126/scitranslmed.aaf9166

29. Trevaskis NL, Kaminskas LM, Porter CJH. From sewer to saviour — targeting the lymphatic system to promote drug exposure and activity. *Nat Rev Drug Discov* (2015) 14(11):781–803. doi: 10.1038/nrd4608

30. Karle AC. Applying MAPPs assays to assess drug immunogenicity. *Front Immunol* (2020) 11:698. doi: 10.3389/fimmu.2020.00698

31. Sekiguchi N, Kubo C, Takahashi A, Muraoka K, Takeiri A, Ito S, et al. MHC-associated peptide proteomics enabling highly sensitive detection of immunogenic sequences for the development of therapeutic antibodies with low immunogenicity. *MAbs* (2018) 10(8):1168–81. doi: 10.1080/19420862.2018.1518888

32. Ducret A, Ackaert C, Bessa J, Bunce C, Hickling T, Jawa V, et al. Assay format diversity in pre-clinical immunogenicity risk assessment: Toward a possible harmonization of antigenicity assays. *MAbs* (2022) 14(1):1993522. doi: 10.1080/19420862.2021.1993522

33. Siegel M, Steiner G, Franssen LC, Carratu F, Herron J, Hartman K, et al. Validation of a dendritic cell and CD4+ T cell restimulation assay contributing to the immunogenicity risk evaluation of biotherapeutics. *Pharmaceutics* (2022) 14(12)1–14. doi: 10.3390/pharmaceutics14122672

34. Jenkins MK, Moon JJ. The role of naive T cell precursor frequency and recruitment in dictating immune response magnitude. *J Immunol (Baltimore Md 1950)* (2012) 188(9):4135–40. doi: 10.4049/jimmunol.1102661

35. Ben Tran LH, Dorff T, Rettig M, Lolkema MP, Jean-Pascal M, Rottey S. Interim Results from AMG 160 a half-life extended (HLE), PSMA-targeted, bispecific T-cell engager (BiTE®) immune therapy for metastatic castration-resistant prostate cancer (mCRPC). *ESMO Virtual Congress* (2020) 2020.

36. Hamuro L, Kijanka G, Kinderman F, Kropshofer H, Bu DX, Zepeda M, et al. Perspectives on subcutaneous route of administration as an immunogenicity risk factor for therapeutic proteins. *J Pharm Sci* (2017) 106(10):2946–54. doi: 10.1016/j.xphs.2017.05.030

37. Mianowska B, Szadkowska A, Pietrzak I, Zmysłowska A, Wegner O, Tomczonek J, et al. Immunogenicity of different brands of human insulin and rapid-acting insulin analogs in insulin-naïve children with type 1 diabetes. *Pediatr Diabetes* (2011) 12 (2):78–84. doi: 10.1111/j.1399-5448.2010.00659.x

38. Peng A, Gaitonde P, Kosloski MP, Miclea RD, Varma P, Balu-Iyer SV. Effect of route of administration of human recombinant factor VIII on its immunogenicity in Hemophilia A mice. *J Pharm Sci* (2009) 98(12):4480–4. doi: 10.1002/jps.21765

39. Schellekens H. The immunogenicity of therapeutic proteins. *Discov Med* (2010) 9(49):560–4.

40. Gerd RB, Andrea R-R, Alain C, Stephen H, Piotr L, Daniel F, et al. A randomised, double-blind, parallel-group study of the safety and efficacy of subcutaneous tocilizumab versus intravenous tocilizumab in combination with traditional disease-modifying antirheumatic drugs in patients with moderate to severe rheumatoid arthritis (SUMMACTA study). *Ann Rheumatic Dis* (2014) 73(1):69. doi: 10.1136/annrheumdis-2013-203523

41. Schiff M. Subcutaneous abatacept for the treatment of rheumatoid arthritis. *Rheumatol (Oxford England)* (2013) 52(6):986–97. doi: 10.1093/rheumatology/ket018

42. Rosenberg AS, Worobec AS. A risk-based approach to immunogenicity concerns of therapeutic protein products, part 2: considering host-specific and product-specific factors impacting immunogenicity. *BioPharm Int* (2004) 17(12).

43. Malissen B, Tamoutounour S, Henri S. The origins and functions of dendritic cells and macrophages in the skin. *Nat Rev Immunol* (2014) 14(6):417–28. doi: 10.1038/nri3683

44. Kinderman F, Yerby B, Jawa V, Joubert MK, Joh NH, Malella J, et al. Impact of precipitation of antibody therapeutics after subcutaneous injection on pharmacokinetics and immunogenicity. *J Pharm Sci* (2019) 108(6):1953–63. doi: 10.1016/j.xphs.2019.01.015

45. Wang W, Singh S, Zeng DL, King K, Nema S. Antibody structure, instability, and formulation. *J Pharm Sci* (2007) 96(1):1–26. doi: 10.1002/jps.20727

46. Kearns JD, Wassmann P, Olgac U, Fichter M, Christen B, Rubic-Schneider T, et al. A root cause analysis to identify the mechanistic drivers of immunogenicity against the anti-VEGF biotherapeutic brolucizumab. *Sci Transl Med* (2023) 15(681):. doi: 10.1126/scitranslmed.abq5068

47. Arranz-Gibert P, Ciudad S, Seco J, García J, Giralt E, Teixidó M. Immunosilencing peptides by stereochemical inversion and sequence reversal: retro-D-peptides. *Sci Rep* (2018) 8(1):6446. doi: 10.1038/s41598-018-24517-6

48. Azam A, Mallart S, Illiano S, Duclos O, Prades C, Maillère B. Introduction of non-natural amino acids into T-cell epitopes to mitigate peptide-specific T-cell responses. *Front Immunol* (2021) 12(637963):1–9. doi: 10.3389/fimmu.2021.637963

49. Townsend S, Fennell BJ, Apgar JR, Lambert M, McDonnell B, Grant J, et al. Augmented Binary Substitution: Single-pass CDR germ-lining and stabilization of therapeutic antibodies. *Proc Natl Acad Sci USA* (2015) 112(50):15354–9. doi: 10.1073/pnas.1510944112

50. Hervé M, Maillere B, Mourier G, Texier C, Leroy S, Ménez A. On the immunogenic properties of retro-inverso peptides. Total retro-inversion of T-cell epitopes causes a loss of binding to MHC II molecules. *Mol Immunol* (1997) 34 (2):157–63. doi: 10.1016/s0161-5890(97)00004-7

51. Stern LJ, Brown JH, Jardetzky TS, Gorga JC, Urban RG, Strominger JL, et al. Crystal structure of the human class II MHC protein HLA-DR1 complexed with an influenza virus peptide. *Nature* (1994) 368(6468):215–21. doi: 10.1038/368215a0

52. Santambrogio L. Molecular determinants regulating the plasticity of the MHC class II immunopeptidome. *Front Immunol* (2022) 13(878271):1–8. doi: 10.3389/fimmu.2022.878271

53. Hamuro L, Tirucherai GS, Crawford SM, Nayeem A, Pillutla RC, DeSilva BS, et al. Evaluating a multiscale mechanistic model of the immune system to predict human immunogenicity for a biotherapeutic in phase 1. *AAPS J* (2019) 21(5):94. doi: 10.1208/s12248-019-0361-7

54. Martínez Sánchez P, Gordon P, Schwartz S, Rossi G, Huguet F, Hernández-Rivas JM, et al. Safety and efficacy of subcutaneous (SC) blinatumomab for the treatment of adults with relapsed or refractory B cell precursor acute lymphoblastic leukemia (R/R B-ALL). *Blood* (2021) 138(Supplement 1):2303. doi: 10.1182/blood-2021-150018

55. Rossi G, Prince HM, Tam CS, Ku M, Thieblemont C, Popplewell LL, et al. A phase 1b study of blinatumomab including subcutaneous administration in relapsed / refractory (R/R) indolent non hodgkin's lymphoma (NHL). *Blood* (2021) 138 (Supplement 1):2436–. doi: 10.1182/blood-2021-152822

56. KIMMTRAK®. *(tebentafusp-tebn)*. Conshohocken, Pennsylvania, United States: Immunocore Inc (2022). Available at: https://www.accessdata.fda.gov/drugsatfda_docs/label/2022/761228s000lbl.pdf.

57. Salazar-Fontana LI, Desai DD, Khan TA, Pillutla RC, Prior S, Ramakrishnan R, et al. Approaches to mitigate the unwanted immunogenicity of therapeutic proteins during drug development. *AAPS J* (2017) 19(2):377–85. doi: 10.1208/s12248-016-0030-z

frontiers | Frontiers in Immunology

TYPE Original Research
PUBLISHED 23 January 2024
DOI 10.3389/fimmu.2024.1342477

OPEN ACCESS

EDITED BY
Michael Tovey,
Svar Life Science, France

REVIEWED BY
Zuben E. Sauna,
United States Food and Drug Administration, United States
Stephanie DeStefano,
Hannover Medical School, Germany

*CORRESPONDENCE
Thierry Dervieux
tdervieux@prometheulabs.com

RECEIVED 21 November 2023
ACCEPTED 02 January 2024
PUBLISHED 23 January 2024

CITATION
Spencer EA, Dubinsky MC, Kamm MA, Chaparro M, Gionchetti P, Rizzello F, Gisbert JP, Wright EK, Schulberg JD, Hamilton AL, McGovern DPB and Dervieux T (2024) Poor prognostic factors of pharmacokinetic origin predict outcomes in inflammatory bowel disease patients treated with anti-tumor necrosis factor-α. *Front. Immunol.* 15:1342477. doi: 10.3389/fimmu.2024.1342477

Poor prognostic factors of pharmacokinetic origin predict outcomes in inflammatory bowel disease patients treated with anti-tumor necrosis factor-α

Elizabeth A. Spencer[1], Marla C. Dubinsky[1], Michael A. Kamm[2], Maria Chaparro[3], Paolo Gionchetti[4,5], Fernando Rizzello[4,5], Javier P. Gisbert[3], Emily K. Wright[2], Julien D. Schulberg[2], Amy L. Hamilton[2], Dermot P. B. McGovern[6] and Thierry Dervieux[7]*

[1]Division of Gastroenterology, Icahn School of Medicine Mount Sinai, New York, NY, United States, [2]St Vincent's Hospital and The University of Melbourne, Melbourne, VIC, Australia, [3]Hospital Universitario de La Princesa, Instituto de Investigación Sanitaria Princesa (IIS-Princesa), Universidad Autónoma de Madrid (UAM) and Centro de Investigación Biomédica en Red de Enfermedades Hepáticas y Digestivas (CIBEREHD), Madrid, Spain, [4]IRCCS Azienda Ospedaliero-Universitaria di Bologna Italy, Bologna, Italy, [5]DIMEC University of Bologna-Italy , Bologna, Italy, [6]F. Widjaja Inflammatory Bowel Institute, Cedars-Sinai Medical Center, Los Angeles, CA, United States, [7]Research and Development, Prometheus Laboratories, San Diego, CA, United States

Introduction: We evaluated baseline Clearance of anti-tumor necrosis factors and human leukocyte antigen variant (HLA DQA1*05) in combination as poor prognostic factors (PPF) of pharmacokinetic (PK) origin impacting immune response (formation of antidrug antibodies) and disease control of inflammatory bowel disease (IBD) patients treated with infliximab or adalimumab.

Methods: Baseline Clearance was estimated in IBD patients before starting treatment using weight and serum albumin concentrations. HLA DQA1*05 carrier status (rs2097432 A/G or G/G variant) was measured using real time polymerase chain reaction. The outcomes consisted of immune response, clinical and biochemical remission (C-reactive protein<3 mg/L in the absence of symptoms), and endoscopic remission (SES-CD<3). Statistical analysis consisted of logistic regression and nonlinear mixed effect models.

Results and discussion: In 415 patients enrolled from 4 different cohorts (median age 27 [IQR: 15-43] years, 46% females), Clearance>0.326 L/day and HLA DQA1*05 carrier status were 2-fold more likely to have antidrug antibodies (OR=2.3, 95%CI: 1.7-3.4; p<0.001, and OR=1.9, 95%CI: 1.4-2.8; p<0.001, respectively). Overall, each incremental PPF of PK origin resulted in a 2-fold (OR=2.16, 95%CI: 1.7-2.7; p<0.01) higher likelihood of antidrug antibody formation. The presence of both PPF of PK origin resulted in higher rates of antidrug antibodies (p<0.01) and lower clinical and biochemical remission (p<0.01). Each incremental increase in PPF of PK origin associated with lower likelihood of endoscopic remission (OR=0.4, 95%CI: 0.2-0.7; p<0.001). Prior

biologic experience heightened the negative impact of PPF of PK origin on clinical and biochemical remission ($p<0.01$). Implementation of proactive therapeutic drug monitoring reduced it, particularly during maintenance and in the presence of higher drug concentrations ($p<0.001$). We conclude that PPF of PK origin, including both higher Clearance and carriage of HLA DQA1*05, impact outcomes in patients with IBD.

KEYWORDS

drug response, tumor necrosis factor, clearance, inflammatory bowel disease, pharmacogenetic

1 Introduction

Predicting response to monoclonal antibody therapies remains an unmet need in the management of immune-mediated inflammatory disease, particularly in inflammatory bowel disease (IBD; Crohn's disease [CD] and ulcerative colitis [UC]), that causes progressive intestinal damage, which impacts the quality of life of affected patients (1). After two decades of intensive research, it is clear that the response to anti-tumor necrosis factor-α; (TNF) such as infliximab (IFX) and adalimumab (ADA) is complex and pathway dependent (2, 3). Undoubtedly, the response to anti-TNF is also a function of suboptimal pharmacokinetics (PK) (4) where immune response and formation of neutralizing antibodies preclude the achievement of the minimally effective concentration required for disease control (5). In fact, the prediction of suboptimal baseline PK in patients starting induction is likely to be important, as a countermeasure of simple dose intensification may prevent the potential negative impact of lower concentration on disease control in a susceptible individual.

One of the most promising genetic markers associated with the immune response to anti-TNF and formation of antibodies to IFX (ATI) or ADA (ATA) is HLA DQA1*05 (tagged rs2097432 A/G), and substantial evidence supports the value of the genotype as recently reported in a meta-analysis (6) with 75% higher risk of immunogenicity compared with non-carriers and twofold higher risk of secondary loss of response. The precise mechanism of action is well established and combines the recognition of the antigenic proteolytic fragments of the monoclonal antibody itself by the immune system and clonal expansion to produce neutralizing antibodies. However, HLA DQA1*05 has modest performances when associated with PK and pharmacodynamic outcomes, illustrating the complexity of a low penetrance single variant with outcome.

Recently, several reports have established that baseline clearance calculated from covariates estimated in the population PK model is associated with outcome in IBD (7, 8), where higher clearance reflects intrinsic suboptimal PK (e.g., recirculation of the IgG through the neonatal receptor and/or higher weight) as well as an individual's inflammatory burden, which consumes the drug. This unfavorable state is only worsened in the presence of the HLA DQA1*05 carrier status and the associated immune response.

In this report, we evaluate accelerated baseline clearance and HLA DQA1*05 carrier status as PPFs of PK origin impacting immune response and therapeutic outcomes in IBD. Our results show a significant impact of higher clearance and presence of HLA DQA1*05 carrier status on immune response where the cumulative presence of both PPFs of PK origin is associated with a high likelihood of treatment failure.

2 Methods

2.1 Patients

Patients with IBD were enrolled from four different cohorts starting subcutaneous ADA or intravenous IFX treatment (9–12). Internal review boards approved the studies, and patient informed consent was collected. The first cohort (BOLOGNA) was performed in the context of a 1-year prospective observational clinical trial aimed at identifying biomarkers and predictors of a failure to respond to ADA in patients with CD (11). The second cohort (PREDICROHN) was a prospective multicenter cohort study in patients with CD naïve to biologics with active luminal disease (12); participants were started on ADA and IFX and followed up longitudinally. The third cohort (STRIDENT) was from an open-label, single-center, randomized controlled trial evaluating dose intensity in participants with symptomatic intestinal Crohn's disease strictures (9). The patients in the fourth cohort (Proactive dosing cohort, PRECISION IFX trial [NCT02624037]) received proactive dose intensification using therapeutic drug monitoring (TDM) and iDose dashboard (Baysient, LLC, Fort Myers, FL, USA) to target therapeutic concentrations above 17 μg/mL and 10 μg/mL during induction and maintenance, respectively (10); the impact of proactive TDM in preventing immunization to IFX has been reported elsewhere (13). Patients from each cohort were followed up longitudinally at each visit during their maintenance treatment. Blood specimens were collected periodically during maintenance

and always at the trough for IFX; sera were isolated and stored at subzero temperature (−80°C) until analysis.

2.2 Pharmacokinetic and pharmacogenetic measurements

Serum ADA and IFX concentrations and their respective antibodies (ATA and ATI, respectively) were determined using drug-tolerant homogenous mobility shift assay in the clinical laboratory at Prometheus Laboratories (San Diego, CA, USA) (14, 15). All specimens were collected in serum separator tubes. Pre-analytical experiments have shown that the analytes are stable for at least 14 days at room temperature in serum. Serum was stored at −80°C within 72 hours of isolation. The lower and upper limits of quantification of the drug assay were 1.6 μg/mL and 50 μg/mL, respectively, for ADA and 0.8 μg/mL and 34 μg/mL, respectively, for IFX. The cutoffs associated with ATA and ATI status (corresponding to the 97.5th percentile of normal health) were 1.7 U/mL and 3.1 U/mL, respectively. Serum albumin and C-reactive protein (CRP) were determined using immunochemistry (IMMAGE 800 Protein Chemistry Analyzer, Beckman Coulter, Brea, CA, USA) in the clinical laboratory at Prometheus Laboratories). Carriage of the HLA-DQA1*05 (presence of rs2097432 AG or GG variant) was determined from genomic DNA extracted from serum or whole blood using real-time PCR with allelic discrimination (13).

2.3 Derivatization of baseline clearance

The population PK parameters were estimated from the BOLOGNA and PREDICROHN cohorts (113 patients who received ADA and 553 samples/observations) using non-linear mixed-effects modeling (one compartment with linear elimination), with random effects on apparent clearance (CL/F) with albumin levels and weight as covariates. The covariate estimates of weight and albumin from the population PK model were applied to calculate baseline clearance for ADA and IFX in all patients before starting treatment. Cutoff for higher clearance corresponds to the typical value determined from that population PK model and was applied unmodified to all other cohorts receiving ADA or IFX. This clearance calculation was used for both IFX and ADA baseline clearance.

2.4 Outcome variables and statistical analysis

Immune response to ADA and IFX consisted of antidrug antibody formation (above cutoff) during induction and maintenance, anytime (corresponding to immune response detected at any of the time points where serum was available for PK analysis), and at all cycles (corresponding to immune response detected at all of the time points where serum was available for PK analysis). The clinical outcome determined at each study visit was CRP-based clinical remission status, defined as CRP levels below 3 mg/L in the presence of clinical remission (Crohn's Disease Activity Index<150 points or Harvey–Bradshaw index (HBI) below 5 points for CD, or partial Mayo below 2 points for UC).

Endoscopic remission (ER) was available in CD only and corresponded to the Simple Endoscopic Score for CD (SES-CD< 3 points) available during treatment in the BOLOGNA and STRIDENT cohorts. Statistical analysis consisted of logistic regression with odds ratio (OR; with 95% confidence interval). Results were expressed as median with interquartile ranges (IQRs), as appropriate.

The impact of baseline clearance and HLA DQA1*05 carrier status on outcomes was estimated using longitudinal repeated event analysis using non-linear mixed-effects modeling via Monolix (Lixoft, 2021R2). Prior biologic exposure and implementation of proactive TDM (from the PRECISION cohort) were used as covariates in the analysis, as appropriate. Logistic regression and Mann–Whitney testing were used as appropriate.

3 Results

A total of 415 patients (median age 27 [IQR: 15–43] years, 46% female) were enrolled in the study (n = 185 ADA and n = 230 IFX). PK measurements and CRP-based clinical remission status during maintenance were available in a total of 1,893 cycles collected with PK specimens; antidrug antibodies were detected in 15% of patients at any time point. Results are presented in Table 1. There was no difference in concentrations between IFX and ADA during maintenance (IFX: median of 9.9 μg/mL [IQR 5.0–15.1 μg/mL]; ADA: median of 10.7 μg/mL [IQR 6.9–14.6 μg/mL]; $p > 0.6$).

3.1 Baseline clearance and calculation of PF of PK origin score

Baseline clearance was calculated using the parameter estimates derived from the population PK model from ADA patients (BOLOGNA and PREDICROHN cohorts) as follows:

$$CL = (EXP(LOG(0.326) + 0.458 * LOG(WT/70) - 0.768 * LOG(ALB/4.0)),$$

where *WT* is weight in kg and *ALB* is serum albumin level in g/dL.

The PPF of PK origin score was calculated as the sum of higher clearance (>0.326 L/day, 1 point) and HLA DQA1*05 G carrier status (1 point) and ranged from 0 to 2 (0 corresponding to the absence of both PPFs of PK origin, 1 corresponding to either clearance > 0.326 L/day or HLA DQA1*05 G carrier status, and 2 corresponding to the presence of both PPFs of PK origin).

3.2 Impact of PPFs of PK origin on immune response during treatment

Longitudinal repeated event analysis over the treatment period revealed that longer time on therapy associated with

10.3389/fimmu.2024.1342477

TABLE 1 Patient characteristics.

	BOLOGNA (Italy)	PREDICROHN (Spain)	STRIDENT (Australia)	PRECISION (USA)	All cohorts
Anti-TNFs	ADA	ADA/IFX	ADA	IFX	ADA/IFX
Crohn's disease	100% (53/53)	100% (112/112)	100% (77/77)	73% (125/173)	88%% (367/415)
Prior biologics	30% (16/53)	0% (0/112)	12% (9/77)	22% (38/173)	15% (63/415)
Age (years)	24 (26; 44)	39 (29; 50)	44 (30; 52)	15 (12; 17)	27 (15; 43)
Gender (female)	36% (19/53)	48% (54/112)	51% (39/77)	46% (79/173)	46% (191/415)
Weight at baseline	67 (60; 78)	64 (57; 76)	78 (66; 87)	45 (33; 59)	61 (46; 73)
ALB at baseline	3.9 (3.8; 4.2)	3.8 (3.3; 4.4)	3.7 (3.5; 3.9)	3.2 (2.8; 3.7)	3.6 (3.0; 4.0)
HLA DQA1*05 carriage	47% (25/53)	37% (42/112)	27% (21/77)	46% (80/173)	40% (168/415)
CL > 0.326 L/day	51% (27/53)	49% (55/112)	79% (61/77)	42% (72/173)	52% (215/415)
Responder score >0	79% (42/53)	67% (75/112)	86% (66/77)	69% (120/173)	73% (303/415)
Responder score >1	19% (10/53)	20% (22/112)	21% (16/77)	18% (32/173)	19% (80/415)
Antibodies (anytime)	23% (12/53)	16% (18/112)	14% (11/77)	13% (23/173)	15% (64/415)
Antibodies all cycles	15% (28/182)	11% (70/614)	8% (24/285)	4% (34/930)	8% (156/2011)
CRP-based clinical rem.	47% (28/182)	44% (235/535)	45% (113/250)	52% (487/930)	49% (919/1893)
SES-CD	1 (0; 4)	NA	3 (0; 8)	NA	3 (0; 6)
SES-CD ≥ 3	43% (39/90)	NA	64% (35/55)	NA	51% (74/145)
Maintenance cycles	3.4 (182)	4.5 (507)	2.7 (208)	2.5 (434)	3.2 (1331)
Trough concentrations	10 (5.2; 12.8)	8.0 (3.9; 12.2)	13.2 (8.2; 18.0)	12.3 (8.3; 18.0)	10.2 (6.0; 15.1)

Results are expressed as median IQR or % (n/N), as appropriate.
SES-CD, Simple Endoscopic Score for Crohn's Disease.
NA, not available.

immune response and antidrug antibody formation (θ_{time} = + 0.006 ± 0.001, p< 0.001), where the presence of PPFs of PK origin (clearance > 0.326 L/day; HLA DQA1*05 carrier status) at baseline each independently and significantly contributing to immunization during treatment ($\theta_{Clearance>0.326}$ = +2.2 ± 0.70, p = 0.02, and $\theta_{HLA\ DQA1*05\ carrier}$ = +1.5 ± 0.70, p = 0.03, respectively) (θ_{pop} = −9.6 ± 1.0). Patients with clearance > 0.326 L/day and HLA DQA1*05 carrier status were twofold more likely to present with treatment cycles with antidrug antibodies (OR = 2.3, 95%CI: 1.7–3.4, p< 0.001, and OR = 1.9, 95%CI: 1.4–2.8, p< 0.001, respectively).

When combined, the increased number of PPFs of PK origin resulted in a higher risk of immune response for both ADA and IFX (Table 2). Results by cohort are presented in Supplementary Table 2. The incidence of antidrug antibodies by PPFs of PK origin is presented in Figure 1. Overall, each incremental PPF of PK origin resulted in a 2-fold (OR=2.16, 95%CI: 1.7-2.7; p<0.01) higher likelihood of antidrug antibody formation. Also, antidrug antibodies detected at the time of clinical assessment were associated with a lower likelihood of CRP-based clinical remission (OR = 0.5, 95%CI: 0.3–0.7, p< 0.001) and endoscopic remission (OR = 0.2, 95%CI: 0.1–0.7, p = 0.003). There was no impact of prior biologic treatment on immune response (data not shown).

3.3 Impact of PPFs of PK origin on CRP-based clinical remission

Longitudinal repeated event analysis over the treatment period revealed that longer time on therapy was associated with a higher probability of achieving CRP-based clinical remission (θ_{time} = +0.004 ± 0.001, p< 0.001). Additionally, higher baseline clearance (>0.326 L/day, $\theta_{Clearance>0.326}$ = −1.1 ± 0.2, p< 0.001) and prior biologic therapy (θ_{prior} biologics = −1.2 ± 0.3, p< 0.001) negatively impacted achievement of

TABLE 2 Poor prognostic factors of pharmacokinetic origin and immune response to anti-TNFs.

Parameter	Adalimumab	Infliximab	All cohorts
θ_{pop}	−11.3 ± 2.9 (p< 0.001)	−9.1 ± 1.2 (p< 0.001)	−10.1 ± 1.2 (p< 0.001)
θ_{cov}: score =1 versus 0	+4.5 ± 2.5 (p = 0.07)	+1.8 ± 1.1 (p = 0.102)	+2.5 ± 0.9 (p = 0.006)
θ_{cov}: score =2 versus 0	+6.2 ± 2.6 (p = 0.017)	+2.6 ± 1.2 (p = 0.030)	+3.8 ± 1.1 (p< 0.001)
θ_{time}	+0.006 ± 0.001 (p = 0.030)	+0.006 ± 0.001 (p = 0.030)	+0.006 ± 0.001 (p< 0.001)

Model, logit(Probability of CRP Based Remission) = θ_{pop} + θ_{covi} * cov_i + ….

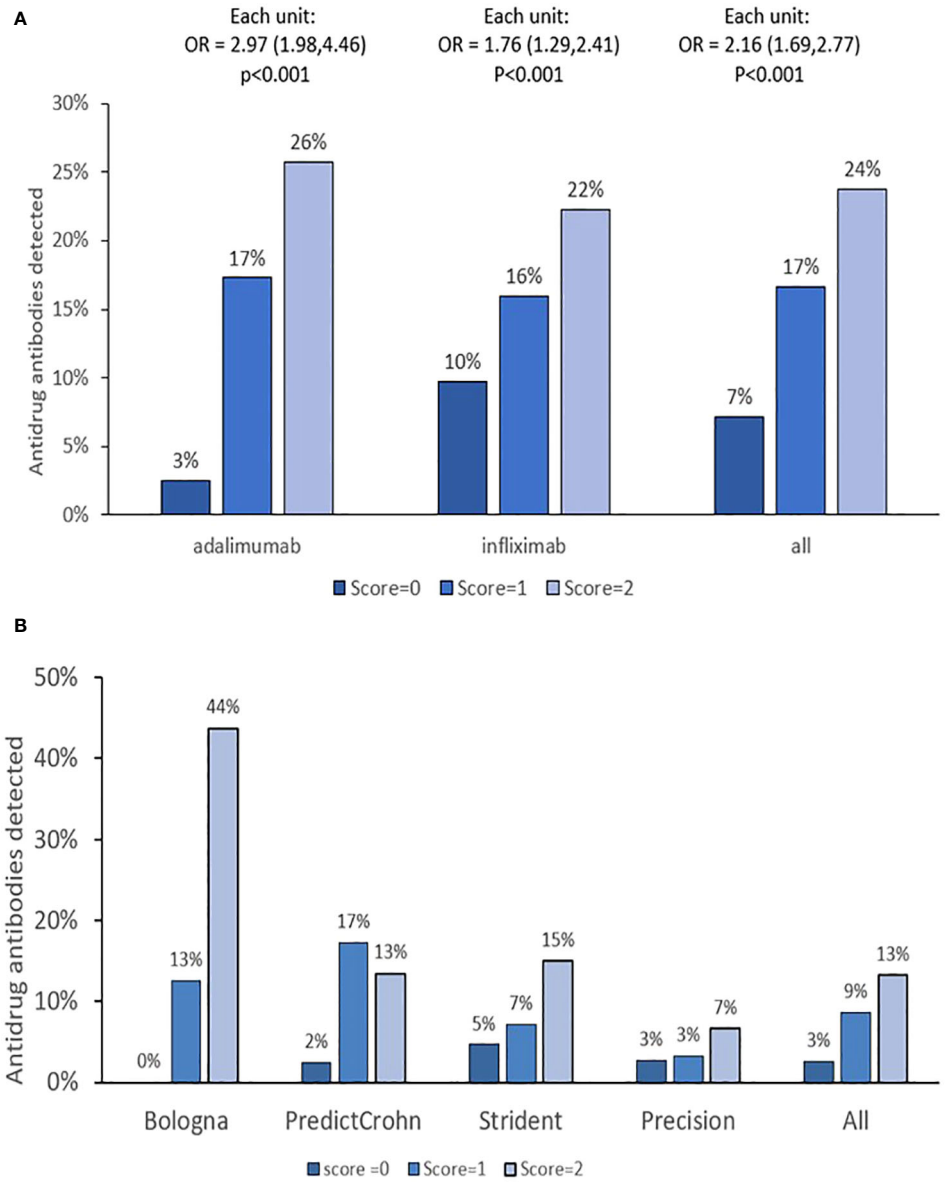

FIGURE 1
PPF of PK origin score and treatment cycles with antidrug antibodies. **(A, B)** The results by monoclonal antibody and cohorts, respectively. OR is given with 95% confidence intervals. Immune response (ATA or ATI) detected anytime during treatment was calculated. PPF, poor prognostic factor.

CRP-based clinical remission, an effect that was modified by proactive TDM ($\theta_{proactive}$ tdm = 0.6 ± 0.2, p< 0.003) but not HLA DQA1*05 carrier status ($\theta_{HLA\ DQA1*05\ carrier}$ = 0.1 ± 0.2, p = 0.62) (θ_{pop} = −0.5 ± 0.2, p = 0.012).

The impact of the PPF of PK score (>0) on CRP-based clinical remission status adjusting for prior biologics, proactive TDM, and time on therapy is presented in Figure 2. The analysis revealed a significant impact of prior biologics on worse outcomes, while proactive TDM was associated with improved disease control, an effect that was also dependent on the presence of PF of PK origin. Results by cohorts and biologics are presented in Supplementary Tables 3, 4, respectively.

During maintenance, longitudinal analysis also revealed that prior biologics, proactive TDM, and the presence of at least one PPF of PK origin impacted therapeutic outcomes with higher concentrations resulting in improved disease control. Results are presented in Figure 3.

3.4 Impact of PPFs of PK origin on endoscopic outcomes

Endoscopic outcomes (n = 145 assessments) were available in ADA-treated patients enrolled in the BOLOGNA and STRIDENT cohorts. ATA status detected anytime during treatment was associated with a 0.2-fold (95%CI 0.1–0.7) (p = 0.002) lower likelihood of having endoscopic remission. Multivariate logistic regression analysis revealed that higher clearance (adjusted OR =

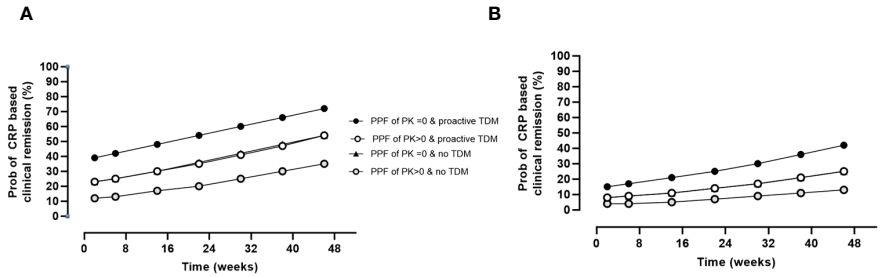

FIGURE 2
Impact of PPFs of PK origin by proactive TDM and prior biologics on CRP-based clinical remission status over time. Estimates are as follows: θ_{po} p = 0.5 ± 0.3 (p = 0.100); θ_{cov}, prior biologics = −1.2 ± 0.3 (p< 0.001); θ_{cov}, PPFs of PK origin >0 = −0.8 ± 0.3 (p = 0.008); θ_{cov}, proactive TDM = 0.8 ± 0.2 (p< 0.001); θ_{Time} = 0.004 ± 0.001 (p< 0.001). **(A)** Probability of CRP-based clinical remission in patients naïve to biologics. **(B)** Probability of CRP-based clinical remission in patients with prior biologics. The probability of CRP-based remission in the presence of proactive TDM and PPK > 0 was indistinguishable from the probability from the probability of with no TDM and PPF of PK = 0. PPF, poor prognostic factor; PK, pharmacokinetic; TDM, therapeutic drug monitoring; CRP, C-reactive protein.

0.3, 95%CI: 0.2–0.7, p = 0.004) and presence of HLA DQA1*05 carriage (adjusted OR = 0.4, 95%CI: 0.2–0.8, p = 0.013) independently and significantly impacted endoscopic remission. Cumulatively, each incremental increase in PPFs of PK origin resulted in a lower likelihood of endoscopic remission (OR = 0.4, 95%CI: 0.2–0.7, p< 0.001). Results are presented in Figure 4. There was no association between prior biologics on worse endoscopic outcomes (data not shown).

4 Discussion

In this report, we have established that the PPFs of PK origin, both higher baseline clearance of IFX and ADA and carriage of HLA DQA1*05, impact immune response and disease control in patients with IBD. These PPFs of PK origin specifically detect a signature associated with suboptimal PK during treatment with anti-TNF-α;. The first PPF of PK origin corresponds to accelerated clearance of the monoclonal antibody itself and is representative of its baseline intrinsic recirculation (with albumin as a proxy) (16) and also the inflammatory burden that accelerates the consumption of the drug from the central compartment (17). The second PPF of PK origin corresponds to the HLA DQA1*05 variant (detected as the A/G and G/G genotype), which informs on the immunization risk by presentation of the monoclonal antibody for clonal expansion and production of antidrug antibodies (6).

Our finding that the combination of these two PPFs of PK origin resulted in worse outcomes was expected. Notably, in addition to increasing immune response and antidrug antibodies, disease control was also worsened with reductions in clinical remission across all four cohorts. Our analysis further revealed that the detrimental effects of the PPFs of PK origin on CRP-based clinical remission were heightened in those who were biologic-experienced and lessened in those utilizing proactive TDM, as seen in the PRECISION cohort (10). With regard to endoscopic outcomes available from two separate cohorts, suboptimal PK secondary to the PPFs of PK origin resulted in worse outcomes with no impact of prior biologics.

Our data have some strengths and limitations in this population of IBD patients who all started an anti-TNF. The strengths include multiple, rich cohorts enrolled, the availability of endoscopic outcomes (at least with ADA) and availability of PK outcomes, and the fact that the responder score and clearance derived from the ADA-treated cohorts (BOLOGNA and PREDICROHN) also

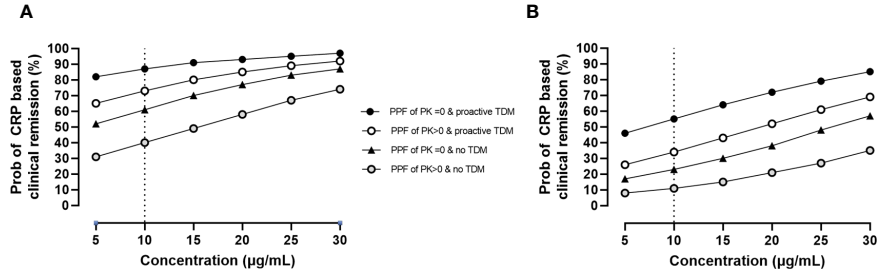

FIGURE 3
Impact of PPFs of PK origin by proactive TDM and prior biologics on CRP-based clinical remission status by exposure during maintenance. Estimates are as follows: θ_{pop} = 0.3 ± 0.4 (p = 0.453); θ_{cov}, prior biologics = −1.7 ± 0.5 (p = 0.001); θ_{cov}, PPFs of PK origin >0 = −0.9 ± 0.4 (p = 0.024); θ_{cov}, proactive TDM = 1.4 ± 0.3 (p< 0.001); $\theta_{concentrations}$ = 0.07 ± 0.01 (p< 0.001). **(A)** Probability of CRP-based clinical remission in patients naïve to biologics. **(B)** Probability of CRP-based clinical remission in patients with prior biologics. PPF, poor prognostic factor; PK, pharmacokinetic; TDM, therapeutic drug monitoring; CRP, C-reactive protein.

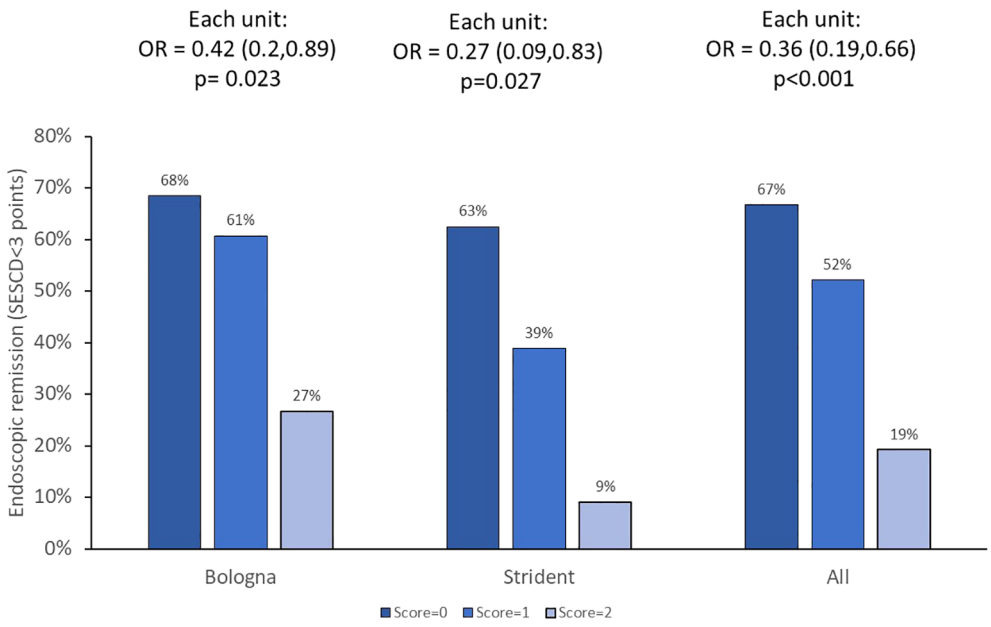

FIGURE 4
Endoscopic remission and PPFs of PK origin. The OR with 95%CI for each incremental unit of the PPF of PK origin is given. PPF, poor prognostic factor; PK, pharmacokinetic.

generally replicated in the IFX cohorts and the STRIDENT ADA cohorts. Limitations arise from the retrospective nature of our study, and it will be important to prospectively evaluate the value of the PPFs of PK origin.

There are potential direct clinical applications of these findings. The measurement and presence of the PPFs of PK origin before starting treatment could inform providers on the appropriateness of drug selection and dose intensification strategies to achieve exposure commensurate with disease control and thus remediate any suboptimal PK. Results may also identify which patients may benefit from combination therapy with a thiopurine to decrease the formation of antidrug antibodies, allowing for more sophisticated therapeutic decision-making and limiting unnecessary risk of adverse events in patients where there is an absence of PPFs of PK origin (18).

In conclusion, a serogenetic panel combining higher baseline clearance and HLA DQA1*05 is associated with outcomes in patients with IBD treated with anti-TNF therapies. Whether these PPFs of PK origin are also associated with outcomes in other immune-mediated inflammatory diseases is not known, but we hypothesize that their presence resulting in suboptimal PK is likely to result in lesser disease control as well, at least among the group of patients with active disease and high inflammatory burden.

Data availability statement

The original contributions presented in the study are included in the article/Supplementary Material, further inquiries can be directed to the corresponding author/s.

Ethics statement

The studies involving humans were approved by Mount Sinai Medical Center, St Vincent Hospital, University de la Princessa, University de Bologna. The studies were conducted in accordance with the local legislation and institutional requirements. Written informed consent for participation in this study was provided by the participants' legal guardians/next of kin.

Author contributions

ES: Conceptualization, Data curation, Formal analysis, Methodology, Writing – review & editing. MD: Conceptualization, Data curation, Formal analysis, Writing – review & editing, Funding acquisition, Investigation, Project administration, Supervision. MK: Conceptualization, Data curation, Project administration, Supervision, Writing – review & editing. MC: Data curation, Project administration, Supervision, Writing – review & editing, Conceptualization. PG: Data curation, Project administration, Conceptualization, Writing – review & editing. FR: Writing – review & editing, Conceptualization, Data curation. JG: Conceptualization, Data curation, Writing – review & editing, Project administration. EW: Conceptualization, Data curation, Writing – review & editing, Methodology. JS: Conceptualization, Data curation, Writing – review & editing. AH: Conceptualization, Data curation, Writing – review & editing. DM: Conceptualization, Writing – review & editing, Investigation, Validation. TD: Conceptualization, Data curation, Formal analysis, Investigation, Methodology, Project administration, Validation, Writing – original draft.

Funding

The author(s) declare financial support was received for the research, authorship, and/or publication of this article. This study was supported by Prometheus Laboratories.

Acknowledgments

We acknowledge Jordan Stachelski, Judson McFarland, and Patty Hughes for the management of testing in the Prometheus Laboratories, and Manny Ma and Annelie Everts van der Wind for the data management. We also acknowledge Carl Panetta for the statistical support and pharmacokinetic modeling.

Conflict of interest

JG has served as speaker, consultant, and advisory member for or has received research funding from MSD, Abbvie, Pfizer, Kern Pharma, Biogen, Mylan, Takeda, Janssen, Roche, Sandoz, Celgene/Bristol Myers, Gilead/Galapagos, Lilly, Ferring, Faes Farma, Shire Pharmaceuticals, Dr. Falk Pharma, Tillotts Pharma, Chiesi, Casen Fleet, Gebro Pharma, Otsuka Pharmaceutical, Norgine and Vifor Pharma. MD is a consultant for Prometheus Laboratories, Janssen, Abbvie, Takeda, Celgene, Gilead, U.C.B., Pfizer, Arena, and Eli Lilly as well as co-Founder of Mi Test Health and Trellus Health. TD is employee of Prometheus Laboratories; MK, AH, and EW: research grants from Prometheus Laboratories; DM: consultant Prometheus Laboratories, Merck; Palatin Bio; Takeda; Prometheus Biosciences; Palisade Bio.s.

The remaining authors declare that the research was conducted in the absence of any commercial or financial relationships that could be construed as a potential conflict of interest.

Publisher's note

All claims expressed in this article are solely those of the authors and do not necessarily represent those of their affiliated organizations, or those of the publisher, the editors and the reviewers. Any product that may be evaluated in this article, or claim that may be made by its manufacturer, is not guaranteed or endorsed by the publisher.

Supplementary material

The Supplementary Material for this article can be found online at: https://www.frontiersin.org/articles/10.3389/fimmu.2024.1342477/full#supplementary-material

References

1. Podolsky DK. Inflammatory bowel disease. *N Engl J Med* (2002) 347:417–29. doi: 10.1056/NEJMra020831

2. Jurgens M, Laubender RP, Hartl F, Weidinger M, Seiderer J, Wagner J, et al. Disease activity, ANCA, and IL23R genotype status determine early response to infliximab in patients with ulcerative colitis. *Am J Gastroenterol* (2010) 105:1811–9. doi: 10.1038/ajg.2010.95

3. Strand V, Cohen SB, Curtis JR, Zhang L, Kivitz AJ, Levin RW, et al. Clinical utility of therapy selection informed by predicted nonresponse to tumor necrosis factor-a inhibitors: an analysis from the Study to Accelerate Information of Molecular Signatures (AIMS) in rheumatoid arthritis. *Expert Rev Mol Diagn* (2022) 22:101–9. doi: 10.1080/14737159.2022.2020648

4. Tutuncu Z, Kavanaugh A, Zvaifler N, Corr M, Deutsch R, Boyle D, et al. Fcgamma receptor type IIIA polymorphisms influence treatment outcomes in patients with inflammatory arthritis treated with tumor necrosis factor alpha-blocking agents. *Arthritis Rheum* (2005) 52:2693–6. doi: 10.1002/art.21266

5. Cheifetz AS, Abreu MT, Afif W, Cross RK, Dubinsky MC, Loftus EV, et al. A comprehensive literature review and expert consensus statement on therapeutic drug monitoring of biologics in inflammatory bowel disease. *Am J Gastroenterol* (2021). doi: 10.14309/ajg.0000000000001396

6. Solitano V, Facciorusso A, McGovern DPB, Nguyen T, Colman RJ, Zou L, et al. HLA-DQA1 *05 genotype and immunogenicity to tumor necrosis factor-alpha antagonists: A systematic review and meta-analysis. *Clin Gastroenterol Hepatol* (2023). doi: 10.1016/j.cgh.2023.03.044

7. McGovern DPB, Kamm MA, Li D, Hamilton AL, Wright EK, Schulberg JD, et al. Tu1767 BASELINE CLEARANCE FOR ANTI TUMOR NECROSIS FACTORS PREDICTS LACK OF DISEASE CONTROL DURING MAINTENANCE TREATMENT OF CROHN'S DISEASE WITH INFLIXIMAB AND ADALIMUMAB. *Gastroenterology* (2023) 164:S–1117-S-1118. doi: 10.1016/S0016-5085(23)03582-5

8. Battat R, Hemperly A, Truong S, Whitmire N, Boland BS, Dulai PS, et al. Baseline clearance of infliximab is associated with requirement for colectomy in patients with acute severe ulcerative colitis. *Clin Gastroenterol Hepatol* (2021) 19:511–518.e6. doi: 10.1016/j.cgh.2020.03.072

9. Schulberg JD, Wright EK, Holt BA, Hamilton AL, Sutherland TR, Ross AL, et al. Intensive drug therapy versus standard drug therapy for symptomatic intestinal Crohn's disease strictures (STRIDENT): an open-label, single-centre, randomised controlled trial. *Lancet Gastroenterol Hepatol* (2022) 7:318–31. doi: 10.1016/S2468-1253(21)00393-9

10. Dubinsky MC, Mendiolaza ML, Phan BL, Moran HR, Tse SS, Mould DR. Dashboard-driven accelerated infliximab induction dosing increases infliximab durability and reduces immunogenicity. *Inflammation Bowel Dis* (2022). doi: 10.1093/ibd/izab285

11. Rizzello F, Gionchetti P, Spisni E, Saracino IM, Bellocchio I, Spigarelli R, et al. Dietary habits and nutrient deficiencies in a cohort of european crohn's disease adult patients. *Int J Mol Sci* (2023) 24. doi: 10.3390/ijms24021494

12. Chaparro M, Guerra I, Iborra M, Cabriada JL, Bujanda L, Taxonera C, et al. Usefulness of monitoring antitumor necrosis factor serum levels during the induction phase in patients with Crohn's disease. *Eur J Gastroenterol Hepatol* (2020) 32:588–96. doi: 10.1097/MEG.0000000000001706

13. Spencer EA, Stachelski J, Dervieux T, Dubinsky MC. Failure to achieve target drug concentrations during induction and not HLA-DQA1 *05 carriage is associated with antidrug antibody formation in patients with inflammatory bowel disease. *Gastroenterology* (2022) 162:1746–1748 e3. doi: 10.1053/j.gastro.2022.01.009

14. Wang SL, Hauenstein S, Ohrmund L, Shringarpure R, Salbato J, Reddy R, et al. Monitoring of adalimumab and antibodies-to-adalimumab levels in patient serum by the homogeneous mobility shift assay. *J Pharm BioMed Anal* (2013) 78-79:39–44. doi: 10.1016/j.jpba.2013.01.031

15. Wang SL, Ohrmund L, Hauenstein S, Salbato J, Reddy R, Monk P, et al. Development and validation of a homogeneous mobility shift assay for the measurement of infliximab and antibodies-to-infliximab levels in patient serum. *J Immunol Methods* (2012) 382:177–88. doi: 10.1016/j.jim.2012.06.002

16. Sand KM, Bern M, Nilsen J, Noordzij HT, Sandlie I, Andersen JT. Unraveling the interaction between fcRn and albumin: opportunities for design of albumin-based therapeutics. *Front Immunol* (2014) 5:682.

17. Wright EK, Chaparro M, Gionchetti P, Hamilton AL, Schulberg J, Gisbert JP, et al. Adalimumab Clearance, rather than Trough Level, May Have Greatest Relevance to Crohn's Disease Therapeutic Outcomes Assessed Clinically and Endoscopically. *J Crohns Colitis* (2023). doi: 10.1093/ecco-jcc/jjad140

18. Ungaro RC, Colombel JF, Dubinsky MC, Jain A, Dervieux T. Impact of thiopurine exposure on immunogenicity to infliximab is negligible in the setting of elevated infliximab concentrations. *Inflammation Bowel Dis* (2022) 28:649–51. doi: 10.1093/ibd/izab232

frontiers | Frontiers in Immunology

TYPE Correction
PUBLISHED 27 February 2024
DOI 10.3389/fimmu.2024.1383704

OPEN ACCESS

EDITED AND REVIEWED BY
Michael Tovey,
Svar Life Science, France

*CORRESPONDENCE
Thierry Dervieux
tdervieux@prometheulabs.com

RECEIVED 07 February 2024
ACCEPTED 16 February 2024
PUBLISHED 27 February 2024

CITATION
Spencer EA, Dubinsky MC, Kamm MA, Chaparro M, Gionchetti P, Rizzello F, Gisbert JP, Wright EK, Schulberg JD, Hamilton AL, McGovern DPB and Dervieux T (2024) Corrigendum: Poor prognostic factors of pharmacokinetic origin predict outcomes in inflammatory bowel disease patients treated with anti-tumor necrosis factor-α. *Front. Immunol.* 15:1383704. doi: 10.3389/fimmu.2024.1383704

Corrigendum: Poor prognostic factors of pharmacokinetic origin predict outcomes in inflammatory bowel disease patients treated with anti-tumor necrosis factor-α

Elizabeth A. Spencer[1], Marla C. Dubinsky[1], Michael A. Kamm[2], Maria Chaparro[3], Paolo Gionchetti[4,5], Fernando Rizzello[4,5], Javier P. Gisbert[3], Emily K. Wright[2], Julien D. Schulberg[2], Amy L. Hamilton[2], Dermot P. B. McGovern[6] and Thierry Dervieux[7]*

[1]Division of Gastroenterology, Icahn School of Medicine Mount Sinai, New York, NY, United States, [2]St Vincent's Hospital and The University of Melbourne, Melbourne, VIC, Australia, [3]Hospital Universitario de La Princesa, Instituto de Investigación Sanitaria Princesa (IIS-Princesa), Universidad Autónoma de Madrid (UAM) and Centro de Investigación Biomédica en Red de Enfermedades Hepáticas y Digestivas (CIBEREHD), Madrid, Spain, [4]IRCCS Azienda Ospedaliero-Universitaria di Bologna Italy, Bologna, Italy, [5]DIMEC University of Bologna-Italy, Bologna, Italy, [6]F. Widjaja Inflammatory Bowel Institute, Cedars-Sinai Medical Center, Los Angeles, CA, United States, [7]Research and Development, Prometheus Laboratories, San Diego, CA, United States

KEYWORDS

drug response, tumor necrosis factor, clearance, inflammatory bowel disease, pharmacogenetic

A Corrigendum on

Poor prognostic factors of pharmacokinetic origin predict outcomes in inflammatory bowel disease patients treated with anti-tumor necrosis factor-α

By Spencer EA, Dubinsky MC, Kamm MA, Chaparro M, Gionchetti P, Rizzello F, Gisbert JP, Wright EK, Schulberg JD, Hamilton AL, McGovern DPB and Dervieux T (2024) *Front. Immunol.* 15:1342477. doi: 10.3389/fimmu.2024.1342477

In the published article, there was an error. In **Table 1**, the percentage of HLA DQA1*05 carriage for "all cohort" was incorrect and was corrected to 40% (168/415).

In the Abstract, and Results, section 3.2. *Impact of PPF of PK origin on Immune response during treatment*, there was an error in the p value reported: "Overall, each incremental PPF of PK origin resulted in a 2-fold (OR=2.16, 95%CI: 1.7-2.7; p<0.11) higher likelihood of antidrug antibody formation".

10.3389/fimmu.2024.1383704

The corrected sentence appears below:

"Overall, each incremental PPF of PK origin resulted in a 2-fold (OR=2.16, 95%CI: 1.7-2.7; $p<0.01$) higher likelihood of antidrug antibody formation".

The authors apologize for these errors and state that this does not change the scientific conclusions of the article in any way. The original article has been updated.

Publisher's note

frontiers | Frontiers in Immunology

TYPE Original Research
PUBLISHED 26 January 2024
DOI 10.3389/fimmu.2024.1345473

OPEN ACCESS

EDITED BY
Michael Dougan,
Massachusetts General Hospital and Harvard Medical School, United States

REVIEWED BY
Erwan Mortier,
Centre National de la Recherche Scientifique (CNRS), France
Moutih Rafei,
Montreal University, Canada

*CORRESPONDENCE
Mark A. Kroenke
mkroenke@amgen.com

†PRESENT ADDRESSES
Christina L. Zuch de Zafra,
Nonclinical Sciences, Seagen, South San Francisco, CA, United States
Michael Archer,
Drug Safety and Pharmacovigilance, Atara Biotherapeutics, Thousand Oaks, CA, United States
Gurleen Saini,
Immunogenicity Characterization, Boehringer Ingelheim, Ridgefield, CT, United States

RECEIVED 27 November 2023
ACCEPTED 12 January 2024
PUBLISHED 26 January 2024

CITATION
Kroenke MA, Starcevic Manning M, Zuch de Zafra CL, Zhang X, Cook KD, Archer M, Lolkema MP, Wang J, Hoofring S, Saini G, Aeffner F, Ahern E, Cabanas EG, Govindan R, Hui M, Gupta S and Mytych DT (2024) Translatability of findings from cynomolgus monkey to human suggests a mechanistic role for IL-21 in promoting immunogenicity to an anti-PD-1/IL-21 mutein fusion protein.
Front. Immunol. 15:1345473.
doi: 10.3389/fimmu.2024.1345473

Translatability of findings from cynomolgus monkey to human suggests a mechanistic role for IL-21 in promoting immunogenicity to an anti-PD-1/IL-21 mutein fusion protein

Mark A. Kroenke[1]*, Marta Starcevic Manning[2], Christina L. Zuch de Zafra[3†], Xinwen Zhang[4], Kevin D. Cook[5], Michael Archer[6†], Martijn P. Lolkema[7], Jin Wang[2], Sarah Hoofring[2], Gurleen Saini[2†], Famke Aeffner[3], Elizabeth Ahern[8], Elena Garralda Cabanas[9], Ramaswamy Govindan[10], Mun Hui[11], Shalini Gupta[2] and Daniel T. Mytych[1]

[1]Clinical Immunology, Amgen, Thousand Oaks, CA, United States, [2]Translational Safety & Bioanalytical Sciences, Amgen, Thousand Oaks, CA, United States, [3]Translational Safety & Bioanalytical Sciences, Amgen, South San Francisco, CA, United States, [4]Clinical Pharmacology, Modeling, and Simulation, Amgen, South San Francisco, CA, United States, [5]Pharmacokinetics and Drug Metabolism, Amgen, South San Francisco, CA, United States, [6]Global Safety, Amgen, Thousand Oaks, CA, United States, [7]Early Development, Amgen, Thousand Oaks, CA, United States, [8]Medical Oncology, Monash Health, Clayton, VIC, Australia, [9]Research Unit, Hospital Universitario Vall d'Hebron, Barcelona, Spain, [10]Division of Hematology and Oncology, Washington University Medical School, St. Louis, MO, United States, [11]Chris O'Brien Lifehouse, Camperdown, NSW, Australia

AMG 256 is a bi-specific, heteroimmunoglobulin molecule with an anti-PD-1 antibody domain and a single IL-21 mutein domain on the C-terminus. Nonclinical studies in cynomolgus monkeys revealed that AMG 256 administration led to the development of immunogenicity-mediated responses and indicated that the IL-21 mutein domain of AMG 256 could enhance the anti-drug antibody response directed toward the monoclonal antibody domain. Anti-AMG 256 IgE were also observed in cynomolgus monkeys. A first-in-human (FIH) study in patients with advanced solid tumors was designed with these risks in mind. AMG 256 elicited ADA in 28 of 33 subjects (84.8%). However, ADA responses were only robust and exposure-impacting at the 2 lowest doses. At mid to high doses, ADA responses remained low magnitude and all subjects maintained exposure, despite most subjects developing ADA. Limited drug-specific IgE were also observed during the FIH study. ADA responses were not associated with any type of adverse event. The AMG 256 program represents a unique case where nonclinical studies informed on the risk of immunogenicity in humans, due to the IL-21-driven nature of the response.

KEYWORDS

PD-1, IL-21, immunogenicity, anti-drug antibodies, mutein, IgE

1 Introduction

Inhibition of the PD-1/PD-L1 T cell checkpoint pathway has been established as an effective and generally well-tolerated approach to stimulating an immune response to tumor cells (1). While improved objective responses and/or improved overall survival have been observed in numerous patients, a significant subset of patients do not benefit from monotherapy (2). Consequently, various types of combination approaches are being investigated, including recombinant human IL-21 (rhIL-21).

IL-21 is a pleiotropic cytokine with the potential to catalyze a variety of downstream signaling events (3). In the context of immunotherapy for oncology indications, it has the potential to synergize with blockade of PD-1/PD-L1 by supporting a gene expression profile consistent with immature effector CD8 T cells (4). Furthermore, the combination of PD-1 blockade with IL-21 has shown remarkable efficacy in mouse tumor models, largely by enabling enhanced infiltration of CD8 T cells into the tumor (5).

To capitalize on the synergistic therapeutic potential of PD-1/PD-L1 inhibition and IL-21 signaling, a bifunctional fusion protein was created. AMG 256 is a fully human, aglycosylated heteroimmunoglobulin molecule, with 2 different heavy chains held together by charge pair mutations. One heavy chain is linked to an affinity-attenuated, monovalent, human IL-21 mutein. The monoclonal antibody domain (clone 22D4) is specific for PD-1. AMG 256 was designed to deliver an IL-21 signal specifically to PD-1^+ CD8 T cells, while simultaneously inhibiting PD-1 signaling (6).

The nonclinical safety and pharmacokinetic (PK) profile of AMG 256 was evaluated in exploratory and Good Laboratory Practice (GLP) PK/pharmacodynamic (PD) and toxicology studies in cynomolgus monkeys because it binds with similar high affinity to the extracellular domains of human and cynomolgus monkey PD-1, but not to rodent PD-1. This is consistent with expectations of species specificity based on the protein sequence similarity which is 96% for cynomolgus monkey PD-1, but only 62.4% for mouse PD-1, relative to human PD-1 (7). Additionally, AMG 256 blocks the interaction of the human and cynomolgus monkey receptors with the human ligands, PD-L1 and PD-L2 (data not shown). Furthermore, the amino acid sequence homology between human and cynomolgus monkey IL-21 receptor (IL-21R) is 96.5% (7), but between human and mouse is only 62% (8).

A phase 1, first-in-human (FIH) study was designed to assess the safety, tolerability, pharmacokinetic, and pharmacodynamic properties of AMG 256 in patients with advanced solid tumors. Nonclinical studies had indicated that fusion of the IL-21 mutein domain to the monoclonal antibody domain could result in enhanced anti-drug antibody (ADA) responses, and potential class switching to the IgE isotype. Consequently, the FIH study was specifically designed to mitigate the risk of immunogenicity and hypersensitivity.

2 Materials and methods

2.1 Nonclinical study designs

A series of Investigational New Drug (IND)-enabling PK/PD and toxicology studies were conducted in cynomolgus monkeys at AAALAC-accredited facilities. All procedures conducted in animals complied with the Animal Welfare Act, the Guide for the Care and Use of Laboratory Animals, and the Office of Laboratory Animal Welfare. Protocols were approved by the applicable Institutional Animal Care and Use Committees.

In an exploratory PK/PD study, AMG 256 (5 mg/kg) or 22D4 (5 mg/kg) were administered to male cynomolgus monkeys by IV bolus injection on days 1 and 15 (n=4/group). A third group was dosed with 22D4 (5 mg/kg) on days 1 and 15 and rhIL-21 (0.1 mg/kg) on days 1, 4, 7, 15, 18, and 21. Blood samples for evaluation of serum chemistry parameters were obtained predose on day 1 and at 24 and 168 hours postdose, and predose on day 15 and at 24 and 168 hours postdose. Serum samples for the evaluation of PK were obtained on day 1 at 5 and 15 minutes and 1, 24, 72, 120, 168, and 240 hours post dose, and predose on day 15 and at 5 and 15 minutes and 1, 24, 72, 120, 168, and 240 hours post dose. Serum samples for evaluation of immunogenicity were obtained predose on day 15 (336 hours) and on day 25 (576 hours) after the first dose administration on day 1.

In an exploratory toxicology study, male cynomolgus monkeys were administered 3 weekly doses of AMG 256 by IV bolus injection at 10 or 30 mg/kg (n=3/group). Blood samples for the evaluation of clinical chemistry and hematology were collected prestudy and on days 2, 8, 9, 15, and 19. Blood samples for evaluation of coagulation parameters were collected prestudy and on days 2, 9, and 19. Serum samples for the evaluation of toxicokinetics (TK) were collected at 5 minutes and 1, 24, 72, 96, and 168 hours after the day 1 dose administration; at 5 minutes and 96 and 168 hours after the day 8 dose administration; and at 5 minutes and 1, 24, 72, and 96 hours after the day 15 dose administration. Serum samples for the evaluation of immunogenicity were obtained predose on days 1 and 8, and on day 19. Plasma samples for the analysis of the complement split products Bb, C3a, C5a, and sC5b9 and serum samples for CH50 analysis were collected prestudy and 30 minutes postdose on days 1, 8, and 15. Necropsy was conducted on day 19.

In a GLP toxicology study, male and female cynomolgus monkeys were administered 4 weekly doses of AMG 256 by IV bolus injection at doses of 0, 6, 30, or 150 mg/kg (n=3/sex/group). Blood samples for the evaluation of clinical chemistry and hematology were obtained prestudy and on days 2, 9, 16, 23, and 29. Blood samples for evaluation of coagulation parameters were collected prestudy and on day 29. Serum samples for evaluation of toxicokinetics were obtained predose on days 1, 15, and 22; 15 minutes postdose on days 1, 8, 15, and 22; and 4, 24, 48, 72, 96, and 168 hours postdose on days 1 and 22. Samples for evaluation of immunogenicity were obtained at baseline, predose on days 8, 15, and 22, and on day 29. Necropsy was conducted on day 29.

2.2 Nonclinical assays

Quantitation of AMG 256 and 22D4 in cynomolgus monkey serum was performed using electrochemiluminescent (ECL)-based immunoassays. For the exploratory PK/PD and toxicology studies, the method used biotinylated PD-1 (R&D Systems; Minneapolis, MN) as the capture reagent and ruthenylated mouse anti-human Fc (Amgen Inc.; Thousand Oaks, CA) as the detection reagent. For the

GLP toxicology study, the validated method used rhPD-1 (Amgen Inc.) as the capture regent and ruthenylated mouse anti-human Fc (Amgen Inc.) as the detection reagent. Analyte serum concentrations were interpolated from standard curves using the corresponding analytes.

Anti-AMG 256 IgG was assessed in the nonclinical studies using the universal indirect species-specific assay (UNISA) (9). AMG 256 or 22D4 (if applicable) was coated on a bare Mesoscale Discovery plate (MSD; Rockville, MD), then washed and blocked. Serum samples were diluted and incubated on the drug-coated plate before washing and addition of a ruthenylated anti-cyno IgG detection reagent. Plates were washed and ECL signal was read using an MSD plate reader. Specificity was confirmed by incubating diluted serum samples with excess drug.

Anti-AMG 256 IgE was assessed in the nonclinical studies using an ECL-based immunoassay. Anti-cynomolgus monkey IgE antibody was coated on a standard bare MSD plate, then washed and blocked. Diluted serum samples were added to the plate to capture total IgE antibodies. Plates were washed and ruthenylated AMG 256 was utilized to detect drug-specific IgE bound to the plate. Specificity was confirmed by adding excess unlabeled AMG 256 to the detection reagent.

Several assays were performed to evaluate complement activation following 3 weekly doses of AMG 256 in the exploratory toxicology study. CH50 was measured by a hemolytic assay based on lysis of antibody-coated sheep red blood cells due to activation of complement on the cell's surface. Serial dilutions of the test specimen were mixed with equal volumes of sheep red blood cells and the amount of hemoglobin released when the target cells were lysed by the action of complement was measured. Serial dilutions of a human serum standard with known CH50 activity were used to establish its 50% lysis point; each specimen was diluted in the same manner, and individual 50% lysis points were determined by linear regression.

Bb, C3a, and soluble C5b-9 (sC5b-9) were measured by ELISA. Assay standards, controls, and test specimens were diluted and placed in duplicate into wells precoated with a monoclonal antibody against Bb or C3a. After washing to remove unbound proteins, a second anti-Bb, anti-C3a, or sC5b-9 antibody conjugated to horseradish peroxidase was added; after an appropriate incubation time and washing, a chromogenic substrate was added, and the wells were assessed spectrophotometrically.

C5a was assessed using a competitive radioimmunoassay. Cross-reacting high molecular weight antigen (native C5) was removed from specimens by precipitation, and radiolabeled (^{125}I) C5a antigen of known concentration was mixed with the plasma specimen. The mixtures were precipitated by adding a limited quantity of polyclonal human C5/C5a antibody. As C5a from the specimen competed with labeled C5a for binding to the antibody, the amount of radiolabeled antigen that precipitated was inversely proportional to the amount of C5a antigen present in the specimen.

2.3 Human *in vitro* T cell assay

Donors were recruited at phase 1 clinical trial units and selected to represent the global frequency of HLA-DRB1 alleles. A dendritic cell and T cell co-culture (DC:T) assay was performed by Lonza (Saffron Walden, UK). Briefly, monocytes were isolated from PBMCs through positive selection, and differentiated into immature dendritic cells using GM-CSF and IL-4. Immature dendritic cells were loaded with test proteins and matured using TNFα and IL-1β. Autologous CD4 T cells were isolated from PBMCs using negative selection and co-cultured with the mature dendritic cells for 6 days before $CD3^+$ $CD4^+$ Edu^+ cells were measured by flow cytometry, with each condition carried out in 6 replicates. The stimulation index (SI) was calculated by dividing the test condition by the media alone control (baseline). A donor is generally considered a responder if SI ≥ 2.

2.4 FIH study design

The phase 1 study (NCT04362748) was designed to evaluate the safety, tolerability, pharmacokinetics, and pharmacodynamics of AMG 256 in patients with advanced solid tumors. The study was a non-randomized, open-label study with AMG 256 administered by intravenous (IV) infusion on days 1, 8, 15, and 22 of every 28-day cycle (QW dosing), or days 1 and 15 of every 28-day cycle (Q2W dosing). Dose escalation began at 0.6 mg IV QW and increased up to 1400 mg IV QW, with two additional cohorts dosed with 1000 mg or 2000 mg AMG 256 Q2W. Immunogenicity was monitored every week for the first cycle, every 2 weeks for cycle 2, and at the start of each cycle for cycles 3 and beyond. Subjects were observed for 24 hours after each infusion during cycles 1 and 2, and for 1 hour after each infusion during cycle 3 and all subsequent cycles. Dosing was staggered for the first 2 cycles to minimize the potential for multiple subjects experiencing hypersensitivity reactions on the same day. Informed consent was obtained from all subjects before participation.

2.5 Anti-drug antibody methods

Two different antibody assay methods were validated; one to detect all anti-AMG 256 antibodies in human serum and another to detect only antibodies that bind to endogenous human IL-21. The cut points for both assays were calculated from 30 healthy donor serum samples and 30 donor serum samples from patients with solid tumors, in accordance with regulatory guidance. Both assays were composed of screening and confirmatory components. Samples with a signal to noise (S/N) ratio higher than the assay cut point in the screening assay were analyzed with excess AMG 256 or IL-21 in the confirmatory assay to assess specificity. Percent depletion was calculated by subtracting the mean electrochemiluminescent (ECL) value of the treated specimen from the mean ECL value of the untreated specimen and dividing by the untreated specimen mean ECL value.

Anti-AMG 256 antibodies were measured using a validated, affinity capture elution (ACE) method. Maxisorp plates were coated with AMG 256, washed, and blocked. Samples were diluted 1:10 in 300 mM acetic acid to enable antibody-drug complex dissociation prior to analysis. The coated and blocked plates were washed, 1 M

Tris pH 9.5 was added to each well, followed immediately by acid-diluted serum samples. Plates were incubated overnight to allow the coated drug to capture ADA from the neutralized sample. Plates were then washed, and 300 mM acetic acid was added to the plate to elute the bound ADA. The acid eluted samples were then neutralized with 1 M Tris pH 9.5, added to bare MSD high bind plates and allowed to incubate. The plates were then washed and blocked. Next, untreated or drug-treated detection buffer containing ruthenylated AMG 256 and excess unlabeled drug (confirmatory assay only) was added to the plates. Lastly, the plates were washed and tripropylamine MSD read buffer was added to each well. An electrical current was placed across the plate-associated electrodes using an MSD plate reader, resulting in a series of electrically induced oxidation-reduction reactions involving ruthenium and tripropylamine. The overall assay sensitivity was 3.2 ng/mL of anti-AMG 256 polyclonal antibody. At 100 ng/mL of anti-AMG 256 antibody, the assay could tolerate at least 200 µg/mL of excess AMG 256.

Antibodies against endogenous IL-21 were measured using a validated, ECL bridging method. Prior to analysis, samples were treated with 300 mM acetic acid (1:40) to enable antibody-IL-21 complex dissociation. Then, acid treated samples were neutralized and incubated overnight in a mixture of biotinylated-IL-21 and ruthenylated-IL-21 (and excess unlabeled IL-21 in the confirmatory assay). ADA present in serum samples form a bridge between the two IL-21 conjugates. The formed antibody complex was captured on a blocked streptavidin plate, washed, and analyzed on a plate reader where signal was produced from an electrically induced oxidation-reduction reaction involving ruthenium and tripropylamine. The overall assay sensitivity was 4.3 ng/mL of anti-IL-21 monoclonal antibody. At 100 ng/mL of anti-IL-21 antibody, the assay could tolerate at least 250 µg/mL of excess AMG 256.

Anti-AMG 256 IgE antibodies were detected using an ECL-based method consisting of a screening and confirmatory assay. Total IgE antibodies from serum samples (diluted 1:40 in assay diluent) were captured onto a bare standard-bind MSD plate coated with anti-human IgE capture antibody. The MSD plate was washed and a detection reagent containing either ruthenylated AMG 256 (screening assay) or ruthenylated AMG 256 with excess unlabeled AMG 256 (confirmatory assay) was added to the plate. The plate was washed and tripropylamine-containing MSD read buffer was added to each well. Using an MSD plate reader, an electrical current was placed across the plate-associated electrodes, inducing a series of reactions involving ruthenium and tripropylamine and resulting in an ECL signal. Sample results were expressed as a S/N ratio, calculated by dividing sample signal by the signal of the negative control. Samples with a S/N greater than or equal to the screening assay cut point that demonstrated signal inhibition greater than or equal to the confirmatory cut point in the presence of excess unlabeled AMG 256 were considered positive for AMG 256-specific IgE antibodies. Cut points were established according to regulatory guidance using data from 103 individual donor serum samples (61 healthy and 42 solid tumor), including 28 baseline samples from the FIH study. A chimeric mouse/human IgE antibody that binds a modified component of the AMG 256 Fc domain was used as a positive control to determine method parameters and monitor assay performance. Assay sensitivity was determined to be 111 pg/mL or 151 pg/mL in the screening or confirmatory assays, respectively. The screening assay was qualified to detect 0.5 ng/mL of anti-AMG 256 IgE antibody in the presence of 200 µg/mL of soluble AMG 256. The confirmatory assay was qualified to detect 0.5 ng/mL or 1 ng/mL of anti-AMG 256 IgE antibody in the presence of 50 µg/mL or 200 µg/mL, respectively, of soluble AMG 256. In addition, high concentrations of total IgE (up to 10 µg/mL) or AMG 256-specific IgG (up to 200 µg/mL) did not result in false positives or false negatives at 200 pg/mL of positive control.

2.6 Neutralizing antibody assay

A cell-based neutralizing antibody assay was developed and validated by PPD (Richmond, VA) to assess the ability of anti-IL-21 antibodies to neutralize endogenous IL-21. Briefly, Hut78 cells were stimulated with rhIL-21 and phosphorylation of STAT3 was measured using an MSD kit. In the presence of a neutralizing antibody, STAT3 phosphorylation was lost. The overall sensitivity of the assay was 128 ng/mL. At 0.5 µg/mL of excess AMG 256 in serum, the assay could detect at least 500 ng/mL of anti-IL-21 neutralizing antibodies.

2.7 Pharmacokinetic assay

AMG 256 was measured in human serum using a validated sandwich immunoassay. An anti-idiotype monoclonal antibody against the 22D4 domain was used for capture and a biotin conjugated anti-IL-21 monoclonal antibody was used for detection. The assay range was 10.0 to 1,000 ng/mL.

3 Results

3.1 *In vitro* T cell assay to assess sequence-based risk of immunogenicity

Prior to initiation of a clinical study, an *in vitro* T cell assay was performed to identify T cell epitopes and assess immunogenic risk of AMG 256. A DC:T assay format was utilized to eliminate the possibility that neutralization of PD-1 and/or IL-21 signaling could influence the result.

All donors demonstrated an SI of greater than 2 in response to keyhole limpet hemocyanin (KLH) which was used as a positive control. The CD4 response to AMG 256 and the 22D4 monoclonal antibody domain alone was similar, with 10 of 50 and 11 of 50 donors, respectively, responding with an SI of greater than 2 (Figure 1). This indicates that the IL-21 mutein domain of AMG 256 contributes minimal sequence-based immunogenic risk. An additional anti-PD-1 clone, 20A2, was also tested as a potential alternative to 22D4. For 20A2, 14 of 50 donors had an SI greater than 2, with several large magnitude responses, indicating the risk of

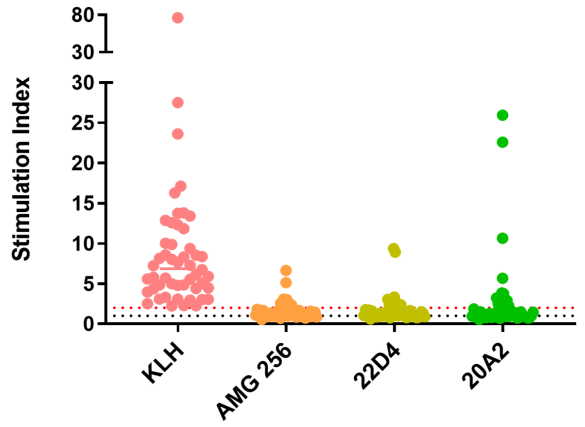

FIGURE 1
In vitro T cell assays did not suggest significant sequence-based risk of immunogenicity for AMG 256. A DC:T assay was performed with naïve donors representative of global HLA allele frequencies. Results are shown as stimulation index, or test protein divided by the baseline condition (media alone). Monocytes from 50 PBMC donors were differentiated into dendritic cells, loaded with test protein, and matured. Autologous CD4 T cells were isolated and co-cultured with mature dendritic cells presenting test protein agretopes for 6 days prior to assessment of CD4 T cell proliferation by flow cytometry. KLH was used as a positive control. Additional controls included 22D4 (AMG 256 MAb domain alone) and 20A2 (unrelated anti-PD-1 MAb). The black dashed line indicates an SI of 1 (no change from baseline) and the red dashed line indicates an SI of 2 (response).

a T-dependent antibody response being elicited was lower for 22D4 than for 20A2. These data contributed to the selection of the 22D4 clone to comprise the antibody portion of AMG 256.

3.2 Clinical observations, loss of exposure, and ADA response in a cynomolgus monkey PK/PD study

The safety and PK profile of AMG 256 were characterized through a series of IND-enabling studies in cynomolgus monkeys, the most relevant nonclinical species for evaluation of the PK/PD and toxicity of AMG 256. In a PK/PD study, animals were dosed IV with AMG 256 or the 22D4 monoclonal antibody on days 1 and 15; a third group was dosed with 22D4 (5 mg/kg) on days 1 and 15 and rhIL-12 (0.1 mg/kg) on days 1, 4, 7, 15, 18, and 21. Within 6 to 10 minutes of administration of the second AMG 256 dose on day 15, 2 of 4 animals in the AMG 256 group showed signs of hypersensitivity-type reactions including decreased activity, dilated pupils, pale mucous membranes, salivation, and reddened facial skin; 1 of these 2 animals also transiently lost consciousness, had severe emesis, and was treated with diphenhydramine, dexamethasone, oxygen, oral honey, and intravenous fluids. Both animals were placed in incubators for observation. By approximately 6.5 hours after dosing, both animals appeared normal and were returned to their home cages without further need for medical treatment.

In the AMG 256 group, clinical chemistry alterations were generally small in magnitude, sporadic, and transient. They were consistent with hemolysis and/or altered hepatobiliary function included minimal to mild sporadic, transient increases in AST, ALT, ALP, and total bilirubin. Hematology was not evaluated in this study, therefore the relative contribution of hemolysis and/or hepatobiliary function to these changes cannot be determined. Inflammation was indicated by minimal to mild increases in CRP. Altered mineral and electrolyte metabolism was indicated by minimal sporadic, transient decreases in calcium, potassium, and phosphorus and minimal increases in sodium and chloride. None of the observations were considered adverse because they were of small magnitude, sporadic, and transient.

While it was anticipated that 22D4 would have slightly higher exposure than AMG 256 (6), rapid loss of exposure was observed in the terminal phase of the first dose interval and upon subsequent dosing of AMG 256 (Figure 2A). All AMG 256-dosed animals were positive for anti-AMG 256 IgG on days 15 and 25 (hours 336 and 576 after the day 1 dose, respectively). Surprisingly, the antibody response in animals dosed with AMG 256 was uniformly and remarkably enhanced relative to animals dosed with 22D4 alone (Figure 2B). The antibody response magnitude for animals dosed with 22D4 and 22D4+rhIL-21 was similar, indicating that either the IL-21 mutations and/or the fusion to the 22D4 domain was required in order to observe this enhanced response.

One possible explanation for this observation was that the cynomolgus monkey response was primarily directed against the IL-21 domain of AMG 256, and consequently when this domain was not present, fewer antibodies were detected. In order to assess this, serum samples from animals dosed with AMG 256 were pre-treated with either AMG 256 or 22D4 and re-tested in the AMG 256 antibody assay. Assay signal was depleted to a similar extent with both AMG 256 and 22D4, demonstrating that the bulk of the antibody response was directed against the 22D4 domain of AMG 256 (Figure 2C). These data indicate that the IL-21 mutein domain of AMG 256 enhanced the 22D4 directed antibody response in cynomolgus monkey.

Based on the hypersensitivity-type clinical signs observed following the day 15 dose in 2 of 4 animals dosed with AMG 256, additional immunogenicity assessment was conducted to evaluate the presence of IgE isotype ADAs. It was important to assess this because there are plausible mechanisms by which the IL-21 mutein domain of AMG 256 could trigger class switching to IgE (10, 11). If this was observed in cynomolgus monkey studies, similar mechanisms may trigger drug-specific IgE in the FIH study, posing a safety risk to patients. All animals (4 of 4) administered AMG 256 were positive for IgE ADAs on days 15 and 25, except for a single animal that was IgE ADA-negative on day 15. IgE ADAs were not detected in any of the animals administered 22D4.

3.3 Activation of classical and alternative complement pathways in a cynomolgus monkey exploratory toxicology study

Following 3 weekly IV doses of AMG 256 to male cynomolgus monkeys at doses of 10 or 30 mg/kg, transient clinical signs including decreased activity, dilated pupils, pale skin, and loss of

10.3389/fimmu.2024.1345473

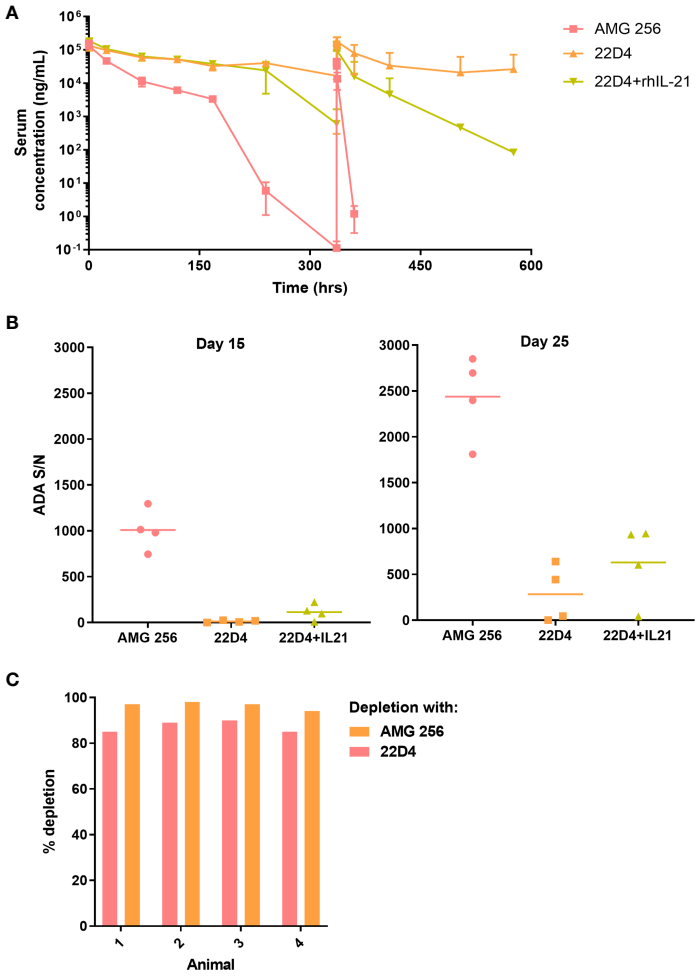

FIGURE 2
IL-21 mutein domain enhanced the antibody response to 22D4 in cynomolgus monkeys. Cynomolgus monkeys were dosed with 5 mg/kg AMG 256, 5 mg/kg 22D4, or 5 mg/kg 22D4 plus 0.1 mg/kg recombinant human IL-21. **(A)** AMG 256 or 22D4 serum levels were measured over time in each of the 3 treatment groups. **(B)** The ADA response in each dosing group was assessed on day 15 and day 25 by UNISA. **(C)** Domain characterization was performed on AMG 256 dosed animals at the day 25 time point. Serum samples were pre-treated with either AMG 256 or 22D4 and re-tested in the antibody assay. Percent depletion indicates the signal change from the pre-treated sample relative to the untreated sample.

coordination were observed in 1 of 3 animals in the 30 mg/kg dose group. Anti-AMG 256 IgG antibodies were observed in all animals at the day 19 time point, resulting in loss of exposure similar to the PK/PD study (data not shown). A subset of animals was also tested for anti-AMG 256 IgE. This subset was composed of 1 animal from the 30 mg/kg group with potentially IgE-mediated clinical observations and 2 animals with no evidence of IgE (one from each group). The animal suspected of being IgE positive was confirmed positive for anti-AMG 256 IgE at day 19, along with one other animal from the 30 mg/kg group.

Based on the clinical observations and ADA responses in this study as well as the previous PK/PD study, samples were evaluated for evidence of complement pathway activation. Results were consistent with dose-dependent activation of both classical and the alternative complement pathways. CH50 values for all 10 mg/kg animals and 2 of 3 30 mg/kg animals remained relatively unchanged on days 1 and 8 when compared to prestudy levels. One of 3 animals in the 30 mg/kg group had a significant decrease in CH50 values, reflecting complement activation, following dosing on day 8, and all animals in both dose groups had dramatic decreases in CH50 values (down to 0 U/mL) following the third dose of AMG 256 on day 15. Increases in Bb, C3a, and sC5b-9 were observed in all animals, and the magnitude of the changes increased progressively over the course of the study. No notable changes were seen in C5a levels at all sampling timepoints; however, C5a has a relatively short half-life and is cleared rapidly from circulation, so it is possible that it was undetectable even in samples collected at 30 minutes post-dose (earliest sampling timepoint).

3.4 Consistent, robust anti-AMG 256 IgG response in a GLP cynomolgus monkey toxicology study

In a GLP toxicology study, cynomolgus monkeys were administered AMG 256 IV at 0, 6, 30, or 150 mg/kg once weekly for 4 weeks. Three animals displayed serious clinical signs, including pallor, weakness, petechia, hypothermia, and

dehydration, leading to the unscheduled euthanasia of 2 animals in the 150 mg/kg dose group (on day 9 and day 11), and 1 animal in the 30 mg/kg dose group on day 22. The cause of moribundity in these animals was attributed to IgM ADA-mediated immune complex disease resulting in thrombocytopenia, consumptive coagulopathy, and circulatory collapse. Clinical pathology changes included decreased red blood cell (RBC) mass (hemoglobin, RBC count, and hematocrit), reticulocytes, and platelets; prolonged PT and aPTT and altered fibrinogen; decreased albumin; and/or increased C-reactive protein (CRP).

Clinical observations in several animals surviving to scheduled termination included emesis, discolored skin, salivation, weakness, hunched posture, decreased activity, diarrhea, and coughing/sneezing in individual animals at all dose levels. These signs were transient and generally occurred after at least 2 doses. AMG 256-related hematology alterations included decreased RBC mass with decreased then increased reticulocytes, decreased platelets, and decreased white blood cell count. AMG 256-related changes in clinical chemistry parameters included an acute phase response characterized by increased CRP, globulins, and triglycerides and/or decreased albumin and albumin/globulin ratio at all dose levels. Alanine aminotransferase, AST, and LDH were increased at ≥ 30 mg/kg and total bilirubin was increased at all dose levels. Alkaline phosphatase and GGT levels were decreased at 150 mg/kg and cholesterol was increased at all dose levels. Creatinine was increased at 150 mg/kg.

AMG 256 exposure increased with dose, and an impact of anti-AMG 256 ADAs on exposure was observed in all animals except the 150 mg/kg dose group animal euthanized on day 11. At the day 8 predose time point, IgG ADAs were detected in 1 of 6 animals in the 6 mg/kg dose group; at the day 15 predose time point and onward, IgG ADAs were observed in all surviving animals. While it is not possible to differentiate immunogenicity driven by foreign human sequence from IL-21-driven immunogenicity, it was noted that every animal developed a robust anti-AMG 256 IgG response, and results were consistent across animals (Figure 3).

Some reduction in assay signal was observed as the dose of AMG 256 was increased, however, this is likely due to the impact of higher levels of circulating drug on S/N values, rather than a real reduction in antibody magnitude. This uniform ADA response was distinct from what is typically observed following administration of biotherapeutic molecules to cynomolgus monkeys, which is a varied ADA response driven by the diversity of cynomolgus monkey HLA alleles and T/B cell repertoires (9). These data further support the hypothesis that fusing an IL-21 mutein domain to a monoclonal antibody can enhance the ADA response to the antibody domain.

Based on observations of hypersensitivity and/or IgE ADA in prior cynomolgus monkey studies, together with the clinical observations in this study, drug-specific IgE was assessed. No animals in the control group tested positive for anti-AMG 256 IgE at any time point. IgE ADAs were detected in 2 animals at 6 mg/kg and 1 animal at 30 mg/kg on day 15, and by day 29 all 6 animals at 6 mg/kg, 4 of 6 animals at 30 mg/kg, and none of the animals at 150 mg/kg were IgE positive (Table 1). The two animals at 150 mg/kg that were euthanized at unscheduled time points were negative for both IgG and IgE ADAs at their last sampling time point on day 8 or day 9. The IgE response was low magnitude relative to IgG, as expected based on the relative concentration of IgE compared to IgG in serum. The decreased incidence of anti-AMG 256 IgE with increasing dose of AMG 256 was likely due to the concentration of AMG 256 in serum exceeding the drug tolerance of the IgE assay, and not an actual drop in ADA incidence.

3.5 Immunogenicity assessment in the AMG 256 FIH study

Prior to initiating the FIH study, an immunogenicity risk assessment was conducted based on *in vitro* and nonclinical data as well as relevant literature. It was recognized that AMG 256 had the potential for mechanism of action (MOA)-driven immunogenicity as well as elicitation of drug-specific IgE. Due to these risks, a conservative approach to dosing human subjects was taken. Some examples of mitigations put in place included a low 0.6 mg starting dose (based on a minimally anticipated biological effect level [MABEL] approach), beginning the study with single subject dose escalation cohorts, staggering dosing in later multi-subject cohorts, long infusion times, and frequent ADA sampling (Figure 4A). Furthermore, the study was conducted at centers prepared with trained clinical personnel and resources to respond appropriately should severe hypersensitivity responses (i.e. anaphylaxis) occur. These safeguards ensured, among other things, that any AMG 256 hypersensitivity or anaphylactic reaction would be limited initially to one subject and mitigated to the extent possible.

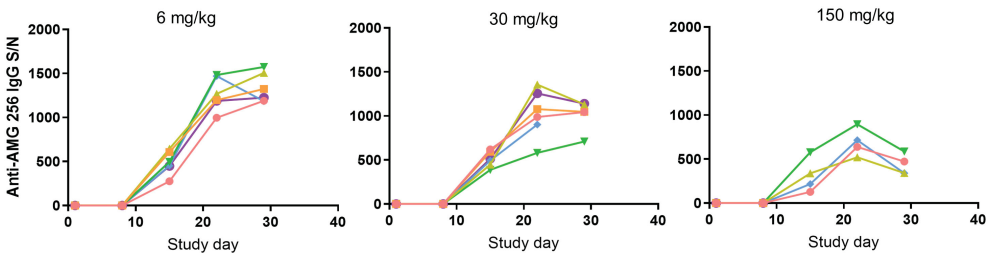

FIGURE 3
Antibody response in cynomolgus monkeys was robust and uniform. Cynomolgus monkeys were dosed with 6, 30, or 150 mg/kg AMG 256. UNISA was used to assess anti-AMG 256 IgG antibodies at baseline and 4 post-baseline time points. In the 30 mg/kg group, one animal was euthanized early on day 22, and in the 150 mg/kg group, two animals were euthanized early on days 9 and 11. Each color represents an individual animal.

10.3389/fimmu.2024.1345473

TABLE 1 Drug-specific IgE results from GLP cynomolgus monkey study.

Group	Dose	Anti-drug IgE incidence	Positive sample peak S/N range
Group 1	Placebo	0/6	–
Group 2	6 mg/kg	6/6	1.97 – 3.61
Group 3	30 mg/kg	4/6	1.54 – 4.98
Group 4	150 mg/kg	0/6	–

Aside from the risk of IgG or IgE-mediated hypersensitivity, there was an additional risk that antibodies elicited to AMG 256 could cross-react with and neutralize endogenous IL-21. A tailored antibody monitoring strategy was devised to specifically address this risk. First, all antibody samples were screened for binding to AMG 256 using a sensitive and drug-tolerant ACE assay. If a sample tested positive for anti-AMG 256 antibodies, the sample was subsequently tested for antibodies that cross-react with endogenous human IL-21 using an independent assay. Lastly, if positive for binding to both AMG 256 and endogenous human IL-21, the sample was also tested for the ability to neutralize endogenous IL-21 in a cell-based assay (Figure 4B). A human anti-AMG 256 IgE assay was also developed in the event that hypersensitivity was observed and required further investigation.

Upon dosing cohorts 1 and 2, a robust antibody response to AMG 256 was observed. For the cohort 1 subject, the magnitude of the response increased steadily throughout the first 11 cycles and likely saturated the immunoassay at a S/N of over 10,000 (Figure 5A). In cohort 2, the magnitude of the ADA response increased nearly 1000-fold between the 2nd and 3rd doses of AMG 256. The anti-AMG 256 antibodies observed in cohorts 1 and 2 also cross-reacted with endogenous IL-21 with much lower magnitude (Figure 5B), supporting the hypothesis that the IL-21 mutein was driving the antibody response to the 22D4 domain. Both subjects with anti-IL-21 antibodies also tested positive for neutralizing antibodies to endogenous IL-21 throughout most of their time on study (Supplementary Table 1).

As the study progressed to higher doses in cohorts 3 and beyond, the incidence of anti-AMG 256 antibodies remained high (Table 2); however, the magnitude of the antibody responses was significantly reduced compared to cohorts 1 and 2, and most subjects had S/N values in the single digits (Figure 5C). Only one

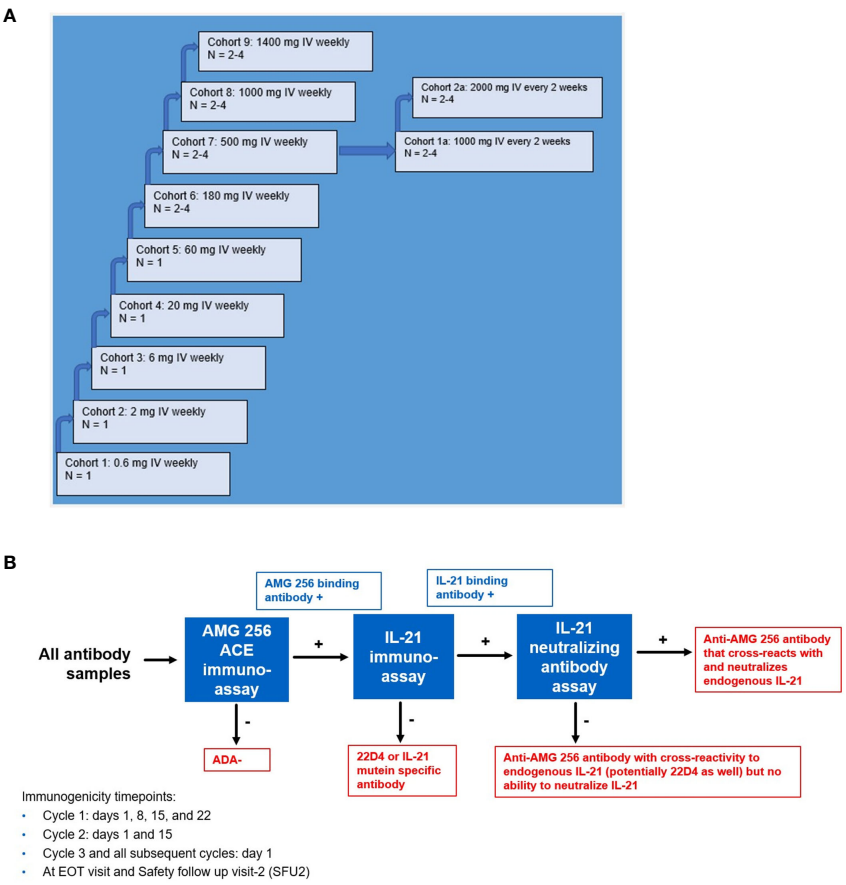

FIGURE 4
Study schema for first-in-human NCT04362748 and immunogenicity testing strategy. **(A)** NCT04362748 was designed as a multiple ascending dose phase 1 study to assess safety, tolerability, and PK/PD. **(B)** A comprehensive antibody testing strategy was implemented to monitor all anti-AMG 256 antibodies and the possibility of anti-AMG 256 antibodies that cross-react with and neutralize endogenous IL-21. End results are shown in red boxes. Results that require further characterization are shown in blue boxes.

10.3389/fimmu.2024.1345473

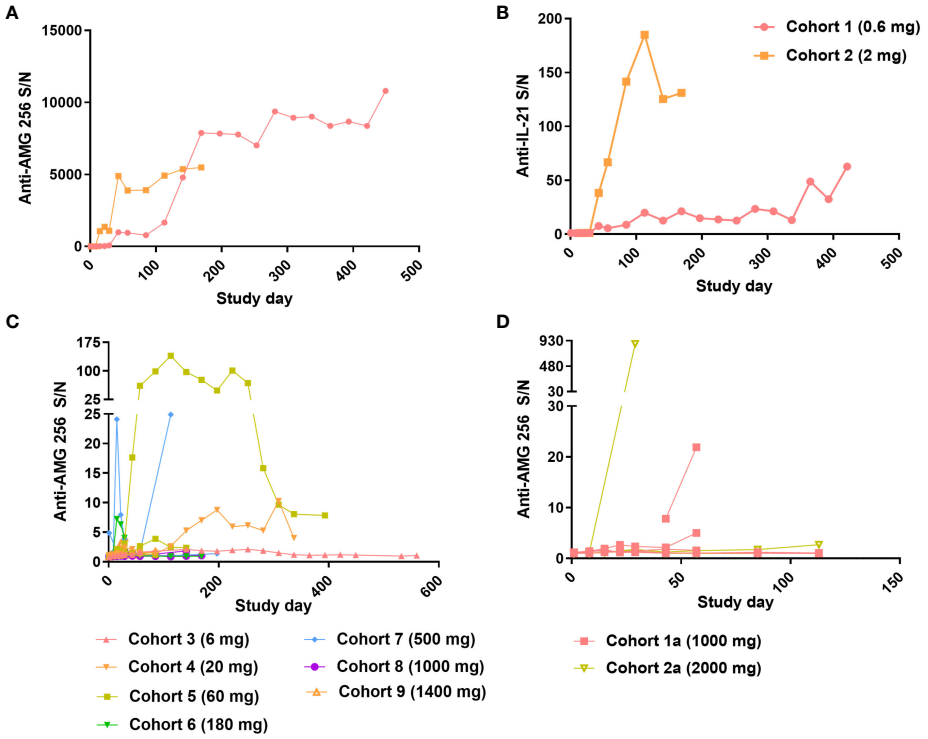

FIGURE 5
Robust antibody response observed at low doses of AMG 256. For cohorts 1 and 2, Anti-AMG 256 S/N **(A)** and anti-IL-21 S/N **(B)** are plotted by study day. For QW dosing cohorts 3 through 9 **(C)** and Q2W dosing cohorts 1a and 2a **(D)**, anti-AMG 256 S/N is shown by study day. Only subjects with at least one positive anti-AMG 256 antibody test result are shown, and individual subjects are shown for each cohort using the same color.

TABLE 2 Incidence of treatment emergent[a] binding and neutralizing antibodies in NCT04362748.

Cohort	Dose (IV)	Anti-AMG 256 antibody incidence	Anti-IL-21 antibody incidence	Neutralizing anti-IL-21 incidence
1	0.6 mg QW	1/1	1/1	1/1
2	2 mg QW	1/1	1/1	1/1
3	6 mg QW	1/1	0/1	–
4	20 mg QW	2/2	0/2	–
5	60 mg QW	3/3	0/3	–
6	180 mg QW	2/3	0/2	–
7	500 mg QW	3/4[b]	1/3	0/1
8	1000 mg QW	2/4	1/2	0/1
9	1400 mg QW	4/4	1/4	0/1
1a	1000 mg Q2W	5/6[c]	0/5	–
2a	2000 mg Q2W	4/4	1/4	0/1
	Total	28/33	6/28	2/6

[a]Treatment emergent defined as a subject who is antibody positive post-baseline with a negative or no result at baseline, or a subject who is positive at baseline with a >4-fold increase in antibody magnitude (S/N value) post-baseline.
[b]All subjects in cohort 7 were ADA positive, however, 1 subject was ADA positive at baseline and did not qualify as treatment emergent.
[c]One subject had a baseline antibody sample only (ADA negative) and was excluded from the table.

subject in cohort 2a had an antibody response somewhat similar to that observed in cohorts 1 and 2 (Figure 5D).

3.6 Impact of immunogenicity on exposure

Given the high incidence of anti-AMG 256 antibodies throughout the study, it was important to assess the impact on AMG 256 exposure. In cohorts 1 and 2, AMG 256 became undetectable in serum shortly after the development of anti-AMG 256 antibodies (Figures 6A, B). In all other cohorts, exposure to AMG 256 was maintained, with no apparent impact of anti-AMG 256 antibodies (Figure 6C). One subject in cohort 2a developed a larger magnitude anti-AMG 256 antibody response with no apparent impact on exposure, however, the subject left the study before exposure could be thoroughly evaluated. Only 4 subjects were antibody negative throughout the study, and all 4 had comparable AMG 256 exposures relative to the antibody positive subjects within the same cohort.

3.7 Anti-AMG 256 IgE detected at late time points

A subset of subjects and time points in NCT04362748 were assessed for drug-specific IgE antibodies. This testing was performed to further characterize the antibody response, and was not triggered by an adverse event. Samples were selected to cover a range of doses, both early and late time points, and the full range of anti-AMG 256 antibody responses, based on the ACE assay. Post-baseline samples from a total of 16 subjects were analyzed. In the single subject cohorts 1-3, the cohort 1 subject was the only subject to test positive for anti-AMG 256 IgE, despite the cohort 2 subject exhibiting a similar, high magnitude anti-AMG 256 response by ACE (Figure 7A). Of the three subjects in cohort 5, only 1 tested positive for anti-AMG 256 IgE (Figure 7B). Both subjects positive for anti-AMG 256 IgE were positive at cycle 6 day 1 and cycle 12 day 1 (Supplementary Table 2). IgE responses were low magnitude, consistent with the low concentration of IgE in human serum relative to other immunoglobulin isotypes.

3.8 No impact of immunogenicity on safety observed

The impact of immunogenicity on safety was carefully assessed, especially in cohorts 1 and 2 given the presence of anti-IL-21 neutralizing antibodies. To determine what types of adverse events could potentially manifest as a result of an anti-IL-21 neutralizing antibody, a comprehensive literature search of compounds blocking IL-21 signaling was carried out. Several anti-IL-21 antibodies (12, 13) and an anti-IL-21R antibody (14) were identified and available clinical data were assessed. Overall, a decrease or loss of IL-21 signaling was well-tolerated, but theory and some studies suggested that loss of IL-21 signaling could cause immunosuppression relative to placebo. Based on this, adverse events in subjects with IL-21 neutralizing antibodies were carefully evaluated for any evidence of increased infections (Table 3). Subjects with neutralizing antibodies to IL-21 and subjects with anti-AMG 256 antibodies only (no cross-reactivity to endogenous IL-21) had adverse event profiles similar to antibody negative subjects, and there was no discernable impact of immunogenicity on safety.

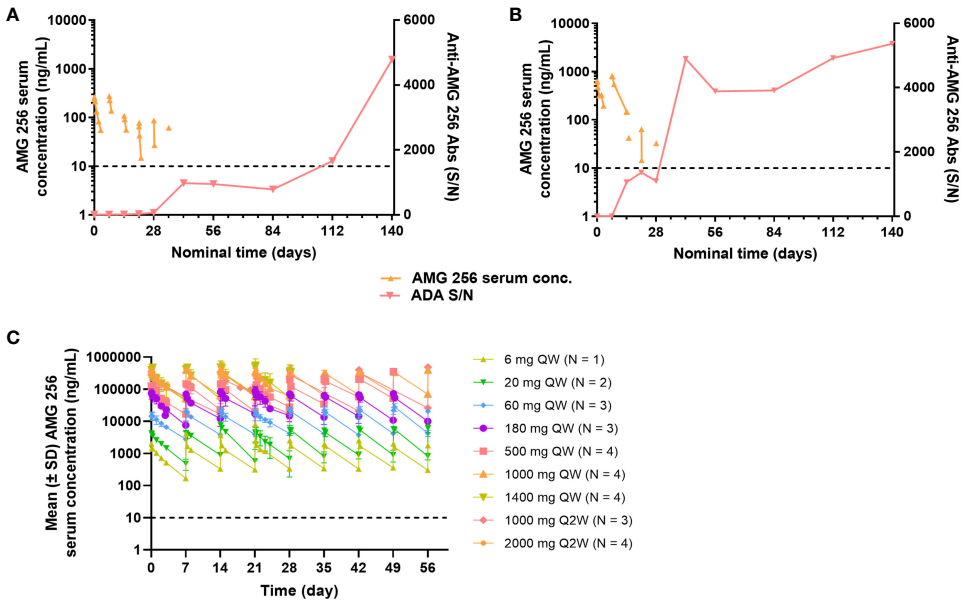

FIGURE 6
Anti-AMG 256 antibodies significantly impact exposure at low doses. The anti-AMG 256 antibody response S/N is plotted with serum concentration of AMG 256 for cohort 1 **(A)** and cohort 2 **(B)**. **(C)** Serum levels of AMG 256 are shown for cohort 3 and all subsequent cohorts. The lower limit of quantitation for the PK assay (10 ng/mL) is indicated by the dashed line.

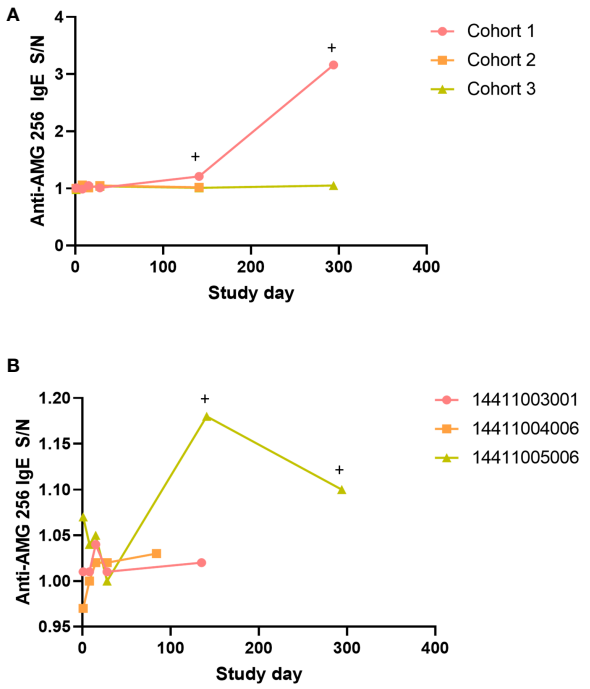

FIGURE 7
Anti-AMG 256 IgE antibodies detected in two subjects. The anti-AMG 256 IgE antibody response S/N is plotted for the single dose cohorts 1-3 **(A)** and cohort 5 **(B)**. Positive time points are denoted by a +. No anti-AMG 256 IgE positive subjects were identified in the other cohorts tested (4, 7, 1a).

Furthermore, given the risk of an anti-AMG 256 IgE response based on IL-21 biology and observations in AMG 256 nonclinical studies, subjects were carefully monitored for hypersensitivity reactions. The presence of anti-AMG 256 IgE in two subjects from NCT04362748 confirmed that all the precautions taken in the study design were appropriate. However, there was no apparent impact of the drug-specific IgE on safety (Table 3).

4 Discussion

Many of the observed effects of AMG 256 in the nonclinical studies in cynomolgus monkeys were consistent with expected pharmacology (15–20). Observations in each AMG 256 study were consistent in their timing (occurring after administration of at least two doses, typically being noted on day 15) and were suggestive of hypersensitivity (including observations of redness, mydriasis, emesis, salivation, decreased activity, coughing, and sneezing). Evidence of complement activation was demonstrated in the exploratory toxicology study, confirming the presence of immune complexes. The administration of biotherapeutics to nonclinical species often leads to the development of immunogenicity and formation of ADAs (21–23); consistent with data reported in these published case studies, observations in monkeys administered AMG 256 included weakness, hunched posture, decreased activity, mydriasis, emesis, hypersalivation, red or pale skin, diarrhea, and loss of consciousness. Clinical pathology changes included reductions in red cell parameters (RBC count, hemoglobin concentration, and hematocrit), thrombocytopenia, prolonged coagulation parameters (PT and aPTT), and acute phase reactions (ie, decreased albumin and increased globulin, increased fibrinogen). Together, these data were indicative of an immunogenicity-related response and are broadly consistent with published case studies.

In the first in human study, a high incidence of anti-AMG 256 antibodies was observed. Based on the amino acid sequence of AMG 256, together with the results of the *in vitro* immunogenicity risk assessment, this was unexpected. The 22D4 clone is a fully human antibody, and the IL-21 mutein domain contains only two point mutations.

While nonclinical studies typically do not predict the risk of immunogenicity in humans (24), in this case, they were informative. Because the fundamental function of IL-21 is similar in cynomolgus monkeys and humans, the IL-21-dependent enhancement of the anti-22D4 antibody response observed in cynomolgus monkey PK/PD and toxicology studies indicated a heightened risk of immunogenicity in humans. While a high incidence of anti-AMG 256 antibodies was observed in NCT04362748, no consequences of this immune response were observed during the study, except for loss of exposure at the two lowest doses.

There are at least 2 potential mechanisms for the unique, dose-dependent immunogenicity observed in NCT04362748. One hypothesis is that when the complementarity-determining regions of the 22D4 domain of AMG 256 are recognized by a B cell, AMG 256 has the potential to both cross-link the BCR receptor and deliver an IL-21 signal, which can lead to plasma cell differentiation (25). Such a mechanism could lead to selective plasma cell expansion of drug-specific B cells. As the dose is increased, cross-linking of the BCR becomes less optimal, and thus the antibody response is mitigated.

An alternative hypothesis is that AMG 256 effectively signals to follicular T helper cells (T_{FH}) in the germinal center (GC T_{FH}), which highly express PD-1 (26). At low doses of AMG 256, this PD-1-targeted IL-21 signal could lead to enhancement of antibody responses by mediating expansion of GC T_{FH} and/or enhancement of GC T_{FH} activity. At high doses of AMG 256, the IL-21 mutein domain could lead to activation induced cell death of B cells, largely countering the GC T_{FH} -driven mechanism and keeping the antibody response in check (27).

Given the small number of subjects in cohorts 1 and 2, the antibody responses observed may have been due to chance and unrelated to dose. Given the robust nature and unique characteristics of these responses relative to all other dosed subjects, this seems unlikely, but cannot entirely be ruled out without dosing additional subjects at these levels (not feasible for ethical reasons as the dose levels in cohorts 1 and 2 are expected to be sub-efficacious).

While the incidence of ADA often fades as dose increases due to insufficient drug tolerance of the ADA assay, this does not appear to be the case in this study. The ACE method was validated to detect low levels of ADA in the presence of trough levels of AMG 256 throughout the dose escalation cohorts. The nature of the anti-AMG 256 antibody response changed in cohort 3, at which point the levels of AMG 256 in serum are approximately 500-fold below where drug would start to interfere in ADA detection.

10.3389/fimmu.2024.1345473

TABLE 3 Treatment-related, treatment-emergent adverse events and immunogenicity in NCT04362748[a,b].

Cohort	1[d,e] (n=1)	2[d] (n=1)	3 (n=1)	4 (n=2)	5[e] (n=3)	6 (n=3)		7 (n=4)	8[f] (n=4)		9 (n=4)	1a (n=7)		2a (n=4)
ADA status[c]	Pos	Pos	Pos	Pos	Pos	Pos	Neg	Pos	Pos	Neg	Pos	Pos	Neg	Pos
All treatment-related, treatment-emergent AEs	1	1	1	2	3	2	1	1	1	1	2	4	2	4
Blood and lymphatic system disorders	0	0	0	0	0	1	0	0	0	0	1	1	1	1
Endocrine disorders	0	0	0	2	2	1	0	0	0	1	0	1	0	1
Eye disorders	0	0	0	0	0	0	0	0	1	0	0	0	0	0
Gastrointestinal disorders	0	0	0	0	1	0	0	0	0	0	0	1	1	1
General disorders and administration site conditions	0	0	1	2	0	2	0	0	0	0	1	2	0	1
Hepatobiliary disorders	0	0	0	0	0	0	0	0	1	0	0	0	0	0
Immune system disorders	0	0	0	0	1	0	0	0	0	0	1	0	0	0
Infections and infestations	0	0	0	0	1	0	0	0	0	0	0	0	0	0
Injury, poisoning and procedural complications	0	0	0	0	0	0	0	0	0	1	0	0	0	0
Investigations[g]	0	1	1	1	1	1	1	0	1	0	0	1	0	1
Metabolism and nutrition disorders	0	0	0	0	0	1	0	0	0	0	0	0	0	0
Musculoskeletal and connective tissue disorders	0	0	0	0	1	0	0	0	1	0	0	0	1	3
Neoplasms benign, malignant, and unspecified	0	0	0	0	0	0	0	0	1	0	0	0	0	0
Nervous system disorders	1	0	0	1	0	0	0	0	0	0	0	0	0	1
Renal and urinary disorders	0	0	0	0	0	0	0	0	0	0	0	0	1	0
Skin and subcutaneous tissue disorders	0	0	0	1	3	0	0	1	1	1	0	0	0	0
Vascular disorders	0	0	0	0	1	0	0	0	0	0	0	0	0	0

[a]Subject incidence of adverse events by System Organ Class (SOC), for adverse events considered by the study investigator to be at least possibly related to investigative product.
[b]Medical Dictionary for Regulatory Activities version 25.1 (MedDRA).
[c]Defined as positive for anti-AMG 256 antibodies at any time.
[d]One subject in each of cohorts 1 and 2 developed neutralizing antibodies to endogenous IL-21. In theory, these two subjects may have been considered at increased risk of experiencing infection events. However, these two subjects experienced no adverse events considered causally related to investigative product within the SOC "Infections and Infestations.".
[e]Each of cohorts 1 and 5 included one subject positive for anti-AMG 256 IgE. In theory, these two subjects may have been considered at increased risk of experiencing hypersensitivity adverse events. Adverse events of hypersensitivity would be reported generally within the SOC "Immune System Disorders." For these cohorts, within "Immune System Disorders," the only adverse event considered causally related to investigative product was one subject (IgE negative) who experienced CRS in cohort 5. (One subject in cohort 9 also experienced a causally related CRS.) Notably, no study subject in any cohort experienced any reported hypersensitivity event considered causally related to investigative product.
[f]One ADA negative cohort 8 subject experienced a causally related Infusion-related reaction event, falling within the "Injury, poisoning and procedural complications" SOC.
[g]Investigations comprised of an increase in alanine aminotransferase, aspartate aminotransferase, blood creatine phosphokinase, blood creatinine, gamma-glutamyltransferase, troponin, or a decrease in white blood count.

AMG 256 represents a rare instance where drug-specific IgE was assessed both nonclinically and in humans using sensitive and drug tolerant assays. The literature on the role of IL-21 and class switching to IgE is mixed with most studies indicating that IL-21 is a negative regulator of IgE class switching (28–31). However, a small set of studies indicate IL-21 can induce IgE secretion (10, 11, 32). Consequently, there are two plausible pathways by which AMG 256 could potentiate a class switch to IgE. One possibility is that in the context of AMG 256 administration, the IL-21 domain directly promotes IgE production. Alternatively, it's possible that AMG 256 administration elicits an anti-IL-21 antibody response that cross-reacts with and neutralizes IL-21 (a negative regulator of IgE in this case), thereby promoting class switching to IgE. The human IgE data favor the hypothesis that AMG 256-induced IL-21 signaling promotes the switch to IgE, since there was no apparent association between drug-specific IgE and neutralizing antibodies to IL-21.

While drug-specific IgE was detected in both nonclinical and human studies, hypersensitivity was only observed nonclinically. There are several potential reasons for this discrepancy. In cynomolgus monkey studies, only a subset of IgE positive animals developed hypersensitivity. It's possible hypersensitivity was not observed in NCT04362748 because of the small number of subjects evaluated (2 of 16 subjects were IgE positive). Drug concentrations, levels of anti-AMG 256 IgG (and perhaps other isotypes), and receptor expression levels could all impact the likelihood of type I hypersensitivity, with a reaction only occurring when each of these variables are within a certain range (33). Furthermore, drug-specific IgE was not observed until cycle 6 in NCT04362748, compared to in nonclinical studies where it was observed as early as day 15, suggesting that the underlying mechanism for elicitation of IgE may differ between the cynomolgus monkey and human studies.

Overall, the nonclinical and FIH study data described in this report highlight a novel mechanism of immunogenicity, where a cytokine mutein domain facilitates an ADA response. As protein therapeutics become more complex and incorporate varied functional domains, it will be important to consider all the potential ways each domain can signal to immune cells and contribute to the development of immunogenicity. This MOA-based assessment of immunogenic risk is as important as traditional sequence-based assessments (ie looking for T cell epitopes). This study also yields important insights into how nonclinical studies can, in rare cases, be used to inform on the risk of immunogenicity in humans.

Data availability statement

Qualified researchers may request data from Amgen clinical studies. Requests to access the datasets should be directed to https://wwwext.amgen.com/science/clinical-trials/clinical-data-transparency-practices/clinical-trial-data-sharing-request/.

Ethics statement

The studies involving humans were approved by the Institutional Review Board for each study site. The studies were conducted in accordance with the local legislation and institutional requirements. The participants provided their written informed consent to participate in this study. The animal study was approved by Charles River Laboratories Institutional Animal Care and Use Committee. The study was conducted in accordance with the local legislation and institutional requirements.

Author contributions

MK: Conceptualization, Data curation, Formal analysis, Methodology, Writing – original draft, Writing – review & editing. MM: Conceptualization, Data curation, Methodology, Writing – original draft, Writing – review & editing. CZ: Conceptualization, Data curation, Formal analysis, Investigation, Methodology, Supervision, Writing – original draft, Writing – review & editing. XZ: Conceptualization, Data curation, Formal analysis, Writing – original draft, Writing – review & editing. KC: Conceptualization, Data curation, Formal analysis, Supervision, Writing – original draft, Writing – review & editing. MA: Conceptualization, Data curation, Formal analysis, Writing – original draft, Writing – review & editing. ML: Data curation, Formal analysis, Supervision, Writing – original draft, Writing – review & editing. JW: Data curation, Formal analysis, Methodology, Writing – original draft, Writing – review & editing. SH: Formal analysis, Methodology, Writing – original draft, Writing – review & editing. GS: Data curation, Methodology, Writing – original draft, Writing – review & editing. FA: Conceptualization, Data curation, Formal analysis, Methodology, Writing – original draft, Writing – review & editing. EA: Conceptualization, Data curation, Supervision, Writing – review & editing. EC: Conceptualization, Data curation, Supervision, Writing – review & editing. RG: Conceptualization, Data curation, Supervision, Writing – review & editing. MH: Conceptualization, Data curation, Supervision, Writing – review & editing. SG: Conceptualization, Methodology, Writing – review & editing. DM: Conceptualization, Methodology, Supervision, Writing – original draft, Writing – review & editing.

Funding

The author(s) declare financial support was received for the research, authorship, and/or publication of this article. This research was funded by Amgen.

Acknowledgments

NCT04362748 was sponsored by Amgen. The authors would like to thank Hansen Wong, Nooshin Hashemi Sadraei, Stephanie Lee, and Pablo Martinez for their support of AMG 256 and NCT04362748.

Conflict of interest

MK, MS, CZ, XZ, KC, MA, ML, JW, SH, GS, FA, SG, and DM were employees of Amgen during the time the study was being conducted.

The remaining authors declare that the research was conducted in the absence of any commercial or financial relationships that could be construed as a potential conflict of interest.

Publisher's note

All claims expressed in this article are solely those of the authors and do not necessarily represent those of their affiliated organizations, or those of the publisher, the editors and the reviewers. Any product that may be evaluated in this article, or claim that may be made by its manufacturer, is not guaranteed or endorsed by the publisher.

Supplementary material

The Supplementary Material for this article can be found online at: https://www.frontiersin.org/articles/10.3389/fimmu.2024.1345473/full#supplementary-material

References

1. Ohaegbulam KC, Assal A, Lazar-Molnar E, Yao Y, Zang X. Human cancer immunotherapy with antibodies to the PD-1 and PD-L1 pathway. *Trends Mol Med* (2015) 21(1):24–33. doi: 10.1016/j.molmed.2014.10.009

2. Seidel JA, Otsuka A, Kabashima K. Anti-PD-1 and Anti-CTLA-4 Therapies in Cancer: Mechanisms of Action, Efficacy, and Limitations. *Front Oncol* (2018) 8:86. doi: 10.3389/fonc.2018.00086

3. Leonard WJ, Spolski R. Interleukin-21: a modulator of lymphoid proliferation, apoptosis and differentiation. *Nat Rev Immunol* (2005) 5(9):688–98. doi: 10.1038/nri1688

4. Hinrichs CS, Spolski R, Paulos CM, Gattinoni L, Kerstann KW, Palmer DC, et al. IL-2 and IL-21 confer opposing differentiation programs to CD8+ T cells for adoptive immunotherapy. *Blood* (2008) 111(11):5326–33. doi: 10.1182/blood-2007-09-113050

5. Lewis KE, Selby MJ, Masters G, Valle J, Dito G, Curtis WR, et al. Interleukin-21 combined with PD-1 or CTLA-4 blockade enhances antitumor immunity in mouse tumor models. *Oncoimmunology* (2017) 7(1):e1377873. doi: 10.1080/2162402X.2017.1377873

6. Shen S, Sckisel G, Sahoo A, Lalani A, Otter DD, Pearson J, et al. Engineered IL-21 Cytokine Muteins Fused to Anti-PD-1 Antibodies Can Improve CD8+ T Cell Function and Anti-tumor Immunity. *Front Immunol* (2020) 11:832. doi: 10.3389/fimmu.2020.00832

7. UniProt: the universal protein knowledgebase. *Nucleic Acids Res* (2017) 45(D1):D158–d69. doi: 10.1093/nar/gkw1099

8. Parrish-Novak J, Dillon SR, Nelson A, Hammond A, Sprecher C, Gross JA, et al. Interleukin 21 and its receptor are involved in NK cell expansion and regulation of lymphocyte function. *Nature* (2000) 408(6808):57–63. doi: 10.1038/35040504

9. Bautista AC, Salimi-Moosavi H, Jawa V. Universal immunoassay applied during early development of large molecules to understand impact of immunogenicity on biotherapeutic exposure. *AAPS J* (2012) 14(4):843–9. doi: 10.1208/s12248-012-9403-0

10. Avery DT, Ma CS, Bryant VL, Santner-Nanan B, Nanan R, Wong M, et al. STAT3 is required for IL-21-induced secretion of IgE from human naive B cells. *Blood* (2008) 112(5):1784–93. doi: 10.1182/blood-2008-02-142745

11. Caven TH, Sturgill JL, Conrad DH. BCR ligation antagonizes the IL-21 enhancement of anti-CD40/IL-4 plasma cell differentiation and IgE production found in low density human B cell cultures. *Cell Immunol* (2007) 247(1):49–58. doi: 10.1016/j.cellimm.2007.07.007

12. Ignatenko S, Skrumsager BK, Mouritzen U. Safety, PK, and PD of recombinant anti-interleukin-21 monoclonal antibody in a first-in-human trial. *Int J Clin Pharmacol Ther* (2016) 54(4):243–52. doi: 10.5414/CP202474

13. Hussaini A, Mukherjee R, Berdieva DM, Glogowski C, Mountfield R, Ho PTC. A Double-Blind, Phase I, Single Ascending Dose Study to Assess the Safety, Pharmacokinetics, and Pharmacodynamics of BOS161721 in Healthy Subjects. *Clin Transl Sci* (2020) 13(2):337–44. doi: 10.1111/cts.12715

14. Hua F, Comer GM, Stockert L, Jin B, Nowak J, Pleasic-Williams S, et al. Anti-IL21 receptor monoclonal antibody (ATR-107): Safety, pharmacokinetics, and pharmacodynamic evaluation in healthy volunteers: a phase I, first-in-human study. *J Clin Pharmacol* (2014) 54(1):14–22. doi: 10.1002/jcph.158

15. Davis ID, Skrumsager BK, Cebon J, Nicholaou T, Barlow JW, Moller NP, et al. An open-label, two-arm, phase I trial of recombinant human interleukin-21 in patients with metastatic melanoma. *Clin Cancer Res* (2007) 13(12):3630–6. doi: 10.1158/1078-0432.CCR-07-0410

16. Davis ID, Brady B, Kefford RF, Millward M, Cebon J, Skrumsager BK, et al. Clinical and biological efficacy of recombinant human interleukin-21 in patients with stage IV malignant melanoma without prior treatment: a phase IIa trial. *Clin Cancer Res* (2009) 15(6):2123–9. doi: 10.1158/1078-0432.CCR-08-2663

17. Grunwald V, Desar IM, Haanen J, Fiedler W, Mouritzen U, Olsen MW, et al. A phase I study of recombinant human interleukin-21 (rIL-21) in combination with sunitinib in patients with metastatic renal cell carcinoma (RCC). *Acta Oncol* (2011) 50(1):121–6. doi: 10.3109/0284186X.2010.509104

18. Thompson JA, Curti BD, Redman BG, Bhatia S, Weber JS, Agarwala SS, et al. Phase I study of recombinant interleukin-21 in patients with metastatic melanoma and renal cell carcinoma. *J Clin Oncol* (2008) 26(12):2034–9. doi: 10.1200/JCO.2007.14.5193

19. Timmerman JM, Byrd JC, Andorsky DJ, Yamada RE, Kramer J, Muthusamy N, et al. A phase I dose-finding trial of recombinant interleukin-21 and rituximab in relapsed and refractory low grade B-cell lymphoproliferative disorders. *Clin Cancer Res* (2012) 18(20):5752–60. doi: 10.1158/1078-0432.CCR-12-0456

20. Waggie KS, Holdren MS, Byrnes-Blake K, Pedersen S, Ponce R, Hughes S, et al. Preclinical safety, pharmacokinetics, and pharmacodynamics of recombinant human interleukin-21 in cynomolgus macaques (Macaca fascicularis). *Int J Toxicol* (2012) 31(4):303–16. doi: 10.1177/1091581812449661

21. Heyen JR, Rojko J, Evans M, Brown TP, Bobrowski WF, Vitsky A, et al. Characterization, biomarkers, and reversibility of a monoclonal antibody-induced immune complex disease in cynomolgus monkeys (Macaca fascicularis). *Toxicol Pathol* (2014) 42(4):765–73. doi: 10.1177/0192623314522559

22. Kronenberg S, Husar E, Schubert C, Freichel C, Emrich T, Lechmann M, et al. Comparative assessment of immune complex-mediated hypersensitivity reactions with biotherapeutics in the non-human primate: Critical parameters, safety and lessons for future studies. *Regul Toxicol Pharmacol* (2017) 88:125–37. doi: 10.1016/j.yrtph.2017.06.004

23. Leach MW, Rottman JB, Hock MB, Finco D, Rojko JL, Beyer JC. Immunogenicity/hypersensitivity of biologics. *Toxicol Pathol* (2014) 42(1):293–300. doi: 10.1177/0192623313510987

24. Ponce R, Abad L, Amaravadi L, Gelzleichter T, Gore E, Green J, et al. Immunogenicity of biologically-derived therapeutics: assessment and interpretation of nonclinical safety studies. *Regul Toxicol Pharmacol* (2009) 54(2):164–82. doi: 10.1016/j.yrtph.2009.03.012

25. Ettinger R, Sims GP, Fairhurst AM, Robbins R, da Silva YS, Spolski R, et al. IL-21 induces differentiation of human naive and memory B cells into antibody-secreting plasma cells. *J Immunol* (2005) 175(12):7867–79. doi: 10.4049/jimmunol.175.12.7867

26. Kroenke MA, Eto D, Locci M, Cho M, Davidson T, Haddad EK, et al. Bcl6 and Maf cooperate to instruct human follicular helper CD4 T cell differentiation. *J Immunol* (2012) 188(8):3734–44. doi: 10.4049/jimmunol.1103246

27. Leonard WJ, Zeng R, Spolski R. Interleukin 21: a cytokine/cytokine receptor system that has come of age. *J Leukoc Biol* (2008) 84(2):348–56. doi: 10.1189/jlb.0308149

28. Suto A, Nakajima H, Hirose K, Suzuki K, Kagami S, Seto Y, et al. Interleukin 21 prevents antigen-induced IgE production by inhibiting germ line C(epsilon) transcription of IL-4-stimulated B cells. *Blood* (2002) 100(13):4565–73. doi: 10.1182/blood-2002-04-1115

29. Ozaki K, Spolski R, Feng CG, Qi CF, Cheng J, Sher A, et al. A critical role for IL-21 in regulating immunoglobulin production. *Science* (2002) 298(5598):1630–4. doi: 10.1126/science.1077002

30. Minegishi Y, Saito M, Tsuchiya S, Tsuge I, Takada H, Hara T, et al. Dominant-negative mutations in the DNA-binding domain of STAT3 cause hyper-IgE syndrome. *Nature* (2007) 448(7157):1058–62. doi: 10.1038/nature06096

31. Yang Z, Wu CM, Targ S, Allen CDC. IL-21 is a broad negative regulator of IgE class switch recombination in mouse and human B cells. *J Exp Med* (2020) 217(5). doi: 10.1084/jem.20190472

32. Caven TH, Shelburne A, Sato J, Chan-Li Y, Becker S, Conrad DH. IL-21 dependent IgE production in human and mouse *in vitro* culture systems is cell density and cell division dependent and is augmented by IL-10. *Cell Immunol* (2005) 238(2):123–34. doi: 10.1016/j.cellimm.2006.03.001

33. Finkelman FD, Khodoun MV, Strait R. Human IgE-independent systemic anaphylaxis. *J Allergy Clin Immunol* (2016) 137(6):1674–80. doi: 10.1016/j.jaci.2016.02.015

frontiers | Frontiers in Immunology

TYPE Review
PUBLISHED 15 May 2024
DOI 10.3389/fimmu.2024.1399438

OPEN ACCESS

EDITED BY
Michael Tovey,
Svar Life Science, France

REVIEWED BY
Alastair Dg Lawson,
UCB Pharma, United Kingdom
Piero Pileri,
Toscana Life Sciences, Italy
Pierpaolo Bruscolini,
University of Zaragoza, Spain

*CORRESPONDENCE
Charlotte M. Deane
deane@stats.ox.ac.uk

RECEIVED 11 March 2024
ACCEPTED 02 May 2024
PUBLISHED 15 May 2024

CITATION
Gordon GL, Raybould MIJ, Wong A and Deane CM (2024) Prospects for the computational humanization of antibodies and nanobodies.
Front. Immunol. 15:1399438.
doi: 10.3389/fimmu.2024.1399438

Prospects for the computational humanization of antibodies and nanobodies

Gemma L. Gordon, Matthew I. J. Raybould, Ashley Wong and Charlotte M. Deane*

Oxford Protein Informatics Group, Department of Statistics, University of Oxford, Oxford, United Kingdom

To be viable therapeutics, antibodies must be tolerated by the human immune system. Rational approaches to reduce the risk of unwanted immunogenicity involve maximizing the 'humanness' of the candidate drug. However, despite the emergence of new discovery technologies, many of which start from entirely human gene fragments, most antibody therapeutics continue to be derived from non-human sources with concomitant humanization to increase their human compatibility. Early experimental humanization strategies that focus on CDR loop grafting onto human frameworks have been critical to the dominance of this discovery route but do not consider the context of each antibody sequence, impacting their success rate. Other challenges include the simultaneous optimization of other drug-like properties alongside humanness and the humanization of fundamentally non-human modalities such as nanobodies. Significant efforts have been made to develop *in silico* methodologies able to address these issues, most recently incorporating machine learning techniques. Here, we outline these recent advancements in antibody and nanobody humanization, focusing on computational strategies that make use of the increasing volume of sequence and structural data available and the validation of these tools. We highlight that structural distinctions between antibodies and nanobodies make the application of antibody-focused *in silico* tools to nanobody humanization non-trivial. Furthermore, we discuss the effects of humanizing mutations on other essential drug-like properties such as binding affinity and developability, and methods that aim to tackle this multi-parameter optimization problem.

KEYWORDS

humanization, humanness, antibody, nanobody, computational, therapeutics

Introduction

An immunogenic response against a therapeutic antibody, including the production of anti-drug antibodies (ADAs), can reduce drug efficacy and negatively impact the patient (1). It is critical that this risk is minimized ahead of a drug entering human trials.

The earliest experimental approaches to discover target-specific therapeutic antibodies involved inoculating a non-human organism with the antigen of interest to raise

complementary antibodies. If these antibody clones were to be injected directly into a human patient, an anti-drug immune response would be a very likely outcome, as was found to be the case for the first monoclonal antibody therapy, Muromonab (2).

Logic would suggest that the immunogenicity of a non-human biologic might be mitigated by somehow increasing its 'humanness', loosely defined as similarity to antibodies raised naturally and tolerated by healthy human immune systems. This theory has sparked the development of an array of technologies to 'humanize' non-human antibodies. Though numerous techniques to discover genetically human antibodies have also been developed, such as constructing phage/yeast display libraries, using transgenic mice, or isolating antibodies directly from convalescent humans (3), it is striking that most recent therapeutics still derive from non-human organism inoculation followed by humanization (Figure 1; 4).

Therefore, resolving outstanding challenges within this long-established field remains highly relevant. For example, grafting strategies that load non-human complementary-determining regions (CDRs) onto human framework scaffolds are unsuccessful when the variable loops play a role in immunogenicity and can compromise other key developability properties. Increasingly, computational approaches are offering a route toward identifying and mitigating factors contributing to immunogenicity, as well as enabling the simultaneous optimization of other drug-like properties alongside humanness (5).

Additional challenges are posed by nanobodies, a fundamentally non-human modality deriving from camelids (VHHs) or cartilaginous fish (VNARs) (6, 7), which are emerging as a promising therapeutic format. Their smaller size facilitates expression, improves tumor penetration, and increases solubility, while maintaining comparable binding affinity to conventional antibodies (8–13). However, structural differences between antibodies and nanobodies affect how they interact with their antigens (14). Therefore, it is likely that many humanization protocols designed for conventional antibodies, particularly computational tools, are not immediately applicable to nanobodies.

Previous reviews cover experimental humanization approaches for conventional antibodies, such as CDR grafting or resurfacing (15, 16). More recent publications address the use of machine learning in the antibody discovery field, including *in silico* methods for humanization, humanness scoring and immunogenicity prediction within the broader scope of antibody design (5, 17–22), and draw attention to the need for multi-parameter optimization (23, 24). Focus is largely placed on the development of conventional antibodies as opposed to alternative formats, though the need for work on nanobodies is highlighted in Norman et al. (17). Rossotti et al. (7) consider nanobody humanization but focus on experimental rather than computational methods.

In this review, we start by introducing early approaches to humanization and, more broadly, how the immunogenicity of an antibody can be quantified. We cover computational methodologies designed to measure humanness and direct humanization (Table 1), including the degree of evidence to support the efficacy of each protocol and their potential applicability to nanobodies. Finally, we place humanization in the wider context of antibody design and multi-parameter optimization, highlighting the need for high-quality, unbiased data to overcome the challenges that persist in this field.

Experimental approaches to humanization

Experimental methods seek to reduce the immunogenicity of an antibody by increasing the human portion of its variable domains (Figure 2). The first broadly applicable strategy to achieve this was chimerization, the grafting of a non-human variable region onto human constant domains (44).

Further increases in the humanness of the antibody sequence were made possible by humanization techniques such as only grafting the CDRs (complementarity-determining regions) of a non-human antibody onto a human framework region (45). In theory, this approach serves to preserve binding activity, since the CDR loops tend to form most of the binding site, alongside the structural stability provided by a native framework. However, CDR grafting has often been found to require additional changes to the framework, such as back-mutations to the original non-human residue, to improve or even rescue binding (46).

Reducing the number of non-human residues even further, structures of antibody-antigen complexes have been used to determine the binding site residues of a non-human antibody and use only these from the non-human CDR loops (specificity-determining region (SDR) grafting) (47, 48). Similarly, Apgar et al. (2016) (49) developed a method to identify important binding residues and reduce immunogenic residues in non-human CDR loops, after CDR grafting.

To preserve favorable properties of the non-human antibody, humanization has also been carried out using the most closely related human germline sequences or homologous framework regions as a template (16). Alternative approaches include framework shuffling (50), where a set of framework regions representative of all human germline genes were iteratively combined with the CDR loops of a non-human antibody and their binding activity assessed. Another method, resurfacing, preserves the non-human frameworks: only surface-exposed residues which differ from human are replaced on the basis that buried residues will not impact the level of immunogenicity (51, 52).

Collectively, these experimental strategies have been widely integrated into pharmaceutical companies' preclinical therapeutic development pipelines and have yielded developable molecules, as evidenced by the ever-growing number of humanized antibodies progressing through first-in-human clinical trials (Figure 1C). Nevertheless, success remains clone dependent, and efficiencies could certainly be found in directing the humanization process, in which amino acid mutations are frequently introduced *via* trial-and-error. The concurrent integration of computational methods, which attempt to learn sequence and structural features of antibodies to predict the impact of modifications, promises to lead to more rational and efficacious humanization.

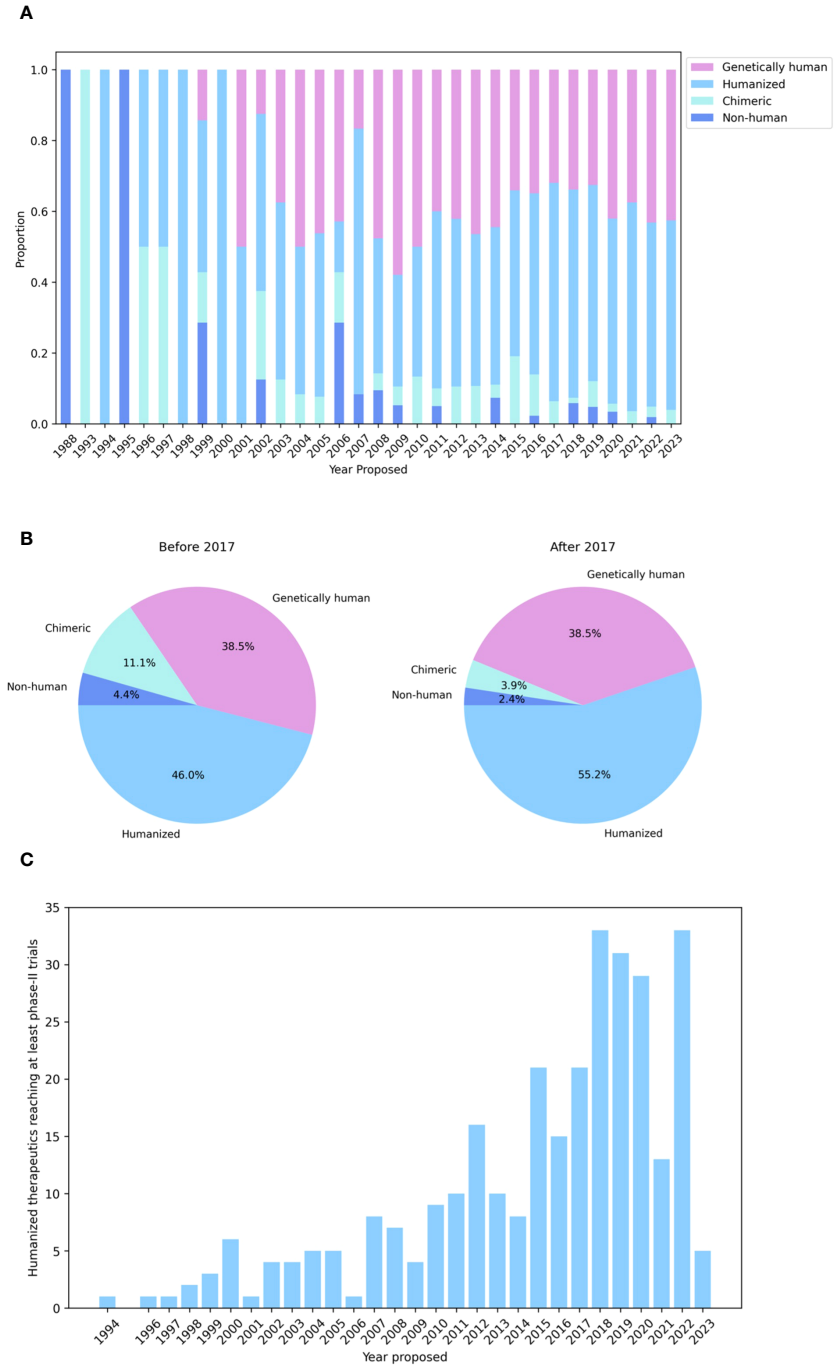

FIGURE 1
Humanization is the leading method for generating antibody therapeutics compatible with the human immune system. **(A)** Genetics of all WHO-recognized antibody- and nanobody-derived therapeutics included in the Thera-SAbDab database (4), by year of proposed International Nonproprietary Name (INN). **(B)** Developmental origins of therapeutics with a proposed INN before and after 2017 show that humanization is still the predominant means of generating antibodies for therapeutic use. **(C)** Cumulative number of humanized therapeutics recorded in Thera-SAbDab reaching at least phase-II clinical trials, by year of proposed INN. Statistics for recent therapeutics are likely to increase with time.

Quantifying the "humanness" of an antibody and its utility for computational humanization

While the most direct measure of immunogenicity is the quantification of anti-drug antibodies (ADAs), T cells, or inflammatory cytokines raised upon injection of the drug into an organism, this carries an inherent safety risk, and so indicative assays are used during early-stage development.

Computational methods have gained traction in the quantification of the humanness of a sequence, hypothesized as a proxy metric for the likelihood of immunogenicity due to the evident success of experimental grafting strategies.

TABLE 1 Summary of available computational methods for humanness scoring and humanization, in order of reference in this review.

Authors	Year	Name	Web server	Reference
Abhinandan and Martin	2007	H-score	http://www.bioinf.org.uk/abs/shab/	(25)
Thullier et al.	2010	G-score	N/A	(26)
Gao et al.	2013	T20 score	https://sam.curiaglobal.com/t20/	(27)
Lazar et al.	2007	Human String Content	N/A	(28)
Seeliger	2013	N/A	N/A	(29)
Clavero-Álvarez et al.	2018	MG-score	N/A	(30)
Schmitz et al.	2020	PGSSM score	N/A	(31)
Marks et al.	2021	Hu-mAb	https://opig.stats.ox.ac.uk/webapps/sabdab-sabpred/sabpred/humab	(32)
Prihoda et al.	2022	BioPhi	https://biophi.dichlab.org/	(33)
Uçar et al.	2023	SelfPAD	N/A	(34)
Zou et al.	2023	PLAN	N/A	(35)
Wollacott et al.	2019	N/A	N/A	(36)
Vashchenko et al.	2022	AbBERT	N/A	(37)
Choi et al.	2015, 2016	CoDAH	N/A	(38, 39)
Hsieh et al.	2022	N/A	N/A	(40)
Tennenhouse et al.	2023	CUMAb	https://cumab.weizmann.ac.il/step/cumab-terms/	(41)
Sang et al.	2022	Llamanade	http://www.llamanade.app	(42)
Ramon et al.	2023	AbNatiV	www-cohsoftware.ch.cam.ac.uk/index.php/abnativ	(43)

The expanded form for 'N/A' would be 'Not available'.

An early example of a computational humanness score is the H-score (25), which uses pairwise sequence identity to distinguish between human and non-human variable regions. The G-score was later derived from the H-score to account for the effects of the size of the corresponding human germline family (26). This was further refined to the T20 metric by Gao et al. (27), who incorporate a BLAST search, scoring by taking the average percentage sequence identity of the top 20 matching sequences. Lazar et al. (28) break sequences down into 9-mers, proposing the Human String Content (HSC) score, which is calculated by comparing the sequence identity of each 9-mer frame in a sequence to human germline sequences. Together, these methods were validated simply by demonstrating distinct distributions of humanness scores between human and non-human species. For example, Abhinandan and Martin (25) showed a separation between the mean 'raw humanness' scores and Z-scores of human and murine antibodies. Improving on this, the T20 score was shown to distinguish between chimeric, humanized, and human sequences with greater specificity than the H-score or G-score on a set of 98 therapeutic antibodies. Further to this, Gao et al. present perhaps the first quantitative benchmark between an *in silico* humanness metric and a direct measure of immunogenicity, having demonstrated on a dataset of 65 therapeutic antibodies that higher (more human) T20 scores correlate, albeit weakly (Pearson's correlation of 0.21), with lower ADA abundance.

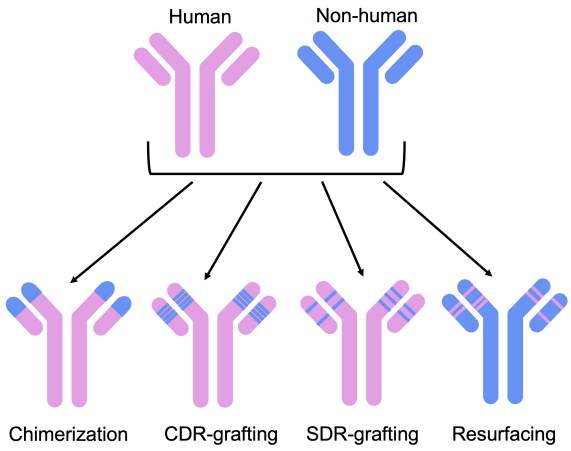

FIGURE 2
Humanization methods have evolved from initial chimerization approaches, aiming to reduce non-humanness without compromising functionality. These include CDR-grafting, where non-human CDR loops are grafted on to a human framework, SDR-grafting, where only the binding residues of the CDRs are grafted on to the framework, and resurfacing, where exposed non-human residues are replaced by human ones.

To capture higher-order relationships between amino acid residues, Seeliger (29) designed a heuristic scoring function to distinguish between human and murine antibodies, using commonly occurring mutations as a fingerprint for the species. Like previous work, their humanness scores show a small overlap between murine and human antibodies, given the shared sequence

identity of the two species. Using a statistical inference method to account for correlations between residue pairs at different positions, Clavero-Álvarez et al. (30) created an 'MG-Score' metric, finding that their approach outperforms the T20 score at differentiating between human and murine sequences, although these methods are equally predictive for the smaller therapeutic datasets tested.

Schmitz et al. (31) introduce a position- and gene-specific scoring matrix (PGSSM) metric, which uniquely uses single nucleotide frequencies to measure the similarity of a sequence to a human antibody repertoire. The authors found that human sequences scored significantly higher than other species including non-human primates, using their metric. In a broader application to antibody developability, Petersen et al. (53) use a position-specific scoring matrix representing antibody repertoire data to predict high-frequency framework mutations that could improve therapeutic properties.

Although sequence identity indicates how closely related a human antibody and non-human antibody are, it may not be the most informative metric for the purpose of humanization. More recent strategies such as those from Seeliger (29) and Clavero-Álvarez et al. (30), or those using scoring matrices could offer an advantage in that they provide insight into higher-order features: it is possible to determine which residues are most important in contributing to humanness versus which are common across species. This in turn can be used to inform the choice of mutations for humanization.

Naturally, the greater availability of sequence data (54, 55) has made *in silico* humanness scoring and humanization amenable to machine-learning methods. Hu-mAb (32) approaches this problem as a classification task, using random forest models to distinguish human from non-human sequences, achieving ROC AUC values across all classification models of 1 or close to 1. Similarly to Gao et al. (27), the authors curated an ADA benchmark dataset, this time for an enhanced set of 217 therapeutics, demonstrating a stronger correlation between higher Hu-mAb humanness scores and lower immunogenicity. They also demonstrated that therapeutics with the most severe ADAs frequently had Hu-mAb scores below 0.9.

The same dataset of 217 therapeutics was used for evaluation by Prihoda et al. (33) and Uçar et al. (34). Uçar et al. used a contrastive-learning model to predict humanness, leveraging a large body of patent data, while Prihoda et al. present the BioPhi platform, developed using Transformer architecture. BioPhi consists of tools for both humanization (Sapiens) and humanness scoring (OASis), the latter derived from the use of 9-mer peptides in the HSC scoring method (28). The platform can operate at different levels of stringency: at a medium level (a peptide is defined as human if it is found in at least 50% of subjects), OASis outperformed other humanness scoring methods, such as the aforementioned T20 and MG-scores, with a ROC AUC of 0.966, though it was comparable to the PGSSM metric from Schmitz et al. (31). Authors find a similar correlation between their humanness scores and the ADA responses to the therapeutic set, though do not outperform Hu-mAb (achieving a Pearson correlation of 0.28, compared to Hu-mAb's 0.34).

Marks et al. (2021) further validate Hu-mAb by comparing their computationally suggested mutations against a ground truth of experimentally chosen mutations for a set of 25 humanized therapeutics, all of which showed reduced immunogenicity upon humanization. Overall, they found Hu-mAb more efficiently suggested mutations that overlapped considerably with the mutations made experimentally (77%, or 85% when including residues of similar types). A similar approach is taken by Prihoda et al., (33) and Zou et al. (35), who adopt the BioPhi OASis humanness scoring method in their proposed humanization approach, which makes use of protein language models alongside a k-nearest-neighbors method to optimally select residues for humanization. Prihoda et al. expand their test set to include 152 humanized antibodies and putative parental sequences.

A metric often used to validate humanization is the change in humanness score after mutation, where scoring methods are developed using a dataset of human antibodies as a benchmark. Assuming a reliable and valid negative correlation between this humanness metric and immunogenicity, an increase in the humanness score of a putatively humanized sequence before and after mutation would indicate that humanization has been successful. This is adopted by Marks et al. (32), Zou et al. (35), Wollacott et al. (35, 36) and Vashchenko et al. (37). Long short-term memory (LSTM) models trained by Wollacott et al. on natural antibodies can be used to quantify the nativeness of antibody sequences and to select templates for humanization, based on changes in their LSTM humanness score. AbBERT (37) is an attention-based Transformer trained on 20 million unpaired sequences from OAS (55) primarily to determine humanness (for which greater humanness scores are demonstrated for human sequences over humanized and murine sequences), but embeddings can be used to optimize *in silico* antibody design. Vashchenko et al. (37) are additionally conscious of the balance between humanness and optimization of other antibody properties such as stability: authors test for expression levels, finding that in general, more human antibodies were better expressed.

Structure-guided methods for computational humanization can make use of means of validation that cannot be adopted by methods built on sequence data, given the intrinsic differences in the nature of the data used. For example, Choi et al. (38, 39), Hsieh et al. (40) and Tennenhouse et al. (41) all adopt binding affinity as their main indicator for the success of their humanization, specifically whether the affinities of their proposed humanized variants are comparable to their parental antibody.

Choi et al. present CoDAH (38, 39), which aims to produce designs that increase humanness without disrupting stability. Hsieh et al. (40) implement homology modeling and molecular dynamics simulations to compare murine and humanized CDR structures, as changes in these residues impact the resulting binding affinity. Given the effect that CDR-grafting can have on stability and affinity, Tennenhouse et al. (41) present CUMAb, which seeks to simulate this CDR-grafting onto human frameworks and select designs using an energy-based ranking. Computationally, this can be carried out at much higher throughput and CUMAb searches a more diverse structural space, testing non-homologous frameworks as well as homologous templates that are the default for CDR-grafting.

The combination of close similarity between a proposed humanized variant and human antibodies, and maintaining binding affinity, imply that humanization has successfully increased humanness without compromising native features which may contribute to binding or other favorable properties of the therapeutic. However, to evaluate the performance of these tools more robustly, the reliability of the humanness scoring method must also be considered. Additionally, while maintaining affinity is undoubtedly important in the success of a humanized antibody, relying solely on affinity for the validation of these humanization methods will not fully encapsulate their capabilities.

Overall, these computational methods capture humanness in different ways, and each have their own merits as measurements, but vary as to what extent, and by what means, they are validated as predictors of immunogenicity. An increased humanness score, the most-used validation metric across all tools, does not *de facto* guarantee reduced immunogenicity. Humanness metrics which are validated against experimental data, such as those that exhibit a correlation to the incidence of ADAs across therapeutics, or whose values support experimental humanization decisions for a case study antibody that were proven to decrease immunogenicity, might reasonably be considered more robust predictors. Furthermore, it is important to consider that machine learning approaches, which are now abundant in this field, are reliant on the data that they are built upon: humanized antibodies generated by these models will harbor the inherent biases of the training set, which could limit their real-world applicability.

Applicability of antibody humanization software to nanobodies

MAbs are significantly more established as biotherapeutics than nanobodies, meaning benchmark datasets are more readily available and so efforts thus far have been focused on developing *in silico* methods for conventional antibodies. For example, as illustrated above, a dataset of 217 therapeutics with ADA data has been used for validation of antibody-focused computational approaches. In comparison, to our knowledge, ADA data only exists for 10 nanobody therapeutics (Table 2, 56–73). This discrepancy extends to a differential availability of natural sequence data from which to build models. There are far more publicly available antibody repertoire data than nanobody repertoire data: at present, approximately 1.6 million nanobody sequences are deposited in the OAS database, compared to over 2 million paired and 2.4 billion unpaired antibody sequences (55).

However, given the increasing application of nanobodies in the therapeutic space, future work developing humanization approaches should consider their applicability to other formats and modalities. General principles for the experimental humanization of nanobodies are akin to those for antibodies, such as CDR grafting and back-mutation, resurfacing and the use of germline sequences as templates (74). However, there are additional considerations to make since antibodies and nanobodies have distinct structural features (Figure 3). Vincke et al. (9) outline the humanization of a camelid nanobody (VHH) and observe the importance of residues in the FR2 region in contributing to binding affinity. These hallmark residues, located at an equivalent position to those at the VH-VL interface in antibodies, are usually hydrophilic and are hypothesized to contribute to the increased solubility of the single-domain antibody (8, 75). Since these residues are buried and hydrophobic in conventional antibodies, *in silico* humanization tools built for antibodies may suggest changes to these residues. Although this may increase their humanness, it may also diminish the favorable properties that nanobodies possess. Furthermore, this could decrease developability and increase immunogenicity, since exposed hydrophobic residues increase aggregation propensity (76–78).

In addition to their distinct hallmark residues, nanobodies more often incorporate framework residues into their paratopes (the antigen binding site) (12, 14, 79, 80). This is critical to consider in developing computational methods based on protocols such as CDR grafting, where it may be assumed that only the CDRs contribute to antigen-binding. As highlighted by Hummer and Deane (81), this is a pitfall encountered with CUMAb (41), where their approach to entirely replace the framework during *in silico* CDR-grafting may remove critical binding residues in nanobodies.

Bespoke computational methods for nanobody humanization

Therefore, there is a need for computational methods that take the characteristic topology of nanobodies into account; the structure modeling software NanoBodyBuilder2, which outperforms AlphaFold2 by 0.55 Å over the CDR3 region, exemplifies the advantages of nanobody-specific tools (82). The development of humanization software dedicated to nanobodies is still a relatively new endeavor, the first being Llamanade (42). Sang et al. identify properties specific to Nbs by comparison with IgGs and use this as the basis for rational Nb humanization, avoiding humanization of residues that are integral to the nanobody physicochemical properties, such as highly conserved framework residues in the FR2 region and those which may contribute to the conformation of the CDR3 loop. This balance between nativeness (keeping residues critical to the unique structural properties of the nanobody) and humanness is also prioritized in AbNatiV (43), a deep-learning-based pipeline for nanobody (and antibody) humanization. Sequence data is used to train variational auto-encoders (VQ-VAE) models which quantify the similarity of a sequence to human VH or camelid VHH domains. This measure of nanobody or antibody nativeness is coupled with a sequence profile that can be used to inform engineering.

The Llamanade pipeline was assessed by calculating T20 scores (27) and conducting ELISA tests for 9 SARS-CoV-2 binders. The authors observed an increase in humanness scores, and, upon expression, 8 out of the 9 structures exhibited binding capabilities comparable to the original structures. The use of the T20 score in

TABLE 2 Nanobody therapeutics with available ADA data.

Name	Phase	Therapeutic (T)/ Placebo (P)	Total participants	% Patients with ADA	Reference
2Rs15d	-	T	20	0	(56, 57)
	-	T	20	5	
ALX-0061	I/II	T	37	0	(58–61)
	II	T	250	41	
		P	62	52	
	IIb	T	187	31	
ALX-0081	I/Ib	T	64	0	(62–64)
	II	T	36	9	
	III	T	145	3	
ALX-0141	I	T	42	0	(65)
ALX-0171	I	T	60	0	(66, 67)
	IIb	T	135	34	
		P	39	26	
ALX-0761	I	T	33	30.3	(68)
		P	8	37.5	
ATN-103	I/II	T	266	3	(69–71)
M6495: Construct 579 (2F3*SO35GS linker093*SO linkerAlb11)	-	T	50	6	(72)
M6495: Construct 581 (2F3*SO35GS linker Alb11)	-	T	50	0	(72)
TAS266	I	T	4	75	(73)

Where applicable, dose-dependent figures have been aggregated for total participants and percentage of patients with ADAs.

their evaluation invites confidence in their approach, given that Gao et al. (27) previously demonstrated some correlation between increased humanness and decreased immunogenicity. AbNatiV takes a similar approach to verify their humanness scoring, finding a negative correlation between humanness and the percentage of patients who developed ADAs for 216 therapeutic antibodies. Following Llamanade, humanization conducted by the AbNatiV pipeline is validated by the characterization of humanized variants of two nanobodies: Ramon et al. (43) find that their method improves or retains thermostability and binding compared to wild-

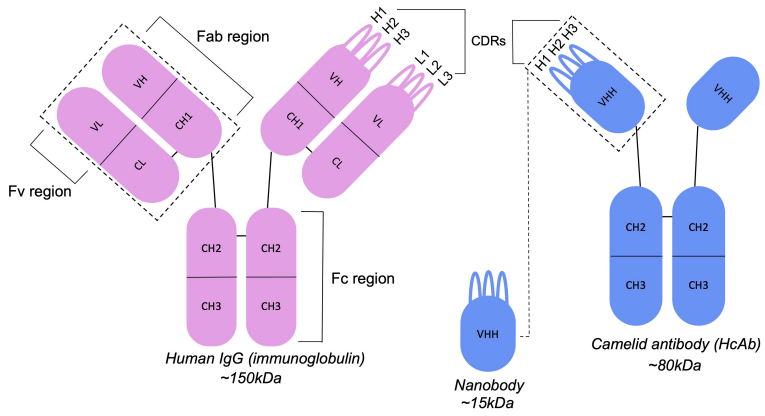

FIGURE 3
Antibodies and nanobodies differ in their structural features. Camelid nanobodies (VHHs) are derived from heavy-chain antibodies and lack the light-chain partner seen in conventional antibodies, exposing residues that would otherwise be buried at the VH-VL interface.

type variants. Both works by Sang et al. (42) and Ramon et al. (43) are subject to the same difficulties in their use of humanness scoring and affinity as their primary means of validation, as was previously discussed. This is only exacerbated by the more restricted sequence and structural data available for nanobodies, which, as highlighted by Sang et al. (42), limits opportunities to quantify the uncertainty of proposed designs.

Humanization within the multi-parameter optimization problem

All previously outlined computational approaches consider humanization in isolation, however, when designing an antibody therapeutic, it is important to be aware of the full landscape of properties that need to be optimized. Immunogenicity can originate not only from intrinsic humanness but also from developability factors, including solubility, aggregation likelihood, cross reactivity, and product heterogeneity deriving from sub-optimal chemical or thermal stability of the antibody (83–85). More broadly, the multi-parameter optimization problem may pertain to patient or treatment-related factors affecting therapeutic success. For example, a patient's immune status, such as having a chronic infection or being depleted of B cells, might impact the likelihood of observing ADAs. The personalized combination of human leukocyte antigen (HLA) alleles in each patient influences the propensity of autologous helper T cells to recognize drug fragments, and therefore activate B lymphocytes toward the expression of ADAs (86); tools such as NetMHCIIpan-4.0 (87) can survey whether drugs contain peptide fragments able to be displayed by certain Class II HLA alleles. Meanwhile, more convenient routes of administration that increase the global accessibility of a medication, such as subcutaneous injection, typically require more concentrated doses that are more susceptible to molecular aggregation and thus the induction of ADAs.

The use of computation to simultaneously optimize or select antibodies (or nanobodies) with a general set of drug-like properties represents a compelling strategy toward reducing the failure rate of candidate therapeutics and accelerating the antibody design pipeline. Excitingly, such approaches are already coming to the fore. Makowski et al. (88) assess how machine learning can be used to co-optimize the affinity and specificity of Emibetuzumab through a joint reward function. Furthermore, Bachas et al. (89) use language models to predict binding affinity alongside a 'naturalness' metric. They show that this naturalness relates to developability and immunogenicity and, as such, optimizing both affinity and naturalness together using a genetic algorithm may help to solve this multi-parameter optimization problem. There are also increasing examples of work using machine-learning to generate new sequences using antibody libraries with favorable properties as a source of high-throughput data (90, 91). Arras et al. (92) developed a semi-synthetic method to generate humanized and developable nanobodies (VHH) from camelid immunization, with minimal need for further optimization. Camelid CDR3 loops are grafted onto humanized VHH backbone libraries with diverse combinations of camelid CDR1 and CDR2 loops. The library is then filtered for developability attributes and biophysical properties are tested experimentally. In subsequent work, they combine their library approach with an LSTM model, training the model on promising sequences selected from the library, to design new humanized and developable nanobodies (93).

These library approaches show that there is potential to achieve multi-parameter optimization provided there is access to high-throughput and high-quality data for model training. However, if we are to address this problem computationally, the necessity for robust validation methods becomes even greater, since the entanglement of different antibody properties will make assessment ever more complex. In some cases, the complex interplay between developability properties may even render complete multi-parameter optimization impossible to achieve.

Discussion

Humanization is the leading technique for mitigating the immunogenicity associated with therapeutics derived from non-human sources. Primarily, this has been achieved using traditional experimental strategies such as chimerization and CDR loop grafting, alongside necessary back mutations. Nonetheless, the increased availability of sequence and structural data has now facilitated the development of machine learning-based tools for humanness scoring and humanization, which suggest case-by-case engineering strategies for each input variable region sequence and are beginning to yield promising results. While most efforts are directed toward antibody humanization, the growing interest in nanobodies and their distinct structural characteristics necessitates the consideration of humanization tools tailored for this alternative scaffold. However, these efforts are hampered by the fact that nanobody data are currently relatively limited and dispersed (Table 2, 4, 54, 55, 94). For the plethora of alternative engineered formats now available, including bispecific or multi-specific antibodies, or those with enhanced effector functions, such as an scFv-Fc, these challenges are only enhanced and currently remain understudied (95, 96).

If *in silico* humanization tools are to be routinely implemented into therapeutic design pipelines, they must be thoroughly validated, such that computationally humanized variants can be considered confidently de-risked candidates. However, an additional layer of complexity is added since validation methods themselves vary in their reliability and proximity to the overarching phenotype of immunogenicity. Furthermore, the sensitivity of direct measures of immunogenicity such as ADA detection assays has increased over time, reflected in the surprisingly high numbers of ADAs recorded in the placebo arms of recent nanobody clinical trials (Table 2). This complicates the use of aggregate ADA data over the past 40 years as a benchmark and perhaps contributes to the relatively weak correlations observed between humanness metrics and the recorded abundance of ADAs (97). Even successful transition of a drug beyond Phase-I clinical trials has its limitations as a metric, due to the differential toleration of ADAs based on the severity of the indication. A better understanding of

the factors underlying ADA production may be gained through investigation of healthy or immunocompromised humanized mouse immune systems (98).

Broader issues emerge across the full landscape of antibody properties, where the successful humanization of candidates might inadvertently compromise other developability attributes. These can often be addressed successfully during formulation, but formulation choices can equally yield their own developability challenges, such as anti-polyethylene glycol antibodies induced by recent biopharmaceuticals including modular mRNA vaccine technologies (99, 100). Consequently, there are growing attempts to address this multi-parameter optimization problem computationally, leveraging machine-learning techniques and the greater data availability, though these fall prey to the same need for more routine and systematic experimental validation.

More generally, the field at present functions on a certain definition of humanness. This definition is challenged by the fact that apparently genetically human antibodies can still provoke ADA production (1). This is unsurprising due to the genetic diversity sampled across humans, perhaps most pronounced in our highly personalized sets of HLA alleles that influence T cell-assisted B cell activation. Moreover, it remains hard to robustly capture the humanness of non-germline regions such as the recombination junctions or of randomness introduced by somatic hypermutation. Particularly, we highlight the emergence of machine-learning methods in antibody humanization, built using resources such as OAS (54, 55). There is an urgent need for wider representation in the available repertoire sequence datasets, since any tools trained on them will inherit their underlying biases (101). Ensuring this heterogeneity will be crucial toward accurately quantifying humanness and creating computationally designed therapeutics that exhibit general compatibility across populations.

Author contributions

GG: Writing – original draft, Writing – review & editing. MR: Supervision, Writing – review & editing. AW: Data curation, Writing – review & editing. CD: Supervision, Writing – review & editing.

Funding

The author(s) declare financial support was received for the research, authorship, and/or publication of this article. This work was supported by an Engineering and Physical Sciences Research Council DPhil studentship awarded to GG (grant number EP/S024093/1), and a Boehringer Ingelheim Postdoctoral Research Fellowship awarded to MR.

Conflict of interest

The authors declare that the research was conducted in the absence of any commercial or financial relationships that could be construed as a potential conflict of interest.

Publisher's note

All claims expressed in this article are solely those of the authors and do not necessarily represent those of their affiliated organizations, or those of the publisher, the editors and the reviewers. Any product that may be evaluated in this article, or claim that may be made by its manufacturer, is not guaranteed or endorsed by the publisher.

References

1. Harding FA, Stickler MM, Razo J, DuBridge RB. The immunogenicity of humanized and fully human antibodies: residual immunogenicity resides in the CDR regions. *MAbs*. (2010) 2:256–65. doi: 10.4161/mabs.2.3.11641

2. Hansel TT, Kropshofer H, Singer T, Mitchell JA, George AJ. The safety and side effects of monoclonal antibodies. *Nat Rev Drug Discovery*. (2010) 9:325–38. doi: 10.1038/nrd3003

3. Lu R-M, Hwang Y-C, Liu IJ, Lee C-C, Tsai H-Z, Li H-J, et al. Development of therapeutic antibodies for the treatment of diseases. *J Biomed Science*. (2020) 27:1. doi: 10.1186/s12929-019-0592-z

4. Raybould MIJ, Marks C, Lewis AP, Shi J, Bujotzek A, Taddese B, et al. Thera-SAbDab: the therapeutic structural antibody database. *Nucleic Acids Res*. (2020) 48: D383–d8. doi: 10.1093/nar/gkz827

5. Kim J, McFee M, Fang Q, Abdin O, Kim PM. Computational and artificial intelligence-based methods for antibody development. *Trends Pharmacol Sci*. (2023) 44:175–89. doi: 10.1016/j.tips.2022.12.005

6. Wesolowski J, Alzogaray V, Reyelt J, Unger M, Juarez K, Urrutia M, et al. Single domain antibodies: promising experimental and therapeutic tools in infection and immunity. *Med Microbiol Immunol*. (2009) 198:157–74. doi: 10.1007/s00430-009-0116-7

7. Rossotti MA, Bélanger K, Henry KA, Tanha J. Immunogenicity and humanization of single-domain antibodies. *FEBS J*. (2022) 289:4304–27. doi: 10.1111/febs.15809

8. Krah S, Schröter C, Zielonka S, Empting M, Valldorf B, Kolmar H. Single-domain antibodies for biomedical applications. *Immunopharmacol Immunotoxicol*. (2016) 38:21–8. doi: 10.3109/08923973.2015.1102934

9. Vincke C, Loris R, Saerens D, Martinez-Rodriguez S, Muyldermans S, Conrath K. General strategy to humanize a camelid single-domain antibody and identification of a universal humanized nanobody scaffold. *J Biol Chem*. (2009) 284:3273–84. doi: 10.1074/jbc.M806889200

10. Czajka TF, Vance DJ, Mantis NJ. Slaying SARS-coV-2 one (Single-domain) antibody at a time. *Trends Microbiol*. (2021) 29:195–203. doi: 10.1016/j.tim.2020.12.006

11. Bannas P, Hambach J, Koch-Nolte F. Nanobodies and nanobody-based human heavy chain antibodies as antitumor therapeutics. *Front Immunol*. (2017) 8:1603. doi: 10.3389/fimmu.2017.01603

12. Zavrtanik U, Lukan J, Loris R, Lah J, Hadži S. Structural basis of epitope recognition by heavy-chain camelid antibodies. *J Mol Biol*. (2018) 430:4369–86. doi: 10.1016/j.jmb.2018.09.002

13. Muyldermans S. Nanobodies: natural single-domain antibodies. *Annu Rev Biochem*. (2013) 82:775–97. doi: 10.1146/annurev-biochem-063011-092449

14. Gordon GL, Capel HL, Guloglu B, Richardson E, Stafford RL, Deane CM. A comparison of the binding sites of antibodies and single-domain antibodies. *Front Immunol*. (2023) 14:1231623. doi: 10.3389/fimmu.2023.1231623

15. Almagro JC, Fransson J. Humanization of antibodies. *Front Biosci*. (2008) 13:1619–33. doi: 10.2741/2786

16. Safdari Y, Farajnia S, Asgharzadeh M, Khalili M. Antibody humanization methods - a review and update. *Biotechnol Genet Eng Rev*. (2013) 29:175–86. doi: 10.1080/02648725.2013.801235

17. Norman RA, Ambrosetti F, Bonvin A, Colwell LJ, Kelm S, Kumar S, et al. Computational approaches to therapeutic antibody design: established methods and emerging trends. *Brief Bioinform*. (2020) 21:1549–67. doi: 10.1093/bib/bbz095

18. Wilman W, Wróbel S, Bielska W, Deszynski P, Dudzic P, Jaszczyszyn I, et al. Machine-designed biotherapeutics: opportunities, feasibility and advantages of deep learning in computational antibody discovery. *Briefings Bioinf.* (2022) 23:bbac267. doi: 10.1093/bib/bbac267

19. Akbar R, Bashour H, Rawat P, Robert PA, Smorodina E, Cotet TS, et al. Progress and challenges for the machine learning-based design of fit-for-purpose monoclonal antibodies. *MAbs*. (2022) 14:2008790. doi: 10.1080/19420862.2021.2008790

20. Wang B, Gallolu Kankanamalage S, Dong J, Liu Y. Optimization of therapeutic antibodies. *Antibody Ther*. (2021) 4:45–54. doi: 10.1093/abt/tbab003

21. Zhou Y, Huang Z, Li W, Wei J, Jiang Q, Yang W, et al. Deep learning in preclinical antibody drug discovery and development. *Methods*. (2023) 218:57–71. doi: 10.1016/j.ymeth.2023.07.003

22. Makowski EK, Wu L, Gupta P, Tessier PM. Discovery-stage identification of drug-like antibodies using emerging experimental and computational methods. *MAbs*. (2021) 13:1895540. doi: 10.1080/19420862.2021.1895540

23. Khetan R, Curtis R, Deane CM, Hadsund JT, Kar U, Krawczyk K, et al. Current advances in biopharmaceutical informatics: guidelines, impact and challenges in the computational developability assessment of antibody therapeutics. *MAbs*. (2022) 14:2020082. doi: 10.1080/19420862.2021.2020082

24. Evers A, Malhotra S, Sood VD eds. *In Silico Approaches to Deliver Better Antibodies by Design: The Past, the Present and the Future* (2023) [preprint].

25. Abhinandan KR, Martin AC. Analyzing the "degree of humanness" of antibody sequences. *J Mol Biol*. (2007) 369:852–62. doi: 10.1016/j.jmb.2007.02.100

26. Thullier P, Huish O, Pelat T, Martin AC. The humanness of macaque antibody sequences. *J Mol Biol*. (2010) 396:1439–50. doi: 10.1016/j.jmb.2009.12.041

27. Gao SH, Huang K, Tu H, Adler AS. Monoclonal antibody humanness score and its applications. *BMC Biotechnol*. (2013) 13:55. doi: 10.1186/1472-6750-13-55

28. Lazar GA, Desjarlais JR, Jacinto J, Karki S, Hammond PW. A molecular immunology approach to antibody humanization and functional optimization. *Mol Immunol*. (2007) 44:1986–98. doi: 10.1016/j.molimm.2006.09.029

29. Seeliger D. Development of scoring functions for antibody sequence assessment and optimization. *PloS One*. (2013) 8:e76909. doi: 10.1371/journal.pone.0076909

30. Clavero-Álvarez A, Di Mambro T, Perez-Gaviro S, Magnani M, Bruscolini P. Humanization of antibodies using a statistical inference approach. *Sci Rep*. (2018) 8:14820. doi: 10.1038/s41598-018-32986-y

31. Schmitz S, Soto C, Crowe JE Jr., Meiler J. Human-likeness of antibody biologics determined by back-translation and comparison with large antibody variable gene repertoires. *MAbs*. (2020) 12:1758291. doi: 10.1080/19420862.2020.1758291

32. Marks C, Hummer AM, Chin M, Deane CM. Humanization of antibodies using a machine learning approach on large-scale repertoire data. *Bioinformatics*. (2021) 37:4041–7. doi: 10.1093/bioinformatics/btab434

33. Prihoda D, Maamary J, Waight A, Juan V, Fayadat-Dilman L, Svozil D, et al. BioPhi: A platform for antibody design, humanization, and humanness evaluation based on natural antibody repertoires and deep learning. *MAbs*. (2022) 14:2020203. doi: 10.1080/19420862.2021.2020203

34. Uçar T, Ramon A, Oglic D, Croasdale-wood R, Diethe T, Sormanni P. Improving antibody humanness prediction using patent data. *ArXiv*. (2024). abs/2401.14442. doi: 10.48550/arXiv.2401.14442

35. Zou H, Yuan R, Lai B, Dou Y, Wei L, Xu J. Antibody humanization via protein language model and neighbor retrieval. *bioRxiv*. (2023). doi: 10.1101/2023.09.04.556278

36. Wollacott AM, Xue C, Qin Q, Hua J, Bohnuud T, Viswanathan K, et al. Quantifying the nativeness of antibody sequences using long short-term memory networks. *Protein Engineering Design Selection*. (2019) 32:347–54. doi: 10.1093/protein/gzz031

37. Vashchenko D, Nguyen S, Goncalves A, FLd S, Petersen B, Desautels T, et al. AbBERT: learning antibody humanness via masked language modeling. *bioRxiv*. (2022). doi: 10.1101/2022.08.02.502236

38. Choi Y, Hua C, Sentman CL, Ackerman ME, Bailey-Kellogg C. Antibody humanization by structure-based computational protein design. *MAbs*. (2015) 7:1045–57. doi: 10.1080/19420862.2015.1076600

39. Choi Y, Ndong C, Griswold KE, Bailey-Kellogg C. Computationally driven antibody engineering enables simultaneous humanization and thermostabilization. *Protein Engineering Design Selection*. (2016) 29:419–26. doi: 10.1093/protein/gzw024

40. Hsieh Y-C, J-m L, Chuang K-H, Ho K-W, Hong S-T, Liu H-J, et al. A universal in silico V(D)J recombination strategy for developing humanized monoclonal antibodies. *J Nanobiotechnology*. (2022) 20:58. doi: 10.1186/s12951-022-01259-2

41. Tennenhouse A, Khmelnitsky L, Khalaila R, Yeshaya N, Noronha A, Lindzen M, et al. Computational optimization of antibody humanness and stability by systematic energy-based ranking. *Nat Biomed Engineering*. (2024) 8:30–44. doi: 10.1038/s41551-023-01079-1

42. Sang Z, Xiang Y, Bahar I, Shi Y. Llamanade: An open-source computational pipeline for robust nanobody humanization. *Structure*. (2022) 30:418–29.e3. doi: 10.1016/j.str.2021.11.006

43. Ramon A, Ali M, Atkinson M, Saturnino A, Didi K, Visentin C, et al. Assessing antibody and nanobody nativeness for hit selection and humanization with AbNatiV. *Nat Mach Intelligence*. (2024) 6:74–91. doi: 10.1038/s42256-023-00778-3

44. Morrison SL, Johnson MJ, Herzenberg LA, Oi VT. Chimeric human antibody molecules: mouse antigen-binding domains with human constant region domains. *Proc Natl Acad Sci U S A*. (1984) 81:6851–5. doi: 10.1073/pnas.81.21.6851

45. Jones PT, Dear PH, Foote J, Neuberger MS, Winter G. Replacing the complementarity-determining regions in a human antibody with those from a mouse. *Nature*. (1986) 321:522–5. doi: 10.1038/321522a0

46. Baca M, Presta LG, O'Connor SJ, Wells JA. Antibody humanization using monovalent phage display. *J Biol Chem*. (1997) 272:10678–84. doi: 10.1074/jbc.272.16.10678

47. De Pascalis R, Iwahashi M, Tamura M, Padlan EA, Gonzales NR, Santos AD, et al. Grafting of "abbreviated" complementarity-determining regions containing specificity-determining residues essential for ligand contact to engineer a less immunogenic humanized monoclonal antibody. *J Immunol*. (2002) 169:3076–84. doi: 10.4049/jimmunol.169.6.3076

48. Kashmiri SV, De Pascalis R, Gonzales NR, Schlom J. SDR grafting–a new approach to antibody humanization. *Methods*. (2005) 36:25–34. doi: 10.1016/j.ymeth.2005.01.003

49. Apgar JR, Mader M, Agostinelli R, Benard S, Bialek P, Johnson M, et al. Beyond CDR-grafting: Structure-guided humanization of framework and CDR regions of an anti-myostatin antibody. *MAbs*. (2016) 8:1302–18. doi: 10.1080/19420862.2016.1215786

50. Dall'Acqua WF, Damschroder MM, Zhang J, Woods RM, Widjaja L, Yu J, et al. Antibody humanization by framework shuffling. *Methods*. (2005) 36:43–60. doi: 10.1016/j.ymeth.2005.01.005

51. Padlan EA. A possible procedure for reducing the immunogenicity of antibody variable domains while preserving their ligand-binding properties. *Mol Immunol*. (1991) 28:489–98. doi: 10.1016/0161-5890(91)90163-E

52. Roguska MA, Pedersen JT, Keddy CA, Henry AH, Searle SJ, Lambert JM, et al. Humanization of murine monoclonal antibodies through variable domain resurfacing. *Proc Natl Acad Sci U S A*. (1994) 91:969–73. doi: 10.1073/pnas.91.3.969

53. Petersen BM, Ulmer SA, Rhodes ER, Gutierrez-Gonzalez MF, Dekosky BJ, Sprenger KG, et al. Regulatory approved monoclonal antibodies contain framework mutations predicted from human antibody repertoires. *Front Immunol*. (2021) 12:728694. doi: 10.3389/fimmu.2021.728694

54. Kovaltsuk A, Leem J, Kelm S, Snowden J, Deane CM, Krawczyk K. Observed antibody space: A resource for data mining next-generation sequencing of antibody repertoires. *J Immunol*. (2018) 201:2502–9. doi: 10.4049/jimmunol.1800708

55. Olsen TH, Boyles F, Deane CM. Observed Antibody Space: A diverse database of cleaned, annotated, and translated unpaired and paired antibody sequences. *Protein Sci*. (2022) 31:141–6. doi: 10.1002/pro.4205

56. Ackaert C, Smiejkowska N, Xavier C, Sterckx YGJ, Denies S, Stijlemans B, et al. Immunogenicity risk profile of nanobodies. *Front Immunol*. (2021) 12:632687. doi: 10.3389/fimmu.2021.632687

57. Keyaerts M, Xavier C, Heemskerk J, Devoogdt N, Everaert H, Ackaert C, et al. Phase I study of 68Ga-HER2-nanobody for PET/CT assessment of HER2 expression in breast carcinoma. *J Nucl Med*. (2016) 57:27–33. doi: 10.2967/jnumed.115.162024

58. Ablynx aSc. *A Phase II Multicenter, Randomized, Double- blind, Placebo Controlled, Dose-range Finding Study to Evaluate the Safety and Efficacy of ALX-0061 Administered Subcutaneously in Subjects With Moderate to Severe Active Systemic Lupus Erythematosus*. clinicaltrials.gov (2019).

59. Ablynx aSc. *A Phase IIb Multicenter, Randomized, Double- blind Study of ALX-0061 Administered Subcutaneously as Monotherapy, in Subjects With Moderate to Severe Rheumatoid Arthritis Who Are Intolerant to Methotrexate or for Whom Continued Methotrexate Treatment is Inappropriate*. clinicaltrials.gov (2019).

60. Holz J-B, Sargentini-Maier L, Bruyn SD, Gachályi B, Udvaros I, Rojkovich B, et al. OP0043 twenty- four weeks of treatment with a novel anti-IL-6 receptor nanobody® (ALX- 0061) resulted in 84% ACR20 improvement and 58% DAS28 remission in a phase I/ii study in RA. *Ann Rheumatic Dis*. (2013) 72:A64–4. doi: 10.1136/annrheumdis-2013-eular.248

61. Van Roy M, Ververken C, Beirnaert E, Hoefman S, Kolkman J, Vierboom M, et al. The preclinical pharmacology of the high affinity anti-IL-6R Nanobody® ALX-0061 supports its clinical development in rheumatoid arthritis. *Arthritis Res Ther*. (2015) 17:135. doi: 10.1186/s13075-015-0651-0

62. Bartunek J, Barbato E, Heyndrickx G, Vanderheyden M, Wijns W, Holz J-B. Novel antiplatelet agents: ALX-0081, a Nanobody directed towards von Willebrand factor. *J Cardiovasc Transl Res*. (2013) 6:355–63. doi: 10.1007/s12265-012-9435-y

63. Peyvandi F, Scully M, Kremer Hovinga JA, Knöbl P, Cataland S, De Beuf K, et al. Caplacizumab reduces the frequency of major thromboembolic events, exacerbations and death in patients with acquired thrombotic thrombocytopenic purpura. *J Thromb Haemost*. (2017) 15:1448–52. doi: 10.1111/jth.13716

64. Scully M, Cataland SR, Peyvandi F, Coppo P, Knöbl P, Kremer Hovinga JA, et al. Caplacizumab treatment for acquired thrombotic thrombocytopenic purpura. *N Engl J Med*. (2019) 380:335–46. doi: 10.1056/NEJMoa1806311

65. Schoen P, Jacobs S, Verschueren K, Ottevaere I, Sobry S, Holz J-B. Anti-RANKL nanobody ALX-0141 shows sustained biomarker inhibition in a Phase I study in healthy postmenopausal Women. *Bone Abstracts*. (2013). Presented at the European Calcified Tissue Society Congress 2013, Bioscientifica. 1:PP135 doi: 10.1530/boneabs.1.PP135

66. Detalle L, Stohr T, Palomo C, Piedra PA, Gilbert BE, Mas V, et al. Generation and characterization of ALX-0171, a potent novel therapeutic nanobody for the treatment of respiratory syncytial virus infection. *Antimicrobial Agents Chemotherapy*. (2015) 60:6–13. doi: 10.1128/AAC.01802-15

67. Cunningham S, Piedra PA, Martinon-Torres F, Szymanski H, Brackeva B, Dombrecht E, et al. Nebulised ALX-0171 for respiratory syncytial virus lower respiratory tract infection in hospitalised children: a double-blind, randomised, placebo-controlled, phase 2b trial. *Lancet Respir Med*. (2021) 9:21–32. doi: 10.1016/S2213–2600(20)30320–9

68. Merck KGaA D, Germany. *Multicenter, Phase I, Randomized, Double-Blind, Placebo-Controlled Trial to Assess the Safety, Tolerability, Immunogenicity, Pharmacokinetics, Pharmacodynamics and Efficacy of Multiple Ascending Doses of Subcutaneous MSB0010841 (Anti-IL17A/F Nanobody) in Male and Female Subjects With Moderate to Severe Psoriasis (Clinical trial registration No. results/NCT02156466)*. clinicaltrials.gov (2016).

69. Ablynx aSc. *An Open-Label Extension Study To Assess The Long-term Safety And Tolerability Of ATN-103 In Subjects With Rheumatoid Arthritis (Clinical trial registration No. NCT01063803)*. clinicaltrials.gov (2016).

70. Ablynx aSc. *A Randomized, Multicenter, Double-Blind, Placebo-Controlled, Multiple Ascending Dose Study Of The Safety, Tolerability, Pharmacokinetics, Pharmacodynamics, And Clinical Efficacy Of ATN-103 Administered To Japanese Subjects With Active Rheumatoid Arthritis On A Background Of Methotrexate (Clinical trial registration No. NCT01007175)*. clinicaltrials.gov (2013).

71. Ablynx aSc. *A Seamless, Phase 1/2, Multiple Ascending Dose, Proof Of Concept Study Of ATN-103 Administered To Subjects With Active Rheumatoid Arthritis On A Background Of Methotrexate (Clinical trial registration No. NCT00959036)*. clinicaltrials.gov (2013).

72. Buyse M-A, Hermans G, Lindemann S, Guehring H, Guenther R, Kellner R. Adamts binding immunoglobulins. Patent number: WO2018220234A1 (2017).

73. Papadopoulos KP, Isaacs R, Bilic S, Kentsch K, Huet HA, Hofmann M, et al. Unexpected hepatotoxicity in a phase I study of TAS266, a novel tetravalent agonistic Nanobody® targeting the DR5 receptor. *Cancer Chemother Pharmacol*. (2015) 75:887–95. doi: 10.1007/s00280-015-2712-0

74. Sulea T. Humanization of camelid single-domain antibodies. *Methods Mol Biol*. (2022) 2446:299–312. doi: 10.1007/978-1-0716-2075-5_14

75. Conrath K, Vincke C, Stijlemans B, Schymkowitz J, Decanniere K, Wyns L, et al. Antigen binding and solubility effects upon the veneering of a camel VHH in framework-2 to mimic a VH. *J Mol Biol*. (2005) 350:112–25. doi: 10.1016/j.jmb.2005.04.050

76. Gentiluomo L, Roessner D, Streicher W, Mahapatra S, Harris P, Frieß W. Characterization of native reversible self-association of a monoclonal antibody mediated by fab-fab interaction. *J Pharm Sci*. (2020) 109:443–51. doi: 10.1016/j.xphs.2019.09.021

77. Voynov V, Chennamsetty N, Kayser V, Helk B, Trout BL. Predictive tools for stabilization of therapeutic proteins. *MAbs*. (2009) 1:580–2. doi: 10.4161/mabs.1.6.9773

78. Waibl F, Fernández-Quintero ML, Kamenik AS, Kraml J, Hofer F, Kettenberger H, et al. Conformational ensembles of antibodies determine their hydrophobicity. *Biophys J*. (2021) 120:143–57. doi: 10.1016/j.bpj.2020.11.010

79. Mitchell LS, Colwell LJ. Comparative analysis of nanobody sequence and structure data. *Proteins*. (2018) 86:697–706. doi: 10.1002/prot.25497

80. Kelow SP, Adolf-Bryfogle J, Dunbrack RL. Hiding in plain sight: structure and sequence analysis reveals the importance of the antibody DE loop for antibody-antigen binding. *MAbs*. (2020) 12:1840005. doi: 10.1080/19420862.2020.1840005

81. Hummer AM, Deane CM. Designing stable humanized antibodies. *Nat Biomed Engineering*. (2024) 8:3–4. doi: 10.1038/s41551-023-01168-1

82. Abanades B, Wong WK, Boyles F, Georges G, Bujotzek A, Deane CM. ImmuneBuilder: Deep-Learning models for predicting the structures of immune proteins. *Commun Biol*. (2023) 6:575. doi: 10.1038/s42003-023-04927-7

83. Jain T, Boland T, Vásquez M. Identifying developability risks for clinical progression of antibodies using high-throughput in *vitro* and in silico approaches. *MAbs*. (2023) 15:2200540. doi: 10.1080/19420862.2023.2200540

84. Heads JT, Kelm S, Tyson K, Lawson ADG. A computational method for predicting the aggregation propensity of IgG1 and IgG4(P) mAbs in common storage buffers. *MAbs*. (2022) 14:2138092. doi: 10.1080/19420862.2022.2138092

85. Zhang W, Wang H, Feng N, Li Y, Gu J, Wang Z. Developability assessment at early-stage discovery to enable development of antibody-derived therapeutics. *Antib Ther*. (2023) 6:13–29. doi: 10.1093/abt/tbac029

86. Vaisman-Mentesh A, Gutierrez-Gonzalez M, DeKosky BJ, Wine Y. The molecular mechanisms that underlie the immune biology of anti-drug antibody formation following treatment with monoclonal antibodies. *Front Immunol*. (2020) 11:1951. doi: 10.3389/fimmu.2020.01951

87. Reynisson B, Alvarez B, Paul S, Peters B, Nielsen M. NetMHCpan-4.1 and NetMHCIIpan-4.0: improved predictions of MHC antigen presentation by concurrent motif deconvolution and integration of MS MHC eluted ligand data. *Nucleic Acids Res*. (2020) 48:W449–W54. doi: 10.1093/nar/gkaa379

88. Makowski EK, Kinnunen PC, Huang J, Wu L, Smith MD, Wang T, et al. Co-optimization of therapeutic antibody affinity and specificity using machine learning models that generalize to novel mutational space. *Nat Commun*. (2022) 13:3788. doi: 10.1038/s41467-022-31457-3

89. Bachas S, Rakocevic G, Spencer D, Sastry AV, Haile R, Sutton JM, et al. Antibody optimization enabled by artificial intelligence predictions of binding affinity and naturalness. *bioRxiv*. (2022). doi: 10.1101/2022.08.16.504181

90. Liu G, Zeng H, Mueller J, Carter B, Wang Z, Schilz J, et al. Antibody complementarity determining region design using high-capacity machine learning. *Bioinformatics*. (2020) 36:2126–33. doi: 10.1093/bioinformatics/btz895

91. Saka K, Kakuzaki T, Metsugi S, Kashiwagi D, Yoshida K, Wada M, et al. Antibody design using LSTM based deep generative model from phage display library for affinity maturation. *Sci Rep*. (2021) 11:5852. doi: 10.1038/s41598-021-85274-7

92. Arras P, Yoo HB, Pekar L, Schröter C, Clarke T, Krah S, et al. A library approach for the *de novo* high-throughput isolation of humanized VHH domains with favorable developability properties following camelid immunization. *MAbs*. (2023) 15:2261149. doi: 10.1080/19420862.2023.2261149

93. Arras P, Yoo HB, Pekar L, Clarke T, Friedrich L, Schröter C, et al. AI/ML combined with next-generation sequencing of VHH immune repertoires enables the rapid identification of *de novo* humanized and sequence-optimized single domain antibodies: a prospective case study. *Front Mol Biosci*. (2023) 10:1249247. doi: 10.3389/fmolb.2023.1249247

94. Raybould MIJ, Kovaltsuk A, Marks C, Deane CM. CoV-AbDab: the coronavirus antibody database. *Bioinformatics*. (2020) 37:734–5. doi: 10.1093/bioinformatics/btaa739

95. Brinkmann U, Kontermann RE. The making of bispecific antibodies. *MAbs*. (2017) 9:182–212. doi: 10.1080/19420862.2016.1268307

96. Keri D, Walker M, Singh I, Nishikawa K, Garces F. Next generation of multispecific antibody engineering. *Antibody Ther*. (2023) 7:37–52. doi: 10.1093/abt/tbad027

97. Song S, Yang L, Trepicchio WL, Wyant T. Understanding the supersensitive anti-drug antibody assay: unexpected high anti-drug antibody incidence and its clinical relevance. *J Immunol Res*. (2016) 2016:3072586. doi: 10.1155/2016/3072586

98. Chen J, Liao S, Xiao Z, Pan Q, Wang X, Shen K, et al. The development and improvement of immunodeficient mice and humanized immune system mouse models. *Front Immunol*. (2022) 13:1007579. doi: 10.3389/fimmu.2022.1007579

99. Kozma GT, Shimizu T, Ishida T, Szebeni J. Anti-PEG antibodies: Properties, formation, testing and role in adverse immune reactions to PEGylated nano-biopharmaceuticals. *Adv Drug Delivery Rev*. (2020) 154–155:163–75. doi: 10.1016/j.addr.2020.07.024

100. Ju Y, Carreño JM, Simon V, Dawson K, Krammer F, Kent SJ. Impact of anti-PEG antibodies induced by SARS-CoV-2 mRNA vaccines. *Nat Rev Immunol*. (2023) 23:135–6. doi: 10.1038/s41577-022-00825-x

101. Olsen TH, Moal IH, Deane CM. Addressing the antibody germline bias and its effect on language models for improved antibody design. *bioRxiv*. (2024). doi: 10.1101/2024.02.02.578678

frontiers | Frontiers in Immunology

TYPE Original Research
PUBLISHED 15 May 2024
DOI 10.3389/fimmu.2024.1377911

OPEN ACCESS

EDITED BY
Daniel T. Mytych,
Amgen, United States

REVIEWED BY
Lisbeth Guethlein,
Stanford University, United States
Randi Vita,
La Jolla Institute for Immunology (LJI),
United States

*CORRESPONDENCE
Naonobu Sugiyama
Naonobu.sugiyama@pfizer.com
Anne S. De Groot
annied@epivax.com

†PRESENT ADDRESS
Frances E. Terry,
Division of Research, Brown University,
Providence, RI, United States

RECEIVED 28 January 2024
ACCEPTED 24 April 2024
PUBLISHED 15 May 2024

CITATION
Sugiyama N, Terry FE, Gutierrez AH, Hirano T, Hoshi M, Mizuno Y, Martin W, Yasunaga S, Niiro H, Fujio K and De Groot AS (2024) Individual and population-level variability in HLA-DR associated immunogenicity risk of biologics used for the treatment of rheumatoid arthritis.
Front. Immunol. 15:1377911.
doi: 10.3389/fimmu.2024.1377911

Individual and population-level variability in HLA-DR associated immunogenicity risk of biologics used for the treatment of rheumatoid arthritis

Naonobu Sugiyama[1]*, Frances E. Terry[2†], Andres H. Gutierrez[2], Toshitaka Hirano[1], Masato Hoshi[1], Yasushi Mizuno[1], William Martin[2], Shin'ichiro Yasunaga[3], Hiroaki Niiro[4], Keishi Fujio[5] and Anne S. De Groot[2]*

[1]Rheumatology, Inflammation and Immunology Medical Affairs, Pfizer Japan Inc., Tokyo, Japan, [2]EpiVax, Inc., Providence, RI, United States, [3]Department of Biochemistry, Faculty of Medicine, Fukuoka University, Fukuoka, Japan, [4]Department of Medical Education, Kyushu University Graduate School of Medical Sciences, Fukuoka, Japan, [5]Department of Allergy and Rheumatology, Graduate School of Medicine, The University of Tokyo, Tokyo, Japan

Hypothesis: While conventional in silico immunogenicity risk assessments focus on measuring immunogenicity based on the potential of therapeutic proteins to be processed and presented by a global population-wide set of human leukocyte antigen (HLA) alleles to T cells, future refinements might adjust for HLA allele frequencies in different geographic regions or populations, as well for as individuals in those populations. Adjustment by HLA allele distribution may reveal risk patterns that are specific to population groups or individuals, which current methods that rely on global-population HLA prevalence may obscure.

Key findings: This analysis uses HLA frequency-weighted binding predictions to define immunogenicity risk for global and sub-global populations. A comparison of assessments tuned for North American/European versus Japanese/Asian populations suggests that the potential for anti-therapeutic responses (anti-therapeutic antibodies or ATA) for several commonly prescribed Rheumatoid Arthritis (RA) therapeutic biologics may differ, significantly, between the Caucasian and Japanese populations. This appears to align with reports of differing product-related immunogenicity that is observed in different populations.

Relevance to clinical practice: Further definition of population-level (regional) and individual patient-specific immunogenic risk profiles may enable prescription of the RA therapeutic with the highest probability of success to each patient, depending on their population of origin and/or their individual HLA background. Furthermore, HLA-specific immunogenicity outcomes data are limited, thus there is a need to expand HLA-association studies that examine the relationship between HLA haplotype and ATA in the clinic.

KEYWORDS

immunogenicity, HLA-DR, T-cell, rheumatoid arthritis, personalized medicine, immunoinformatics

1 Introduction

1.1 Natural history of RA

Rheumatoid arthritis (RA) is a chronic inflammatory disorder that primarily affects the joints, leading to swelling, pain, stiffness, and gradual joint destruction. It is a global disease with varying prevalence rates in different populations; although estimates suggest that approximately 1% of the world's population is affected. In the United States and Japan, the prevalence of RA is approximately 0.3-1.0% (1–3). The etiology of RA is multifactorial and results from a complex interplay of genetic, environmental, and hormonal factors.

Among genetic factors, as is true for many autoimmune diseases, specific variants of the human leukocyte antigen (HLA) gene, particularly the HLA-DRB1 alleles, have been strongly associated with RA. This association is more pronounced in certain ethnic populations. Notably, the "shared epitope" (SE) hypothesis postulates that a specific sequence of amino acids in the HLA-DRB1 region is a common feature for most RA patients (4–6). A list of SE alleles can be found in a recent publication by Viatte et al. (7). Other genetic aspects of genetic RA susceptibility are also discussed in the Viatte publication.

More specific examples of differences related to the HLA-DRB1 alleles follow: The HLA-DR*04 allele is frequently found in individuals of European ancestry who have been diagnosed with RA in the United States. Conversely, in the Japanese population, the HLA-DR*09 allele is more commonly associated with RA along with the HLA-DOA gene (see reference (6) for a discussion of these contributors to RA risk). Thus, the prevalence of HLA-DR alleles that are found in native RA patients in the US may differ from the HLA-DR prevalence of native Japanese patients with RA.

These differences in HLA-DR distribution found in RA patient populations may also be relevant to the development of immune responses to RA therapies, since HLA-DR presentation of T cell epitopes derived from therapeutic proteins has been identified as a risk factor for the development of anti-therapeutic antibodies (ATA) (8, 9). RA patients are often treated with biologic protein drugs (also known as biological DMARDs: disease-modifying antirheumatic drugs) that are known to be processed and presented by antigen presenting cells, in the context of HLA-DR molecules, to T cells that can drive ATA responses to the drugs.

Since these ATA can interfere with the efficacy of the biological DMARDs, and HLA-DR-restricted epitopes are the root cause of the ATA, we have hypothesized that regional HLA distributions may help to explain observed differences in immunogenicity (ATA) between global patient groups. In fact, a link between HLA-DR and CD4 T cell activation has already been identified as a factor underlying RA disease activity in studies of patients in Japan (10).

1.2 Impact of RA on immune cell populations that can drive ATA

RA also has a direct impact on immune cell populations. T cells, particularly CD4+ T cells, and B cells play key roles in the pathogenesis of RA. They contribute to the chronic inflammation of the joints, and are responsible for the production of autoantibodies, including rheumatoid factor (RF) and anti-citrullinated protein antibodies (ACPAs). In addition, RA patients are noted to have abnormally activated immune cells such as macrophages and dendritic cells, activity (11).

Impaired regulatory T cell responses can also contribute to the development of anti-therapeutic antibodies (ATA) to RA therapies (12, 13). RA patients reportedly have changes to the ratio of T effector helper (Teff) to regulatory T cells (Treg), which can contribute to ATA (14). Effective treatment strategies for RA often target these immune cell populations to reduce inflammation and joint damage (15). The immune system environment is extremely dynamic, and modulatory therapies can have an impact on both local (joint) and systemic (lymphoid system) environments, resulting in changes to joint inflammation and reduction in B cell responses systemically. Likewise, systemic therapies may have an influence on the activation of T helper cells driving ATA. Thus, it is not surprising that effective therapy of RA can also be associated with a reduction in T cell inflammatory responses, an increase in regulatory T cell responses, and a decrease in the inflammatory profile of the immune response which, at the same time, may contribute to a reduction in the anti-therapeutic immune response (ATA) (16).

1.3 Biologic DMARDs and JAK inhibitors to treat RA

Biologic therapies for RA known as biologic disease-modifying antirheumatic drugs (bDMARDs) and JAK (Janus kinase) inhibitors have transformed the treatment landscape for rheumatoid arthritis. They work by targeting specific components of the immune system to inhibit the inflammatory processes that are driving inflammation in RA. Readers are referred to an excellent review article by Di Matteo, Bathon, and Emery on therapy for Rheumatoid Arthritis in the Lancet, published in October 2023, for additional information on RA therapy (17). Drugs that are used to treat RA are classified as follows:

1.3.1 TNF inhibitors

These drugs block the cytokine tumor necrosis factor (TNF), which plays a major role in promoting inflammation. Monoclonal antibodies that target TNF include Infliximab (Remicade), Adalimumab (Humira), Certolizumab pegol (Cimzia), and Golimumab (Simponi). Etanercept (Enbrel) is an Fc-fusion of the TNF receptor that also traps TNF, rather than directly inhibiting the cytokine.

1.3.2 Non TNF inhibitors

Both TNFα and IL-6 contribute to inflammation in RA, therefore IL-6 is another inflammatory cytokine that is targeted in RA treatment. IL-6 inhibitors include anti–IL-6 receptor monoclonal antibodies such as Tocilizumab (Actemra) and Sarilumab (Kevzara). Abatacept (Orencia) is a fusion protein comprised of IgG Fc fused to the extracellular domain of CTLA-

4, which can bind to the B7 molecules (CD80 and CD86) on antigen-presenting cells. By binding to B7, abatacept prevents a critically important costimulatory signal to T cells, thereby reducing the activity of T cells and the consequent inflammatory response.

1.3.3 JAK inhibitors

RA is also treated using Janus kinase (JAK) inhibitors, a newer class of small molecules (not therapeutic proteins) that block the Janus kinase pathway, which plays a role in the immune response.

1.4 Immunogenicity of therapeutic proteins in RA

1.4.1 Clinical observations

Several publications have addressed and reported the incidence and prevalence of ATA in RA. See for example the systemic review by Thomas et al. (18), Woblink et al. (19), and an earlier publication by Garces and Demengeot (20). As discussed above, the recognition and response to these therapeutic proteins is likely heightened in RA due to the underlying dysregulated immune response. For example, approximately 12% of patients treated with therapeutic monoclonal antibodies against TNF develop ATA, but the incidence is much higher in RA patients.

One systemic review found that ATA were involved in decreased response to TNF inhibitors by 27% of patients in RA and by 18% in spondyloarthritis (18). Another systemic review has demonstrated that patients with RA who are treated with TNF inhibitors, such as infliximab or adalimumab, have a higher incidence of developing ATAs compared to those with other inflammatory conditions like Crohn's disease (13). This propensity to develop ATAs can have important clinical implications, as the presence of these antibodies has been linked to decreased drug efficacy, increased risk of adverse reactions, and reduced treatment durability. Immune response to prescribed RA medication is a problem that affects a significant number of RA patients.

As hypothesized above, the HLA-DR of the individual patient or patient population, as well as to their ability to present natural Treg epitopes may be related to the development of ATA to the individual RA product. This underscores the need for personalized approaches in treating RA, including careful selection of therapeutic agents, taking into consideration the risk of immunogenicity for each individual patient, and monitoring therapeutic response and drug levels over time. Here we focus on populations at the level of geography, but sub populations, disease-specific populations, and individuals may each have different immune responses to therapeutic proteins based on differences in their HLA-DR alleles [Makuch, Van Hamm et al, manuscript in final revision].

1.4.2 Population-level immunogenicity risk assessment with iTEM

To address better understand the influence of HLA distributions on RA therapy, we developed a weighted immunogenicity risk assessment score for populations of patients, that was previously applied to measuring immune responses for individual patients, called the "Individualized T-cell epitope measure" (iTEM) tool. This tool makes it possible to estimate the risk of immune response to a protein antigen based on the HLA-DR frequency in a population, or the combination of HLA-DRs in a single individual (21, 22). The individual score is calculated by counting the number of T effector epitopes, presented by any given HLA-DR that is identified in a monoclonal or DMARD, and adjusted for the presence of validated Treg epitopes (also known as Tregitopes) that are known to occur in monoclonal antibody sequences (8), as described in greater detail below.

Since HLA typing is not routinely performed as an aspect of clinical care for RA patients, we used population-based HLA-DR-adjusted immunogenicity risk assessments to evaluate whether differences in immune responses to biologic products may be related to differences in the HLA prevalence in populations, beginning with HLA prevalence in RA populations in Japan and in the US (to establish an approach that could be used for additional regional populations and sub-populations). iTEM was used to convert HLA-DRB1 allele binding predictions generated by EpiMatrix, an epitope-mapping tool, into an allele-specific scoring system for the HLA distributions observed in Japanese (East Asian) and US (Caucasian) populations. We also identified combinations of HLA-DR alleles for which differences in the predicted immune responses were the greatest (highest risk) or the least (lowest risk).

We then demonstrated that iTEM (HLA-DR-restricted haplotype) analysis of immunogenicity risk appears to differentiate populations in which a specific RA drug may be more likely to activate an immune response and below which immune response is likely to be absent. iTEM may be a useful tool for selecting populations or individuals for which RA drugs may be less likely to elicit ATA, and iTEM may be a useful tool for pre-clinical evaluation of biologic products tailored to selected (different) population groups.

2 Methods

2.1 Compiling HLA expression frequencies

HLA-DR allele expression frequencies were calculated using gold standard data extracted from The Allele Frequency Net Database (23) with a minimum of four-digit (two field) resolution (e.g., DRB1*01:01). To optimize specificity, population samples were selected based on ethnic origin filters ("Caucasoid" vs. "Oriental" are the terms used in the Database). For the Japanese population, seven population samples with matching ethnic origin ("Oriental") and geographic filters ("Japan") were available (Supplementary Table 1A). For the Caucasian population, 27 population samples were available across North American and European regions (Supplementary Table 1B). Allele frequencies were calculated based on the reported "Total % of individuals that have the allele", scaled by sample size and aggregated. Alleles expressed at greater than 1% frequency for at least one population were selected (Table 1, Supplementary Table 2).

2.2 Compiling observed immunogenicity data for monoclonal antibodies & fusion proteins

A fair estimate of ATA response rate to a given biologic includes clinical data from any available study with significant numbers of systematically chosen participants; however, study size may vary from biologic to biologic and target population to target population. In most cases, an average ATA response rate was calculated based on the rates reported in FDA package inserts using a method described in detail for global population groups in a previous publication by Jawa et al. (24). As previously described, where multiple clinical studies were included, this average was weighted by the number of study participants included for each reported rate. Rates associated with monotherapy were preferred. Where no rates were reported without concomitant medication, a systematic review was performed to justify the inclusion of certain datapoints. Rates associated with very small samples or concomitant medications expected to have significant confounding impacts on ATA response were excluded. Due to measurement inconsistency across product studies, no attempts were made to specify "neutralizing" antibody response rate.

2.3 Calculating immunogenic potential scores

Methods to assess the immunogenic potential of a complete protein are available on several public and academic platforms such as the Immune Epitope Database (25), in some cases paired with mathematical models based on hypothetical binding affinities and T cell precursor frequencies (26), or with MAPPs-determined peptidomes (27–29). Here, we used the EpiMatrix scoring system that has been described previously (30, 31). EpiMatrix was developed by De Groot and colleagues at Brown University and licensed to EpiVax in 1998. EpiMatrix and JanusMatrix have been applied and validated in the field of vaccine development, most recently for personalized cancer vaccine development (31)(. Substantial improvements to the EpiMatrix algorithm have resulted in a high degree of accuracy for class II epitopes (77-100%) and higher than 95% for most class I epitopes (32, 33).

Briefly, the EpiMatrix algorithm maps putative ligands to globally representative HLA-DRB1 supertype alleles (34) and calculates a length-normalized score to represent aggregate T cell epitope density. This is called the "Raw" EpiMatrix Score. An adjustment to this score in which the putative ligands specific for known regulatory Tregitopes are excluded from the aggregate calculation has been shown to correlate with the observed immunogenicity of monoclonal antibodies in the clinic (24). This is called the "Tregitope-adjusted" EpiMatrix Score. An adaptation of the EpiMatrix Score for use in personalized medicine is called the individualized T cell Epitope Measure, or "iTEM" Score (21). This score restricts the aggregation of epitope content to a set of two HLA-DR alleles, in order model the scenario of an individual patient, who may be homozygous or heterozygous.

The iTEM Score has been applied to the personalized immunogenicity risk assessment for replacement enzymes (22, 35) and peptides derived from vaccine candidate antigens (36). In previous iterations of iTEM, corrections have been applied for "cross-conservation with self-epitopes" (using the JanusMatrix tool). As this tool has not yet been adjusted for Tregitopes and therefore cannot be applied to antibody-derived biological DMARDs without significant modification, we elected to use the well-standardized Tregitope correction (8) to the EpiMatrix analysis in the models that were applied below (22, 37) instead of the JanusMatrix-corrected version of iTEM (J-iTEM).

3 Approach and calculations

3.1 Modeling population distributions

To understand the relative immunogenic potential of each biologic specific to distinct populations, we first created 100 iterative random samples of allele frequencies from each population. We used these frequencies to weight the epitope content in each biologic according to the HLA frequency sample, generating an allele frequency-weighted score. The distribution of 100 allele frequency-weighted scores for each biologic for each population was visualized as a violin plot and compared to the conventional EpiMatrix Score based on global HLA supertype alleles (Supplementary Figure 1).

3.2 Statistical analysis

Medians of Raw and Tregitope-adjusted EpiMatrix Scores by population were compared for each biologic by Wilcoxon signed rank test; p-values <0.05 were considered significant. Results were confirmed with multiple approaches to adjusting p-values for multiple comparisons and quantifying effect sizes (Supplementary Table 3).

3.3 Modeling risk for individuals in populations

An iTEM Score was calculated for each biologic and each potential combination of HLA alleles in each population. Both "Raw" and "Tregitope-adjusted" iTEM Scores were calculated (Supplementary Figure 2).

3.4 Differentiation by absolute difference between populations according to joint probability of allele pairs

To compare and visualize the impact of HLA expression frequency on immunogenic risk, box and whisker plots of Tregitope-adjusted iTEM Scores for all potential pairs of HLA alleles were generated. Pairs of alleles with joint probabilities greater than 5%, and absolute differences of greater than 5% between Japanese and Caucasian populations are shown.

4 Results

4.1 Observed HLA frequencies

Available population data were less abundant for Japanese populations than for Caucasian populations (Supplementary Tables 1A, B). Still, sample sizes were sufficient to calculate expression frequencies for multiple common HLA alleles. As shown in Table 1, alleles expressed at similar frequencies in both populations include HLA-DRB1*0101 and *1501 (Supplementary Figure 3).

Notable differences in the HLA-DR distribution between US and Japanese populations are highlighted here: HLA-DRB1*0901 and *1502 are expressed at high frequency in the Japanese population but not in the Caucasian population, whereas HLA-DRB1*0301 and *0701 are expressed at high frequency in the Caucasian population, but not in the Japanese population. Based on the potential for HLA-DR-restricted T cell epitopes to drive immunogenicity (as measured by ATA), these differences indicate at least some potential for population-specific immunogenic risk based on differential presentation of HLA ligands. A complete, annotated list of evaluated alleles can be seen in Supplementary Table 2.

TABLE 1 Expression frequency of HLA alleles in Japanese and Caucasian populations.

Allele	HLA Allele Frequency, %	
	Japanese Population	Caucasian Population
DRB1*01:01**	**13.51**	**15.02**
DRB1*01:03	0.00	1.96
DRB1*01:04	**0.00**	**4.02**
DRB1*03:01	0.72	29.04
DRB1*04:01**	**2.28**	**7.82**
DRB1*04:04**	**12.23**	**8.41**
DRB1*04:05**	**25.70**	**6.54**
DRB1*04:08**	**0.92**	**1.94**
DRB1*04:10	**3.80**	**0.09**
DRB1*07:01	0.41	24.05
DRB1*08:01	16.78	3.98
DRB1*08:02	7.38	0.34
DRB1*08:73	3.02	0.01
DRB1*09:01**	28.77	0.71
DRB1*11:01	4.00	11.47
DRB1*11:02	0.20	6.60
DRB1*11:04	4.09	8.29
DRB1*11:58	2.40	0.03
DRB1*12:01	8.93	2.58
DRB1*13:01	1.22	11.39
DRB1*13:02	12.49	7.28
DRB1*13:03**	0.00	2.58
DRB1*14:01	5.10	4.83
DRB1*15:01	13.99	16.04
DRB1*15:02	22.89	1.86
DRB1*16:01**	1.53	6.98

Bold font indicates classical "shared epitope" allele.
**Indicates RA risk allele based on 95% confidence interval of OR>1 (Raychaudhuri et al., 2012).
Details of population frequencies are described in Supplementary Table 2.

4.2 Immunogenicity scores of RA biologics

4.2.1 Range of scores calculated for global supertypes

On an overall, global level (not restricted by population-level prevalence data), the Tregitope-adjusted EpiMatrix Immunogenicity Scores of the evaluated RA biologics range from positive 16.99 (Tocilizumab) to negative 60.58 (Etanercept) on the normalized scale illustrated in Figure 1. The highest scores are above the average score of a benchmark set of monoclonal antibodies known to simulate ATA in >5% of exposed patients, while the lowest scores are well below the average score of a benchmark set of monoclonal antibodies known to stimulate ATA in <5% of exposed patients (Figure 1) (30).

4.2.2 Medians of scores for regional populations

On a population level, all the medians of the simulated population distributions of Raw EpiMatrix Scores for most RA biologics differ significantly between Japanese and Caucasian populations, except for Sarilumab (Figure 2, Table 2). Tregitope-adjusted EpiMatrix Score simulated population distribution medians also differ significantly between Japanese and Caucasian populations, with Adalimumab falling near the threshold for significance after adjusting for multiple comparisons (Supplementary Table 3). Fusion proteins consistently have the lowest median scores, both Raw and Tregitope-adjusted, but also differ significantly between populations (Figure 2). The effect sizes showed that the differences in scores between populations are meaningful except for EpiMatrix scores for Sarilumab and Tregitope-adjusted EpiMatrix for Adalimumab.

4.2.3 EpiMatrix and Tregitope-adjusted scores

As is also shown in Figure 2, the unweighted (calculated using supertype HLA-DRB1 alleles) Raw EpiMatrix Scores (not corrected based on Tregitope content) are consistently higher than HLA allele expression frequency-weighted Raw EpiMatrix Scores. After Tregitope-adjustment, unweighted scores for selected DMARDS, specifically Adalimumab, Certolizumab, Golimumab and Sarilumab fall within the distributions of HLA allele expression frequency-weighted scores. In other words, the Tregitope-adjusted score calculated for supertypes is no longer higher than those of the weighted scores for Caucasian and Japanese populations. This result suggests that HLA expression frequencies have differential effects in the immunogenicity risk assessment scores among RA biologics, in particular for those with high Tregitope content. For these biologics,

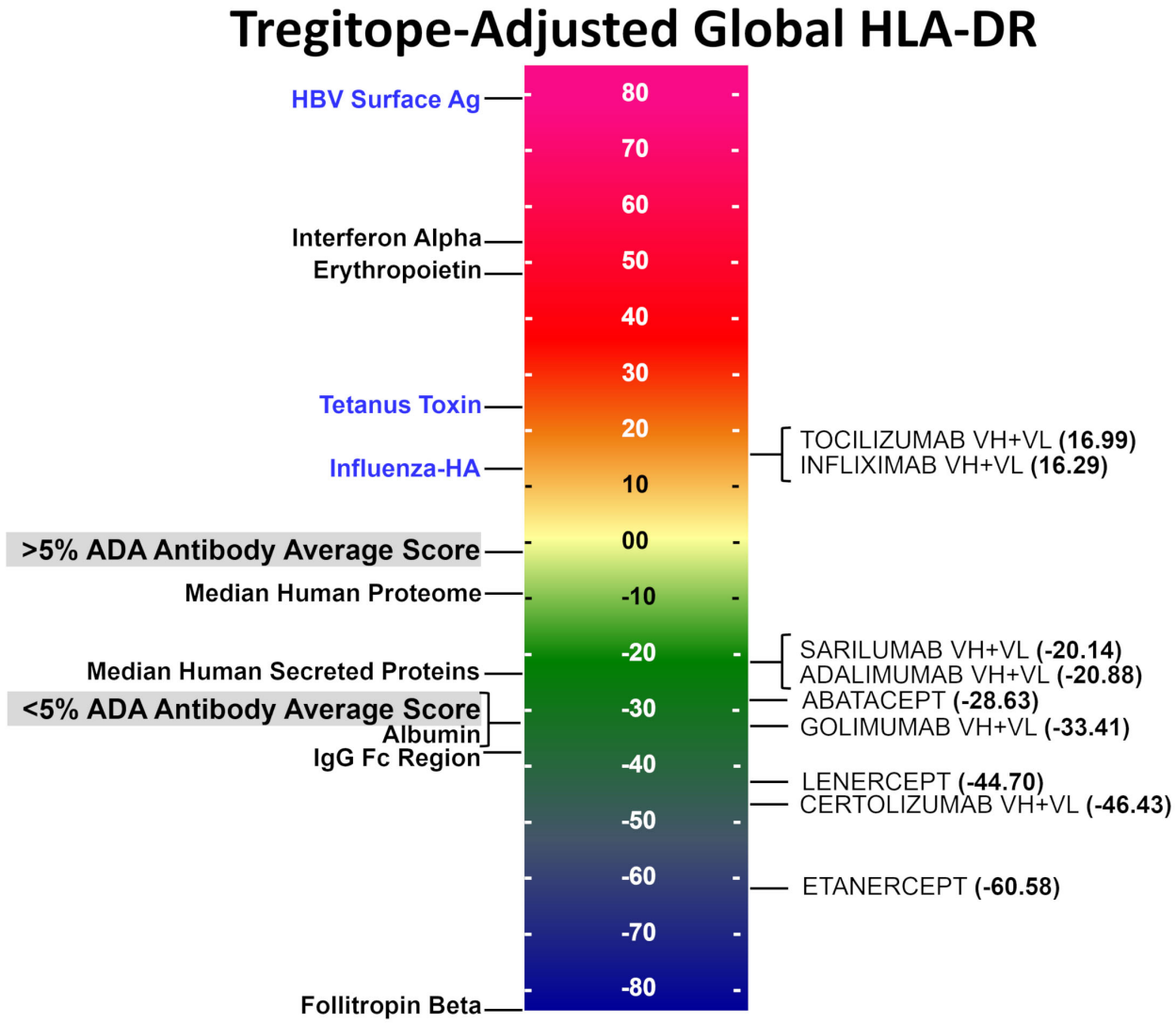

FIGURE 1
Tregitope-adjusted Immunogenicity Risk Potential Scores of RA Biologics and Benchmark Proteins. The EpiMatrix Tregitope-adjusted Protein Immunogenicity Risk Potential Score represents the aggregate predicted T cell epitope content in each protein, per unit protein length, relative to the expected T cell epitope content in a protein of equivalent length. Proteins with positive scores carry more epitope content than the random expectation, and thereby, increased risk for immunogenic response. Proteins with negative scores carry less epitope content than random expectation, and reduced risk for immunogenic response. These scores are adjusted for the presence of epitopes known to stimulate regulatory T cells, called Tregitopes. Human proteins have a wide distribution of Immunogenicity Risk Potential Scores, whose median is -9.05. The median Immunogenicity Risk Potential Score of secreted human proteins is even lower, at -23.08. Protein Immunogenicity Risk Potential Scores above the median of the human proteome may indicate elevated immunogenic risk for therapeutic protein candidates.

the relationship between potential T effector and Tregitope content is more likely to be affected by variations in HLA expression frequencies.

4.2.4 Impact of population HLA expression frequencies is strongest when Tregitope or T effector epitope content is high

Biologics with high Tregitope content (Supplementary Table 4) are more likely to change the Tregitope-adjusted EpiMatrix score/Tregitope content (i.e., T effector/Tregitope) relationship because they have more chances to be affected by HLA frequencies. However, both Tregitope content and potential T effector content can be altered by the HLA frequencies. If the T effector content is lower for one population, and the Tregitope content is identical both populations, differences in the T effector/Tregitope relationship are expected.

4.2.5 Identification of higher risk HLA pairs

Further analysis of pairs of HLA-DR alleles identifies haplotypes that could be 'higher risk' in each population, and that may be contributing most to regional differences. Considering the pairs of HLA alleles that might be expressed by individual patients, just three pairs of alleles are expressed at >5% greater joint probabilities in Caucasian populations compared to Japanese populations, while six pairs of alleles are expressed at >5% greater joint probabilities in Japanese populations compared to Caucasian

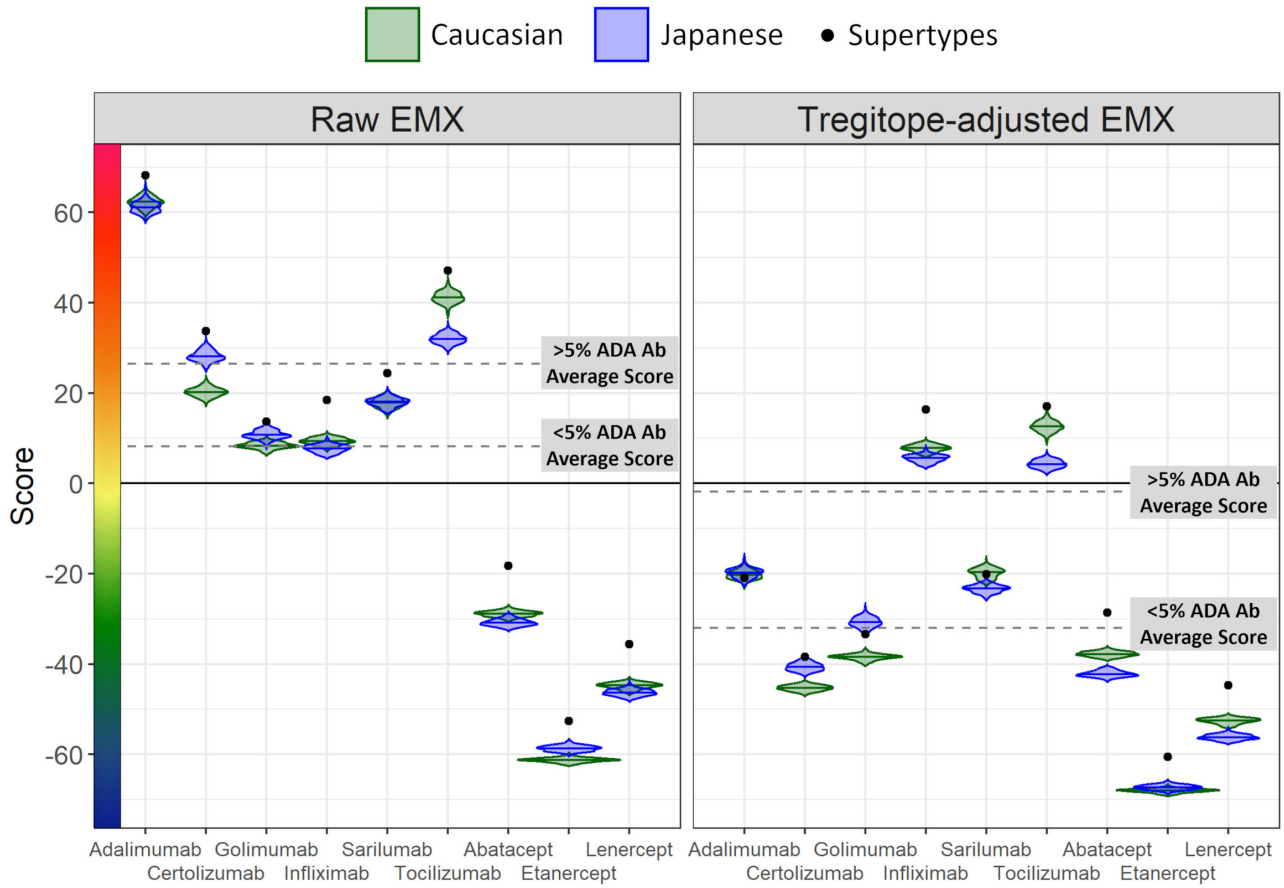

FIGURE 2
Population-specific EpiMatrix Scores of RA Biologics. We used 100 iterative random samples of allele frequencies from each population to weight the epitope content in each biologic according to the HLA frequency sample, generating an allele frequency-weighted score for the Caucasian (green) and Japanese (blue) populations. Supertype scores (black dot) are not weighted for allele frequency. Raw and Tregitope-adjusted EpiMatrix (EMX) scores were calculated. Applying allele frequency weights to scores reveals variation in distributions by population. In most cases, unweighted scores (calculated using HLA-DRB1 alleles) are higher than frequency-weighted scores.

TABLE 2 Raw and Tregitope-adjusted EpiMatrix Score distributions for RA biologics.

Biologic	Raw EpiMatrix			Tregitope-adjusted EpiMatrix		
	Median Caucasian	Median Japanese	p-value	Median Caucasian	Median Japanese	p-value
Adalimumab	62.38	61.18	1.48E-08	-20.26	-19.71	0.0027
Certolizumab	20.22	28.05	2.71E-18	-45.28	-40.73	2.71E-18
Golimumab	8.32	10.68	3.76E-18	-38.41	-30.74	2.71E-18
Infliximab	9.34	7.79	2.58E-16	7.84	5.61	4.77E-18
Sarilumab	17.9	18.05	0.265	-19.6	-23.24	2.71E-18
Tocilizumab	41.16	32.01	2.71E-18	12.58	4.27	2.71E-18
Abatacept	-28.83	-30.9	4.23E-18	-37.81	-42.27	2.71E-18
Etanercept	-61.26	-58.66	2.71E-18	-68.01	-67.29	6.80E-15
Lenercept	-44.74	-46.33	2.94E-17	-52.47	-56.25	2.71E-18

populations (Figure 3). Tregitope-adjusted iTEM Scores for the highest differential frequency HLA allele pairs tend to fall in the top quartile of the distributions, especially for the monoclonal antibody biologics, suggesting higher immunogenicity potential for frequently expressed population-specific HLA allele pairs.

5 Discussion

To better understand the impact of different HLA distributions in distinct population groups on immunogenicity risk potential of RA therapies, we developed a weighted immunogenicity risk assessment score for populations of patients, and for individual patients, called the "T-cell epitope measure" (iTEM) tool. This tool makes it possible to estimate the risk of immune response to a protein antigen based on HLA prevalence in a population, or in an individual (21).

5.1 Summary of key findings

The Human Leukocyte Antigen (HLA) system, specifically the HLA-DR alleles, play a crucial role in the immune response. They are responsible for presenting peptides, including those derived from foreign substances like drugs or pathogens, to the immune system, specifically to CD4+ T cells. The type of HLA-DR allele that is expressed by each individual can influence which peptides are presented to their immune system, which will impact the overall immune response, especially the production of antibodies. HLA-DR differences can also have implications for the generation of anti-

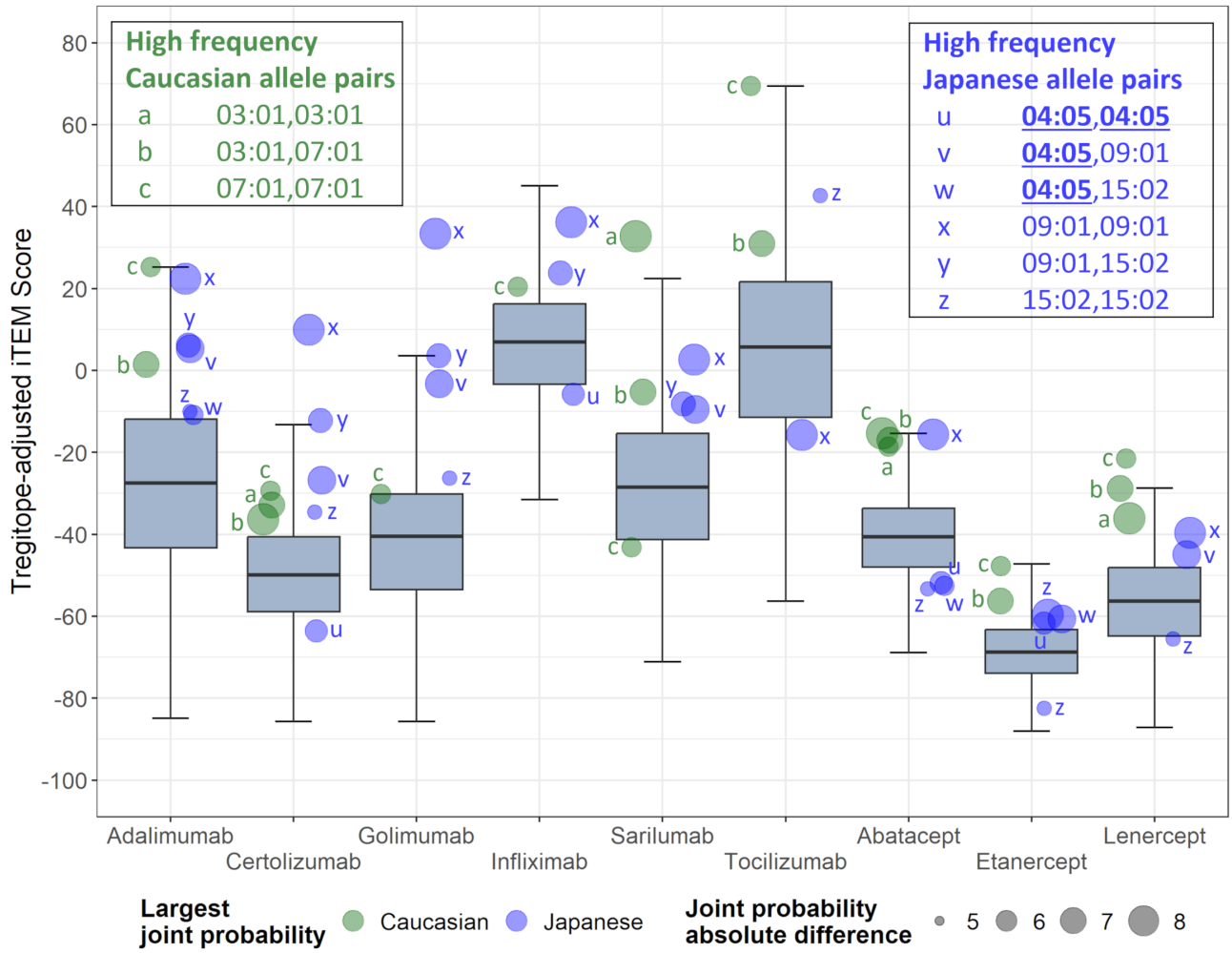

FIGURE 3
RA biologic patient-specific immunogenic risk varies according to HLA expression frequency in Caucasian and Japanese populations. Figure illustrates the distribution of Tregitope-adjusted iTEM Scores for each biologic. The "box" in the box and whisker plot indicates the second and third quartile of each distribution, separated by a median line, while the "whiskers" indicate the first and fourth quartiles. HLA allele pairs are shown in the colored circles to highlight those pairs which have the greatest difference in joint probability between the Caucasian and Japanese populations. Circles shaded green reflect an allele pair whose joint probability is higher in the Caucasian population than the Japanese population; blue-shaded circles indicate allele pairs whose joint probability is higher in the Japanese population. The size of the circle marker indicates the absolute difference in the joint possibility of the allele pair between the two populations. Only pairs whose absolute joint probability difference is greater than 5% are shown.

therapeutic antibodies (ATAs) to biologic therapeutics. Simply stated, a sequence in each biologic drug might be presented as a foreign peptide by a particular HLA-DR allele that is common in one population, triggering an immune response and ATA production, while the same drug might not trigger the same response in a population where that HLA-DR allele is less common. Geographic variations in HLA-DR alleles have been well documented, reflecting the genetic diversity and evolutionary pressures of different human populations (38).

Here, we have focused on two populations in which similar biological DMARDs are used to treat RA, with potentially different outcomes. We note that HLA-DRB1*09:01 and *15:02 are expressed at high frequency in the Japanese population but not in the Caucasian population, whereas HLA-DRB1*03:01 and *07:01 are expressed at high frequency in the Caucasian population, but not in the Japanese population.

Based on the key contribution of HLA-DR-restricted T cell epitopes to immunogenicity risk potential, these differences indicated at least some potential for population-specific immunogenic risk based on differential presentation of HLA ligands. These differences may be exacerbated in the context of autoimmune diseases such as RA, as certain HLA-DR alleles have been associated the condition. Possessing these specific alleles not only predisposes individuals to RA, but also to a more robust or dysregulated immune response to foreign substances, including biologic therapeutics, which can contribute to increased ATA production.

Differences in the potential immunogenicity risk, based on regional HLA-DR allele differences, are summarized in Figure 3. As shown in this figure, on a population level, all the medians of the simulated population distributions of Raw EpiMatrix Scores for most RA biologics differ significantly between Japanese and Caucasian populations, except for Sarilumab.

Take for example, Tocilizumab. Significant differences in the ATA formation to this very important anti-IL-6 therapeutic have been noted in certain populations and could be explained by the fact the HLA-DR*09 allele is highly prevalent among Japanese RA patients. Tocilizumab is known to be associated with limited ATA formation in Japanese patients. The Tregitope adjusted iTEM Scores for DRB1*09:01 homozygous patients fall in the bottom quartile of the distribution for Tocilizumab. In this case, HLA-DRB1*09:01 patients are not expected to develop ATA response to the drug. However, some RA patients in Japan may not carry the HLA-DRB1*09:01 allele that "protects" against ATA for Tocilizumab. In those cases, Fc-fusion proteins such as Abatacept or Etanercept is predicted to be less immunogenic. It is interesting to note that in a previous study, *in vitro* analysis and transcriptomic pathway analysis suggested that a higher frequency of memory CXCR4(+)CD4(+) T cells predicted a better response to CTLA4-Ig (Abatacept) (13). It is not clear whether the memory CD4 T cells in the above study were regulatory T cells, which could explain the observation.

5.1.1 Interpretation of frequency weighted scores, especially iTEM

We evaluated whether the distributions of scores in the violin plots are different between populations. We tried a few tests and found that based on p-values, the populations were different, with EpiMatrix scores for Sarilumab as the only exception. P-values were adjusted for multiple comparisons using 6 different approaches. P-values only tell us whether an effect exists, but do not tell us whether the effect is large enough to be practically meaningful. P-values are influenced by the sample size, so increasing the sample size makes it more likely to find a statistically significant effect, no matter how small the effect truly is in the real world. In contrast, effect sizes are independent of the sample size. For non-parametric tests that used paired samples, effect sizes are calculated using rank-biserial correlations. Categorical effect size interpretations based on criteria defined by different authors were applied, see Supplementary Table 3. Only the effect size for Sarilumab EpiMatrix and Tregitope-adjusted EpiMatrix Adalimumab are not classified as large, very strong, or very large. This means that with exception of EpiMatrix scores for Sarilumab and Tregitope-adjusted EpiMatrix for Adalimumab, the scores are significantly different between populations and the differences can be considered meaningful or they suggest practical significance.

5.1.2 Discussion of potential impact of T cell function during treatment

Tregs play a crucial role in maintaining immune tolerance and controlling excessive immune responses. Restoration of regulatory T cell (Treg) function during rheumatoid arthritis (RA) treatment could potentially have a significant impact on disease activity and progression. In the context of RA, their function is often impaired, contributing to the chronic inflammation and tissue damage characteristic of the disease. Enhancing Treg function may not only help manage the symptoms of RA but could also address some of the underlying immune dysregulation driving ATA responses. Some DMARDs have been shown to enhance Treg function (39). The re-activation of regulatory T cell responses may be responsible for some of the "treatment-induced tolerance" that has been observed in many clinical studies (16), and this effect may be more evident for those individuals that carry HLA-DR alleles that are able to present T reg epitopes (Tregitopes), and for DMARDS that contain more Tregitopes.

5.1.3 Consideration of other (non HLA-DR) HLA

Differences in the HLA-DR distributions between Japanese and Caucasian populations are outlined in Table 1. Notable differences include HLA-DRB1*01:04, *04:01 and *04:05, all of which are alleles that have a shared amino acid pattern known as the "shared epitope" (Table 1). These distinct differences in shared epitope frequency are seen in RA patients from both populations, confirming previous observations that HLA-DR does not directly predict the development of RA. The differences are, however, likely to have an impact on the development of ATA, a hypothesis that is validated in Table 2 (see significant differences in immunogenicity risk potential, as calculated using EpiMatrix); and in Figures 2 and 3 as contrasted with Figure 1, which compares the relative immunogenicity risk potential of RA therapeutics for global, rather than geographically defined populations.

Other HLA effects such as HLA-DP, DQ, and that of the non-classical DOA HLA gene were not measured in this analysis, for several reasons. Firstly, a significant correlation between ATA and T

cell epitope content has been defined previously (24), and this correlation is not preserved when HLA-DP and -DQ predictions are included in the calculation (33). Second, models assessing the impact of the DOA-gene have not been established (6). Additional prospective and retrospective studies may be necessary to define the contributions of alleles beyond HLA-DR.

As can be seen by Table 1, the impact of shared epitope alleles on potential for immunogenicity cannot be distinguished from general HLA prevalence frequency in the two populations. Thus, the contribution of SE to differences in immunogenicity risk cannot be quantified in this study.

5.2 Advantages and limitations of study

A significant limitation of this study is that it only addresses the risk of immunogenicity in two regional populations – Japanese and American Caucasians. Clearly, there can be significant intra-regional HLA-DR differences in populations (such as can be observed between Caucasian-Americans and African Americans) and there are many global populations for which HLA-DR typing is inconsistent and incomplete. More information on HLA-DR haplotypes is a critical need for improving our understanding of ATA responses to immunomodulatory therapeutics in RA.

Furthermore, while we found that differences in the estimated immunogenicity risk potential that could be associated with the frequency of HLA-DR alleles in each of the regional populations we evaluated to be significant for some of the biological DMARDs, we evaluated relying solely on HLA-DR-associated immunogenicity risk assessment which may be insufficient for predicting anti-therapeutic antibody (ATA) development. This is because ATA formation is a complex process influenced by a multitude of factors, both patient-related and drug-related, and not just by the presence of specific HLA-DR alleles. It is important to note that decreased TCR diversity has been identified in some RA subjects that have the "shared epitope" alleles (40). While we did not find an association between SE and immunogenicity risk in this study, constraints on TCR diversity may have an important impact on ATA responses.

Notably, several GWAS studies have identified a specific HLA-DQ allele (HLA-DQA1*05) as being associated with anti-DMARD antibodies (ATA). In a study of Crohn's disease subjects, immunogenicity was linked to HLA-DQA1*05 by GWAS for two disparate biologics [adalimumab, and infliximab, (26, 41)]. These two biologic products are significantly different in terms of their protein sequences. A second publication (42), evaluated linkages between ATA to eight different biologics with significantly different mechanisms of actions and protein sequences, and also found a linkage to HLA-DQLA1*05 along with several other HLA-DR alleles (some of which were found to be protective).

Since the correlation with ATA was found irrespective of the sequence of the biologic in these two studies, it is possible that the association with HLA-DQA1*05 is related to a link between the gene and Treg function in the lymphoid follicle, rather than HLA allele restriction of T effector epitopes which are more likely to be found in the CDR regions and less likely to be found in the common framework regions (where Tregitopes are present). An association with Treg function or Tregitopes could also explain linkages to HLA-DRB1*01:01, 03:01, and 07:01 (these are prevalent alleles in European/Caucasian populations) (43). The potential linkages to epitopes (such as Tregitopes) that are conserved between biologics would require further study.

In addition to HLA-DR alleles, other genes involved in the immune response may influence ATA formation, such as genes coding for cytokines and cytokine receptors, T-cell receptors, and B-cell activating factors. Use of other drugs, especially immunosuppressants, can affect the immune response and the risk of ATA development. The presence of aggregates, post-translational modifications, and impurities can also increase the risk of ATA formation. Both the dose and frequency of administration of biological DMARDs can influence the risk of ATA development. Environmental factors, including exposure to pathogens or other foreign antigens, can stimulate the immune system and potentially influence ATA formation. Given the multifactorial nature of immunogenicity, a comprehensive risk assessment for ATA development would need to consider all these factors and their potential interactions, rather than focusing solely on HLA-DR-associated risk.

Lastly, we must address the accuracy of the HLA ligand predictions that are based on EpiMatrix, a tool that has been in continuous use (with updates) since the early 2000's. In support of the accuracy of this tool, we compiled a retrospective evaluation of EpiMatrix results to internal HLA binding assays which demonstrated that EpiMatrix ranking has a Positive Predictive Value (PPV) of 81% and that the HLA class II predictions were 74% accurate. This study involved more than 1600 assays, performed in house, using the same methodology as published in De Groot et al., 2020 (33).

In addition, for this publication, we performed a high-level analysis of HLA-DR-eluted peptides that have been compiled in the IEDB database (25) to EpiMatrix HLA-DR predictions. We identified 70,594 peptides in the IEDB that were reported (as of March 26, 2024) to have been eluted from human HLA-DR molecules. Using our usual threshold for binding (EpiMatrix Z-score of 1.64), 58,335 (83%) of these peptides contained at least one HLA-allele-specific epitope that is also identified by EpiMatrix. At a slightly lower cutoff that includes "likely" HLA-binding 9-mers (Z-score of 1.28), 64,064 or 91% of the reported eluted peptides contain at least one HLA-allele-specific EpiMatrix ligand (unpublished data analysis by Bill Martin).

Additional T cell epitope and HLA binding validation studies have been published in the course of grant-funded research collaborations, describing T cell immune responses to predicted epitopes *in vitro* using human lymphocytes. For example, 100% of subjects exposed to either Tularemia or Vaccinia responded to pools of T cell epitope clusters that score higher than 20 on the EpiMatrix immunogenicity scale (44–46). In a recent head-to-head comparison, the ClustiMer approach outperformed the standard overlapping peptide approach (usually 15mer peptides overlapping by five amino acids) used by many biologics' researchers (44). In that comparison, T cell responses to the 15mer overlapping peptides

were lower, on average, than the maximal responses induced by the pools predicted using immunoinformatic tools (32).

Overall, the HLA-DR-assessments that are included in this study can be considered to be highly correlated with HLA binding data, HLA ligand elution studies, and T cell assays as currently performed and compiled in public databases.

6 Conclusions

In conclusion, analysis of HLA-DR allele haplotypes in rheumatoid arthritis (RA) patient populations could potentially improve the selection of disease-modifying antirheumatic drugs (DMARDs) because these alleles can influence the immune response, including the response to therapeutics. As we have shown here, certain HLA-DR alleles might predispose individuals to a heightened immune response towards specific biologic DMARDs, increasing the risk of developing ATA that can neutralize the drug or accelerate its clearance, thereby reducing their efficacy. Identifying these HLA-DR risk alleles may make possible to select drugs with a lower risk of immunogenicity for these patients. Differences in the frequencies of higher risk HLA pairs in regional populations could also explain any differences in the immunogenicity of biologics that are observed in regional cohorts participating in studies that measure ATA.

In clinical practice, understanding the relationship between HLA-DR alleles and ATA formation could potentially guide personalized therapeutic decisions and the selection of one biological DMARD over another. HLA haplotyping has improved recently, due to the availability of algorithms that deduce HLA haplotype from NGS sequencing of genetic material in peripheral blood (47, 48). Making these decisions will depend on the ability of clinicians to access therapeutic drug monitoring and HLA-DR typing for their patients. In addition, treatment with certain therapeutic agents likely modifies the inflammatory response, leading to the induction of tolerance. Thus, a full understanding of the disease state of the patient, their specific RA-risk factor and phenotype, as well as their HLA-DR allele may be required prior to planning to introduce personalized therapy. More research is needed to fully understand the implications of HLA-DR variations on ATA formation and biologic drug response in different populations.

Achieving the full potential of pharmaceutical products for treatment of Rheumatoid Arthritis (RA) depends on the appropriate selection of the best product for the stage of disease, as well as for the individual patient. Each stage of RA may be phenotypically different, just as each patient may be somewhat genetically unique. Advances have been made in the field of medicine to improve the efficacy of therapy by linking the specific type of therapy by disease characteristic or to stage of disease. Similarly, improvements in RA therapy may be possible if therapy is tailored to characteristics that are unique to populations of patients, and/or to individual patients, based on their individual HLA haplotype and disease phenotype. In other fields, tailored therapy is already being selected. For example, selection of the specific cancer therapy and the design of cancer vaccines can be based on oncogenes that are detected in the patients' tumors, and on the patient's HLA alleles (49–51).

7 Future directions

This study indicates that HLA-DR genotyping could potentially contribute to the optimization of therapeutic selection. Other factors, such as other genetic factors, the patient's disease activity and severity, comorbidities, and concomitant medications, should also be considered. Additional prospective studies are needed to support the role of HLA-DR genotyping in guiding biological DMARD selection in clinical practice.

This information could be made available to clinicians who would like to select therapies for their patients that are unlikely to drive ATA. A website devoted to identifying individualized risk of ATA for patients treated with enzyme replacement therapies (Pompe-PIMA) has already been imagined (22). A similar website could also be developed for selecting the best biological DMARD for an individual patient based on their HLA-DR allele haplotype and other genetic factors that are known to be associated with RA. This website could for example take into consideration RA-specific disease states and pre-disposing genetic factors such as mutations associated with regulatory T cell, T follicular helper cell, and cytokine receptor deficiencies (52). One potential use of such a website would be to retrospectively evaluate the association between HLA-DR haplotypes and ATA data generated in the context of clinical trials. A "batch upload" feature was recently added to the PIMA website to facilitate such studies. Both retrospective and prospective studies should be conducted prior to implementing analyses such as PIMA for RA in clinical settings.

Data availability statement

The original contributions presented in the study are included in the article/Supplementary Material. Further inquiries can be directed to the corresponding authors.

Author contributions

NS: Conceptualization, Funding acquisition, Investigation, Supervision, Writing – review & editing, Data curation, Methodology. FT: Conceptualization, Investigation, Methodology, Formal analysis, Visualization, Writing – original draft. AHG: Writing – review & editing, Data curation, Investigation, Methodology. TH: Writing – review & editing. MH: Writing – review & editing. YM: Writing – review & editing. WM: Writing – review & editing, Investigation, Methodology, Supervision, Validation. SY: Writing – review & editing. HN: Writing – review & editing, Data curation. KF: Writing – review & editing, Conceptualization, Supervision. ADG: Writing – review & editing, Conceptualization, Formal analysis, Funding acquisition, Investigation, Project administration, Supervision, Visualization, Writing – original draft.

Funding

The author(s) declare that financial support was received for the research, authorship, and/or publication of this article. Funding for the research activities related to the development of this manuscript was provided by internal funds from Pfizer Japan, and EpiVax.

Acknowledgments

We are grateful for the review of this manuscript by Sophie Tourdot at Pfizer, in Boston MA. Stephanie Elkins provides significant support for the management of the editorial process. We would also like to thank the EpiVax informatics team including Matt Ardito, Jacob Tivin and Mark Bushnell for their technical and programming support and for the development of the ISPRI toolkit.

Conflict of interest

ADG and WM are senior officers and majority shareholders of EpiVax, Inc, a privately owned immunoinformatics and vaccine design company. ADG, WM and AHG are employees of EpiVax, Inc. Due to this relationship with EpiVax, these authors acknowledge that there is a potential conflict of interest inherent in the publication of this manuscript, and attest that the work contained in this research report is free of any bias that might be associated with the commercial goals of the company. NS, TH, MH, YM are employed by Pfizer Japan. These authors acknowledge that there is a potential conflict of interest inherent in the publication of this manuscript, and attest that the work contained in this research report is free of any bias that might be associated with the commercial goals of the company.

The remaining authors declare that the research was conducted in the absence of any commercial or financial relationships that could be construed as a potential conflict of interest.

The author ADG declared that they were an editorial board member of Frontiers, at the time of submission. This had no impact on the peer review process and the final decision.

Publisher's note

Supplementary material

The Supplementary Material for this article can be found online at: https://www.frontiersin.org/articles/10.3389/fimmu.2024.1377911/full#supplementary-material

References

1. Finckh A, Gilbert B, Hodkinson B, Bae SC, Thomas R, Deane KD, et al. Global epidemiology of rheumatoid arthritis. *Nat Rev Rheumatol.* (2022) 18(10):591–602. doi: 10.1038/s41584-022-00827-y

2. Yamanaka H, Sugiyama N, Inoue E, Taniguchi A, Momohara S. Estimates of the prevalence of and current treatment practices for rheumatoid arthritis in Japan using reimbursement data from health insurance societies and the IORRA cohort (I). *Mod Rheumatol.* (2014) 24(1):33–40. doi: 10.1007/s10165-013-0863-6

3. Nakajima A, Sakai R, Inoue E, Harigai M. Prevalence of patients with rheumatoid arthritis and age-stratified trends in clinical characteristics and treatment, based on the National Database of Health Insurance Claims and Specific Health Checkups of Japan. *Int J Rheum Dis.* (2020) 23(12):1676–84. doi: 10.1111/1756-185X.13974

4. Gregersen PK, Silver J, Winchester RJ. The shared epitope hypothesis. an approach to understanding the molecular genetics of susceptibility to rheumatoid arthritis. *Arthritis Rheumatol.* (1987) 30(11):1205–13. doi: 10.1002/art.1780301102

5. Raychaudhuri S, Sandor C, Stahl EA, Freudenberg J, Lee HS, Jia X, et al. Five amino acids in three HLA proteins explain most of the association between MHC and seropositive rheumatoid arthritis. *Nat Genet.* (2012) 44(3):291–6. doi: 10.1038/ng.1076

6. Okada Y, Suzuki A, Ikari K, Terao C, Kochi Y, Ohmura K, et al. Contribution of a non-classical HLA gene, HLA-DOA, to the risk of rheumatoid arthritis. *Am J Hum Genet.* (2016) 99(2):366–74. doi: 10.1016/j.ajhg.2016.06.019

7. Viatte S, Plant D, Bowes J, Lunt M, Eyre S, Barton A, et al. Genetic markers of rheumatoid arthritis susceptibility in anti-citrullinated peptide antibody negative patients. *Ann Rheum Dis.* (2012) 71(12):1984–90. doi: 10.1136/annrheumdis-2011-201225

8. Jawa V, Terry F, Gokemeijer J, Mitra-Kaushik S, Roberts BJ, Tourdot S, et al. T-cell dependent immunogenicity of protein therapeutics pre-clinical assessment and mitigation–updated consensus and review 2020. *Front Immunol.* (2020) 11. doi: 10.3389/fimmu.2020.01301

9. Pratt KP. Anti-drug antibodies: Emerging approaches to predict, reduce or reverse biotherapeutic immunogenicity. *Antibodies.* (2018) 7(2):19. doi: 10.3390/antib7020019

10. Nagafuchi Y, Shoda H, Sumitomo S, Nakachi S, Kato R, Tsuchida Y, et al. Immunophenotyping of rheumatoid arthritis reveals a linkage between HLA-DRB1 genotype, CXCR4 expression on memory CD4+ T cells, and disease activity. *Sci Rep.* (2016) 6:29338. doi: 10.1038/srep29338

11. Lucas C, Perdriger A, Amé P. Definition of B cell helper T cells in rheumatoid arthritis and their behavior during treatment. *Semin Arthritis Rheum.* (2020) 50 (5):867–72. doi: 10.1016/j.semarthrit.2020.06.021

12. Mehta P, Manson JJ. What is the clinical relevance of TNF inhibitor immunogenicity in the management of patients with rheumatoid arthritis? *Front Immunol.* (2020) 11. doi: 10.3389/fimmu.2020.00589

13. Strand V, Balsa A, Al-Saleh J, Barile-Fabris L, Horiuchi T, Takeuchi T, et al. Immunogenicity of biologics in chronic inflammatory diseases: A systematic review. *BioDrugs.* (2017) 31(4):299–316. doi: 10.1007/s40259-017-0231-8

14. Cao G, Wang P, Cui Z, Yue X, Chi S, Ma A, et al. An imbalance between blood CD4+CXCR5+Foxp3+ Tfr cells and CD4+CXCR5+Tfh cells may contribute to the immunopathogenesis of rheumatoid arthritis. *Mol Immunol.* (2020) 125:1–8. doi: 10.1016/j.molimm.2020.06.003

15. Szalay B, Vásárhelyi B, Cseh Á, Tulassay T, Deák M, Kovács L, et al. The impact of conventional DMARD and biological therapies on CD4+ cell subsets in rheumatoid arthritis: A follow-up study. *Clin Rheumatol.* (2014) 33(2):175–85. doi: 10.1007/s10067-013-2352-x

16. Atiqi S, Hooijberg F, Loeff FC, Rispens T, Wolbink GJ. Immunogenicity of TNF-inhibitors. *Front Immunol.* (2020) 11:312. doi: 10.3389/fimmu.2020.00312

17. Di Matteo A, Bathon JM, Emery P. Rheumatoid arthritis. *Lancet.* (2023) 402 (10416):2019–33. doi: 10.1016/S0140-6736(23)01525-8

18. Thomas SS, Borazan N, Barroso N, Duan L, Taroumian S, Kretzmann B, et al. Comparative immunogenicity of TNF inhibitors: impact on clinical efficacy and tolerability in the management of autoimmune diseases. A systematic review and meta-analysis. *BioDrugs.* (2015) 29(4):241–58. doi: 10.1007/s40259-015-0134-5

19. Van Schouwenburg PA, Rispens T, Wolbink GJ. Immunogenicity of anti-TNF biologic therapies for rheumatoid arthritis. *Nat Rev Rheumatol.* (2013) 9(3):164–72. doi: 10.1038/nrrheum.2013.4

20. Garcês S, Demengeot J. The immunogenicity of biologic therapies. *Curr Problems Dermatol (Switzerland).* (2017) 53:37–48. doi: 10.1159/000478077

21. De Groot AS, Cohen T, Moise L, Ardito M, Martin W. A method for individualizing the prediction of immunogenicity of protein vaccines and biologic therapeutics: Individualized T cell epitope measure (iTEM). *J BioMed Biotechnol.* (2010) 2010:961752. doi: 10.1155/2010/961752

22. De Groot AS, Desai AK, Lelias S, Miah SMS, Terry FE, Khan S, et al. Immune tolerance-adjusted personalized immunogenicity prediction for Pompe disease. *Front Immunol.* (2021) 12. doi: 10.3389/fimmu.2021.636731

23. Gonzalez-Galarza FF, McCabe A, Dos Santos EJM, Jones J, Takeshita L, Ortega-Rivera ND, et al. Allele frequency net database (AFND) 2020 update: Gold-standard data classification, open access genotype data and new query tools. *Nucleic Acids Res.* (2020) 48. doi: 10.1093/nar/gkz1029

24. Jawa V, Cousens L, De Groot AS. Immunogenicity of therapeutic fusion proteins: contributory factors and clinical experience. In *Fusion Protein Technologies for Biopharmaceuticals*. Schmidt S. R. (Ed.) Wiley, Hoboken, NJ (2013).

25. Vita R, Mahajan S, Overton JA, Dhanda SK, Martini S, Cantrell JR, et al. The immune epitope database (IEDB): 2018 update. *Nucleic Acids Res.* (2019) 47:D339–43. doi: 10.1093/nar/gky1006

26. Yogurtcu ON, Sauna ZE, McGill JR, Tegenge MA, Yang H. TCPro: an in silico risk assessment tool for biotherapeutic protein immunogenicity. *AAPS J.* (2019) 21 (5):96. doi: 10.1208/s12248-019-0368-0

27. Chen B, Khodadoust MS, Olsson N, Wagar LE, Fast E, Liu CL, et al. Predicting HLA class II antigen presentation through integrated deep learning. *Nat Biotechnol.* (2019) 37(11):1332–43. doi: 10.1038/s41587-019-0280-2

28. Racle J, Michaux J, Rockinger GA, Arnaud M, Bobisse S, Chong C, et al. Robust prediction of HLA class II epitopes by deep motif deconvolution of immunopeptidomes. *Nat Biotechnol.* (2019) 37(11):1283–6. doi: 10.1038/s41587-019-0289-6

29. Abelin JG, Harjanto D, Malloy M, Suri P, Colson T, Goulding SP, et al. Defining HLA-II ligand processing and binding rules with mass spectrometry enhances cancer epitope prediction. *Immunity.* (2019) 51(4):766–779.e17. doi: 10.1016/j.immuni.2019.08.012

30. De Groot AS, Martin W. Reducing risk, improving outcomes: Bioengineering less immunogenic protein therapeutics. *Clin Immunol.* (2009) 131(2):189–201. doi: 10.1016/j.clim.2009.01.009

31. De Groot AS, Terry F, Cousens L, Martin W. Beyond humanization and de-immunization: Tolerization as a method for reducing the immunogenicity of biologics. *Expert Rev Clin Pharmacol.* (2013) 6(6):651–62. doi: 10.1586/17512433.2013.835698

32. Eickhoff CS, Meza KA, Terry FE, Colbert CG, Blazevic A, Gutiérrez AH, et al. Identification of immunodominant T cell epitopes induced by natural Zika virus infection. *Front Immunol.* (2023) 14. doi: 10.3389/fimmu.2023.1247876

33. De Groot AS, Moise L, Terry F, Gutierrez AH, Hindocha P, Richard G, et al. Better epitope discovery, precision immune engineering, and accelerated vaccine design using immunoinformatics tools. *Front Immunol.* (2020) 11. doi: 10.3389/fimmu.2020.00442

34. Southwood S, Sidney J, Kondo A, del Guercio MF, Appella E, Hoffman S, et al. Several common HLA-DR types share largely overlapping peptide binding repertoires. *J Immunol.* (1998) 160(7):3363–73. doi: 10.4049/jimmunol.160.7.3363

35. De Groot AS, Kazi ZB, Martin RF, Terry FE, Desai AK, Martin WD, et al. HLA- and genotype-based risk assessment model to identify infantile onset pompe disease patients at high-risk of developing significant anti-drug antibodies (ADA). *Clin Immunol.* (2019) 200:66–70. doi: 10.1016/j.clim.2019.01.009

36. Kotraiah V, Phares TW, Terry FE, Hindocha P, Silk SE, Nielsen CM, et al. Identification and immune assessment of T cell epitopes in five plasmodium falciparum blood stage antigens to facilitate vaccine candidate selection and optimization. *Front Immunol.* (2021) 12. doi: 10.3389/fimmu.2021.690348

37. De Groot AS, Moise L, McMurry JA, Wambre E, Van Overtvelt L, Moingeon P, et al. Activation of natural regulatory T cells by IgG Fc-derived peptide "Tregitopes. *Blood.* (2008) 112(8):3303–11. doi: 10.1182/blood-2008-02-138073

38. Sanchez-Mazas A. A review of HLA allele and SNP associations with highly prevalent infectious diseases in human populations. *Swiss Med Wkly.* (2020) 150: w20214. doi: 10.4414/smw.2020.20214

39. Nguyen DX, Ehrenstein MR. Anti-TNF drives regulatory T cell expansion by paradoxically promoting membrane TNF-TNF-RII binding in rheumatoid arthritis. *J Exp Med.* (2016) 213(7):1241–53. doi: 10.1084/jem.20151255

40. Sakurai K, Ishigaki K, Shoda H, Nagafuchi Y, Tsuchida Y, Sumitomo S, et al. HLA-DRB1 shared epitope alleles and disease activity are correlated with reduced T Cell receptor repertoire diversity in CD4+ T cells in rheumatoid arthritis. *J Rheumatol.* (2018) 45(7):905–14. doi: 10.3899/jrheum.170909

41. Sazonovs A, Kennedy NA, Moutsianas L, Heap GA, Rice DL, Reppell M, et al. HLA-DQA1*05 carriage associated with development of anti-drug antibodies to infliximab and adalimumab in patients with Crohn's disease. *Gastroenterology.* (2020) 158(1):189–99. doi: 10.1053/j.gastro.2019.09.041

42. Hässler S, Bachelet D, Duhaze J, Szely N, Gleizes A, Abina SHB, et al. Clinicogenomic factors of biotherapy immunogenicity in autoimmune disease: A prospective multicohort study of the ABIRISK consortium. *PloS Med.* (2020) 17(10): e1003348. doi: 10.1371/journal.pmed.1003348

43. Liu M, Degner J, Davis JW, Idler KB, Nader A, Mostafa NM, et al. Identification of HLA-DRB1 association to adalimumab immunogenicity. *PloS One.* (2018) 13: e0195325. doi: 10.1371/journal.pone.0195325

44. Mattei AE, Gutierrez AH, Seshadri S, Tivin J, Ardito M, Rosenberg AS, et al. In silico methods for immunogenicity risk assessment and human homology screening for therapeutic antibodies. *MAbs.* (2024) 16:2333729. doi: 10.1080/19420862.2024.2333729

45. McMurry JA, Gregory SH, Moise L, Rivera D, Buus S, De Groot AS. Diversity of Francisella tularensis Schu4 antigens recognized by T lymphocytes after natural infections in humans: identification of candidate epitopes for inclusion in a rationally designed tularemia vaccine. *Vaccine.* (2007) 25:3179–91. doi: 10.1016/j.vaccine.2007.01.039

46. Moise L, Buller RM, Schriewer J, Lee J, Frey SE, Weiner DB, et al. VennVax, a DNA-prime, peptide-boost multi-T-cell epitope poxvirus vaccine, induces protective immunity against vaccinia infection by T cell response alone. *Vaccine.* (2011) 29:501–11. doi: 10.1016/j.vaccine.2010.10.064

47. Nariai N, Kojima K, Saito S, Mimori T, Sato Y, Kawai Y, et al. HLA-VBSeq: Accurate HLA typing at full resolution from whole-genome sequencing data. *BMC Genomics.* (2015) 16 Suppl 2(Suppl 2):S7. doi: 10.1186/1471-2164-16-S2-S7

48. Boegel S, Löwer M, Schäfer M, Bukur T, de Graaf J, Boisguérin V, et al. HLA typing from RNA-Seq sequence reads. *Genome Med.* (2012) 4(12):102. doi: 10.1186/gm403

49. Richard G, Princiotta MF, Bridon D, Martin WD, Steinberg GD, De Groot AS. Neoantigen-based personalized cancer vaccines: the emergence of precision cancer immunotherapy. *Expert Rev Vaccines.* (2022) 21(2):173–84. doi: 10.1080/14760584.2022.2012456

50. Aletaha D. Precision medicine and management of rheumatoid arthritis. *J Autoimmun.* (2020) 110:102405. doi: 10.1016/j.jaut.2020.102405

51. Saxena M, van der Burg SH, Melief CJM, Bhardwaj N. Therapeutic cancer vaccines. *Nat Rev Cancer.* (2021) 21(6):360–78. doi: 10.1038/s41568-021-00346-0

52. Zhu Y, Zou L, Liu YC. T follicular helper cells, T follicular regulatory cells and autoimmunity. *Int Immunol.* (2016) 28(4):173–9. doi: 10.1093/intimm/dxv079

frontiers | Frontiers in Immunology

TYPE Original Research
PUBLISHED 28 May 2024
DOI 10.3389/fimmu.2024.1406040

OPEN ACCESS

EDITED BY
Daniel T. Mytych,
Amgen, United States

REVIEWED BY
Matthew Raybould,
University of Oxford, United Kingdom
Daniel Kramer,
Sanofi, Frankfurt am Main, Germany

*CORRESPONDENCE
Laurent Malherbe
malherbe_laurent@lilly.com

RECEIVED 24 March 2024
ACCEPTED 14 May 2024
PUBLISHED 28 May 2024

CITATION
Walsh RE, Nix A, Ackaert C, Mazy A, Schockaert J, Pattyn S and Malherbe L (2024) Preclinical immunogenicity risk assessment of biotherapeutics using CD4 T cell assays. *Front. Immunol.* 15:1406040. doi: 10.3389/fimmu.2024.1406040

Preclinical immunogenicity risk assessment of biotherapeutics using CD4 T cell assays

Robin E. Walsh[1], Angela Nix[1], Chloé Ackaert[2], Aurélie Mazy[2], Jana Schockaert[2], Sofie Pattyn[2] and Laurent Malherbe[1]*

[1]Lilly Research Laboratories, Eli Lilly and Company, Indianapolis, IN, United States, [2]ImmunXperts SA| Rue August Piccard 48, Gosselies, Belgium

T-cell dependent antibody responses to biotherapeutics remain a challenge to the optimal clinical application of biotherapeutics because of their capacity to impair drug efficacy and their potential to cause safety issues. To minimize this clinical immunogenicity risk, preclinical assays measuring the capacity of biotherapeutics to elicit CD4 T cell response *in vitro* are commonly used. However, there is considerable variability in assay formats and a general poor understanding of their respective predictive value. In this study, we evaluated the performance of three different CD4 T cell proliferation assays in their capacity to predict clinical immunogenicity: a CD8 T cell depleted peripheral blood mononuclear cells (PBMC) assay and two co-culture-based assays between dendritic cells (DCs) and autologous CD4 T cells with or without restimulation with monocytes. A panel of 10 antibodies with a wide range of clinical immunogenicity was selected. The CD8 T cell depleted PBMC assay predicted the clinical immunogenicity in four of the eight highly immunogenic antibodies included in the panel. Similarly, five antibodies with high clinical immunogenicity triggered a response in the DC: CD4 T cell assay but the responses were of lower magnitude than the ones observed in the PBMC assay. Remarkably, three antibodies with high clinical immunogenicity did not trigger any response in either platform. The addition of a monocyte restimulation step to the DC: CD4 T cell assay did not further improve its predictive value. Overall, these results indicate that there are no CD4 T cell assay formats that can predict the clinical immunogenicity of all biotherapeutics and reinforce the need to combine results from various preclinical assays assessing antigen uptake and presentation to fully mitigate the immunogenicity risk of biotherapeutics.

KEYWORDS

immunogenicity, CD4 T cell proliferation, dendritic cells, major histocompatibility complex class II, T cell epitopes, therapeutic proteins

1 Introduction

The immunogenicity of biotherapeutics, i.e., their propensity to evoke an unwanted immune response in patients, is an important consideration in drug development because of its potential to influence the safety, efficacy, and overall therapeutic outcomes. Immunogenicity can manifest in various forms, ranging from the production of neutralizing antibodies to hypersensitivity reactions, which can profoundly impact patient health and treatment success. Consequently, understanding, assessing, and mitigating immunogenicity risks through proper design, characterization, and monitoring strategies are essential steps in the development and regulatory approval process of biotherapeutics.

Pharmaceutical companies, biotechnology companies, and contract research organizations are using a variety of approaches to predict clinical immunogenicity. The most common assays are measuring the capacity of biotherapeutics to elicit CD4 T cell responses *in vitro*. CD4 T cells are essential to the development of the anti-drug antibodies (ADA) responses and unlike B cells their responses can readily be assessed *in vitro* (1). While there is general recognition of the importance of CD4 T cells in the ADA response, there is no agreement on assay format to measure CD4 T cell responses (2, 3) Some companies used peripheral blood mononuclear cells (PBMCs) depleted or not of CD8 T cells (4) and/or regulatory T cells (5) while others used a co-culture with monocyte-derived dendritic cells (DCs) (6) and purified CD4 T cells (7). The duration of the T cell assays varies between laboratories ranging from 2 days (8) to 3 weeks (9) while the number of donors evaluated fluctuates between 10 to 50 donors. Finally, diverse endpoints are used to measure CD4 T cell responses including the expression of T cell activation markers (8), T cell proliferation, or the production of cytokines (IL-2, IFN-γ or IL-5). Whether all these CD4 T cell assays predict equally well clinical immunogenicity is however unclear.

In this study, we reviewed the performance of one assay format, the PBMC assay with CD8 T cell depletion, using 45 homologs of clinically tested monoclonal antibodies (mAbs). We then selected 10 mAbs that were correctly predicted or not by the PBMC assay to determine whether DC-based CD4 T cell assays with or without a restimulation step would have a better predictive value.

2 Materials and methods

2.1 Monoclonal antibodies and proteins

For CD8+ Depleted PBMC assay, the positive assay control (10), keyhole limpet hemocyanin (Imject™ mcKLH), was purchased from Thermo Fisher Scientific and was reconstituted with 2mL of ultrapure water. The final assay concentration for KLH was 0.33μM. KLH used in DC-T assays with (50ug/ml) and without (25ug/ml) stimulation was purchased from Enzo. Proprietary antibodies, mAb1, mAb2, mAb3, mAb4, and mAb5 were supplied by Eli Lilly and Co. Anti-PCSK9-A, anti-PCSK9-B, anti-IL21R, anti-IL7R, and anti-PDL1 homologs were synthesized using the published sequences described by W.H.O. International Nonproprietary Names for Pharmaceutical Substances or U.S. patents. Whole antibody heavy and light chains were subcloned from the VH and VL genes, respectively. The mAbs of interest were produced by transfection into Chinese Hamster Ovary (CHO-GS/Lipase KO(2F9) cells (Lonza, Basel, Switzerland)) cells. A Protein-A affinity chromatography (MabSelect SuRe; GE Healthcare Biosciences, AB, Uppsala, Sweden) and Strong Cation Exchange (SCX/SEC) chromatography (Poros50 HS SCX (Thermo Scientific Cat#1335906, GE Healthcare cat#28922937) were used to purify the respective cell culture fluid for each antibody. The final concentration of all the mAbs used in the assay was 50 μg/ml (0.33 μM).

2.2 CD8 T cell depleted PBMC proliferation assay

Cryopreserved PBMCs were purchased from an HLA-DR1 characterized library available through Cellular Technology Limited (CTL; cat# CTL-CP1) and were thawed according to CTL's instructions using Anti-Aggregate Wash™ Medium (CTL-AA-005). CD8+ T cells were depleted from the PBMCs by immunomagnetic sorting using CD8 Microbeads, human (Miltenyi Biotec, cat # 130–045-201) using an autoMACS Pro separator (Miltenyi Biotec) according to the manufacturer's protocol. CD8 depleted PBMCs were washed, labeled with 1 μM Carboxyfluorescein Diacetate Succinimidyl Ester (CFSE, Molecular Probes, cat # C34554)), and resuspended in AIM-V media (Life Technologies, cat# 12055–083) containing 5% CTS™ Immune Cell SR (Gibco, cat# A2596101). Using several different 10 donor cohorts, the cells then were seeded at 4 x 10^6 cells/ml/well and tested in triplicate in 2.0 mL containing the different test articles, KLH, or media control only. After cultures were incubated for 7 days at 37°C with 5% CO_2, samples were stained with cell surface markers: anti-CD3 (BioLegend, cat# 300424), anti-CD4 (BioLegend, cat# 300530), anti-CD14 (BD Biosciences, cat#563743), anti-CD19 (BD Biosciences, cat#562440), and DAPI (BD Pharmingen, cat#564907) for viability detection by flow cytometry using a BD LSRFortessa™, equipped with a High Throughput Sampler (HTS). FlowJo™ v10.8 Software (BD Life Sciences) was used to analyze data and a Cellular Division Index (CDI) was calculated as described previously (11).

2.3 DC: CD4 T cell proliferation assay

HLA-typed PBMCs isolated from 50 healthy donor whole blood according to the ethical protocol/amendment IXP-001_V3 (Belgium; Reg. Nr. B6702014215858), protocol IXP-003_V1 (Belgium; Reg. Nr. B707201627607) or protocol IXP-004_V1 (The Netherlands; Reg. Nr. NL57912.075.16) and were kept in cryogenic storage (-180°C) until use. PBMCs were thawed in culture

medium. Monocytes were isolated by magnetic separation (Miltenyi (cat#130–050-201)) and cultured for 5 days in DC medium including interleukin 4 (IL-4, Miltenyi Biotech cat# 130–093-922) and granulocyte-macrophage colony-stimulating factor (GM-CSF, Miltenyi Biotech cat# 130–093-866). On day 5, the monocytes were differentiated into immature DCs (iDCs). The iDCs were collected, seeded into cell culture plates, and then pulsed with mAbs, buffer, or controls, while further cultured in medium supplemented with Interleukin-1 beta (IL-1β) and tumor necrosis factor alpha (TNF-α) for overnight maturation. On day 6, monocyte-derived DCs were washed. Autologous CD4 T cells from the respective donors were isolated by negative magnetic separation according to Manufacturer's instructions (StemCell: EasySep™ Human CD4+ T Cell Enrichment Kit; 19052) and co-cultured with the antigen loaded DCs for 6 days. To confirm the differentiation process of monocytes into DCs, samples of monocyte cultures were taken on days 0, 5 and 6, respectively. The cells then were fluorescently stained for a set of differentiation and maturation markers (CD14, CD80, CD83, CD86, CD40, CD209 and HLA-DR). CD4 T cell proliferation was assessed by measuring 5-Ethynyl-2′-deoxyuridine incorporation (12). On day 12, the DC-T cell co-culture was pulsed with EdU for approximately 16 hours. Afterwards, the cells were fluorescently stained for live/dead differentiation, T cell surface markers (CD3 and CD4), fixed, permeabilized, and the incorporated EdU was stained with a fluorescent azide. Flow cytometry data were acquired with a BD FACSymphony™ (BD Biosciences) and analyzed using Flowlogic™ software (Innovai, Australia).

2.4 DC: CD4 T cell re-stimulation assay

PBMCs isolated from 10 healthy donors were retrieved from cryogenic storage and thawed in culture medium. Monocytes were isolated and differentiated into DCs as previously described. DCs were then seeded onto cell culture plates and then pulsed with the therapeutic mAbs (50 μg/ml), buffer, or controls, while further cultured in medium supplemented with IL-1β and TNF-α for overnight maturation. Autologous CD4 T cells were isolated and co-cultured with the antigen loaded DCs. After 5 days of co-culture the CD4 T cells are harvested and seeded on a FluoroSpot plate with and without restimulation with fresh monocytes and the therapeutic mAbs overnight. Then the next day the plate is developed with IFN-γ and IL-5 antibodies. The stimulation index (SI) was calculated by dividing the average number of spots/1 x 10^6 cells by the average number of spots observed in the medium control wells. When control wells were negative for Spot Forming Units (SFU), we set the number of negative wells to 1, since the formula cannot accept the value 0 (13, 14).

2.5 Statistical analysis

All analysis were performed using GraphPad Prism (version 10) or Excel. The specific statistical tests used are indicated in the figure legends.

3 Results

3.1 *In vitro* T cell assays used in preclinical immunogenicity risk assessment

T cell assays assess the immunogenic risk of biotherapeutics by measuring CD4 T cell activation. The complexity of the T cell assays varies from a relatively simple PBMC culture to more elaborate and time-consuming co-culture assays between monocyte-derived DCs and autologous CD4 T cells. The output of these T cell assays ranges from measuring the expression of T cell activation marker, assessing CD4 T cell proliferation, or measuring cytokine secretion via multiplexed cytokine immunoassays or ELISPOT. In this study, we evaluated three different T cell assay platforms for their capacity to predict the clinical immunogenicity of therapeutic mAbs (1): CD8 T cell depleted PBMC assay (2), DC: CD4 T cell proliferation assay, and (3) DC: CD4 T cell restimulation assay. Each assay was performed in HLA-typed PBMCs from healthy donors with keyhole limpet hemocyanin (KLH) as assay control. A schematic overview of the three CD4 T cell assays is shown in Figure 1.

3.2 Immunogenicity risk assessment using CD8 T cell depleted PBMC assay

One of the most commonly performed *in vitro* cell based assay for measuring the potential of immunogenicity is the PBMC assay (2) (Figure 1A). We have previously shown that a CD4 T cell proliferative assay using CD8 T cell depleted PBMC predicted the clinical immunogenicity of most of the 12 biotherapeutics tested (4). To better assess the specificity and sensitivity of this assay, we have since tested 45 homologs of mAbs and compared them with the various ADA rates in the clinic using the most up to date information available from FDA labels and publications and used the data and split the mAbs into 3 categories based on their reported clinical ADA responses in the labels or publications: high immunogenicity (treatment-emergent anti-drug antibodies (TE-ADA >40%), intermediate (20%<TE-ADA<40%) and low (TE-ADA ≤ 20%). When looking at mAbs that elicited a strong response in the CD8 T cell depleted PBMC assay (≥40% positive donors), all were classified as mAbs with either high or intermediate clinical ADAs (Figure 2), demonstrating the high specificity of the assay. However, only half of the mAbs with high clinical ADA (9 out of 17) elicited a response in this assay, suggesting the assay is not sensitive enough for a standalone assay for preclinical immunogenicity risk assessment (4).

To better understand whether different T cell assay formats would have superior predictive value, we selected 10 mAbs for a comparative analysis: 2 low immunogenicity mAbs serving as negative controls, 4 high immunogenicity mAbs correctly predicted by the PBMC assay and 4 high immunogenicity mAbs that were not predicted (Table 1). Each mAb was evaluated in the CD8 T cell depleted PBMC assay using independent 10 donor cohorts selected based on their HLA-DR alleles to reflect the distribution of HLA types within the U.S. population. The CD4 T cell proliferative response to the mAbs was analyzed by flow

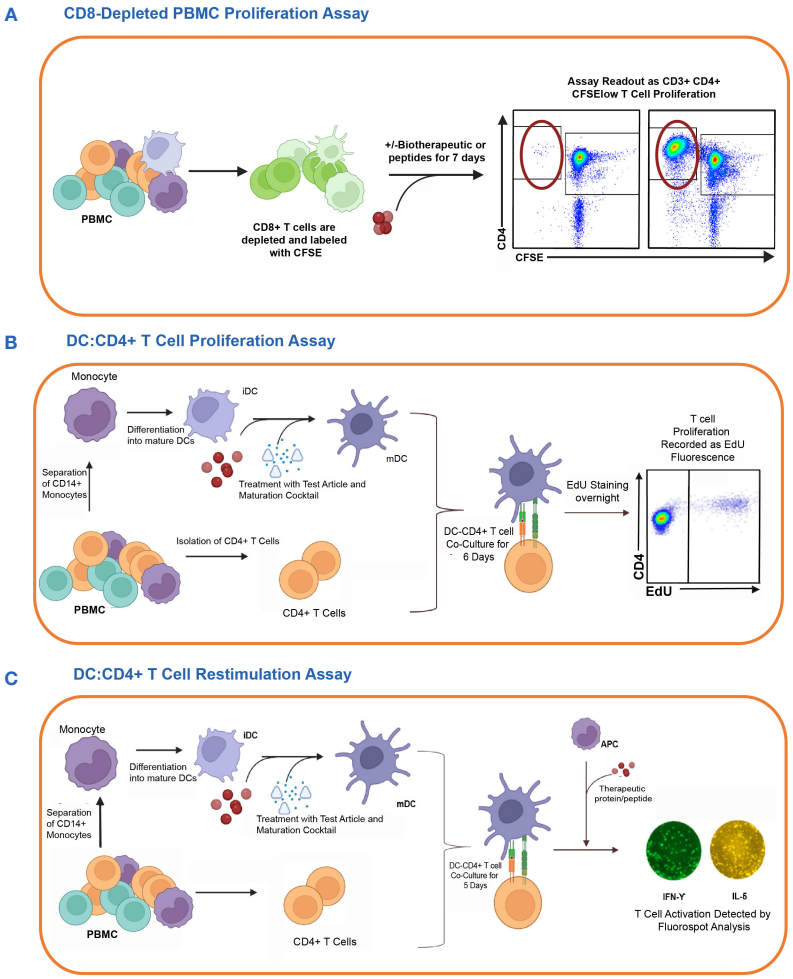

FIGURE 1
In vitro cell-based assay methods used to detect CD4 T cell responses to therapeutic proteins in healthy donors. The figure shows the schematic representation of three different T cell assay formats used to assess the risk of raising a CD4 T cell response. **(A)** First, the CD8 T cell depleted PBMC Proliferation Assay. Briefly, CD8 T cell depleted CFSE-labeled PBMCs are incubated for 7 days with media only, KLH, or one of the eleven therapeutic antibodies. CD3+CD4+CFSElow T cell proliferation is detected by flow cytometry analysis. **(B)** Second is the DC: CD4 T cell Proliferation Assay. Monocyte-derived DCs are exposed to the therapeutic proteins or controls and then co-cultured with autologous CD4 T cells. The proliferation of T cells in response to the activated DC is measured by flow cytometry analysis of CD3+CD4+ T cells using Click-IT® EdU Cell proliferation kit. **(C)** Lastly, the DC: CD4 T cell re-stimulation assay measures the recall response of previously co-cultured CD4 T cells by re-stimulating them with or without the test articles and autologous monocytes. After 24 hours, readouts for this assay are determined by the detection of IFN-γ and IL5 cytokines by FluoroSpot. Figure created with BioRender.com.

cytometry after 7 days incubation using CFSE (Figure 3A). Individual responses were considered positive when the cell division index (CDI) was ≥2.5. With this criterion, all 10 healthy donors responded positively to the assay control KLH (Median CDI = 248.7). As expected, the low immunogenicity mAbs (mAb1 and anti-PCSK9A homolog) elicited a minimal response in the assay (1 positive donors). In contrast, the high immunogenicity mAbs ((anti-IL21R homolog, mAb2 and anti-PCSK9B homolog) elicited a CD4 T cell response in over 50% of the donors (70%, 87% and 56% positive donor frequency, respectively, Figure 3B). The magnitude of the T cell response in these positive donors was well above the positivity threshold of 2.5 (positive donors median CDIs of 18.2, 29, and 4.9, respectively, Figures 3B, C). The high immunogenicity mAb5 elicited a more moderate response in the assay with 30% positive donors and a median for positive donors of only 2.7. In contrast, four high immunogenicity mAbs (mAb3, mAb6, anti-IL7R homolog, and anti-PDL1 homolog) elicited minimal to no response in the assay. Overall, mAbs with high clinical immunogenicity exhibited a wide range of response in the CD8 T cell depleted PBMC assay.

3.3 Immunogenicity risk prediction by DC: CD4 T cell proliferation assay

One limitation of the PBMC assay is the low frequency in peripheral blood of DC, a critical cell for the initiation of CD4 T cell response. To circumvent this issue, some laboratories co-cultured monocyte-derived DC with autologous CD4 T cells to predict clinical immunogenicity. To assess the performance of the DC: CD4 T cell assay, we tested the same 10 mAbs described previously as well as a second homolog of the anti-IL21R ATR-107 (IL21R-

10.3389/fimmu.2024.1406040

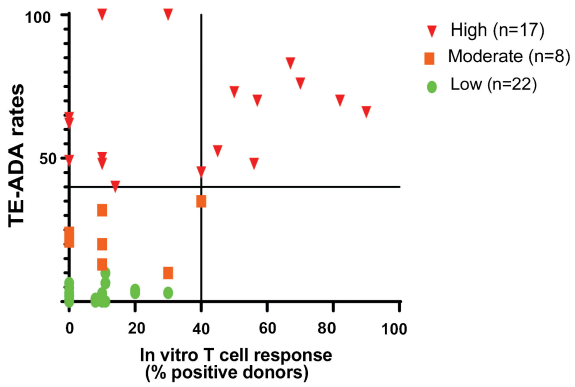

FIGURE 2
CD8 T Cell Depleted PBMC Assay Performance. The CD4 T cell Proliferation assay is suitable to detect biotherapeutics that elicit a strong CD4 T cell proliferation response (≥40% positive donor frequency) and suggests a high risk of clinical immunogenicity. The graph shows the distribution of 45 mAbs based on their performance in the CD8 T cell depleted PBMC proliferation assay compared to the clinical immunogenicity homologs with known clinical immunogenicity. mAbs were categorized into high (TE-ADA≥40%; n=15), moderate (20%<TE-ADA<40%; n=8), and low immunogenicity (TE-ADA ≤ 20%; n=23). The y-axis represents clinical immunogenicity and the x- axis depicts the evaluation of antibodies in a T cell proliferation assay.

IMXP) in 50 HLA-typed healthy donors (Figure 1B) selected to best represent the number and frequency of HLA-DR allotypes expressed in the US and world population (Supplementary S1). In this assay, the assay control KLH led to a positive response in all the donors tested (Median SI = 14) while the two negative control mAbs, mAb1 and anti-PCSK9A homolog, did not elicit a response in most donors [0% and 4% positive donors, respectively (Figure 4A)]. Surprisingly, the two anti-IL21R ATR-107 homologs triggered very different CD4 T cell responses. The Lilly anti-IL21R homolog elicited a weak response (8% positive donors) while the anti-IL21R-IMXP homolog triggered a response in 36% of the donors. Consistent with the PBMC assay, mAb2 induced the highest proliferative response in the DC: CD4 T cell assay (54% positive donors) but the magnitude of the response in positive donors was noticeably lower than the response triggered in the PBMC assay (median SI = 1.8). Three highly immunogenic mAbs (mAb5, anti-PDL1 homolog and anti-PCSK9-B homolog) elicited moderate responses in this assay with 14% positive donors and median SIs for positive donors hovering over 2 (2.2, 2.0, and 1.9, respectively). However, similar to what was observed for the PBMC assay, three mAbs with high clinical immunogenicity (mAb3, mAb4, and anti-IL7R homolog) triggered minimal to no response in the DC: CD4 T cell assay (0%, 0%, and 4% positive donors, respectively). Overall, the DC: CD4 T cell assay did not significantly

TABLE 1 Performance of different CD4 T cell assay formats in predicting the clinical immunogenicity of therapeutic mAbs.

Biologic (mAb)	Description	Subtype	Rate of Clinical Immunoge-nicity	CD8 Depleted PBMC Assay %Positive Donors	DC-T Cell Assay %Positive Donors	DC-T Cell Restimulation Assay %Positive Donors
mAb1		IgG4	1%[a]	10%	0%	40%
anti-PCSK9 A	Evolocumab Homolog	IgG2	<1%[b]	10%	4%	NT
anti-IL21R	ATR-107 Homolog	IgG1	76%[a]	78%	8%	NT
anti-IL21R-IMXP	ATR-107 Homolog	IgG4	NA	NT	36%	90%
mAb2		IgG4	65%[a]	80%	54%	NT
mAb3		IgG1	90%[a]	10%	0%	10%
mAb4		IgG4	62%[a]	0%	0%	10%
mAb5		IgG1	100%[a]	30%	14%	40%
anti-IL7R	GSK2618960 Homolog	IgG1	100%[a]	0%	2%	NT
anti-PDL1	Atezolizumab Homolog	IgG1	13–54%[b]	10%	14%	NT
anti-PCSK9 B	Bococizumab Homolog	IgG2	48%[a]	56%	14%	NT

[a]The clinical immunogenicity rates are based on early clinical trial testing.
[b]The clinical immunogenicity rates are based on FDA labeling and package inserts.
Rates are based on the ADA response associated with diverse disease indications and assay testing platforms with variable sensitivity.

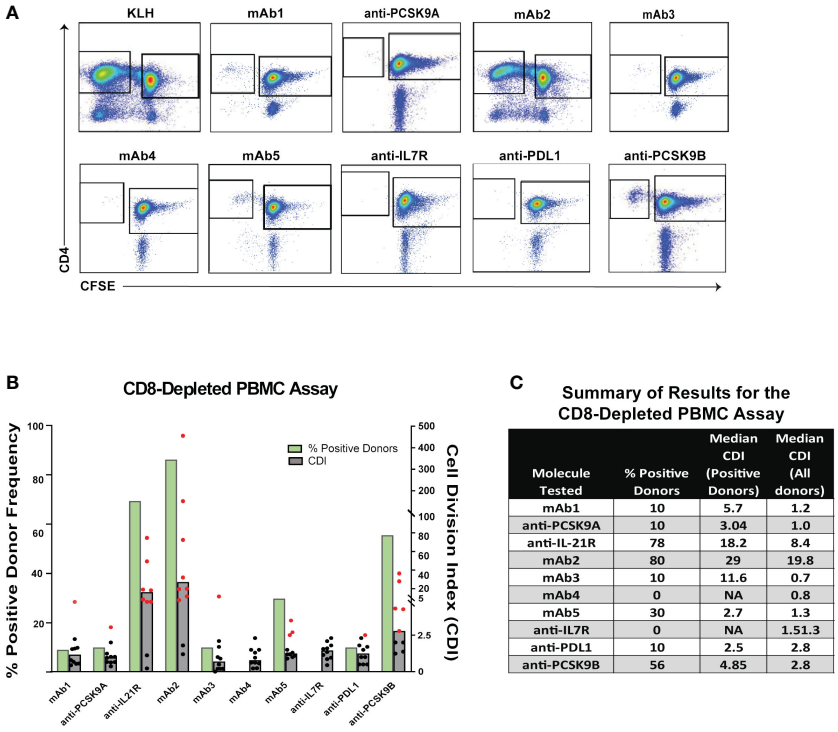

C

Summary of Results for the CD8-Depleted PBMC Assay

Molecule Tested	% Positive Donors	Median CDI (Positive Donors)	Median CDI (All donors)
mAb1	10	5.7	1.2
anti-PCSK9A	10	3.04	1.0
anti-IL-21R	78	18.2	8.4
mAb2	80	29	19.8
mAb3	10	11.6	0.7
mAb4	0	NA	0.8
mAb5	30	2.7	1.3
anti-IL7R	0	NA	1.51.3
anti-PDL1	10	2.5	2.8
anti-PCSK9B	56	4.85	2.8

FIGURE 3
CD4 T Cell Responses to Immunogenic mAbs in CD8 T Cell Depleted PBMC Assay. **(A)** Representative plots showing flow cytometric analysis of CD4 T cell proliferative response from PBMC 7 days after incubation with media only, KLH, mAb1, anti-PCSK9A homolog, anti-IL21R homolog, mAb2, mAb3, mAb4, mAb5, anti-IL7R homolog, anti-PDL1 homolog, and anti-PCSK9B homolog. PBMCs were labeled with CFSE prior to incubation with test articles. Cells in plots were gated from DAPI$^-$CD14$^-$CD19$^-$CD3$^+$. **(B)** Bar graph summarizing the % positive donor frequency (green bars) and the magnitude of the response (grey bars represent the median CDI from 10 donors while dots represent CDIs from individual donors). If CDI $\geq$ 2.5, the donor is considered as positive for the tested mAb (individual red dots). Black dots represent negative donors. **(C)** Table summarizing for each mAb tested, the frequency of positive donor, median CDI of positive donors, and median CDI for all donors.

improve the immunogenicity risk prediction for the 10 selected mAbs. With the notable exception of the anti-PDL1 homolog, mAbs that triggered a response in the DC: CD4 T cell assay also triggered a response in the PBMC assay, but the responses were of lower magnitude.

3.4 Immunogenicity risk prediction by DC: CD4 restimulation assay

To improve the low signal window of the DC: CD4 T cell assay, a second round of stimulation using antigen-pulsed monocytes can be added Figure 1C (15). To determine whether this restimulation step could improve the overall predictive value of the DC: CD4 T cell assay, we tested 5 out of the 10 mAbs: one negative control mAb1, two highly immunogenic mAbs predicted in the PBMC and DC: CD4 T cell assays ((anti-IL21R homolog, mAb5), and 2 highly immunogenic mAbs not predicted by any platform (mAb3 and mAb4). Ten healthy donors were selected based on their HLA-DRB1 alleles to reflect the U.S. population. Monocyte-derived DCs were loaded with each mAbs, matured with a cytokine cocktail, and culture with autologous CD4 T cells. After five days of co-culture, CD4 T cells were harvested and seeded onto a FluoroSpot plate with freshly isolated autologous monocytes in the presence of the respective mAb. IFN-γ Fluorospot was developed after overnight incubation. As expected, the assay control KLH triggered an IFN-γ response in all donors tested. The anti-IL21R-IMXP homolog was again the most potent mAb tested in this platform inducing an IFN-γ response in 9 out of the 10 donors tested with a median SI of 15.2 (Figure 4B). Surprisingly, the low immunogenicity control mAb1 and the highly immunogenic mAb5 triggered similar strong IFN-γ response (40% positive donors) while the other two immunogenic mAbs, mAb3 and mAb4 did not elicit significant response (1/10 positive donor). Overall, the restimulation step with autologous monocytes did not enhance the predictive value of the DC: CD4 T cell assay with this limited set of mAbs.

4 Discussion

The development of ADA of the IgG class following the administration of a biotherapeutic generally indicates that the therapeutic is driving a T-dependent immune response (16). In contrast, T-cell independent humoral immune responses that are dominated by IgMs are typically triggered by repeating polymers such as polysaccharides, glycolipids, and nucleic acids. For this reason, preclinical assays to predict clinical immunogenicity of biotherapeutics frequently rely on CD4 T cell assays. However, a

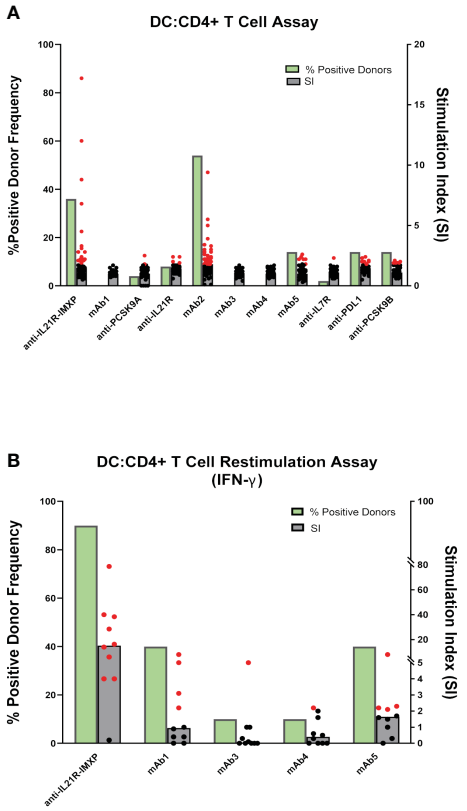

FIGURE 4
CD4 T cell responses to immunogenic mAbs in DC: CD4 T cell assays. **(A)** CD4 T cell proliferation after 6 days of co-culture of DCs pulsed with the indicated mAbs with autologous CD4 T cells. Cell proliferation was monitored by EdU incorporation. Bar graphs summarizing the percent of positive donors (green bar) and the magnitude of the response (grey bars represent the median SI from the fifty donors tested while dots represent SIs from individual donors). **(B)** IFN-γ response after 7 days of co-culture of DCs pulsed with indicated mAbs with autologous CD4 T cells and restimulation with autologous monocytes pulsed with mAbs. IFN-γ response was measured by ELISPOT. SI represents the number of IFN-γ positive cells over baseline. Bar graphs summarizing the percent of positive donors (green bars) and the magnitude of the response (grey bars represent the median SI from the ten donors tested while dots represent SIs from individual donors). If the calculated SI was above 2 (SI > 2) the donor is considered as positive for the tested mAb, represented by the red dots. Black dots represent negative donors.

wide diversity of CD4 T cell assay platforms exists with little indication of their relative performance. In this study, we compared the performance of three different CD4 T cell assays in predicting the clinical immunogenicity of 10 mAbs. This panel contained 2 non-immunogenic and 8 immunogenic mAbs. Out of the 8 immunogenic mAbs, 4 (anti-IL21R homolog, mAb2, anti-PCSK9B homolog, and mAb5) were correctly predicted by both the CD8 T cell depleted PBMC assay and the DC: CD4 T cell assay, but the magnitude of the response elicited in the DC: CD4 T cell assay was lower than the one observed in the PBMC assay. One immunogenic mAb (anti-PDL1 homolog) was only predicted by the DC: CD4 T cell assay while four mAbs (mAb3, mAb4, mAb6, and the anti-IL7R homolog) were not predicted by any of the platforms tested. Furthermore, adding a restimulation step to the DC: CD4 T cell assay did not improve the predictive value of the DC: CD4 T cell platform and instead enhanced the response to one of the negative control non-immunogenic mAb (mAb1).

One possible interpretation of the inability of the CD8 T cell depleted PBMC assay to predict the immunogenicity of some biotherapeutics could stem from the fact that DCs, key antigen-presenting cells for the initiation of the CD4 T cell response, are rare in PBMC and their numbers vary from donor to donor (15, 17). However, the lack of significant improvement in the prediction by the DC: CD4 T cell assay where antigen presentation is driven by human DC matured with inflammatory cytokines suggest that the nature of the antigen-presenting cells may not be the key issue in these assays. The only antibody that triggered a better response in the DC assay is a homolog of atezolizumab that targets PD-L1, a target that is expressed on DCs and may facilitate the antibody uptake and presentation.

Another explanation for the lack of T cell response against some immunogenic mAbs is the short duration of the assay (7 days) which may not be sufficient to efficiently stimulate the expansion of the rare antigen-specific T cells. Recent studies have shown that adding a monocyte restimulation step after the 7 days culture with DC could increase the likelihood of capturing a T cell response (15, 18). However, in our study, the restimulation step did not significantly increase the response to immunogenic mAbs and in fact enhanced the response against one of our negative controls, mAb1, that did not trigger ADA response in clinic. An alternative method that could help with the expansion of the small pre-existing CD4 T cell repertoire reactive to the drug is to add a T cell growth factor such as IL-2 during *in vitro* culture to enhance the expansion of antigen-specific CD4 T cells. Liao et al. reported a strong CD4 T cell response to the anti-IL7R GSK2618960 homolog in their PBMC assay but the assay required a 10 day-stimulation period and the presence of IL2 (19). The use of restimulation steps and T cell growth factors have been indeed very successful at promoting the expansion of drug-specific T cells (20, 21). Whether adding cytokines that promote T cell expansion in preclinical assays used for immunogenicity risk assessment will improve or hurt the predictive value of these assays is however unclear.

One of the challenges for the development and comparison of preclinical *in vitro* immunogenicity risk assays is the lack of availability of standard positive and negative control therapeutic proteins for use in assay qualification and as benchmarks for comparison of relative immunogenicity (2, 3). The different CD4 T cell responses elicited by the two anti-IL21R ATR107 homologs used in this study are an illustration of the challenge. The basis for this discrepancy is not clear and may be caused by differences in the encoding amino acid sequences, the isotype used to produce the mAb homologs, or the level of aggregates or impurities present in the two homologs. To address this issue, the Therapeutic Product Immunogenicity Community within the American Association of Pharmaceutical Scientists (AAPS) in collaboration with the Immuno-Safety Technical Committee within the Health and Environmental Sciences Institute are currently promoting the development of a reference panel of lyophilized mAbs composed of high, moderate, low immunogenicity mAbs that would facilitate cross-organization assay comparison and assay harmonization (3).

Overall, our study highlights the limitation of a preclinical immunogenicity risk assessment solely based on CD4 T cell assays with intact biotherapeutics and emphasizes the importance of additional assays to refine the preclinical immunogenicity risk assessment. The MAPPS assay that identifies MHC II-restricted peptides that are naturally presented by DCs can for example be leveraged to map potential T cell epitopes in biotherapeutics that could he be assessed for their capacity to induce CD4 T cell responses (4).

Data availability statement

The original contributions presented in the study are included in the article/Supplementary Material. Further inquiries can be directed to the corresponding author.

Ethics statement

Ethical approval was not required for the studies on humans in accordance with the local legislation and institutional requirements because only commercially available established cell lines were used.

Author contributions

RW: Writing – original draft, Methodology, Investigation, Formal analysis, Conceptualization. AN: Writing – review & editing, Methodology, Investigation, Formal analysis. CA: Writing – review & editing, Methodology, Investigation, Formal analysis. AM: Writing – review & editing, Methodology, Investigation, Formal analysis. JS: Writing – review & editing, Methodology, Investigation. SP: Writing – review & editing, Project administration, Methodology, Investigation. LM: Writing – review & editing, Supervision, Resources, Project administration, Conceptualization.

Funding

The author(s) declare that no financial support was received for the research, authorship, and/or publication of this article.

Acknowledgments

The authors would like to thank Sarah Labra for her excellent technical assistance.

Conflict of interest

RW, AN, and LM are employees of Eli Lilly and Company and own stock in Eli Lilly and Company. CA, AM, JS, and SP are employed with ImmunXperts, a Q2 Solutions Company.

Publisher's note

All claims expressed in this article are solely those of the authors and do not necessarily represent those of their affiliated organizations, or those of the publisher, the editors and the reviewers. Any product that may be evaluated in this article, or claim that may be made by its manufacturer, is not guaranteed or endorsed by the publisher.

Supplementary material

The Supplementary Material for this article can be found online at: https://www.frontiersin.org/articles/10.3389/fimmu.2024.1406040/full#supplementary-material

References

1. Baker MP, Reynolds HM, Lumicisi B, Bryson CJ. Immunogenicity of protein therapeutics: The key causes, consequences and challenges. *Self Nonself*. (2010) 1:314–22. doi: 10.4161/self.1.4.13904

2. Gokemeijer J, Wen Y, Jawa V, Mitra-Kaushik S, Chung S, Goggins A, et al. Survey outcome on immunogenicity risk assessment tools for biotherapeutics: an insight into consensus on methods, application, and utility in drug development. *AAPS J*. (2023) 25:55. doi: 10.1208/s12248-023-00820-7

3. Ducret A, Ackaert C, Bessa J, Bunce C, Hickling T, Jawa V, et al. Assay format diversity in pre-clinical immunogenicity risk assessment: Toward a possible harmonization of antigenicity assays. *MAbs*. (2022) 14:1993522. doi: 10.1080/19420862.2021.1993522

4. Walsh RE, Lannan M, Wen Y, Wang X, Moreland CA, Willency J, et al. *Post-hoc* assessment of the immunogenicity of three antibodies reveals distinct immune stimulatory mechanisms. *mAbs*. (2020) 12:1764829. doi: 10.1080/19420862.2020.1764829

5. Ito S, Ikuno T, Mishima M, Yano M, Hara T, Kuramochi T, et al. *In vitro* human helper T-cell assay to screen antibody drug candidates for immunogenicity. *J Immunotoxicology*. (2019) 16:125–32. doi: 10.1080/1547691X.2019.1604586

6. Soto JA, Melo-Gonzalez F, Gutierrez-Vera C, Schultz BM, Berrios-Rojas RV, Rivera-Perez D, et al. Inactivated vaccine-induced SARS-coV-2 variant-specific immunity in children. *mBio*. (2022) 13:e0131122. doi: 10.1128/mbio.01311-22

7. Moser JM, Sassano ER, Leistritz del C, Eatrides JM, Phogat S, Koff W, et al. Optimization of a dendritic cell-based assay for the in vitro priming of naive human CD4+ T cells. *J Immunol Methods*. (2010) 353:8–19. doi: 10.1016/j.jim.2009.11.006

8. Cohen S, Myneni S, Batt A, Guerrero J, Brumm J, Chung S. Immunogenicity risk assessment for biotherapeutics through in *vitro* detection of CD134 and CD137 on T helper cells. *MAbs*. (2021) 13:1898831. doi: 10.1080/19420862.2021.1898831

9. Delluc S, Ravot G, Maillere B. Quantitative analysis of the CD4 T-cell repertoire specific to therapeutic antibodies in healthy donors. *FASEB J*. (2011) 25:2040–8. doi: 10.1096/fj.10-173872

10. Schlienger K, Craighead N, Lee KP, Levine BL, June CH. Efficient priming of protein antigen–specific human CD4+ T cells by monocyte-derived dendritic cells. *Blood*. (2000) 96:3490–8. doi: 10.1182/blood.V96.10.3490.h8003490_3490_3498

11. Mannering SI, Morris JS, Jensen KP, Purcell AW, Honeyman MC, van Endert PM, et al. A sensitive method for detecting proliferation of rare autoantigen-specific human T cells. *J Immunol Methods*. (2003) 283:173–83. doi: 10.1016/j.jim.2003.09.004

12. Sun X, Zhang C, Jin H, Sun G, Tian Y, Shi W, et al. Flow cytometric analysis of T lymphocyte proliferation in *vivo* by EdU incorporation. *Int Immunopharmacol*. (2016) 41:56–65. doi: 10.1016/j.intimp.2016.10.019

13. Schultz HS, Reedtz-Runge SL, Backstrom BT, Lamberth K, Pedersen CR, Kvarnhammar AM, et al. Quantitative analysis of the CD4+ T cell response to therapeutic antibodies in healthy donors using a novel T cell:PBMC assay. *PloS One*. (2017) 12:e0178544. doi: 10.1371/journal.pone.0178544

14. Petrich de Marquesini LG, Fu J, Connor KJ, Bishop AJ, McLintock NE, Pope C, et al. IFN-gamma and IL-10 islet-antigen-specific T cell responses in autoantibody-negative first-degree relatives of patients with type 1 diabetes. *Diabetologia*. (2010) 53:1451–60. doi: 10.1007/s00125-010-1739-3

15. Wullner D, Zhou L, Bramhall E, Kuck A, Goletz TJ, Swanson S, et al. Considerations for optimization and validation of an in *vitro* PBMC derived T cell assay for immunogenicity prediction of biotherapeutics. *Clin Immunol*. (2010) 137:5–14. doi: 10.1016/j.clim.2010.06.018

16. Jawa V, Terry F, Gokemeijer J, Mitra-Kaushik S, Roberts BJ, Tourdot S, et al. T-cell dependent immunogenicity of protein therapeutics pre-clinical assessment and mitigation-updated consensus and review 2020. *Front Immunol*. (2020) 11:1301. doi: 10.3389/fimmu.2020.01301

17. Patente TA, Pinho MP, Oliveira AA, Evangelista GCM, Bergami-Santos PC, Barbuto JAM. Human dendritic cells: their heterogeneity and clinical application potential in cancer immunotherapy. *Front Immunol*. (2018) 9:3176. doi: 10.3389/fimmu.2018.03176

18. Siegel M, Steiner G, Franssen LC, Carratu F, Herron J, Hartman K, et al. Validation of a dendritic cell and CD4+ T cell restimulation assay contributing to the immunogenicity risk evaluation of biotherapeutics. *Pharmaceutics*. (2022) 14. doi: 10.3390/pharmaceutics14122672

19. Liao K, Chen K, Brett S, Gehman A, Schwartz AM, Gunn GR, et al. Characterization of the robust humoral immune response to GSK2618960, a humanized anti-IL-7 receptor monoclonal antibody, observed in healthy subjects in a Phase 1 study. *PloS One*. (2021) 16:e0249049. doi: 10.1371/journal.pone.0249049

20. Delluc S, Ravot G, Maillere B. Quantification of the preexisting CD4 T-cell repertoire specific for human erythropoietin reveals its immunogenicity potential. *Blood*. (2010) 116:4542–5. doi: 10.1182/blood-2010-04-280875

21. Hamze M, Meunier S, Karle A, Gdoura A, Goudet A, Szely N, et al. Characterization of CD4 T cell epitopes of infliximab and rituximab identified from healthy donors. *Front Immunol*. (2017) 8:500. doi: 10.3389/fimmu.2017.00500

frontiers | Frontiers in Immunology

TYPE Original Research
PUBLISHED 31 May 2024
DOI 10.3389/fimmu.2024.1406353

OPEN ACCESS

EDITED BY
Daniel T. Mytych,
Amgen, United States

REVIEWED BY
Linlin Luo,
Merck, United States
Stephanie DeStefano,
Hannover Medical School, Germany

*CORRESPONDENCE
Gregor P. Lotz
gregor.lotz@roche.com

RECEIVED 24 March 2024
ACCEPTED 06 May 2024
PUBLISHED 31 May 2024

CITATION
Lotz GP, Lutz A, Martin-Facklam M, Hansbauer A, Schick E, Moessner E, Antony M, Stuchly T, Viert M, Hosse RJ, Freimoser-Grundschober A, Klein C, Schäfer M, Ritter M and Stubenrauch K-G (2024) Characterization of anti-drug antibody responses to the T-cell engaging bispecific antibody cibisatamab to understand the impact on exposure.
Front. Immunol. 15:1406353.
doi: 10.3389/fimmu.2024.1406353

Characterization of anti-drug antibody responses to the T-cell engaging bispecific antibody cibisatamab to understand the impact on exposure

Gregor P. Lotz[1*], Achim Lutz[1], Meret Martin-Facklam[2], Andre Hansbauer[1], Eginhard Schick[2], Ekkehard Moessner[3], Michael Antony[1], Thomas Stuchly[1], Maria Viert[1], Ralf J. Hosse[3], Anne Freimoser-Grundschober[3], Christian Klein[3], Martin Schäfer[1], Mirko Ritter[4] and Kay-Gunnar Stubenrauch[1]

[1]Roche Pharma Research and Early Development, Roche Innovation Center Munich, Penzberg, Germany, [2]Roche Pharma Research and Early Development, Roche Innovation Center Basel, Basel, Switzerland, [3]Roche Pharma Research and Early Development, Roche Innovation Center Zurich, Schlieren, Switzerland, [4]Roche Diagnostics GmbH, Antibody Development Technologies, Penzberg, Germany

An appropriately designed pharmacokinetic (PK) assay that is sensitive for anti-drug antibody (ADA) impact on relevant exposure is an alternative strategy to understand the neutralizing potential of ADAs. However, guidance on how to develop such PK assays and how to confirm the functional ADA impact on exposure is missing. Here, the PK assay of a T-cell-engaging bispecific antibody, cibisatamab, was developed based on its mechanism of action (MoA). Using critical monoclonal anti-idiotypic (anti-ID) antibody positive controls as ADA surrogates, the impact on exposure was evaluated pre-clinically. In a phase I clinical trial (NCT02324257), initial data suggest that the combination of ADA and PK assays for correlation of the ADA response with cibisatamab exposure. To understand the neutralizing potential of patient-derived ADAs on drug activity, advanced ADA characterization has been performed. Structural binding analysis of ADAs to antibody domains of the drug and its impact on targeting were assessed. For this purpose, relevant patient ADA binding features were identified and compared with the specific monoclonal anti-ID antibody-positive controls. Comparable results of target binding inhibition and similar impacts on exposure suggest that the observed reduction of Cmax and Ctrough levels in patients is caused by the neutralizing potential of ADAs and allows a correlation between ADA response and loss of exposure. Therefore, the described study provides important functional aspects for the development of an appropriately designed PK assay for bispecific antibodies as an alternative option towards understanding the neutralizing ADA impact on exposure.

KEYWORDS

PK, exposure, immunogenicity, ADA, T cell engager

Introduction

It is critical during the clinical development of biotherapeutics to generate precise pharmacokinetic (PK) data to understand the relationship between exposure and pharmacodynamic (PD) response, safety, and efficacy as a prerequisite for dose and schedule selection (1). The analysis of relevant drug exposure becomes particularly important when patients demonstrate an anti-drug antibody (ADA) response during treatment. In such cases, it is necessary to understand the impact of ADAs on drug exposure, which is ideally correlated with the corresponding PD effect.

A key aspect of assessing ADA impact on exposure is the combination of ADA analysis with PK analysis using a PK assay that is sensitive for ADA impact on the pharmacologically relevant drug exposure. The combination of both assay data allows the correlation of drug exposure with the ADA response for a given patient. A prerequisite for the development of a PK assay analyzing relevant drug exposure is the generation of specific reagent assay tools such as the target antigen or, alternatively, anti-idiotypic (anti-ID) antibodies directed to epitopes of the binding sites that are involved in target binding (2). Using antigen-reagents or appropriate anti-ID antibodies as reagents ensures coverage of the united functionalities of the drug and allows the development of a PK assay based on its mechanism of action (MoA).

Another important step during the development of the PK assay is an adequate evaluation of the impact of ADAs on exposure. However, it is difficult to address the ADA impact on drug exposure pre-clinically due to a lack of patient-derived ADA characteristics. At present, the widely accepted standard is the use of ADA surrogate tools often generated in animal models as positive controls for the development of ADA assays and the pre-clinical evaluation of ADA impact on clinical PK assays (3). What is often missing is the retrospective validation of the ADA positive controls to confirm that they are comparable to patient-derived ADAs, thus evaluating and confirming that the PK assay is indeed sensitive to the impact of ADAs on exposure.

In this study, the development of a PK assay for the bispecific T-cell engager cibisatamab based on its MoAs is described, and its performance in clinical trials is shown. The ADA impact on exposure was evaluated using ADA-positive controls and compared with functional patient-derived ADA binding to the drug, and its interference with target antigen binding was demonstrated. Based on the patient's ADA binding features, appropriate anti-ID ADA-positive controls with similar binding features were identified and selected to validate the PK assay. Comparable results of impact on exposure by patient-derived ADAs and selected ADA positive controls suggest that the observed reduction of Cmax and Ctrough level in patients is caused by neutralizing ADAs and allows a correlation between ADA response and loss of exposure. Taken together, the results of this study may provide criteria to be considered for the development of appropriate PK assays to understand the impact of potential neutralizing ADAs.

Abbreviations: PK, pharmacokinetic; ADA, anti-drug antibodies; MoA, Mechanism of action; Anti-ID, anti-idiotypic; Cmax, maximum serum concentration; Ctrough, trough concentration before next dosing; PD, Pharmacodynamic; CDR, complementary determining regions; IgM, Immunoglobulin M; IgG, immunoglobulin G; HC, Heavy chain; LC, Light chain.

Results

Development of a mechanism of action-based PK assay that is sensitive for ADA impact to analyze relevant exposure

The design of the assay format to develop an appropriate PK assay is a key prerequisite to enable the detection of relevant drug exposure (4–6). The first important aspect to consider is the MoA of the drug. The MoA of cibisatamab is based on the simultaneous binding of cibisatamab to CEA/CEACAM5 on tumor cells and to the CD3ε chain on T cells, which results in T-cell activation and subsequent tumor cell killing (7, 8). This dual binding functionality was implemented for the development of a MoA-based PK assay (Figures 1A, B). A second important aspect of assay development is the production and characterization of high-quality reagents (2). To mimic the MoA, monoclonal anti-ID antibodies were generated, purified, and characterized for each specific functional binding site of cibisatamab (Figure 1B). These anti-ID antibody reagents directed to the target-binding relevant complementarity-determining regions (CDRs) of the anti-CEA and to the anti-CD3 domains of cibisatamab allow the quantification of drug concentration, exposing its free binding moieties to both targets along with an ultrasensitive detection of <1 ng/ml. In Table 1, inter-assay statistics of standards and quality control drug concentrations result in accuracy and precision assay performance within the acceptance criteria during validation and the clinical phase of study I.

To evaluate the ADA impact on target-binding competent drug exposure, the recovery of a constant cibisatamab serum concentration (120 ng/ml) was analyzed in the absence (control) and presence of different ADA positive control concentrations (10, 100, and 1000 ng/ml) containing an equimolar mix of two monoclonal anti-ID antibodies, one directed to the anti-CEA and one directed to the anti-CD3 domain (Supplementary Figure 1A, C). Each monoclonal anti-ID antibody had comparable binding parameters. Fast association and slow dissociation kinetics with comparable affinities (KD 1 nM to anti-CD3 and 0.64 nM to anti-CEA), respectively, were measured using surface plasmon resonance (not shown) and biolayer interferometry analysis (Supplementary Figure 1B/sensogram).

In Supplementary Figure 1C, keeping the cibisatamab serum concentration constant at 120 ng/ml, the anti-ID ADA control mix at a concentration of 10 ng/ml reduced the recovery of the drug slightly by ~20%. At a concentration of 100 ng/ml anti-ID ADA PCs, a strong reduction in recovery >90% was observed, suggesting that comparable molar concentrations of anti-ID ADA positive controls and cibisatamab led to a significant decrease in the target-binding-competent drug concentration. Consequently, an anti-ID

10.3389/fimmu.2024.1406353

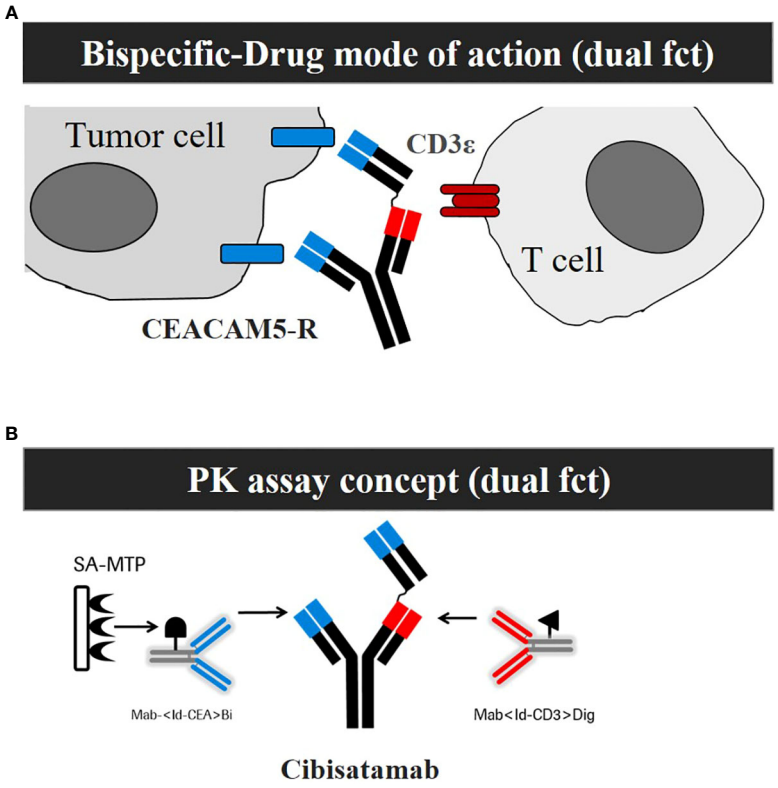

FIGURE 1
Development of a mechanism of action (MoA) based Pharmacokinetic (PK) assay that is sensitive for ADA impact on exposure. **(A)** Schemata of the MoA of cibisatamab with its dual functionality (dual fct). **(B)** Schemata of the PK Assay concept with its dual functionality (dual fct).

ADA positive control concentration that is ~10-fold higher results in a complete loss of target-binding-competent drug detection (Supplementary Figure 1C). These data suggest that the MoA-based PK assay detects critical target-binding-competent drug exposure and is sensitive to interference by binding of anti-ID ADA positive controls.

To prove the concept of the PK assay, the impact of patient-related ADA responses to cibisatamab exposure was evaluated. In Figure 2, the ADA titer over time was compared with the drug exposure data in one ADA-negative patient (patient A) and in one patient (patient B) with a persistent ADA response. In patient A, who did not develop ADAs, the detectable drug concentrations of cibisatamab were maintained over time, whereas in patient B, a significant reduction of the detectable drug concentration was already observed at the onset of an ADA response after week 1, resulting in a complete loss of exposure from week 4 onwards and a persistently high ADA titer. These data indicate that an increase in cibisatamab ADA titer is associated with a decrease in target-binding competent cibisatamab exposure (patient B), in contrast to an ADA-negative patient where drug exposure is maintained

TABLE 1 Determination of high accuracy and precision of a MoA-based PK assay.

Cibisatamab PK assay validation					
Dynamic range	**Sensitivity**	**Inter-assay statistics (Cals; n=20)**		**Inter-assay statistics (QC samples; n=40)**	
		Accuracy	**Precision**	**Accuracy**	**Precision**
0.925–120 ng/mL	0.925 ng/mL	98.1%–102.9%	≤ 4.4% CV	94.8%–100.0%	≤ 12.3% CV
Cibisatamab sample analysis (FiH Study)					
Inter-assay statistics (Cals; n=256)		**Inter-assay statistics (QC samples; n=512)**			
Accuracy	**Precision**	**Accuracy**		**Precision**	
99.6%–101.0%	≤ 3.4% CV	94.4%–100.0%		≤ 12.0% CV	

Assay parameters of the MoA-based PK assay demonstrate accurate and precise performance of calibration (Cals) and quality control (QC) samples of recovery and CV values within acceptance criteria during the validation and FiH study.

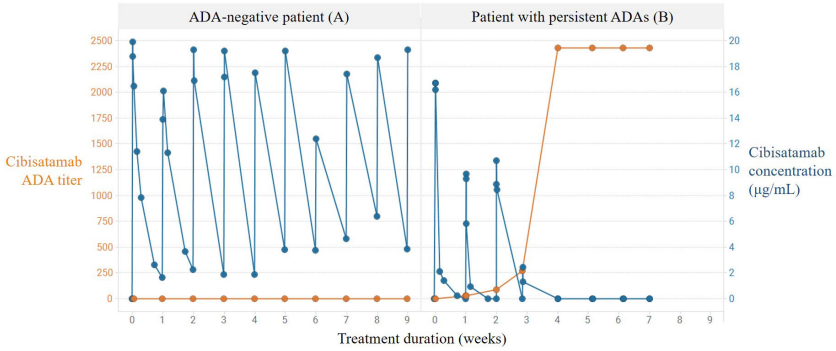

FIGURE 2
Correlation of persistent ADA response and loss of exposure using MoA-based PK assay. Increase in cibisatamab ADA titer and associated decrease in active cibisatamab exposure (patient B) in contrast to ADA negative patient with maintained active exposure (patient A).

over time (patient A). These data confirm that the use of a MoA-based PK assay allows the correlation of patient-derived ADA responses to exposure.

Persistent patient-derived ADA response dominantly consists of IgG isotypes and is directed to the anti-CD3 domain, leading to relevant loss of exposure

To better understand the neutralizing potential of the patient-derived ADAs for functional binding and their impact on exposure, an advanced ADA response characterization was performed. Samples of 10 patients were further analyzed to determine (a) the specific ADA-reactive drug domain using an ADA domain detection assay (9, 10) (Supplementary Figure 2) and (b) the isotype of the ADA response using ADA immune-complex assays for IgM and IgG detection (11–13) (Supplementary Figure 3). Patient serum samples taken 4 weeks after ADA onset were selected and analyzed with domain detection ELISAs specific for ADA detection in the anti-CEA domain or anti-CD3 domain (Table 2). In all 10 samples, a strong signal towards the anti-CD3 was detected, whereas only in 3/10 samples, a weak signal towards the anti-CEA domain slightly above the cut point (CP: 0.04 OD) was detected. In Supplementary Figure 3, a characteristic ADA response detected in one patient with cibisatamab treatment is shown. At ADA onset, IgM triggered the initial response with a lower titer, whereas at a later time point, the response was mainly determined by the ADA-IgG response with a high titer alongside loss of drug exposure. At 4 weeks after ADA onset (Supplementary Figure 3, black arrow), the IgG detection was saturated, the IgM detection was below the cut point, and exposure was lost. Similarly, in all ten selected patient samples collected 4 weeks after ADA onset, the ADA immune-complex analysis using a FcγR1-based detection reagent indicated a strong IgG-related ADA response but hardly any IgM response (Table 3). There is no drug that could be detected using the MoA-based PK assay at that time point in all 10 patient samples (Table 3). These data suggest that the ADA response in these patients leading to significant loss of exposure was caused by ADA-IgG and mainly directed to the anti-CD3 domain at 4 weeks after ADA onset.

Advanced characterization of anti-ID antibodies as ADA-positive controls

The deeper characterization of patient-derived ADAs 4 weeks after onset determined IgG as the major isotype and anti-CD3 domain binding specificity to cibisatamab. However, whether ADAs were anti-ID with neutralizing potential was not yet clear. To explore these questions, first, anti-ID antibodies were further evaluated to establish adequate ADA-positive controls for advanced binding and neutralizing studies. Four purified, monoclonal anti-IDs were selected to analyze their specific binding to the anti-CD3 domain of cibisatamab individually (Supplementary Figure 4). All four anti-IDs showed similar binding features to the anti-CD3 domain of cibisatamab, including a strong signal using an ELISA assay (Supplementary Figure 4A) and fast association and slow dissociation kinetics using biolayer interferometry analysis (Supplementary Figure 4B).

Based on structural data, the heavy chain (HC) plays an important role in recognizing the CD3ε receptor (data not shown). To understand if the anti-IDs were directed to the CDRs of the HC or to the CDRs of the light-chain (LC) of the anti-CD3 domain, specific anti-CD3 domain constructs were engineered, purified, and used as capture reagents for CDR-specific domain detection assays (Supplementary Figure 5). The specific anti-CD3 domain constructs had either functional CDRs in the V-domain of the heavy chain with germline CDRs in the V-domains of the light chain or vice versa. Corresponding controls, such as a construct with both functional CDRs in the antibody paratope, were used as a positive control, or germline CDR sequences in the antibody paratope were used as a negative control. In Figure 3A, each anti-ID antibody was able to bind to the HC/LC positive control but did not bind to the negative control construct (germline in HC/LC) using an ELISA assay. Interestingly, only one anti-ID (anti-ID 4) bound to the anti-CD3 domain construct with functional CDRs in the HC, whereas the other three anti-ID antibodies did not. Similarly, using the anti-CD3 domain constructed with the functional CDRs of the LC, another

10.3389/fimmu.2024.1406353

TABLE 2 Patient-derived ADAs are mainly directed to the anti-CD3 domain at 4 weeks after ADA onset.

Patient (Samples taken 4 weeks after ADA onset)	Total ADA assay (Screening)	ADA CD3-Domain assay	ADA CEA-domain assay
1	Positive	+++	Negative
2	Positive	+++	Negative
3	Positive	++	Negative
4	Positive	+++	Negative
5	Positive	+++	+
6	Positive	+++	Negative
7	Positive	++	Negative
8	Positive	+++	+
9	Positive	+++	Negative
10	Positive	+++	+
Strong: +++ (> OD 1.0) Medium: ++ (> OD 0.3) Low: + (> CP) Negative: (< CP)	Cut Point (OD): 0.04; baseline control mean: 0.035		

Ten patient serum samples collected 4 weeks after ADA onset were analyzed with anti-CD3 and anti-CEA domain binding assays.

anti-ID antibody (ADA anti-ID 2) was able to bind, and the other three were not. These results were additionally confirmed with an orthogonal binding readout using biolayer interferometry (Figure 3B). In summary, all four monoclonal anti-ID antibodies with similar binding affinities showed strong binding to fully functional CDRs. The anti-ID antibodies were directed to distinct CDR epitopes in the anti-CD3 variable domains and, consequently, might have different neutralizing interference potentials from cibisatamab binding to its CD3ϵ antigen receptor target.

Anti-ID antibodies inhibit receptor antigen-target engagement of an anti-CD3 IgG drug in a CD3-receptor reporter cell assay

To analyze the neutralizing potential of the four selected anti-ID antibodies as relevant ADA positive controls, a CD3ϵ antigen receptor-specific reporter cell line was used. Stimulation of the highly expressed CD3ϵ antigen receptors on the cell surface activates a reporter gene expressing luciferase. The corresponding luminescence signal correlates

TABLE 3 The ADA response leading to loss of exposure at the end of infusion to the signal below LoQ is mainly caused by ADA IgG isotypes at 4 weeks after ADA onset.

Patient (Samples taken 4 weeks after ADA onset)	Total ADA assay (Screening)	ADA IgG assay	ADA IgM assay	Loss of exposure (PK assay)
1	Positive	+++	Negative	Yes
2	Positive	+++	Negative	Yes
3	Positive	+++	Negative	Yes
4	Positive	+++	Negative	Yes
5	Positive	+++	Negative	Yes
6	Positive	+++	Negative	Yes
7	Positive	+++	Negative	Yes
8	Positive	+++	Negative	Yes
9	Positive	+++	+	Yes
10	Positive	+++	Negative	Yes
Strong: +++ (> OD 1.5) Medium: ++ (> OD 0.75) Low: + (>CP) Negative: (<CP)	Individual patient-specific Cut Point (OD) IgG and IgM assay: double pre-dose patient sample signal (blank)			Signal below the LoQ

10.3389/fimmu.2024.1406353

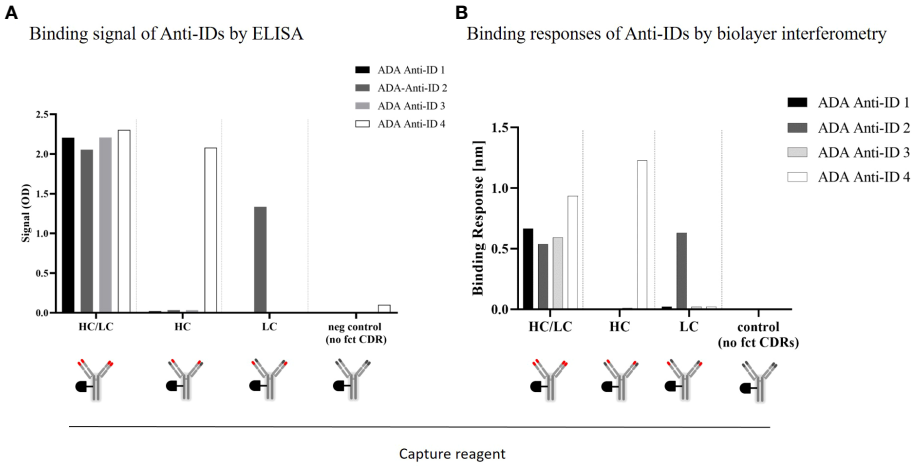

FIGURE 3
ADA anti-CD3/CDR domain specificity characterization: Binding characteristics of four different monoclonal anti-idiotypic antibodies to modified anti-CD3 domains analyzed by ELISA **(A)** and biolayer interferometry **(B)**. HC, heavy chain; LC, light chain; CDR, complementarity-determining region.

with the CD3ε-mediated luciferase activation (Figure 4). To enable the best possible read-out, an anti-CD3 IgG antibody was used as a stimulating control for maximal signal response. This anti-CD3 control contains the same binding sequence in the CDR as in the cibisatamab anti-CD3 domain. The interference of the four anti-IDs with CD3ε-mediated activation was tested by pre-incubation in different ratios with an anti-CD3 IgG control. All four monoclonal anti-ID antibodies abolished CD3ε-mediated cell activation completely when the anti-ID concentration was in at least 10-fold excess over the anti-CD3 IgG control concentration (anti-ID-control ratio 10 or 100) (Figure 4). At a ratio of 1.2, two anti-ID antibodies (Anti-ID 2; Anti-ID 4) still abolished the signal significantly, from 80% to 100%, and two anti-ID antibodies (Anti-ID 1; Anti-ID 3) showed a reduction of 50% of the signal. Although not all anti-ID antibodies at equimolar concentrations to the anti-CD3 IgG control suppressed CD3ε-mediated activation equally, each selected anti-ID that bound to functional binding sites of the anti-CD3 drug domain strongly interfered with CD3ε receptor antigen binding. These data demonstrate that all anti-ID antibodies are valid ADA-positive controls with a neutralizing effect on drug-antigen target binding and on CD3ε-mediated signaling.

Patient-derived ADAs are anti-ID antibodies and predominantly directed at the heavy-chain CDRs of the anti-CD3 domain

The ADA positive controls used for the evaluation of the PK assay to measure if the assay is sensitive for ADA impact on free-drug exposure were anti-IDs and able to interfere with antigen-target binding. To understand if patient-derived ADAs are also anti-ID antibodies and directed to functional CDRs, the same-engineered anti-CD3 domain constructs with modified functional CDR (HC, LC, or both) were used to analyze the same 10 patient samples, taken 4 weeks after ADA onset.

In Table 4, all 10 patient samples were shown to be ADA positive using an ADA screening bridging ELISA (total ADA/

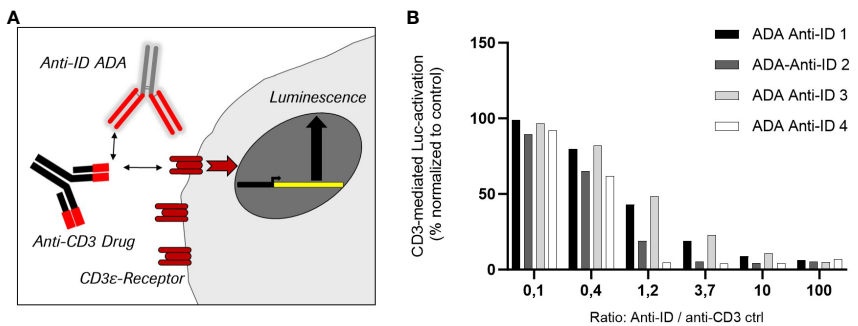

FIGURE 4
Inhibition of cell-based target CD3 receptor mediated luciferase activity by four different monoclonal anti-idiotypic antibodies as potential ADA positive controls. **(A)** Schemata of CD3ε-receptor mediated reporter cell line using anti-CD3 antibodies as stimulating control. **(B)** Effect of the four anti-idiotypic antibodies in CD3-mediated luciferase activation.

10.3389/fimmu.2024.1406353

TABLE 4 ADAs to the anti-CD3 domain are anti-idiotypic and directed dominantly to the CDRs of the heavy chain.

	Column 1	Column 2	Column 3	Column 4	Column 5	Column 6	Column 7
Patient (Samples 4 weeks after ADA onset)	Pre-dose baseline sample (Screening)	Total ADA assay ADA screen	Anti-CD3 domain	Anti-CD3 full CDR	Anti-CD3 HC-CDR	Anti-CD3 LC-CDR	Unrelated CDR germline control
ADA +/sample	0/10	10/10	10/10	10/10	9/10	5/10	4/10
1	Negative	+++	+++	+++	++	+ (0.078)	+ (0.077)
2	Negative	+++	+++	+++	++	+ (0.034)	Negative
3	Negative	+	+	+	Negative	Negative	Negative
4	Negative	+++	+++	+++	+	Negative	Negative
5	Negative	++	++	+++	+	Negative	Negative
6	Negative	++	++	+++	+	Negative	Negative
7	Negative	++	++	+++	++	+ (0.039)	+ (0.042)
8	Negative	+++	+++	++	+	Negative	Negative
9	Negative	+++	+++	+++	+++	+ (0.042)	+ (0.04)
10	Negative	+++	+++	+++	+++	+ (0.064)	+ (0.062)
Cut point (CP)	CP: 0.04	CP: 0.04	CP: 0.04	CP: 0.04	CP: 0.034	CP: 0.029	CP: 0.032

Strong: +++ (> OD 1.0); Medium: ++ (> OD 0.3); Low: + (>CP); Negative: (<CP).

column 2). In addition, all samples were detected ADA-positive using either the anti-CD3 domain capture (Table 4/Column 3) or the construct with full functional CDRs (Table 4/Column 4), suggesting that the patient-derived ADAs were anti-ID and directed to the anti-CD3 domain of cibisatamab. Baseline pre-dose samples (Table 4/Column 1) were instead negative in all 10 samples. A second control using constructs with unrelated CDRs (Table 4/Column 7) showed 4/10 positive, but all signals were borderline and only slightly above the very low cut point of 0.032 OD, indicating that these signals were rather falsely positive than real positive signals. Interestingly, 9/10 patient samples showed reactivity to the anti-CD3 construct with functional CDRs of the HC (Table 4/column 5), whereas only 5/10 have shown a binding signal towards the anti-CD3 construct with functional LC CDRs (Table 4/column 6). The signal strength of the HC anti-CD3 construct was high (> 1.0 OD), whereas the five positive samples in the LC anti-CD3 construct were borderline signals slightly above the cut point. These results indicate that patient-derived ADAs were anti-ID antibodies and mainly directed to the HC of the cibisatamab anti-CD3 domain rather than to the LC, suggesting a specific, immune-dominant epitope on the HC.

Patient-derived ADAs strongly inhibit receptor antigen-target engagement of an anti-CD3 IgG drug in a CD3-receptor cell assay

To demonstrate the neutralizing interference of the CD3-specific ADA response in patients, the CD3ε-specific reporter cell line was used with the same ADA-positive samples taken 4 weeks after the onset of ADA in the selected ten patients. As expected, the anti-CD3 IgG antibody control mediated strong luminescence signals in pre-dose samples (Figure 5, pt1 and pt8 predose) and control samples with a human serum pool (Figure 5, NC). Two concentrations of the anti-ID antibody mix were used as neutralizing positive controls (nAb PC1, nAb PC2). All treatment-induced, patient-derived ADAs inhibited the signal completely (Figure 5A, pt1–10). These data indicate that patient-derived ADAs interfered with drug binding to the CD3ε receptor and elicited the neutralizing potential of ADAs similar to the tested monoclonal anti-ID antibodies.

ADA inhibition of drug-target binding is dependent on the molar ADA-drug ratio. To demonstrate this in patient samples of the cibisatamab study, samples of patient 5 were diluted with ADA-free serum by maintaining a constant stimulating anti-CD3 IgG control concentration to evaluate if full recovery of the signal could be reached. Before diluting the samples, the anti-CD3 IgG control activated the Jurkat T cells in the reporter assay in the pre-dose sample, whereas the post-dose sample showed complete inhibition (Figure 5B, pre- and post-dose). ADA dilutions of 1:10 and 1:100 in ADA-free serum allowed increased recovery of the signal, and dilutions of 1:1000 and 1:10000 in ADA-free serum brought the luciferase signal back to full recovery. In total, the data suggest that ADAs collected 4 weeks after the onset of an ADA response were directed to the functional target binding sites of the CD3 domain of cibisatamab and neutralized drug target binding to CD3ε receptors.

Exposure to cibisatamab is impacted by ADAs in the phase I study using the MoA-based PK assay

The MoA-based PK assay used to detect the cibisatamab concentration has been demonstrated to be sensitive for potential

10.3389/fimmu.2024.1406353

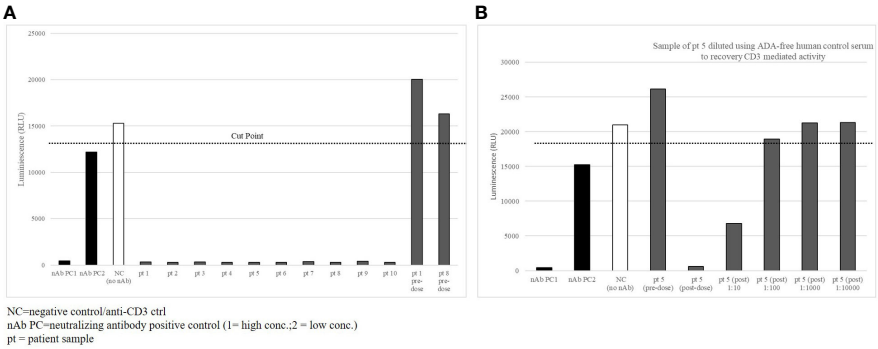

FIGURE 5
Patient-derived ADAs inhibit CD3ε-receptor mediated activation. **(A)** 10 selected patient samples with high titer ADA detection were tested in the CD3ε receptor mediated reporter assay with a complete loss of signal **(B)** Sample of patient 5 diluted in ADA-free human control serum to recovery CD3ε mediated activity.

neutralizing anti-ID ADA responses. To investigate the correlation in the clinic, PK and ADA data were collected in a phase I dose-escalation and expansion study of cibisatamab monotherapy (NCT02324257) in patients with advanced CEA-positive solid tumors. An increase in cibisatamab ADA titers was associated with a decrease in target-binding competent cibisatamab exposure (Figure 6). Usually, the concentration prior to the next infusion (Ctrough) decreases first, followed by a decrease in the maximum concentration after the infusion (Cmax). Patients with low ADA titers (<810) tended to have Cmax values that were not significantly lower than in ADA-negative patients, although a decrease in Ctrough may have been more pronounced. Strikingly, in patients with high ADA-titers (>810), both Cmax and Ctrough were significantly decreased, even to a complete loss of exposure, i.e., no target-binding-competent cibisatamab is detectable in serum directly, even shortly after dosing, when cmax is expected.

Discussion

To inform decision-making during clinical development, it is critical to rely on exposure data that can be correlated with efficacy and safety data. Therefore, it is important to understand which drug species (e.g., total, target binding competent, complexed) are being measured (4–6, 14). This process is even more important when multiple functionalities and binding sites are combined in one drug (15). It is thus essential to consider and involve all functionalities of the drug in the PK assay(s) to be used for sample analysis.

This study describes the development of a MoA-based PK assay of the T-cell engaging bispecific antibody cibisatamab using anti-ID antibodies to allow analysis of functionally relevant target-binding-competent drug exposure. To mimic the MoA appropriately, it is fundamental to select high-quality reagents to enable such a development and to transfer the dual intra-dependent functionality of the drug molecule into the assay format design.

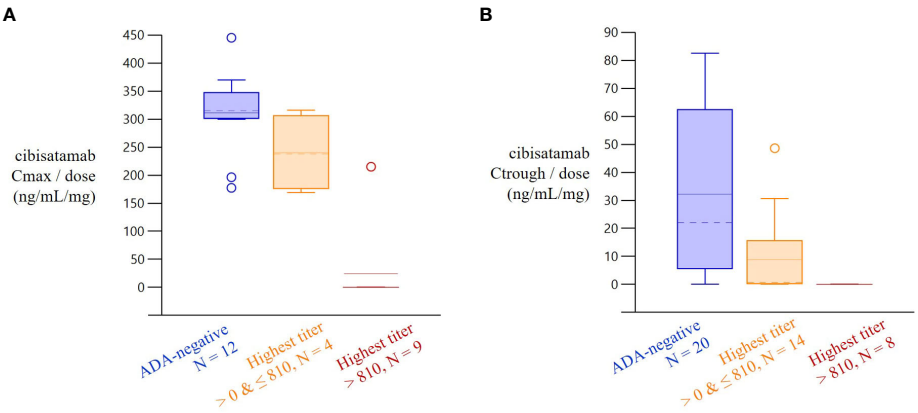

FIGURE 6
Increase in Cibisatamab ADA titer and associated decrease in cibisatamab exposure. Dose-normalized cibisatamab Cmax and Ctrough by highest ADA-titer 4 weeks after treatment start. In patients with high ADA-titers (>810), both Cmax and Ctrough/min were relevantly decreased. Patients with low ADA titers (<810) tended to have Cmax values that were not relevantly smaller than in ADA-negative patients, although decrease in Ctrough/min may be more pronounced.

Here, it is necessary to prove the capability of the anti-ID reagent to bind to relevant drug binding sites involved in target interaction (2). Another important aspect of a MoA-based assay is to capture information about the molecular integrity of the drug during analysis and to exclude the detection of potential structurally misfolded, dysfunctional drugs. Long-term supply of these reagents with high quality, low batch-to-batch variability, and high production yield are further advantages of using anti-ID reagent tools (2).

Immediately after the MoA-based PK assay is developed, it is critical to evaluate the sensitivity of the PK assay to potential biological interferences on drug detection, e.g., due to bound ADAs (6). In this study, multiple ADA-positive controls were characterized in depth to prove their validity to interfere with the drug's functionality and its drug-target binding. It was demonstrated that all ADA-positive controls inhibit drug-CD3ϵ target-mediated activation and, therefore, indicate a loss of drug function. This deeper pre-clinical evaluation of appropriate ADA positive controls on PK assay performance allowed retrospective translation of clinical exposure data along with ADA response data. Indeed, a broader evaluation of the clinical data in the phase I study suggests a strong correlation between high-titer ADAs and a significant loss of cibisatamab exposure and proves the concept of a MoA-based PK assay performance to measure target binding competent drug exposure.

The deeper characterization of ADA-positive controls was an advantage in identifying relevant patient ADA-binding features. Specific CDRs of cibisatamab were identified as being involved in the binding of ADA-positive controls and also in the binding of patient ADAs. CDRs of the heavy chain seem to play an essential role in terms of ADA binding. Interestingly, CDRs of the heavy chain were critical for CD3ϵ receptor antigen binding (data not shown), suggesting that ADAs (controls and patient ADAs) interfere with functional antigen binding. Indeed, the one anti-ID ADA PC (anti-ID 4) that specifically reacted with the CDRs of the HC was the most efficient inhibitor of CD3ε receptor-mediated activation.

Domain characterization data shows that patient-derived ADAs were anti-ID antibodies and dominantly directed to the CDRs of the anti-CD3 domain when collected 4 weeks after ADA onset. An anti-ID ADA response to drug-specific CDRs interferes with drug target binding and results in a neutralizing impact on drug function (16). ADA isotype characterization further demonstrated that the evaluation of the ADA responses revealed a class switch from an initial IgM response to a stronger (high titer) IgG response as described for classical immune responses (17). Maturation to the ADA IgG isotype response in these patients might be an indication of a more drug-specific epitope along with an increased ADA affinity for the drug. The characterized ADA positive controls used in this study seem to be directed to such an epitope and serve not only as appropriate and important tools to understand the neutralizing impact on PK exposure analyses but can also be used for further epitope characterization and/or complex analyses. The identification of specific B-cell epitopes via ADA binding evaluation combined with screening of potential drug-sequence-related T-cell epitopes might be an interesting evaluation to better understand the T-B-cell interaction of the ADA immune response in cibisatamab, similar to what was demonstrated in natalizumab (16).

Another advantage of using a MoA-based PK assay and understanding the neutralizing impact of ADAs is the quantitative free-drug concentration analysis over time. These quantitative PK analyses are more informative to support decision-making during clinical development than neutralizing ADA assays (nAb assays), which usually only have qualitative read-outs and no information about whether the remaining functional target-binding competent drug is still in circulation (18, 19).

In summary, the development of an appropriate MoA-based PK assay called for deeper exploration of appropriate assay reagent tools. The retrospective control analysis with clinical data and an advanced patient-derived ADA characterization for pre-clinical assay evaluation supplemented the essential proof of assay performance. The availability of correct target-binding, competent exposure data sensitive to ADAs is fundamental for adequate correlation with safety and efficacy to support informed decision-making during drug development. Target-binding PK assays might be used in lieu of qualitative nAb assays.

Materials and methods

Antibodies and reagents

The test compound cibisatamab is a bispecific therapeutic antibody in a head-to-tail 2:1 format and is described in previous publications (7, 8).

Murine monoclonal anti-ID antibodies against CDRs of cibisatamab mAb<Id-mAb<H-CEA>>IgG-Bi as a biotin-labeled capture reagent and mAb<Id-mAb<H-CD3>>IgG-Dig as a digoxigenin-labeled detection reagent was produced by Roche Diagnostics GmbH, Penzberg, Germany, for the development of the PK assay.

Cibisatamab was labeled with biotin or digoxigenin by Roche Diagnostics GmbH for the development of the ADA-bridging ELISA assay.

Murine monoclonal anti-ID antibodies 1–4 as ADA positive controls, specifically generated against CDRs of the anti-CD3 domain of cibisatamab, were produced and labeled by Roche Diagnostics GmbH, Germany.

Specific domains of cibisatamab and anti-CD3 antibody variants with different functional CDRs (at LC and HC or germline) were generated by pRED Large Molecule Research at Roche Innovation Center Zurich and Munich.

Study samples

Clinical serum samples were collected from the first-in-human, phase I cibisatamab monotherapy study (NCT02324257), an open-label, multicenter, dose escalation study. This study was approved by each center's ethics committee or institutional review board and was conducted in conformance with the Declaration of Helsinki, the International Conference on Harmonization Guidelines for Good Clinical Practice, and appropriate laws and regulations. All enrolled participants supplemented written, informed consent.

Biolayer interferometry analysis to characterize anti-ID binding

The binding properties of the anti-ID reagents (including ADA-positive controls) to cibisatamab or anti-CD3 domain variants were evaluated using biolayer interferometry (Octet). All steps of the analytics were defined (baseline, loading, association, and dissociation). The BLI baseline signal is established by calibrating the SA-sensor tip in an assay buffer (PBS, 0.5% RPLA1, 0.002% Bronidox) for 300 s (5 min). Streptavidin sensor tips were saturated with biotin-labeled cibisatamab or anti-CD3 variants. To establish baseline signal 2, the loaded sensor tip was incubated another 300 s (5 min) in the assay buffer. The kinetic rate constants were monitored by adjusting the association time when a saturated concentration of the binding partner approached the equilibrium-binding signal (~10–30 min). Dissociation time was at least 600 s (10 min).

Pharmacokinetic assay to analyze active cibisatamab

To determine the concentration of cibisatamab in human serum, a serial sandwich enzyme-linked immunosorbent assay (ELISA) was developed and validated based on regulatory guidelines (20, 21). Purified and biochemically characterized anti-ID antibodies were specifically selected as capture and detection reagent tools to develop a target-binding-competent PK assay to measure active exposure. Here, critical conditions to avoid dissociation of the drug-ADA complexes (e.g., dilution or incubation times) were considered (4–6). In detail, capture anti-ID antibody (mAb<Id-mAb<H-CEA>>IgG-Bi), calibrators (cibisatamab) and diluted serum samples, detection anti-ID antibody (mAb<Id-mAb<H-CD3>>IgG-Dig), and anti-digoxigenin-POD are added serially to a streptavidin-coated microtiter plate (SA-MTP). Each reagent was incubated for no longer than 1 h on a MTP shaker at 500 rpm, and after each step, the MTP was washed three times. Finally, the immobilized immune complexes were analyzed via ABTS and HRP substrates and photometrically determined. The quantification of cibisatamab is performed by back-calculating the absorbance values using the corresponding calibration curve with a non-linear 4-parameter Wiemer-Rodbard curve fitting function.

Anti-drug antibody assay to analyze ADA responses to cibisatamab

A bridging enzyme-linked immunosorbent assay (ELISA) was developed and validated to detect cibisatamab antibodies in human serum based on regulatory guidelines (22–24) and as described by Shankar (3). As a positive control, a mixture containing equimolar concentrations of two monoclonal antibodies (mAb<Id-mAb<CD3>>IgG; mAb<Id-mAb<CEA>>IgG) with similar binding features was used.

Characterization of ADA-specific domain binding: domain-detection assay

The classical ADA bridging screening assay is not designed to identify a single drug-binding domain of ADA or to identify CDR-specific epitopes of ADA binding.

To distinguish between ADAs that bind to different domains, domain detection ELISA assays were developed for the detection of anti-CD3 antibodies or anti-CEA antibodies (Supplementary Figure 2), similar to previous approaches (9). Monoclonal anti-ID antibodies mAb<Id<CD3>> IgG or mAb<Id-mAb<CEA>>IgG were used as ADA-positive controls for corresponding domain detection assays. Capture antibody biotinylated cibisatamab, or anti-CD3 fab domain, or anti-CEA fab´2 domain, calibrators (ADA positive controls), along with detection antibody (digoxigenin-labeled cibisatamab) and POD-conjugated anti-digoxigenin Fab fragments, were added to a streptavidin-coated microtiter plate (SA-MTP). Each reagent was incubated for 1 h on an MTP shaker at 500 rpm, and after each step, the MTP was washed three times and residual fluids were removed. Next, the immobilized immune complexes were visualized by the addition of ABTS solution, an HRP substrate, which converted to a colored reaction product. Finally, the color intensity is photometrically determined, and the signal is proportional to the analyte concentration in the serum sample.

Similarly, to determine the binding of anti-ID antibodies directed to specific CDRs of the anti-CD3 domain, different engineered constructs with modified anti-CD3 binding sites were generated and used as biotinylated capture reagents. These constructs include fully functional HC and LC CDRs, functional HC CDRs but germline on LC, functional LC CDRs but germline on HC, or negative control germline LC and HC (with abrogated CD3e specificity and CD3e binding).

ADA isotype determination by ELISA

To detect IgG-specific ADAs directed to cibisatamab, a specific drug-ADA-IgG complex assay was used as previously described (11, 12).

IgM-specific ADAs detection was performed as previously described (13). Here, cibisatamab has been biotin-labeled and bound onto an SA-MTP to capture IgMs.

Cut point determination of ADA assays

CP determination for ADA bridging ELISA: The ADA screening and confirmatory cut points (SCP and CCP) were evaluated according to Shankar et al. by triplicate analysis of 100 individual samples collected from healthy volunteers (50 men and 50 women). Following pooling of all data points and exclusion of technical outliers, the remaining 299 data points showing a non-normal distribution were used to establish a screening cut point applying a 95th percentile leading to an expected false positive rate of 5% and a confirmatory cut point applying a 99th percentile leading to an expected false positive rate of about 1% (3). For the screening

assay, an additive normalization factor was used to establish analytical run-specific cut points during sample analysis. Samples showing signals below the plate-specific SCP were rated as negative. Samples with signals equal to or above the plate-specific CP were rated as putatively positive and were reanalyzed in the confirmatory assay in the absence or presence of an excess drug concentration. Samples showing a signal inhibition equal to or greater than the CCP were deemed confirmed positive and were tittered.

CP determination for ADA Domain ELISA: The ADA domain-specific cut points were established as described before for the ADA screening assay by triplicate analysis of 40 healthy individual samples using either the anti-CD3 fab domain or the anti-CEA fab´2 domain of cibisatamab instead of the whole molecule as capture molecules, in combination with analyte-specific positive controls (monoclonal anti-idiotypic antibodies). Additive normalization factors were used to calculate analytical run-specific cut points.

CP determination for ADA Isotype Analysis: For this exploratory analysis, individual-specific cut points of patient serum samples were determined by averaging the OD values of every pre-dose sample of each patient and multiplying it by factor 2. These cut points were used for the evaluation of the study samples to reduce the effect of individual variations of baseline signals. Study samples with signals equal to or above the individual-specific cut point were rated as ADA IgG/IgM positive. Study samples with signals below the individual-specific cut point were rated as ADA-negative.

Cell-based CD3ϵ receptor-reporter assay

The Jurkat NFAT reporter cells (Promega, Madison, WI, USA) were cultured at 0.1–0.5 Mio cells/mL in RPMI 1640 (Thermo Fisher Scientific, Waltham, MA, USA) containing HEPES, GlutaMax and additionally 10% FBS, 1 × NEAA, and 1x SoPyr (Thermo Fisher Scientific, Waltham, MA, USA). For the analysis, negative/positive control or samples were added in triplicate with a final serum concentration of 10% in white flat bottom 96-well plates. The plate was incubated for 4 h 45 min at 37°C, 5% CO2, brought to room temperature, and finally 35 µl of OneGlo Ex substrate were added. After 2 min of shaking at 1.000 rpm, the luminescence signals were measured on a Tecan Infinite F500.

Data availability statement

The orginial contribution presented in the study are included in the article/Supplementary Material. Specific data availability statement to the clinical trial NCT02324257 has been published (25). Further inquiries can be directed to the corresponding author.

Ethics statement

The studies involving humans were approved by each center's ethics committee or institutional review board and was conducted in conformance with the Declaration of Helsinki, International Conference on Harmonization Guidelines for Good Clinical Practice, and appropriate laws and regulations. The studies were conducted in accordance with the local legislation and institutional requirements. The participants provided their written informed consent to participate in this study. Written informed consent was obtained from the individual(s) for the publication of any potentially identifiable images or data included in this article.

Author contributions

GL: Conceptualization, Data curation, Formal Analysis, Investigation, Methodology, Supervision, Visualization, Writing – original draft, Writing – review & editing. AL: Data curation, Formal Analysis, Investigation, Methodology, Validation, Writing – review & editing. MM-F: Data curation, Formal Analysis, Writing – review & editing. AH: Data curation, Formal Analysis, Investigation, Methodology, Writing – review & editing. ES: Data curation, Formal Analysis, Methodology, Validation, Writing – review & editing. EM: Data curation, Formal Analysis, Methodology, Writing – review & editing. MA: Data curation, Formal Analysis, Writing – review & editing. TS: Data curation, Formal Analysis, Methodology, Writing – review & editing. MV: Data curation, Formal Analysis, Methodology, Writing – review & editing. RH: Data curation, Writing – review & editing. AF-G: Data curation, Formal Analysis, Methodology, Writing – review & editing. CK: Investigation, Supervision, Writing – review & editing. MS: Data curation, Formal Analysis, Writing – review & editing. MR: Methodology, Writing – review & editing. K-GS: Investigation, Resources, Supervision, Writing – review & editing.

Funding

The author(s) declare that no financial support was received for the research, authorship, and/or publication of this article.

Conflict of interest

CK is employed at F. Hoffman-La Roche AG and holds ownership of stocks and patents of the company.

All authors were employees of Roche Diagnostics GmbH or F. Hoffman-La Roche AG during the time this study and associated analyses were being conducted. Authors might hold shares or patents of the company.

Publisher's note

Supplementary material

The Supplementary Material for this article can be found online at: https://www.frontiersin.org/articles/10.3389/fimmu.2024.1406353/full#supplementary-material

References

1. Chirmule N, Jawa V, Meibohm B. Immunogenicity to therapeutic proteins: impact on PK/PD and efficacy. *AAPS J*. (2012) 14:296–302. doi: 10.1208/s12248-012-9340-y

2. Staack RF, Stracke JO, Stubenrauch K, Vogel R, Schleypen J, Papadimitriou A. Quality requirements for critical assay reagents used in bioanalysis of therapeutic proteins: what bioanalysts should know about their reagents. *Bioanalysis*. (2011) 3:523–34. doi: 10.4155/bio.11.16

3. Shankar G, Devanarayan V, Amaravadi L, Barrett YC, Bowsher R, Finco-Kent D, et al. Recommendations for the validation of immunoassays used for detection of host antibodies against biotechnology products. *J Pharm Biomed Anal*. (2008) 48:1267–81. doi: 10.1016/j.jpba.2008.09.020

4. Staack RF, Jordan G, Dahl U, Heinrich J. Free analyte QC concept: a novel approach to prove correct quantification of free therapeutic protein drug/biomarker concentrations. *Bioanalysis*. (2014) 6:485–96. doi: 10.4155/bio.13.316

5. Staack RF, Jordan G, Viert M, Schäfer M, Papadimitriou A, Heinrich J. Quantification of a bifunctional drug in the presence of an immune response: a ligand-binding assay specific for A'ctive' drug. *Bioanalysis*. (2015) 7:3097–106. doi: 10.4155/bio.15.213

6. Schick E, Staack RF, Haak M, Jordan G, Dahl U, Heinrich J, et al. Validation of a ligand-binding assay for active protein drug quantification following the 'free analyte QC concept. *Bioanalysis*. (2016) 8:2537–25494. doi: 10.4155/bio-2016-0172

7. Bacac M, Klein C, Umana P. CEA TCB: A novel head-to-tail 2:1 T cell bispecific antibody for treatment of CEA-positive solid tumors. *Oncoimmunology*. (2016) 5: e1203498. doi: 10.1080/2162402X.2016.1203498

8. Bacac M, Fauti T, Sam J, Colombetti S, Weinzierl T, Ouaret D, et al. A novel carcinoembryonic antigen T-cell bispecific antibody (CEA TCB) for the treatment of solid tumors. *Clin Cancer Res*. (2016) 22:3286–97. doi: 10.1158/1078-0432.CCR-15-1696

9. Stubenrauch K, Künzel C, Vogel R, Tuerck D, Schick E, Heinrich J. Epitope characterization of the ADA response directed against a targeted immunocytokine. *J Pharm BioMed Anal*. (2015) 114:296–304. doi: 10.1016/j.jpba.2015.05.029

10. Gorovits B, Peng K, Kromminga A. Current considerations on characterization of immune response to multi-domain biotherapeutics. *BioDrugs*. (2020) 34:39–54. doi: 10.1007/s40259-019-00389-8

11. Wessels U, Schick E, Ritter M, Kowalewsky F, Heinrich J, Stubenrauch K. Novel drug and soluble target tolerant antidrug antibody assay for therapeutic antibodies bearing the P329G mutation. *Bioanalysis*. (2017) 9:849–59. doi: 10.4155/bio-2017-0048

12. Wessels U, Poehler A, Moheysen-Zadeh M, Zadak M, Staack RF, Umana P, et al. Detection of antidrug antibodies against human therapeutic antibodies lacking Fc-effector functions by usage of soluble Fcγ receptor I. *Bioanalysis*. (2016) 8:2135–45. doi: 10.4155/bio-2016-0182

13. Künzel C, Abdolzade-Bavil A, Engel AM, Pleitner M, Schick E, Stubenrauch K. Assay concept for detecting anti-drug IgM in human serum samples by using a novel recombinant human IgM positive control. *Bioanalysis*. (2021) 13:253–63. doi: 10.4155/bio-2020-0308

14. Heinrich J, Staack RF, Stubenrauch KG, Papadimitriou A. Proposal for a harmonized descriptive analyte nomenclature for quantitative large-molecule bioanalysis. *Bioanalysis*. (2015) 7:3057–62. doi: 10.4155/bio.15.218

15. Zhou Y, Penny HL, Kroenke MA, Bautista B, Hainline K, Chea LS, et al. Mytych DT Immunogenicity assessment of bispecific antibody-based immunotherapy in oncology. *J Immunother Cancer*. (2022) 10:e004225. doi: 10.1136/jitc-2021–004225

16. Cassotta A, Mikol V, Bertrand T, Pouzieux S, Le Parc J, Ferrari P, et al. A single T cell epitope drives the neutralizing anti-drug antibody response to natalizumab in multiple sclerosis patients. *Nat Med*. (2019) 25:1402–7. doi: 10.1038/s41591-019-0568-2

17. Gorovits B. Current considerations for immunoglobulin isotype characterization of antibody response against biotherapeutics. *AAPS J*. (2020) 22:144. doi: 10.1208/s12248–020-00530–4

18. Piccoli S, Mehta D, Vitaliti A, Allinson J, Amur S, Eck S, et al. White paper on recent issues in bioanalysis: FDA immunogenicity guidance, gene therapy, critical reagents, biomarkers and flow cytometry validation (Part 3 – recommendations on 2019 FDA immunogenicity guidance, gene therapy bioanalytical challenges, strategies for critical reagent management, biomarker assay validation, flow cytometry validation & CLSI H62). *Bioanalysis*. (2019) 2019):11 (24). doi: 10.4155/bio-2019-0271

19. Corsaro B, Yang T, Murphy R, Sonderegger I, Exley A, Bertholet S, et al. White paper on recent issues in bioanalysis: vaccine assay validation, qPCR assay validation, QC for CAR-T flow cytometry, NAb assay harmonization and ELISpot validation (Part 3 – recommendations on immunogenicity assay strategies, NAb assays, biosimilars and FDA/EMA immunogenicity guidance/guideline, gene & Cell therapy and vaccine assays). *Bioanalysis*. (2020) 13(6):415–63. doi: 10.4155/bio-2021-0007

20. Food & Drug Administration (FDA). *Bioanalytical Method Validation - Guidance for Industry*. (2018). FDA-2013-D-1020.

21. European Medicines Agency (EMA). *Guideline on bioanalytical method validation*. (2011), Draft ICH M10, 2023.

22. Food & Drug Administration (FDA). *Assay Development and Validation for Immunogenicity Testing of Therapeutic Protein Products - Guidance for Industry*. (2016). ID FDA-2009-D-0539-0023.

23. Food & Drug Administration (FDA). *Immunogenicity testing of therapeutic protein products - developing and validating assays for anti-drug antibody detection. Guidance for Industry*. (2019). ID FDA-2009-D-0539-0055.

24. Committee for Medicinal Products for Human Use (CHMP). *Guideline on immunogenicity assessment of therapeutic proteins*. (2017). EMEA/CHMP/BMWP/14327/2006 Rev 1.

25. Segal NH, Melero I, Moreno V, Steeghs N, Marabelle A, Rohrberg K, et al. CEA-CD3 bispecific antibody cibisatamab with or without atezolizumab in patients with CEA-positive solid tumours: results of two multi-institutional Phase 1 trials. *Nat Commun*. (2024) 15(1):4091. doi: 10.1038/s41467-024-48479-8

frontiers | Frontiers in Immunology

TYPE Original Research
PUBLISHED 15 July 2024
DOI 10.3389/fimmu.2024.1395854

OPEN ACCESS

EDITED BY
Michael Tovey,
Svar Life Science, France

REVIEWED BY
Heinz Kohler,
Retired, Carlsbad, CA, United States
Klaus R. Liedl,
University of Innsbruck, Austria

*CORRESPONDENCE
Chunhe Wang
wangc@simm.ac.cn
Zuoquan Xie
zqxie@simm.ac.cn
Guifeng Wang
gfwang@simm.ac.cn

†These authors have contributed equally to this work and share first authorship

RECEIVED 04 March 2024
ACCEPTED 26 June 2024
PUBLISHED 15 July 2024

CITATION
Wang Y, Chen Y-L, Xu H, Rana GE, Tan X, He M, Jing Q, Wang Q, Wang G, Xie Z and Wang C (2024) Comparison of "framework Shuffling" and "CDR Grafting" in humanization of a PD-1 murine antibody.
Front. Immunol. 15:1395854.
doi: 10.3389/fimmu.2024.1395854

Comparison of "framework Shuffling" and "CDR Grafting" in humanization of a PD-1 murine antibody

Yongmei Wang[1,2†], Yi-Li Chen[3,4†], Hui Xu[1,2†], Gul E. Rana[1,2], Xiaorong Tan[1], Mengying He[1], Qingqing Jing[5], Qi Wang[1], Guifeng Wang[1,2*], Zuoquan Xie[1,2*] and Chunhe Wang[1,2,3*]

[1]Shanghai Institute of Materia Medica, Chinese Academy of Sciences, Shanghai, China, [2]University of Chinese Academy of Sciences, Beijing, China, [3]Dartsbio Pharmaceuticals Ltd., Zhongshan, Guangdong, China, [4]Shanghai Mabstone Biotechnology Ltd., Shanghai, China, [5]Antibody Development Department, Shanghai Genechem Co., Ltd., Shanghai, China

Introduction: Humanization is typically adopted to reduce the immunogenicity of murine antibodies generated by hybridoma technology when used in humans.

Methods: Two different strategies of antibody humanization are popularly employed, including "complementarity determining region (CDR) grafting" and "framework (FR) shuffling" to humanize a murine antibody against human programmed death-1 (PD-1), XM PD1. In CDR-grafting humanization, the CDRs of XM PD-1, were grafted into the human FR regions with high homology to the murine FR counterparts, and back mutations of key residues were performed to retain the antigen-binding affinities. While in FR-shuffling humanization, a combinatorial library of the six murine CDRs in-frame of XM PD-1 was constructed to a pool of human germline FRs for high-throughput screening for the most favorable variants. We evaluated many aspects which were important during antibody development of the molecules obtained by the two methods, including antibody purity, thermal stability, binding efficacy, predicted humanness, and immunogenicity, along with T cell epitope prediction for the humanized antibodies.

Results: While the ideal molecule was not achieved through CDR grafting in this particular instance, FR-shuffling proved successful in identifying a suitable candidate. The study highlights FR-shuffling as an effective complementary approach that potentially increases the success rate of antibody humanization. It is particularly noted for its accessibility to those with a biological rather than a computational background.

Discussion: The insights from this comparison are intended to assist other researchers in selecting appropriate humanization strategies for drug development, contributing to broader application and understanding in the field.

KEYWORDS

antibody humanization, programmed death-1, FR shuffling, CDR grafting, immunogenicity

1 Introduction

Antibody therapeutics have emerged as the fastest growing field of drugs in the world. To date, FDA has approved over 100 monoclonal antibodies (mAbs) (1), extensively utilized in treating conditions such as tumors, viral infections, autoimmune diseases, and organ transplantation (2). Most antibodies were generated through the classic murine hybridoma technology. However, the use of murine antibodies poses high risk of immunogenicity, which diminishes the biological activities and hastens the clearance of therapeutic mAbs by anti-drug antibodies (ADA), and results in side effects in clinical applications (3, 4). Even chimeric antibodies, which retain about 66% of human-like characteristics, have substantial murine sequences (5). Consequently, further humanization is required for most therapeutical applications in human patients. The past three decades have witnessed the evolution of several humanization methods, encompassing CDR grafting, specificity-determining residues (SDR) grafting, resurfacing, framework (FR) shuffling, FR libraries, and guided selection, etc. (6). Two primary trends in the field of humanization include computer- and structure-based rational design, and library-based empirical methods. As a classic method, CDR grafting involves transferring specific antigen-binding CDRs onto human FRs with high homology to murine FRs (7–10). However, it typically results in a substantial reduction in antigen affinity (11, 12), as some key murine residues are crucial for adjusting the conformation of CDRs loop change. The absence of these residues leads to incompatibility between human FRs and non-human CDRs (12–14). Back mutation of these key residues has been typically employed to restore binding affinity (15). CDR grafting relies on computer modeling to identify canonical structure determining residues and design back mutation variants. CDR grafting depends on the precision of computational structural models and the depth of experiential knowledge. If computational predictions are imprecise, or if there is a deficiency in expert knowledge which leads to inadequate selection of critical amino acids for back mutation, the production of an optimal molecule might be compromised. Unlike rational methods that depend on antibody structure or sequence information, FR shuffling is an empirical method relying on constructing and screening large and diverse combinatorial libraries through phage display to select variants with desired properties. This library comprises six CDRs from murine antibodies fused with a pool of diverse human germline FRs, which contains almost all human germline genes of heavy and light chains suitable for antibody humanization (16). The substantial diversity facilitates the selection of optimal human FR combinations that can maintain the dominant conformation of non-human CDRs (17), allowing for sustained high affinities.

In this study, both CDR grafting and FR shuffling were conducted to humanize a chimeric human PD-1 antibody, XM Ch PD-1, with murine CDRs from XM PD-1, a murine antibody. The two strategies were directly compared using evaluation parameters such as production yield, thermal stability, binding activity, blocking efficacy, humanness, and immunogenicity. Notably, the most promising antibody, T5, emerged from the FR-shuffling process. The study highlights FR-shuffling as an effective complementary approach that can potentially increase the success rate of antibody humanization. Although the results are based on a single case study, the dissemination of these comparative insights will hopefully assist other researchers in the pharmaceutical field in selecting effective antibody humanization techniques.

2 Materials and methods

2.1 Cell lines and reagents

CHO-PD-1 and HEK293F cells were procured from the National Collection of Authenticated Cell Cultures (Shanghai, China). CHO-PD-1 cells were cultured in CD CHO medium (Gibco, New York, USA) supplemented with 0.7 mg/ml geneticin (Gibco, Paisley, UK) and 10 mM glutamine (Gibco, New York, USA). HEK293F cells were cultured in OPM-293 CD05 medium (OPM BiosciencesCo., Ltd., Shanghai, China). Human peripheral blood mononuclear cells (PBMCs) were purchased from MiaoTong Biotechnology (Shanghai, China). E.coli DH10B was a product of Invitrogen(Carlsbad, CA, USA). E.coli XL-1Blue was obtained from Agilent Technologies (USA). M13KO7 helper phage was obtained from NEB (Beijing, China).

PrimeSTAR ® HS DNA Polymerase was from Takara(Beijing, China). T4 DNA ligase and T4 DNA polymerase were purchased from NEB(Beijing, China). Triethylamine was purchased from Sigma (Shanghai, China), and the nitrocellulose filter was purchased from Whatman(Germany). Polyethylenimine (PEI) was purchased from Polysciences(Warrington, PA, USA). Goat anti-human kappa-unlabeled antibodies were procured from Southern Biotech (Birmingham, AL, USA), and PE-labeled goat-anti-human antibodies were purchased from BioLegend(San Diego, CA, USA). Enzymes EcoR I and Nhe I, streptavidin magnetic beads, 1% casein, Immunotube, TMB Substrate Kit, neutravidin-alkaline phosphatase-conjugated, alkaline phosphatase substrate (NBT-BCIP), 5000×SYPRO Orange, and high sensitivity streptavidin-HRP were purchased from Thermo Fisher Scientific. Additional reagents included anti-M13 antibody HRP, PD-1-6xHis, PD-L1-6xHis, GM-CSF, IL-4 TNF-α, IL-1β, IL-6, IL-10 ELISA Kit, IFN-γ ELISA Kit from SinoBiological(Beijing, China). PGE2 was sourced from Absin(Shanghai, China). The EasySep™ Human CD4+ T Cell Isolation Kit was purchased from Stemcell Technologies (Canada), and the CD14 MicroBeads human lyophilized kit was obtained from Miltenyi Biotec(Bergisch Gladbach, Germany).

2.2 CDR grafting

The amino acid sequence of murine antibody XM PD-1 was discovered in a previous study (18)and incorporated into the library. Molecular Operating Environment (MOE, version 2019.0102) was utilized for modeling and humanization.

The murine amino acid sequence was loaded into MOE, with annotations made for the regions of FRs and CDRs. The 3D structure model of the antibody was constructed based on FR and CDR templates, respectively. The best mode was selected based on sequence similarity and energy minimization. MOE identified three

types of canonical structure determining residues, and the roles of residues in maintaining conformation were confirmed through 3D visualization of the structure. Subsequently, a few human FRs with the highest homology in the Fab sequence database were chosen, and the murine CDRs were grafted onto the selected human FRs. Finally, key residues were designed for back-mutation based on the previously identified canonical structure determining residues and predictions of their effects on structure maintenance and binding ability.

2.3 FR shuffling

2.3.1 Construction of the FR shuffling libraries

The process was performed according to the previous literature (16). Oligonucleotides encoding human germline heavy chain FRs served as templates, paired with different primers encoding part of CDRs as homologous arms. The combinatorial library was assembled using overlap extension PCR with biotinylated primers. After capture by streptavidin-labeled magnetic beads, single-strand DNA was obtained by denaturing PCR products in 0.15M NaOH, and the minus single-stranded DNA (non-biotinylated ssDNA) was isolated through 70% EtOH and 3M NAOAc precipitation. The shuffled library, comprising a mixture of light and heavy chains, was annealed simultaneously with the M13 vector containing two palindromic loops. The minus strand was synthesized using T4 DNA ligase and T4 DNA polymerase. The parental template was then digested by *Eco*R I and *Nhe* I restriction enzyme, leaving vectors incorporating both VL and VH. The synthesized DNA was electroporated into DH10B cells for phage packaging (19). A phage solution was prepared through phage amplification in XL-1 Blue cells.

2.3.2 Solution panning

The procedures were carried out as previously reported (19). A total of 5×10^{12} phages were incubated with streptavidin beads for 15 min after being blocked with 1% casein. Subsequently, the solution was pipetted out, and the phages were transferred to a new tube. The bio-PD-1 antigen was then added to the tube and rocked for 1 h. New beads were introduced to pull down the antibody phage-biotinylated antigen complex, and the bound antibody phage was eluted using 100 mM Triethylamine and neutralized with 1 M Tris-HCl at pH 6.4. The XL-1 Blue cells were cultured with the eluted phage for amplification. The phage display library underwent panned for three consecutive rounds.

2.3.3 Immunotube panning

One immunotube was coated with PD-1 antigen protein, and another with phosphate buffered saline (PBS), both standing overnight at 4°C. A total of 5×10^{12} pfu phage was incubated with the PBS immunotube for 1.5 h, rolling up and down, and then standing for an additional 0.5 h for negative selection. Subsequently, the phage was transferred to the immunotube coated with PD-1 antigen, undergoing the same process. The desired phages were eluted with 100mM Triethylamine, and the eluted phages were amplified by infection into XL-1 Blue cells, prepared for the next panning.

2.3.4 Filter lift assay

The procedure was operated following the methods previously reported (19, 20). Phage clones were plated on the bacterial lawn at a density of $2\sim3\times10^3$ pfu plaques per dish. A nitrocellulose filter was overlaid with 5 ml of 2 μg/ml goat anti-human κ antibody-unlabeled for 2 h. Subsequently, the nitrocellulose filter was blocked with 1% casein, air-dried, and applied to the plaque lawn at 22°C overnight. The filter was then exposed to biotinylated PD-1 antigen for 1 h, followed by incubation with neutravidin-alkaline phosphatase for 30 min. Positive clones were ultimately detected using the alkaline phosphatase substrate (NBT-BCIP).

2.3.5 Single point ELISA

50 μl of phage supernatant was incubated with a plate coated with PD-1 antigen for 1 h. Subsequently, the signals were detected using anti-M13 antibody HRP and TMB substrate at OD_{450} nm.

2.4 Expression and purification

Regarding the CDR grafting method, the VH and VL sequences were synthesized as designed by Sangon Biotech (shanghai). Conversely, for the FR shuffling method, the VH and VL containing CDRs and shuffled FRs were identified through phage sequencing. The VH and VL regions of the two methods were fused with human IgG1 heavy and light constant domains using DNA recombinant technology. The expression plasmids of heavy chains (HC) and light chains (LC) were co-transfected into HEK293 cells at the ratio of HC: LC=1:3 using polyethylenimine (PEI). The supernatant was harvested after 5-6 days of cell culture, and the antibodies were purified using a protein A column (Smart-lifesciences) and eluted with 0.1M glycine on the AKTA Pure FPLC system (GE Healthcare).

2.5 Size-exclusion chromatography

Analytical SEC was performed using the Agilent 1260 HPLC system (Agilent), which was equipped with a Thermo MAbPac SEC-1, 5 μm, 7.8 × 300 mm column (P/N 088460, Thermo Fisher Scientific). A total of 10 μl of sample was injected into the column at a concentration of 1mg/ml. Sodium phosphate (pH 6.8) served as the mobile phase with a flow rate of 1 ml/min. Protein detection was carried out using a UV detector at OD280.

2.6 Differential scanning fluorimetry

A working solution of SYPRO Orange 250× was freshly prepared by diluting 1 μl of 5,000×SYPRO Orange in 19μl of water. Subsequently, 1μl of SYPRO Orange working solution was added to 24 μl of PBS-diluted antibodies at a 20 μM. Fluorescence intensities were measured at every 1°C interval within the temperature range of 25 to 95°C using the CF×96 Touch qPCR machine (Bio-Rad). The melting temperature (*Tm*) was calculated from the derivative Relative Fluorescence Unit (RFU) against temperature (dRFU/dT) curve.

2.7 Enzyme-linked immunosorbent assay

The 96-well plate (Greiner) was coated with 2 μg/ml PD1-Fc at 4°C overnight, then blocked with 1% casein for 1 h. After washing, three-fold series dilutions from 100nM of antibodies were added to the plates. The color was developed using goat anti human kappa-HRP and TMB substrate at room temperature. After being stopped by 2M H_2SO_4, the absorbance was measured at OD_{450} using SpectraMax M5e (Molecular Devices).

2.8 Biolayer interferometry

Binding kinetics analysis was conducted on the Octet RED96e system (ForteBio). Protein A biosensors (Sartorius) were pre-wetted in the kinetics buffer (PBS with 0.05% Tween 20) for 10 min. The antibodies were immobilized on the protein A biosensor at a signal level of 1.5 nm. Various concentrations of PD-1-his were applied in a two-fold series dilution in the kinetics buffer (from 100 to 1.56 nM). The association step was set for 120 s, and the disassociation step was set for 180 s. The binding curves were fitted using a global fit 1:1 binding model with ForteBio Data Analysis software 9.0 (ForteBio).

In the self-binding assay, a protein A biosensor captured the antibody to be tested. To ensure specificity, a non-binding antibody blocked any remaining Fc binding sites on the biosensor. The antibody to be tested then underwent a 120s association followed by a 180s dissociation. The signal measured during the association was used to assess the self-binding capabilities of the antibody to be tested, indicating its tendency to interact with itself.

2.9 Surface plasmon resonance

The binding kinetics of CDR grafting humanized antibodies were verified by SPR using Biacore T200 (GE Healthcare). The running buffer employed was HBS-EP, consisting of 10 mM HEPES, 150 mM NaCl, 3 mM EDTA at pH 7.4 and 0.005% (v/v) Tween-20. Purified antibodies were diluted to 2 μg/ml and immobilized on Series S Sensor Chip Protein A (GE Healthcare, Cat: 29127556) at 250 response units (RU). The gradient PD-1-ECD-his flowed over the immobilized antibodies starting from 50nM in a two-fold serial dilution, at a flow rate of 30ul/min, with 180 s for association and 1200 s for disassociation. After each cycle, the sensor chip was regenerated with 10mM glycine at pH1.5 for 30 s. The binding kinetics were analyzed using Biacore T200 Evaluation software version 3.1 with a 1:1 Langmuir binding model.

2.10 Flow cytometry

Binding of the humanized antibodies to the cell surface PD-1 was measured using Fluorescence-Activated Cell Sorting (FACS). CHO cells overexpressing PD-1 (CHO-PD-1) were aliquoted into FACS tubes at 3×10^5 cells/tube and then incubated with 2 μg/ml PD-1 antibody at 4°C for 30 min. After washing with PBS twice, the cells were incubated in 100 μl staining buffer containing PE-labeled goat-anti human antibody in the dark for 30 min. The mean fluorescence intensity (MFI) of binding was measured by CytoFLEX flow cytometer (Beckman), and the data were analyzed using FlowJo software (BD Biosciences).

2.11 Competitive ELISA

A concentration of 1 μg/ml of recombinant human PD-1-6xHis was coated on 96-well plates (Greiner) at 4°C overnight. Testing antibodies in a 2-fold series dilution were then added to the plates along with 1 μg/ml biotinylated PD-L1. Following a 1 h incubation, the bound ligand was detected using streptavidin-HRP and developed with TMB substrate. The reaction was halted by 2M H_2SO_4, and the absorbance was measured using SpectraMax M5e (Molecular Devices).

2.12 Mixed lymphocyte reaction assays

$CD14^+$ and $CD4^+$ cells were isolated from frozen PBMCs from different donors using the CD14 MicroBeads human lyophilized kit and EasySep™ Human $CD4^+$ T Cell Isolation Kit. The isolated $CD14^+$ cells were cultured with 500 ng/ml GM-CSF and 500 ng/ml IL-4 for 5 days to generate immature DCs. Subsequently, they were treated with 30 ng/ml TNF-α, 300 ng/ml IL-1β, 300 ng/ml IL-6, and 3 μg/ml PGE2 for an additional two days to induce DC maturation. On day 8, $CD4^+$ T cells (1×10^5 cells) were co-cultured with allogeneic DCs (1×10^4 cells) in the presence of T5, Pembrolizumab, Nivolumab, and isotype. After 5 days of culture, the supernatant was collected to measure the production of IL-10 and INF-γ using ELISA.

2.13 Prediction of humanness and immunogenicity

BioPhi was a platform designed for antibody design, humanization, and humanness evaluation, which leveraged natural antibody repertoires and deep learning technologies (21). It incorporated a component called OASis, which provided a detailed, interpretable humanness score. The sequences of the light chain and heavy chain were inputted on this website https://biophi.dichlab.org, and the OASis score was outputted.

T20 humanness analyzer was another classic prediction tool (22). The sequences of the light and heavy chains were inputted on this website http://abAnalyzer.lakepharma.com, and the T20 score was outputted.

2.14 Molecular dynamics simulations

The structures of the murine antibody was obtained by homology modeling by MOE. The antibodies were annotated according to Kabat. The antibody Fv was solvated in a cubic water box that is sufficiently large to provide a minimum buffer zone of 14 Å between biological

material and the cubic system boundaries. Na^+ and Cl^- ions were randomly placed to neutralize the system electrostatically at a physiological salt concentration of 0.150 M. The CHARMM36m force field (23) and the three-site OPC water model were used subject to periodic boundary conditions (24). The initial energy minimization was performed using the steepest descent method. Later, the system was equilibrated in the NVT ensemble at 310 K for 100 ps, using a small integration time step of 2 fs. Production trajectories were recorded in the NPT ensemble at 310 K and 1 atm atmospheric pressure using a 2 fs of integration time steps for a total of 100 ns. Atomic coordinates were saved every 10 ps. The long simulation utilized similar parameter settings, with a total duration of 1 μs. Gromacs 2024.1 was used for simulation setups and trajectory collection. Gromacs and in-house Python scripts were used for all analyses.

2.15 Comparative analysis of residual interactions across predicted protein structures

We developed a comprehensive method to analyze protein-protein interactions within a structure, utilizing the Bio.PDB module from the BioPython library. Our method focuses on identifying four primary types of molecular interactions critical to protein function and stability:

Hydrogen Bonds: Analyzed between nitrogen (N) and oxygen (O) atoms within a 3.5 Å threshold.

Hydrophobic Contacts: Evaluated between side-chain carbons of hydrophobic residues (Leucine, Isoleucine, Valine, Phenylalanine, Tryptophan, Methionine) excluding alpha carbons, with a distance limit of 5.0 Å.

Salt Bridges: Assessed between oppositely charged residues (Arginine, Lysine, Histidine; Aspartic acid, Glutamic acid) within a 4.0 Å range.

Pi-Pi Stacking: Investigated between aromatic rings (Phenylalanine, Tyrosine, Tryptophan, Histidine) up to 6.5 Å apart.

2.16 Statistical analysis

Statistical evaluation was conducted using GraphPad Prism 8.0 (GraphPad Software Inc.). P values were calculated using a one-way ANOVA multiple comparison test (*P < 0.05, **P < 0.01, ***P < 0.001, ns: not significant).

3 Results

3.1 Generation, screening and sequence analysis of humanized antibodies

The design of CDR-grafting humanization was conducted using software Molecular Operating Environment (MOE) (25). The annotation of antibodies was performed using the IMGT(The International ImMunoGeneTics information system). The murine antibody structure model was built based on the FR and CDR templates retrieved from the PDB database. The templates and corresponding similarity scores were shown in Supplementary Table 1. Three types of canonical structure determining residues were identified through the predicted 3D structure (Supplementary Tables 2, 3). Type 1 residues, located at the binding interface between VL and VH, play key roles in the packing of the two structural domains. Type 2 residues, positioned close to the CDR region and embedded in the protein interior, may affect the overall antigen-antibody binding conformation. Type 3 residues have direct interactions with the CDR region, including hydrophobic interactions, hydrogen bonds, and salt bridges. The robustness of our MOE template modeling has been validated through comparative analyses with models generated by ABodyBuilder (26) and ImmuneBuilder (27). The results, as shown in Supplementary Figure 1, indicate that the overall structural frameworks were consistent across the models, with RMSD values of 0.48 Å between MOE and ABodyBuilder, and 0.393 Å between MOE and ImmuneBuilder. This consistency underscores the reliability of the MOE model, especially within the framework regions (FR).The RMSDs calculated separately for the CDR loops and the remaining Fv regions were shown in Supplementary Table 4). Static modeling provides a single, often idealized snapshot of the molecular structure, without accounting for the natural fluctuations and movements that molecules undergo in their native environments. Molecular Dynamics (MD) simulation captures the time-dependent behavior of molecules and incorporates environmental effects, enabling researchers to observe how structures and interactions evolve over time. Supplementary Figure 2A displayed the Root Mean Square Deviation (RMSD) values for XM Ch PD1 in MD simulations (100 ns), showing fluctuations between 6.5 and 12.5 ns, yet not exceeding 0.23 nm. After approximately 15 ns of MD simulation, the system began to stabilize, ultimately settling at 0.09-0.17 nm. This suggested that the simulated structure closely matched the predicted structure from homology modeling. Additionally, long simulations (1 μs) were employed to gain deeper insights into the dynamic behavior of conformation-stabilizing contacts and to potentially correct minor inaccuracies in the modeled structures. The RMSD values, ranging from 0.069 to 0.258 nm (Supplementary Figure 2B), indicated that the antibody maintained a relatively stable structure with some conformational flexibility over the 1 μs MD simulation. This further indicated that the simulation conditions were appropriately set, and the initial model was reliable, without resulting in significant structural changes.

The conventional CDR-grafting method employs a single human germline sequence for grafting parent CDRs, often failing to satisfy all key requirements: low immunogenicity, high stability, and high expression. To address this, each non-human FR was individually humanized by selecting the most homologous human germline FR, allowing the preservation of the original antibody's properties to the greatest extent. The chosen germlines of CDR grafting were shown in Table 1. After grafting the CDRs onto human FRs, the designed molecule was named 'human-germline-grafted'. By comparing the designed one and the murine antibody XM Ch PD-1, the residues different in the FR region were identified. Three types of canonical structure determining residues listed by the MOE were only for reference, we determined the key residues by comprehensive considerations. To determine which key residues need back-mutation to retain the binding ability, their roles in conformation maintenance were checked using the constructed parental structure

model. The sites involved in the mutations include K19, T40, E42, R44, P61, A63, V70, E76, E77, I78, K87, and S88 in the heavy chain and the sites involved mutations include M37, H38, and P47 in the light chain(Supplementary Figure 3). Finally, eight humanized heavy chains and four humanized light chains were designed. We generated 32 humanized antibodies. Through single point ELISA screening, four candidates with the highest binding, named BS#3, BS#5, BS#11, BS#31 were selected for subsequent studies.

FR-shuffling humanization was executed by selecting different human heavy and light (κ) germline genes into each of the four FRs while keeping the CDRs fixed (16). The full-length variable structural domains were generated by fusing CDRs with the FR pool. The gene diversity of the library exceeded 4×10^6, which was ample for selecting the optimal matches between CDRs and FRs. After multiple rounds of solution panning and immunotube panning, the capture lift assay was developed for the initial screening of the large library (19, 20). Only deep colored spots were isolated as positive clones. Single point ELISA was employed for the secondary screening. The schematic diagrams of the FR shuffling and CDR grafting methods are shown in Figure 1. We selected the top nine candidate molecules with the highest OD values from a single-point ELISA binding assay, representing the molecules with the best binding affinity, named T1-T9.

The humanized heavy and light chains were completely shuffled as they derived from various human germline families. For example, T1 Ab contained VH5/VH3 and VK6/VK3, respectively (Table 2). With a more nuanced insight, three FRs of individual heavy and light chains may derive from different human germline genes with in a given family, such as T5 Ab compromised VH3-15 and VH3-53 in the heavy chain. Overall, the humanized PD-1 antibodies' heavy chain showed a preference for the VH3 germline family. This inclination could be attributed to the greater homology of this class with the parental FR, thereby increasing the likelihood of preserving essential parental residues (16). Besides, various germline families were exhibited in the humanized light chain.

3.2 FR shuffling-humanized antibodies showed higher titers and purities

The top mammalian expression titers of selected CDR grafting antibodies (BS# series) were approximately 100 mg/L, and most of the FR shuffling-humanized antibodies (T series) yielded titers higher than 100 mg/L, except T6 and T8 (Table 3). Size exclusion chromatography (SEC) were used to assess the purities of antibodies after a single-step purification with Protein A columns. Peaks that elute faster in the chromatogram represented larger aggregates. All the CDR grafting-humanized antibodies aggregated to an extent of about 20% (Figure 2A).

TABLE 1 The germlines used for CDR-grafting humanization.

	FR1	FR2	FR3	FR4
VH	IGHV3-15*01	IGHV3-7*01	IGHV3-74*01	JH5
VL	IGKV3D-11*02	IGKV3-11*01	IGKV6-21*01	JK4

In comparison, all nine FR shuffling-humanized antibodies exhibited minimal aggregation with >90% purity as revealed by analytical SEC (Figure 2B). Thus, T1-5, T7 and T9 were selected for further studies. For subsequent head-to-head comparison, we used SEC for secondary purification to remove aggregates and improved the antibody purities to nearly 100%. Once the aggregates were removed, the CDR grafting-humanized remained stable in the PBS buffer.

3.3 FR shuffling-humanized antibodies exhibited better thermal stability

After being heated at 60°C for one hour, the purity of the humanized antibodies was analyzed by SEC to determine their thermal stabilities. Protein peaks that elute after the main peak were typically degraded smaller fragments, which traveled through the gel matrix slower than the intact antibody molecules. The four candidates obtained by CDR grafting were not thermally stable, and degraded more when compared to the chimeric antibody XM Ch PD-1 (Figure 3A). In contrast, the nine candidates obtained by FR shuffling were thermally stable after being heated (Figure 3B).

Additionally, Differential Scanning Fluorimetry (DSF) was used to measure the thermal stability of the antibodies. Using extrinsic fluorescent probes and real-time PCR apparatus, DSF can monitor unfolding transition of specific proteins with increasing temperature (28). As shown in Figure 3C, all the *Tm* values of the antibodies' Fc domains were at 68.2°C, consistent with the chimeric antibody. The melting temperatures were shown in Supplementary Table 5. The Fab domains of T1, T3, T5 and T6-9 exhibited enhanced thermal stability compared with its murine counterpart XM Ch PD-1, and the *Tm* values of the antibodies were all above 73.9°C. Thus, the selected FRs and CDRs are compatible to each other. In contrast, the *Tm* values of the Fabs of the four CDR grafting-generated variants were under 68.2°C (Figure 3C). Thus, they are inferior to FR shuffling-generated variants generated in thermal stability.

3.4 FR shuffling-humanized antibodies retained binding affinities

The binding affinities of humanized antibodies were compared by ELISA. The two CDR grafting-humanized variant BS#5 and BS#11, and the nine FR shuffling-humanized variants all showed high affinities similar to that of the chimeric antibody (Figures 4A, B).

The binding kinetics was evaluated by biolayer interferometry (BLI), which monitors the rates of association and disassociation in real-time with precision and accuracy (29). The nine FR shuffling-humanized variants showed high binding affinities in BLI (Figure 4C), with T5 as the highest affinity antibody. In contrast, CDR grafting-humanized variant BS#3, BS#5, BS#11 and BS#31 exhibited much lower binding affinities than XM Ch PD-1 and the positive control pembrolizumab. Surface plasmon resonance (SPR) is another reliable label-free detection method for biomolecular interactions (30), which showed similar results to BLI (Figures 4D, E).

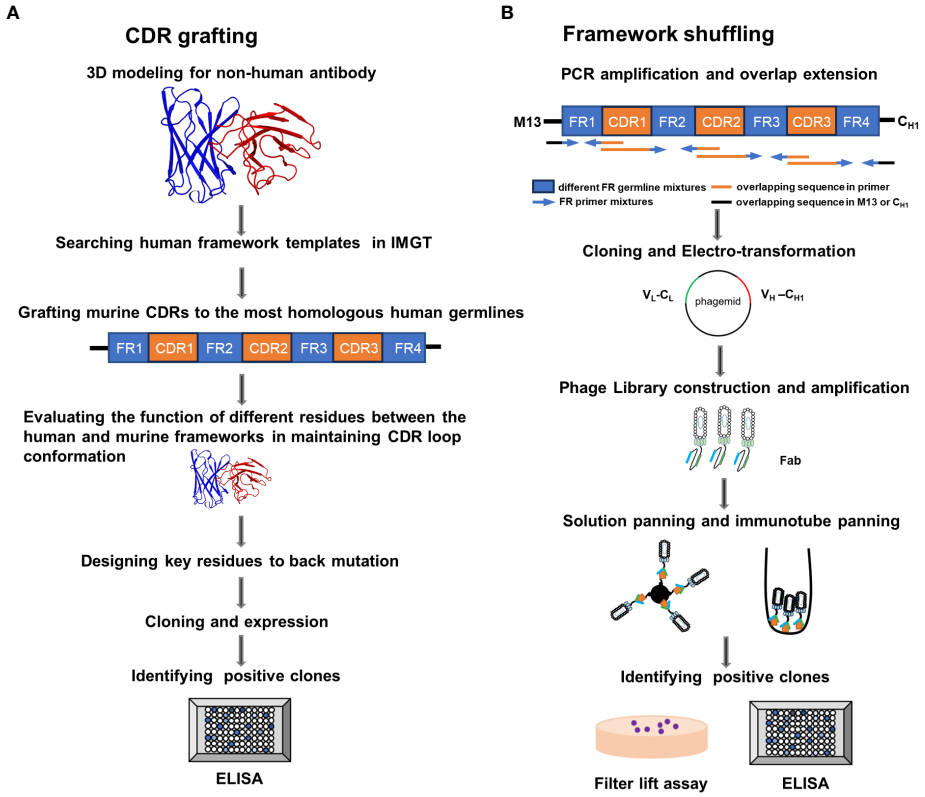

FIGURE 1
Schematic illustration of the complementarity determining region (CDR) grafting and framework (FR) shuffling humanization strategies. **(A)** The main procedure of the CDR grafting. **(B)** The main process of the FR shuffling.IMGT, the international ImMunoGeneTics database; ELISA, enzyme-linked immunosorbent assay; PCR, polymerase chain reaction; Fab, fragment of antigen binding. V_L, Light chain variable region; C_L, light chain constant region; V_H, heavy chain variable region , C_{H1}, heavy chain constant region 1.

Next, we compared the binding activities of the variants after being heated, which demonstrated that FR shuffling-humanized variants were superior to CDR grafting-humanized ones (Figure 5A).

Based on the results above, we focused on developing molecules of FR shuffling. The nine FR-shuffling variants were assayed for binding abilities to PD-1 overexpressed on CHO cells. They showed comparable binding activities to XM Ch PD-1 and pembrolizumab, with T5 as the highest-binding variant (Figure 5B).

3.5 Humanized antibodies blocked PD-1/PD-L1 interaction

The effects of the FR shuffling-humanized variants on the interaction between PD-1 and PD-L1, were measured (31). All nine variants could effectively block the binding between PD-1 and PD-L1. The IC_{50} values of the variants ranged from 0.45 to 0.84 nM, slightly better than pembrolizumab. Among them, T5 was the best

TABLE 2 Sequence analysis of FR-shuffled antibodies.

mAbs	Human VH germline				Human VL germline			
	FR1	FR2	FR3	FR4	FR1	FR2	FR3	FR4
T1	IGHV5-51	IGHV3-15	IGHV3-23	JH5	IGKV6-21	IGKV3-15	IGKV6-21	JK4
T2	IGHV3-15	IGHV1-46	IGHV1-46	JH5	IGKV1-5	IGKV3-15	IGKV2-28	JK4
T3	IGHV3-23	IGHV1-46	IGHV3-53	JH5	IGKV5-2	IGKV3-15	IGKV4-1	JK4
T4	IGHV3-23	IGHV3-15	IGHV3-72	JH5	IGKV5-2	IGKV4-1	IGKV3-15	JK4
T5	IGHV3-15	IGHV3-15	IGHV3-53	JH5	IGKV5-2	IGKV3-15	IGKV2-28	JK4
T6	IGHV3-72	NA	IGHV3-72	JH5	IGKV5-2	IGKV3-15	IGKV4-1	JK4
T7	IGHV3-23	IGHV3-72	IGHV3-72	JH5	IGKV5-2	IGKV3-15	IGKV4-1	JK4
T8	IGHV3-53	IGHV4-4	IGHV3-72	JH5	IGKV1D-43	IGKV3-15	IGKV6-21	JK4
T9	IGHV3-15	NA	IGHV3-53	JH5	IGKV1-5	IGKV3-15	IGKV4-1	JK4

FR, framework; NA, not applicable, for the mutations in the region.

TABLE 3 Production yields of humanized PD-1 antibodies in HEK 293 cells.

Antibodies	Production (mg/L)
BS#3	97
BS#5	117
BS#11	101
BS#31	99
T1	172
T2	160
T3	150
T4	133
T5	159
T6	86
T7	156
T8	28
T9	114

variants with IC_{50} values of 0.45 nM (Figure 6A). In addition, the functional activity of FR-shuffling variant T5 was analyzed by MLR assay (32). As shown in Figure 6B, T5 significantly stimulated IL-10 and INF-γ production at both 1 and 10 μg/ml, which was comparable to positive control pembrolizumab and nivolumab.

3.6 Prediction of humanness and immunogenicity for humanized antibodies

We used two different methods to predict the humanness of the humanized antibodies, BioPhi and T20 humanness analyzer, as shown in Table 4. The results showed that the variants from both humanization strategies were similar in degrees of humanness and all had improved humanness compared to the murine counterpart. FR-shuffling variant T5 was one of the variants with the highest humanness.

Analyzing the potential T cell epitopes has been suggested to provide valuable forecasts for immunogenicity estimation. Thus, netMHCIIpan (4.0) was implemented to predict the potential peptides binding to HLA II. Due to the extensive polymorphism of HLA II in the general population, which presents a formidable obstacle in T cell epitope identification, we chose the most frequent alleles in loci DRB1 to represent the coverage of HLA II in the population (33, 34). As shown in Table 5, T5 demonstrated a reduction in affinity for HLA II alleles when compared to its murine counterpart, suggesting a decrease in potential immunogenicity.

4 Discussion

For murine antibodies generated using hybridoma technology, humanization is typically necessary before clinical applications to minimize potential immunogenicity in human. This study compared two popular strategies of antibody humanization in the industry: CDR grafting and FR shuffling.

The comparative analysis of two humanization methods was applied to a PD-1 antibody, revealing distinct advantages of FR shuffling over CDR grafting. CDR grafting-humanized variants exhibited a higher propensity for aggregation (nearly 20%), whereas FR shuffling-humanized variants demonstrated higher purity post-purification. Antibody aggregation reduces biological activity and may elicit immunological responses *in vivo* (35–37). The initial purification step involved Protein A column, which did not effectively remove aggregates. Subsequent size exclusion chromatography (SEC) was employed as a secondary purification step, successfully eliminating the aggregates. The cessation of antibody aggregation following the second purification indicates that most aggregation likely occurred during cell culture or the binding and elution process on Protein A, where antibodies were exposed to physical stress, pH fluctuations, and changes in ionic strength, potentially destabilizing their structure and leading to aggregation. Despite these challenges, the antibody T series exhibited superior structural and conformational stability, maintaining structural integrity under such stressful conditions.

Furthermore, the CDR grafting-humanized variants exhibited poor thermal stability, leading to significant antibody degradation upon heating. Additionally, these variants demonstrated markedly lower binding responses in BLI and SPR assays. In contrast, the FR shuffling-humanized variants exhibited robust binding responses and higher affinities compared to both the chimeric version and pembrolizumab. The discrepancy in antigen-antibody binding signals observed between ELISA and binding kinetics assays indicates more efficient and stable binding of FR shuffling-humanized variants relative to CDR grafting-humanized ones. This discrepancy in maximum binding between ELISA and kinetics assays can be attributed to several factors. Firstly, ELISA employs enzymatic amplification to enhance assay sensitivity, facilitating detection of even low-affinity interactions. In contrast, BLI and SPR directly measure changes in interference pattern or refractive index due to binding events without amplification, potentially rendering them less sensitive to weak interactions. Secondly, ELISA, being an end-point assay, quantifies the total amount of bound antigen after a specific incubation period, which can capture slow or weak interactions. In contrast, BLI and SPR measure binding kinetics in real-time, allowing differentiation of signals for weak or fast-dissociating interactions. Importantly, it was confirmed that there was no self-binding between the variant molecules, thereby excluding self-binding as a cause for the observed performance differences (Supplementary Figure 4).

The stability of the antibodies was further assessed using DSF. The *Tm* values of the CDR grafting-humanized antibodies were found to be below 68.5°C, whereas those of the FR shuffling-humanized variants exceeded 73°C. A higher *Tm* value indicates greater thermal stability, indicative of a well-packed structure that requires more energy to unfold and is less likely to undergo aggregation (38). Noteworthy, all nine variants generated through FR shuffling retained their binding ability even after undergoing accelerated thermal treatment. The lower thermal stability observed in CDR grafting-humanized antibodies may lead to increased

10.3389/fimmu.2024.1395854

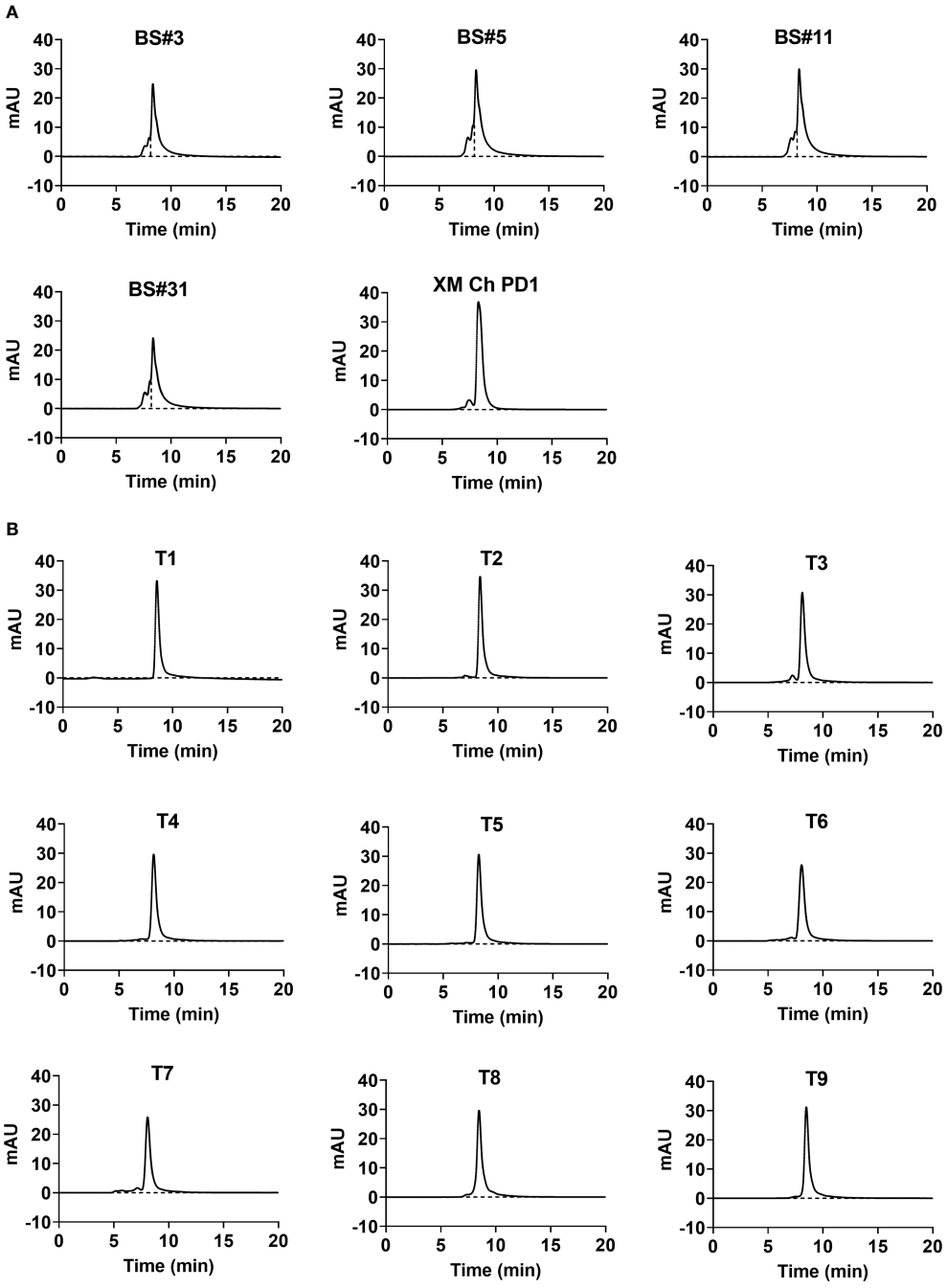

FIGURE 2
The aggregation and purity of humanized antibodies. The purity of humanized variants generated by **(A)** CDR grafting and **(B)** FR shuffling detected by size-exclusion chromatography (SEC).

aggregation propensity, susceptibility to degradation, and challenges in manufacturing, shipping, and storage. These factors can contribute to delays and escalate costs in drug development processes.

After humanization, humanness was evaluated for immunogenicity prediction. BioPhi was a platform designed for antibody design, humanization, and humanness evaluation, which leveraged natural antibody repertoires and deep learning technologies. The OASis score was calculated based on a search of 9-mer peptides within the Observed Antibody Space (OAS) database, ensuring a diverse and granular evaluation of antibody sequences for their similarity to natural human antibodies (21). The T20 humanization assessment tool was developed based on an in-depth analysis of the humanness of therapeutic antibodies using a large number of human antibody sequences from the NCBI Igblast database. It can efficiently distinguish human sequences from non-human sequences (22). As expected, both CDR grafting and FR shuffling improved the humanness of XM Ch PD-1. Besides, T5 exhibited superior biophysical and biological features in comprehensive consideration.

The netMHCII 4.0 tool was trained on natural ligands eluted from HLA II by mass spectrometry and binding affinity to HLA II, a state-of-

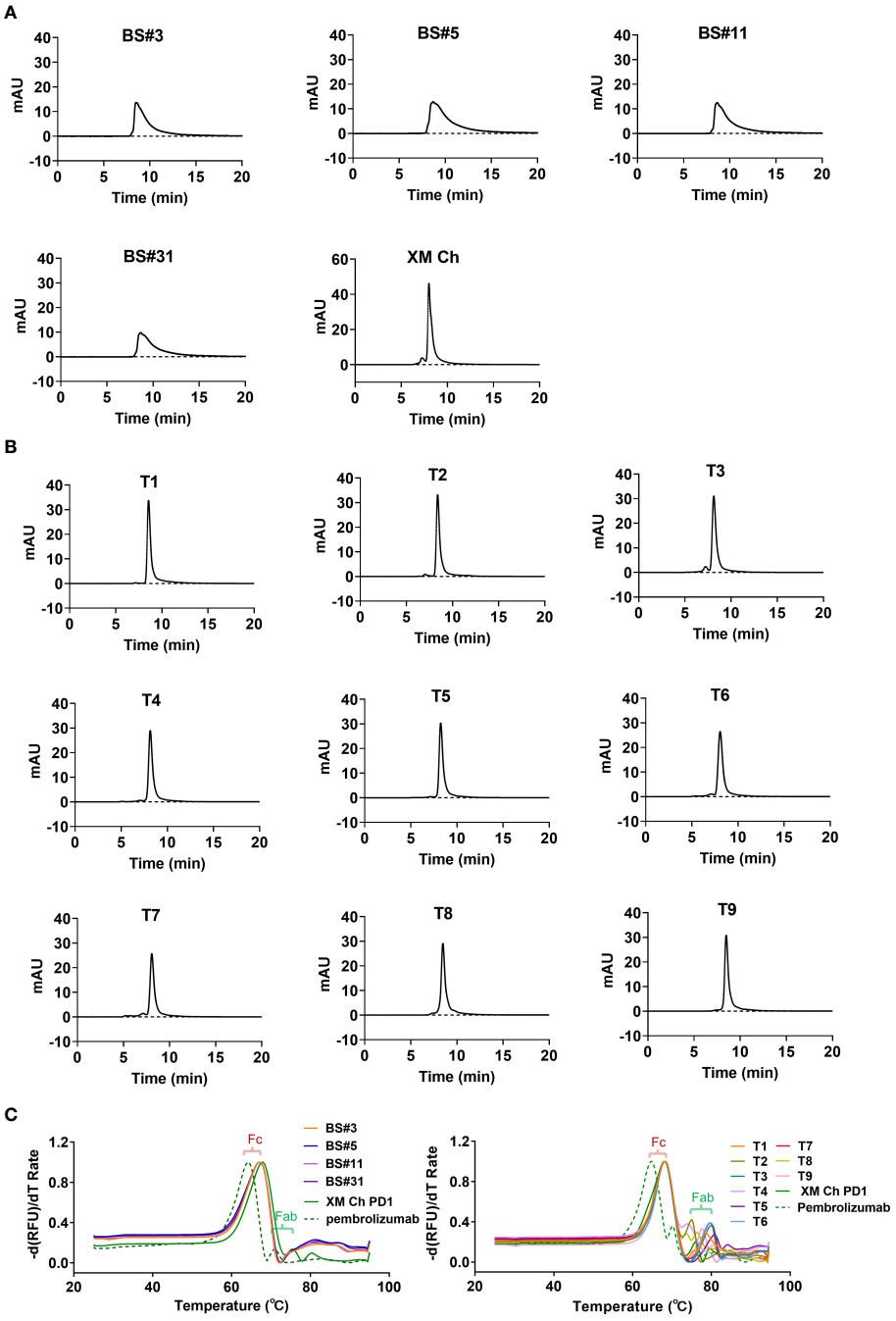

FIGURE 3
The thermal stabilities of the antibodies obtained from the two different humanization methods. **(A, B)** The detection of degradation using SEC after heating at 60°C for one hour for CDR grafting- and FR shuffling-humanized antibodies. **(C)** Differential scanning fluorimetry (DSF) was used to determine the melting temperature (*Tm*) values of proteins.

the-art predictor tool for the analysis of T cell epitopes considering biological features in the process (39, 40). It seemed that T5 decreased the number of T cell epitopes compared with the murine counterpart. However, given the MHC-II polymorphism and diverse allotype tolerance of patients in clinic, it's still a great challenge to predict the immunogenicity of therapeutic antibodies in the field.

The orientation of the heavy and light chain in the interface is heavily influenced by crystal packing effects. The templates for the homology model are based on crystal structures. This factor sometimes compromises the reliability of residues identified as type 1 canonical structure determining residues. To address this issue, we compared the residues and their interactions across three predictive models: MOE, ABodyBuilder, and ImmuneBuilder(Supplementary Tables 6 and 7). Importantly, discrepancies observed among these models did not involve mutated residues. Moreover, interactions identified across the different models exhibited a high degree of similarity, underscoring the robustness and consistency of our modeling approach. MD simulations capture the evolution of

10.3389/fimmu.2024.1395854

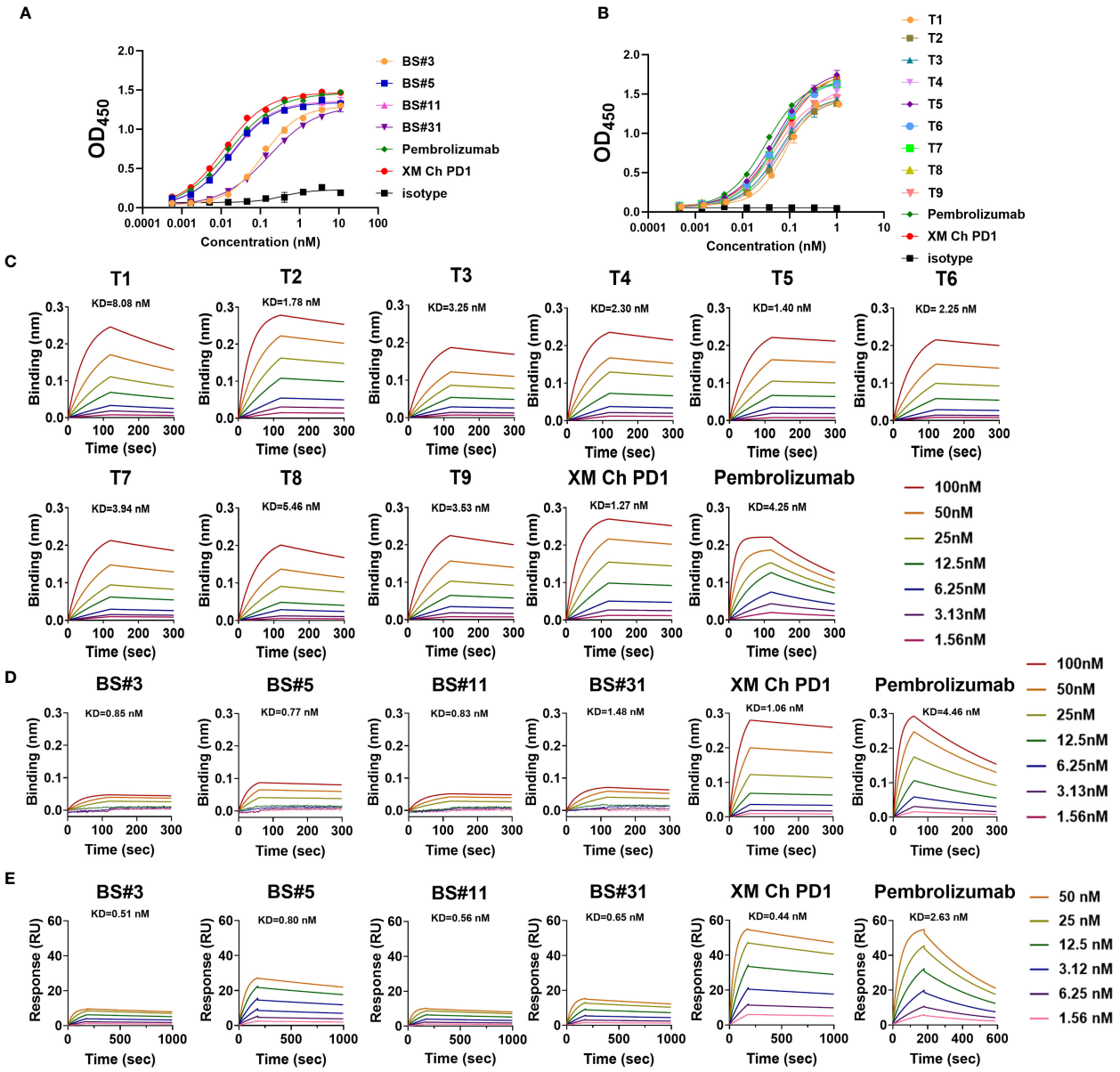

FIGURE 4
The binding abilities of humanized antibodies. **(A, B)** The binding affinity for CDR grafting variants and FR shuffling variants with PD-1 protein measured by enzyme-linked immunosorbent assay (ELISA), respectively. **(C)** The binding kinetics of FR shuffling variants detected by biolayer interferometry (BLI). **(D, E)** The low binding response of CDR grafting variants verified by BLI and surface plasmon resonance (SPR). The positive control pembrolizumab was approved by the FDA in 2014 for use in unresectable or metastatic solid tumors.

molecular structures and interactions over time, providing insights into processes like protein folding and conformational changes. Integrating MD simulations with traditional homology modeling can significantly enhance the precision and efficacy of antibody engineering and development process.

The CDR grafting dataset is characterized by a fixed combination of germlines, whereas the framework shuffling dataset exhibits considerably more diversity. To optimize the CDR grafting process, it is advisable to consider incorporating the top three germlines instead of solely relying on the single best match, unless there is a significant decrease in homology. By employing multiple germline datasets in CDR grafting, there is potential to achieve enhanced results. This approach facilitates a broader exploration of germline diversity, which can improve the efficacy of the humanization process. It also allows for a more comprehensive evaluation of candidate molecules, potentially leading to better outcomes in terms of antibody stability, affinity, and other critical properties. Incorporating multiple germline datasets thus represents a strategic enhancement in optimizing CDR grafting for antibody engineering and therapeutic development.

Both CDR grafting and FR shuffling stand as pivotal methodologies in the humanization of antibodies. While CDR

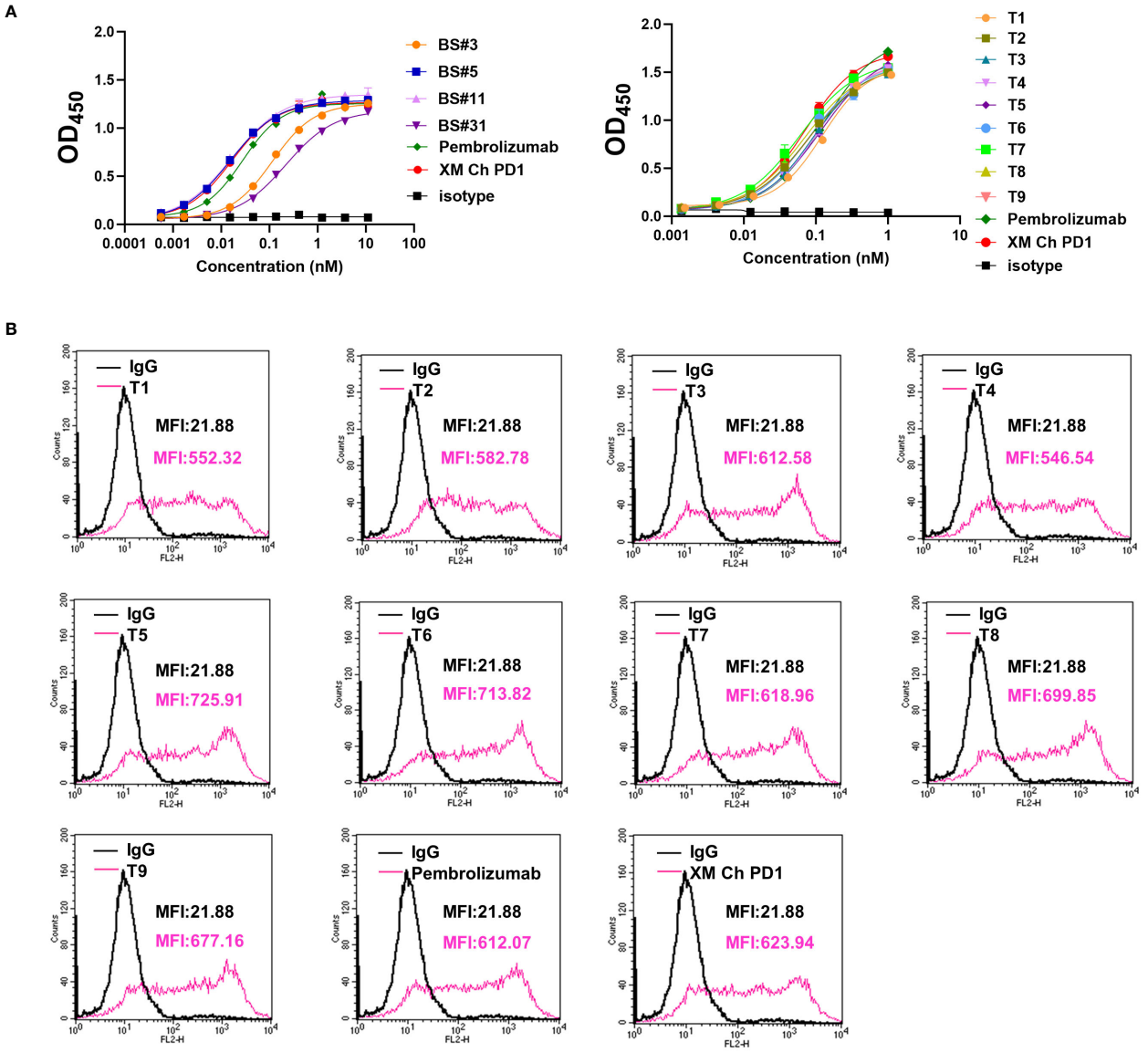

FIGURE 5
The binding properties of FR shuffling antibodies were further analyzed. **(A)** The binding activities of humanized antibodies after heating to PD-1 protein. **(B)** The binding activities of humanized antibodies to PD-1 on the CHO cells. PE-labeled anti-human IgG was used, and the mean fluorescence intensity (MFI) of binding was measured by flow cytometry.

grafting holds a historical precedence in antibody humanization, its efficacy can be hindered by the intricate task of identifying suitable residues for back mutations, a process reliant on precise structural modeling. Moreover, the iterative nature of designing and evaluating variants in CDR grafting can prolong the humanization process. Furthermore, CDR grafting is inherently personalized, with back mutations varying from one antibody to another, thus placing a heavy emphasis on the expertise and experience of the designer. In contrast, the adoption of the FR shuffling method offers a promising avenue to enhance the success rate of antibody humanization. Through the utilization of a highly diverse FR shuffling library, optimal combinations of CDRs and FRs can be selected, thereby increasing the likelihood of retaining affinities. Notably, the comprehensive nature of the FR library, encompassing a wide array of human heavy and light chain germline genes, renders this method applicable across various antibody targets. Illustratively, our laboratory has successfully employed the FR shuffling method in the humanization of antibodies targeting PD-L1 (41) and TIGIT (42), among others. These humanized antibodies have demonstrated satisfactory thermal stabilities, affinities, and biological functionalities underscoring the effectiveness of the FR shuffling approach in antibody engineering.

FR shuffling is particularly accessible to those with a biological rather than computational background, contributing to the growing popularity of humanized techniques in the industry. The insights

10.3389/fimmu.2024.1395854

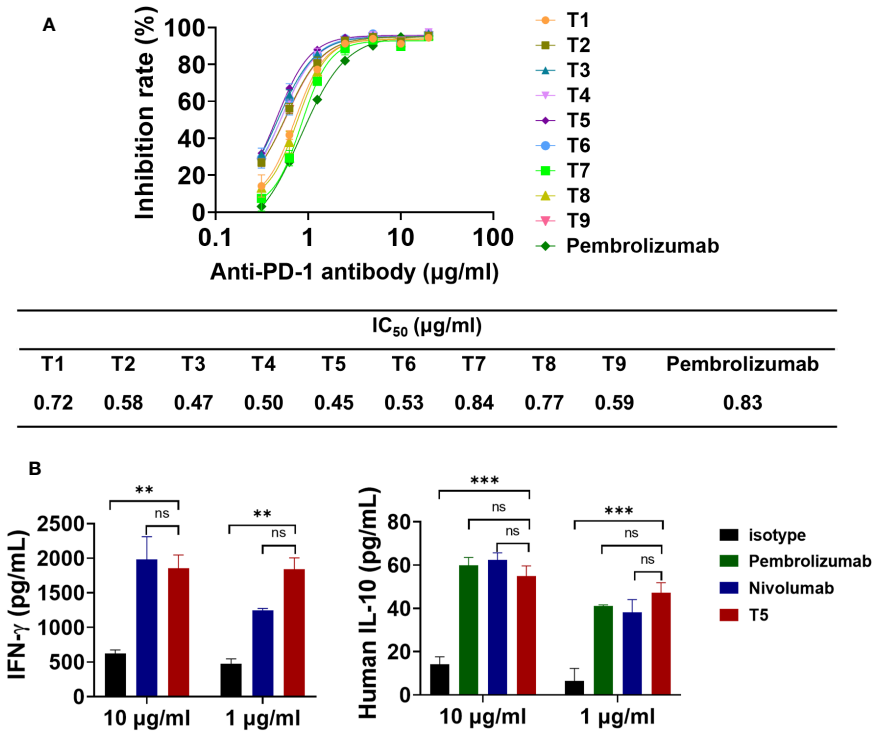

IC_{50} (μg/ml)									
T1	T2	T3	T4	T5	T6	T7	T8	T9	Pembrolizumab
0.72	0.58	0.47	0.50	0.45	0.53	0.84	0.77	0.59	0.83

FIGURE 6
The blocking effects of FR shuffling antibodies on PD-1/PD-L1 interaction. **(A)** The humanized variants of FR shuffling suppressed PD-1/PD-L1 interaction by competitive ELISA. Data are presented as means ± SEM of triple replicates. **(B)** The promising candidate T5 activated T cell responses and induced INF-γ and IL-10 secretion in mixed lymphocyte reaction(MLR) assays. Nivolumab (Opdivo®) was one of the first PD-1 antibodies to receive FDA approval. The data were presented as mean ± SEM and were analyzed by one-way ANOVA. ***P < 0.001, **P < 0.01 were regarded as statistically significant and ns as not significant.

TABLE 4 Humanness prediction *in silico* by OASis Identity and T20.

Antibodies	OASis Identity			T20	
	whole antibody	VH	VL	VH	VL
XM Ch PD-1	59.15%	60.36%	57.84%	69.96%	65.23%
T1	71.36%	73.87%	68.63%	72.82%	75.63%
T2	70.89%	72.97%	68.63%	70.97%	70.68%
T3	71.83%	75.68%	67.65%	82.56%	67.61%
T4	71.83%	74.77%	68.63%	78.61%	68.02%
T5	72.30%	76.58%	67.65%	81.39%	65.95%
T6	69.48%	73.87%	64.71%	77.52%	67.61%
T7	72.30%	76.58%	67.65%	80.84%	67.61%
T8	70.42%	75.68%	64.71%	78.49%	69.73%
T9	72.30%	74.77%	69.61%	82.06%	74.32%
BS3#	72.30%	71.17%	73.53%	75.34%	78.33%
BS5#	69.95%	71.17%	68.63%	75.34%	75.77%
BS11#	70.89%	71.17%	70.59%	75.34%	76.53%
BS31#	72.30%	71.17%	73.53%	75.34%	77.39%

TABLE 5 The potential immunogenicity by predicting the number of strong binders to HLA II alleles.

Alleles	XM PD-1 VH	T5 VH	XM PD-1 VL	T5 VL
DRB1*0101	1	1	0	0
DRB1*0301	1	0	0	0
DRB1*0401	2	1	1	1
DRB1*0405	2	1	2	1
DRB1*0701	0	0	0	0
DRB1*0901	0	0	0	0
DRB1*1101	1	1	0	0
DRB1*1201	0	0	0	0
DRB1*1302	0	0	1	1
DRB1*1501	0	0	1	1
total	7	4	5	4

The HLA II alleles were selected as the most frequent in the general worldwide population according to the literature (34). Each allele has a different frequency in population. The threshold for a strong binder was set at 1% rank in default.

derived from this comparison aim to assist researchers in selecting suitable humanization strategies for drug development, thereby fostering broader application and a deeper understanding of this field.

Data availability statement

The raw data supporting the conclusions of this article will be made available by the authors, without undue reservation.

Ethics statement

Ethical approval was not required for the studies on humans in accordance with the local legislation and institutional requirements because only commercially available established cell lines were used. The study was conducted in accordance with the local legislation and institutional requirements.

Author contributions

YW: Data curation, Formal analysis, Investigation, Methodology, Software, Validation, Visualization, Writing – original draft, Writing – review & editing. Y-LC: Data curation, Formal analysis, Methodology, Software, Validation, Visualization, Writing – review & editing. HX: Data curation, Formal analysis, Methodology, Software, Validation, Visualization, Writing – review & editing. GR: Formal analysis, Visualization, Writing – original draft, Writing – review & editing. XT: Data curation, Formal analysis, Methodology, Software, Validation, Visualization, Writing – review & editing. ZX: Conceptualization, Funding acquisition, Resources, Supervision, Writing – review & editing. MH: Data curation, Formal analysis, Investigation, Methodology, Validation, Visualization, Writing – review & editing. QJ: Data curation, Formal analysis, Methodology, Software, Writing – review & editing. QW: Software, Conceptualization, Funding acquisition, Investigation, Project administration, Resources, Supervision, Writing – review & editing. GW: Formal analysis, Investigation, Writing – original draft, Conceptualization, Funding acquisition, Project administration, Resources, Supervision, Visualization, Writing – review & editing. CW: Funding acquisition, Project administration, Resources, Supervision, Visualization, Writing – review & editing, Conceptualization.

Funding

The author(s) declare financial support was received for the research, authorship, and/or publication of this article. This work was supported by the Key-Area Research and Development Program of Guangdong Province (2022B1111070007), the National Natural Science Foundation of China (81872785 and 32370958), Shanghai Municipal Commission of Science and Technology of China (21S11904500), Major Scientific and Technological Special Project of Zhongshan City (210205143867019), and the CAS Bohai Rim Advanced Research Institute for Drug Discovery Project (LX211005).

Conflict of interest

Author Y-LC was employed by the companies Shanghai Mabstone Biotechnologies, Ltd and Dartsbio Pharmaceuticals Ltd. Author CW was employed by the company Dartsbio Pharmaceuticals Ltd. Author CW received compensation from Dartsbio Pharmaceuticals Ltd. Author QJ was employed by the company Shanghai Genechem Co., Ltd.

The remaining authors declare that the research was conducted in the absence of any commercial or financial relationships that could be construed as a potential conflict of interest.

Publisher's note

All claims expressed in this article are solely those of the authors and do not necessarily represent those of their affiliated organizations, or those of the publisher, the editors and the reviewers. Any product that may be evaluated in this article, or claim that may be made by its manufacturer, is not guaranteed or endorsed by the publisher.

Supplementary material

The Supplementary Material for this article can be found online at: https://www.frontiersin.org/articles/10.3389/fimmu.2024.1395854/full#supplementary-material

References

1. Mullard A. Fda approves 100th monoclonal antibody product. *Nat Rev Drug Discovery*. (2021) 20:491–5. doi: 10.1038/d41573-021-00079-7

2. Weiner GJ. Building better monoclonal antibody-based therapeutics. *Nat Rev Cancer*. (2015) 15:361–70. doi: 10.1038/nrc3930

3. Hwang WY, Foote J. Immunogenicity of engineered antibodies. *Methods*. (2005) 36:3–10. doi: 10.1016/j.ymeth.2005.01.001

4. Cheung NK, Guo H, Hu J, Tassev DV, Cheung IY. Humanizing murine Igg3 anti-Gd2 antibody M3f8 substantially improves antibody-dependent cell-mediated cytotoxicity while retaining targeting *in vivo*. *Oncoimmunology*. (2012) 1:477–86. doi: 10.4161/onci.19864

5. Singh A, Chaudhary S, Agarwal A, Verma AS. Chapter 15 - antibodies: monoclonal and polyclonal. In: Verma AS, Singh A, editors. *Animal Biotechnology*. Academic Press, San Diego (2014). p. 265–87.

6. Almagro JC, Fransson J. Humanization of antibodies. *Front Biosci*. (2008) 13:1619–33. doi: 10.2741/2786

7. Lo BK. Antibody humanization by Cdr grafting. *Methods Mol Biol*. (2004) 248:135–59. doi: 10.1385/1-59259-666-5:135

8. Jones PT, Dear PH, Foote J, Neuberger MS, Winter G. Replacing the complementarity-determining regions in a human antibody with those from a mouse. *Nature*. (1986) 321:522–5. doi: 10.1038/321522a0

9. Riechmann L, Clark M, Waldmann H, Winter G. Reshaping human antibodies for therapy. *Nature*. (1988) 332:323–7. doi: 10.1038/332323a0

10. Verhoeyen M, Milstein C, Winter G. Reshaping human antibodies: grafting an antilysozyme activity. *Science*. (1988) 239:1534–6. doi: 10.1126/science.2451287

11. Pavlinkova G, Colcher D, Booth BJ, Goel A, Wittel UA, Batra SK. Effects of humanization and gene shuffling on immunogenicity and antigen binding of anti-tag-72 single-chain Fvs. *Int J Cancer*. (2001) 94:717–26. doi: 10.1002/(ISSN)1097-0215

12. Lazar GA, Desjarlais JR, Jacinto J, Karki S, Hammond PW. A molecular immunology approach to antibody humanization and functional optimization. *Mol Immunol*. (2007) 44:1986–98. doi: 10.1016/j.molimm.2006.09.029

13. Foote J, Winter G. Antibody framework residues affecting the conformation of the hypervariable loops. *J Mol Biol*. (1992) 224:487–99. doi: 10.1016/0022-2836(92)91010-M

14. Ahmadzadeh V, Farajnia S, Feizi MA, Nejad RA. Antibody humanization methods for development of therapeutic applications. *Monoclon Antib Immunodiagn Immunother*. (2014) 33:67–73. doi: 10.1089/mab.2013.0080

15. Bai Z, Xu M, Mei Y, Hu T, Zhang P, Chen M, et al. Generation of a novel high-affinity antibody binding to Pcsk9 catalytic domain with slow dissociation rate by Cdr-grafting, alanine scanning and saturated site-directed mutagenesis for favorably treating hypercholesterolemia. *Biomedicines*. (2021) 9:1783. doi: 10.3390/biomedicines9121783

16. Dall'Acqua WF, Damschroder MM, Zhang J, Woods RM, Widjaja L, Yu J, et al. Antibody humanization by framework shuffling. *Methods*. (2005) 36:43–60. doi: 10.1016/j.ymeth.2005.01.005

17. Damschroder MM, Widjaja L, Gill PS, Krasnoperov V, Jiang W, Dall'Acqua WF, et al. Framework shuffling of antibodies to reduce immunogenicity and manipulate functional and biophysical properties. *Mol Immunol*. (2007) 44:3049–60. doi: 10.1016/j.molimm.2006.12.019

18. Chu W, Xu H, Wang Y, Xie Y, Chen YL, Tan X, et al. Her2/Pd1 bispecific antibody in Igg4 subclass with superior anti-tumour activities. *Clin Transl Med*. (2022) 12:e791. doi: 10.1002/ctm2.791

19. Wu H. Simultaneous humanization and affinity optimization of monoclonal antibodies. In: Welschof M, Krauss J, editors. *Recombinant Antibodies for Cancer Therapy: Methods and Protocols*. Humana Press, Totowa, NJ (2003). p. 197–212.

20. Wu H, An L-L. Tailoring kinetics of antibodies using focused combinatorial libraries. In: Welschof M, Krauss J, editors. *Recombinant Antibodies for Cancer Therapy: Methods and Protocols*. Humana Press, Totowa, NJ (2003). p. 213–33.

21. Prihoda D, Maamary J, Waight A, Juan V, Fayadat-Dilman L, Svozil D, et al. Biophi: A platform for antibody design, humanization, and humanness evaluation based on natural antibody repertoires and deep learning. *MAbs*. (2022) 14:2020203. doi: 10.1080/19420862.2021.2020203

22. Gao SH, Huang K, Tu H, Adler AS. Monoclonal antibody humanness score and its applications. *BMC Biotechnol*. (2013) 13:55. doi: 10.1186/1472-6750-13-55

23. Huang J, MacKerell AD Jr. Charmm36 all-atom additive protein force field: validation based on comparison to Nmr data. *J Comput Chem*. (2013) 34:2135–45. doi: 10.1002/jcc.23354

24. Izadi S, Anandakrishnan R, Onufriev AV. Building water models: A different approach. *J Phys Chem Lett*. (2014) 5:3863–71. doi: 10.1021/jz501780a

25. Sun F, Wang T, Jiang J, Wang Y, Ma Z, Li Z, et al. Engineering a high-affinity humanized anti-Cd24 antibody to target hepatocellular carcinoma by a novel Cdr grafting design. *Oncotarget*. (2017) 8:51238–52. doi: 10.18632/oncotarget.v8i31

26. Leem J, Dunbar J, Georges G, Shi J, Deane CM. Abodybuilder: automated antibody structure prediction with data-driven accuracy estimation. *MAbs*. (2016) 8:1259–68. doi: 10.1080/19420862.2016.1205773

27. Abanades B, Wong WK, Boyles F, Georges G, Bujotzek A, Deane CM. Immunebuilder: deep-learning models for predicting the structures of immune proteins. *Commun Biol*. (2023) 6:575. doi: 10.1038/s42003-023-04927-7

28. Qin K, Shi W, Zhao L, Li M, Tang Y, Faridoon, et al. Thermostability detection and optimization of glycoengineered antibodies and antibody-drug conjugates based on differential scanning flouremitry analysis. *Bioorganic Chem*. (2020) 94:103391. doi: 10.1016/j.bioorg.2019.103391

29. Abdiche Y, Malashock D, Pinkerton A, Pons J. Determining kinetics and affinities of protein interactions using a parallel real-time label-free biosensor, the octet. *Anal Biochem*. (2008) 377:209–17. doi: 10.1016/j.ab.2008.03.035

30. Abbas A, Linman MJ, Cheng Q. New trends in instrumental design for surface plasmon resonance-based biosensors. *Biosens Bioelectron*. (2011) 26:1815–24. doi: 10.1016/j.bios.2010.09.030

31. Kim JH, Kim YS, Kim TI, Li W, Mun JG, Jeon HD, et al. Unripe black raspberry (*Rubus coreanus* Miquel) extract and its constitute, ellagic acid induces T cell activation and antitumor immunity by blocking PD-1/PD-L1 interaction. *Foods*. (2020) 9 (11):1590. doi: 10.3390/foods9111590

32. Phakham T, Bulaon CJI, Khorattanakulchai N, Shanmugaraj B, Buranapraditkun S, Boonkrai C, et al. Functional characterization of pembrolizumab produced in Nicotiana benthamiana using a rapid transient expression system. *Front Plant Sci*. (2021) 12:736299. doi: 10.3389/fpls.2021.736299

33. Greenbaum J, Sidney J, Chung J, Brander C, Peters B, Sette A. Functional classification of class ii human leukocyte antigen (Hla) molecules reveals seven different supertypes and a surprising degree of repertoire sharing across supertypes. *Immunogenetics*. (2011) 63:325–35. doi: 10.1007/s00251-011-0513-0

34. Paul S, Lindestam Arlehamn CS, Scriba TJ, Dillon MB, Oseroff C, Hinz D, et al. Development and validation of a broad scheme for prediction of Hla class ii restricted T cell epitopes. *J Immunol Methods*. (2015) 422:28–34. doi: 10.1016/j.jim.2015.03.022

35. Rosenberg AS. Effects of protein aggregates: an immunologic perspective. *AAPS J*. (2006) 8:E501–7. doi: 10.1208/aapsj080359

36. Braun A, Kwee L, Labow MA, Alsenz J. Protein aggregates seem to play a key role among the parameters influencing the antigenicity of interferon alpha (Ifn-alpha) in normal and transgenic mice. *Pharm Res*. (1997) 14:1472–8. doi: 10.1023/A:1012193326789

37. Chennamsetty N, Voynov V, Kayser V, Helk B, Trout BL. Design of therapeutic proteins with enhanced stability. *Proc Natl Acad Sci*. (2009) 106:11937–42. doi: 10.1073/pnas.0904191106

38. Mehta SB, Bee JS, Randolph TW. Carpenter JF. Partial unfolding of a monoclonal antibody: role of a single domain in driving protein aggregation. *Biochemistry*. (2014) 53:3367–77. doi: 10.1021/bi5002163

39. Reynisson B, Alvarez B, Paul S, Peters B, Nielsen M. Netmhcpan-4.1 and netmhciipan-4.0: improved predictions of Mhc antigen presentation by concurrent motif deconvolution and integration of Ms Mhc eluted ligand data. *Nucleic Acids Res*. (2020) 48:W449–w54. doi: 10.1093/nar/gkaa379

40. Reynisson B, Barra C, Kaabinejadian S, Hildebrand WH, Peters B, Nielsen M. Improved prediction of mhc ii antigen presentation through integration and motif deconvolution of mass spectrometry mhc eluted ligand data. *J Proteome Res*. (2020) 19:2304–15. doi: 10.1021/acs.jproteome.9b00874

41. Li HY, Chen YL, Deng XN, Li HH, Tan J, Liu GJ, et al. Bispecific antibody targeting both B7-H3 and Pd-L1 exhibits superior antitumor activities. *Acta Pharmacol Sin*. (2023) 44:2322–30. doi: 10.1038/s41401-023-01118-2

42. Mu S, Liang Z, Wang Y, Chu W, Chen YL, Wang Q, et al. Pd-L1/tigit bispecific antibody showed survival advantage in animal model. *Clin Transl Med*. (2022) 12:e754. doi: 10.1002/ctm2.754

frontiers | Frontiers in Immunology

TYPE Original Research
PUBLISHED 20 August 2024
DOI 10.3389/fimmu.2024.1406804

OPEN ACCESS

EDITED BY
Urban Švajger,
Blood Transfusion Centre of Slovenia, Slovenia

REVIEWED BY
Miguel Alvaro-Benito,
Free University of Berlin, Germany
Li-Tzu Wang,
National Taiwan University, Taiwan

*CORRESPONDENCE
Céline Marban-Doran
celine.marban-doran@roche.com

†These authors have contributed equally to this work and share senior authorship

RECEIVED 15 April 2024
ACCEPTED 12 July 2024
PUBLISHED 20 August 2024

CITATION
Siegel M, Padamsey A, Bolender A-L, Hargreaves P, Fraidling J, Ducret A, Hartman K, Looney CM, Bertinetti-Lapatki C, Rohr O, Hickling TP, Kraft TE and Marban-Doran C (2024) Development and characterization of dendritic cell internalization and activation assays contributing to the immunogenicity risk evaluation of biotherapeutics.
Front. Immunol. 15:1406804.
doi: 10.3389/fimmu.2024.1406804

Development and characterization of dendritic cell internalization and activation assays contributing to the immunogenicity risk evaluation of biotherapeutics

Michel Siegel[1], Aman Padamsey[2], Anna-Lena Bolender[2], Patrick Hargreaves[1], Johannes Fraidling[2], Axel Ducret[1], Katharina Hartman[1], Cary M. Looney[1], Cristina Bertinetti-Lapatki[1], Olivier Rohr[3,4], Timothy P. Hickling[1], Thomas E. Kraft[2†] and Céline Marban-Doran[1*†]

[1]Roche Pharmaceutical Research and Early Development, Pharmaceutical Sciences, Roche Innovation Center Basel, Basel, Switzerland, [2]Roche Pharmaceutical Research and Early Development, Pharmaceutical Sciences, Roche Innovation Center Penzberg, Penzberg, Germany, [3]University of Strasbourg, UPR CNRS 9002 ARN, IUT Louis Pasteur, Schiltigheim, France, [4]Institut Universitaire de Technologie Louis Pasteur, Université de Strasbourg, Schiltigheim, France

Introduction: Immunogenicity refers to the ability of a substance, such as a therapeutic drug, to elicit an immune response. While beneficial in vaccine development, undesirable immunogenicity can compromise the safety and efficacy of therapeutic proteins by inducing anti-drug antibodies (ADAs). These ADAs can reduce drug bioavailability and alter pharmacokinetics, necessitating comprehensive immunogenicity risk assessments starting at early stages of drug development. Given the complexity of immunogenicity, an integrated approach is essential, as no single assay can universally recapitulate the immune response leading to the formation of anti-drug antibodies.

Methods: To better understand the Dendritic Cell (DC) contribution to immunogenicity, we developed two flow cytometry-based assays: the DC internalization assay and the DC activation assay. Monocyte-derived dendritic cells (moDCs) were generated from peripheral blood mononuclear cells (PBMCs) and differentiated over a five-day period. The internalization assay measured the accumulation rate of therapeutic antibodies within moDCs, while the activation assay assessed the expression of DC activation markers such as CD40, CD80, CD86, CD83, and DC-SIGN (CD209). To characterize these two assays further, we used a set of marketed therapeutic antibodies.

Results: The study highlights that moDCs differentiated for 5 days from freshly isolated monocytes were more prone to respond to external stimuli. The internalization assay has been shown to be highly sensitive to the molecule tested, allowing the use of only 4 donors to detect small but significant differences. We also demonstrated that therapeutic antibodies were efficiently taken up by moDCs, with a strong correlation with their peptide presentation on MHC-II. On the other hand, by monitoring DC activation through a limited set of activation markers including CD40, CD83, and DC-SIGN, the DC activation assay has the potential to compare a series of compounds. These two assays provide a more comprehensive

understanding of DC function in the context of immunogenicity, highlighting the importance of both internalization and activation processes in ADA development.

Discussion: The DC internalization and activation assays described here address key gaps in existing immunogenicity assessment methods by providing specific and reliable measures of DC function. The assays enhance our ability to pre-clinically evaluate the immunogenic potential of biotherapeutics, thereby improving their safety and efficacy. Future work should focus on further validating these assays and integrating them into a holistic immunogenicity risk assessment framework.

KEYWORDS

immunogenicity, immunomodulation, biotherapeutics, dendritic cells, assay development

Introduction

Immunogenicity, defined here as the propensity of a substance to elicit an immune response, is a double-edged sword in the realm of biomedicine. While immunogenicity can be desirable in some contexts, such as vaccine development, undesirable immunogenicity can negatively impact the safety and efficacy of biotherapeutics. Anti-drug antibodies (ADAs) can compromise the therapeutic efficacy and safety by diminishing drug bioavailability or altering its pharmacokinetic profile. It is therefore critical to assess the immunogenic potential of biotherapeutics during their early development stages.

The complexity of immunogenicity necessitates a multifaceted assessment approach, as no single assay can universally predict the immunogenic response to protein therapeutics. This has been acknowledged by experts who recognize the limitations of current preclinical tools in forecasting clinical immunogenicity (1). A holistic strategy that interrogates various aspects of the immune system may improve the predictability of clinical outcomes and foster the development of safer, more efficacious treatments.

ADA production is triggered by a cascade of immunological events initiated by antigen (Ag) uptake by professional antigen-presenting cells (APCs), particularly dendritic cells (DCs). These cells process the internalized Ag and display peptide fragments as peptide-MHC-II (pMHC-II) complexes on their surface. T cells that recognize these complexes, along with receiving additional co-stimulatory signals, can trigger B cell activation and maturation into plasmablasts and plasma cells, which then secrete ADAs. Given the pivotal role of DCs in this process, assays such as MHC-II Associated Peptide Proteomics (MAPPs) are frequently employed in drug development to evaluate their capacity to present drug-derived peptides (2). However, other aspects of DC biology, such as antigen internalization and activation, are less explored. This is despite their importance in ADA development, recognized by studies like those by Xue et al. (3) and others focusing on protein aggregates (4, 5).

In this manuscript, we present a novel *in vitro* approach to quantify the internalization of therapeutic antibodies by monocyte-derived dendritic cells (moDCs) and to assess their subsequent activation, which is a prerequisite for an immunogenic response. Activation markers such as CD40, B7 (CD80, CD86), CD83, DC-SIGN (CD209), and HLA-DR are commonly used as indicators of the status of DC activation (6–8). Despite the challenges in detecting moDC activation by non-aggregated, monomeric antibodies, recent advancements have been made (9) building on this progress, we present novel techniques for assessing antibody internalization and DC activation, providing a more comprehensive assessment of the risk for immunogenicity. The characterization of these methods highlights the critical role of DCs in initiating immunogenic responses, one that is of high relevance in the development of biotherapeutics (10).

Results

Development and characterization of a DC activation assay

Activation, internalization, processing and presentation of biotherapeutics into antigen presenting cells (APCs) are the first step in the immunogenic response to protein based therapeutics. We therefore used moDCs as APCs to look into their activation status, their propensity to internalize therapeutic antibodies and to present drug-derived T cell epitopes. The workflow of the three immunogenicity assays used in the present manuscript are depicted in Figure 1.

Numerous protocols for differentiating monocytes into moDCs *in vitro* have been documented in the literature (11). Drawing from our experience and the internal use of moDCs in the MAPPs assay (2), we chose a five-day differentiation period as our initial approach for cell generation, as it has been published that this timeframe is

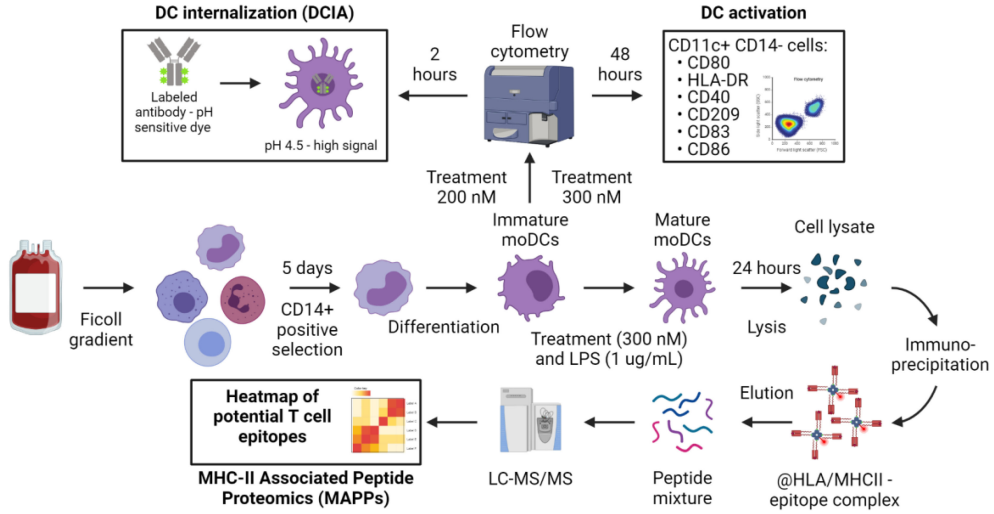

FIGURE 1
Overview of the experimental procedure to assess the contribution of dendritic cells to immunogenicity. The common starting point of the assays is the PBMC isolation according to standard protocols. CD14+ cells isolation and differentiation into immature moDCs are also shared between the procedures. Immature moDCs are challenged with the treatment as described in Material and Methods for the DC internalization and DC activation assays. Matured moDCs are used for MHC-II Associated Peptide Proteomics (MAPPs).

sufficient to differenciate CD14+ cells into moDCs. To ensure optimal moDC phenotype on the day of antigen challenge with the antibody, we compared this differentiation protocol to a shorter version of 3 days published recently (9). The assessment was conducted using flow cytometry, as detailed in the Materials and Methods section. In summary, cells were selected based on singlets, morphology, and viability. We then measured the Mean Fluorescence Intensities (MFI) for HLA-DR and CD209 and the percentage of positive cells for other activation markers (CD80, CD86, CD83, and CD40) on viable CD11c+ CD14- cells (Figure 2A).

The assay was initially evaluated for its sensitivity to lipopolysaccharide (LPS) treatment, which is known to activate moDCs through the TLR-4 signaling pathway (Supplementary Figure 1A). The panel of activation markers we examined (HLA-DR, CD40, CD86, CD83, CD209, and CD80) exhibited similar responses under both differentiation protocols (3 versus 5 days). Notably, all markers were upregulated in a dose-dependent manner, with the exception of CD209, which was downregulated as anticipated (Supplementary Figure 1B). However, since LPS induces activation of moDCs through receptor-mediated pathways, we also tested keyhole limpet hemocyanin (KLH), an antigen that does not engage with specific surface receptors on moDCs (Figure 2B) and is expected to therefore activate comparable pathways to those activated by drug internalization. The moDC response to KLH was less pronounced than to LPS, allowing us to more clearly discern the nuances in response dynamics. moDCs demonstrated an upregulation of all markers to KLH following 5 day period of differentiation, with the sole exception being the downregulation of CD209. Another critical factor was the origin of the monocytes. We observed significant differences in moDC responsiveness to KLH when comparing moDCs derived from freshly isolated peripheral blood mononuclear cells (PBMCs) with those derived from frozen PBMCs (Figure 2C). Indeed, the median SI for CD40 increased approximately by 4-fold while for CD80, CD83, CD86 it increased by 1.1, 1.3 and 2 respectively. Consequently, we recommend using freshly isolated PBMCs and employing the response to KLH as a positive control to verify cell viability and functionality.

The parameters for the assay as mentioned above were used to qualify the DC activation assay using a set of commercially available therapeutic antibodies (Figure 3).

None of the tested therapeutic antibodies significantly affected the phenotype of the moDC, with the exception of CD209 expression, which was increased (15% increase above medium-treated control) by the TNFα targeted antibodies adalimumab and infliximab. We observed a similar, albeit non-significant (when compared to the medium treated control) increase in CD40 expression following treatment with the PCSK9 targeting antibodies alirocumab and evolocumab, but not for bococizumab. Of note, this observation might be a consequence of a decreased expression of CD40 following bococizumab challenge.

Development and characterization of a DC internalization assay

In addition to providing a costimulation signal to T cells, APCs should ensure the specificity of the response by presenting an epitope derived from the antigen, which starts with its internalization into APCs. Measurement of the cellular accumulation of drug candidates in a meaningful way during preclinical development of therapeutic antibodies could therefore improve the understanding of their immunogenicity risk and aid in the selection and engineering of a clinical lead molecule. We therefore developed an assay to measure the internalization and

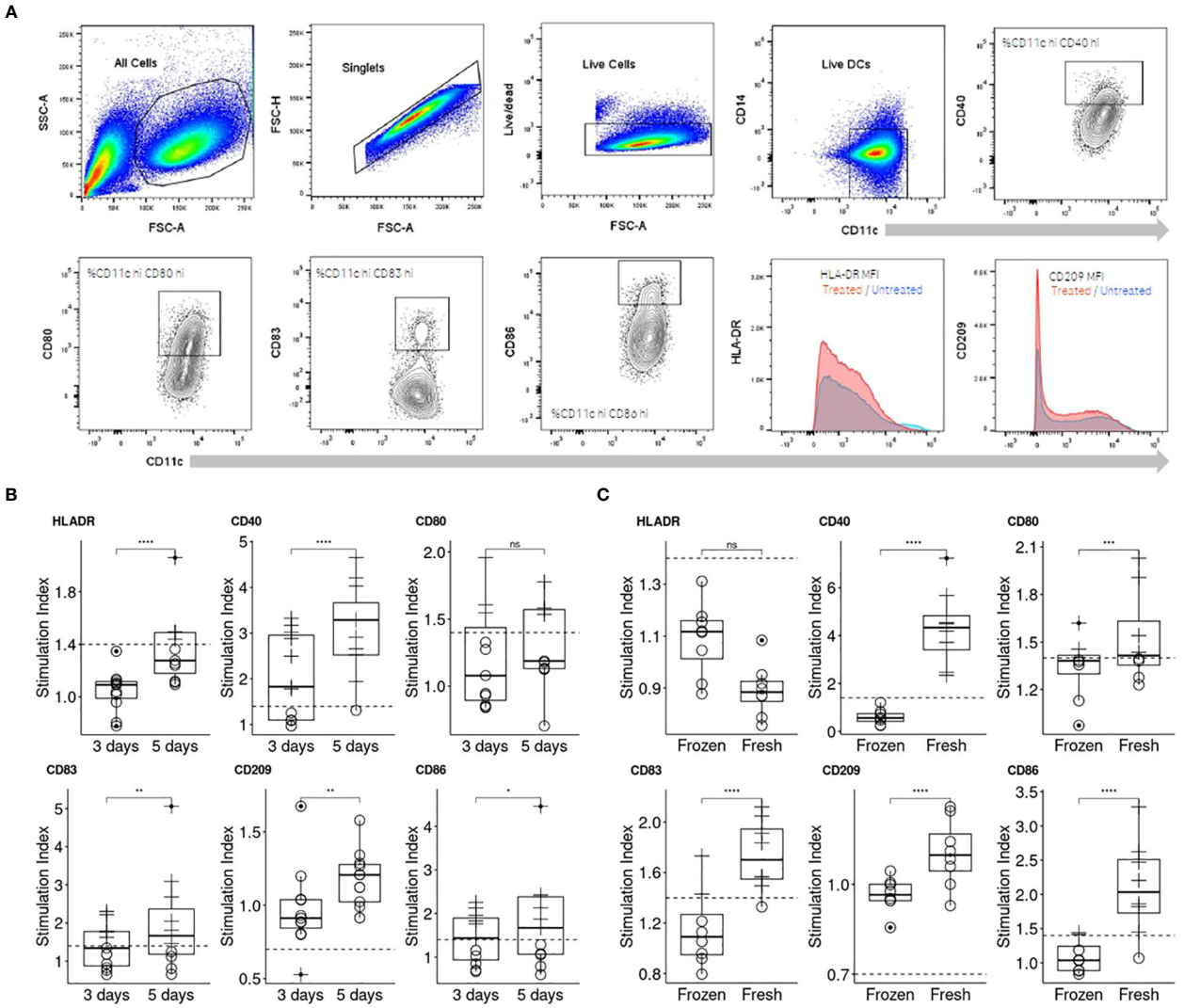

FIGURE 2
Comparison of two moDC differentiation durations and cell sources on their response to KLH. **(A)** Representation of the flow cytometry gating strategy applied for the assessment of DC activation. **(B)** Three days of differentiation was compared to an extended differentiation of five days by assessing the moDC response to KLH (n=10). Individual moDCs SI were calculated (see Material and Methods, "Data analysis" section for more information) and a plot per activation marker generated. **(C)** Freshly isolated and frozen PBMCs were compared for their ability to respond to KLH (n=8). To compare the differentiation periods and the PBMC source, one-sided paired t test for each activation marker were performed (p< 0.0001****; p< 0.001***; p< 0.01**; p< 0.05*; not significant, ns).

accumulation rate of mAbs in human moDCs. We first labeled antibodies with a pH-sensitive fluorophore, site directed to their Fc glycosylation; this avoids the alteration of biophysical and target binding properties, as no amino acid is modified. We then incubated these labeled mAbs with moDCs and determined the relative amount of accumulated antibody through FACS measurement and normalization to dosing solution fluorescence. The fluorophore shows low to no fluorescence at physiological pH outside the cell and an 50-100 fold increase in fluorescence intensity at acidic pH, found in the late endosome and lysosome (details can be found in Figure 1 and in the material and methods section together with the Equations 1, 2).

A set of 8 commercially available therapeutic antibodies comprised of ixekizumab, alirocumab, evolocumab, bevacizumab, briakinumab, adalimumab, bococizumab, and ATR-107, as well as two additional internal control mAbs (var1 and var112, with IgG typical and high internalization rates respectively) (12), were tested to evaluate the performance of the DCIA and to better understand properties that could influence internalization.

ATR-107 and bococizumab showed significantly higher DC internalization as compared to var1, the internal control. This was also observed to a lesser extent for adalimumab and briakinumab. The other benchmark molecules (alirocumab, evolocumab and bevacizumab) were internalized at a similar rate as the internal control, while ixekizumab showed a significantly lower internalization rate.

The rate of compound internalization, as calculated by dividing the mean fluorescent intensity by the incubation time, varied by donor as well as between the different compounds (Figure 4A). Since our goal was to capture compound specific differences in

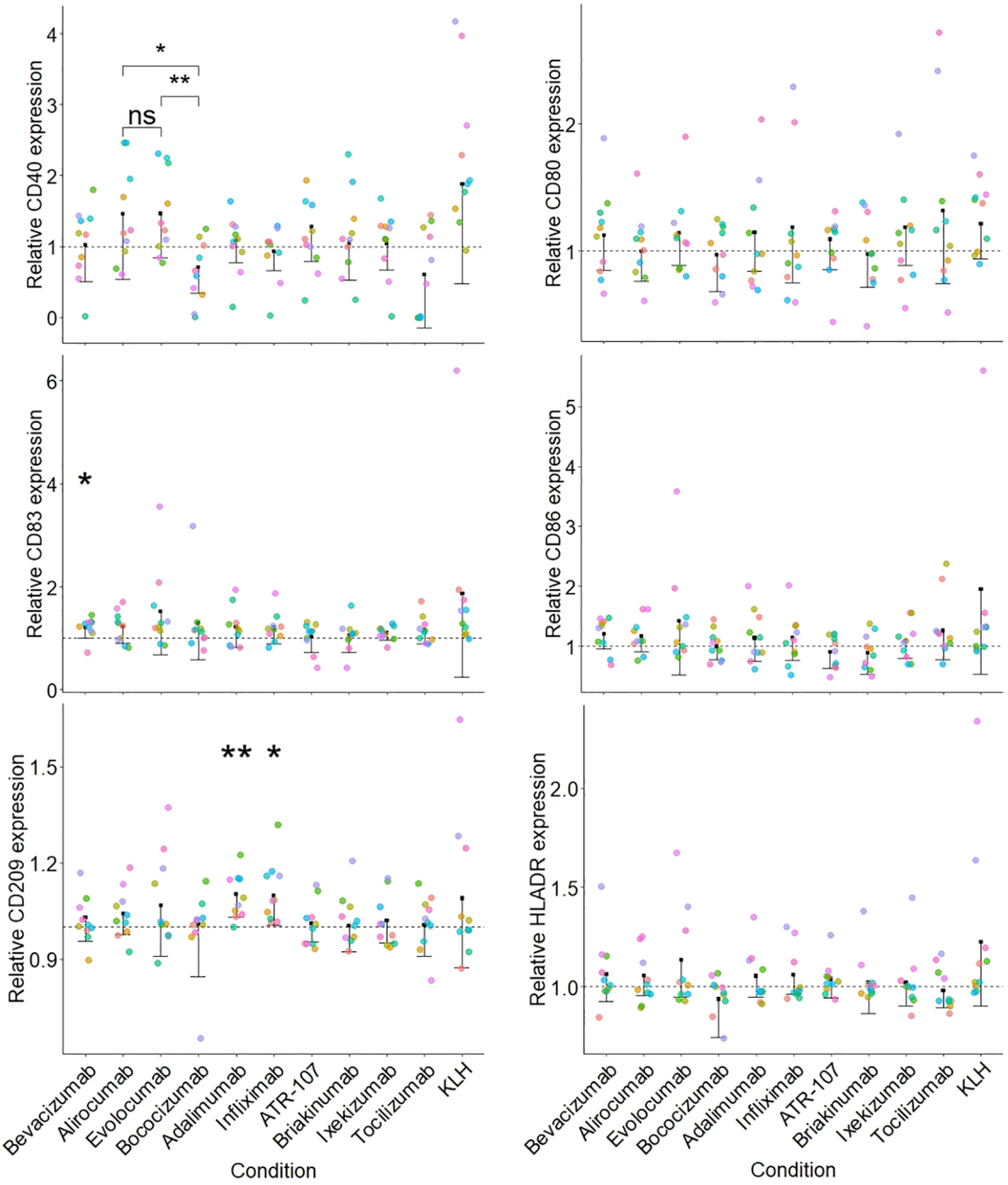

FIGURE 3
Activation of moDCs by a set of therapeutic antibodies. Each sub-figure represents the stimulation index (SI) for a particular surface marker and the dotted line corresponds to 1 (value for the medium treated condition). The SI was calculated for each donor/surface marker pair using the corresponding medium treated control as described in the Material and Methods section. Each individual donor tested is indicated by a different color (n=10) and a one-sided paired t test was applied for the comparison of antibodies against the medium treated control (p< 0.01**; p< 0.05*) displayed along with a one-sided confidence interval (level = 0.95). Additionally, a paired one-sided t test between the PCSK9 targeting antibodies (alirocumab, evolocumab and bococizumab) was performed (p< 0.01**; p< 0.05*; not significant, ns).

internalization in order to rank drug candidates within a series and to flag high internalization molecules, the inter-donor variability was controlled for by normalizing the slope of each test antibody for each donor with the slope of our internal control var1 (untargeted IgG1) measured in the same donor, thus yielding relative internalization rates (Figure 4B). On performing a Variance Component Analysis, it was shown that this method of normalization almost completely accounted for donor specific variance (Figure 4C and Supplementary Table 1). The normalization procedure reduces donor based variance from ~31% to 0%, suggesting that the residual variance was compound-specific. This inter-donor baseline correction also allows us to detect smaller differences between compounds, with high statistical significance.

For routine use of the DCIA, we aim to reduce the number of donors to optimize throughput, save resources, and decrease time and cost. This reduction still enables the detection of large enough differences between compounds to be useful in informing decisions regarding immunogenicity risk and compound ranking, as

10.3389/fimmu.2024.1406804

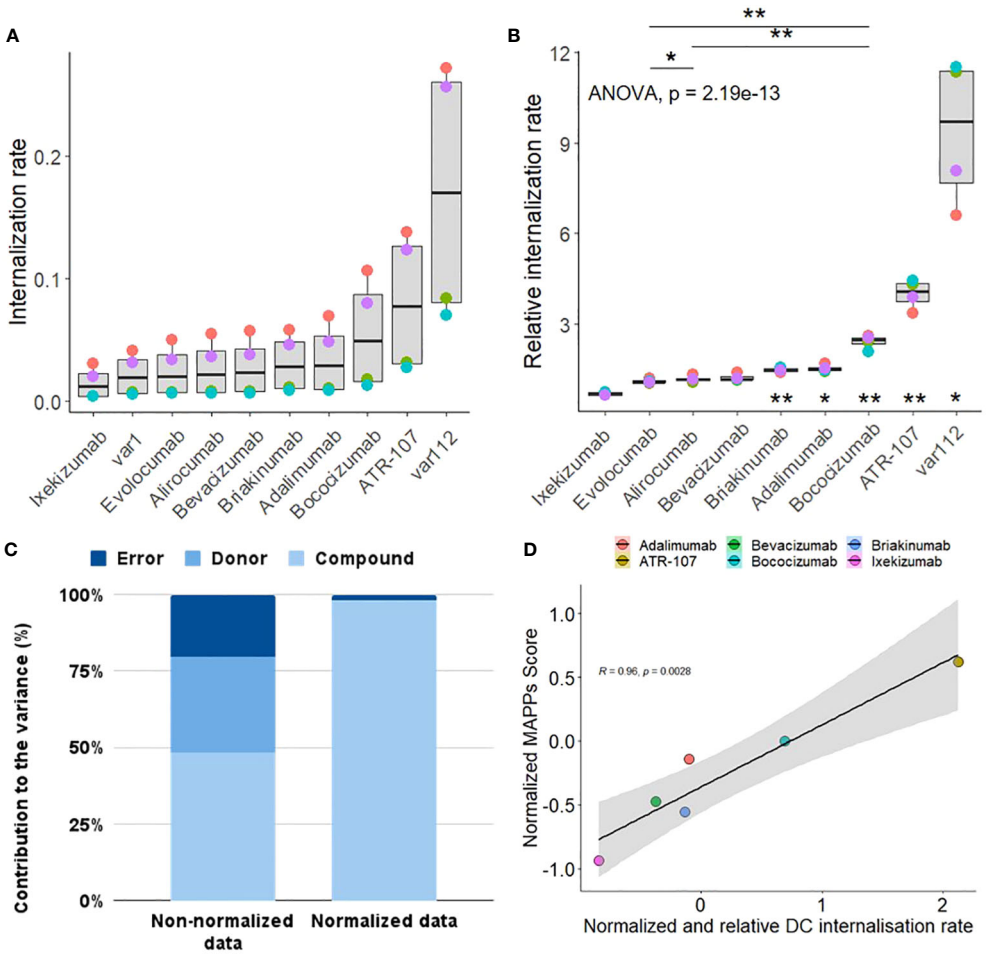

FIGURE 4
Characterization Qualification of DC internalization assay. **(A)** The internalization rate represents the internalization efficiency as calculated by the slope of the mean fluorescence intensity (MFI) values of antibodies coupled to a pH sensitive fluorophore into the acidic lysosome of CD11c+ moDCs from 4 human healthy blood donors (color coded) at 120 min, normalized to the fluorescence of the antibody dosing solution to account for differences in labeling efficiency between antibodies. **(B)** The relative internalization rate uses the slope of an internal control antibody to normalize the donor specific internalization rate (according to the Material and Methods section). A one-sided paired t-test was applied for the comparison of antibodies sharing the same target (displayed at the top, p< 0.01**; p< 0.05*). A one sample two-sided paired T-test between each group (antibody) and the internal control antibody has been performed (corrected for multiple testing, displayed at the bottom, p< 0.01**; p< 0.05*). **(C)** Comparison of the contribution of donor, compound and residual error on the total variance for the non-normalized **(A)** vs normalized internalization data **(B)**. **(D)** Correlation plot between the normalized MAPPs score (see Material and Methods for the equation used and Supplementary Figure 3 for the heatmap of the detected peptide clusters) and the normalized and relative (to var1) DC internalization rate. Normalization for each treatment has been achieved by subtracting the corresponding assay dataset mean and dividing it by the corresponding standard deviation.

immunogenicity risk is only one of several factors defining a successful clinical lead molecule, and internalization is only one of several contributing factors for immunogenicity risk (12). We therefore decided on a minimum effect size of 2, based on internal experience with the assay, to be able to capture large, relevant differences between internalization rates of compounds and used a power analysis to determine a suitable sample size of 4 donors (Supplementary Figure 2).

Additionally, we explored the relevance of the observations made about the cellular accumulation rates for the therapeutic antibodies tested by comparing it to the outcome of a well-established assay, the MHC-II Associated Peptide Proteomics (MAPPs, Supplementary Figure 3). The set of therapeutic antibodies tested, in both the DCIA and MAPPs, exhibited a wide range of risk for immunogenicity. Interestingly, our results revealed a linear correlation between the cellular accumulation of these antibodies and their presentation by Major Histocompatibility Complex class II (MHC-II) molecules (Figure 4D). This correlation suggests that the extent to which an antibody accumulates within cells may be predictive of its ability to be processed and presented as peptides on MHC-II, a key step in the activation of the adaptive immune response.

Discussion

The studies presented here focus on enhancing our understanding of the mechanisms underlying clinical immunogenicity in response to

therapeutic antibodies. This can be achieved by focusing on the early stages of the immunogenic response that leads to the development of anti-drug antibodies (ADAs), specifically the internalization and presentation of antigens by dendritic cells and their activation.

The differentiation of moDCs was found to be critically dependent on both the presence and incubation conditions of IL-4, as previously reported (11). This finding reinforces the importance of standardizing differentiation protocols to ensure reproducibility and reliability in moDC-based assays. The use of serum-free media was a key factor in minimizing assay variability, given the complex and potentially variable composition of serum, and the potential uptake of serum proteins by moDCs that could interfere with the assay, as noted by Sauter et al. (13). Furthermore, our choice of ultra-low binding surfaces was based both on past experience and literature, as their use did not impair the T cell activation capacity of moDCs (13), suggesting that these surfaces are suitable for culturing cells in the context of our assays. The exclusion of LPS as a co-treatment was based on the understanding that DC maturation and/or activation could inhibit macropinocytosis, possibly confounding assay results (14, 15). This decision highlights the need to carefully consider the addition of maturation agents in assays designed to measure antigen uptake and processing.

Using the optimized protocol for moDCs differentiation, we propose an improved method for the dendritic cell (DC) activation assay with increased specificity and applicability. Here, we evaluated the ability of different therapeutic antibodies to modulate the expression of various activation markers on moDCs. Our data suggest that CD209 and CD40 are the most informative markers for assessing DC activation and should be prioritized in the assay panel. Additionally, while HLA-DR expression is more reflective of inter-donor variability than a direct response to treatment, its inclusion may remain important for capturing individual immune response differences. To streamline the assay and reduce redundancy, we recommend selecting a single co-stimulatory molecule—either CD83, CD86, or CD80—as all three have shown similar degrees of activation in the assay. For assay characterization qualification and consistency, Keyhole Limpet Hemocyanin (KLH) should be incorporated as a positive control, given its greater relevance to the tested mechanisms versus a receptor-mediated activation agent such as LPS. Finally, the inclusion of relevant comparator (e.g. sequence variants, antibody with the same target allows for a more meaningful analysis of DC activation potential.

The results of our study underscore the complex interplay between cell culture conditions, antibody characteristics, and assay protocols in influencing the phenotype and function of moDCs, with direct implications for testing the *in vivo* immunogenicity potential of therapeutic antibodies.

In addition to optimized cell culture conditions, the right assay setup and optimal controls are crucial for generating meaningful data, as shown by the use of internal antibody controls. By normalizing the cellular accumulation rate of each test compound to the rate of the negative control, we substantially reduced the donor contribution to the total variance, highlighting compound-specific differences. This is particularly important when comparing compounds.

Cellular accumulation in APCs is only one of several mechanisms that potentially contributes to the risk of immunogenicity for a therapeutic antibody. Furthermore, other parameters, like potency, pharmacokinetics and technical developability also need to be taken into account when selecting a suitable clinical lead. Therefore, the ability to measure significantly large differences between compounds regarding their DC cellular accumulation rate can be seen as a key first step for clinical lead selection.

The number of healthy donor samples required for investigating DC internalization was determined by the calculation of the effect size according to the sample size. The effect size, which indicates practical significance, was used instead of relying solely on statistical significance (p-values), which can be misleading due to its dependence on sample size. An effect size value of 2 (Cohen's D factor >0.8 considered as large), was observed with a sample size of 4 healthy donors. This suggests that 4 samples are sufficient to detect a meaningful difference in DC internalization rates using a paired t-test. The results of a power analysis in combination with the reduction in donor and residual error by normalization enabled us to increase the throughput and number of test compounds per assay run compared to other preclinical immunogenicity assays requiring between 13-30 donors (16, 17). In addition, we recommend an internal negative control for normalization; while we used var1 in this study, bevacizumab would be a potential alternative, given its low cellular accumulation in the DCIA. Similarly, while we used var112 as a positive control, bococizumab or ATR-107 could be used as a positive control, according to our results.

Antibody characteristics such as surface charges, FcRn binding, and glycosylation patterns were shown to have significant effects on the internalization and activation of moDCs (18, 19). The increased internalization of bococizumab, which exhibits a positive surface charge patch (20) and the occurrence of ADAs in 50% of patients within a year of treatment (21) compared to other PCSK9 targeting antibodies, suggests that charge interactions may enhance uptake by moDCs and potentially increase the risk of immunogenicity. The role of target binding in antibody uptake was exemplified by the TNF-α targeting antibody adalimumab, which showed increased cellular accumulation, potentially leading to DC activation and increased immunogenicity (22, 23). The TNFα-targeting antibodies adalimumab and infliximab also showed an increased expression of C-type lectin receptors (CD209/DC-SIGN) on moDCs, a molecule associated with increased presentation on DCs. Furthermore, this assay enables the comparison of molecules sharing the same target such as evolocumab, alirocumab and bococizumab, all three targeting PCSK9. The reduced expression of CD40 observed after treatment with bococizumab, compared to evolocumab and alirocumab, could result from a less mature phenotype of the moDCs. This may be a consequence of the higher cellular accumulation of bococizumab compared to evolocumab and alirocumab, and potentially account for a more efficient internalization into DCs.

The impact of antibody formulation on DC uptake and activation by such antibody-independent considerations as

aggregation and their subsequent effect on immunogenicity also must be considered. Aggregates can profoundly influence antibody internalization and moDC activation, as demonstrated by the historical use of DC activation assays to describe the immunogenicity of antibody aggregates (24). This is particularly relevant to bococizumab and ATR-107, which were not evaluated in this context with their clinical formulation and concentration.

Immunogenicity is influenced by a multitude of factors, one of which is the efficacy of synapse formation between T lymphocytes and DCs. This interaction is enhanced when DCs display a high density of peptide epitopes on their surface, increasing the avidity of TCR/MHC interactions (25). Considering the observed positive correlation between the DCIA and MAPPs data, an increased internalization of antigens by DCs may lead to a more abundant presentation of epitopes, potentially indicating a higher risk of immunogenicity.

The production of ADAs is influenced by a wide range of risk factors, including those related to the product, the treatment regimen, and the patient population, thus making immunogenicity risk assessment complex and challenging. On the one hand, product-related risks such as the sequence or the biophysical properties of biotherapeutics are often evaluated early in the development, employing in silico and *in vitro* tools to guide candidate selection. This often involves predicting T cell epitopes via in silico tools, in parallel with conducting MHC-II Associated Peptide Proteomics (MAPPs and T cell activation assays (2, 17). On the other hand, we present the DCIA and DC activation assays to provide a more mechanistic understanding of immunogenicity. Gaining a deeper understanding of the mechanisms driving immunogenicity is critical to minimize immunogenic potential of candidates and ensure the delivery of safe biotherapeutics to patients.

Materials and methods

Compounds

Stock solutions of keyhole limpet hemocyanin (KLH-Imject Maleimide-Activated mcKLH, Thermo Fisher Scientific, #77600) were reconstituted and stored at -80°C in single-use aliquots according to the manufacturer's recommendations under sterile conditions. All biotherapeutics; were either produced internally (briakinumab, ixekizumab, bococizumab, ATR-107, var1 and var112) or bought from Runge Pharma GmbH & Co in their respective formulation and stored according to the manufacturer's recommendations.

Antibody labeling

For the DC internalization assay, antibodies were labeled using the SiteClick Antibody Azido Modification Kit (Thermo Fisher, #S20026) according to the manufacturer's instructions. Briefly, N-linked galactose residues of the Fc region were removed by β-galactosidase and replaced by an azide-containing galactose via the β-1,4-galactosyltransferase. This azide modification enables a copper-free conjugation of sDIBO-modified dyes. The pH-sensitive amine-reactive dye was coupled to a sulfo-DBCO PEG4 amine. Antibodies were labeled with a molar dye excess of 3.5. Excess dye was removed using the Amicon Ultra-2 Centrifugal Filter (Merck, #UFC205024) with a MWCO of 50 kD and antibodies were re-buffered in 20 mM histidine 140 mM NaCl buffer (pH 5.5). The fluorescence of the dosing solution was measured in a Tecan Infinite Pro 300 fluorometer. 50µl of dosing solution was mixed with 150µl citric acid buffer (0.2 M Citrate-Phosphate buffer pH 4.5) and the fluorescence was measured with an excitation at 532 nm and emission at 560 nm. The absorbances of the labeled molecules at 280 nm and 532 nm were determined using a Nanodrop spectrometer and the concentration [1] as well as the dye-to-antibody ratio (DAR) [2] was calculated as follows.

$$c(AB) = [A280nm - A[280nm^{*} \ CF(Dye)]] \ / \ \varepsilon(AB) \quad (1)$$

$$DAR = [A532nm^{*}MW(AB)] \ / \ [c(AB) \ ^{*} \varepsilon(Dye)] \quad (2)$$

(A, absorbance; AB, antibody; c, concentration; DAR, dye to antibody ratio; ε (dye), extinction coefficient dye, 47225; CF, correction factor = 0.36)

Quality control of the labeled antibodies

To confirm the efficient removal of unbound dye and to exclude possible antibody aggregates or fragments, a size exclusion chromatography of the labeled antibodies and their unlabeled counterparts was performed. Samples were separated using a BioSuite Diol (OH) column (Waters, 186002165) with a potassium dihydrogen phosphate buffer (pH 6.2) as the mobile phase at a flow rate of 0.5 ml/min. Detectors at 280 nm and 532 nm were used to quantify and analyze the labeled antibodies.

Cell culture and maintenance

Human peripheral blood mononuclear cells were isolated by Pancoll density gradient centrifugation from whole blood according to the manufacturer's instructions. Therefore, EDTA-whole blood donations from healthy volunteers were diluted 1:2 with PBS. For each experiment, different donors were used. For further enrichment of monocytes, magnetic activated cell sorting was performed using anti-huCD14 beads (Miltenyi, #130-050-201) and LS columns (Miltenyi, #130-042-401) according to the manufacturer's instructions. Briefly, monocytes and beads were incubated in MACS Buffer for 15 min on ice and separated by a magnet. The isolated monocytes were suspended in a pre-warmed medium.

Internalization assay

CD14+ monocytes were differentiated into monocyte derived DCs (moDCs), by culturing within a DC medium (sterile filtered CellGenix GMP DC medium, with GlutaMAX, non-essential amino acids, sodium pyruvate and Penicillin-Streptomycin) supplemented

with 5 ng/mL rhIL4 (R&D systems, #204-IL) and 50 ng/mL rhGM-CSF (R&D system, #215GM-500) for 5 days at 37°C and 5% CO2 ambient on ultra-low attachment culture dishes ($0.3x10^6$ cells/ml, Corning, #354407). On the day of the experiment, cells were detached from the ultra-low attachment culture dishes by pipetting and plated into ultra-low attachment 96-well plates at a density of 8x104 cells/well (50µl/well). Antibody solutions were prepared at a concentration of 400 nM in DC medium (dosing solution) and 50 µl were applied to the cells for a final concentration of 200 nM. Cells were incubated for two and four hours at 37°C and 5% CO2. Cells were transferred into U-bottom 96-well plates for sedimentation (300 g, 5 min), the pellet was washed with 200 µl ice cold PBS, centrifuged and resuspended in 200 µl FACS buffer containing 50 ng/mL DAPI.

MHC-II associated peptide proteomics

MAPPs assay was performed according to the standard protocol and analyzed according to Steiner et al. (2). In short, 2.5 million moDCs (at 0.3 x 106 cells/mL) cells were challenged with the test protein at 300 nM in the presence of 1 µg/mL of lipopolysaccharide (LPS) from Salmonella abortus equi (Sigma-Aldrich Chemie GmbH, Buchs, Switzerland) for 24 h. Mature moDCs were harvested, washed with PBS and the cell pellets were frozen at −80°C. Frozen cell pellets were lysed in 20 mM Tris-buffer solution pH 7.8 containing 1% (v/v) Digitonin and protease inhibitors (Roche Diagnostics GmbH, Mannheim, Germany) for 1 h at 4°C on a ThermoMixer at 1100 rpm. The HLA-DR immune complexes were isolated by immunoprecipitation using the biotin-conjugated anti-human HLA-DR monoclonal antibodies (10 µg, clone L243, BioLegend) in a total volume of 50 µL lysis buffer (described above) per sample. Lysates were incubated with the antibody on a rotator overnight at 4° C. Samples were washed five times with a buffer containing 20 mM N-(2-hydroxyethyl)piperazine-N′-ethanesulfonic acid-NaOH (pH 7.9), 150 mM KCl, 1 mM MgCl2, 0.2 mM CaCl2, 0.2 mM ethylenediaminetetraacetate, 10% (v/v) glycerol, and 0.1% (v/v) Digitonin and five times with purified water. MHC-II peptides were eluted twice from HLA-DR molecules by adding 18 µL of 0.1% trifluoroacetic acid. The eluates were collected and analyzed by tandem mass spectrometry. Detected peptides were grouped into clusters and represented along the sequence of the corresponding antibody. A numerical estimation of the MAPPs assay outcome was calculated using the number of epitopes detected and their signal intensities like follows:

$$n_{epitopes} \times \text{mean}(\log2(\text{signal}))$$

DC activation assay

CD14+ monocytes were differentiated into dendritic cells (DCs), by culturing within medium supplemented with 10 ng/mL rhIL4 (R&D systems, #204-IL) and 100 ng/mL rhGM-CSF (R&D system, #215GM-500) for 5 days at 37°C and 5% CO_2 ambient on ultra-low attachment 96-well culture plates (200 µL, $3x10^6$ cells/ml, Corning, #3262). At day 5 the cells are seeded (300 g, 5 min) and half of the medium was changed for the treatment of interest containing medium (100 µL at 600 nMol/L or 100 µg/mL for a final concentration of 300 nMol/L or 50 µg/mL) and incubated for 48 hours at 37°C and 5% CO_2 ambient.

The cells were then spun down (300 g, 5 min) and resuspended in 200 µL PBS containing a Fixable Viability Stain BV510 (BD, #564406) and a FcR blocking agent (Miltenyi, #130-059-901) for 15 minutes at room temperature. The medium was changed for the antibody mastermix composed of CD80 BUV 737 (clone L307, BD, #741865), HLA-DR FITC (clone G46-6, BD, #555811), CD40 BV786 (clone 5C3, BD, #740985), CD209 BV421 (clone DCN46, BD, #564127), CD11c BUV395 (clone B-ly6, BD, #563787), CD14 PerCP (clone M5E2, BioLegend, #301848), CD83 APC (clone HB15E, BD, #551073), CD86 PE (clone 2331, BD, #555658) in a brilliant stain buffer (BD, #566349) - PBS solution and incubated 30 minutes at 4°C. Cells were finally washed twice in FACS buffer and the fluorescence was acquired using the Fortessa X20 (BD).

Data analysis

The mean fluorescent intensity (MFI) of the internalized antibodies was acquired using a Fortessa X20 flow cytometer (BD) equipped with a 532 nm emitting laser. Signals were collected at 572 nm ± 35 nm. The exact same conditions, gains, and gates were used for all time points. Data extraction was performed using the FlowJo-V10.8.1 software (BD Life Sciences). Cells were gated for singlets, morphology and viability. Values of the negative control were subtracted from all geo-mean values, followed by normalization to the fluorescence intensity of the dosing solution and to our internal untargeted IgG1 control. The normalized geo-mean values from each antibody were plotted as a linear regression using R Statistical Software (v4.1.2; 26) to extract the slope (Geo Mean MFI/min for 120 min).

Concerning the activation assay, data extraction was performed using the FloJo_V10 software as well. Cells were gated for singlets, morphology and viability. MFI were extracted for CD209 and HLA-DR while % positive were used for the other activation markers (CD80, CD86, CD83 and CD40) on $CD11c^+$ $CD14^-$ viable cells. Values of the non-treated control were used to calculate the Stimulation Index (SI) specific to each activation marker and individual. The SI were plotted for each treatment to compare for their ability to activate moDCs. Keyhole Limpet Hemocyanin (KLH, Sigma, #SRP6195) response was used as a positive control. Statistical significance of differences in internalization rates and DC activation SI were calculated by a paired T-test. Statistical analysis was performed using R (v4.1.2; 26). Significance level: p< 0.0001= ****; p< 0.001= ***; p< 0.01=**; p< 0.05= *; not significant= ns.

Data availability statement

The raw and processed mass spectrometric data have been deposited to the PRIDE archive (https:proteomecentral.proteomexchange.org/cgi/GetDataset?ID=PXD054823) via the MassIVE partner repository (MassIVE dataset identifier: MSV000095578).

Ethics statement

Ethical approval was not required for the studies involving humans because blood or peripheral blood mononuclear cells (PBMCs) from healthy donors were sourced from either the Blood Donation Center in Aarau, Switzerland (for more information, visit https://www.blutspende-ag-so.ch/ueber-uns/unterrichtsmaterial/) or from Lonza (additional details can be found at https://bioscience.lonza.com/lonza_bs/DE/en/Primary-and-Stem-Cells/p/000000000000185248/Human-PeripheralBlood-Mononuclear-Cells-%28hPBMC%29%2C-Cryopreserved%2C-50-million-). The studies were conducted in accordance with the local legislation and institutional requirements. The participants provided their written informed consent to participate in this study.

Author contributions

MS: Writing – original draft, Writing – review & editing. AP: Writing – review & editing. A-LB: Writing – review & editing. PH: Writing – review & editing. JF: Writing – review & editing. AD: Conceptualization, Data curation, Visualization, Writing – review & editing. KH: Writing – review & editing. CL: Writing – review & editing. CB-L: Conceptualization, Writing – review & editing. OR: Writing – review & editing. TH: Writing – review & editing. TK: Writing – original draft, Writing – review & editing. CM-D: Writing – original draft, Writing – review & editing.

Funding

The author(s) declare that no financial support was received for the research, authorship, and/or publication of this article.

Acknowledgments

We would like to extend our sincere thanks to Guido Steiner and Linnéa Franssen for their expert contribution to the data analysis, which greatly enhanced the quality of this publication. We are extremely grateful to the Large Molecule Drug Discovery Department of Genentech and especially Dr Paul Carter for providing briakinumab, ixekizumab, bococizumab and ATR-107.

Conflict of interest

MS, AP, A-LB, PH, JF, AD, KH, CL, CB-L, OR, TH, TEK and CM-D were employed by Roch. The authors declare that the research was conducted in the absence of any commercial or financial relationships that could be construed as a potential conflict of interest.

The author(s) declared that they were an editorial board member of Frontiers, at the time of submission. This had no impact on the peer review process and the final decision.

Publisher's note

Supplementary material

The Supplementary Material for this article can be found online at: https://www.frontiersin.org/articles/10.3389/fimmu.2024.1406804/full#supplementary-material

SUPPLEMENTARY FIGURE 1
Comparison of two moDCs differentiation durations using LPS. **(A)** Three days of differentiation was compared to an extended differentiation of five days by assessing the moDCs response to 1 ug/mL of LPS (n=10). **(B)** A dose response to increasing LPS concentrations using the 5 days differentiation period (n=10). Individual moDCs SI for the different LPS concentrations were calculated and a plot per activation marker generated (see Material and Methods sections "DC activation assay" and "Data Analysis").

SUPPLEMENTARY FIGURE 2
Sample size estimation for the DC internalization assay. An *a priori* power analysis was performed using R (27) to estimate sample size for a paired t-test. Based on experience, we set an effect size of 2 to be able to capture large, relevant differences between internalization rates of compounds, along with a power of 80% and p of 0.05. The power curve indicated that at least 4 donors were required to capture effect sizes of this magnitude.

SUPPLEMENTARY FIGURE 3
Heatmaps depicting the cluster profile of MAPPs-identified peptides. The sequence regions are organized according to the antibody domains (i.e., variable domain of the heavy chain (VH), constant domain of the heavy chain (CH1), variable domain of the light chain (VL), constant region of the kappa-type light chain (Ck), and the fragment crystallizable (Fc) region). Vertical pink, green, and blue lines along the sequence of the VH and VL domains correspond to the position of the complementarity-determining regions (CDRs) 1 to 3. Identified peptide clusters are depicted as colored regions with varying abundances (as a log score) per sequence position, spanning from dark red to yellow. Donor number is denoted on the vertical axis.

SUPPLEMENTARY TABLE 1
Variance Component Analysis (28) comparing the origins of variance in non-normalized and normalized data. * VC coefficient for "Donor" assigned 0 (shrinkage) VC (Variance Component) denotes extent of the variance emanating from the corresponding variable. Error denotes residual error of the fit.

References

1. Rosenberg AS, Sauna ZE. Immunogenicity assessment during the development of protein therapeutics. *J Pharm Pharmacol*. (2018) 70:584–94. doi: 10.1111/jphp.12810

2. Steiner G, Marban-Doran C, Langer J, Pimenova T, Duran-Pacheco G, Sauter D, et al. Enabling routine MHC-II-associated peptide proteomics for risk assessment of drug-induced immunogenicity. *J Proteome Res*. (2020) 19:3792–806. doi: 10.1021/acs.jproteome.0c00309

3. Xue L, Hickling T, Song R, Nowak J, Rup B. Contribution of enhanced engagement of antigen presentation machinery to the clinical immunogenicity of a human interleukin (IL)-21 receptor-blocking therapeutic antibody. *Clin Exp Immunol*. (2016) 183:102–13. doi: 10.1111/cei.12711

4. Gallais Y, Szely N, Legrand F, Leroy A, Pallardy M, Turbica I. Effect of growth hormone and IgG aggregates on dendritic cells activation and T-cells polarization. *Immunol Cell Biol*. (2017) 95:306–15. doi: 10.1038/icb.2016.100

5. Rombach-Riegraf V, Karle AC, Wolf B, Sordé L, Koepke S, Gottlieb S, et al. Aggregation of human recombinant monoclonal antibodies influences the capacity of dendritic cells to stimulate adaptive T-cell responses. *In Vitro*. *PLoS One*. (2014) 9:e86322. doi: 10.1371/journal.pone.0086322

6. Ahmadi M, Bryson CJ, Cloake EA, Welch K, Filipe V, Romeijn S, et al. Small amounts of sub-visible aggregates enhance the immunogenic potential of monoclonal antibody therapeutics. *Pharmaceut Res*. (2015) 32:1383–94. doi: 10.1007/s11095-014-1541-x

7. Groell F, Jordan O, Borchard G. *In vitro* models for immunogenicity prediction of therapeutic proteins. *Eur J Pharm Biopharm*. (2018) 130:128–42. doi: 10.1016/j.ejpb.2018.06.008

8. Morgan H, Tseng S-Y, Gallais Y, Leineweber M, Buchmann P, Riccardi S, et al. Evaluation of in *vitro* assays to assess the modulation of dendritic cells functions by therapeutic antibodies and aggregates. *Front Immunol*. (2019) 10:601. doi: 10.3389/fimmu.2019.00601

9. Wickramarachchi D, Steeno G, You Z, Shaik S, Lepsy C, Xue L. Fit-for-purpose validation and establishment of assay acceptance and reporting criteria of dendritic cell activation assay contributing to the assessment of immunogenicity risk. *AAPS J*. (2020) 22:114. doi: 10.1208/s12248-020-00491-8

10. Paul S, Grifoni A, Peters B, Sette A. Major histocompatibility complex binding, eluted ligands, and immunogenicity: benchmark testing and predictions. *Front Immunol*. (2020) 10:3151. doi: 10.3389/fimmu.2019.03151

11. Sander J, Schmidt SV, Cirovic B, McGovern N, Papantonopoulou O, Hardt A-L, et al. Cellular differentiation of human monocytes is regulated by time-dependent interleukin-4 signaling and the transcriptional regulator NCOR2. *Immunity*. (2017) 47:1051–1066.e12. doi: 10.1016/j.immuni.2017.11.024

12. Siegel M, Bolender A-L, Ducret A, Fraidling J, Hartman K, Looney CM, et al. Internalization of therapeutic antibodies into Dendritic cells as a risk factor for immunogenicity. *Front Immunol*. (2024).

13. Sauter A, Yi DH, Li Y, Roersma S, Appel S. The culture dish surface influences the phenotype and cytokine production of human monocyte-derived dendritic cells. *Front Immunol*. (2019) 10:2352. doi: 10.3389/fimmu.2019.02352

14. Kim MK, Kim J. Properties of immature and mature dendritic cells: phenotype, morphology, phagocytosis, and migration. *RSC Adv*. (2019) 9:11230–8. doi: 10.1039/C9RA00818G

15. Roche PA, Furuta K. The ins and outs of MHC class II-mediated antigen processing and presentation. *Nat Rev Immunol*. (2015) 15:203–16. doi: 10.1038/nri3818

16. Walsh RE, Lannan M, Wen Y, Wang X, Moreland CA, Willency J, et al. *Post-hoc* assessment of the immunogenicity of three antibodies reveals distinct immune stimulatory mechanisms. *mAbs*. (2020) 12:1764829. doi: 10.1080/19420862.2020.1764829

17. Siegel M, Steiner G, Franssen LC, Carratu F, Herron J, Hartman K, et al. Validation of a dendritic cell and CD4+ T cell restimulation assay contributing to the immunogenicity risk evaluation of biotherapeutics. *Pharm*. (2022) 14:2672. doi: 10.3390/pharmaceutics14122672

18. Wolf B, Piksa M, Beley I, Patoux A, Besson T, Cordier V, et al. Therapeutic antibody glycosylation impacts antigen recognition and immunogenicity. *Immunology*. (2022) 166:380–407. doi: 10.1111/imm.13481

19. Baker K, Rath T, Pyzik M, Blumberg RS. The role of fcRn in antigen presentation. *Front Immunol*. (2014) 5:408. doi: 10.3389/fimmu.2014.00408

20. Dyson MR, Masters E, Pazeraitis D, Perera RL, Syrjanen JL, Surade S, et al. Beyond affinity: selection of antibody variants with optimal biophysical properties and reduced immunogenicity from mammalian display libraries. *mAbs*. (2020) 12:1829335. doi: 10.1080/19420862.2020.1829335

21. Sun A, Benet LZ. Late-stage failures of monoclonal antibody drugs: A retrospective case study analysis. *Pharmacology*. (2020) 105:145–63. doi: 10.1159/000505379

22. Deora A, Hegde S, Lee J, Choi C-H, Chang Q, Lee C, et al. Transmembrane TNF-dependent uptake of anti-TNF antibodies. *Mabs*. (2017) 9:680–95. doi: 10.1080/19420862.2017.1304869

23. Kroenke MA, Milton MN, Kumar S, Bame E, White JT. Immunogenicity risk assessment for multi-specific therapeutics. *AAPS J*. (2021) 23:115. doi: 10.1208/s12248-021-00642-5

24. Dingman R, Balu-Iyer SV. Immunogenicity of protein pharmaceuticals. *J Pharm Sci*. (2018) 108:1637–54. doi: 10.1016/j.xphs.2018.12.014

25. Osugi Y, Vuckovic S, Hart DNJ. Myeloid blood CD11c+ dendritic cells and monocyte-derived dendritic cells differ in their ability to stimulate T lymphocytes. *Blood*. (2002) 100:2858–66. doi: 10.1182/blood.V100.8.2858

26. R Core Team. _R: A Language and Environment for Statistical Computing_. Vienna, Austria: R Foundation for Statistical Computing (2023). Available at: https://www.R-project.org/.

frontiers | Frontiers in Immunology

TYPE Original Research
PUBLISHED 22 August 2024
DOI 10.3389/fimmu.2024.1429544

OPEN ACCESS

EDITED BY
Michael Tovey,
Svar Life Science, France

REVIEWED BY
Julian Q. Zhou,
Washington University in St. Louis, United States
Susan Richards,
Sanofi Genzyme, United States

*CORRESPONDENCE
Liyan Miao
miaolysuzhou@163.com
Jian Wu
njwujian@163.com

†These authors have contributed equally to this work

RECEIVED 08 May 2024
ACCEPTED 05 August 2024
PUBLISHED 22 August 2024

CITATION
Ding X, Xue L, Wang M, Zhu S, Zhu K, Jiang S, Wu J and Miao L (2024) Dynamics and implications of anti-drug antibodies against adalimumab using ultra-sensitive and highly drug-tolerant assays.
Front. Immunol. 15:1429544.
doi: 10.3389/fimmu.2024.1429544

Dynamics and implications of anti-drug antibodies against adalimumab using ultra-sensitive and highly drug-tolerant assays

Xiaoliang Ding[1,2†], Ling Xue[1,2†], Mingjun Wang[3], Shengxiong Zhu[1,2,4], Kouzhu Zhu[1,2,4], Sheng Jiang[1,2,4], Jian Wu[3*] and Liyan Miao[1,2,4*]

[1]Department of Pharmacy, The First Affiliated Hospital of Soochow University, Suzhou, China, [2]Institute for Interdisciplinary Drug Research and Translational Sciences, Soochow University, Suzhou, China, [3]Department of Rheumatology, The First Affiliated Hospital of Soochow University, Suzhou, China, [4]College of Pharmaceutical Sciences, Soochow University, Suzhou, China

Background: Adalimumab induces the production of anti-drug antibodies (ADA) that may lead to reduced drug concentration and loss-of-response, posing significant clinical challenges. However, traditional immunoassays have limitations in terms of sensitivity and drug-tolerance, hindering the insights of ADA response.

Methods: Herein, we developed an integrated immunoassay platform combining the electrochemiluminescence immunoassay with immunomagnetic separation strategy. A longitudinal cohort study involving 49 patients with ankylosing spondylitis was carried out to analyze the dynamic profiles of ADA and to investigate the impact of ADA on adalimumab pharmacokinetics using a population pharmacokinetic model. Additionally, cross-sectional data from 12 patients were collected to validate the correlation between ADA levels and disease relapse.

Results: The ADA assay demonstrated high sensitivity (0.4 ng/mL) and drug-tolerance (100 μg/mL), while the neutralizing antibodies (NAB) assay showed a sensitivity of 100 ng/mL and drug-tolerance of 20 μg/mL. Analysis of the longitudinal cohort revealed that a majority of patients (44/49, 90%) developed persistent ADA within the first 24 weeks of treatment. ADA levels tended to plateau over time after an initial increase during the early immune response phase. Further, nearly all of the tested patients (26/27, 96%) were classified as NAB positive, with a strong correlation between ADA levels and neutralization capacity (R^2 = 0.83, P < 0.001). Population pharmacokinetic modeling revealed a significant positive association between model-estimated individual clearance and observed ADA levels. Higher ADA levels were associated with adalimumab clearance and disease relapse in a cross-sectional cohort, suggesting a promising ADA threshold of 10 for potential clinical application. Moreover, the IgG class was the primary contributor to ADA against adalimumab and the apparent affinity exhibited an increasing trend over time, indicating a T-cell dependent mechanism for ADA elicitation by adalimumab.

10.3389/fimmu.2024.1429544

Conclusion: In summary, this integrated immunoassay platform shows promise for in-depth analysis of ADA against biologics, offering fresh insights into immunogenicity and its clinical implications.

KEYWORDS

adalimumab, anti-drug antibodies, electrochemiluminescence, immunogenicity, neutralizing antibodies

1 Introduction

Monoclonal antibody-based biopharmaceuticals have significantly advanced current therapies for cancer and autoimmune diseases. However, a major concern with long-term clinical use is the immunogenicity elicited by repeated drug administration (1). The host immune system recognizes the differing relevant epitopes in the biologic drug as foreign and then triggers the specific anti-drug antibodies (ADA) against it, leading to the formation of drug–ADA immune complexes and accelerated drug clearance. Neutralizing antibodies (NAB), a subset of ADA, have the ability to directly block the drug from binding to its target, thereby neutralizing its pharmacological activity. The development of ADA and NAB can potentially impact drug pharmacokinetics, pharmacodynamics and safety.

Adalimumab has been approved for the treatment of various inflammation-mediated diseases, including inflammatory bowel diseases, rheumatoid arthritis, ankylosing spondylitis, and psoriasis. Its high specificity for the target and strong binding to tumor necrosis factor α (TNF-α) have made it the most widely prescribed biological agent globally for the past decade. Initially, adalimumab was perceived as less immunogenic since it is a fully human monoclonal antibody derived from phage display technology. However, recent advancements in bioanalysis have revealed that the prevalence and impact of ADA formation were previously underestimated (2). Numerous studies have explored the relationships between ADA formation, drug concentrations, and treatment effectiveness (3–5).

Nevertheless, there are major gaps in the knowledge on the characteristics of ADA against adalimumab, which hinder a comprehensive understanding of immunogenicity and its clinical implications. For example, limited data exists on the dynamic profile of ADA against adalimumab, including onset time, response duration and magnitude evolution following initial and subsequent doses. Critical information is missing about the threshold relevant to adalimumab pharmacokinetics and treatment effectiveness. Moreover, the kinetics of NAB development and its correlation with ADA are poorly understood. Additionally, detailed features of ADA against adalimumab, such as isotype switching and affinity maturation, remain unclear. Utilizing immunoassays with high sensitivity and drug-tolerance is expected to help fill these knowledge gaps. Existing knowledge on ADA against adalimumab has mainly been obtained using drug-sensitive assays, like traditional bridging ELISA and radioimmunoassay, which can only detect ADA in the presence of low concentrations or absence of the drug (6, 7). Currently, the electrochemiluminescence (ECL) platform is now widely used in the pharmaceutical industry due to its drug-tolerance and sensitivity (8). However, the bridging-ECL immunoassay format may not effectively capture IgG4 and IgM class ADA due to the nature of monovalent antibodies of IgG4 and weak affinity of IgM. NAB are typically detected using cell-based assays or competitive immunoassays (9, 10), but challenges related to sensitivity and drug-tolerance hinder the accurate detection and interpretation of NAB data. Hence, there is a need for immunoassays with high sensitivity, drug-tolerance, and the ability to recognize all ADA isotypes to fully comprehend the landscape of ADA against adalimumab.

Herein, an integrated analytical platform was developed to comprehensively evaluate ADA against adalimumab. This platform utilizes immunomagnetic separation in combination with the ECL detection system, enhancing the drug-tolerance and sensitivity. A longitudinal cohort study was conducted to analyze the dynamics of ADA and NAB levels and their quantitative impact on adalimumab pharmacokinetics. Furthermore, a cross-sectional cohort study investigated the relationship between ADA levels and disease relapse. Additionally, the analytical platform was used to explore class switching and affinity maturation of enriched ADA. These methodologies provide valuable insights into the mechanisms underlying ADA formation and improve the clinical applicability of ADA data in patient care.

2 Materials and methods

2.1 Patients

Two distinct groups of patients were enrolled in this study, each with access to different types of data. The first group consisted of forty-nine patients with ankylosing spondylitis who were either initiating or continuing adalimumab therapy. This prospective observational single-center cohort study was conducted between September 2021 and May 2023 at the Department of Rheumatology, the First Affiliated Hospital of Soochow University (Suzhou, China). The patients included in the study were either biologically naïve or had prior experience with biological treatment for at least 6 months. None of the patients received concomitant immunomodulatory drugs. Longitudinal blood

samples were collected at baseline and prior to each subsequent adalimumab injection randomly in a clinical setting.

To investigate the relationships between adalimumab levels, magnitude of ADA and disease relapse, we analyzed cross-sectional therapeutic drug monitoring data and retrospective electronic medical records from a separate set of 12 patients who had been receiving adalimumab maintenance therapy for more than 3 months. This group comprised 8 patients with Crohn's disease and 4 patients with ankylosing spondylitis. Among these patients, four experienced disease flare leading to drug discontinuation, while clinical remission was maintained in eight patients as evaluated by a physician using disease activity scores or clinical symptoms (Crohn's Disease Activity Index for Crohn's disease, Ankylosing Spondylitis Disease Activity Score for ankylosing spondylitis).

All protocols were approved by the Institutional Review Board of the First Affiliated Hospital of Soochow University (No. 2021–078), and all patients provided written informed consent.

2.2 Immunomagnetic separation of ADA

To isolate ADA from plasma while minimizing carryover of the residual drug or biotinylated drug leaching, magnetic beads covalently crosslinked with adalimumab (25 μg protein/mg beads) were prepared according to the manufacturer's instructions (BeaverBio, BeaverBeads Mag NHS Kit, 300 nm) prior to affinity separation. Before use, glycine buffer (100 mM, pH 2.0) was added to wash the beads, and then the beads were washed three times with PBST (0.1% Tween in phosphate buffer solution) using a magnetic rack. Beads covalently coupled with adalimumab were finally resuspended in Tris buffer (1.5 M, pH 9.6).

Ten-microliter plasma samples were diluted with 300 mM acetic acid at a ratio of 1:9 on a shallow 96-well plate, followed by incubation for 15–20 min with shaking at room temperature. After the ADA-drug complexes were dissociated, 0.1 mg of beads/24 μL buffer were added to each acidified sample to capture ADA at room temperature for 1 h at 1200 rpm. After incubation, the beads were washed three times with PBST using a magnetic separator. Finally, 100 μL of glycine buffer (100 mM, pH 2.0) was added to each sample to elute the ADA from the beads, and the mixture was shaken for 15–20 min at 1200 rpm. The elution supernatant was transferred for subsequent analysis.

2.3 Measurement of ADA and NAB with the Meso Scale Discovery (MSD®) platform

An ECL technique based on the MSD platform was used to measure ADA and NAB against adalimumab after ADA purification. Pooled biological-naïve human plasma (n = 20) was used as the negative control (NC). NC samples spiked with rabbit-anti-adalimumab idiotype polyclonal antibodies (pAb, made by Abcepta Biotech) were prepared to assess the performance of the ADA assay as positive control (PC), and NC samples spiked with an anti-idiotype antibody against adalimumab (Bio-Rad, AbD18655_hIgG1, catalogue no. HCA204) were used as PC samples for the NAB assay.

The ADA assay was configured in direct ligand binding format. In brief, the eluted supernatant was directly coated on an MSD high-bind plate, which was incubated for 1 h at 37°C with shaking at 500 rpm. Then, the plate was washed using a microplate washer (BioTek, 405LS) and blocked with 1% BSA in PBS for 1 h at 37°C with shaking at 500 rpm. The plate-bound ADA was detected with ruthenium-labeled adalimumab. After the final incubation step and washing, 2X Read Buffer was added, and the ECL signal of the plate was read on a QuickPlex SQ120 Reader (MSD). The ECL signal was proportional to the ADA level, and each result was converted to a signal-to-NC ratio (S/N). The assay was validated according to white paper (11).

For the NAB assay, a competitive ligand binding (CLB) assay in drug capture format was used to evaluate the neutralization capacity of the ADA. As ruthenium-labeled TNF-α would be unable to bind the adalimumab pre-coated on the plate if the ADA had neutralization capacity, a high ADA neutralization capacity would result in a reduction in the ECL signal. Thirty microliters (5 ng/mL in PBS) of biotin-labeled adalimumab was coated on the MSD streptavidin plate for 1 h at room temperature, followed by the addition of 50 μL of ADA supernatant and 7 μL of neutralization buffer (1 M Tris buffer, pH 8.8). After incubation, the residual adalimumab was detected by ruthenium-labeled TNF-α (100 ng/mL in PBS) and the ECL signal of the plate was read on a QuickPlex SQ120 Reader (MSD) by adding 2X Read Buffer. The sample ECL signal relative to the blank ECL signal (B/B0) reflected the neutralization capacity. The assay was validated according to white paper (12).

2.4 Measurement of IgG, IgM or IgA class antibodies to adalimumab

Adalimumab-Fab was prepared to mitigate interference with the IgG detection procedure. Adalimumab was digested by papain to produce specific Fab fragments of adalimumab, according to the manufacturer's instructions (Pierce™ Fab Preparation Kit, Thermo Scientific). MSD high-binding plate was coated overnight with adalimumab-Fab (1 μg/mL in PBS). After washing and blocking, 50 μL of ADA supernatant and 7 μL of neutralization buffer (1 M Tris buffer, pH 8.8) were added and the plate was incubated at 37°C for 60 min with shaking at 500 rpm. For detection, ruthenium-labeled anti-human IgG (GenScript, catalogue no. V90401), anti-human IgM (GenScript, catalogue no. A02128) antibody, or anti-human IgA antibody (Merck, Rabbit monoclonal, catalogue no. SAB5600221) with ruthenium-labeled anti-rabbit antibody (Abcepta Biotech) was added, and the ECL signal of the plate was read on a QuickPlex SQ120 Reader (MSD). The positive cut-off signal was calculated based on the mean ECL signal obtained with a panel of 10 adalimumab naïve samples plus 3 standard deviations.

2.5 Solution equilibrium titration for apparent affinity estimation

In brief, a fixed concentration of enriched ADA was incubated with a series of concentrations of biotin-labeled adalimumab (1–10000 pM) until equilibrium was reached, and then the ADA-biotin-labeled

adalimumab complexes were removed using streptavidin-beads (Beaver, BeaverBeads Streptavidin, 1 μm) under a magnetic rack. The unbound ADA that remained in solution were measured using a direct ADA assay, and a kinetic equation was fitted to determine K_D value using the custom program in GraphPad (Prism 8, La Jolla, CA). The equation was as follows (13):

$$\text{ECL signal} = \text{ECL}_{max}\left(1 - \frac{1}{\left(\frac{K_D}{Dose} + 1\right)^2}\right)$$

where ECL_{max} is the maximum signal when no drug is added, K_D is the apparent equilibrium dissociation constant, Dose is the amount of biotin-labeled adalimumab added to the enriched ADA.

2.6 Measurement of adalimumab levels

The plasma adalimumab concentration was quantified using a validated sandwich ELISA. Microtiter plates (Thermo, catalogue no. 446469) were coated with an anti-idiotype antibody, a mouse monoclonal antibody specific to adalimumab (GenScript, catalogue no. A01954). The bound adalimumab was then detected using biotinylated mouse anti-adalimumab antibody (GenScript, catalogue no. A01956). Horseradish peroxidase-labeled streptavidin (Solarbio, catalogue no. SE068) and 1-Step Ultra TMB-ELISA substrate solution (Thermo, catalogue no. 34028) were consecutively added to the plate to generate a chromophore, and the color development was stopped by adding a 2 N H_2SO_4 solution. The colorimetric intensity was determined by a microplate reader (Thermo, Multiskan Go) at 450 nm with correction based on the signal at 630 nm.

2.7 Population pharmacokinetic analysis

Population pharmacokinetic analysis was performed by NONMEN (version 7.5.0; ICON Development Solutions) with Wing for NONMEM (version 750), R (version 3.5.2) and the Pirana interface (version 2.9.4, Certara).

A one-compartment pharmacokinetic model with first-order absorption and elimination (ADVAN2 and TRANS2) was selected to describe the pharmacokinetics of adalimumab based on published data (14). The apparent clearance (CL/F) and apparent volume of distribution (V/F) were estimated, while the absorption rate constant (KA) was fixed due to the limited sampling time points. All parameters were estimated with the first-order conditional estimation with interaction (FOCE-I) algorithm.

The interindividual variability (IIV) of the parameters was modeled using an exponential model as follows:

$$P_{ij} = \text{TVP} \times \exp(\eta_{ij})$$

where P_{ij} represents the *i*-th individual value of the parameter on the *j*-th occasion, TVP represents the typical population value of the parameter, and η represents the interindividual variability of the pharmacokinetic parameter and is normally distributed with a mean of 0 and a variance of ω^2.

The residual error of the model using a combined (proportional plus additive) model was calculated as follows:

$$Y = \text{CONC} + \text{sqrt}(\text{CONC}^2 \times \theta_{PROP}^2 + \theta_{ADD}^2) \times \varepsilon$$

where θ_{PROP} represents the parameter of the proportion residual error, θ_{ADD} represents the parameter of the additional residual error, CONC represents the individual predicted adalimumab concentration, Y represents the observed value, and ε represents the residual error and is assumed to be normally distributed with a mean of 0 and variance of σ^2.

Based on prior knowledge, normal fat mass (NFM) and ADA levels were introduced into the model using the following general equation:

$$\theta = \theta_1 \times \left(\frac{\text{Covariate}}{\text{mean}}\right)^{\theta_2}$$

where θ_1 is the population estimate of the parameter, Covariate is the continuous covariate, mean is the average of the continuous covariate, and θ_2 is the estimated coefficient of the continuous covariate. The NFM was calculated based on our previously published model (15). These covariates were retained in the final model with a significant decrease in the objective function value (dOFV, $P < 0.001$). The final model was evaluated with a goodness-of-fit plot, bootstrap and prediction-corrected visual predictive check (pc-VPC).

2.8 Statistical analysis

Continuous variables are expressed as medians and interquartile ranges (IQRs), and categorical variables are expressed as percentages. Unpaired continuous variables were compared using the Mann-Whitney U test, and paired continuous variables were compared using the Wilcoxon test. Kaplan-Meier curves were plotted to determine the overall cumulative percentage of patients who developed ADA. The relationship between the values of ADA-S/N and NAB-B/B0 was analyzed via linear regression. To visually check the relationship between ADA-S/N values and *post hoc* individual estimates of apparent clearance, a restricted cubic spline curve was generated. Differences with a two-tailed *P* value < 0.05 were considered statistically significant. All statistical analysis and graphical figures were performed with GraphPad Prism 8 (La Jolla, CA).

3 Results

3.1 An integrated immunoassay platform for detecting ADA and NAB against adalimumab

The schematic diagram and work flow are shown in Figure 1. NHS-activated magnetic-beads were utilized to covalently immobilize adalimumab via stable amide linkages formed between NHS and primary amines, thereby enhancing binding

10.3389/fimmu.2024.1429544

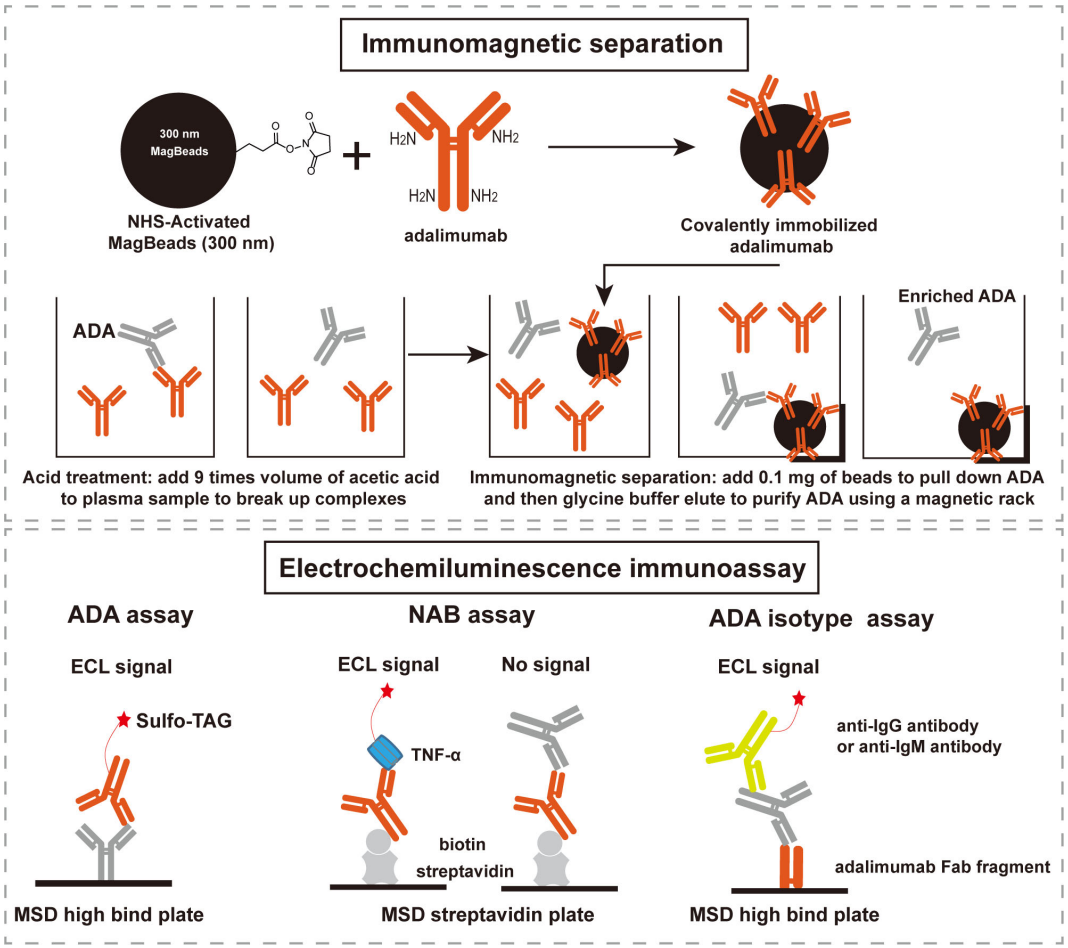

FIGURE 1
Scheme of the integrated immunoassay platform comprised of immunomagnetic separation and electrochemiluminescence immunoassay. ADA: anti-drug antibodies, NAB: neutralizing antibodies, ECL: electrochemiluminescence, MSD: meso scale discovery.

capacity and reducing leaching of the immobilized-adalimumab. Subsequently, ADA in the plasma matrix were captured and purified using the functionalized beads, followed by acid dissociation to minimize residual adalimumab from the sample itself. The enriched ADA were then detected using adalimumab labeled with SULFO-TAG after direct coating onto the MSD high-binding plate. The NAB assay was developed using a drug capture and competitive ligand binding format. In the absence of NAB, SULFO-TAG labeled TNF-α binds to the coated biotin adalimumab, resulting in a signal. However, in the presence of NAB, the signal is suppressed. The class of enriched ADA was determined using an indirect ECL immunoassay, where the enriched ADA were captured by the Fab fragment of adalimumab and subsequently detected by specific anti-human IgG or IgM antibody.

To reveal the detection performance of ADA assay, a panel of 51 adalimumab naïve samples was used to establish the screen cut point factor (SCPF, absence of spiked adalimumab) and confirmatory cut point (CCP, presence of spiked adalimumab) (16). From the 153 values obtained from the 51 individual samples determined three times, a sample was deemed positive if the S/N value from the screening assay exceeded 1.05 (Supplementary Figure S1A), and the percent inhibition by the spiked adalimumab in the confirmatory assay was above 10.6% (Supplementary Figure S1B). The assay sensitivity was calculated to be 0.4 ng/mL for surrogate pAb in the neat matrix based on the assay's cut point (Figure 2A). Drug-tolerance was assessed by using pAb at concentrations of 10 ng/mL and 100 ng/mL in the presence of adalimumab at varying concentrations (0, 10, 30, and 100 μg/mL). The signal decreased as the adalimumab increased concentration up to 100 μg/mL but remained above the SCPF (Figure 2B), indicating a drug-tolerance above 100 μg/mL at 10 ng/mL pAb (drug-tolerance: adalimumab:ADA=10,000:1). Furthermore, TNF-α spiked in the NC at concentrations up to 1000 ng/mL showed no interference (Figure 2C).

For validation of the NAB assay, the neutralizing cut point (NCP) was determined to be 0.85 (Supplementary Figure S1C), and the sensitivity of the surrogate HCA204 in the neat matrix was found to be 100 ng/mL (Figure 2D). The signal of PC sample at 500 ng/mL HCA204 remained below the NCP even with increasing adalimumab concentrations up to 20 μg/mL (Figure 2E). Additionally, spiking the NC sample with the target at concentrations up to 1000 ng/mL did not impact the results of the NAB assay (Figure 2F). A summary of the key parameters

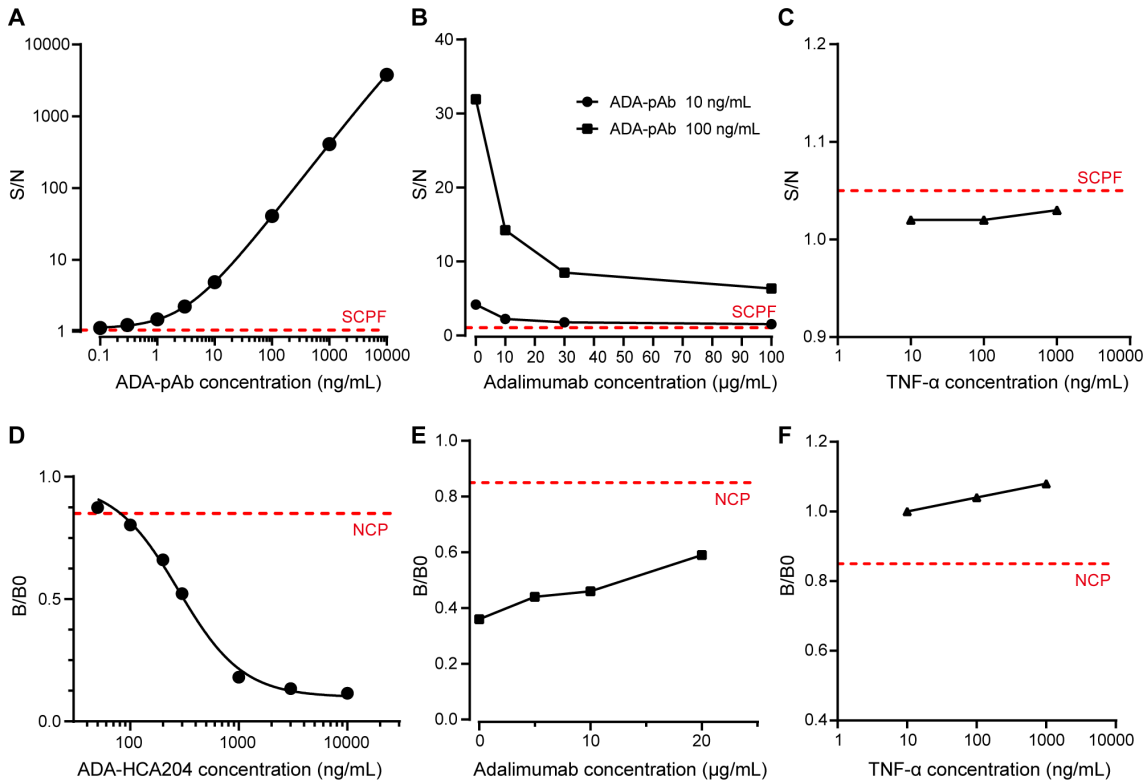

FIGURE 2
Performance of ADA and NAB assay. **(A)** A typical dose-response curve of ADA-pAb ranging from 0.1 to 10000 ng/mL is generated and fitted by a four-parameter logistic model. **(B)** Positive control samples containing ADA-pAb at 10 ng/mL or 100 ng/mL in the presence of adalimumab at various concentrations (0, 10, 30 and 100 μg/mL) were evaluated in the ADA screening assay. **(C)** Blank plasma matrix with TNF-α at concentrations ranging from 10 to 1000 ng/mL were assessed in the ADA screening assay. **(D)** A typical dose-response curve of ADA-HCA204 ranging from 50 to 10000 ng/mL. The graph is fitted by four-parameter logistic fitting. **(E)** Positive control samples containing ADA-HCA204 at 500 ng/mL in the presence of adalimumab at various concentrations (0, 5, 10 and 20 μg/mL) were assessed in the NAB assay. **(F)** Blank plasma matrixes with TNF-α at concentrations ranging from 10 to 1000 ng/mL was assessed in the NAB assay. The red dotted line illustrates the SCPF in A-C and the NCP in **(D–F)**. ADA, anti-drug antibodies; NAB, neutralizing antibodies; SCPF, screening cut point factor; NCP, neutralizing cut point.

validated for assessing ADA and NAB against adalimumab in human plasma is presented in Supplementary Table S1. Therefore, the integrated immunoassay platform consisting of immunomagnetic separation and ECL technique demonstrates high sensitivity and high drug-tolerance, making it suitable for ADA and NAB assessment.

3.2 Longitudinal profiles of ADA and NAB against adalimumab

Having defined the sensitivity and drug-tolerance of ADA and NAB assays, we proceeded to examine their kinetic profiles. A longitudinal cohort comprising of 49 patients with ankylosing spondylitis who were initially treated with adalimumab in a real-life clinical setting was analyzed (Supplementary Table S2). A total of 201 plasma samples were examined, with no presence of ADA detected in samples collected prior to adalimumab treatment. The overall cumulative percentage of patients testing ADA-positive showed that 90% (44 out of 49) developed ADA during the follow-up period (Figure 3A). Out of the five patients who remained ADA-negative, two were lost to follow-up on days 14 and 23, respectively. The ADA-S/N generally increased over time in the early phase and subsequently reached a relative plateau in late phase, with notable variation observed among patients (Figure 3B). The enlarged section highlighting early phase showed that 7 out of 43 patients developed ADA after first dosage, and 73% (11/15) of patients developed ADA after second dosage (Supplementary Figure S2A). The late response period was observed in eight patients (Supplementary Figure S2B), showing relatively flat response. It is noteworthy that all ADA responses were persistent and no transient response was observed. When referring to the sensitivity threshold (100 ng/mL) required by regulatory agency (17) (ADA-S/N=40 based on the ADA calibration curve), only one-third of patients were considered positive (Supplementary Figure S3).

Due to the sensitivity considerations, samples with ADA-S/N value exceeding 10 underwent further neutralizing activity assessment, containing 47 samples from 27 patients. Our results revealed that the neutralization capacity and ADA levels displayed similar kinetic profiles (Figure 3C). Almost all patients (26 out of 27, 96%) tested positive for NAB during follow-up, with one exception likely attributed to the short duration of follow-up (40 days since the initial dose). We observed a strong correlation between the ADA

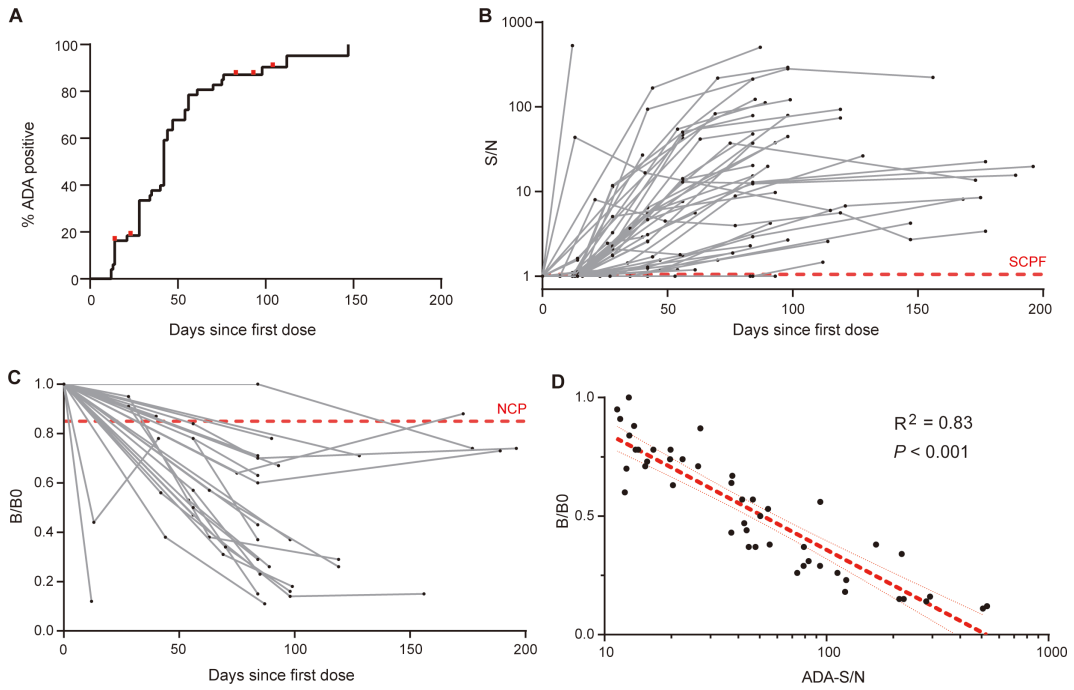

FIGURE 3
Dynamic profiles of ADA and NAB against adalimumab. **(A)** The overall cumulative percentage of patients who developed ADA during follow-up, with red dots representing censored data for five ADA-negative patients. **(B)** The kinetics of ADA response over treatment time in individual patients, measured by the signal-to-NC ratio (S/N), with the red dotted line indicating the screening cut point factor. **(C)** Kinetics of the NAB response over treatment time in individual patients. The sample signal relative to the blank signal (B/B0) reflects the neutralization capacity, and the red dotted line illustrates the neutralizing cut point. **(D)** There was a strong correlation between ADA levels (S/N) and neutralization activity (B/B0). The red line indicates the linear regression and 95% confidence intervals.

levels and neutralizing capacity (R^2 = 0.83, P < 0.001, Figure 3D), indicating that ADA against adalimumab primarily possess neutralizing properties. Overall, our in-house ADA and NAB assays shed light on the kinetics of ADA and NAB against adalimumab, following the nature of human immune system.

3.3 Adalimumab elicits ADA in a T-cell dependent manner

In addition to evaluating the onset, duration and neutralizing activity of ADA response, other characteristics of ADA, such as class-switch recombination and affinity maturation, can offer further insights into antibody response in a T-cell dependent or T-cell independent manner (18). We observed a similar kinetic profile between IgG class and total ADA in the ten patients (Figures 4A, B). IgM class signals with no increasing trend were observed only in a minority of the samples (Figure 4C), and IgA class signals were relatively negative in all tested samples (Figure 4D). Profiles of total ADA, IgG class, and IgM class ADA in individual patients were shown in Supplementary Figure S4, suggesting that the IgG class is the most prevalent type of ADA against adalimumab.

ADA signals of immunoassays are dependent on both antibody affinity and concentrations (19). We have developed an ECL-based solution equilibrium titration method for apparent affinity estimation of enriched ADA. Our observations in a representative patient showed that the signals of unbound ADA decreased gradually as the concentrations of biotin-adalimumab increasing (Supplementary Figure S5), reflecting the principle of solution-phase equilibrium binding interaction. The apparent K_D values showed a decreasing trend over time in a subgroup of 9 patients (Figure 4E), suggesting an enhancement in affinity with longer treatment duration. Statistical analysis revealed a significant decrease in apparent K_D values with prolonged treatment time (P = 0.004, Figure 4F), supporting the concept of a maturing immune response. In conclusion, the primary mechanism underlying the formation of ADA against adalimumab involves T-cell dependent B cell activation, including class switching from IgM to IgG and the production of antibodies with higher affinity.

3.4 Clinical relevance of ADA against adalimumab

After revealing the characteristics of ADA toward adalimumab, we focused on exploring its clinical relevance with adalimumab concentrations and disease relapse. The plasma adalimumab concentrations were measured using a validated sandwich ELISA method. The lower limit of quantification was 62.5 ng/mL, and standard curve fitting with a four-parameter curve ranged from 62.5–2000 ng/mL (Supplementary Figure S6). The intra-assay and inter-assay coefficients of variation were ≤6% and ≤10%, respectively (Supplementary Table S3).

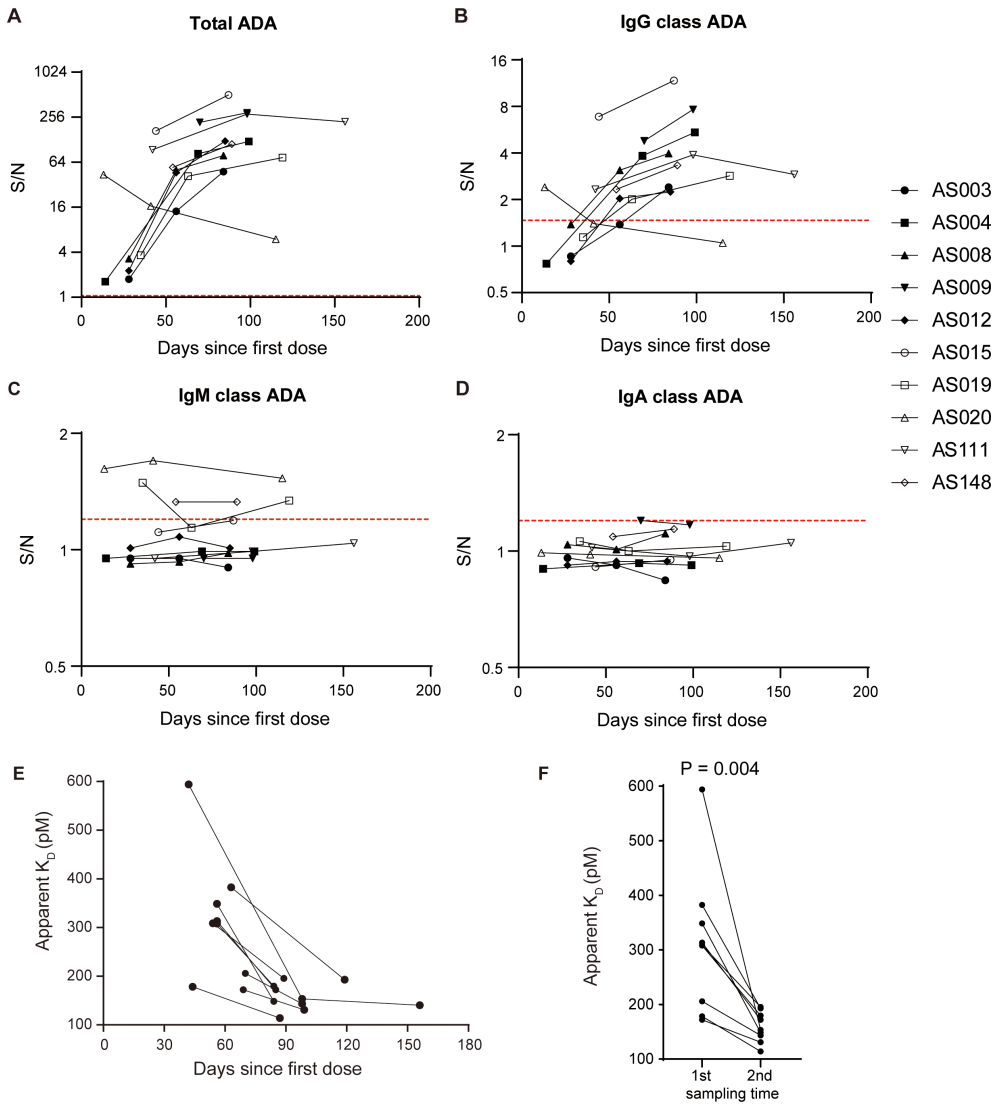

FIGURE 4
Adalimumab elicits ADA formation in T-cell dependent manner. Profiles of total ADA **(A)**, IgG class ADA **(B)**, IgM class ADA **(C)**, and IgA class ADA **(D)** in ten patients over the course of treatment. The red dotted lines illustrate the corresponding cut points. **(E)** The apparent K_D showed a decreasing trend with treatment time in a subset of 9 patients, suggesting an increase in affinity over time. **(F)** The apparent K_D values significantly decreased with time extension, as evidenced by the comparison between the first sample and the second sample (median 308.8 vs. 153.3, Wilcoxon test, $P = 0.004$).

A population pharmacokinetic model was established to quantitatively investigate the impact of ADA levels on adalimumab pharmacokinetics using data from a longitudinal cohort of 49 patients. The parameters and evaluations of the model are presented in Supplementary Figures S7, S8. The addition of ADA levels into the final model reduced interindividual variability in clearance (CL/F) from 53.5% to 35.4% (Supplementary Table S4). A scatter plot illustrated a positive correlation between model-estimated individual clearance and observed ADA-S/N values (Figure 5A), suggesting that an ADA-S/N > 10 could be a noteworthy threshold affecting adalimumab exposure based on visual inspection. Figures 5B, C demonstrate that adalimumab trough concentration initially rose post-administration in the absence of ADA formation, with levels stabilizing in a patient with low ADA levels (Figure 5B). In contrast, a patient with high ADA levels experienced a decline in adalimumab trough levels (Figure 5C).

To further investigate the relationship between ADA levels and disease relapse, we conducted a retrospective analysis using data from 12 patients (Supplementary Table S5). The median ADA-S/N values were found to be higher in patients who experienced disease relapse compared to those who maintained remission (68.25, n=4 vs. 2.49, n=8, $P = 0.004$, Figure 5D). Notably, there was no overlap between the two groups. Furthermore, the adalimumab concentrations were considerably lower in patients with disease relapse compared to those in remission (median 0.19 µg/mL vs. 9.8 µg/mL, $P = 0.004$, Figure 5E). Based on these findings regarding ADA levels, drug exposure and disease relapse, it is postulated that an ADA-S/N > 10 could potentially be a clinically relevant threshold.

10.3389/fimmu.2024.1429544

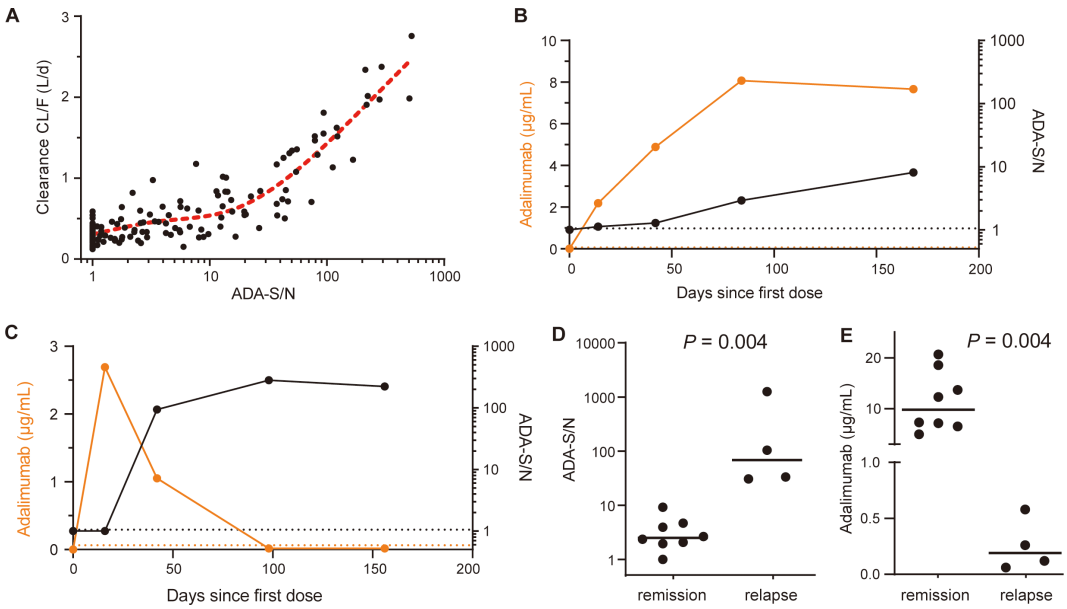

FIGURE 5
Clinical relevance of ADA against adalimumab. **(A)** Relationship between ADA-S/N values and *post hoc* individual estimates of apparent clearance (CL/F). The red dotted line indicates a restricted cubic spline curve (knots=3). **(B)** The kinetics of adalimumab concentrations (orange dots; left y axis) and ADA-S/N values (black dots; right y axis) in a single representative patient with low ADA levels. The black and orange dotted lines indicate the screening cut point factor of the ADA assay and the lower limit of quantitation of adalimumab, respectively. **(C)** The kinetics of adalimumab concentrations (orange dots; left y axis) and ADA-S/N values (black dots; right y axis) in a single representative patient with high ADA levels. Black and orange dotted lines indicate the screening cut point factor of the ADA assay and the lower limit of quantitation of adalimumab, respectively. **(D)** Median ADA-S/N values were significantly higher for patients at disease relapse than for patients in remission (68.25, n=4 vs. 2.49, n=8, Mann-Whitney test, $P = 0.004$). The black lines show the medians. **(E)** Median adalimumab concentrations were significantly lower for patients at disease relapse than for patients in remission (0.19 µg/mL vs. 9.8 µg/mL, Mann-Whitney test, $P = 0.004$). The black lines show the medians.

4 Discussion

Here, a highly sensitive and drug-tolerant immunoassay platform was developed for evaluating immunogenicity against adalimumab. This platform involved an affinity separation procedure using drug-specific covalently coupled magnetic beads combined with the MSD-ECL system. The method allowed us to uncover the broad complexity of ADA response against adalimumab, such as kinetics profile, neutralizing capacity, class switching, and affinity maturation. The study also highlighted the implications of these findings on the drug's pharmacokinetics and effectiveness, proposing a potentially clinically meaningful threshold for clinical applications.

The innovative analytical platform has demonstrated exceptional performance and shows promising as a versatile analytical protocol for evaluating the immunogenicity to biopharmaceuticals. Compared to our previous method involving biotin-drug extraction and acid dissociation (20), the preparation of beads covalently coupled with adalimumab was found to be crucial in minimizing drug carryover during sample treatment, thereby preventing biotin-drug leaching from streptavidin beads (21). Particularly, the magnetic bead separation procedure plays a vital role in achieving drug-tolerance of at least 20 µg/mL for assessing NAB using competitive immunoassay, as drug carryover significantly impacts the subsequent NAB assay (22, 23). Furthermore, MSD-ECL technology offers highly sensitive and robust assays, enhancing sensitivity down to 0.4 ng/mL and broadening the dynamic range up to 10000 ng/mL for ADA assay (24). Advanced technology provides a strong foundation for assessing ADA magnitude with a suitable signal to noise ratio (25). Notably, ADA enrichment using magnetic bead separation is a simpler strategy compared to drug removal methods in reducing residual drug interference (26). The overall workflow can be carried out in a semi-automated manner using a 96-well microtiter plate.

Utilizing the integrated analytical platform, we successfully elucidated the comprehensive profiles of ADA against adalimumab, such as onset time, duration, kinetics, class-switching and affinity maturation. These findings suggest that existing information on immunogenicity against adalimumab from development and early studies may now be outdated. A critical next step lies in translating these findings into clinical practice. Our novel immunoassay revealed that approximately 90% of the patients will persistently develop ADA against adalimumab, representing one of the highest incidences reported in literatures (7, 27). Our observations revealed a distinct pattern in ADA formation kinetics, reminiscent of the kinetic view in adaptive immune responses to vaccines or foreign antigens (28, 29). This pattern is characterized by an initial phase of ADA production within 2–4 weeks, followed by a maturation of the immune response over approximately 3 months. Significant variation were noted in ADA magnitude among individuals, with the underlying mechanism still elusive. Notably, our study emphasizes the importance of monitoring individual ADA dynamics rather than

focusing solely on absolute concentrations, as this idea may offer valuable predictive information regarding the potential loss-of-response to infliximab treatment (30). Our data also suggest that proactive monitoring of ADA formation could aid in early prediction of treatment response issues prior to the occurrence of clinical symptoms (31). However, the clinical implications of this strategy warrant further investigation. Additionally, our findings indicate that all patients were persistently positive according to the supersensitive assay, leading us to speculate that transient ADA may be caused by less sensitive assays (31). It is generally believed that transient ADA, which are typically present at low titers, may not significantly impact treatment efficacy (20, 32). Furthermore, our observations suggest that the humoral response to biopharmaceuticals resembles that of a vaccine-like immune response, with repeated administrations potentially eliciting a stronger immune response akin to booster vaccines (33). The development of high-affinity IgG class antibodies following repeated adalimumab dosing indicates T-cell dependent immune response dominance. Conversely, an extrafollicular T-cell independent immune response was noted following initial infliximab administration (34). It is important to consider that alterations in antibody affinity over time could affect results when relying solely on the quantification of enriched ADA masses through LC-MS/MS techniques (35). While the format in which ADA are enriched by protein-A beads and detected by the Fab fragment of adalimumab may be an alternative method (36).

The strong correlation between the ADA-S/N and the neutralization capacity of NAB suggests that the ADA response to adalimumab could be characterized as anti-idiotype responses. This indicates that nearly all ADA are anti-idiotype antibodies and NAB under the conditions of the supersensitive assay. Previous studies using cell-based or immunoassays had limited sensitivity, resulting in only a minority of ADA being tested as NAB and complicating the interpretation of NAB results (37). Patient-derived monoclonal antibodies in studies involving the antibody repertoire of ADA-positive patients showed a restricted response, with all ADA competing for TNF-α binding (38, 39). In addition, ADA epitopes were identified mostly located in the adalimumab variable region by epitope mapping assay via peptide microarray (40). The presence of ADA leads to suboptimal drug exposure and treatment response by increasing drug clearance and blocking the pharmacological effect of adalimumab. Therefore, assessing NAB results does not seem to provide additional value compared to the more readily available ADA results.

Establishing a clinically meaningful threshold relevant to adalimumab pharmacokinetics and clinical efficacy is crucial for guiding clinical practice. Our study propose a provisional threshold of ADA-S/N above 10, showing correlation with disease relapse and lower adalimumab concentrations. When high ADA levels are detected, patients should receive increased attention in terms of treatment decisions, potentially including the addition of immune-modulators or adjustments to dosing intervals. It is important to note that different bioanalysis methods may yield varying results, typically of a qualitative nature. Although ADA-S/N value correlates well with titer and could serve as an equivalent (25), single S/N value is highly dependent on the assay and its performance, which pose significant challenges for its harmonization and application in clinical practice.

A limitation of the present study is the lack of efficacy data from the longitudinal cohort. The association between ADA levels and treatment relapse was established in a cross-sectional cohort with a small sample size. Notably, the absence of overlap in ADA levels between the relapse and remission groups strengthened the validity of the findings. Therefore, the clinical significance of the provisional threshold based on a limited data set requires additional validation and refinement through well-designed prospective trials. Additionally, the limited sensitivity of NAB assay in comparison to ADA assay prevented the detection of samples with low ADA levels. Fortunately, the NAB assay can cover the samples exceeding the clinical significance threshold (ADA-S/N>10). Moreover, enriched ADA were not typed to subclasses of IgG, which can be performed using specific antibodies if necessary.

Collectively, our study presented an integrated immunoassay platform that combines immunomagnetic separation and ECL technique, tailored for evaluating immunogenicity against adalimumab. By utilizing the highly sensitive and drug-tolerant assays, we were able to comprehensively outline the characteristics of ADA against adalimumab, offering fresh insights into immunogenicity and its clinical implications. Future clinical trials will be essential to determine whether proactive monitoring of ADA levels and drug concentrations is correlated with favorable outcomes.

Data availability statement

The original contributions presented in the study are included in the article/Supplementary Material. Further inquiries can be directed to the corresponding authors.

Ethics statement

The studies involving humans were approved by Institutional Review Board of the First Affiliated Hospital of Soochow University. The studies were conducted in accordance with the local legislation and institutional requirements. The participants provided their written informed consent to participate in this study.

Author contributions

XD: Conceptualization, Data curation, Formal analysis, Funding acquisition, Investigation, Methodology, Project administration, Writing – original draft. LX: Formal analysis, Investigation, Methodology, Writing – original draft. MW: Data curation, Investigation, Resources, Writing – review & editing. SZ: Data curation, Investigation, Writing – review & editing. KZ: Data curation, Investigation, Writing – review & editing. SJ: Data curation, Investigation, Writing – review & editing. JW: Conceptualization, Resources, Writing – review & editing. LM: Conceptualization, Funding acquisition, Project administration, Resources, Writing – review & editing.

Funding

The author(s) declare financial support was received for the research, authorship, and/or publication of this article. This work was supported by National Natural Science Foundation of China (82003857), Jiangsu Provincial Science and Technology Plan Special Fund (BM2023003), Jiangsu Provincial Medical Key Discipline (ZDXK202247), Key R&D Program of Jiangsu Province (BE2021644), Suzhou Health Leading Talent (GSWS2019001), and the Priority Academic Program Development of the Jiangsu Higher Education Institutes (PAPD).

Acknowledgments

We would like to thank the patients. Thanks to Zhongping Yuan Ph.D. (Meso Scale Discovery company) for the technical support.

Conflict of interest

The authors declare that the research was conducted in the absence of any commercial or financial relationships that could be construed as a potential conflict of interest.

Publisher's note

Supplementary material

The Supplementary Material for this article can be found online at: https://www.frontiersin.org/articles/10.3389/fimmu.2024.1429544/full#supplementary-material

References

1. Strand V, Goncalves J, Isaacs JD. Immunogenicity of biologic agents in rheumatology. *Nat Rev Rheumatol*. (2021) 17:81–97. doi: 10.1038/s41584-020-00540-8

2. Atiqi S, Hooijberg F, Loeff FC, Rispens T, Wolbink GJ. Immunogenicity of TNF-inhibitors. *Front Immunol*. (2020) 11:312. doi: 10.3389/fimmu.2020.00312

3. Bartelds GM, Krieckaert CL, Nurmohamed MT, van Schouwenburg PA, Lems WF, Twisk JW, et al. Development of antidrug antibodies against adalimumab and association with disease activity and treatment failure during long-term follow-up. *JAMA*. (2011) 305:1460–8. doi: 10.1001/jama.2011.406

4. Bitoun S, Hassler S, Ternant D, Szely N, Gleizes A, Richez C, et al. Response to biologic drugs in patients with rheumatoid arthritis and antidrug antibodies. *JAMA Netw Open*. (2023) 6:e2323098. doi: 10.1001/jamanetworkopen.2023.23098

5. Baert F, Kondragunta V, Lockton S, Vande Casteele N, Hauenstein S, Singh S, et al. Antibodies to adalimumab are associated with future inflammation in Crohn's patients receiving maintenance adalimumab therapy: a *post hoc* analysis of the Karmiris trial. *Gut*. (2016) 65:1126–31. doi: 10.1136/gutjnl-2014-307882

6. Gorovits B, Baltrukonis DJ, Bhattacharya I, Birchler MA, Finco D, Sikkema D, et al. Immunoassay methods used in clinical studies for the detection of anti-drug antibodies to adalimumab and infliximab. *Clin Exp Immunol*. (2018) 192:348–65. doi: 10.1111/cei.13112

7. Borrega R, Araujo C, Aguiam N, Magro F, Fonseca JE, Danese S, et al. Systematic review and principal components analysis of the immunogenicity of adalimumab. *BioDrugs*. (2021) 35:35–45. doi: 10.1007/s40259-020-00458-3

8. Suh K, Kyei I, Hage DS. Approaches for the detection and analysis of antidrug antibodies to biopharmaceuticals: A review. *J Sep Sci*. (2022) 45:2077–92. doi: 10.1002/jssc.202200112

9. Ogric M, Zigon P, Lakota K, Praprotnik S, Drobne D, Stabuc B, et al. Clinically important neutralizing anti-drug antibodies detected with an in-house competitive ELISA. *Clin Rheumatol*. (2019) 38:361–70. doi: 10.1007/s10067-018-4213-0

10. Wu B, Chung S, Jiang XR, McNally J, Pedras-Vasconcelos J, Pillutla R, et al. Strategies to determine assay format for the assessment of neutralizing antibody responses to biotherapeutics. *AAPS J*. (2016) 18:1335–50. doi: 10.1208/s12248-016-9954-6

11. Myler H, Pedras-Vasconcelos J, Phillips K, Hottenstein CS, Chamberlain P, Devanaryan V, et al. Anti-drug antibody validation testing and reporting harmonization. *AAPS J*. (2021) 24:4. doi: 10.1208/s12248-021-00649-y

12. Myler H, Pedras-Vasconcelos J, Lester T, Civoli F, Xu W, Wu B, et al. Neutralizing antibody validation testing and reporting harmonization. *AAPS J*. (2023) 25:69. doi: 10.1208/s12248-023-00830-5

13. Joyce A, Shea C, You Z, Gorovits B, Lepsy C. Determination of anti-drug antibody affinity in clinical study samples provides a tool for evaluation of immune response maturation. *AAPS J*. (2022) 24:114. doi: 10.1208/s12248-022-00759-1

14. Zeng X, Zhang J, Yu J, Wu X, Chen Y, Wu J, et al. Comparative assessment of pharmacokinetic parameters between HS016, an adalimumab biosimilar, and adalimumab (Humira(R)) in healthy subjects and ankylosing spondylitis patients: Population pharmacokinetic modeling. *Adv Clin Exp Med*. (2022) 31:499–509. doi: 10.17219/acem/145947

15. Xue L, Holford N, Ding XL, Shen ZY, Huang CR, Zhang H, et al. Theory-based pharmacokinetics and pharmacodynamics of S- and R-warfarin and effects on international normalized ratio: influence of body size, composition and genotype in cardiac surgery patients. *Br J Clin Pharmacol*. (2017) 83:823–35. doi: 10.1111/bcp.13157

16. Devanarayan V, Smith WC, Brunelle RL, Seger ME, Krug K, Bowsher RR. Recommendations for systematic statistical computation of immunogenicity cut points. *AAPS J*. (2017) 19:1487–98. doi: 10.1208/s12248-017-0107-3

17. U.S. Food & Drug Administration. Guidance for industry: immunogenicity testing of therapeutic protein products - developing and validating assays for anti-drug antibody detection. (2019).

18. Jawa V, Terry F, Gokemeijer J, Mitra-Kaushik S, Roberts BJ, Tourdot S, et al. T-cell dependent immunogenicity of protein therapeutics pre-clinical assessment and mitigation-updated consensus and review 2020. *Front Immunol*. (2020) 11:1301. doi: 10.3389/fimmu.2020.01301

19. Macdonald PJ, Ruan Q, Grieshaber JL, Swift KM, Taylor RE, Prostko JC, et al. Affinity of anti-spike antibodies in SARS-CoV-2 patient plasma and its effect on COVID-19 antibody assays. *EBioMedicine*. (2022) 75:103796. doi: 10.1016/j.ebiom.2021.103796

20. Ding X, Zhu R, Wu J, Xue L, Gu M, Miao L. Early adalimumab and anti-adalimumab antibody levels for prediction of primary nonresponse in ankylosing spondylitis patients. *Clin Transl Sci*. (2020) 13:547–54. doi: 10.1111/cts.12738

21. Jiang H, Xu W, Titsch CA, Furlong MT, Dodge R, Voronin K, et al. Innovative use of LC-MS/MS for simultaneous quantitation of neutralizing antibody, residual drug, and human immunoglobulin G in immunogenicity assay development. *Anal Chem*. (2014) 86:2673–80. doi: 10.1021/ac5001465

22. Jiang Z, Kamerud J, Zhang M, Ruiz CC, Guadiz C, Fichtner A, et al. Strategies to develop highly drug-tolerant cell-based neutralizing antibody assay: neutralizing antidrug antibodies extraction and drug depletion. *Bioanalysis*. (2020) 12:1279–93. doi: 10.4155/bio-2020-0091

23. Wickramarachchi D, Wagner J, Woo T, Ferrari F, Steinmetz T, Helmy R, et al. A novel neutralization antibody assay method to overcome drug interference with better compatibility with acid-sensitive neutralizing antibodies. *AAPS J*. (2023) 25:18. doi: 10.1208/s12248-023-00783-9

24. Ren A, Sohaei D, Ulndreaj A, Pons-Belda OD, Fernandez-Uriarte A, Zacharioudakis I, et al. Ultrasensitive assay for saliva-based SARS-CoV-2 antigen detection. *Clin Chem Lab Med*. (2022) 60:771–7. doi: 10.1515/cclm-2021-1142

25. Starcevic Manning M, Hassanein M, Partridge MA, Jawa V, Mora J, Ryman J, et al. Comparison of titer and signal to noise (S/N) for determination of anti-drug antibody magnitude using clinical data from an industry consortium. *AAPS J*. (2022) 24:81. doi: 10.1208/s12248-022-00728-8

26. Partridge MA, Karayusuf EK, Shyu G, Georgaros C, Torri A, Sumner G. Drug removal strategies in competitive ligand binding neutralizing antibody (NAb) assays: highly drug-tolerant methods and interpreting immunogenicity data. *AAPS J*. (2020) 22:112. doi: 10.1208/s12248-020-00497-2

27. Su J, Li M, He L, Zhao D, Wan W, Liu Y, et al. Comparison of the efficacy and safety of adalimumab (Humira) and the adalimumab biosimilar candidate (HS016) in chinese patients

with active ankylosing spondylitis: A multicenter, randomized, double-blind, parallel, phase III clinical trial. *BioDrugs*. (2020) 34:381–93. doi: 10.1007/s40259-020-00408-z

28. Ungar B, Engel T, Yablecovitch D, Lahat A, Lang A, Avidan B, et al. Prospective observational evaluation of time-dependency of adalimumab immunogenicity and drug concentrations: the POETIC study. *Am J Gastroenterol*. (2018) 113:890–8. doi: 10.1038/s41395-018-0073-0

29. Cortese M, Sherman AC, Rouphael NG, Pulendran B. Systems biological analysis of immune response to influenza vaccination. *Cold Spring Harb Perspect Med*. (2021) 11:a038596. doi: 10.1101/cshperspect.a038596

30. Grasmeier MK, Langmann AF, Langmann P, Treiber M, Thaler MA, Luppa PB. Dynamics of serum concentrations of antibodies to infliximab: a new approach for predicting secondary loss of response in inflammatory bowel diseases. *Therap Adv Gastroenterol*. (2021) 14:17562848211037849. doi: 10.1177/17562848211037849

31. van Schouwenburg PA, Krieckaert CL, Rispens T, Aarden L, Wolbink GJ, Wouters D. Long-term measurement of anti-adalimumab using pH-shift-anti-idiotype antigen binding test shows predictive value and transient antibody formation. *Ann Rheum Dis*. (2013) 72:1680–6. doi: 10.1136/annrheumdis-2012-202407

32. Sandborn WJ, Wolf DC, Kosutic G, Parker G, Schreiber S, Lee SD, et al. Effects of transient and persistent anti-drug antibodies to certolizumab pegol: longitudinal data from a 7-year study in crohn's disease. *Inflammation Bowel Dis*. (2017) 23:1047–56. doi: 10.1097/MIB.0000000000001100

33. Arunachalam PS, Scott MKD, Hagan T, Li C, Feng Y, Wimmers F, et al. Systems vaccinology of the BNT162b2 mRNA vaccine in humans. *Nature*. (2021) 596:410–6. doi: 10.1038/s41586-021-03791-x

34. Vaisman-Mentesh A, Rosenstein S, Yavzori M, Dror Y, Fudim E, Ungar B, et al. Molecular landscape of anti-drug antibodies reveals the mechanism of the immune response following treatment with TNFalpha antagonists. *Front Immunol*. (2019) 10:2921. doi: 10.3389/fimmu.2019.02921

35. Huang X, Xu X, Partridge MA, Chen J, Koehler-Stec E, Sumner G, et al. Isotyping and semi-quantitation of monkey anti-drug antibodies by immunocapture liquid chromatography-mass spectrometry. *AAPS J*. (2021) 23:16. doi: 10.1208/s12248-020-00538-w

36. van Strien J, Dijk L, Atiqi S, Schouten R, Bloem K, Wolbink GJ, et al. Drug-tolerant detection of anti-drug antibodies in an antigen-binding assay using europium chelate fluorescence. *J Immunol Methods*. (2023) 514:113436. doi: 10.1016/j.jim.2023.113436

37. Vaisman-Mentesh A, Gutierrez-Gonzalez M, DeKosky BJ, Wine Y. The molecular mechanisms that underlie the immune biology of anti-drug antibody formation following treatment with monoclonal antibodies. *Front Immunol*. (2020) 11:1951. doi: 10.3389/fimmu.2020.01951

38. van Schouwenburg PA, Kruithof S, Votsmeier C, van Schie K, Hart MH, de Jong RN, et al. Functional analysis of the anti-adalimumab response using patient-derived monoclonal antibodies. *J Biol Chem*. (2014) 289:34482–8. doi: 10.1074/jbc.M114.615500

39. van Schie KA, Hart MH, de Groot ER, Kruithof S, Aarden LA, Wolbink GJ, et al. The antibody response against human and chimeric anti-TNF therapeutic antibodies primarily targets the TNF binding region. *Ann Rheum Dis*. (2015) 74:311–4. doi: 10.1136/annrheumdis-2014-206237

40. Homann A, Rockendorf N, Kromminga A, Frey A, Platts-Mills TA, Jappe U. Glycan and peptide igE epitopes of the TNF-alpha blockers infliximab and adalimumab - precision diagnostics by cross-reactivity immune profiling of patient sera. *Theranostics*. (2017) 7:4699–709. doi: 10.7150/thno.20654

frontiers | Frontiers in Immunology

TYPE Original Research
PUBLISHED 11 November 2024
DOI 10.3389/fimmu.2024.1438251

OPEN ACCESS

EDITED BY
Michael Tovey,
Svar Life Science, France

REVIEWED BY
Gerson D. Keppeke,
Universidad Católica del Norte, Chile
Linlin Luo,
Merck, United States

*CORRESPONDENCE
Charlotte Hagman
charlotte.hagman@novartis.com

RECEIVED 25 May 2024
ACCEPTED 16 October 2024
PUBLISHED 11 November 2024

CITATION
Hagman C, Chasseigne G, Nelson R, Anlauff F, Kagan M, Goldfine AB, Terszowski G and Jadhav M (2024) Immunogenicity assessment strategy for a chemically modified therapeutic protein in clinical development.
Front. Immunol. 15:1438251.
doi: 10.3389/fimmu.2024.1438251

Immunogenicity assessment strategy for a chemically modified therapeutic protein in clinical development

Charlotte Hagman[1]*, Gaetan Chasseigne[1], Robert Nelson[2], Florian Anlauff[2], Mark Kagan[3], Allison B. Goldfine[4], Grzegorz Terszowski[1] and Maria Jadhav[5]

[1]Pharmacokinetic Sciences - Drug Disposition, Biomedical Research, Novartis, Basel, Switzerland, [2]BioAgilytix Laboratories, Hamburg, Germany, [3]Pharmacokinetic Sciences, Biomedical Research, Novartis, East Hanover, NJ, United States, [4]Translational Medicine, Biomedical Research, Novartis, Cambridge, MA, United States, [5]Pharmacokinetic Sciences - Drug Disposition, Biomedical Research, Novartis, Cambridge, MA, United States

The clinical immunogenicity assessment for complex multidomain biological drugs is challenging due to multiple factors that must be taken into consideration. Here, we describe a strategy to overcome multiple bioanalytical challenges in order to assess anti-drug antibodies (ADA) for a novel and unique chemically modified protein therapeutic. A risk-centered approach was adopted to evaluate the immunogenic response to a modified version of human growth differentiation factor 15 (GDF15) connected to an albumin-binding fatty acid via a polyethylene glycol (PEG) linker. Key steps include monitoring anti-drug antibodies (ADAs), using a standard tiered approach of screening and confirmation. To deepen our understanding of ADA response, as a third tier of immunogenicity assessment, novel extensive characterization using a set of assays was developed, validated, and used routinely in clinical sample analysis. This characterization step included performance of titration, mapping of ADA response including anti-GDF15 and anti-PEG–fatty-acid antibody characterization, and assessment of the neutralizing anti-drug antibodies (NAbs) using cell-based assays for immunogenicity in parallel. The analytical methods were applied during two clinical trials involving both healthy volunteers and overweight or obese patients. We observed low incident rates for ADA and no ADAs against the PEG linker with fatty acid conjugation. In one of the clinical studies, we identified neutralizing ADAs. The proposed novel strategy of extensive characterization proved effective for monitoring the presence of ADAs and NAbs and can be used to support clinical development of a broad range of chemically modified proteins and multidomain biotherapeutics.

KEYWORDS

immunogenicity, clinical development, therapeutic proteins, chemical modification, endogenous counterpart

Introduction

The first monoclonal antibody therapeutic was approved by the Food and Drug Administration (FDA) in 1986 (1), consisting of human/mouse chimeric sequences. Since this time, drug developers have worked extensively to improve the pharmacokinetic (PK), pharmacodynamic (PD), and immunogenicity profile of therapeutic antibodies and proteins primarily through sequence optimization. More recently, structural and chemical modifications such as PEGylation (2), glycosylation (3), and lipidation (4) have been introduced resulting in multidomain biotherapeutics (MDB) (5, 6) with enhancements in stability, aggregation, adsorption, and degradation, in addition to PK, PD, and immunogenicity improvements. For example, in 2013, a recombinant anti-hemophilic factor VIII was approved to treat and prevent bleeding in patients with hemophilia A (7, 8). The medicine required several doses per day during bleeding episodes. To improve the pharmacokinetic properties and reduce the patient burden of frequent administration, the active substance was chemically modified by linking a polyethylene glycol (PEG) polymer chain (PEGylation) resulting in a new active substance with reduced clearance and a longer half-life, which was approved by the FDA in 2019 (9). However, these modifications may lead to anti-drug antibody (ADA) formation not only to the protein itself but also to the newly formed potentially immunogenic epitopes at points of chemical modification or to the PEG part of the molecule (10). Considering this, the bioanalytical strategy to monitor ADAs during clinical development must address these concerns by developing multiple assays for the ADA characterization.

Immunogenicity can lead to failure of a product in the late stages of clinical development and is a critical consideration in the development of biotherapeutics. Most biologic molecules induce different levels of immune response in treated individuals, potentially leading to the formation of ADAs, the impact of which can range from no observable consequence to, in more extreme cases, substantial impacts on exposure, efficacy, and safety of the administrated drug (11). The situation becomes more complex when the drug contains homology, or partial homology, with an endogenous peptide or protein. In these cases, antibodies raised to the drug may cross-react with the endogenous counterpart, increasing the potential risk of safety-related events. Antibodies to the endogenous peptide can be sustained. Additionally, the presence and impact of preexisting antibodies is often a concern for modified or multidomain proteins, with a high prevalence reported for antibody fragments (12) and PEG (2, 10, 13).

Industry best practices (14–16) and regulatory guidance (14, 17) provide a framework to assess the incidence, magnitude, and clinical impact of the humoral (antibody) immune response to biotherapeutics. It is recommended to establish assays to monitor ADAs throughout the whole life cycle of drug development (14, 17). In the case of antibodies induced against a drug containing an endogenous counterpart, assessment of the neutralization potential of these ADAs to the drug and also to the endogenous counterpart at the entry into clinical development is often a requirement (15, 18, 19). The existence of neutralizing ADAs (NAb) is often correlated with a lower clinical response to the administered drug (20, 21).

An immunogenicity monitoring strategy was developed and implemented to support the clinical development program of a novel complex biologic therapeutic in early clinical development. For a multidomain biotherapeutics drug of this format, several aspects were considered when defining the strategy since each conjugation results in unique domain interfaces (22, 23). The risk assessment is based on numerous factors such as B lymphocyte and T lymphocyte cell epitopes, the presence of endogenous counterparts, and the formulation and availability of pharmacodynamic biomarkers (15, 17).

At the time of the initiation of the first in human (FIH) study for the described drug, no reliable clinical pharmacodynamic biomarkers for target engagement or response prediction had been previously identified that could serve as indicators of safety and efficacy. GDF15 is involved in energy regulation by suppressing food intake and is thought to play an important role in metabolic disease (24); thus, a conservative immunogenicity approach was developed. From an immunogenicity risk assessment standpoint, we assessed the drug as a high-risk molecule as it is additionally chemically modified, thereby justifying the extensive immunogenicity strategy that was proposed and implemented.

Taking into consideration the unique and novel structure of the chemically modified drug, while designing a bioanalytical strategy, we had to take into consideration both the high-risk nature of the protein part of the biotherapeutic, chemical modification that could potentially create novel immunogenic epitopes and the PEG linker. To address these considerations, a conventional assessment ADA-tiered approach with a novel extensive panel of characterization assays run in parallel was used.

The ADA assays developed for the protein therapeutic consisted of a screening assay and a confirmatory assay to detect ADA against the whole protein including modifications, and an extended set of characterization assays which were requested by regulatory authorities (14, 17). These characterization assays consisted of a titration assay to evaluate the magnitude of ADA response to the whole protein, and then two domain-specific characterization assays to assess whether ADAs were specific for endogenous GDF15 and or specific for the modification with PEG linker + fatty acid. Furthermore, two neutralizing cellular assays were developed, one for the detection of neutralizing antibodies against the whole therapeutic protein (GDF15 and PEG linker + fatty acid) and one against the protein domain of the therapeutic protein (GDF15). Together, an approach of performing these five assays applied in parallel allowed for detailed characterization of the immunogenicity response to this multidomain biotherapeutics to support a first-in-man and a proof-of-concept study.

Materials and methods

Source of human serum samples

Human serum samples were obtained from two clinical studies. The first was an exploratory, randomized, investigator- and subject-blinded, sponsor open-label, placebo-controlled first in-human-study of single ascending subcutaneous doses (SAD) of the therapeutic protein. The study was conducted from August 2019

through November 2021, at two research sites in the United States. The second was a non-confirmatory, randomized, placebo-controlled, participant- and investigator-blinded, sponsor open-label study in which participants received up to eight biweekly subcutaneous doses of the therapeutic protein. The study was conducted from February 2022 to May 2023, at four clinical research sites in the United States. Institutional Review Board approvals were obtained for each site for both studies from Advarra (Columbia, MD), and trials were conducted according to the Declaration of Helsinki.

Detection of anti-drug antibodies with acid dissociation

Anti-drug antibodies (ADAs) to the chemically modified GDF15 (the drug) were detected using a validated electrochemiluminescence (ECL) assay on the Meso Scale Discovery (MSD) platform. According to the Health Authorities guidelines, the assays were developed to detect both IgG and IgM, (Figure 1, AI). An equimolar mix of three anti-human GDF15 monoclonal antibodies was used as a surrogate positive control antibody pool (SPC) (14).

The poor solubility of the protein therapeutic at neutral pH did not allow chemical conjugation with biotin or SULFO-TAG necessary to set up ADA bridging, and industry-standard SPEAD (Solid Phase with Extraction Acid Dissociation) and PandA (Precipitation and Acid dissociation) assay formats were implemented (25, 26). Instead, a sequential ECL immunoassay was developed with a drug-target-mediated drug removal pretreatment step to improve drug tolerance. For this purpose, complexes of anti-drug antibodies with the drug in samples were dissociated with 300 mM acetic acid (Figure 1, AII). Following neutralization of the acidified samples with Tris buffer, the samples were immediately transferred to nickel plates on which a His-tagged drug target (GDNF family receptor alpha-like, GFRAL) was immobilized. At neutral pH, the drug target competed with ADAs for drug binding; the drug was captured by its target and thereby removed from the samples. To reach sufficient drug tolerance, this drug removal step was repeated with a second drug-target-immobilized nickel plate (Figure 1, AIII). The supernatants from the nickel plates contained the un-complexed ADAs (pretreated samples). For screening and titration assays, the supernatant was then diluted with low cross buffer; for the confirmatory assays, it was diluted with the respective confirmatory agent (the drug, the GDF15 protein, or the PEG-fatty acid residue) and preincubated for 30 min before being transferred to MSD standard plates coated with the drug (Figure 1, AIV). Bound ADAs were then detected via their Fc region by using a combination of SULFO-TAG-conjugated goat polyclonal anti-human IgG (Southern Biotech 2049-01; Sulfo-Tag NHS Ester (MesoScale Discovery R91AO-1) and SULFO-TAG-conjugated goat anti-human IgM antibody [Southern Biotech 2020-01; Sulfo-Tag NHS Ester (MesoScale Discovery R91AO-1)] (Figure 1, AV). The electrical excitation of the Sulfo-Tag is mediated by a redox reaction and leads to light emission. The light intensity quantified by the system is proportional to the amount of bound antibody complexes and is output in the form of relative light units (RLUs) (Figure 1, I).

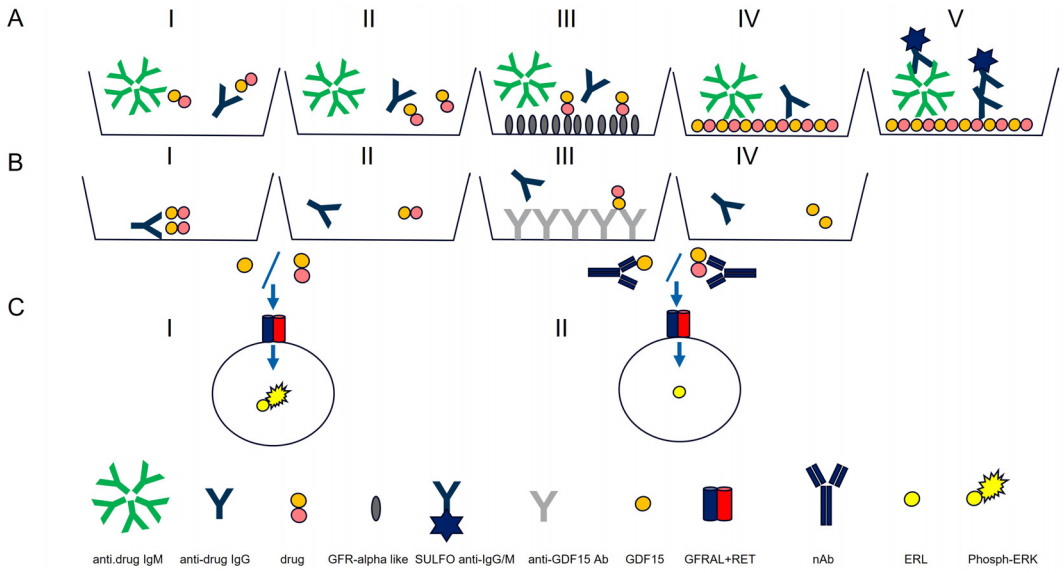

FIGURE 1
Antibody assay **(A)** and neutralizing antibody assays (Nab) **(B, C)**. Antibody assay: AI) ECL assay for IgG and IgM detection. AII) Acid dissociation to improve drug tolerance. AIII) Drug capture with immobilized GFRAL to remove access of drug. AIV) Drug-coated MSD plate used to capture IgG and IgMs. AV) Detection with SULFO-TAG polyclonal anti-human IgG and IgM. Neutralizing antibody assays: BI) PEG treatment. BII) Acid dissociation of co-precipitated drug. BIII) Drug capture by immobilized anti-GDF15 antibodies. BIV) Purified sample. Neutralizing antibody assays: CI) Purified sample mixed with GDF15 or drug and incubated with HEK293-hGFRAL/RET cells (29). Sample with no NAbs results in high ERK phosphorylation). CII) Purified sample containing NAbs mixed with GDF15 or drug and incubated with HEK293-hGFRAL/RET cells. The presence of neutralizing ADAs decreases the interaction with the hGFRAL/RET receptor resulting in a lower ERK phosphorylation.

To distinguish between the ADA directed against the chemically modified GDF15 (the drug), the protein backbone (GDF15) and the PEG linker + fatty acid domain, three confirmatory assays were established in which an excess of chemically modified GDF15 (confirmatory I), GDF15 protein (confirmatory II), or PEG linker + fatty acid residue (confirmatory III) domain-specifically suppresses the ADA-induced signals. Validation of the confirmatory assay included definition of the confirmatory cut point (CCP) for all three confirmatory assays. Due to the exploratory nature of ADA cross-reactivity assessments in confirmatory II (GDF15) and confirmatory III (PEG-fatty acid) assays, evaluations of precision, sensitivity, and matrix effects were not conducted for these confirmatory assays, whereas the same parameters have been assessed for anti-drug confirmatory assay.

The minimum required dilution (MRD) of 1:50 in the screening and confirmatory assays represents the cumulative dilution of the samples during sample pretreatment and final dilution in LowCross-Buffer.

Screening cut point

The screening cut point (SCP) is defined as the level of response at which a sample is screening assay positive for the presence of anti-drug antibodies. As assay responses vary between plates, a floating screening cut point is generally recommended (16, 27, 28). The requirement of a floating screening CP was shown by a positive correlation of mean sample signal level per plate versus mean negative control (NC) signal level per plate for all CP runs in scatter plot analyses. A floating screening cut point was established that uses a statistically determined screening cut point factor (SCPF) to normalize the CP to the NC of the respective plates: The plate-specific CP = SCPF × (plate mean NC). To establish the SCPF, 51 individual samples from untreated healthy subjects were analyzed in duplicate in six independent preparations in a semi-balanced design (see "Statistical Evaluation").

Confirmatory cut points

The CCP is defined as the inhibition percentage at or above which a sample is considered confirmed positive for anti-drug antibodies. Three CCPs were established, CCP-I, specific for the chemically modified GDF15, a characterizing CCP-II, specific for the protein backbone of the drug (GDF15), and another characterizing CCP-III, specific for the PEG linker + fatty acid moiety of the drug. To establish the CCP-I for the drug, 51 drug-naïve serum samples from untreated healthy subjects were analyzed in the presence (i.e., inhibited sample) and absence (i.e., uninhibited sample) of the drug in six independent determinations. The percentage of signal inhibition between drug-spiked and non-spiked samples is determined for each individual serum sample as follows: Signal inhibition % = [1-(signal of drug spiked sample/signal of neat sample)] * 100%. A non-parametric approach was used, with analytical outliers being removed based on Tukey box plot outlier test on stacked subject-level residuals (see "Statistical Evaluation" in "Materials and Methods". The target false positive rate was 1% (16, 27).

To establish the CCP-II (for GDF15) and CCP-III (for PEG linker + fatty acid), respectively, 30 drug-naïve serum samples from untreated healthy subjects were analyzed in the presence (i.e., inhibited sample) and absence (i.e., uninhibited sample) of GDF15 (5 µg/mL) or PEG linker + fatty acid (1.14 µg/mL equimolar to 20 µg/mL drug) in six independent determinations. Analytical outliers were removed based on Tukey box plot outlier test on stacked subject-level residuals (see "Statistical Evaluation"). The target false positive rate was 1%.

MBL949 and GDF15 neutralizing antibody assays

The ability of anti-drug antibodies to inhibit the drug's or endogenous GDF-15 activity was explored in a HEK293 cell line co-expressing the human GFRAL receptor and RET receptor on the surface. pIRES plasmid including subcloned sequences encoding hGFRAL and hRET51 was used for creation of a stably transfected cell line. Alternatively, a commercially available source can be used (29). Stimulation of the HEK293-hGFRAL/RET cells with drug or GDF15 triggered an intracellular signaling cascade leading to ERK phosphorylation. ERK phosphorylation in relation to total non-phosphorylated ERK was used as assay readout. Assay controls were prepared with a surrogate positive control antibody (monoclonal antibody directed against GDF15).

Similarly to the ADA assay, the inability to chemically conjugate the drug did not allow SPEAD NAb assay formats, which would have been ideal to remove interfering matrix components such as growth factors causing unspecific ERK phosphorylation in this assay and to remove free drug to improve drug tolerance of the assay (26). Instead, all confirmed ADA-positive serum samples were pretreated by PEG treatment (12.5% PEG 6000) that precipitated unspecific antibodies, drug, and drug–ADA complexes (Figure 1, BI) (30, 31). To improve drug tolerance, the co-precipitated drug was released from antibody–drug complexes by 300 mM acetic acid (Figure 1, BII) and captured by immobilized anti-GDF15 antibodies (II) (Figure 1, BIII). Purified samples (Figure 1, BIV) were mixed with drug or GDF-15 depending on the specificity of the NAb assay (detection of neutralizing antibody assays (NAbs) against drug or against GDF15) at a concentration of 0.3 nM and added to pre-seeded HEK293-hGFRAL/RET cells. The binding of the drug or GDF15 to the GFRAL/RET complex induces ERK phosphorylation (Figure 1, CI). After 20 min of incubation, cells were lysed with a lysis buffer (Tris Lysis buffer, MSD R60TX-3; Protease Inhibitor Solution, MSD K15707D-3: Phosphatase Inhibitor Solution I, MSD K15707D-3; Phosphatase Inhibitor Solution I, MSD K15707D-3; AEBSF, Sigma A8456; SDS solution MSD K15707D-3), lysates were stored at −80°C till further measurement. The level of ERK phosphorylation in the cell lysates was measured as a drug/ligand activity marker using the Phospho/Total ERK1/2 Whole Cell Lysate Kit from Meso Scale Discovery. In the presence of neutralizing antibodies, drug/GDF-15 binding to the hGFRAL/RET receptor complex was inhibited, leading to a lower ERK phosphorylation

level (Figure 1, CII). The ERK phosphorylation level inversely correlated with the amount of neutralizing antibodies present in the sample.

The ERK phosphorylation level was calculated with the phospho-ERK1/2 and total ERK1/2 signals obtained from each sample by converting them to respective % phosphoprotein values, as described in the MSD manual (Phospho/Total ERK1/2 Whole Cell Lysate Kit) using the following formula:

$$\%\,\text{phospho} - \text{protein} = ((2 \times \text{pERK} - \text{signal}) / (\text{pERK} - \text{signal} + \text{Erk1/2} - \text{signal})) \times 100$$

The % phospho-protein values were further normalized to the upper and lower signal controls that defined the dynamic range of the assay (upper signal controls = whole drug or GDF15 added to cells = 0% of inhibition; low signal control = cells without whole drug/GDF15 stimulation = 100% of whole drug/GDF15 inhibition).

$$\%\ \text{inhibition} = 100 - ((\%\ \text{phospho} - \text{protein of sample} - \%\ \text{phospho} - \text{protein of low signal control}) / (\%\ \text{phospho} - \text{protein of high signal control} - \%\ \text{phospho} - \text{protein of low signal control})) * 100$$

Cut point determination for anti-drug/anti-GDF-15 neutralizing antibody assays

The assay cut point (CP) is defined as the level of response of the assay at and above which a sample is positive for the presence of neutralizing antibodies. Assay cut points for the anti-drug and anti-GDF15 neutralizing assays were determined by using 30 individual drug-naive self-declared healthy subjects. Those samples were analyzed in duplicate in six independent preparations (see Statistical Evaluation). To calculate the CP, the readout of each sample was normalized to internal run controls that determine the plate specific upper and lower dynamic range level (negative control without stimulating drug/negative control sample with stimulating drug) to minimize inter-run variability of the assay signal. Due to the fast ERK phosphorylation kinetics after cell stimulation, depending on the location of the sample on the plate (left third, center third, or right third), an individual normalization routine was applied to corresponding location-specific upper and lower dynamic range controls. Samples and assay performance controls located in the left third of the plate in columns 1–4 were normalized to upper and lower dynamic range controls located in the left third of the plate, whereas samples and assay performance controls located in the right third of the plate in columns 9–12 were normalized to upper and lower dynamic range controls located in the right third of the plate and samples located in the center third of the plate in columns 5–8 were normalized to the mean of the upper and lower dynamic range controls located in the left third and the right third of the plate. In total, there was one upper and one lower dynamic range control each in duplicates placed in the left third of the plate, and one upper and one lower dynamic range control each in duplicates placed in the right third of the plate. This normalization routine reduced the effect of the unpreventable plate drift effects in the raw signals on normalized signals.

Analytical outlier values in both neutralizing assays were identified using a box-plot analysis from stacked subject-level residuals (27). Subsequently, a biological outlier was identified by Tukey box plot analysis and excluded from CP determination (see "Statistical Evaluation"). The CPs for drug NAb and GDF15 NAb employed a parametric approach.

Statistical evaluation

The statistical analysis performed to determine the ADA assay cut point was based on the strategy and considerations outlined by Shankar et al.; the concept was further developed by Devanarayan et al. Following the recommendation of using at least 50 drug-naive individual samples for cut point determination, the experimental set up of the cut point assessment was designed in a balanced fashion (27) with three sample groups (A, B, and C) comprising 17 individual samples each. Each sample group was analyzed on each of the three plates per assay run, leading to 306 data points (51 individuals, analyzed 6 times). Samples were analyzed in the screening non-drug spiked and whole-drug confirmatory in parallel.

The ADA screening cut point factor was established with mean plate NC-normalized (signal to noise) and log-transformed values with outliers being removed. Analytical outliers were identified by the evaluation of the differences of signal-to-noise results of each determination of a subject sample from the median signal-to-noise value of the corresponding subject. These obtained subject-level residuals were analyzed stacked using Tukey's outlier box plot, where samples above and below the defined limits were considered as analytical outlier:

$$\text{Upper outlier limit}: 75\text{th percentile} + 1.5 \times (75\text{th percentile} - 25\text{th percentile}),$$

$$\text{Lower outlier limit}: 25\text{th percentile} - 1.5 \times (75\text{th percentile} - 25\text{th percentile}).$$

Acknowledging a heterogenous signal distribution in the cut point data set and the fact that excluding statistical outlier from the data set lowers the determined screening cut point factor, a conservative strategy for cut point determination was chosen with box plot constant k = 1.5 instead of k = 3, as recommended by Devanarayan et al. (27). This lowered the threshold for outlier selection and allowed the removal of more outlier values from the data set resulting in a lower screening cut point factor which enabled the detection of signal increase in low signal samples at the expense of a higher false positive rate in the screening assay.

After analytical outlier elimination (37 out of 306 data points), the medians of the remaining subject-specific signal-to-noise determinations were assessed for biological outliers using Tukey's box plot (27). Subjects with signal-to-noise medians above or below the defined limits were considered as biological outliers and removed (three subjects with a total of eight remaining data points out of 269 data points after analytical outlier removal).

The 261 remaining data points were stacked and assessed for normality. As the dataset was abnormally distributed and skewness <1, the robust parametric approach was followed. The screening cut point factor was determined as the anti-log of the median of log-transformed signal to noise values + 1.645 × (1.4826 × median absolute deviation) targeting a false positive rate of >5%.

The ADA confirmatory cut point determination for drug (CCP-I) was based on 306 data points, using the same strategy as for the screening cut point factor result. In short, % inhibition values obtained for the 51 individuals analyzed six times were assessed for analytical outlier by applying Tukey's box plot analysis on stack subject-level residuals (individual differences of each determination to the median of the respective subject specific determinations). Analytical outliers were removed (22 out of 306 data points), and the remaining data set was assessed for biological outliers (three subjects with a total of 16 data points out of 284 data points after analytical outlier removal) by applying again Tukey's box plot analysis on the subject specific medians. The final outlier cleaned data set (268 data points) was assessed for normality using the Shapiro–Wilk normality test, and the data set was abnormally distributed with skewness < 1. The robust-parametric method was not considered as it would result in a lower confirmatory cut point factor compared with the non-parametric approach with a confirmatory assay sensitivity < screening assay sensitivity. Considering the tired approach in which only preselected samples from the screening assay are intended for confirmatory assay analysis, for the sake of assay robustness, the higher CCP-I determined by the non-parametric approach was selected (99th percentile of all signal inhibitions excluding outliers). The CCP-I targets a false positive rate of 1%.

The ADA confirmatory cut points for the characterizing assays (GDF15 and PEG linker + fatty acid modification, CCP-II and CCP-III respectively) followed the same rationale as outlined above only that the number of drug-naive samples to be assessed six times was reduced to 30 leading to a data set with 180 data points. A parametric approach was used for CCP-II (GDF15), and a non-parametric approach was used for CCP-III (PEG linker + fatty acid), with analytical outliers (18 out of 180 data points for CCP-II, 15 out of 180 data points for CCP-III) being removed based on the box plot outlier test on stacked differences of each sample to the respective median of samples of each subject. Biological outliers (one subject with three data points out of remaining 162 data points for CCP-II after removal of analytical outlier and one subject with four data points out of remaining 165 data points for CCP-III after removal of analytical outlier) were subsequently removed based on a box plot outlier test on the respective medians of the six values for the 30 samples, leaving a final data set of 159 data points for CCP-II and 161 data points for CCP-III. CCP-II (GDF15) was calculated using the mean + 2.33* SD of all signal inhibitions excluding outliers, whereas CCP-III (PEG linker + fatty acid) was calculated using the 99th percentile of all signal inhibitions excluding outliers (27). Both CCP-II and CCP-III target a false positive rate of 1%.

For the drug and GDF15 NAb assays, 30 drug-naive samples were assessed six times (total of 180 datapoints) to establish the two cut points. The % inhibition values obtained for the 30 individuals were assessed for analytical outlier by applying Tukey's box plot analysis on stack subject-level residuals (individual differences of each determination to the median of the respective subject-specific determinations). For the drug NAb assay cut point, 11 analytical outliers and one subject with five remaining data points as biological outliers were removed from the data set leading to 164 remaining data points. The final data set was normally distributed, and the cut point established the anti-log of the mean of % inhibition values + 2.33 × SD targeting a false positive rate of 1%. For the GDF15 NAb assay cut point, 11 analytical outliers and one subject with five remaining data points as biological outliers were removed from the data set leading to 164 remaining data points. The final data set was normally distributed, and the cut point established the anti-log of the mean of % inhibition values + 2.33 × SD targeting a false positive rate of 1% (27).

Results

Immunogenicity assessment strategy

The clinical testing strategy for immunogenicity involves the use of screening and confirmatory assays to detect ADAs, followed by extensive characterization including titration, domain mapping, and assessment for neutralizing anti-drug antibodies (NAb) (Figure 2). This strategy is in line with the current recommendation of Health Authorities, *i.e.*, EMA 2017 and FDA 2019 (14, 17). The ADA assay initially screens to identify samples that show a positive ADA response, and the screening assay detects both anti-drug IgG and IgM antibodies (14). To confirm the presence of ADAs, the drug-specific confirmatory assay is conducted. Once the drug-specific confirmatory assay yields positive results, a panel of parallel analysis is performed to characterize the ADA response further. Taking into consideration chemical modification of the therapeutic protein, characterization of the ADA response to evaluate drug domain specificity is employed. Here, a GDF15 spike to the sample leads to ADA/GDF15 complex formation and suppression of GDF15-specific ADA signals in comparison with a buffer-spiked sample. Similarly, the ADA confirmatory PEG linker + fatty acid assay focuses on the ADA response related to the PEG linker + fatty acid domain, when signals induced by PEG linker + fatty acid domain-spiked samples are compared with respective buffer-spiked sample signals. ADA titration provided semiquantitative characterization of the magnitude of the immune response in study samples.

Since the therapeutic drug is designed to mimic the endogenous counterpart (GDF15), in addition to the ADA characterization assays, the corresponding samples were analyzed using the drug and GDF15 NAb assays. The drug-specific NAb assay is designed to detect neutralizing antibodies against the drug, whereas the NAb GDF15 assay specifically targets the neutralizing antibodies against the endogenous GDF15.

A pseudo polyclonal positive control (PC) was created by combining three monoclonal antibodies in equal amounts to produce an equimolar mixture (14, 18). The pseudo-PC was then used to characterize the assays and served as a control to ensure consistent performance for ADA assays. This novel approach allowed a streamlined process of resupplying critical reagents and

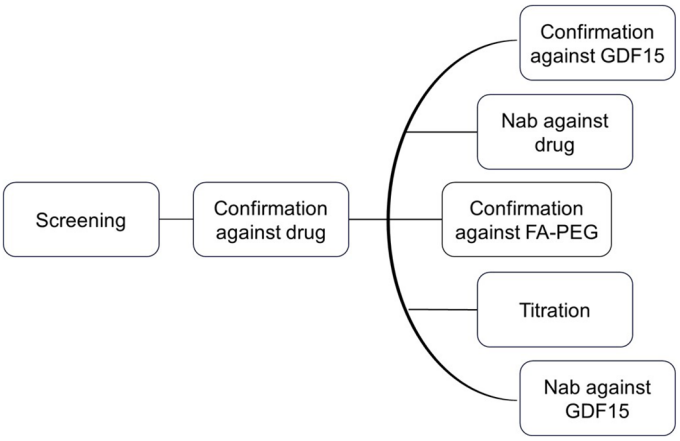

FIGURE 2
Clinical testing strategy for immunogenicity. The ADA assay initially screens for samples with a positive ADA response. To confirm the presence of ADAs, a drug-specific confirmatory assay is conducted. If the confirmatory assay is positive, a panel of parallel analyses is performed to further characterize the ADA response.

simplifying the assessment as well as requalification of assays of an extensive immunogenicity assessment package.

ADA validation results

The determined screening assay cut point (SCP) factor was 1.35. The SCP data set was characterized by an inhomogeneous signal distribution with elevated signals in several drug-naive samples. Most of these high signal samples were identified as outliers in the Tukey box plot analyses and thus removed prior to SCPF calculation. Therefore, the false positive rate (FPR) on the cut point data set including outliers was 17.6% and the FPR excluding outliers was 9.6% (27). While the 9.6% is significantly larger than the targeted FPR of 5%, following a conservative screening strategy, a higher false positivity was accepted to be able to detect induced immunogenicity in low signal samples.

Multiple confirmatory cut points corresponding to the different domains were assessed. The Confirmatory cut point for the drug (CCP-I) was 29.5%. Even though in both SCP and CCP-I data sets three biological outliers were identified, these outlier samples were different for screening and confirmatory assay and none of the samples with high signals in the screening assay could be confirmed in the confirmatory assay. This suggested that the high signals in part of the SCP data set were not caused by preexisting ADAs (*e.g.*, against the PEG linker + fatty acid domain). The FPR on data set including outliers was 2.0%, and the FPR excluding outliers was 0.7% which is considered acceptable for the drug confirmatory assay, where 1% FPR was targeted (27). The confirmatory cut point for GDF15 (CCP-II) was 24.8%. The FPR on the cut point data set including outliers was 1.7%, and the FPR excluding outliers was 0.6%. Considering the data set size (total n = 180), 0.6% FPR is considered acceptable for the characterizing confirmatory assays, where 1% FPR was targeted (27). The confirmatory cut point for PEG linker + fatty acid (CCP-III) was 18.0%. The FPR on the cut point data set including outliers was 2.2%, and the FPR excluding outliers was 0.6%. Considering the data set size (total n = 180), 0.6% FPR is considered acceptable for the characterizing confirmatory assays, where 1% FPR was targeted (27). The titer cut point factor (TCPF) was determined based on the screening cut point (CP) dataset. The TCPF was defined with a robust-parametric approach in the log-transformed data set with outliers removed as 2.2 (anti-log of median + 3.09*1.4826*MAD). The TCPF targets a 0.1% false positive rate (27).

The high positive control concentration level for the ADA assay was set to be at the upper third of the linear range of a surrogate antibody titration. The low positive control level was determined statistically to fail in 1% of cases as recommended by Shankar et al. (16). An intermediate LPC (LPC2) was selected as 1.5× of the 1% failure LPC level.

The developed ADA assays were validated in line with guidance document (14) evaluating parameters such as the screening assay cut point factor (SCPF), the titration assay cut point factor (TCPF), confirmatory cut points for drug (confirmatory I), GDF15 (confirmatory II) and PEG linker + fatty acid (confirmatory III), assay sensitivity and precision for screening and drug confirmatory (not for GDF15 and PEG linker + fatty acid confirmatory), assessment of the assay selectivity and specificity (interference with BMP-7), short-term stability, drug tolerance, robustness, and hook effect (see Table 1).

Neutralizing antibody assay validation

The ability to inhibit the activity of the drug and its endogenous counterpart GDF-15 has been addressed with the use of a cell-based assay. Downstream phosphorylation of ERK in cells expressing the human GFRAL and RET receptor served as a marker of tested protein activity after exposure to patient sera.

For the NAb assay, considering its low dynamic range, the HPC concentration level was set at the upper inhibition plateau. The low positive control level was determined statistically to fail in 1% of

cases, as recommended by Shankar et al. (16). An intermediate LPC (1.5× LPC) was selected as 1.5× of the 1% failure LPC level.

The developed NAb assays were validated with respect to the following parameters: assay cut point (CP), assay sensitivity, assay precision/reproducibility, robustness, assessment of the assay selectivity (interference with drug), hemolyzed or lipemic sample, and structurally similar compound (BMP-7) (NCBI protein blast showed 33% amino acid identity)). BMP7 in human serum can interfere with MAPK signaling and ERK phosphorylation (32, 33). All validation parameters performed well within the acceptance limits required for support of clinical trials (see Table 2).

Evaluation of clinical immunogenicity

The described methodology for ADA assessment was implemented in two clinical trials to measure clinical samples and evaluate the immunogenicity of the drug.

In the first clinical trial, which involved a population of healthy volunteers, a single subcutaneous ascending dose of the drug was administered. None of the pre-dose samples analyzed showed positive ADA results. Out of the 47 subjects, emergent ADAs against the drug were confirmed in only two individuals. The two ADA-positive individuals showed scores just above the confirmatory cutoff point (CP) in the drug confirmatory assay. Upon GDF15 and PEG-fatty acid characterization of the response, the two ADA confirmatory characterization assays could not confirm the positive results from the drug confirmatory assay. Also, a titer was not detectable at 1:2 dilution in both samples (assuming prior MRD 50). For one of the subjects, later timepoints assessed scored negative in the ADA assay, indicating a transient nature of ADA response. For the second subject, the ADA-positive sample was detected at the end of a study visit, therefore indicating a persistent nature of a response. Furthermore, no neutralizing capacity of the ADA was detected for the drug when performing a cell-based NAb assay analysis.

In the second clinical study, which involved an overweight or obese population, the drug was administered subcutaneously with different dosing regimens. ADAs against the drug were confirmed in 3 of the 82 patients. One individual showed a confirmed positive ADA result in the pre-dose sample, whereas two individuals had emergent confirmed positive ADA results after the dose administration. Similar to the outcome in the first clinical trial, domain characterization for PEG-fatty acid showed a negative result. However, the characterizing ADA confirmatory assay for GDF15 confirmed the two positive results obtained from the drug confirmatory assay. Further characterization for the neutralizing capacities of ADA revealed positive data in the NAb assay for GDF15, but not for the drug itself. The NAb GDF15 results for the three ADA-confirmed positive samples were all in the range between CP and LPC, suggesting low neutralizing activity. Interestingly, the drug NAb assay detected those samples as negative. Their inhibition level in the drug NAb assay was elevated but below the CP. The different outcome in scoring above CP (NAb GDF15) and below CP (NAb whole drug) can be attributed to the subtle differences in assay sensitivity between one NAb assay format vs. the other and run-to-run variability, which also was observed during assay validation. No detectable titer was observed at a 1:2 dilution in all samples, assuming a prior MRD of 50. In each case, ADAs were detected in the patients only once throughout the studies, indicating the transient nature of their appearance (see Table 3). In both clinical trials, the observed incidents of ADA did not have any impact on drug exposure.

TABLE 1 ADA validation parameters for screening, confirmatory, and titration assays.

ADA assay	Cut point (% inhibition)	Sensitivity (ng/mL)	Positive control (ng/mL)	Intra (I) and inter (II) precision (CV%)	Drug tolerance (µg/mL)	Interference (hemolysis, lipemic, structurally similar compound)	Robustness
Screening	SCPF: 1.35	65.5 SPC	High PC: 10000 SPC Low PC1: 89.7 SPC Low PC2: 134.5 SPC	(I) HPC: 5.6%, LPC1: 10.9%, LPC2: 5.2% (II) HPC: 46.6%, LPC1: 18.6%, LPC2: 19.9%	Up to 4 µg/mL drug for SPC at 100 ng/mL	No interference in hemolyzed nor lipemic samples. Up to 200 pg/mL BMP-7 for SPC at LPC1, LPC2 and HPC levels	Yes
Confirmatory	CCP-I (drug): 29.5% CCP-II (GDF15): 24.8% CCP-III (PEG-fatty acid): 18.0%	67.8 SPC (drug confirmatory assay)	High PC: 10,000 SPC Low PC1: 89.7 SPC Low PC2: 134.5 SPC	Drug confirmatory assay (I) HPC: 0.2%, LPC1: 15.2%, LPC2: 3.3% (II) HPC: 1.4%, LPC1: 24.3%, LPC2: 15.3%			
Titer	TCPF: 2.2	n.a.	High PC: 10,000 SPC Low PC1: 89.7 SPC Low PC2: 134.5 SPC	n.a.			

n.a., not applicable.

10.3389/fimmu.2024.1438251

TABLE 2 Assay validation parameters for neutralizing anti-drug and neutralizing anti-GDF-15 assays.

Assay	Cut point (% inhibition)	Sensitivity (ng/mL)	Positive control (ng/mL)	Intra (I) and inter (II) precision (CV%)	Drug tolerance (µg/mL)	Interference (hemolysis)	Interference (lipemic)	Interference (structurally similar compound)	Robustness
Neutralizing anti-drug	38.4	2110	HPC: 10 000 1.5 × LPC1: 3730 LPC1: 2,480	I) HPC: 1.5 1.5× LPC: 2.4 LPC: 6.0 II) HPC: 1.7 1.5× LPC: 9.1 LPC: 13.0	≥ 0.427 at LPC1	No interference	No interference	No interference	Yes
Neutralizing Anti-GDF-15	28.2	1980	HPC: 10 000 1.5× LPC1: 3,220 LPC1: 2,140	I) HPC: 1.7 1.5× LPC: 4.7 LPC: 29.0 II) HPC: 2.8 1.5× LPC: 12.6 LPC: 24.6	> 0.68 at LPC1	No interference	No interference	No interference	Yes

Discussion

Described in the current case study, the proposed strategy of conventical ADA detection and extensive ADA response characterization proved effective for monitoring the presence of ADAs and NAbs and could be used to support clinical development of a broad range of chemically modified proteins and multidomain biotherapeutics.

The industry advocates a risk-based approach considering drug exposure, efficacy, and patient safety when developing an immunogenicity strategy. The immune response to chemically modified endogenous molecules can be directed either to multiple epitopes across the non-modified biologics or to the chemically modified parts. For this molecule, one of the domains is a GDF15 protein with an endogenous counterpart, which is conjugated with a PEG linker coupled to a fatty acid. Since an immune response to the GDF15 domain could potentially have an impact on the regulation of multiple physiological functions, it was essential to investigate and characterize the neutralizing capacities of potential ADAs. Therefore, this novel chemically modified endogenous molecule was assessed as a high-risk biologic from the immunogenicity risk standpoint, warranting development of two neutralizing assays, one targeting the entire multidomain therapeutic and a second neutralizing assay for the GDF15 domain only. This risk assessment was reflected in the request from regulatory authorities to perform the described characterization.

A strategy of creating a pseudo polyclonal positive control was adopted during the development and validation of ADA assays. This involved the combination of three different monoclonal antibodies, derived specifically against the human GDF15, in equimolar ratios. By adopting this approach, a reliable and reproducible source of a critical reagent was established (34). This pseudo polyclonal positive control played a pivotal role in consistently evaluating the performance of ADA assays throughout the entire clinical development process, in our case consisting of two clinical studies. Moreover, the establishment of pseudo positive control that specifically binds to variable regions of the drug aligns with Health Authority guidelines (14). This original approach ensured that the control maximally represented the interaction between the drug and potential anti-drug antibodies and is highly recommended for bioanalytical community to further evaluate.

During the clinical study in a healthy volunteer population, 2 out 47 dosed individuals were confirmed ADA positive, but no neutralizing antibodies were detected. In the clinical study with an overweight or obese population, 3 of 82 patients were confirmed positive. While the observed incidence of ADA was low, through the characterization assessments performed, we were able to establish that the ADAs were cross-reactive against GDF15 and most importantly that these ADA were able to neutralize the function of GDF15, albeit at a very low titer. These observations highlight the advantage of a parallel and unbiased ADA characterization process in high-risk modalities and justify the investment in the extensive suite of assays for development of this high-risk therapeutic.

It has been reported in literature that protein conjugation with PEG may trigger an immune response and the developed anti-PEG antibodies can impact the safety and efficacy of the administered drug

TABLE 3 Characterization of immunogenicity from two clinical trials.

Clinical study	Confirmed ADA patients Cross-reactive to the drug	Cross-reactive to FA PEG	Cross-reactive to GDF15	NAb for drug	NAb for GDF15	Titer
Healthy volunteers, 47 dosed and 64 enrolled	2 out of 47 1 transient 1 persistent	NO	NO	NO	NO	Low
Disease population, 82 dosed	3 out of 82 1 preexisting 2 transient	NO	YES 2 out of 3	NO	YES 3 out of 3	Low

(10, 13). When administering therapeutics using PEG liposomes, anti-PEG IgM antibodies were detected, which could trigger the complement system, leading to accelerated blood clearance and reduced exposure and efficacy due to anti-PEG antibodies. Since this was the first time the current biotherapeutics with this PEG linker was introduced into clinical development, it was of high importance to gain understanding of potential ADA response and develop an assay which would allow the characterization of potential anti-PEG antibodies. However, for the fatty acid domain within the chemically modified therapeutic protein, the requirement to develop an assay for the characterization of the immune response was questionable. To our knowledge, anti-fatty acid antibodies have not been associated with loss of efficacy or safety concerns; therefore, this domain was not included by itself in the characterization using bioanalytical methodology (35) but rather in combination with the applied PEG linker.

No ADAs against PEG linker–fatty acid conjugates were detected while characterizing detected ADAs in two clinical studies for the current biotherapeutic. One explanation could be that preexisting ADAs against PEG known for their high prevalence would not cross-react to the PEG linker as the linker is relatively short in comparison with a PEGylated domain. It is also possible that the frequency was too low to be observed in the participants treated with the respective drug. Based on current analysis, the PEG linker can be considered suitable for conjugation of other molecules as a domain with low immunogenic potential.

Each clinical development program administrating a multidomain biotherapeutic should consider whether each domain or component requires its own specificity assay and the extent of ADA characterization to be performed. In addition to the different functional domains, it must also be considered that inter-domain interfaces created within each chemically modified biotherapeutic can themselves also trigger an immune response (34, 36, 37). Including domain characterization as part of a validated ADA assay as described in the current strategy can be analytically and operationally challenging, requiring specific critical reagents and considerable scientific effort. Although the described and successfully implemented strategy allowed us to assess and understand the clinical immunogenicity of the current drug, we propose several reflections when considering the ADA detection and characterization for multidomain biotherapeutics.

The risk assessment of the therapeutic molecule will be the major factor when deciding the extent of the characterization required. With a lower-risk molecule, a more exploratory approach to the domain specificity assessment may be sufficient in the early stages of clinical development and an assessment of the neutralizing potential may be deferred until later clinical phases. In case one of the domains has a particular impact on the ADA formation, this can support either further clinical development of respective biotherapeutics or back-translational efforts. Even within a high-risk molecule, there are likely to be domains with lower and higher risks of clinical consequences for immunogenicity. Here for example, we considered that the fatty acid domain did not require its own domain specificity assay, whereas the GDF15 domain had both ADA specificity and NAb assays.

To assess the pharmacological neutralization of a chemically modified endogenous molecule, either a cell-based or a ligand-binding assay can used to assess the capacity of the ADA to reduce the multidomain biotherapeutics potency by blocking the target binding domain. For high-risk molecules, a functional cell-based assay is generally regarded as more appropriate to characterize a potential neutralizing effect already at the Phase I entry into the human stage of clinical development since they are considered to better represent the physiological mode of action (19). Following our safety-driven conservative immunogenicity monitoring approach, in this program a cellular assay had already been developed to support the early characterization at Phase I. The engineered HEK-cell line expressing the target receptor complex hGFRAL/hRET has been utilized to assess the NAb capacity of anti-drug and anti-GDF15 antibodies.

During NAb assay development, known analytical challenges of a cell-based system, *i.e.*, sensitivity and drug tolerance compared with the corresponding ADA screening ligand-binding assay, were faced. To overcome the limitation, extensive sample preparation to break apart NAb/drug complexes and remove interfering drug and other interfering matrix components from the sample were introduced (38–40). The poor solubility of the drug prevented standard approaches for chemical conjugation with biotin that would have allowed a SPEAD pretreatment approach. Alternative sample pretreatment that did not require any chemical conjugation had to be envisioned. PEG precipitation combined with acid treatment and anti-drug antibody-mediated drug capture was therefore implemented that 1) removed interfering matrix components that would trigger unspecific ERK phosphorylation in the cellular assay and 2) removed some but not all of the drugs present in clinical samples, thereby improving the drug tolerance of the assay.

Thanks to the multiple mitigation strategies described here, we were able to achieve successful analytical validation of two NAb assays. Our methodology allowed detection of neutralizing antibodies at the expected drug concentration in the clinical studies. While performing clinical sample analysis in healthy and overweight or obese populations, we could also confirm the presence of neutralizing antibodies in three samples. Interestingly, all the samples showed a positive result only in the assay addressing the impact on GDF-15 but not on the drug itself. These unexpected results can be explained by a small difference in activity between the drug and recombinant GDF-15, which may impact the assay sensitivity at the tested conditions. However, this small distinction may lead to a different outcome if the signal inhibition is at the detection threshold.

Considering the analytical challenges related to sensitivity of the cellular NAb assays even after implementing sample pretreatment, which have been also demonstrated in the current case study, it is advised to plan for NAb assessments only at later sampling timepoints and particularly in the washout phase in studies when multiple ascending doses are explored (34). To streamline analytics development and characterization of ADAs, one could develop only one NAb assay to assess neutralizing ADAs against the endogenous counterpart, but not against the whole drug itself, which would still address the major safety concerns. Additionally, a non-cell-based competitive ligand-binding assay-based NAb assay might allow better analytical performance to assess neutralizing ADA, particularly with respect to sensitivity and drug tolerance. One could consider implementation of competitive ligand-binding assay NAb assay at the earlier stages of clinical development instead of a cell-based assay. Depending on the mechanism of action of the therapeutic, such an approach may be appropriate to support the entire clinical development (40).

For a complex multidomain therapeutic, particularly one with higher-risk components, it is recommended that the strategy for ADA detection and characterization, including the approach for neutralizing ADA assessment, be discussed with Health Authorities prior to the Investigational New Drug (IND) applications stage of drug development.

Data availability statement

The original contributions presented in the study are included in the article/supplementary material. Further inquiries can be directed to the corresponding author.

Ethics statement

The studies involving humans were approved by Food and Drug Administration, USA IND140386. The studies were conducted in accordance with the local legislation and institutional requirements. The participants provided their written informed consent to participate in this study.

Author contributions

CH: Data curation, Formal analysis, Methodology, Supervision, Validation, Writing – original draft, Writing – review & editing. GC: Data curation, Formal analysis, Investigation, Methodology, Writing – original draft. GT: Formal analysis, Methodology, Writing – original draft, Writing – review & editing. FA: Data curation, Formal analysis, Methodology, Validation, Writing – original draft, Writing – review & editing. RN: Writing – original draft, Writing – review & editing. MK: Data curation, Writing – review & editing. AG: Data curation, Project administration, Writing – review & editing. MJ: Conceptualization, Data curation, Formal analysis, Investigation, Methodology, Project administration, Supervision, Validation, Writing – original draft, Writing – review & editing.

Funding

The author(s) declare that no financial support was received for the research, authorship, and/or publication of this article.

Acknowledgments

The authors would like to express their deep gratitude to Florent Bender, Franck Picard, and Lydia Michaut (PK Sciences, Novartis, Basel) for fruitful discussions. Moreover, we would like to acknowledge Julia Owoh from BioAgilytix for constant support.

Conflict of interest

FA and RN are employees of BioAgilytix with all remaining authors employees of Novartis. The authors have no other relevant affiliations or financial involvement with any organization or entity with a financial interest in or financial conflict with the subject matter or materials discussed in the manuscript apart from those disclosed.

Publisher's note

References

1. Cosimi AB. Clinical development of orthoclone OKT3. *Transplant Proc*. (1987) 14:7–16.

2. Harris JM, Chess RB. Effect of pegylation on pharmaceuticals. *Nat Rev Drug Discovery*. (2003) 2:214–21. doi: 10.1038/nrd1033

3. Elliott S, Lorenzini T, Asher S, Aoki K, Brankow D, Buck L, et al. Enhancement of therapeutic protein in vivo activities through glycoengineering. *Nat Biotechnol*. (2003) 21:414–21. doi: 10.1038/nbt799

4. Rosenstock J, Bajaj HS, Janež A, Silver R, Begtrup K, Hansen MV, et al. Once-weekly insulin for type 2 diabetes without previous insulin treatment. *N Engl J Med*. (2020) 383:2107–16. doi: 10.1056/NEJMoa2022474

5. Shin M, Lee H-A, Lee M, Shin Y, Song J-J, Kang S-W, et al. Targeting protein and peptide therapeutics to the heart via tannic acid modification. *Nat Biomed Eng*. (2018) 2:304–17. doi: 10.1038/s41551-018-0227-9

6. Dixon JE, Osman G, Morris GE, Markides H, Rotherham M, Bayoussef Z, et al. Highly efficient delivery of functional cargoes by the synergistic effect of GAG binding motifs and cell-penetrating peptides. *Proc Natl Acad Sci*. (2016) 113:E291–9. doi: 10.1073/pnas.1518634113

7. Kulkarni R, Karim FA, Glamocanin S, Janic D, Vdovin V, Ozelo M, et al. Results from a large multinational clinical trial (guardian™3) using prophylactic treatment with turoctocog alfa in paediatric patients with severe haemophilia A: safety, efficacy and pharmacokinetics. *Haemophilia*. (2013) 19:698–705. doi: 10.1111/hae.12165

8. Khawaji M, Astermark J, Berntorp E. Lifelong prophylaxis in a large cohort of adult patients with severe haemophilia: a beneficial effect on orthopaedic outcome and quality of life. *Eur J Haematol*. (2012) 88:329–35. doi: 10.1111/j.1600-0609.2012.01750.x

9. Giangrande P, Abdul Karim F, Nemes L, You CW, Landorph A, Geybels MS, et al. Long-term safety and efficacy of N8-GP in previously treated adults and adolescents with hemophilia A: final results from pathfinder2. *J Thromb Haemost*. (2020) 18:5–14. doi: 10.1111/jth.14959

10. Kozma GT, Shimizu T, Ishida T, Szebeni J. Anti-PEG antibodies: Properties, formation, testing and role in adverse immune reactions to PEGylated nano-biopharmaceuticals. *Adv Drug Deliv Rev*. (2020) 154-155:163–75. doi: 10.1016/j.addr.2020.07.024

11. Vaisman-Mentesh A, Gutierrez-Gonzalez M, DeKosky BJ, Wine Y. The molecular mechanisms that underlie the immune biology of anti-drug antibody formation following treatment with monoclonal antibodies. *Front Immunol*. (2020) 11:1951. doi: 10.3389/fimmu.2020.01951

12. Shiwatari-Ogata C, Kyuuma M, Ogata H, Yamakawa M, Iwata K, Ochi M, et al. Ozoralizumab, a humanized anti-TNFα NANOBODY® compound, exhibits efficacy not only at the onset of arthritis in a human TNF transgenic mouse but also during secondary failure of administration of an anti-TNFα IgG. *Front Immunol*. (2022) 13:853008. doi: 10.3389/fimmu.2022.853008

13. Freire Haddad H, Burke JA, Scott EA, Ameer GA. Clinical relevance of pre-existing and treatment-induced anti-poly(ethylene glycol) antibodies. *Regen Eng Transl Med*. (2022) 8:32–42. doi: 10.1007/s40883-021-00198-y

14. *Immunogenicity Testing of Therapeutic Protein Products — Developing and Validating Assays for Anti-drug Antibody Detection, U.S. Department of Health and Human Services Food and Drug Administration Center for Drug Evaluation and Research (cder) Center for Biologics Evaluation and Research (CBER)* (2019). Available online at: https://www.fda.gov/media/119788/download.

15. Koren E, Smith HW, Shores E, Shankar G, Finco-Kent D, Rup B, et al. Recommendations on risk-based strategies for detection and characterization of antibodies against biotechnology products. *J Immunol Methods*. (2008) 333:1–9. doi: 10.1016/j.jim.2008.01.001

16. Shankar G, Devanarayan V, Amaravadi L, Barrett YC, Bowsher R, Finco-Kent D, et al. Recommendations for the validation of immunoassays used for detection of host antibodies against biotechnology products. *J Pharm BioMed Anal*. (2008) 48:1267–81. doi: 10.1016/j.jpba.2008.09.020

17. *Guideline on Immunogenicity assessment of therapeutic proteins*. European Medicines Agency (2017). EMEA/CHMP/BMWP/14327/2006 Rev 1. Available online at: https://www.ema.europa.eu/en/documents/scientific-guideline/guideline-immunogenicity-assessment-therapeutic-proteins-revision-1_en.pdf.

18. Myler H, Pedras-Vasconcelos J, Phillips K, Hottenstein CS, Chamberlain P, Devanaryan V, et al. Anti-drug antibody validation testing and reporting harmonization. *AAPS J*. (2021) 24:4. doi: 10.1208/s12248-021-00649-y

19. Myler H, Pedras-Vasconcelos J, Lester T, Civoli F, Xu W, Wu B, et al. Neutralizing antibody validation testing and reporting harmonization. *AAPS J*. (2023) 25:69. doi: 10.1208/s12248-023-00830-5

20. Chirmule N, Jawa V, Meibohm B. Immunogenicity to therapeutic proteins: impact on PK/PD and efficacy. *AAPS J*. (2012) 14:296–302. doi: 10.1208/s12248-012-9340-y

21. Ehrenpreis ED, Ehrenpreis ED. Pharmacokinetic effects of antidrug antibodies occurring in healthy subjects after a single dose of intravenous infliximab. *Drugs R D*. (2017) 17:607–13. doi: 10.1007/s40268-017-0211-y

22. Gorovits B, Peng K, Kromminga A. Current considerations on characterization of immune response to multi-domain biotherapeutics. *BioDrugs*. (2020) 34:39–54. doi: 10.1007/s40259-019-00389-8

23. Gorovits B, Azadeh M, Buchlis G, Harrison T, Havert M, Jawa V, et al. Evaluation of the humoral response to adeno-associated virus-based gene therapy modalities using total antibody assays. *AAPS J*. (2021) 23:108. doi: 10.1208/s12248-021-00628-3

24. Wang D, Day EA, Townsend LK, Djordjevic D, Jørgensen SB, Steinberg GR. GDF15: emerging biology and therapeutic applications for obesity and cardiometabolic disease. *Nat Rev Endocrinol*. (2021) 17:592–607. doi: 10.1038/s41574-021-00529-7

25. Smith HW, Butterfield A, Sun D. Detection of antibodies against therapeutic proteins in the presence of residual therapeutic protein using a solid-phase extraction with acid dissociation (SPEAD) sample treatment prior to ELISA. *Regul Toxicol Pharmacol*. (2007) 49:230–7. doi: 10.1016/j.yrtph.2007.07.005

26. Zoghbi J, Xu Y, Grabert R, Theobald V, Richards S, et al. A breakthrough novel method to resolve the drug and target interference problem in immunogenicity assays. *J Immunol Methods*. (2015) 426:62–9. doi: 10.1016/j.jim.2015.08.002

27. Devanarayan V, Smith WC, Brunelle RL, Seger ME, Krug K, Bowsher RR. Recommendations for systematic statistical computation of immunogenicity cut points. *AAPS J*. (2017) 19:1487–98. doi: 10.1208/s12248-017-0107-3

28. Shen M, Dong X, Tsong Y. Statistical evaluation of several methods for cut-point determination of immunogenicity screening assay. *J Biopharm Stat*. (2015) 25:269–79. doi: 10.1080/10543406.2014.979196

29. *Human GFRAL/RET Stable Cell Line - HEK293 (CSC-RO0650)*. Creative Biogene. Available online at: https://www.creative-biogene.com/human-gfral-ret-stable-cell-line-hek293-item-csc-ro0650-470765.html.

30. Scannell MJ, Hyatt MW, Budyak IL, Woldeyes MA, Wang Y. Revisit PEG-Induced precipitation assay for protein solubility assessment of monoclonal antibody formulations. *Pharmaceut Res*. (2021) 38:1947–60. doi: 10.1007/s11095-021-03119-4

31. Hofmann M, Winzer M, Weber C, Gieseler H. Limitations of polyethylene glycol-induced precipitation as predictive tool for protein solubility during formulation development. *J Pharm Pharmacol*. (2018) 70:648–54. doi: 10.1111/jphp.12699

32. Tacke F, Gäbele E, Bataille F, Schwabe RF, Hellerbrand C, Klebl F. Bone morphogenetic protein 7 is elevated in patients with chronic liver disease and exerts fibrogenic effects on human hepatic stellate cells. *Dig Dis Sci*. (2007) 52:3404–15. doi: 10.1007/s10620-007-9758-8

33. Narasimhulu CA, Singla DK. The role of bone morphogenetic protein 7 (BMP-7) in inflammation in heart diseases. *Cells*. (2020) 9:280. doi: 10.3390/cells9020280

34. Gorovits B, Wakshull E, Pillutla R, Xu Y, Manning MS, Goyal J. Recommendations for the characterization of immunogenicity response to multiple domain biotherapeutics. *J Immunol Methods*. (2014) 408:1–12. doi: 10.1016/j.jim.2014.05.010

35. Nicholas DA, Salto LM, Boston AM, Kim NS, Larios M, Beeson WL, et al. Identification of anti-long chain saturated fatty acid IgG antibodies in serum of patients with type 2 diabetes. *Mediators Inflammation*. (2015) 2015:196297. doi: 10.1155/2015/196297

36. Gauba V, Grünewald J, Gorney V, Deaton LM, Kang M, Bursulaya B, et al. Loss of CD4 T-cell-dependent tolerance to proteins with modified amino acids. *Proc Natl Acad Sci United States America*. (2011) 108:12821–6. doi: 10.1073/pnas.1110042108

37. Hock MB, Thudium KE, Carrasco-Triguero M, Schwabe NF. Immunogenicity of antibody drug conjugates: bioanalytical methods and monitoring strategy for a novel therapeutic modality. *AAPS J*. (2015) 17:35–43. doi: 10.1208/s12248-014-9684-6

38. Corsaro B, Yang TY, Murphy R, Sonderegger I, Exley A, Bertholet S, et al. 2020 white paper on recent issues in bioanalysis: vaccine assay validation, qPCR assay validation, QC for CAR-T flow cytometry, NAb assay harmonization and ELISpot validation (part 3 – recommendations on immunogenicity assay strategies, NAb assays, biosimilars and FDA/EMA immunogenicity guidance/guideline, gene & cell therapy and vaccine assays). *Bioanalysis*. (2021) 13:415–63. doi: 10.4155/bio-2021-0007

39. Finco D, Baltrukonis D, Clemens-Egan A, Delaria K, Gunn GR 3rd, Lowe J, et al. Comparison of competitive ligand-binding assay and bioassay formats for the measurement of neutralizing antibodies to protein therapeutics. *J Pharm Biomed Anal*. (2011) 54:351–8. doi: 10.1016/j.jpba.2010.08.029

40. Wu B, Chung S, Jiang XR, McNally J, Pedras-Vasconcelos J, Pillutla R, et al. Strategies to determine assay format for the assessment of neutralizing antibody responses to biotherapeutics. *AAPS J*. (2016) 18:1335–50. doi: 10.1208/s12248-016-9954-6

frontiers | Frontiers in Immunology

TYPE Review
PUBLISHED 16 December 2024
DOI 10.3389/fimmu.2024.1401178

OPEN ACCESS

EDITED BY
Michael Tovey,
Svar Life Science, France

REVIEWED BY
Daniel Kramer,
Sanofi, Frankfurt am Main, Germany
Jack Ragheb,
JoMoCo Inc, United States

*CORRESPONDENCE
Steven James Swanson
stejswanson@gmail.com

RECEIVED 14 March 2024
ACCEPTED 22 November 2024
PUBLISHED 16 December 2024

CITATION
Swanson SJ (2024) What are clinically significant anti-drug antibodies and why is it important to identify them.
Front. Immunol. 15:1401178.
doi: 10.3389/fimmu.2024.1401178

What are clinically significant anti-drug antibodies and why is it important to identify them

Steven James Swanson*

translational Pharmacokinetics Pharmacodynamics (tPKPD), Genentech Inc., San Francisco, CA, United States

The FDA has released new draft guidance to standardize how immunogenicity of protein therapeutics is described in product labels. A key aspect to this new guidance is that companies should describe anti-drug antibodies that have clinical significance in addition to reporting ADAs' incidence. Factors to consider when determining clinical significance include if those antibodies have a significant effect on the drug's pharmacokinetics, pharmacodynamics, efficacy, and/or safety. While in many instances, the humoral response to protein therapeutics does not have any clinical significance, there are cases where there is a clinically significant effect and it is important to communicate this information to physicians and patients. This new guidance also delineates where immunogenicity information should be listed in product labels which should provide consistency in how this information is listed. There are many factors that contribute to a therapeutic's immunogenicity and determining clinical significance is both complex and challenging, requiring that companies perform thorough analyses with scientific rigor. The analysis that is now proposed to understand clinical significance of ADAs is a new concept and will require companies to develop a strategy for compliance. This manuscript sets forth some of the key considerations in answering this important question. One of the benefits that this new guidance will provide is a common approach for describing the immune response to therapeutics that will be located in a dedicated section of the label, providing valuable consistency across protein therapeutics. Section 12.6 in the Clinical Pharmacology portion of the label will contain the relevant immunogenicity information, which will make it much simpler to find immunogenicity information in product labels. This new guidance is currently being utilized for new protein therapeutics and companies are being requested to systematically revise the labels of previously approved drugs for compliance, although an absolute timeline for this has not been established as of this writing.

KEYWORDS

anti-drug antibodies (ADA), clinically significant antibodies, FDA regulations on immunogenicity, neutralizing antibodies (NAB), immunogenicity

Introduction

It is well established that protein therapeutics have the potential to elicit an unwanted immune response when administered to human subjects. A regulatory expectation from health authorities for companies developing therapeutics that have the potential to elicit an immune response is to test and characterize the immune response against their therapeutic. There are a series of documents available on the FDA website that provide guidance on how to assess immunogenicity of therapeutic proteins. These include "Immunogenicity Assessment for Therapeutic Protein Products" and "Immunogenicity Testing of Therapeutic Protein Products-Developing and Validating Assays for Anti-Drug Antibody Detection". These documents can help sponsors develop an immunogenicity assessment strategy. A previous review details the strategic rationale and value in characterizing an ADAs response against a therapeutic protein and is worth revisiting in light of the new FDA guidance (1). This is a clear expectation from regulatory authorities world-wide, and the FDA has also released draft guidance on how to report the clinical significance of anti-drug antibodies (ADAs) (2). One important aspect of this new guidance is that companies are tasked to call out those ADAs with clinical significance. This has not been a clearly defined expectation prior to this guidance. While the incidence of binding, and sometimes neutralizing, antibodies was typically described in product labels, the information to help ascertain the impact of those ADAs was not consistently captured or reported. Clinical significance is defined as those ADAs having an effect on pharmacokinetics (PK), pharmacodynamics (PD), efficacy, and/or safety of the therapeutic. While methods have been established to readily and reliably test for the presence of these ADAs, the ultimate goal of characterizing the antibodies and learning which population of subjects develop clinically significant antibodies is often not met. A white Paper published by an AAPS working group (3) describes in detail how ADAs could be described. The characteristics defined in that paper include descriptions that define binding antibodies, neutralizing antibodies, drug-sustaining antibodies, clearing antibodies and further recommends how these antibodies should be reported. What was not included in this white paper was any guidance on how to describe the impact or clinical significance of these antibodies. While it is often straightforward to learn which subjects in clinical trials develop ADAs and to appropriately report them, understanding the significance of those antibodies requires a more thorough analysis and all too often is not accomplished. It is also important to recognize that a temporal relationship between ADAs' production and a clinical effect is not necessarily a causal relationship. Demonstrating a causal relationship may require even more detailed analysis. The data that must be considered and evaluated to fully understand and characterize the clinical significance of an immune response include the data from immunogenicity assessment assays, functional assays for determining neutralization potential of the ADAs, pharmacokinetic data, pharmacodynamic data which might include results from biomarker analyses, safety data, and efficacy evaluations. When it is not possible to perform these analyses to determine those subjects that have antibodies with potential clinical significance, physicians and regulators often defer to the default interpretation that all detected antibodies have clinical significance. In reality, the vast majority of antibodies against therapeutic proteins have no clinical impact. It has been demonstrated in clinical trials that many subjects that develop ADAs are not affected by the presence of these antibodies. The likely reasons that the antibodies do not cause a clinical effect include being produced in insufficient quantity and/or duration to impact the therapeutic; insufficient affinity and/or avidity to have an impact on the efficacy of the therapeutic; binding to a region of the therapeutic that does not hamper the efficacy of the therapeutic; and/or because tolerance is established before the antibodies can have a clinical effect.

A goal of this manuscript is to describe what a clinically significant immune response looks like and discuss how companies might comply with the new FDA immunogenicity labeling guidance. While this will be a subjective determination, and will involve examination of multiple characteristics of a measured immune response, it is hoped that it clarifies and delineates those universal properties that are shared by immune responses that impact the well-being of patients. It will always be important that analytical procedures are designed to detect all ADAs generated in a relevant patient population during clinical trials, however, what is also vitally important is to help physicians understand the context of that immunogenicity and any resulting impact of ADAs. A key to understanding how to interpret immunogenicity results is comprehensive knowledge regarding how many subjects developed an immune response that impacted patient's health or treatment with the therapeutic.

Clinically significant antibodies are those that have an impact on the patient's health at any time and are associated with their exposure and ability to respond to the therapeutic. That effect can include an impact on PK, PD, efficacy, and/or safety.

What are clinically significant ADAs

There are several factors that must be considered when identifying potentially clinically significant antibodies. Some of these factors to consider when establishing clinical significance include:

Risk of developing an immune response

- Does the patient population have a high degree of autoimmunity?
    - these subjects are more likely to mount an immune response
- Will the therapeutic be dosed acutely or chronically?
    - Acute or single dosing is less likely to induce an immune response than a therapeutic given consistently over a long period of time
- Is the patient population immune-suppressed?
    - A subject that is immune suppressed is less likely to mount an ADAs response

- Does the therapeutic share epitopes with an endogenous counterpart such as a replacement protein?
    - The concern here is that any ADAs against the therapeutic might also bind to the endogenous protein
    - If the patient does not produce the endogenous counterpart or produces an aberrant version of it, it is likely that the patient will not have established tolerance and significant ADAs could be generated upon exposure to the therapeutic
    - The neutralization of the endogenous counterpart could continue after cessation of treatment with the therapeutic as the endogenous counterpart could continue to exacerbate the immune response (4)
- Is the therapeutic a mAb directed against a self-protein
    - When the target is an immunomodulator there may be concerns regarding ADA having clinical significance

What makes an immune response clinically significant can be summarized as affecting the patient's health or causing the patient to receive less benefit from further administration of the therapeutic. Neutralizing antibodies are defined as being able to neutralize the biological effect of the drug. When produced in high enough concentrations, these are often clinically significant, especially if the antibody is also capable of neutralizing an endogenous molecule as in the case of replacement therapies (5). While neutralizing antibodies are most commonly identified using NAB assays, there may be instances where monitoring the effect these antibodies have on PK and/or PD may be sufficient to convince the sponsor that antibodies are clinically neutralizing. Clearing antibodies are defined as causing a more rapid clearance of the drug as evidenced in the pharmacokinetic profile (6). These antibodies will often have clinical significance because the PK of the drug is affected. The drug has less time to work in the patient before it is cleared as evidenced by examining the drug exposure. It will be a responsibility of companies to define what level of impact on PK is necessary to have a clinically significant impact, and this will vary by drug and may in part depend upon whether an increase in dosage can be tolerated by the patient and the clinical indication.

There are examples where ADAs have had a safety impact. In some cases when therapeutics induce hypersensitivity (7), IgE may be produced which can mediate a clinical effect on the patient. When both circulating antibodies and circulating drug levels are high it is possible that immune complexes could form which could deposit in areas where there are extensive capillary networks or on the internal surface of blood vessels. Immune complexes can result in inflammation and vasculitis which can have a clinical effect on the patient (8, 9).

The duration of an immune response is an important consideration when evaluating clinical significance. Once an immune response to a therapeutic is initiated, it can progress or mature, which is often accompanied by one or more of the following: an increase in titer, an increase in binding affinity/avidity, a switch in class or subclass, and epitope spreading. Once the immune response begins to mature it is an indication that this will be a longer lasting or persistent response that may continue to progress until the treatment is withdrawn and circulating antibodies could remain for an extended time even after withdrawal of the therapeutic. Not all immune responses in any given patient mature. In many patients an immune response is triggered but does not get the necessary signal to progress and the production of antibody stops, which can result in the patient becoming tolerant to the drug. Sometimes the immune response is initiated but remains low, and the signs typically seen during a maturing immune response are not demonstrated. In these cases, the level of antibody remains low and may persist throughout treatment. These transient and low-level immune responses very rarely have any clinical consequences as sufficient free drug is available for the patient to derive a clinical benefit.

The disease that the therapeutic is targeting can have an impact on whether a clinically significant immune response is generated. For example, a therapeutic used in an oncology setting, especially if patients are receiving chemotherapeutic agents, is much less likely to induce a clinically significant antibody response than a chronically-administered therapeutic that mimics an endogenous counterpart. When the therapeutic is administered to patients with a background of auto-immunity, there is a greater chance that the protein therapeutic could trigger an ADAs response because the patient's immune system is more prone to produce antibodies when challenged with a foreign protein. An example of this is that rituximab exhibits higher immunogenicity when used to treat autoimmune disorders than when used in an oncology setting (10).

It is important to recognize that important immunogenicity information can also be obtained after a drug is on the market. This information may be gathered through careful pharmacovigilance when warranted and post-marketing surveillance.

Why new guidance is needed

Immunogenicity of therapeutic proteins is complex and depends on the interplay of multiple factors as depicted in Figure 1. Each protein therapeutic has its own characteristics that contributes to its immunogenicity. While those characteristics have been described elsewhere (11, 12), examples of some of these factors include the genetic makeup (presence of T cell epitopes based on the patient's HLA background, and presence of amino acid sequences flagged as non-self by the immune system), structural (stability of

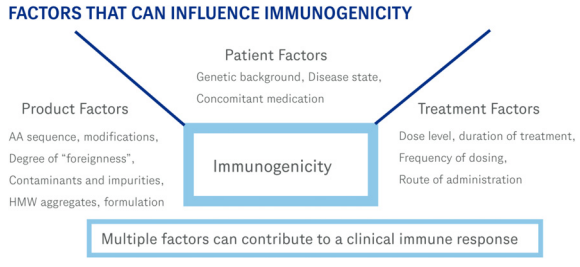

FIGURE 1
These are some of the factors that can contribute to an immune response. Immunogenicity of therapeutic proteins is a complex process involving multiple variables.

the drug, presence of aggregates), purity (presence of host cell proteins or other components that could act as adjuvants that stimulate the immune response), and clinical (route of administration, patient population, concomitant medications). Currently, ADAs data are placed in various sections of the label with most of the information in the Adverse Reactions section (section 6). This is not an ideal placement and can be confusing since most ADAs do not cause adverse reactions. The new guidance will have a dedicated subsection (12.6) and will include language describing clinical significance. This change will benefit both physicians as well as patients in providing clear language in a dedicated location on how many subjects developed clinically significant ADAs. This information can then be used to help evaluate if the therapeutic is a good option for the patient. It is anticipated that the number of subjects that develop clinically significant ADAs will be much lower than the number of subjects that develop ADAs of any type. This also means that many subjects that develop ADAs will not have a significant impact due to those antibodies. When deciding which therapy is best for a patient, this new guidance will provide clear and valuable information on the likelihood that a subject will generate ADAs after administration of the therapeutic that effects how the patient responds to that therapeutic.

One of the many factors a physician should consider when designing a treatment regimen involving a potentially immunogenic therapeutic is how likely the patient is to develop antibodies against the therapeutic and the likelihood of antibodies impacting how the patient responds to the therapeutic. This is why it is important for companies developing these therapeutics to provide the necessary data for physicians as well as regulators to inform the decision on how immunogenic a therapeutic is, and even more importantly, how clinically significant the antibodies induced by the therapeutic are likely to be for any given patient. These data can be valuable as the physician decides which course of treatment is ideal for their patient. Some patients take effort to understand the prescription drugs they are taking and wish to have meaningful conversations with their health care providers regarding their treatment regimen. This change in labeling will facilitate those conversations as the immunogenicity data and potential impact will be more readily available and easier to understand than what is available on most previous drug labels. Further, while it is discouraged to compare immunogenicity rates across different therapeutics, even those addressing the same target (although a head-to-head comparison of a biosimilar to its reference product is legitimate), there may be value in comparing the clinically significant ADAs.

Strategy for adhering to the new guidance

The first step in establishing if subjects administered the drug developed clinically significant ADAs is to verify that the analytical procedures used to assess immunogenicity are adequate. Simply, will the method(s) reliably detect the presence of ADAs with sufficient sensitivity to capture any clinically significant antibodies. The requirements for these assays are delineated in regulatory guidance as well as published white papers (3, 13–15) but include tests for sensitivity, specificity, reproducibility, and the ability to detect ADAs in the presence of circulating drug. Once it is determined that the methods are indeed adequate, those methods can be used to collect data for determination of ADAs incidence as well as clinical significance.

While the concept of clinical significance is clear, the ability to conclusively identify those subjects that have generated antibodies that have clinical significance is quite challenging. This will require that companies perform careful analysis comparing the PK, PD, efficacy, and safety in subjects that developed ADAs with subjects that did not. It will be important for the drug developing companies to identify what level of effect on PK, PD, efficacy, and safety qualifies as being clinically significant. This will require a very careful evaluation on what magnitude of effect impacts the patient and must be determined for each protein therapeutic. For example, a modest drop in drug levels may not impact the patient's ability to achieve benefit from the therapeutic and would therefore not meet the threshold for the ADAs having a "clinically significant" effect. The company will identify those ADAs which they deem to have clinical significance and the Agency will comment and either agree with the assessment or request revision.

When considering whether ADAs have an impact on PD and/or efficacy, the evaluation may need to consider biomarker data collected throughout clinical trials that sheds light on whether the drug is having a clinical impact on the patient. While efficacy is associated with the clinical endpoints defined by the trial, the effect on PD may be much harder to discern unless there exists a clear clinical marker, but the guidance is asking drug development companies to make that determination. Biomarker data are often used as surrogates to the clinical endpoint to help understand the clinical outcome, these data may also prove valuable in determining the clinical significance of ADAs.

It is important to recognize that it will likely be necessary to identify subsets of subjects that develop ADAs in order to find those subjects that develop clinically significant ADAs. A tiered approach may be necessary. This would entail looking at all subjects identified as positive in the screening assay for ADAs, and then performing various subset analyses on different groups of ADAs positive subjects. Evaluating all available data on the characterization of the ADAs including duration, titer, and neutralizing capability will allow appropriate subsets to be identified which can then be assessed for having clinical significance. If one were to only look at the entire population of subjects developing ADAs, it is possible that the threshold established for clinical significance would not be met, especially in a situation where many patients develop a low-level immune response. In this case, there may be a few patients that do develop clinically significant ADAs but that effect is masked by a large population of subjects that have an ADAs response that is not clinically significant. Knowing this is a possibility, it will be imperative for companies to evaluate smaller subsets of subjects to ensure that there is not a small population of subjects with clinically significant ADAs. One approach that could prove useful would be to characterize the immune response as needed in subjects

looking at some or all of these parameters that describe the immune response.

- Magnitude (how much antibody is generated)
  - Titer, S/N ratio, concentration
- Time course (kinetics of the response)
  - Persistent (an immune response that is long lasting)
  - Transient (an immune response that is short lived)
- Maturity (is the response continuing to get stronger)
  - Isotype switching
  - Increasing magnitude of response
  - Increasing binding affinity
- Neutralizing antibodies
  - Are there ADAs that can neutralize the biological effect of the drug

Examination of these characteristics should allow a stratification of subjects that have a more robust immune response and it is these ADAs that are more likely to have clinical significance. It is important to recognize that even if only a small number of subjects develop ADAs with clinical significance, it will be important to identify and describe them in the label but to place into appropriate context to describe the impact.

Recent work focuses on the importance of taking sufficient samples to capture the immune response (16). This analysis points to the net effect of sparse sampling in failing to capture the true ADAs incidence. It also demonstrates that having less than adequate sensitivity and drug tolerance also can lead to an underreporting of ADAs incidence and could prevent capturing ADAs that had clinical significance. While it is true that ADAs that are transient in nature or have a small magnitude of response (such that less sensitive or less drug tolerant assays fail to detect them) are less likely to have clinical significance, it is important that initial screening assays detect as many ADAs as possible to identify the appropriate samples to evaluate for clinical significance.

One aspect of understanding clinical significance is related to the small number of subjects that develop ADAs in many studies. In many clinical trials the number of ADAs positive subjects is below that required to make a meaningful statistical assessment. This small number of subjects can be very challenging for biostatisticians and may require that we think about statistical significance differently and establish revised statistical models to capture clinically significant ADAs. Another aspect that may prove challenging is to establish a causal relationship between the ADAs production and the clinical impact. Establishing a team of scientists including an analytical specialist that understands the assays used, clinical representation to help delineate what constitutes a clinical impact on PD and efficacy, PK scientist, and biostatistician to provide the necessary statistical support will be important for successfully complying with this new guidance.

Case studies

An example of a clinically significant immune response was reported in 2004 (17) and involved epoetin alfa, an erythropoietic stimulating agent which was first approved in 1989. This drug had a strong record of very few cases of ADAs during clinical trials and also in the commercial setting. This drug was used to stimulate red blood cell production as it was a mimetic of erythropoietin. Erythropoietin is produced in the kidney and is required for red blood cell production in the bone marrow. In cases of chronic kidney disease and in some malignancies, the production of endogenous erythropoietin is suppressed to a level that is insufficient to provide the necessary volume of red blood cells to prevent anemia. Erythropoietic stimulating agents are prescribed for these patients.

Eprex® (18) was manufactured for distribution in regions outside of the United States including Europe, Australia, and Canada. In 2002 a report was published (5) that described an emergence of cases in Europe of antibody-mediated pure red cell aplasia (PRCA) that was attributed to patients being treated with Eprex®. Between 2001 and 2004 it was estimated that at least 191 subjects had developed what was described as antibody-mediated PRCA (19). Antibody-mediated PRCA subjects were characterized as having little or no circulating erythropoietin, a bone marrow biopsy devoid of red blood cell precursors, severe anemia, and the presence of antibodies capable of binding to and neutralizing erythropoietin. While the precise reason Eprex® became more immunogenic is still not universally agreed upon, what is evident is that a change in the drug triggered some patients' immune systems to recognize the therapeutic as foreign and mount a robust immune response. In these subjects, treatment with the erythropoietic agent induced antibodies to be formed that were capable of binding both the erythropoietic stimulating agent as well as endogenous erythropoietin. It is also likely that in patients that developed PRCA, that even low levels of endogenous erythropoietin that were produced by the patient acted as a stimulus for the production of more anti-erythropoietin antibodies. Thus, simply withdrawing treatment with the erythropoietic stimulating agent might not be sufficient to stop the patient from producing the antibodies.

Antibodies obtained from Professor Casadevall's subjects were further characterized and a quite consistent pattern was observed. The antibodies were capable of neutralizing the biological effect of erythropoietin; had a relative concentration ranging from 4 to 43 micrograms/ml; had relatively low rates of dissociation; most of the subjects tested had the subclass IgG4 as the most prevalent anti-erythropoietin antibody and IgG1 as the second most prominent subclass. All of the subjects tested had IgG4 present (20). What these data collectively suggest is that the antibodies responsible for the pure red cell aplasia were the product of a mature immune response as indicated by the high concentration of circulating antibodies, neutralizing capacity, low dissociation rate, and presence of high levels of IgG4 antibodies specific for erythropoietin. Because assays were available it was possible to fully characterize the antibodies responsible for the observed clinical events. These data are a clear example of a highly clinically significant immune response.

An important consideration is that during clinical trials, there were no reported cases of antibody-mediated pure red cell aplasia and despite wide use throughout the world, prior to the Casadevall report there were very few incidences of pure red cell aplasia associated with treatment with erythropoietic stimulating agents.

This underscores the importance for manufacturers to remain vigilant for adverse event reports describing a sudden loss of activity for their therapeutic, especially those associated with replacement therapeutics that have an endogenous counterpart that could be affected by antibodies against the therapeutic protein.

Another example of a clinically significant immune response reported in the literature is associated with the use of adalimumab (21). In some patients, ADAs against adalimumab developed and prevented appropriate levels of drug to remain in circulation to provide clinical benefit. In patients that did not develop ADAs against adalimumab there was maintained a high level of circulating drug. However, in patients with moderate levels of ADAs, the level of circulating drug was lower than seen in patients without ADAs and those patients that developed a high titer of ADAs had circulating drug levels that were very low and would likely be insufficient to provide any benefit to those patients. This example demonstrates that the amount of ADAs produced by the patient can have a direct impact on whether the ADAs will have clinical significance or not. There is an increased interest in physicians to better understand the clinical impact of ADAs in patients receiving biological agents for the treatment of autoimmune rheumatic diseases (22).

It was reported in the New England Journal of Medicine (7) that cetuximab was associated with multiple cases of anaphylaxis in patients. In this report the affected patients had preexisting IgE antibodies against galactose-alfa-1,3-galactose. The preexisting antibodies recognized a carbohydrate introduced from a tick bite. The resulting anaphylaxis observed is an example of a clinical safety event that was triggered by exposure to cetuximab. This is another example of a clinically significant immune response to a protein therapeutic that would be specified with this labeling guidance.

Logistics and strategy for compliance

This new guidance is currently being used by the FDA for drugs currently under review for approval and the new language has been incorporated into several drugs approved since late 2022. Companies are urged to consider the new guidance in order to prevent unnecessary delays during the review process. If it is not possible to answer all of the questions related to clinical significance of ADAs, there is prescribed language in the guidance that can be used. It seems likely that for most situations a full description would be preferable as it provides the important information for regulators, prescribers, and patients. It will be important for companies to develop a strategy to comply with this new guidance. This will necessitate early planning to ensure sufficient data are collected, especially during pivotal trials, to be able to answer the immunogenicity questions. Currently, most trials include sufficient data to answer the question of whether the ADAs impact safety and PK. The question of whether there is an impact on PD and efficacy may require additional biomarker data be collected. It will be important when planning the timeline for regulatory submission for the drug that sufficient time be allocated to allow analysis of the necessary data to answer the clinical significance questions. An important strategic point for companies to consider is whether they want to accept the default language when the clinical significance questions cannot be adequately answered or take the additional time to provide the required information prior to drug submission.

It is anticipated that as more labels are approved utilizing this new guidance that effective processes will be developed to perform the necessary data analyses, and that consistency in companies' approaches to compliance will be established. As these analyses become routine, companies will also be tasked with revising the immunogenicity sections of labels from previously approved drugs to comply with the new guidance. This presents another unique set of challenges as it will not be practical (and also not likely beneficial) to generate new data to determine clinical significance of the ADAs. Simply put, many previously approved protein therapeutics were approved without some of the necessary data collected to be able to definitively answer the clinical significance questions. Each company will need to mine their existing data and make the clinical significance evaluation to the best of their ability given existing data and may need to mine real world data for the most thorough approach.

Conclusion

A series of case studies are described that provide examples of when an immune response to a therapeutic protein has clinical significance and when the immune response does not have any clinical impact on the patient. The Eprex® case study describing a clearly clinically significant immune response teaches us that in addition to the importance of neutralizing antibodies, immunogenicity interpretation is always subject to re-evaluation when new data emerge. In most circumstances, the immunogenicity assessment performed during clinical trials, especially those data obtained during long term trials, are sufficient to allow us to understand the immunogenicity of the therapeutic. However, there can be examples where something changes that alters the immunogenicity profile of a therapeutic and underscores the reason for strong pharmacovigilance throughout the life cycle of a protein therapeutic.

The adalimumab example shows that the magnitude of the immune response is an important characteristic to examine and can certainly play a role in determining if a population of ADAs in a patient has clinical significance. It is important for supporting all protein therapeutics that robust ADAs assays are developed with sufficient sensitivity and drug tolerance and that sufficient samples are taken throughout the course of treatment to fully understand the extent of the immune response. When appropriate samples are taken in conjunction with a suitable assay it is more likely to accurately capture and understand the immunogenicity profile. Finally, an example of an ADAs-related clinical safety event, namely anaphylaxis (which is a black box warning on the drug's PI), is shown that warrant inclusion in the drug label as a clinically significant occurrence.

What is proposed is that part of the characterization of an immune response include an evaluation as to whether the presence of these antibodies has a clinical effect. The data to be considered for

this evaluation includes the magnitude and maturity of the antibodies observed in patients; the persistence of the immune response; the ability of the antibodies to alter the PK of the drug; the ability of the antibodies to neutralize the drug and/or an endogenous counterpart; any association of antibodies and adverse events; and the association of antibodies with any hypersensitivity reactions.

When physicians (and patients) examine a drug's label it is important for them to understand what the immunogenicity profile of that drug is. This can help in the evaluation of whether the drug should be administered to the patient. But an important aspect is to understand the context of the information. Adding an evaluation of clinical significance would surely improve the understanding of a product's immunogenicity and hopefully the "clinically significant" language is simple and easy to understand. Immunogenicity assessment is very complicated and the analytical procedures utilized are complex and often very specific for each protein therapeutic. The ability to correctly interpret results from these assays is complex and time consuming and oftentimes, not even possible without access to support documents such as assay development reports and assay validations. It is often difficult to correctly interpret immunogenicity due to the multiple methods used in the process and the many confounding factors in developing and performing these unique assays. Being able to call out a well-defined population of ADAs that have clinical significance should help clarify the importance (if any) of ADAs identified with each therapeutic protein. There is an opportunity for pharmaceutical professional organizations, that rely on collaboration across the industry, to provide leadership and suggestions for compliance. This new guidance is in everyone's best interest, and while it will certainly result in some interesting conversations and efforts in the short term as we all grapple with implementation, will be very beneficial once fully implemented.

Author contributions

SS: Writing – original draft, Writing – review & editing.

Funding

The author(s) declare that no financial support was received for the research, authorship, and/or publication of this article.

Conflict of interest

Author SS was employed by the company Genentech Inc.

The reviewer JR declared a past collaboration with the author at the time of review.

Publisher's note

References

1. Tatarewicz SM, Starcevic-Manning M, Swanson SJ, Moxness MS, Chirmule N. Strategic characterization of anti-drug antibody responses for the assessment of clinical relevance and impact. *Bioanalysis*. (2014) 6:1509–23. doi: 10.4155/bio.14.114

2. Immunogenicity Information in Human Prescription Therapeutic Protein and Select Drug Product Labeling-Content and Format Guidance for Industry. Available online at: www.fda.gov (Accessed March 14, 2024).

3. Shankar G, Arkin S, Cocea L, Devanarayan V, Kirshner S, Kromminga A, et al. Assessment and reporting of the clinical immunogenicity of therapeutic proteins and peptides-harmonized terminology and tactical recommendations. *AAPS J*. (2014) 16:658–73. doi: 10.1208/s12248-014-9599-2

4. Li J, Yang C, Yea X. Thrombocytopenia caused by the development of antibodies to thrombopoietin. *Blood*. (2001) 98:3241–8. doi: 10.1182/blood.V98.12.3241

5. Casadevall N, Nataf J, Viron B, Kolta A, Kiladjian J-J, Martin-Dupont P, et al. Pure red cell aplasia and anti-ertythropoietin antibodies in patients treated with recombinant erythropoietin. *New Engl J Med*. (2002) 346:469–75. doi: 10.1056/NEJMoa011931

6. Chirmule N, Jawa V, Meibohm B. Immunogenicity to therapeutic proteins: impact on PK/PD and efficacy. *AAPS J*. (2012) 14:296–302. doi: 10.1208/s12248-012-9340-y

7. Chung CH, Mirakhur B, Chan E, Le Q-T, Berlin J, Morse M, et al. Cetuximab-induced anaphylaxis and IgE specific for galactose-alfa-1,3-galactose. *NEJM*. (2008) 358:1109–17. doi: 10.1056/NEJMoa074943

8. Krishna M, Nadler SG. Immunogenicity to biotherapeutics – the role of anti-drug immune complexes. *Front Immunol*. (2016) 7:21. doi: 10.3389/fimmu.2016.00021

9. Smiley JD, Moore SE. Southwestern Internal Medicine Conference: Immune-complex vasculitis: role of complement and IgG-Fc receptor functions. *Am J Med Sci*. (1989) 298:267–77. doi: 10.1097/00000441-198910000-00012

10. Saffari F, Jafarzadeh A. Development of antibodies in rituximab-treated patients: related parameters & consequences. *Indian J Med Res*. (2022) 155:335–46. doi: 10.4103/ijmr.IJMR_312_19

11. Schellekens H. Factors influencing the immunogenicity of therapeutic proteins. *Nephrol Dial Transplant*. (2005) 20 [suppl 6]:vi3–9. doi: 10.1093/ndt/gfh1092

12. Jawa V, Terry F, Gokemeijer J, Mitra-Kaushik S, Roberts BJ, Tourdot S, et al. T-cell dependent immunogenicity of protein therapeutics pre-clinical assessment and mitigation-updated consensus and review 2020. *Front Immunol*. (2020) 11:1301. doi: 10.3389/fimmu.2020.01301

13. Gupta S, Indelicato SR, Jethwa V, Kawabata T, Kelley M, Mire-Sluis AR, et al. Recommendations for the design, optimization, and qualification of cell-based assays used for the detection of neutralizing antibody responses elicited to biological therapeutics. *J Immunol Methods*. (2007) 321:1–18. doi: 10.1016/j.jim.2006.12.004

14. Koren E, Smith HW, Shores E, Shankar G, Finco-Kent D, Rup B, et al. Recommendations on risk-based strategies for detection and characterization of antibodies against biotechnology products. *J Immunol Methods*. (2008) 333:1–9. doi: 10.1016/j.jim.2008.01.001

15. Mire-Sluis AR, Barrett YC, Devanarayan V, Koren E, Liu H, Maia M, et al. Recommendations for the design and optimization of immunoassays used in the detection of host antibodies against biotechnology products. *J Immunol Methods*. (2004) 289:1–16. doi: 10.1016/j.jim.2004.06.002

16. Usdin M, Quarmby V, Zanghi J, Bernaards C, Liao L, Laxamana J, et al. Immunogenicity of Atezolizumab: Influence of testing method and sampling frequency on reported anti-drug antibody incidence rates. *AAPSJ*. (2024) 26:84. doi: 10.1208/s12248-024-00954-2

17. Rossert J, Cassadevall N, Eckardt KU. Anti-erythropoietin antibodies and pure red cell aplasia. *JASN*. (2004) 15:398–406. doi: 10.1097/01.ASN.0000107561.59698.42

18. *Eprex® [Product Monograph]*. Toronto Canada, MA: Janssen Inc (2017).

19. Schellekens H, Jiskoot W. Eprex-associated pure red cell aplasia and leachates. *Nat Biotechnol*. (2006) 24:613–4. doi: 10.1038/nbt0606-613

20. Swanson, Steven J, Ferbas J, Mayeux P, Casadevall N. Evaluations of methods to detect and characterize antibodies against recombinant human erythropoietin. *Nephron Clin Pract*. (2004) 96:c88–c95. doi: 10.1159/000076746

21. Bartends GM, Krieckaert CLM, Nurmohamed MT. Development of antidrug antibodies against adalimumab and association with disease activity and treatment failure during long-term follow-up. *JAMA*. (2011) 305:1460–8. doi: 10.1001/jama.2011.406

22. Pizano-Martinez O, Mendieta-Condado E, Vazquez-Del Mercado M, Martinez-Garcia EA, Chavarria-Avila E, Ortuno-Sahagun D, et al. Anti-drug antibodies in the biological therapy of autoimmune rheumatic diseases. *J Clin Med*. (2023) 12:3271. doi: 10.3390/jcm12093271

Frontiers in Immunology

Explores novel approaches and diagnoses to treat immune disorders.

The official journal of the International Union of Immunological Societies (IUIS) and the most cited in its field, leading the way for research across basic, translational and clinical immunology.

Discover the latest Research Topics

See more →

Frontiers

Avenue du Tribunal-Fédéral 34
1005 Lausanne, Switzerland
frontiersin.org

Contact us

+41 (0)21 510 17 00
frontiersin.org/about/contact